Visual system adaptations in the cichlid fish fauna of Lake Tanganyika

Inauguraldissertation

zur

Erlangung der Würde eines Doktors der Philosophie

vorgelegt der

Philosophisch-Naturwissenschaftlichen Fakultät

der Universität Basel

von

Virginie Micheline Irène **Ricci**

2023

Genehmigt von der Philosophisch-Naturwissenschaftlichen Fakultät
auf Antrag von

Erstbetreuer: Prof. Dr. Walter Salzburger
Zweitbetreuer: Prof. Dr. Patrick Tschopp
Externe Expertin: Dr. Maude Baldwin

Basel, den 21. Februar 2023

Prof. Dr. Marcel Mayor
Dekan

Visual system adaptations in the cichlid fish fauna of Lake Tanganyika

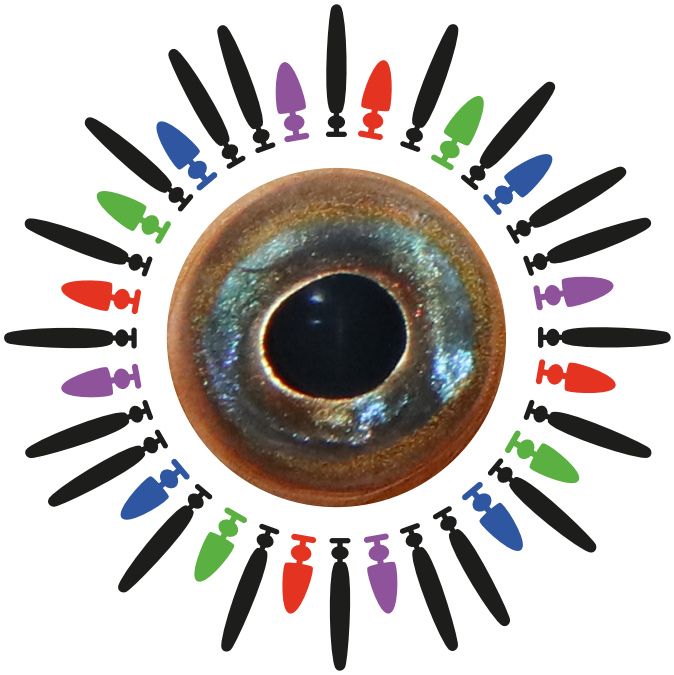

Inauguraldissertation zur
Erlangung der Würde eines Doktors der Philosophie
vorgelegt der Philosophisch-Naturwissenschaftlichen Fakultät
der Universität Basel von

Virginie Micheline Irène **Ricci**

betreut von
Prof. Dr. Walter Salzburger

evaluiert von
Prof. Dr. Walter Salzburger, Prof. Dr. Patrick Tschopp,
Dr. Maude Baldwin & Dr. Fabrizia Ronco

Basel, 2023

CONTENTS

INTRODUCTION

Understanding the genomic basis of evolutionary adaptations has been a central focus in past and current biological research (Byers, Xu, & Schlüter, 2017; Reeve & Sherman, 1993). The organism's ability to adapt to environmental conditions has a strong impact on its survival and has been implicated with diversification and speciation. Among the traits (or trait complexes) that are typically greatly affected by adaptive changes are the sensory systems, i.e. key features for the perception of vital environmental cues (Baldwin & Ko, 2020; Oteiza & Baldwin, 2021; Webster, 2012). Notably, the visual sensory system – detecting visual stimuli – is essential for animals to monitor and situationally respond to their surroundings (e.g., orientate, avoid predators, find shelter, search for edible items, choose reproductive mate, explore new environments, and choose habitat), which in turn has great implications for an individual's fitness.

In many animal groups (fish included), the eye is the main visual sensory organ processing visual information (light) from the environment (**Figure 1A**) (Land, 2005; Land & Nilsson, 2012; Oakley & Speiser, 2015). When a photon enters the eye, it can be absorbed by the photoreceptor cells present in the retina and initiate the phototransduction cascade (Lamb, Collin, & Edward, 2007). The collected visual stimuli are then converted into neuronal signals that are transmitted to the brain via the optic nerve. In vertebrates (fish included), the retina is composed of two types of photoreceptor cells: cones and rods (**Figure 1A**) (Bowmaker, 2008; K. L. Carleton, Escobar-Camacho, Stieb, Cortesi, & Marshall, 2020; Musilova, Salzburger, & Cortesi, 2021). Cone photoreceptor cells are responsible for the photopic vision perceiving chromatic (colour) visual information in bright-light conditions. They can be present in the form of single or double cones (two joined single cones either optically coupled or independent). In contrast, rod photoreceptor cells account for the scotopic vision and detect achromatic visual information (but see Musilova, Cortesi, et al., 2019) primarily in dim-light conditions. Cones and rods carry visual pigments that are composed of an opsin protein bound to a light-sensitive retinal non-protein chromophore (**Figure 1B**) (Fotiadis et al., 2006, 2003; Palczewski et al., 2000). Opsins belong to the transmembrane G protein-couple receptor (GPCRs) gene family that is characterized by conserved structural motifs, including seven transmembrane alpha-helices. The transmembrane domain of visual opsins forms a retinal binding pocket that binds covalently to the chromophore. Each visual pigment has its specific maximal spectral sensitivity (λ_{max}) that indicates the waveband absorbed in the range of the ultraviolet (UV) to the red light spectrum (**Figure 1C**) (Yokoyama, 2000, 2008; Yokoyama & Yokoyama, 1996). Most vertebrates (fish included) harbour a single rod opsin (rhodopsin [RH1], λ_{max} = 444 – 519 nm) and up to four main types of cone

opsins: the UV-sensitive SWS1 (λ_{max} = 347 – 450 nm); the violet/blue-sensitive SWS2 (λ_{max} = 397 – 490 nm); the green-sensitive RH2 (λ_{max} = 452 – 537 nm), and the red-sensitive LWS (λ_{max} = 490 – 570 nm) (Bowmaker, 2008; Davies, Collin, & Hunt, 2012; Lamb et al., 2007; Musilova et al., 2021). Photoreceptor cells are generally organised in a mosaic pattern – with a non-uniform intraretinal spatial distribution – of single cones expressing short-wavelength-sensitive opsins (SWS1 and SWS2) and double cones expressing medium- and long-wavelength sensitive opsins (RH2B and LWS) (**Figure 1D**) (Cortesi et al., 2020; Levine, MacNichol, Kraft, Collins, & BA, 1979; Viets, Eldred, & Johnston, 2016).

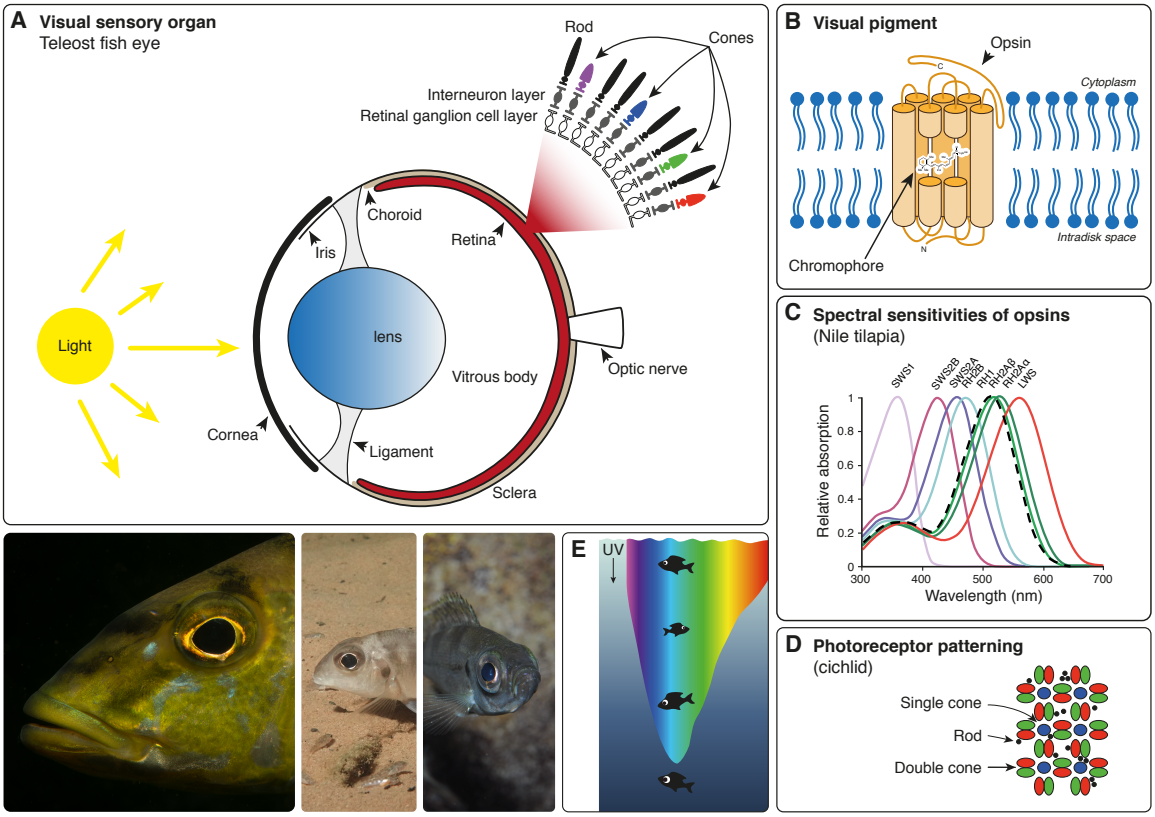

Figure 1 The visual sensory system of teleost (cichlid) fish. Schematic of **(A)** an eye, **(B)** a visual pigment (located in the outer segment of photoreceptor cells), **(C)** the spectral sensitivity of the seven cone opsins and the rod opsin of Nile tilapia (*Oreochromis niloticus*), **(D)** the photoreceptor patterning in the retina, and **(E)** the light gradient along the depth in clear water (UV: ultraviolet). Cichlid pictures kindly provided by Adrian Indermaur (from left to right): *Boulengerochromis microlepis*, *Callochromis macrops*, and *Haplotaxodon microlepis*. Illustrations modified from Hofmann et al. 2009, Carleton et al. 2016, Carleton et al. 2020, and Musilova et al. 2021.

In aquatic environments, the diversity of light conditions is particularly great due to the optical properties of the water that mainly depend on biotic and abiotic factors (Abate & Noakes, 2021; Kirk, 1983; Munz & McFarland, 1977; Warrant & Locket, 2004). In clear water, light is absorbed and scattered through the water column, resulting in a broad spectral waveband from UV to red light in shallow waters to a

prevalence of blue-green light in deep waters (**Figure 1E**). By comparison, the spectral waveband present in turbid water is shifted towards longer (red) wavelength (Musilova et al., 2021). Accordingly, the fish visual sensory system has been extensively studied and different adaptive mechanisms to optimise the perception of light in dim- and bright-light conditions have been uncovered (e.g., Cortesi et al., 2020, 2015; de Busserolles, Fogg, Cortesi, & Marshall, 2020; Fogg et al., 2022; Musilova, Cortesi, et al., 2019; Musilova et al., 2021; Stieb et al., 2019). Among morphological and physiological changes, a modification in eye size and shape, the presence of reflective tapeta as well as a rod-dominated retina can increase the catch of photons, especially in dim-light conditions. Pigmented corneas and lenses can filter out undesirable UV wavelengths and a change from an A1- to an A2-derived chromophore can shift the λ_{max} of visual pigments towards longer wavelengths. At the molecular level, gene duplication followed by functional divergence has also been shown to increase the sensitivity of colour distinction (e.g., RH2Aα and RH2Aβ with distinct λ_{max} in cichlid fish) (Owens & Rennison, 2017; Rennison, Owens, & Taylor, 2012; Spady et al., 2006; Weadick & Chang, 2012). Gene inactivation (pseudogenization) of a present or newly duplicated opsin can adapt the visual system to new spectral light conditions (Cortesi et al., 2015; Davies et al., 2012; Daniel Escobar-Camacho, Ramos, Martins, & Carleton, 2017; Musilova, Cortesi, et al., 2019). In addition, specific amino acid substitutions at so-called "key tuning" sites can induce a shift in λ_{max} towards shorter or longer wavelengths (Musilova, Cortesi, et al., 2019; Schott, Refvik, Hauser, López-Fernández, & Chang, 2014; Spady et al., 2005; Torres-Dowdall, Henning, Elmer, & Meyer, 2015) (see also **Chapter 1**: Ricci, Ronco, Musilova, & Salzburger, 2022). Furthermore, the set of expressed opsins defines visual sensitivity and colour distinction and can differ among species, but also change throughout an organism's life (e.g., ontogeny and heterochrony in cichlid fish) (Karen L. Carleton et al., 2008; Daniel Escobar-Camacho et al., 2017; Lupše et al., 2021; Musilova, Indermaur, et al., 2019; O'Quin, Hofmann, Hofmann, & Carleton, 2010; Spady et al., 2006).

Cichlid fish are a great model system to study evolutionary biology in general (Gavrilets & Losos, 2009; Kocher, 2004; Salzburger, 2018) (see also **Chapter 3**: Ronco et al., 2021) and the visual sensory system in particular (see reviews K. Carleton, 2009; K. L. Carleton & Yourick, 2020; Karen L. Carleton, Dalton, Escobar-Camacho, & Nandamuri, 2016; D Escobar-Camacho & Carleton, 2015). They show an exceptional diversity of ecological, morphological and behavioural traits and represent some of the most spectacular examples of species-rich adaptive radiations in the African

Great Lakes, especially in Lake Tanganyika (Fryer & Iles, 1972; Ronco, Büscher, Indermaur, & Salzburger, 2020; Salzburger, 2018) (see also **Chapter 3**: Ronco et al., 2021). The diversification through adaptive radiation has given rise to closely-related species that have rapidly emerged within a single organismal lineage and have evolved adaptations to distinct ecological niches. Vision has presumably participated in the exploration and hence the establishment of cichlid fish in different ecological niches of freshwater aquatic environments within the African Great Lakes (and surrounding rivers). The visual opsin gene repertoire of cichlids typically includes seven cone opsins (UV-sensitive: SWS1; violet-sensitive: SWS2B; blue-sensitive: SWS2A; green-sensitive RH2B, RH2Aα, and RH2Aβ; and red-sensitive LWS), plus a rod opsin (rhodopsin RH1) (but see Karen L. Carleton et al., 2008; Spady et al., 2005). In principle, adults rely on a dichromatic to tetrachromatic colour vision and generally express a "visual palette" of three cone opsins: short-wavelength (SWS1-RH2B-RH2A), middle-wavelength (SWS2B-RH2B-RH2A), or long-wavelength (SWS2A-RH2A-LWS) (K. Carleton, 2009; K. L. Carleton et al., 2020, 2010; Hofmann & Carleton, 2009; O'Quin et al., 2010). Previous studies have focused on the visual system of cichlids and notably the adaptive changes in visual opsins in relation to the habitat light conditions (between rivers/lakes and within lakes) (see reviews K. Carleton, 2009; K. L. Carleton & Yourick, 2020; Karen L. Carleton et al., 2016; D Escobar-Camacho & Carleton, 2015). For instance, the RH1 protein-coding sequence regularly differs at key tuning sites between shallow- and deep-water living species (Nagai et al., 2011; Sugawara et al., 2005) (see also **Chapter 1**: Ricci et al., 2022). Furthermore, species living in shallow and/or turbid waters primarily express a visual palette dominated by the red-sensitive LWS, while species living in deep waters express predominantly the green-sensitive RH2A (Hofmann et al., 2009; Musilova, Indermaur, et al., 2019; Wright et al., 2019) (see also **Chapter 2**: Ricci et al., submitted).

The major goal of the present thesis was to investigate adaptations in the visual system in the massive adaptive radiation of cichlid fishes in the relatively clear waters of Lake Tanganyika. Based on whole genome and retinal transcriptome data in combination with ecological, phenotypic, as well as phylogenetic information, we explored the diversity and dynamics of the visual opsins of Lake Tanganyika cichlids. More specifically, **Chapter 1** ("Molecular evolution and depth-related adaptations of rhodopsin in the adaptive radiation of cichlid fishes in Lake Tanganyika") focuses on the rhodopsin to assess the evolution of the scotopic vision in virtually the entire adaptive radiation of cichlid fishes in Lake Tanganyika. We primarily investigated the

diversity of the protein-coding sequence of RH1 and the putative molecular adaptations to the different light conditions along the water depth gradient. On the other hand, **Chapter 2** ("Visual opsin gene expression evolution in the adaptive radiation of cichlid fishes of Lake Tanganyika") deals with the visual opsin gene expression patterns in the adaptive radiation of cichlid fishes in Lake Tanganyika. Notably, we retrieved the opsin expression profile and the expressed visual palette per species, and investigated associations between opsin expression levels and eco-morphological traits.

Chapter 3 ("Drivers and dynamics of a massive adaptive radiation in cichlid fishes") was the result of an extensive collaboration that inferred the virtually complete phylogeny of the cichlid fishes from Lake Tanganyika and explored the eco-morphological traits implicated in the course of diversification. More precisely, we performed whole-genome phylogenetic analyses, multivariate morphological measurements of three ecologically relevant trait complexes, scoring of pigmentation patterns and approximations of the ecology of nearly all of the approximately 240 cichlid species endemic to Lake Tanganyika. Note that morphological, ecological, and genomic data, as well as phylogenetic information presented in **Chapter 3** have been used in **Chapter 1** and **Chapter 2**.

My contribution to **Chapter 3** and **Chapter 4** ("QTL study reveals candidate genes underlying host resistance in a Red Queen model system") helped the understanding of the genomic basis of evolutionary adaptations with a focus on the repeat content. Among the repetitive DNA sequences, transposable elements (TEs) are selfish mobile features that can make up to 50% of eukaryotic genomes (Sotero-Caio, Platt, Suh, & Ray, 2017). They are a main source of innovation for genes, regulatory elements, and genome structure (see reviews Bourque, 2009; Bourque et al., 2018; Levin & Moran, 2011; Sotero-Caio et al., 2017). Hence, the characterisation of the repeat content represents a significant part of the genome examination. My contribution to **Chapter 3** was to characterise the species repeat content in order to test for an association between transposable elements content and per-tribe species richness. On the other hand, **Chapter 4** was a collaboration with Maridel Fredericksen who worked on the model system of the crustacean *Daphnia magna* and its bacterial parasite *Pasteuria ramosa*. The goal of this project was to investigate the genetic features that play a role in host resistance. I participated in characterising the repeat content of *Daphnia magna* and investigating the transposable elements present in a newly identified resistance locus.

An overall discussion on the adaptation of the visual system in the adaptive radiation of cichlid fishes in Lake Tanganyika follows the four main chapters. Please, note that the chapters which constitute the present thesis are the results of valuable collaborations. My personal contribution to each chapter is indicated in the authors contribution section.

References

Abate, M. E., & Noakes, D. L. G. (2021). *The Behavior , Ecology and Evolution of Cichlid Fishes*. Springer.

Baldwin, M. W., & Ko, M. C. (2020). Functional evolution of vertebrate sensory receptors. *Hormones and Behavior*, *124*(104771). doi: 10.1016/j.yhbeh.2020.104771

Bourque, G. (2009). Transposable elements in gene regulation and in the evolution of vertebrate genomes. *Current Opinion in Genetics and Development*, *19*(6), 607–612. doi: 10.1016/j.gde.2009.10.013

Bourque, G., Burns, K. H., Gehring, M., Gorbunova, V., Seluanov, A., Hammell, M., … Feschotte, C. (2018). Ten things you should know about transposable elements. *Genome Biology*, *19*(1), 1–12. doi: 10.1186/s13059-018-1577-z

Bowmaker, J. K. (2008). Evolution of vertebrate visual pigments. *Vision Research*, *48*, 2022–2041. doi: 10.1016/j.visres.2008.03.025

Byers, K. J. R. P., Xu, S., & Schlüter, P. M. (2017). Molecular mechanisms of adaptation and speciation: why do we need an integrative approach? *Molecular Ecology*, *26*(1). doi: 10.1111/mec.13678

Carleton, K. (2009). Cichlid fish visual systems: mechanisms of spectral tuning. *Integrative Zoology*, *4*, 75–86. doi: 10.1111/j.1749-4877.2008.00137.x

Carleton, K. L., Escobar-Camacho, D., Stieb, S. M., Cortesi, F., & Marshall, N. J. (2020). Seeing the rainbow: mechanisms underlying spectral sensitivity in teleost fishes. *Journal of Experimental Biology*, *223*. doi: 10.1242/jeb.193334

Carleton, K. L., Hofmann, C. M., Klisz, C., Patel, Z., Chircus, L. M., Simenauer, L. H., … Ser, J. R. (2010). Genetic basis of differential opsin gene expression in cichlid fishes. *Journal of Evolutionary Biology*, *23*(4). doi: 10.1111/j.1420-9101.2010.01954.x

Carleton, K. L., & Yourick, M. R. (2020). Axes of visual adaptation in the ecologically diverse family Cichlidae. *Seminars in Cell and Developmental Biology*, *106*, 43–52. doi: 10.1016/j.semcdb.2020.04.015

Carleton, Karen L., Dalton, B. E., Escobar-Camacho, D., & Nandamuri, S. P. (2016). Proximate and ultimate causes of variable visual sensitivities: Insights from cichlid fish radiations. *Genesis*, *54*(6), 299–325. doi: 10.1002/dvg.22940

Carleton, Karen L., Spady, T. C., Streelman, J. T., Kidd, M. R., McFarland, W. N., & Loew, E. R. (2008). Visual sensitivities tuned by heterochronic shifts in opsin gene expression. *BMC Biology*, *6*, 1–14. doi: 10.1186/1741-7007-6-22

Cortesi, F., Mitchell, L. J., Tettamanti, V., Fogg, L. G., de Busserolles, F., Cheney, K. L., & Marshall, N. J. (2020). Visual system diversity in coral reef fishes. *Seminars in Cell and Developmental Biology*, *106*(March), 31–42. doi: 10.1016/j.semcdb.2020.06.007

Cortesi, F., Musilová, Z., Stieb, S. M., Hart, N. S., Siebeck, U. E., Malmstrøm, M., … Salzburger, W. (2015). Ancestral duplications and highly dynamic opsin gene

evolution in percomorph fishes. *Proceedings of the National Academy of Sciences of the United States of America*, *112*(5), 1493–1498. doi: 10.1073/pnas.1417803112

Davies, W. I. L., Collin, S. P., & Hunt, D. M. (2012). Molecular ecology and adaptation of visual photopigments in craniates. *Molecular Ecology*, *21*(13), 3121–3158. doi: 10.1111/j.1365-294X.2012.05617.x

de Busserolles, F., Fogg, L., Cortesi, F., & Marshall, J. (2020). The exceptional diversity of visual adaptations in deep-sea teleost fishes. *Seminars in Cell and Developmental Biology*, *106*, 20–30. doi: 10.1016/j.semcdb.2020.05.027

Escobar-Camacho, D, & Carleton, K. L. (2015). Sensory modalities in cichlid fish behavior. *Current Opinion in Behavioral Sciences*, *6*, 115–124. doi: 10.1016/j.cobeha.2015.11.002

Escobar-Camacho, Daniel, Ramos, E., Martins, C., & Carleton, K. L. (2017). The opsin genes of amazonian cichlids. *Molecular Ecology*, *26*(5), 1343–1356. doi: 10.1111/mec.13957

Fogg, L. G., Cortesi, F., Lecchini, D., Gache, C., Marshall, N. J., & de Busserolles, F. (2022). Development of dim-light vision in the nocturnal reef fish family Holocentridae I: retinal gene expression. *Journal of Experimental Biology*, *225*. doi: 10.1242/jeb.244513

Fotiadis, D., Jastrzebska, B., Philippsen, A., Müller, D. J., Palczewski, K., & Engel, A. (2006). Structure of the rhodopsin dimer: a working model for G-protein-coupled receptors. *Current Opinion in Structural Biology*, *16*(2), 252–259. doi: 10.1016/j.sbi.2006.03.013

Fotiadis, D., Liang, Y., Filipek, S., Saperstein, D. A., Engel, A., & Palczewski, K. (2003). Rhodopsin dimers in native disc membranes. *Nature*, *421*(6919), 127–128.

Fryer, G., & Iles, T. D. (1972). *The Cichlid Fishes of the Great Lakes of Africa. Their Biology and Evolution*. Oliver and Boyd, Edinburgh.

Gavrilets, S., & Losos, J. (2009). *Adaptive Radiation : Contrasting Theory with Data*. *323*(February), 732–738.

Hofmann, C. M., & Carleton, K. L. (2009). Gene duplication and differential gene expression play an important role in the diversification of visual pigments in fish. *Integrative and Comparative Biology*, *49*(6), 630–643. doi: 10.1093/icb/icp079

Hofmann, C. M., O'Quin, K. E., Justin Marshall, N., Cronin, T. W., Seehausen, O., & Carleton, K. L. (2009). The eyes have it: Regulatory and structural changes both underlie cichlid visual pigment diversity. *PLoS Biology*, *7*(12). doi: 10.1371/journal.pbio.1000266

Kirk, J. T. O. (1983). Light and photosynthesis in aquatic ecosystems. *Light and Photosynthesis in Aquatic Ecosystems.* doi: 10.2307/2405114

Kocher, T. D. (2004). Adaptive evolution and explosive speciation: The cichlid fish model. *Nature Reviews Genetics*, *5*(4), 288–298. doi: 10.1038/nrg1316

Lamb, T. D., Collin, S. P., & Edward, N. P. J. (2007). Evolution of the vertebrate eye: opsins, photoreceptors, retina and eye cup. *Nature Review Neuroscience*, *8*(12), 960–976. doi: 10.1038/nrn2283.

Land, M. F. (2005). The optical structures of animal eyes. *Current Biology*, Vol. 15. doi: 10.1016/j.cub.2005.04.041

Land, M. F., & Nilsson, D.-E. (2012). Animal Eyes. *Zoological Journal of the Linnean Society*, *166*(4), 912–912. doi: 10.1111/j.1096-3642.2012.00849.x

Levin, H. L., & Moran, J. V. (2011). Dynamic interactions between transposable elements and their hosts. *Nature Reviews Genetics*, *12*(9), 615–627. doi: 10.1038/nrg3030

Levine, J., MacNichol, E., Kraft, T., Collins, & BA. (1979). Intraretinal Distribution of Cone Pigments in Certain Teleost Fishes Abstract . Microspectrophotometric investigations of visual pigments in the teleost by PMSP in this manner is both. *Science*, *204*(4392), 523–556.

Lupše, N., Cortesi, F., Freese, M., Marohn, L., Pohlmann, J. D., Wysujack, K., … Musilova, Z. (2021). Visual Gene Expression Reveals a cone-to-rod Developmental Progression in Deep-Sea Fishes. *Molecular Biology and Evolution*, *38*(12), 5664–5677. doi: 10.1093/molbev/msab281

Munz, F. W., & McFarland, W. N. (1977). Evolutionary Adaptations of Fishes to the Photic Environment. In C. F (Ed.), *The Visual System in Vertebrates* (pp. 193–274). Springer Verlag. doi: 10.1007/978-3-642-66468-7_4

Musilova, Z., Cortesi, F., Matschiner, M., Davies, W. I. L., Patel, J. S., Stieb, S. M., … Salzburger, W. (2019). Vision using multiple distinct rod opsins in deep-sea fishes. *Science*, *364*(6440), 588–592. doi: 10.1126/science.aav4632

Musilova, Z., Indermaur, A., Bitja-Nyom, A. R., Omelchenko, D., Kłodawska, M., Albergati, L., … Salzburger, W. (2019). Evolution of the visual sensory system in cichlid fishes from crater lake Barombi Mbo in Cameroon. *Molecular Ecology*, *28*, 5010–5031. doi: 10.1111/mec.15217

Musilova, Z., Salzburger, W., & Cortesi, F. (2021). The Visual Opsin Gene Repertoires of Teleost Fishes: Evolution, Ecology, and Function. *Annual Review of Cell and Developmental Biology*, *37*(1), 441–468. doi: 10.1146/annurev-cellbio-120219-024915

Nagai, H., Terai, Y., Sugawara, T., Imai, H., Nishihara, H., Hori, M., & Okada, N. (2011). Reverse evolution in RH1 for adaptation of cichlids to water depth in Lake Tanganyika. *Molecular Biology and Evolution*, *28*(6), 1769–1776. doi: 10.1093/molbev/msq344

O'Quin, K. E., Hofmann, C. M., Hofmann, H. A., & Carleton, K. L. (2010). Parallel Evolution of opsin gene expression in African cichlid fishes. *Molecular Biology and Evolution*, *27*(12). doi: 10.1093/molbev/msq171

Oakley, T. H., & Speiser, D. I. (2015). How Complexity Originates: The Evolution of Animal Eyes. *Annual Review of Ecology, Evolution, and Systematics*, *46*. doi: 10.1146/annurev-ecolsys-110512-135907

Oteiza, P., & Baldwin, M. W. (2021). Evolution of sensory systems. *Current Opinion in Neurobiology*, *71*, 52–59. doi: 10.1016/j.conb.2021.08.005

Owens, G. L., & Rennison, D. J. (2017). Evolutionary ecology of opsin gene sequence, expression and repertoire. *Molecular Ecology*, *26*(5), 1207–1210. doi: 10.1111/mec.14032

Palczewski, K., Kumasaka, T., Hori, T., Behnke, C. A., Motoshima, H., Fox, B. A., … Miyano, M. (2000). Crystal structure of rhodopsin: A G protein-coupled receptor. *Science*, *289*(5480), 739–745. doi: 10.1126/science.289.5480.739

Reeve, H. K., & Sherman, P. W. (1993). Adaptation and the goals of evolutionary research. *Quarterly Review of Biology*, *68*(1). doi: 10.1086/417909

Rennison, D. J., Owens, G. L., & Taylor, J. S. (2012). Opsin gene duplication and divergence in ray-finned fish. *Molecular Phylogenetics and Evolution*, *62*(3), 986–1008. doi: 10.1016/j.ympev.2011.11.030

Ricci, V., Ronco, F., Musilova, Z., & Salzburger, W. (2022). Molecular evolution and depth-related adaptations of rhodopsin in the adaptive radiation of cichlid fishes in Lake Tanganyika. *Molecular Ecology*, *31*(10), 2882–2897. doi: 10.1111/mec.16429

Ronco, F., Büscher, H. H., Indermaur, A., & Salzburger, W. (2020). The taxonomic diversity of the cichlid fish fauna of ancient Lake Tanganyika, East Africa. *Journal of Great Lakes Research*, *46*(5), 1067–1078. doi: 10.1016/j.jglr.2019.05.009

Ronco, F., Matschiner, M., Böhne, A., Boila, A., Büscher, H. H., El Taher, A., … Salzburger, W. (2021). Drivers and dynamics of a massive adaptive radiation in cichlid fishes. *Nature*, *589*, 76–81. doi: 10.1038/s41586-020-2930-4

Salzburger, W. (2018). Understanding explosive diversification through cichlid fish genomics. *Nature Reviews Genetics*, *19*(11), 705–717. doi: 10.1038/s41576-018-0043-9

Schott, R. K., Refvik, S. P., Hauser, F. E., López-Fernández, H., & Chang, B. S. W. (2014). Divergent positive selection in rhodopsin from lake and riverine cichlid fishes. *Molecular Biology and Evolution*, *31*(5), 1149–1165. doi: 10.1093/molbev/msu064

Sotero-Caio, C. G., Platt, R. N., Suh, A., & Ray, D. A. (2017). Evolution and diversity of transposable elements in vertebrate genomes. *Genome Biology and Evolution*, *9*(1), 161–177. doi: 10.1093/gbe/evw264

Spady, T. C., Parry, J. W. L., Robinson, P. R., Hunt, D. M., Bowmaker, J. K., & Carleton, K. L. (2006). Evolution of the cichlid visual palette through ontogenetic subfunctionalization of the opsin gene arrays. *Molecular Biology and Evolution*, *23*(8), 1538–1547. doi: 10.1093/molbev/msl014

Spady, T. C., Seehausen, O., Loew, E. R., Jordan, R. C., Kocher, T. D., & Carleton, K. L. (2005). Adaptive molecular evolution in the opsin genes of rapidly speciating cichlid species. *Molecular Biology and Evolution*, *22*(6), 1412–1422. doi: 10.1093/molbev/msi137

Stieb, S. M., de Busserolles, F., Carleton, K. L., Cortesi, F., Chung, W. S., Dalton, B. E., … Marshall, N. J. (2019). A detailed investigation of the visual system and visual ecology of the Barrier Reef anemonefish, Amphiprion akindynos. *Scientific Reports*, *9*(1), 1–14. doi: 10.1038/s41598-019-52297-0

Sugawara, T., Terai, Y., Imai, H., Turner, G. F., Koblmüller, S., Sturmbauer, C., … Okada, N. (2005). Parallelism of amino acid changes at the RH1 affecting spectral sensitivity among deep-water cichlids from Lakes Tanganyika and Malawi. *Proceedings of the National Academy of Sciences of the United States of America*, *102*(15), 5448–5453. doi: 10.1073/pnas.0405302102

Torres-Dowdall, J., Henning, F., Elmer, K. R., & Meyer, A. (2015). Ecological and lineage-specific factors drive the molecular evolution of rhodopsin in cichlid fishes. *Molecular Biology and Evolution*, *32*(11), 2876–2882. doi: 10.1093/molbev/msv159

Viets, K., Eldred, K. C., & Johnston, R. J. (2016). Mechanisms of Photoreceptor Patterning in Vertebrates and Invertebrates. *Trends in Genetics*, *32*(10), 638–659. doi: 10.1016/j.tig.2016.07.004

Warrant, E. J., & Locket, N. A. (2004). Vision in the deep sea. *Biological Reviews of the Cambridge Philosophical Society*, *79*, 671–712. doi: 10.1017/S1464793103006420

Weadick, C. J., & Chang, B. S. W. (2012). Complex patterns of divergence among green-sensitive (RH2a) African cichlid opsins revealed by Clade model analyses. *BMC Evolutionary Biology*, *12*(1). doi: 10.1186/1471-2148-12-206

Webster, M. A. (2012). Evolving concepts of sensory adaptation. *F1000 Biology Reports*, *4*(1), 1–7. doi: 10.3410/B4-21

Wright, D. S., Meijer, R., van Eijk, R., Vos, W., Seehausen, O., & Maan, M. E. (2019). Geographic variation in opsin expression does not align with opsin genotype in Lake Victoria cichlid populations. *Ecology and Evolution*, *9*(15), 8676–8689. doi: 10.1002/ece3.5411

Yokoyama, S. (2000). Molecular evolution of vertebrate visual pigments. In *Progress in Retinal and Eye Research* (Vol. 19). doi: 10.1016/S1350-9462(00)00002-1

Yokoyama, S. (2008). Evolution of dim-light and color vision pigments. *Annual Review of Genomics and Human Genetics*, *9*, 259–282. doi: 10.1146/annurev.genom.9.081307.164228

Yokoyama, S., & Yokoyama, R. (1996). Adaptive Evolution of Photoreceptors and Visual Pigments in Vertebrates. *Annual Review of Ecology and Systematics*, *27*, 543–567.

CHAPTER 1

Molecular evolution and depth-related adaptations of rhodopsin in the adaptive radiation of cichlid fishes in Lake Tanganyika

Virginie Ricci, Fabrizia Ronco, Zuzana Musilova & Walter Salzburger

Molecular Ecology (2022)

Received: 26 October 2021 | Revised: 11 February 2022 | Accepted: 4 March 2022

DOI: 10.1111/mec.16429

ORIGINAL ARTICLE

MOLECULAR ECOLOGY WILEY

Molecular evolution and depth-related adaptations of rhodopsin in the adaptive radiation of cichlid fishes in Lake Tanganyika

Virginie Ricci[1] | Fabrizia Ronco[1] | Zuzana Musilova[2] | Walter Salzburger[1]

[1]Department of Environmental Sciences, Zoological Institute, University of Basel, Basel, Switzerland

[2]Department of Zoology, Faculty of Science, Charles University, Prague, Czech Republic

Correspondence
Virginie Ricci and Walter Salzburger, Department of Environmental Sciences, Zoological Institute, University of Basel, Basel, Switzerland.
Emails: virginie.ricci@unibas.ch (V.R.); walter.salzburger@unibas.ch (W.S.)

Funding information
H2020 European Research Council, Grant/Award Number: 617585; Grantová Agentura České Republiky, Grant/Award Number: 21-31712S; Schweizerischer Nationalfonds zur Förderung der Wissenschaftlichen Forschung, Grant/Award Number: 166550 and 176039

Handling Editor: Philine G. D. Feulner

Abstract

The visual sensory system is essential for animals to perceive their environment and is thus under strong selection. In aquatic environments, light intensity and spectrum differ primarily along a depth gradient. Rhodopsin (RH1) is the only opsin responsible for dim-light vision in vertebrates and has been shown to evolve in response to the respective light conditions, including along a water depth gradient in fishes. In this study, we examined the diversity and sequence evolution of RH1 in virtually the entire adaptive radiation of cichlid fishes in Lake Tanganyika, focusing on adaptations to the environmental light with respect to depth. We show that Tanganyikan cichlid genomes contain a single copy of *RH1*. The 76 variable amino acid sites detected in RH1 across the radiation were not uniformly distributed along the protein sequence, and 31 of these variable sites show signals of positive selection. Moreover, the amino acid substitutions at 15 positively selected sites appeared to be depth-related, including three key tuning sites that directly mediate shifts in the peak spectral sensitivity, one site involved in protein stability and 11 sites that may be functionally important on the basis of their physicochemical properties. Among the strongest candidate sites for deep-water adaptations are two known key tuning sites (positions 292 and 299) and three newly identified variable sites (37, 104 and 290). Our study, which is the first comprehensive analysis of RH1 evolution in a massive adaptive radiation of cichlid fishes, provides novel insights into the evolution of RH1 in a freshwater environment.

KEYWORDS
freshwater fish, opsin, photic environment, rod photoreceptor, spectral tuning, vision

1 | INTRODUCTION

The survival of animals depends heavily on their ability to perceive their surroundings (Escobar-Camacho & Carleton, 2015). Among the different sensory systems, vision allows animals to orientate themselves, to escape from predators, to find shelter, to sense potential food items, to communicate amongst each other, to find mates, to choose a habitat and/or to explore new environments (Escobar-Camacho & Carleton, 2015; Musilova et al., 2021). The visual sensory system is thus under strong selection (e.g., Schott et al., 2014; Terai et al., 2002; Torres-Dowdall et al., 2015) and visual adaptations have been implicated with diversification in different terrestrial and

aquatic taxa (Boughman, 2002; Maan et al., 2006; Seehausen et al., 2008; Terai et al., 2006; Wright et al., 2020).

In vertebrates, two types of photoreceptor cells located in the retina—cones and rods—are typically responsible for bright-light (photopic) and dim-light (scotopic) vision, respectively (Bowmaker, 2008; but see Musilova et al., 2021). Cones and rods harbour visual pigments, which are composed of an opsin protein bound to a light-sensitive vitamin A-derived, nonprotein chromophore (Bowmaker, 2008). Each visual pigment absorbs a specific waveband in the range of the ultraviolet (UV) to the red light spectrum, and can be characterized by its maximal spectral sensitivity (λ_{max}) (Carleton et al., 2020). Vertebrates possess up to four main types of cone opsins, the short-wavelength sensitive SWS1 and SWS2, the middle-wavelength sensitive RH2, and the long-wavelength sensitive LWS, plus one rod opsin (rhodopsin, RH1; Bowmaker, 2008; Musilova et al., 2021; Musilova, Cortesi, et al., 2019). These opsins belong to a larger gene family, the transmembrane G protein-coupled receptors (GPCRs), which initiate signalling pathways through the activation of G proteins. GPCRs feature largely conserved structural motifs including seven transmembrane alpha-helices (TM) that form a ligand-binding pocket (Bowmaker, 2008; Palczewski et al., 2000; Terakita, 2005). In visual opsin proteins, the ligand-binding pocket is called retinal binding pocket and binds to the chromophore via a retinal-binding site (located in TM VII) and a Schiff base counterion (in TM III; Bowmaker, 2008; Palczewski et al., 2000; Terakita, 2005). In addition, a disulphide bridge between two amino acid sites maintains the organization of the seven-helix transmembrane motif by bringing together TM III and the extracellular loop between TM IV and V. Visual opsin proteins are hence characterized by conserved amino acid sites (including those responsible for structural stability and chromophore binding) and highly variable sites, whereby a number of amino acid changes at these latter sites have been suggested to be adaptive by fine-tuning the visual sensitivity to match the local light environment (Bowmaker, 2008; Carleton et al., 2020; Hauser & Chang, 2017; Musilova et al., 2021). Next to amino acid substitutions, adaptive changes in opsins may also occur through gene duplication or loss, or the expression of different opsin palettes (e.g., Carleton et al., 2020; Hauser & Chang, 2017; Lin et al., 2017; Musilova, Indermaur, et al., 2019). Thus, different strategies can be applied to assess whether changes in visual opsin proteins are adaptive and correlate with ecology, including positive selection analyses and photoreceptor sensitivity (λ_{max}) estimations (reviewed by Carleton et al., 2020).

In aquatic environments, the visual scenes vary dramatically depending on several different biotic and abiotic factors (Munz & McFarland, 1977; Warrant & Locket, 2004; Yokoyama & Yokoyama, 1996). As light (mostly provided by the sun) passes through the water column, it is continuously absorbed and scattered, resulting in an increasingly narrowed light spectrum with depth. As a consequence, shallow-water species are exposed to UV and a broader range of the visible light spectrum compared to those living in deep waters where blue and blue–green light dominates (Yokoyama & Yokoyama, 1996). In addition, rivers, lakes and oceans have different optical properties that affect light transmission and absorption in the water column (Yokoyama & Yokoyama, 1996). For example, the presence of phytoplankton and dissolved organic material as well as turbidity reduce light penetration, most notably in inshore and inland water bodies. Accordingly, the visual system of fish has been shown to evolve and adapt both anatomically and physiologically to divergent light environments (Carleton et al., 2020; Davies et al., 2012; Musilova, Cortesi, et al., 2019; Seehausen et al., 2008). For instance, deep-sea fishes have evolved different phenotypic adaptations to catch more photons, such as big eyes, tubular eye structures, reflective tapeta that are wavelength-selective, multilayer retinae and lenses containing yellow pigment (Musilova, Cortesi, et al., 2019; Warrant & Locket, 2004).

RH1 is the single opsin in rods and is responsible for perceiving the achromatic visual information from the environment, typically featuring a λ_{max}-value around 500 nm (i.e., in the blue–green part of the light spectrum; Bowmaker, 2008; Hauser & Chang, 2017; Munz & McFarland, 1977). *RH1* is the best studied opsin gene and the first GPCR that had its crystal structure determined (Palczewski et al., 2000). Structural conformation studies found that RH1 exists as dimers and that the oligomeric state of RH1 is important for the activation of G proteins (Fotiadis et al., 2003; Guo et al., 2005). Further, through phylogenetic comparative analyses and *in vitro* protein reconstructions, specific amino acid substitutions at so-called "key tuning" sites have been identified that change λ_{max} and, hence, the function of RH1 (Hunt et al., 2014; Sugawara et al., 2005; Yokoyama et al., 2008). Previous studies also found that deep-water living fishes show specific molecular adaptations and/or have expanded their RH1 repertoire to efficiently adjust their visual system to the light environment at depth (Hunt et al., 1996; Musilova, Cortesi, et al., 2019; Nagai et al., 2011; Sugawara et al., 2005). For example, more than 20 amino acid substitutions at key tuning sites have been identified that mediate a shift in λ_{max} towards shorter wavelengths (blue-shift), and the emergence of differently tuned RH1 copies has been suggested to increase visual sensitivity in deep waters (Hofmann et al., 2009; Musilova, Cortesi, et al., 2019; Sugawara et al., 2005). Such adaptive changes generally optimize visual sensitivity by matching the peak absorbance of RH1 with the peak wavelength of the environmental light (blue and blue–green light in deep waters, as compared to blue-to-red light in shallow waters; Carleton et al., 2020; Yokoyama, 2008). Finally, some fish species living in deep waters, where hydrostatic pressure is elevated, were shown to feature particular amino acid substitutions in RH1 associated with protein stability (Porter et al., 2016). More precisely, the steadiness of the protein structural conformation (opsin dimers) and, hence, the function of RH1 is maintained in deep-water fishes through a reduction of the protein's adiabatic compressibility (Porter et al., 2016).

Cichlid fishes (Cichliformes, Cichlidae), which are currently undergoing dramatic adaptive radiations, most notably in the African Great Lakes, are an important model system in evolutionary biology (Kocher, 2004; McGee et al., 2020; Salzburger, 2018). These radiations have resulted in arrays of closely related species living in various habitats, including at different depths. Cichlids thus also emerge

as a great model system to investigate the visual sensory system in general and visual opsin genes in particular (e.g., Escobar-Camacho & Carleton, 2015; Musilova, Indermaur, et al., 2019; Musilova et al., 2021; Schneider et al., 2020; Torres-Dowdall et al., 2015; Wright et al., 2020). Previous studies investigated the achromatic visual system of a handful of East African cichlid species (Malinsky et al., 2015; Miyagi et al., 2012; Nagai et al., 2011; Schott et al., 2014; Sugawara et al., 2005; Terai et al., 2017; Torres-Dowdall et al., 2015). A common finding so far is that cichlid species living at depth have evolved similar molecular changes at key tuning sites that may shift λ_{max} towards shorter wavelengths (blue-shift; Sugawara et al., 2005) to better match the peak wavelength of the environmental light. On a small subset of Lake Tanganyika (LT) cichlid species, Nagai et al. (2011) found that most deep-water species have a serine (S) at amino acid position 292, while the majority of shallow-water species feature an alanine (A). Note that the substitution A292S is predicted to shift λ_{max} by about −9 nm and has therefore been suggested to mediate a depth-related adaptation (Musilova, Cortesi, et al., 2019; Yokoyama et al., 2008).

In this study, we investigated the molecular evolution of RH1 in virtually the entire adaptive radiation of cichlid fishes from LT, which represents the ecologically, morphologically and behaviourally most diverse cichlid radiation (Ronco et al., 2021; Salzburger, 2018; Salzburger et al., 2014). Making use of available whole genome sequences of nearly all cichlid species occurring in the lake, we (i) identified and newly assembled *RH1* gene sequences and screened for possible gene duplications; (ii) quantified the diversity of both nucleotide and amino acid sequences of RH1; (iii) tested if environmentally selective pressures have shaped RH1 protein sequence evolution; and (iv) screened for candidate amino acid substitutions that are associated with depth and hence potentially represent depth-related adaptations. Our investigation of about 250 closely related taxa provides comprehensive insights into the evolution of RH1 in a freshwater environment.

2 | MATERIALS AND METHODS

2.1 | Data set

For this study, we revisited the Illumina sequence data from our previous work, in which we had produced whole genome sequences for a nearly taxonomically complete sample of the cichlid fish fauna of LT (raw sequencing data are available on NCBI under the BioProject accession no. PRJNA550295, https://www.ncbi.nlm.nih.gov/bioproject/; Ronco et al., 2021). Making use of the available raw DNA reads, we newly assembled the intron-less *RH1* coding sequence (CDS). Our sample included sequence data for 245 taxa belonging to 12 tribes that are part of the adaptive radiation of cichlid fishes in LT, 16 riverine species nested within the Tanganyikan cichlid radiation (from the tribes Haplochromini, Serranochromini and Lamprologini), four Haplochromini species occurring in LT and adjacent rivers, one Oreochromini species that is a secondary colonizer to LT, and five riverine outgroup species (from the tribes Gobiocichlini, Heterotilapini, Tilapiini and Steatocranini; Table S1). In total, we thus used raw read data from 517 specimens, representing one to four male and female individuals of 271 cichlid species in 19 tribes. For depth-related analyses, we refined the species-specific habitat categories from Ronco et al. (2021) into four categories of depth of occurrence, resulting in 61 shallow-water living species (primarily occurring at a depth of 0–10 m); 119 intermediate-water living species (10–20 m); 42 deep-water species (>20 m); and 50 species living at unknown depth or for which the above categories would not capture the ecology of the species adequately (e.g., species occurring in highly variable depth ranges). For analytical reasons, only the categories shallow- and deep-water living species were used in the positive selection tests with the branch-site model (see Section 2.6) and in the depth-related substitutions analysis (see Section 2.7).

2.2 | Identification and assembly of rhodopsin

In a first step, we used BWA-MEM (version 0.7.17, Li & Durbin, 2009) to map all raw reads of each individual to the phylogenetically equidistant Nile tilapia reference genome (*Oreochromis niloticus*; RefSeq accession GCF_001858045.2, female) and extracted all reads that mapped to the Nile tilapia *RH1* CDS (1065 bp). To improve the mapping, we removed the existing trim annotations and performed a second, individual-based, assembly with GENEIOUS (version 2020.1.2, www.geneious.com, parameters: dissolve contigs and re-assemble, GENEIOUS as mapper, Medium Sensitivity/Fast as Sensitivity, Iterate up to 5 times as Fine Tuning). We then obtained the consensus CDS from the individual sequence reads per specimen with GENEIOUS (parameters: 65%—strict as Threshold, Total as Assign quality) and performed a multiple sequence alignment of all consensus CDS plus the reference CDS of Nile tilapia with MAFFT (version 7.310, Katoh & Standley, 2013). One individual of *Neolamprologus multifasciatus* (Neomul, IRF8, Lamprologini) had an additional base in the form of an "N" at nucleotide position 843. However, since the other specimen of this species did not feature this "N" (nor did any other sequence), we deleted this position in specimen IRF8. We then translated every CDS into amino acids (AA) and checked for the presence of start/stop codons, early stop codons or sequence lengths not dividable by 3. Five sequences had early stop codons and were consequently excluded from the downstream analyses (no species had to be removed from the original data set). The resulting 512 RH1 AA sequences were intact with a length of 355 AA.

2.3 | Rhodopsin copy number

To screen for potential duplications of *RH1* (see Musilova, Cortesi, et al., 2019), we performed BLASTN searches (*E*-value cut-off of 1*e*-5; version 2.2.28, https://blast.ncbi.nlm.nih.gov) in all available Tanganyikan cichlid draft genome assemblies (n = 509, see Ronco et al., 2021), using the newly assembled *RH1* CDS as queries. As the

extra-ocular rhodopsin 1 (*exoRH1*) is highly similar to *RH1* (72.39% CDS sequence identity and 74.37% AA sequence identity in the reference genome, see Mano et al., 1999), we used the same workflow to confirm the presence of both genes, *RH1* and *exoRH1*, in the available draft assemblies. As an additional strategy to test for possible *RH1* duplicates, we determined, for each cichlid specimen, the ratio of the median coverage (of mapped reads) in the reference's *RH1* coding region vs. the median coverage of the entire genome. The coverage of the *RH1* coding region was calculated using SAMTOOLS (version 1.7, Li et al., 2009). To obtain an estimate of the genome-wide coverage, we first calculated, for each genome, the coverage distribution of mapped reads to the reference genome using BEDTOOLS (version 2.27.1, Quinlan & Hall, 2010). We then only retained positions with (i) a coverage of at least 1, to not deflate the estimate by regions that are not present in the reference, and (ii) below 50, to exclude sites that are highly duplicated or where mapping is ambiguous (note that this is an arbitrary threshold set after visual inspection of the mapping distributions). Finally, we also manually inspected the raw read alignments to search for an excess of heterozygous sites, which could indicate functionally different *RH1* copies.

2.4 | Rhodopsin gene trees

To decrease the computational complexity of the phylogenetic analyses, we first reduced the multiple alignments for both CDS and AA to unique sequences. This resulted in 238 unique CDS and 158 unique AA sequences (including the reference sequence). Ambiguous characters in the AA alignment (due to heterozygous nucleotide sites) were masked by "X." We then used JMODELTEST (version 2.1.10, Darriba et al., 2012) and PAUP* (version 4.0a, Wilgenbusch & Swofford, 2003) to identify the most appropriate nucleotide substitution models, which turned out to be the GTR+G+I model in both cases (based on Akaike Information Criterion [AIC] values). PROTTEST (version 4.3.2, Darriba et al., 2011) was used to determine the best protein substitution model (JTT+I+G+F, according to AIC). CDS and AA phylogenies were generated using MRBAYES (version 3.2.7, Ronquist & Huelsenbeck, 2003) and IQ-TREE (version 2.0, Nguyen et al., 2014). Bayesian inference calculations with MRBAYES were performed with four chains, 10^7 generations with a sample frequency of 1000 and a burn-in of 25%. The maximum-likelihood (ML) analyses with IQ-TREE were performed with 1000 bootstrap replicates and 1000 iterations for the UFBoot stopping rule, with/without a more thorough NNI (Nearest Neighbour Interchange) search. We ran both analyses four times for CDS and AA, respectively, specifying the Nile tilapia as outgroup. The best topology of these four replicates for Bayesian inference and ML was selected on the basis of topology tests (khtest, shtest and autest) in PAUP*. The topology distance between trees (Robinson–Foulds distance, Robinson & Foulds, 1981) was calculated using the dist.topo function from the R package APE (version 4.0.3 and version 5.4-1, Paradis et al., 2004; Team R Development Core, 2018). Finally, a haplotype genealogy based on the CDS multiple alignment and the best gene tree (ML) was built with HAPLOTYPE VIEWER (http://www.cibiv.at/~greg/haploviewer, Salzburger et al., 2011) and colour-coded according to the depth categories.

2.5 | Rhodopsin amino acid substitutions

To visualize the AA changes in RH1 on the gene trees, we modified the Bayesian and ML trees built with unique CDS sequences (see above), to recover all initial CDS tip labels (reversing the merging of unique CDS sequences). A length of 10^{-4} was assigned to each branch for visualization purposes. We then again reduced each gene tree by pruning tip labels of individuals with identical CDS, but this time only within species (resulting in a total of 343 tip labels including the reference). Using PAUP* (command: describe; parameters: apoList=yes chgList=yes diagnose=yes brlens=yes), we then mapped the AA changes (ambiguous characters as "X") on the gene trees and reported the Consistency Index (CI) and Retention Index (RI) of the respective substitutions. Gene trees were visualized with changes on branches using the R packages APE, PHYTOOLS (version 0.7-47; Revell, 2012), PHANGORN (version 2.5.5; Schliep, 2011), and SEQINR (version 4.2-4; Charif & Lobry, 2007). Moreover, we mapped the substitutions of variable known key tuning sites in the data set on the gene trees and investigated the potential effect of specific changes on the maximal spectral sensitivity value using the reconstructions performed in Yokoyama et al. (2008) and Musilova, Cortesi, et al. (2019). We also mapped the substitutions of variable sites known to be involved in the maintenance of RH1 protein stability along the depth gradient (Porter et al., 2016).

2.6 | Positive selection analysis

Positively selected sites were identified using CodeML from the PAML software package (version 4.9; Yang, 2007). To assess the impact of different tree topologies, we tested random site models (M1a vs. M2a and M7 vs. M8) and branch-site model (H0 vs. HA) on both the Bayesian and ML gene tree. Each pair of models was compared using a Likelihood Ratio Test (LRT) with a χ^2 distribution. For the branch-site model, the background branches included species living in shallow waters (77 CDS tip labels) as opposed to those living in deep waters (58 CDS tip labels). To do so, we used a reduced version of the gene trees that included only species belonging to these two most extreme depth categories. We then filtered the CDS multiple alignment to retain only sequences that are represented in the pruned gene trees. We performed the same analyses with HYPHY (version 2.3.13.20180525beta(MP); Kosakovsky Pond et al., 2005) to confirm our findings using the ML gene tree. FEL (Fixed Effects Likelihood) and FUBAR (Fast Unconstrained Bayesian AppRoximation for inferring selection) were performed to test for pervasive site-level selection, which is equivalent to random site models in CodeML. We also tested for lineage-specific evolution using the branch-site method aBS-REL

(Adaptive Branch-Site Random Effects Likelihood), which is equivalent to branch-site models in CodeML, with shallow- and deep-water living species as categories.

2.7 | Depth-related substitution analysis

To investigate putative depth-related substitutions, we retrieved AAs at variable sites for each species living in the shallow and deep waters included in the species tree from Ronco et al. (2021) and recorded each species as a binary AA score (absence or presence of a particular AA) at each position and the binary depth score (shallow vs. deep). For each site and AA, we then fitted models of trait evolution for discrete characters based on the species tree using BAYESTRAITS (version 3.0.2; http://www.evolution.rdg.ac.uk/). More specifically, for each site we compared the likelihood of an independent model (assuming two binary traits that evolve independently along the phylogeny) and a dependent model (assuming two binary traits that evolve dependently along the phylogeny). We applied the Markov Chain Monte Carlo method with 10^8 iterations and a sample frequency of 2000. We then retained the last 25,000 iterations and assessed the convergence of each chain by calculating the effective sample size (ESS) for each parameter. As all chains converged (ESS > 200), we summarized each model by calculating the mean log-likelihood of the posterior distribution and its derived AIC. Significance was assessed by comparing the difference in AIC of the independent model minus the dependent model, so that positive values indicate that the two traits probably evolved dependently along the phylogeny.

3 | RESULTS

3.1 | Rhodopsin diversity in Tanganyikan cichlids

We identified and newly assembled the intron-less *RH1* gene in 271 cichlid species covering the entire cichlid species flock in LT plus some outgroup taxa and species nested within the radiation. In total, 32 species were represented by one individual, 164 species by two or more individuals that had identical CDS, and 75 species were represented by two or more individuals with different CDS due to incompleteness, homozygous single nucleotide polymorphisms (SNPs) and/or individuals with heterozygous sites (Table S1). Five incomplete CDS with early stop codons were removed from the analysis: JWA8 (*Lamprologus meleagris*, Lamprologini), IZI8 (*Neolamprologus christyi*, Lamprologini), ISA1 (*Trematocara marginatum*, Trematocarini), JXH4 (*Petrochromis orthognathus*, Tropheini) and LCF3 (*Tropheus* sp. "kirschfleck," Tropheini). A visual inspection revealed that all these incomplete CDS were due to regions with no coverage (i.e., lack of raw read data) leading to apparent frame shift mutations (i.e., the lack of nucleotides shifts the reading frame and thereby creates early stop codons). However, because the respective other individual of these five species had a complete CDS and could hence be used for downstream analyses, all species present in the original data set were also included in our analyses. Individuals of 18 species featured differences in the CDS between individuals due to homozygous SNPs, 44 species showed intraspecific differences due to heterozygous sites, and eight species showed differences between individuals due to both homozygous SNPs and heterozygous sites (Figure S1). The minimum CDS and AA sequence identity was 95.3% and 92.5%, respectively, among all pairs of individuals (AA heterozygous sites masked; the CDS multiple alignment is available on Dryad: https://doi.org/10.5061/dryad.4mw6m90c7). No evidence of sex-specific differences was found across the data set. Intraspecific sequence variation was generally low or absent, except for three species that had more than one nucleotide/AA difference due to homozygous SNPs: XenniS (16/12, *Xenotilapia nigrolabiata*, Ectodini), Lamorn (7/6, *Lamprologus ornatipinnis*, Lamprologini) and TelteS (11/8, *Telmatochromis temporalis*, Lamprologini).

Among the 1065 nucleotide positions of *RH1*, 212 positions were variable across the data set (including the reference), of which 57 involved first codon positions, 37 second codon positions and 118 third codon positions (Figure S2A). This resulted in 154 variable codons and 76 variable AA sites (13 variable AA sites due to heterozygosity). Codons were represented by one to 13 codon variants across the data set (median = 1, mean = 1.814) and by one to six different AAs (median = 1, mean = 1.322, Figure S2A). Positions 162 (TM IV), 213 (TM V) and 217 (TM V) showed the greatest AA diversity with six AA variants each. The N-terminal (extracellular side) and the seven transmembrane alpha-helices (TM I–VII), which make up 65.35% (232/355 AA sites) of the whole protein sequence, contained most of the variable AA sites (60/76; 78.95%). The variable AA sites were not uniformly distributed along the alignment and most of them were found in the N-terminal and TM I, IV, V, VI and VII with 10, 6, 7, 8, 10 and 9 changes, respectively (in addition to variable AA sites due to heterozygosity: one in TM IV, two in TM V and one in TM VII; Figure S2A). More than 25% of the AA sites in each of these six regions were variable (with and without positions variable due to heterozygosity; Figure S2B). For all individuals including the reference, the retinal-binding site was fixed at K296 (TM VII), the Schiff base counterion at E113 (TM III), and the disulphide bond sites at C110 (TM III) and C187 (extracellular loop) (Bowmaker, 2008; Terakita, 2005). The conserved tripeptide sequence in TM III involved in G protein interactions was fixed at E134/R135/W136 (Menon et al., 2001). Moreover, of the 27 known key tuning sites in RH1 (Musilova, Cortesi, et al., 2019; Yokoyama et al., 2008), six positions were variable (TM II: site 83, extracellular loop: site 183, TM V: site 214, TM VII: sites 292, 299 and 300). From the AA sites known to be involved in protein stability at depth (Porter et al., 2016), two were fixed (E196 and I275), one was fixed for the majority of species (F159; except for one shallow-water living species with a heterozygous site {FV} and one species living at unknown depth with V), while one site was highly variable (six possible AAs at position 213: A, I, L, M, S, T or {LT}).

3.2 | Rhodopsin copy number

We did not find evidence for multiple *RH1* copies in the Tanganyikan cichlids' draft genome assemblies (the full BLASTN report is available on Dryad: https://doi.org/10.5061/dryad.4mw6m90c7). The BLASTN analysis with the respective *RH1* CDS recovered from the raw reads as query resulted in a highest-scoring hit to *RH1* and a second highest-scoring hit to *exoRH1* for all cichlid genomes. The ratio of the median coverage on the reference's *RH1* CDS vs. the median coverage on the reference's overall genome did not reveal any evidence for a duplication of *RH1*, except for the two *Neolamprologus splendens* individuals that showed a coverage in *RH1* of more than twice the genome-wide median coverage (Figure 1). However, a close inspection of the read data of the two *N. splendens* genomes revealed a coverage distribution with high variance when mapped to the Nile tilapia reference genome. Although many sites showed comparatively high coverage, the highest proportion of positions was covered by only four or fewer reads, pushing down the genome-wide median coverage in these two specimens compared to the other genomes where the coverage was normally distributed with much less variance. We can attribute the much greater variation in coverage in the two *N. splendens* individuals to the comparatively high level of fragmentation of the extracted genomic DNA that was initially recovered from them (the original electropherograms indicated a fragment size distributed around 500–700 bp for the two *N. splendens* individuals, while the other samples' fragments were typically centred around >10 kb). This, in turn, is probably a consequence of these two specimens having been collected more than 30 years ago, whereas the vast majority of the remaining Tanganyikan cichlid genomes were sequenced from recent material producing high-quality DNA extracts (for details see Ronco et al., 2021). Furthermore, since the *RH1* CDS of the two *N. splendens* individuals did not show any excess of heterozygous sites, as would be expected in the presence of a second, functionally different *RH1* copy in a genome, we tentatively assume that the observed signals of an elevated median coverage in *RH1* in *N. splendens* are artefacts.

3.3 | Rhodopsin gene trees

The phylogenetic analyses based on Bayesian and ML of the RH1 CDS and AA sequences resulted in similar tree topologies, with a Robinson–Foulds distance of 125 between gene trees and of 106 between AA trees (Figures S3–S6; the tree files are available on

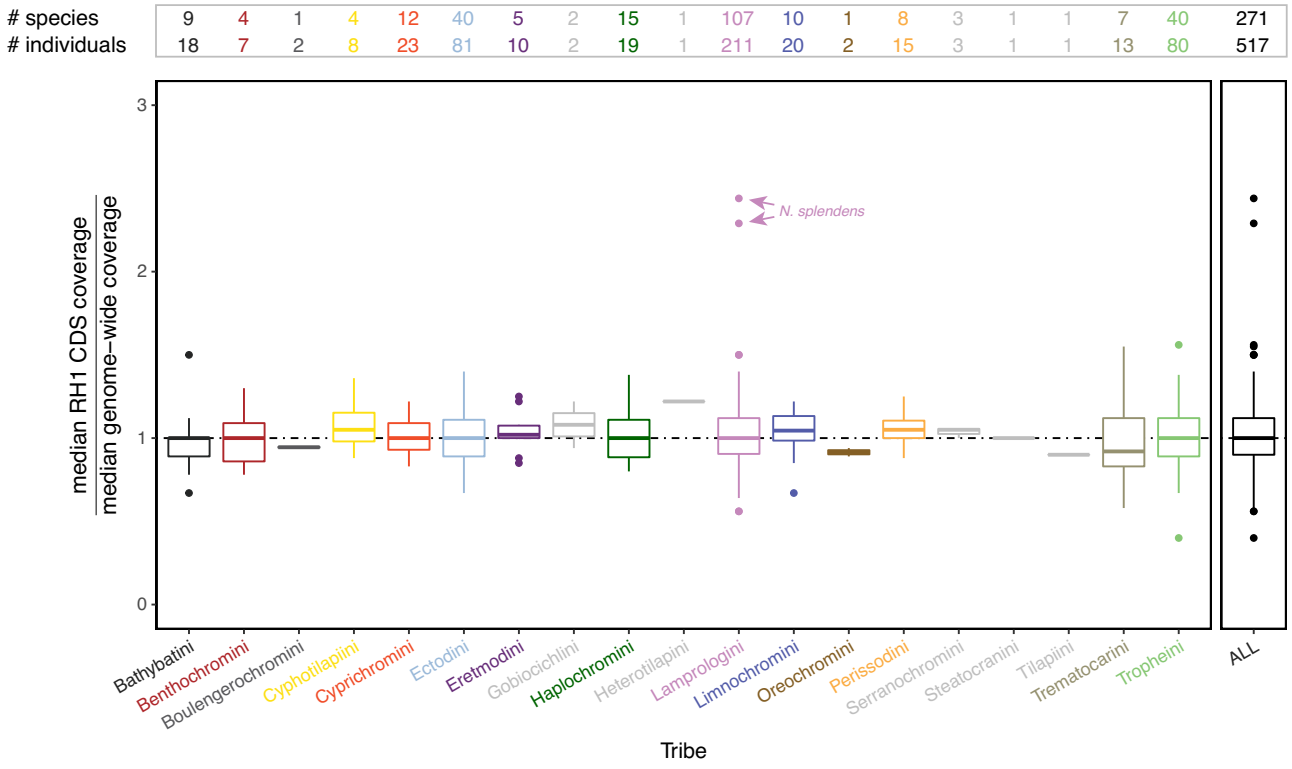

FIGURE 1 Coverage of mapped read estimates. Boxplots showing the median coverage in the CDS (coding sequence) of the *rhodopsin* (*RH1*) gene over an estimate of the median genome-wide coverage in the cichlid fauna of Lake Tanganyika (LT) as well as in outgroup taxa. Boxplots are shown for each cichlid tribe separately and for the entire data set (ALL); the cichlid tribes occurring in LT are colour-coded as in Ronco et al. (2021). The boxes' centre lines show the median, box limits show first and third quartiles, and whiskers show 1.5× the interquartile ranges. Outliers are represented by dots. The horizontal dashed line in black is set to 1 (equal coverage across the whole genome). The number of species and individuals for each tribe is reported at the top. Note that the two genomes of *Neolamprologus splendens* (marked with arrows) show elevated ratios, which we interpret as artefacts (see Section 3.2 Rhodopsin copy number)

Dryad: https://doi.org/10.5061/dryad.4mw6m90c7). Overall, the gene trees resembled the species tree topology at the tribal and genus level (see Ronco et al., 2021), whereas species-level relationships often remained unresolved. This is largely due to the overall short length of the RH1 CDS and AA sequences, and the relatively small number of variable positions (1/5 of the sequences) in proportion to the number of taxa analysed. For the same reasons, the Bayesian posterior probability and ML bootstrap values were low in parts. The topology tests revealed that the ML CDS and AA trees were more likely than the Bayesian trees. Therefore, we mainly present results using the ML trees in the following. The haplotype genealogy based on the ML gene tree (Figure 2) showed that, if species shared the same *RH1* gene sequence (i.e., haplotype), this only occurred between species within but not between tribes (except for Tropheini and Haplochromini, but which should be considered as one clade because Tropheini is phylogenetically nested with Haplochromini; Salzburger et al., 2005). It further appears that within tribes—specifically in the Ectodini, Lamprologini and Tropheini/Haplochromini—shallow-, intermediate-, or deep-water living species can share the same *RH1* haplotype (Figure 2).

3.4 | Rhodopsin amino acid substitutions

RH1 AA changes occurred on both internal (including close to the root) and terminal branches (Figures S3–S6). No major difference in the number and location of AA changes was found between the Bayesian and ML gene trees. Changes mapped on the ML gene tree occurred at different frequency depending on the AA sites and varied from one to 18 changes (median = 3, mean = 5, Table S2). Position 162 featured the highest number of AA changes mapped on the gene tree.

The mapping of changes at (variable) known key tuning sites (positions 83, 183, 214, 292, 299 and 300) revealed that all Tanganyikan cichlids featured at least one change in RH1 that may fine-tune λ_{max} (absent in Oreochromini species, riverine outgroup species, and three riverine Haplochromini species; Figure 3a). Of 28 changes in total, 12 substitutions mapped on the ML gene tree are likely to shift λ_{max} towards shorter (blue-shift) and longer (red-shift) wavelength (nine and three changes, respectively, Figure S7; see Yokoyama et al., 2008 and Musilova, Cortesi, et al., 2019). Interestingly, the mapped changes at the two variable sites involved in protein stability at depth (see Porter et al., 2016) revealed a single change for AA position 159, while 15 changes were mapped at AA position 213 (Figure 3a).

3.5 | Positive selection analysis

Variation in d_N/d_S (the ratio of nonsynonymous to synonymous substitutions) was found when comparing the site models M1a vs. M2a and M7 vs. M8 using both the Bayesian and ML gene trees ($p < 10^{-4}$, Table 1; Table S3). The models M2a and M8 using the ML gene tree revealed similar results with 25 and 31 positively selected sites, respectively (BEB analysis, $p > 95\%$, Figures 3b and 4; Table S4). Hence, 7.04/8.73% of sites showed signals of positive selection with an average d_N/d_S of 10.17/9.68 (under M2a and M8, respectively). The majority of positively selected sites were found in the N-terminal and TM IV, V and VII (Figure 4). Interestingly, no positively selected site was detected in the intracellular loops of RH1. Positive selection results using the Bayesian tree are available in the Supporting Information (including HYPHY results using the ML gene tree, Tables S3–S7).

The majority of changes at positively selected sites mapped on both internal and terminal branches on the ML gene tree (Figure 3b). Moreover, substitutions in positively selected sites belonging to the same region of the protein did not appear to co-occur on specific branches. Among the six key tuning sites variable in our data set, a single site (299) was found to be under positive selection according to M2a, and three sites (214, 292 and 299) according to M8. Moreover, among sites preserving protein stability at depth, a single site (213) was found to be under positive selection according to M2a and M8. The positive selection test using the branch-site models H0 and HA (with both the Bayesian and ML gene trees) and the category "shallow-water living species" as background branches and the category "deep-water living species" as foreground branches did not reveal a difference in RH1 sequence evolution between these groups (Table S6; aBS-REL results using HYPHY were congruent with CodeML results).

3.6 | Depth-related substitution analysis

We found evidence for 23 depth-related substitutions in our data set; that is, AAs at 15 specific RH1 positions are likely to have evolved in dependence on the depth at which a species occurs (Figure 5; Figures S8 and S9). Three of these AA positions were found in the N-terminal (sites 17, 33 and 37), one in TM I (42) and TM II (95), one in the extracellular loop (104), two each in TM IV (162 and 165) and TM V (213 and 214), and five in TM VII (290, 292, 297, 298 and 299). In contrast, no depth-related substitution was found in the intracellular loops and in TM III and TM VI. All detected depth-related substitutions occurred at sites showing signals of positive selection (under M8 using the ML gene tree), including at three known key tuning sites (214, 292 and 299) and one site (213) involved in the maintenance of protein stability.

We found that, among the AA variants at sites probably evolving in dependence on the depth, the commonly observed pattern is that certain AA variants (F37, I104, I290, S292, A297 and A299, and with weaker effect also N33, S42, T95 and A213, Figure 5b; Figures S8 and S9) are found only (or predominantly) in deep-water living species, whereas the alternative variant is found both in shallow- and deep-water living species. The opposite case with AAs exclusively found in the shallow-water living species is rarer (S17, L162, S165 and S298), and similarly, the alternative variants at these positions are then found in both deep- and some shallow-water living species. For eight AA

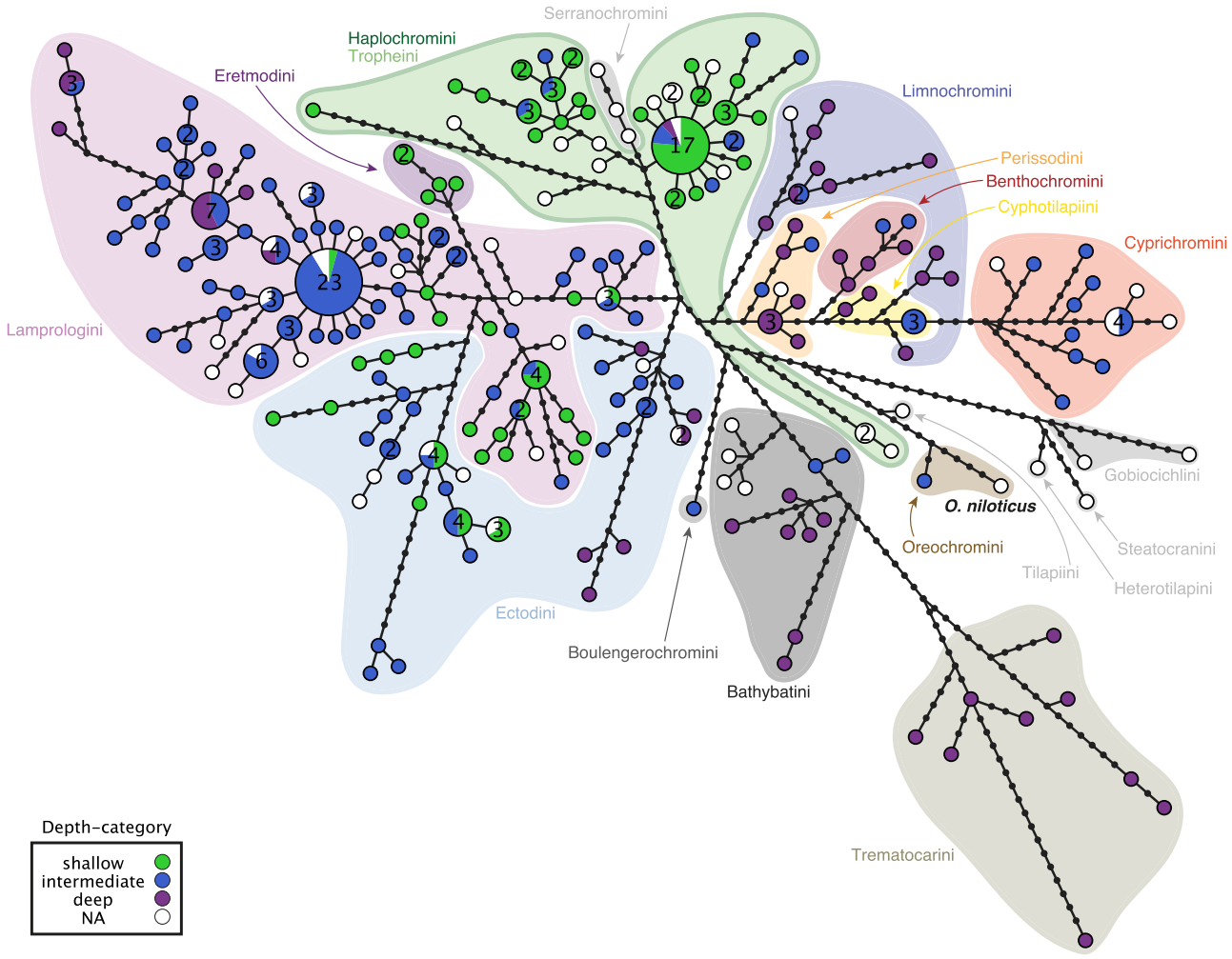

FIGURE 2 *Rhodopsin* nucleotide haplotype genealogy based on the maximum-likelihood gene tree. Each pie chart represents a unique CDS (coding sequence) of the *rhodopsin* gene, and its size corresponds to the number of individuals that share this haplotype (whenever two or more individuals share a haplotype, the number of individuals is reported inside the pie charts). Pie charts are colour-coded according to depth category (see box), and cichlid tribes are indicated with coloured background shadings (according to Ronco et al., 2021); the reference sequence (*Oreochromis niloticus*) is indicated in bold. The black dots represent hypothetical (unsampled) haplotypes. Note that Haplochromini and Tropheini have the same green background shading, because they form one clade, with Tropheini being phylogenetically nested within Haplochromini (Salzburger et al., 2005)

sites, we detected two AA variants associated with depth (sites 17, 33, 37, 104, 162, 290, 292 and 299; Figure 5b), of which a single AA site revealed an almost perfect bidirectional association: S299 is found in most shallow-water living species, while A299 is found in most deep-water living species. Our list of AA sites putatively pertinent for depth-related adaptations thus contains positions previously suggested to be relevant in deep waters (e.g., 292 and 299) as well as candidate positions that have not previously been identified in the context of deep-water adaptations in fishes (e.g., 37, 104 and 290).

4 | DISCUSSION

Rhodopsin (RH1) is the only visual opsin type present in the rod cells of the retina, and is responsible for dim-light vision in vertebrates (Bowmaker, 2008; but see Musilova et al., 2021). While in terrestrial vertebrates adaptive changes in their single copy of RH1 are commonly found in association with a nocturnal lifestyle or crepuscular activity patterns (e.g., Castiglione & Chang, 2018; Hauzman et al., 2017), molecular adaptations in RH1 of fishes—as the main group of vertebrates living in the aquatic realm—are most often associated with the water depth at which a species occurs, and in some cases also with water turbidity (Musilova et al., 2021). In addition to acquiring specific changes in the protein-coding sequence of RH1 in response to the light environment in deeper waters (Hofmann et al., 2009; Hope et al., 1997; Hunt et al., 1996; Malinsky et al., 2015; Musilova, Cortesi, et al., 2019; Nagai et al., 2011; Sugawara et al., 2005), some fishes were shown to have expanded their RH1 repertoire via gene duplication and subsequent functional diversification, resulting in intraspecific arrays of differently tuned copies of RH1

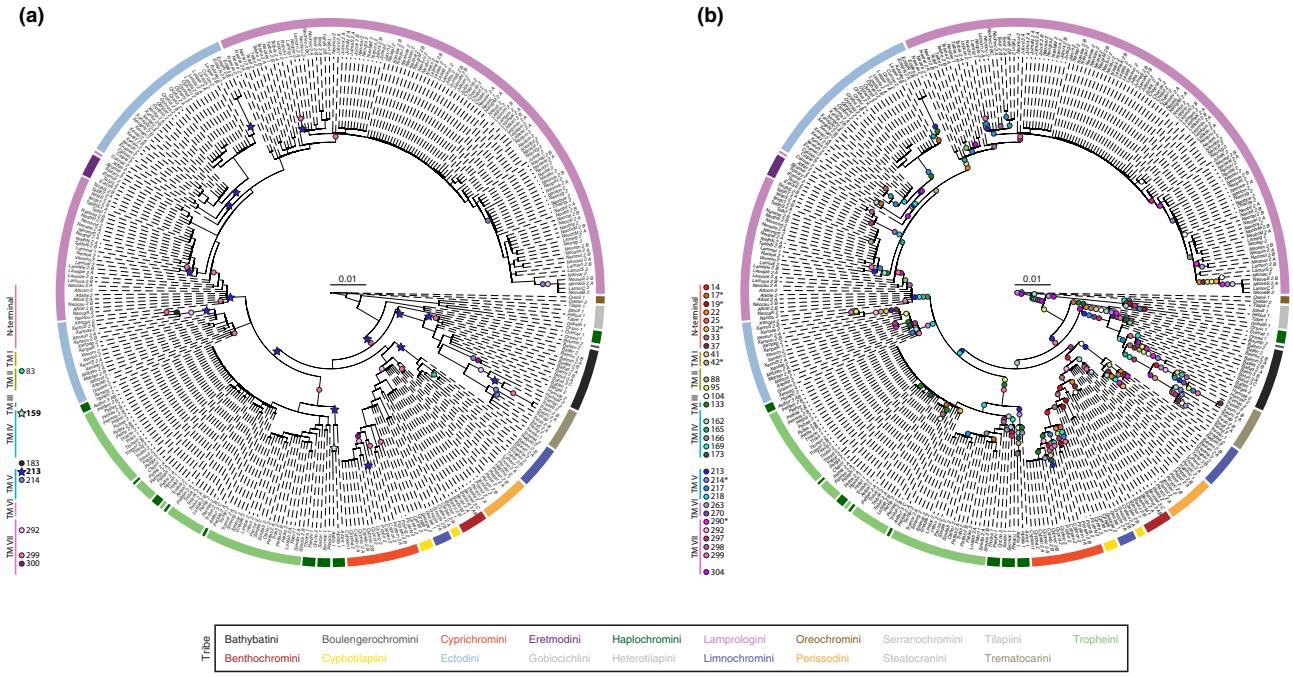

FIGURE 3 Amino acid substitutions in the rhodopsin protein mapped on the maximum-likelihood (ML) gene tree. The coloured arches around the ML gene trees indicate the tribe to which a species belongs (see Figure S3 and Table S1 for full species names). The number and the letter(s) next to each abbreviated species name represent the number of individuals and their IDs (see Table S1 [CDS tip label]). Each coloured circle corresponds to a change occurring at a specific amino acid position along the rhodopsin protein sequence. TM: transmembrane alpha-helix. (a) Amino acid substitutions in known key tuning sites (circles) and in sites involved in protein stability along the depth gradient (in bold, star-shaped symbol). (b) Amino acid substitutions in positively selected sites (CodeML random-site models M2a and M8). Positively selected sites present in M8 but not in M2a are marked with an asterisk (*)

TABLE 1 Rhodopsin positive selection results based on a CodeML random-site model comparison (M1a vs. M2a and M7 vs. M8a) and the maximum-likelihood gene tree. The pairs of models were tested using a Likelihood Ratio Test (LRT) following a χ^2 distribution. Values of each site class ω_0, ω_1 and ω_2 are specified for models M1a and M2a. The shape parameters p and q are specified for models M7 and M8. The value ω_p corresponds to the positively selected site class for M8. The proportion of each site class is given in parentheses

				Parameter						
Model	np	lnL	κ	ω_0/p	ω_1/q	ω_2/ω_p	Null	LRT	*df*	*p*
M1a	3	−5266	2.144	0.001 (91.7%)	1 (8.3%)					
M2a	5	−4999	2.702	0.017 (89.9%)	1 (83%)	9.797 (1.7%)	M1a	534	2	<.0001
M7	3	−5314	2.377	0.007	0.018					
M8	5	−5005	2.807	0.028	0.205	9.548 (2%)	M7	618	2	<.0001

Abbreviations: np, number of parameters; lnL, *ln* likelihood; κ, transition/transversion ratio; Null, null model; *df*, degrees of freedom.

(Musilova, Cortesi, et al., 2019). In the present study, we investigated the evolution of RH1 in the massive adaptive radiation of cichlids in LT, where these fishes have diversified into a multitude of ecological niches in the shallow, intermediate and deep (up to the oxycline at a depth of about 200 m; Talling, 1991) waters (Table S1), starting from a common ancestor that colonized the emerging lake about 10 million years ago (Ronco et al., 2021).

Our in-depth analyses of RH1 in the endemic cichlid fauna of the LT basin based on whole-genome raw sequence data of 517 specimens from 271 species revealed the presence of a single copy of *RH1* per genome across the radiation (Figure 1). We note that for two genomes—namely those of the two representatives of *Neolamprologus splendens*—a coverage pattern in the CDS of *RH1* was retrieved that, when compared to the genome-wide median, would be compatible with a gene duplication scenario for *RH1* (Figure 1). However, upon closer inspection, we tentatively argue that the seemingly higher coverage in the CDS of *RH1* in *N. splendens* is an artefact. Thus, unlike what has been found in deep-sea fishes and in some species of freshwater fishes living in murky waters (Musilova, Cortesi, et al., 2019; Musilova et al., 2021), the adaptation to scotopic light conditions does not seem to have involved lineage- or species-specific duplications of *RH1* in LT cichlids.

When focusing on RH1 sequence evolution in the adaptive radiation of cichlid fishes in LT, we identified a total of 237 unique CDS

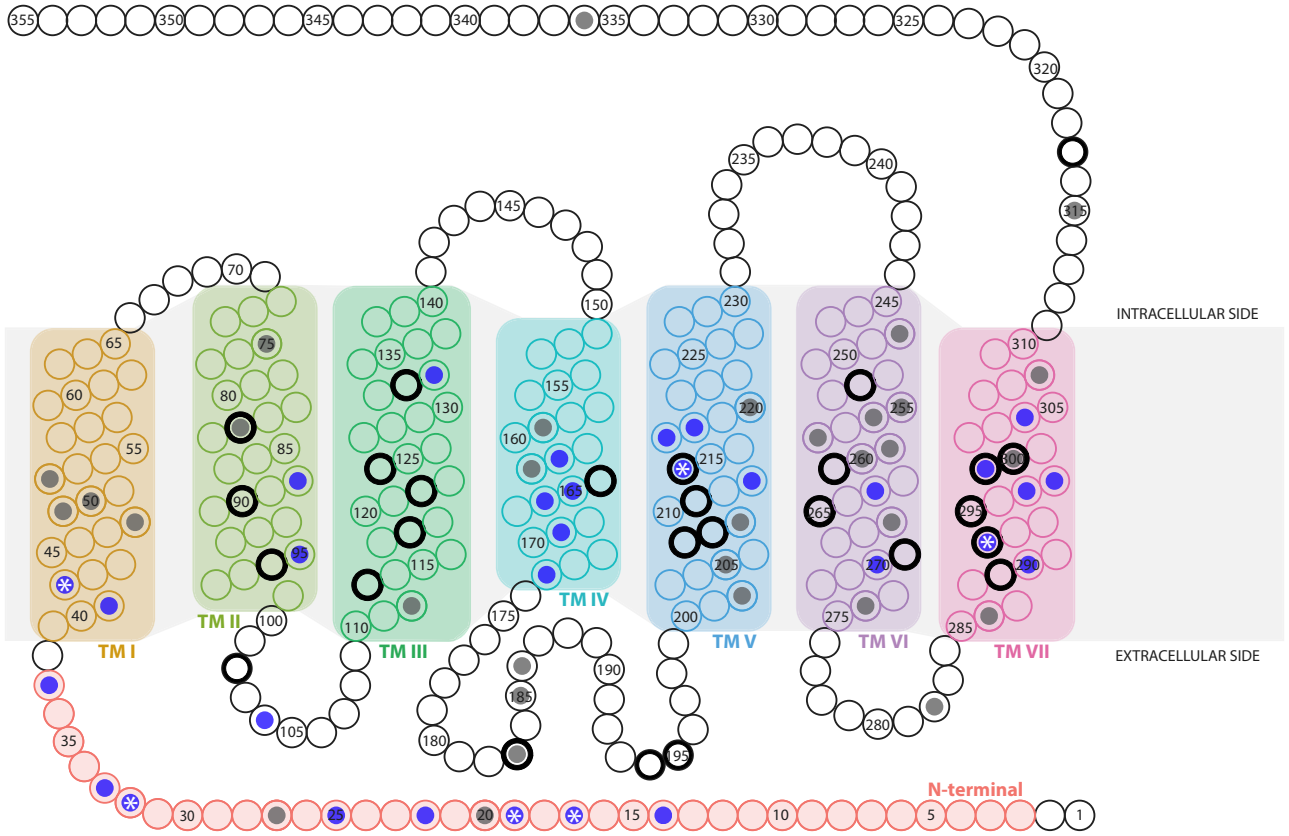

FIGURE 4 Schematic of the rhodopsin (RH1) protein (based on *Oreochromis niloticus*) showing the variable amino acid sites and the positively selected amino acid sites (based on CodeML random site models M1a vs. M2a and M7 vs. M8). Each circle represents an amino acid position in RH1. Variable sites in our data set are colour-coded with a dark grey dot, and positively selected sites among those are highlighted with a blue dot. Positively selected sites present in M8 but not in M2a results are indicated with a white asterisk (*). The 27 key tuning sites in RH1 (see Musilova, Cortesi, et al., 2019; Sugawara et al., 2005) are marked with a black outer circle. The transmembrane alpha-helices (TM) of rhodopsin are highlighted with different background colours (from left to right): TM I, II, III, IV, V, VI, VII. Sites that are part of extra- and intracellular loops are shown in white, except for the N-terminal site that is colour-coded in red

(haplotypes) and 157 unique AA sequences in the data set (excluding the reference sequence in both cases). In the Bayesian and ML gene trees reconstructed from these data, haplotypes and AA sequences clustered according to tribes and genera—thus reflecting phylogenetic relationships as established in a species-tree analysis from genome-wide SNPs (Ronco et al., 2021)—but not according to depth at which a species occurs, nor to feeding ecology (Figure 2; Figures S3 and S4). This is best illustrated by the haplotype genealogy based on unique CDS of the *RH1* gene in LT cichlids (Figure 2), highlighting that no single *RH1* haplotype is shared between tribes (except between Haplochromini and Tropheini, which belong to the same clade with Tropheini being phylogenetically nested in Haplochromini; Salzburger et al., 2005), whereas within tribes, *RH1* haplotypes are occasionally shared between depth categories. When individually mapped on the species tree (Ronco et al., 2021), we found that 56.7% (89 out of 157) of the AA substitutions occurred more than once (up to 20 times; the species tree with mapped AA changes is available on Dryad: https://doi.org/10.5061/dryad.4mw6m90c7), again highlighting that convergent evolution is common in cichlid adaptive radiations (Muschick et al., 2012), in this case on the molecular level. Some of these convergent cases, especially among more closely related species, could also be the result of introgression and/or incomplete lineage sorting (Salzburger, 2018).

Intraspecific sequence variation in *RH1* was very low or absent for the vast majority of species, except for three species that featured noticeable degrees of intraspecific sequence variation between the two specimens examined (Figure S1). There is no obvious reason—for example, with respect to phylogeny, ecology, demography, behaviour or morphology—that could explain why these three species are more diverse in *RH1* than others. To some extent, however, intraspecific variation should be expected in instances of adaptive radiation, which are characterized by incomplete lineage sorting and occasional hybridization (see Salzburger, 2018). Lastly, there was no indication for sex-specific nucleotide differences across the data set.

At the level of the RH1 protein, we found that, out of a total of 355 AA positions, 76 sites were variable across the data set (Figure 4; Figure S2). These included six out of the 27 known key tuning sites (Musilova, Cortesi, et al., 2019; Yokoyama et al., 2008)—namely sites 83, 183, 214, 292, 299 and 300 (Figure S2A)—and two AA sites (159

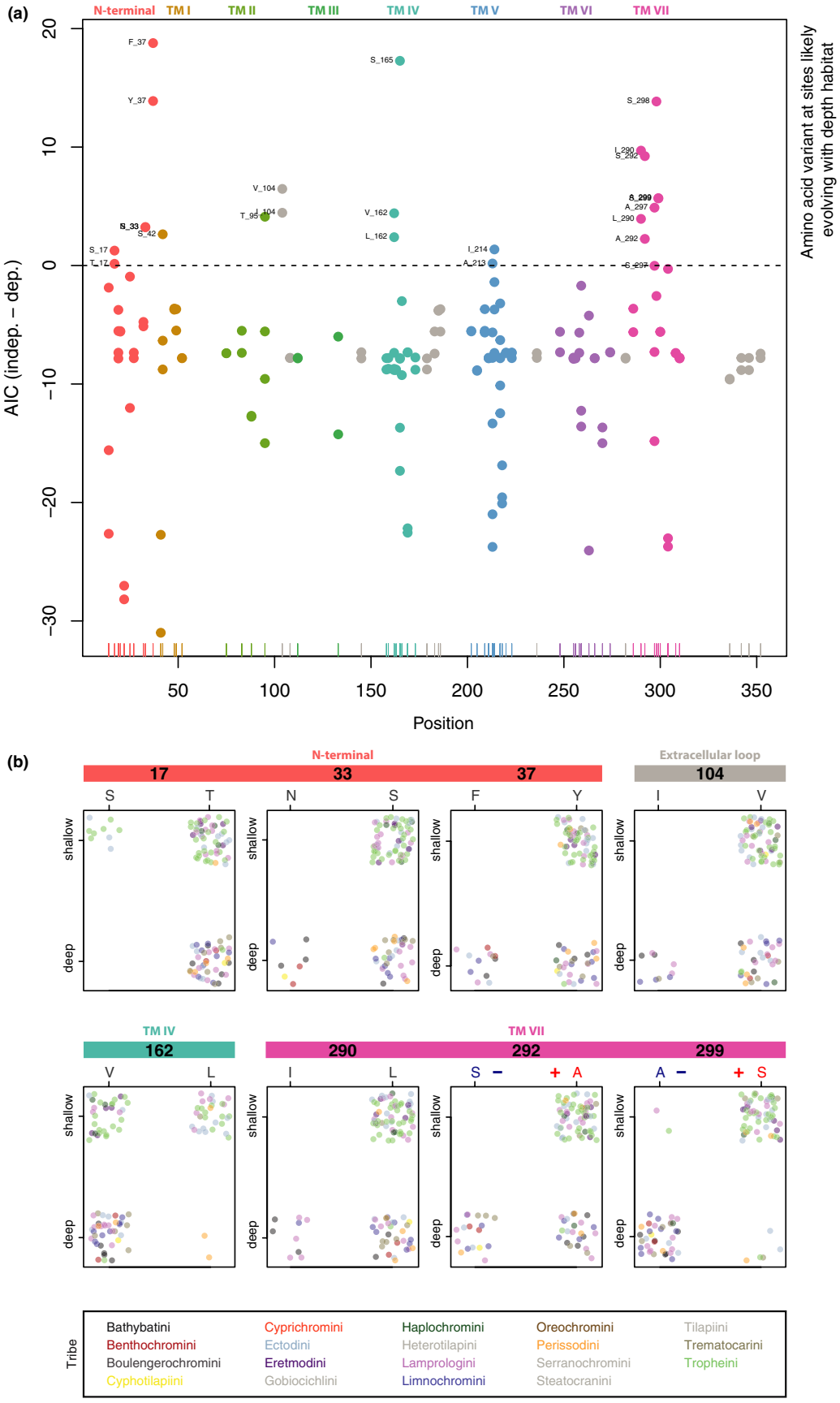

FIGURE 5 Depth-related substitution analysis of rhodopsin (RH1) amino acid sites. (a) Dotplots of BAYESTRAITS results. Each dot corresponds to the difference in AICs of the independent model and the dependent model (absence/presence of an amino acid at a specific site in RH1 and depth at which species occur) and is colour-coded according to the RH1 regions (TM: transmembrane alpha-helix; see Figure 4). The *x*-axis shows the positions along the RH1 protein sequence, and the *y*-axis shows the difference in AICs between the two models. The horizontal dashed line is fixed at zero, meaning that dots above this threshold indicate those amino acids that are associated with the water depth at which a species occurs (shallow- vs. deep-water living species). (b) Dotplots of sites with exactly two amino acid variants associated with water depth (colour-coded as in (a)). Each individual is represented by a single dot, colour-coded according to tribe. The *x*-axis represents the amino acid variants, and the *y*-axis represents the shallow- and deep-water living species (plotted with jitter points and without ambiguous amino acid sites for better visualization). Note that sites 292 and 299 are among the known key tuning sites in RH1, with substitutions predicted to shift the peak spectral sensitivity (the blue "–" symbol indicates a predicted shift towards shorter wavelengths, and the red "+" indicates a predicted shift towards longer wavelengths). An extended version of this figure showing all identified sites is provided as Figure S8

and 213) implicated in protein stability (Porter et al., 2016). Close to half of the variable AA sites (31) were additionally identified as having evolved under positive selection according to the random site model (M8) in PAML (Figure 3b; Table S4). Among these were three key tuning sites (214, 292 and 299; Musilova, Cortesi, et al., 2019; Yokoyama et al., 2008) and one site (213) involved in the maintenance of protein stability at depth (Figure 3a; Porter et al., 2016). The proportion of sites showing a signal of positive selection in RH1 of Tanganyikan cichlids (8.73%; Table 1), as well as the average d_N/d_S (9.68), is in line with what has previously been reported for this group of fishes: examining RH1 in 16 cichlid species from lakes Victoria, Malawi and Tanganyika (three from LT plus *Oreochromis niloticus* in our data set) and using a neighbour-joining tree as a backbone, Spady et al. (2005) found a proportion of positively selected sites of 6.9% and an average d_N/d_S of 14.07; and Schott et al. (2014) found that 7.1% of the sites were under positive selection with an average d_N/d_S of 13.69 in a set of 32 African Great Lake cichlids (20 from LT in our data set) and a Bayesian gene tree as backbone (and 6.6% positively selected sites and a d_N/d_S of 14.37 when using an ML gene tree). A comparison between their (Schott et al., 2014; Spady et al., 2005) and our new findings (Table S4) reveals that 15 positively selected sites (41, 42, 95, 133, 162, 165, 166, 169, 213, 217, 218, 263, 297, 298 and 299) are common to the three studies.

The distribution of the variable (and also of the positively selected) AA sites along the protein was not random in our data set, with the majority of variable sites (60/76) being located in the N-terminal (extracellular side) and the transmembrane alpha-helices I, IV, V, VI and VII (Figure 4; Figure S2A and B), and most (23/31) of the positively selected sites in the N-terminal and TM IV, V and VII (Figure 4). On the other hand, TM II and III, and the intracellular side of RH1 were found to be rather conserved and to have primarily evolved under purifying selection in LT cichlids. Also, the AAs at the retinal-binding site 296, the Schiff base counterion at position 113, and at the disulphide bond sites 110 and 187 were conserved in all cichlid species included in this study, as well as in Nile tilapia, and congruent with what has been reported previously (Bowmaker, 2008; Menon et al., 2001; Terakita, 2005). This suggests that—at least over short evolutionary timescales—some AA sites of RH1 are, more than others, involved in rapid adaptive evolution, which may in part be explained by functional constraints on the respective other regions. For example, the conserved TM III not only contains the disulphide bond site 110 and a fixed tripeptide motif (sites 134, 135 and 136; Menon et al., 2001), but also seven AA sites involved in the formation of the retinal binding pocket (positions 114, 117, 120 and 121, and key tuning sites 113, 118 and 122; Musilova, Cortesi, et al., 2019; Ou et al., 2011; Yokoyama, 2008). By contrast, the regions of RH1 around the dimerization interface (TM IV and V; Fotiadis et al., 2003; Guo et al., 2005) and adjacent to the retinal binding site (position in TM VII) as well as the N-terminal region emerge as mutational hotspots and main targets of positive selection in LT cichlids (Figure 4).

Because, in fishes, adaptive evolution in RH1 is known to be impacted by the ambient light environment along the depth gradient (Hunt et al., 1996; Musilova, Cortesi, et al., 2019; Nagai et al., 2011; Sugawara et al., 2005), and because the roughly 250 cichlid species in LT cover a vast range of niches including from shallow to deep waters, we were particularly interested in depth-related adaptations in RH1 in this spectacular example of adaptive radiation. We thus applied phylogenetic comparative methods to test for potential associations between the variable AAs and depth, and, in doing so, identified 23 substitutions at 15 AA sites that are putatively involved in deep-water visual adaptations in LT cichlids (Figure 5a; Figure S8). This list contains AA sites previously suggested to be involved in deep-water adaptations, including three previously known key tuning sites (214, 292 and 299) and one site (213) likely to be involved in the maintenance of protein stability (Hope et al., 1997; Hunt et al., 1996, 2001; Malinsky et al., 2015; Musilova, Cortesi, et al., 2019; Nagai et al., 2011; Porter et al., 2016; Sugawara et al., 2005; Varela & Ritchie, 2015), as well as 11 novel candidate sites that have not yet been implicated with living at depth and for which the exact functions are currently unknown (sites 17, 33, 37, 42, 95, 104, 162, 165, 290, 297 and 298) (Figure 5a; Figures S8 and S9). Our results may thus serve as a starting point for future functional tests to determine the effect of these particular AA substitutions on λ_{max} of RH1.

Importantly, all AA substitutions in RH1 that we identified as candidates for deep-water adaptations in the cichlid adaptive radiation of LT also show signals of positive selection (Figure 3; Table S4) and occurred repeatedly over the course of the radiation (https://doi.org/10.5061/dryad.4mw6m90c7). Some of these sites, and specific AA substitutions associated with them, emerge as particularly strong candidates for deep-water adaptations, based on what is already known about their function (or their

occurrence) in other deep-living species of fish. For example, previous work in both deep-sea and deep-living freshwater fishes revealed specific depth-related molecular adaptations at key tuning sites in RH1 (Hope et al., 1997; Hunt et al., 1996, 2001; Malinsky et al., 2015; Nagai et al., 2011; Varela & Ritchie, 2015), including N83, S292 and A299, which all mediate a blue-shift in λ_{max} that is considered adaptive at depth. In our data set, all species featured D83, except for the deep-water living *Baileychromis centropomoides* (N83) and two out of three *Bathybates vittatus* individuals (deep-water living; heterozygous site with {DN}); all shallow-water living species had A292, while deep-water living species had either A292 or S292; and most shallow-water living species had S299, while most deep-water living species had A299 (Figure 5b; Figures S8 and S9). This suggests strongly that also in deep-water living LT cichlids the key tuning sites 292 and 299 were involved in adjusting the visual system to the light environment at depth. AA substitutions at sites other than key tuning sites have also been implicated in depth-related adaptations in fishes. Malinsky et al. (2015), for example, identified AAs at four positions to be associated with the deep-water benthic cichlid ecomorph in crater lake Massoko. We found that three of them (V162, S166, A298) are also present in the majority of deep-water living cichlid species in LT, while there is a difference in the fourth one (G297 in the benthic ectomorph in Lake Massoko vs. predominantly A297 in deep-water living species in LT; Figure 5B; Figures S8 and S9). It is of note that V162, which was also among the three sites with the largest number of different AAs across the data set (the others being 213 and 217; Figures S2 and S9), was also retrieved with the depth-related substitution analysis (just as A297 and S298 were). Without doubt, however, it would be necessary to determine the spectral sensitivity properties of the newly identified variants of RH1 by measuring the absorption spectrum of the RH1 pigments (as, e.g., reported in Sugawara et al., 2005), to confirm whether these indeed mediate the hypothesized blue-shift of λ_{max} in deep-water living Tanganyikan cichlid species or contribute to protein stability at depth.

5 | CONCLUSION

Cichlid fishes are an important model group to investigate the visual sensory system in general and visual opsin genes in particular in the aquatic environment. In this study, we present the first all-inclusive analysis of RH1 molecular evolution in an entire massive adaptive radiation, that of cichlid fishes in LT. Our in-depth genomic investigations revealed the presence of a single copy of *RH1* per genome across the cichlid fauna of LT. The AA differences identified across the radiation were not uniformly distributed along the protein, and 31 out of the 76 variable AA sites showed signatures of positive selection. Six out of the 27 known key tuning sites in RH1 are variable in LT cichlids, of which three are likely to have evolved under positive selection. Through phylogenetic comparative analyses, we identified 23 AA substitutions at 15 sites that are associated with water depth. These include three known key-tuning sites, one site with a putative function in protein stability with respect to water depth, as well as 11 novel candidate sites for deep-water adaptations in (cichlid) fishes. Importantly, all the candidates we identified based on the depth-related substitution analyses also emerged as potentially important sites based on our molecular evolutionary inferences, phylogenetic comparisons and positive selection tests. Together, our integrative study on the molecular evolution of the visual system of cichlid fishes in LT provides a comprehensive view on the patterns of RH1 evolution in a freshwater environment and more generally on the evolutionary dynamics of environmentally driven adaptations.

ACKNOWLEDGEMENTS

We thank N. Boileau, F. Cortesi, A. Fages and P. Tschopp for valuable feedback on the project and the analyses; N. Boileau and B. Stelbrink for their help with MRBAYES; R. A. W. Wiberg for advice with CodeML; A. Indermaur for his help categorizing shallow-, intermediate- and deep-water living species; and the Subject Editor as well as two anonymous reviewers for valuable comments. Calculations were performed at sciCORE (https://scicore.unibas.ch/), the Center for Scientific Computing at the University of Basel with support from the Swiss Institute of Bioinformatics (SIB). This work was supported by the European Research Council (ERC, Consolidator Grant No. 617585 "CICHLID~X" to W.S.), the Swiss National Science Foundation (SNF; grant 176039 to W.S.; grant PROMYS 166550 to Z.M.), Charles University (Primus to Z.M.) and the Czech Science Foundation (21-31712S to Z.M.). Open access funding provided by Universitat Basel.

CONFLICT OF INTEREST

The authors declare that they have no competing interests.

AUTHOR CONTRIBUTIONS

V.R., W.S. and Z.M. designed the project. V.R. performed the rhodopsin analyses under the supervision of F.R., Z.M. and W.S. V.R. and F.R. performed the coverage calculations and the depth-related substitution analysis. V.R. and W.S. wrote the initial manuscript draft. All authors commented on the manuscript and approved the final version.

DATA AVAILABILITY STATEMENT

The sequenced genomes and their raw reads are available from NCBI under the BioProject accession no. PRJNA550295 (https://www.ncbi.nlm.nih.gov/bioproject/; Ronco et al., 2021). BLASTN results, gene multiple alignments and phylogenetic trees have been deposited on Dryad (https://doi.org/10.5061/dryad.4mw6m90c7). Scripts as well as data have been deposited on GitHub (https://github.com/Ninet93/RH1_Ricci_et_al.git).

ORCID

Virginie Ricci https://orcid.org/0000-0001-6466-1930
Fabrizia Ronco https://orcid.org/0000-0003-1583-8108
Zuzana Musilova https://orcid.org/0000-0001-8759-8663
Walter Salzburger https://orcid.org/0000-0002-9988-1674

REFERENCES

Boughman, J. W. (2002). How sensory drive can promote speciation. *Trends in Ecology and Evolution*, *17*(12), 571–577. https://doi.org/10.1016/S0169-5347(02)02595-8

Bowmaker, J. K. (2008). Evolution of vertebrate visual pigments. *Vision Research*, *48*, 2022–2041. https://doi.org/10.1016/j.visres.2008.03.025

Carleton, K. L., Escobar-Camacho, D., Stieb, S. M., Cortesi, F., & Marshall, N. J. (2020). Seeing the rainbow: Mechanisms underlying spectral sensitivity in teleost fishes. *Journal of Experimental Biology*, *223*(8), jeb193334. https://doi.org/10.1242/jeb.193334

Castiglione, G. M., & Chang, B. S. W. (2018). Functional trade-offs and environmental variation shaped ancient trajectories in the evolution of dim-light vision. *eLife*, *7*, 1–30. https://doi.org/10.7554/eLife.35957

Charif, D., & Lobry, J. R. (2007). SeqinR 1.0-2: A contributed package to the R project for statistical computing devoted to biological sequences retrieval and analysis. In U. Bastolla, M. Porto, H. E. Roman, & M. Vendruscolo (Eds.), *Structural approaches to sequence evolution: Molecules*, *networks*, *populations*, *series Biological and Medical Physics*, *Biomedical Engineering* (pp. 207–232). Springer Verlag.

Darriba, D., Taboada, G. L., Doallo, R., & Posada, D. (2011). ProtTest 3: Fast selection of best-fit models of protein evolution. *Bioinformatics*, *27*(8), 1164–1165. https://doi.org/10.1093/bioinformatics/btr088

Darriba, D., Taboada, G. L., Doallo, R., & Posada, D. (2012). JModelTest 2: More models, new heuristics and parallel computing. *Nature Methods*, *9*(8), 772. https://doi.org/10.1038/nmeth.2109

Davies, W. I. L., Collin, S. P., & Hunt, D. M. (2012). Molecular ecology and adaptation of visual photopigments in craniates. *Molecular Ecology*, *21*(13), 3121–3158. https://doi.org/10.1111/j.1365-294X.2012.05617.x

Escobar-Camacho, D., & Carleton, K. L. (2015). Sensory modalities in cichlid fish behavior. *Current Opinion in Behavioral Sciences*, *6*, 115–124. https://doi.org/10.1016/j.cobeha.2015.11.002

Fotiadis, D., Liang, Y., Filipek, S., Saperstein, D. A., Engel, A., & Palczewski, K. (2003). Rhodopsin dimers in native disc membranes. *Nature*, *421*(6919), 127–128.

Guo, W., Shi, L., Filizola, M., Weinstein, H., & Javitch, J. A. (2005). Crosstalk in G protein-coupled receptors: Changes at the transmembrane homodimer interface determine activation. *Proceedings of the National Academy of Sciences of the United States of America*, *102*(48), 17495–17500. https://doi.org/10.1073/pnas.0508950102

Hauser, F. E., & Chang, B. S. (2017). Insights into visual pigment adaptation and diversity from model ecological and evolutionary systems. *Current Opinion in Genetics and Development*, *47*(November), 110–120. https://doi.org/10.1016/j.gde.2017.09.005

Hauzman, E., Bonci, D. M. O., Suárez-Villota, E. Y., Neitz, M., & Ventura, D. F. (2017). Daily activity patterns influence retinal morphology, signatures of selection, and spectral tuning of opsin genes in colubrid snakes. *BMC Evolutionary Biology*, *17*(1), 1–14. https://doi.org/10.1186/s12862-017-1110-0

Hofmann, C. M., O'Quin, K. E., Marshall, N. J., Cronin, T. W., Seehausen, O., & Carleton, K. L. (2009). The eyes have it: Regulatory and structural changes both underlie cichlid visual pigment diversity. *PLoS Biology*, *7*(12), e1000266. https://doi.org/10.1371/journal.pbio.1000266

Hope, A. J., Partridge, J. C., Dulai, K. S., & Hunt, D. M. (1997). Mechanisms of wavelength tuning in the rod opsins of deep-sea fishes. *Proceedings of the Royal Society B: Biological Sciences*, *264*(1379), 155–163. https://doi.org/10.1098/rspb.1997.0023

Hunt, D. M., & Collin, S. P. (2014). The evolution of photoreceptors and visual photopigments in vertebrates. In D. M. Hunt, M. W. Hankins, S. P. Collin & N. J. Marshall (Eds.), *Evolution of visual and non-visual pigments* (pp. 163–217). https://doi.org/10.1007/978-1-4614-4355-1

Hunt, D. M., Dulai, K. S., Partridge, J. C., Cottrill, P., & Bowmaker, J. K. (2001). The molecular basis for spectral tuning of rod visual pigments in deep-sea fish. *Journal of Experimental Biology*, *204*(19), 3333–3344. https://doi.org/10.1242/jeb.204.19.3333

Hunt, D. M., Fitzgibbon, J., Slobodyanyuk, S. J., & Bowmaker, J. K. (1996). Spectral tuning and molecular evolution of rod visual pigments in the species flock of cottoid fish in Lake Baikal. *Vision Research*, *36*(9), 1217–1224. https://doi.org/10.1016/0042-6989(95)00228-6

Katoh, K., & Standley, D. M. (2013). MAFFT multiple sequence alignment software version 7: Improvements in performance and usability. *Molecular Biology and Evolution*, *30*(4), 772–780. https://doi.org/10.1093/molbev/mst010

Kocher, T. D. (2004). Adaptive evolution and explosive speciation: The cichlid fish model. *Nature Reviews Genetics*, *5*(4), 288–298. https://doi.org/10.1038/nrg1316

Kosakovsky Pond, S. L., Frost, S. D. W., & Muse, S. V. (2005). HyPhy: Hypothesis testing using phylogenies. *Bioinformatics*, *21*(5), 676–679. https://doi.org/10.1093/bioinformatics/bti079

Li, H., & Durbin, R. (2009). Fast and accurate short read alignment with Burrows-Wheeler transform. *Bioinformatics*, *25*(14), 1754–1760. https://doi.org/10.1093/bioinformatics/btp324

Li, H., Handsaker, B., Wysoker, A., Fennell, T., Ruan, J., Homer, N., Marth, G., Abecasis, G., & Durbin, R. (2009). The sequence alignment/map format and SAMtools. *Bioinformatics*, *25*(16), 2078–2079. https://doi.org/10.1093/bioinformatics/btp352

Lin, J. J., Wang, F. Y., Li, W. H., & Wang, T. Y. (2017). The rises and falls of opsin genes in 59 ray-finned fish genomes and their implications for environmental adaptation. *Scientific Reports*, *7*(1), 1–13. https://doi.org/10.1038/s41598-017-15868-7

Maan, M. E., Hofker, K. D., Van Alphen, J. J. M., & Seehausen, O. (2006). Sensory drive in cichlid speciation. *The American Naturalist*, *167*(6), 947–954. https://doi.org/10.1086/503532

Malinsky, M., Challis, R. J., Tyers, A. M., Schiffels, S., Terai, Y., Ngatunga, B. P., Miska, E. A., Durbin, R., Genner, M. J., & Turner, G. F. (2015). Genomic islands of speciation separate cichlid ecomorphs in an East African crater lake. *Science*, *350*(6267), 1493–1498. https://doi.org/10.1126/science.aac9927

Mano, H., Kojima, D., & Fukada, Y. (1999). Exo-rhodopsin: A novel rhodopsin expressed in the zebrafish pineal gland. *Molecular Brain Research*, *73*(1–2), 110–118. https://doi.org/10.1016/S0169-328X(99)00242-9

McGee, M. D., Borstein, S. R., Meier, J. I., Marques, D. A., Mwaiko, S., Taabu, A., Kishe, M. A., O'Meara, B., Bruggmann, R., Excoffier, L., & Seehausen, O. (2020). The ecological and genomic basis of explosive adaptive radiation. *Nature*, *586*, 75–79. https://doi.org/10.1038/s41586-020-2652-7

Menon, S. T., Han, M., & Sakmar, T. P. (2001). Rhodopsin: Structural basis of molecular physiology. *Physiological Reviews*, *81*(4), 1659–1688. https://doi.org/10.1152/physrev.2001.81.4.1659

Miyagi, R., Terai, Y., Aibara, M., Sugawara, T., Imai, H., Tachida, H., Mzighani, S. I., Okitsu, T., Wada, A., & Okada, N. (2012). Correlation between nuptial colors and visual sensitivities tuned by opsins leads to species richness in sympatric Lake Victoria cichlid fishes. *Molecular Biology and Evolution*, *29*(11), 3281–3296. https://doi.org/10.1093/molbev/mss139

Munz, F. W., & McFarland, W. N. (1977). Evolutionary adaptations of fishes to the photic environment. In F. Crescitelli (Ed.), *The visual system in vertebrates* (pp. 193–274). Springer Verlag. https://doi.org/10.1007/978-3-642-66468-7_4

Muschick, M., Indermaur, A., & Salzburger, W. (2012). Convergent evolution within an adaptive radiation of cichlid fishes. *Current Biology*, *22*(24), https://doi.org/10.1016/j.cub.2012.10.048

Musilova, Z., Cortesi, F., Matschiner, M., Davies, W. I. L., Patel, J. S., Stieb, S. M., De Busserolles, F., Malmstrøm, M., Tørresen, O. K., Brown, C. J., Mountford, J. K., Hanel, R., Stenkamp, D.

L., Jakobsen, K. S., Carleton, K. L., Jentoft, S., Marshall, J., & Salzburger, W. (2019). Vision using multiple distinct rod opsins in deep-sea fishes. *Science*, *364*(6440), 588–592. https://doi.org/10.1126/science.aav4632

Musilova, Z., Indermaur, A., Bitja-Nyom, A. R., Omelchenko, D., Kłodawska, M., Albergati, L., Remišová, K., & Salzburger, W. (2019). Evolution of the visual sensory system in cichlid fishes from crater lake Barombi Mbo in Cameroon. *Molecular Ecology*, *28*, 5010–5031. https://doi.org/10.1111/mec.15217

Musilova, Z., Salzburger, W., & Cortesi, F. (2021). The visual opsin gene repertoires of teleost fishes: Evolution, ecology, and function. *Annual Review of Cell and Developmental Biology*, *37*(1), 441–468. https://doi.org/10.1146/annurev-cellbio-120219-024915

Nagai, H., Terai, Y., Sugawara, T., Imai, H., Nishihara, H., Hori, M., & Okada, N. (2011). Reverse evolution in RH1 for adaptation of cichlids to water depth in Lake Tanganyika. *Molecular Biology and Evolution*, *28*(6), 1769–1776. https://doi.org/10.1093/molbev/msq344

Nguyen, L. T., Schmidt, H. A., Von Haeseler, A., & Minh, B. Q. (2014). IQ-TREE: A fast and effective stochastic algorithm for estimating maximum-likelihood phylogenies. *Molecular Biology and Evolution*, *32*(1), 268–274. https://doi.org/10.1093/molbev/msu300

Ou, W.-b., Yi, T., Kim, J. M., & Khorana, H. G. (2011). The roles of transmembrane domain helix-III during rhodopsin photoactivation. *PLoS One*, *6*(2), 1–13. https://doi.org/10.1371/journal.pone.0017398

Palczewski, K., Kumasaka, T., Hori, T., Behnke, C. A., Motoshima, H., Fox, B. A., Le Trong, I., Teller, D. C., Okada, T., Stenkamp, R. E., Yamamoto, M., & Miyano, M. (2000). Crystal structure of rhodopsin: A G protein-coupled receptor. *Science*, *289*(5480), 739–745. https://doi.org/10.1126/science.289.5480.739

Paradis, E., Claude, J., & Strimmer, K. (2004). APE: Analyses of phylogenetics and evolution in R language. *Bioinformatics*, *20*(2), 289–290. https://doi.org/10.1093/bioinformatics/btg412

Porter, M. L., Roberts, N. W., & Partridge, J. C. (2016). Evolution under pressure and the adaptation of visual pigment compressibility in deep-sea environments. *Molecular Phylogenetics and Evolution*, *105*, 160–165. https://doi.org/10.1016/j.ympev.2016.08.007

Quinlan, A. R., & Hall, I. M. (2010). BEDTools: A flexible suite of utilities for comparing genomic features. *Bioinformatics*, *26*(6), 841–2. https://doi.org/10.1093/bioinformatics/btq033

Revell, L. J. (2012). phytools: An R package for phylogenetic comparative biology (and other things). *Methods in Ecology and Evolution*, *3*(2), 217–223. https://doi.org/10.1111/j.2041-210X.2011.00169.x

Robinson, D. F., & Foulds, L. R. (1981). Comparison of phylogenetic trees. *Mathematical Biosciences*, *53*(1–2), https://doi.org/10.1016/0025-5564(81)90043-2

Ronco, F., Matschiner, M., Böhne, A., Boila, A., Büscher, H. H., El Taher, A., Indermaur, A., Malinsky, M., Ricci, V., Kahmen, A., Jentoft, S., & Salzburger, W. (2021). Drivers and dynamics of a massive adaptive radiation in cichlid fishes. *Nature*, *589*(February), 76–81. https://doi.org/10.1038/s41586-020-2930-4

Ronquist, F., & Huelsenbeck, J. P. (2003). MrBayes 3: Bayesian phylogenetic inference under mixed models. *Bioinformatics*, *19*(12), 1572–1574. https://doi.org/10.1093/bioinformatics/btg180

Salzburger, W. (2018). Understanding explosive diversification through cichlid fish genomics. *Nature Reviews Genetics*, *19*(11), 705–717. https://doi.org/10.1038/s41576-018-0043-9

Salzburger, W., Bocxlaer, B. V., & Cohen, A. S. (2014). Ecology and evolution of the African great lakes and their faunas. *Annual Review of Ecology, Evolution, and Systematics*, *45*, 519–545. https://doi.org/10.1146/annurev-ecolsys-120213-091804

Salzburger, W., Ewing, G. B., & Von Haeseler, A. (2011). The performance of phylogenetic algorithms in estimating haplotype genealogies with migration. *Molecular Ecology*, *20*(9), 1952–1963. https://doi.org/10.1111/j.1365-294X.2011.05066.x

Salzburger, W., Mack, T., Verheyen, E., & Meyer, A. (2005). Out of Tanganyika: Genesis, explosive speciation, key-innovations and phylogeography of the haplochromine cichlid fishes. *BMC Evolutionary Biology*, *5*(1983), 1–15. https://doi.org/10.1186/1471-2148-5-17

Schliep, K. P. (2011). phangorn: Phylogenetic analysis in R. *Bioinformatics*, *27*(4), 592–593. https://doi.org/10.1093/bioinformatics/btq706

Schneider, R. F., Rometsch, S. J., Torres-Dowdall, J., & Meyer, A. (2020). Habitat light sets the boundaries for the rapid evolution of cichlid fish vision, while sexual selection can tune it within those limits. *Molecular Ecology*, *29*(8), 1476–1493. https://doi.org/10.1111/mec.15416

Schott, R. K., Refvik, S. P., Hauser, F. E., López-Fernández, H., & Chang, B. S. W. (2014). Divergent positive selection in rhodopsin from lake and riverine cichlid fishes. *Molecular Biology and Evolution*, *31*(5), 1149–1165. https://doi.org/10.1093/molbev/msu064

Seehausen, O., Terai, Y., Magalhaes, I. S., Carleton, K. L., Mrosso, H. D. J., Miyagi, R., Van Der Sluijs, I., Schneider, M. V., Maan, M. E., Tachida, H., Imai, H., & Okada, N. (2008). Speciation through sensory drive in cichlid fish. *Nature*, *455*(7213), 620–626. https://doi.org/10.1038/nature07285

Spady, T. C., Seehausen, O., Loew, E. R., Jordan, R. C., Kocher, T. D., & Carleton, K. L. (2005). Adaptive molecular evolution in the opsin genes of rapidly speciating cichlid species. *Molecular Biology and Evolution*, *22*(6), 1412–1422. https://doi.org/10.1093/molbev/msi137

Sugawara, T., Terai, Y., Imai, H., Turner, G. F., Koblmüller, S., Sturmbauer, C., Shichida, Y., & Okada, N. (2005). Parallelism of amino acid changes at the RH1 affecting spectral sensitivity among deep-water cichlids from Lakes Tanganyika and Malawi. *Proceedings of the National Academy of Sciences of the United States of America*, *102*(15), 5448–5453. https://doi.org/10.1073/pnas.0405302102

Talling, J. F. (1991). Lake Tanganyika and its life. G. W. Coulter (Ed.) with contributions from J.-J. Tiercelin, A. Mondegver, R.E. Hecky and R.H. Spigel. *Aquatic conservation: Marine and freshwater ecosystems* (pp. 190-191). British Museum (Natural History) Publications — Oxford University Press. https://doi.org/10.1016/0169-5347(91)90231-I

Team R Development Core (2018). *A language and environment for statistical computing*. R Foundation for Statistical Computing (p. 2). https://www.R-project.org

Terai, Y., Mayer, W. E., Klein, J., Tichy, H., & Okada, N. (2002). The effect of selection on a long wavelength-sensitive (LWS) opsin gene of Lake Victoria cichlid fishes. *Proceedings of the National Academy of Sciences of the United States of America*, *99*(24), 15501–15506. https://doi.org/10.1073/pnas.232561099

Terai, Y., Miyagi, R., Aibara, M., Mizoiri, S., Imai, H., Okitsu, T., Wada, A., Takahashi-Kariyazono, S., Sato, A., Tichy, H., Mrosso, H. D. J., Mzighani, S. I., & Okada, N. (2017). Visual adaptation in Lake Victoria cichlid fishes: Depth-related variation of color and scotopic opsins in species from sand/mud bottoms. *BMC Evolutionary Biology*, *17*(1), 1–12. https://doi.org/10.1186/s12862-017-1040-x

Terai, Y., Seehausen, O., Sasaki, T., Takahashi, K., Mizoiri, S., Sugawara, T., Sato, T., Watanabe, M., Konijnendijk, N., Mrosso, H. D. J., Tachida, H., Imai, H., Shichida, Y., & Okada, N. (2006). Divergent selection on opsins drives incipient speciation in Lake Victoria cichlids. *PLoS Biology*, *4*(12), 2244–2251. https://doi.org/10.1371/journal.pbio.0040433

Terakita, A. (2005). The opsins. *Genome Biology*, *6*(3), 1–9. https://doi.org/10.1186/gb-2005-6-3-213

Torres-Dowdall, J., Henning, F., Elmer, K. R., & Meyer, A. (2015). Ecological and lineage-specific factors drive the molecular evolution of rhodopsin in cichlid fishes. *Molecular Biology and Evolution*, *32*(11), 2876–2882. https://doi.org/10.1093/molbev/msv159

Varela, A. I., & Ritchie, P. A. (2015). Critical amino acid replacements in the rhodopsin gene of 19 teleost species occupying different light environments from shallow-waters to the deep-sea. *Environmental Biology of Fishes*, *98*, 193–200. https://doi.org/10.1007/s10641-014-0249-4

Warrant, E. J., & Locket, N. A. (2004). Vision in the deep sea. *Biological Reviews of the Cambridge Philosophical Society*, *79*, 671–712. https://doi.org/10.1017/S1464793103006420

Wilgenbusch, J. C., & Swofford, D. (2003). Inferring evolutionary trees with PAUP *. *Current Protocols in Bioinformatics*, *00*(1), 6.4.1-6.4.28. https://doi.org/10.1002/0471250953.bi0604s00

Wright, D. S., van Eijk, R., Schuart, L., Seehausen, O., Groothuis, T. G. G., & Maan, M. E. (2020). Testing sensory drive speciation in cichlid fish: Linking light conditions to opsin expression, opsin genotype and female mate preference. *Journal of Evolutionary Biology*, *33*, 422–434. https://doi.org/10.1111/jeb.13577

Yang, Z. (2007). PAML 4: Phylogenetic analysis by maximum likelihood. *Molecular Biology and Evolution*, *24*(8), 1586–1591. https://doi.org/10.1093/molbev/msm088

Yokoyama, S. (2008). Evolution of dim-light and color vision pigments. *Annual Review of Genomics and Human Genetics*, *9*, 259–282. https://doi.org/10.1146/annurev.genom.9.081307.164228

Yokoyama, S., Tada, T., Zhang, H., & Britt, L. (2008). Elucidation of phenotypic adaptations: Molecular analyses of dim-light vision proteins in vertebrates. *Proceedings of the National Academy of Sciences of the United States of America*, *105*(36), 13480–13485. https://doi.org/10.1073/pnas.0802426105

Yokoyama, S., & Yokoyama, R. (1996). Adaptive evolution of photoreceptors and visual pigments in vertebrates. *Annual Review of Ecology and Systematics*, *27*, 543–567.

SUPPORTING INFORMATION

Additional supporting information may be found in the online version of the article at the publisher's website.

How to cite this article: Ricci, V., Ronco, F., Musilova, Z., & Salzburger, W. (2022). Molecular evolution and depth-related adaptations of rhodopsin in the adaptive radiation of cichlid fishes in Lake Tanganyika. *Molecular Ecology*, *31*, 2882–2897. https://doi.org/10.1111/mec.16429

MOLECULAR ECOLOGY

Supplemental Information for:

Molecular evolution and depth-related adaptations of rhodopsin in the adaptive radiation of cichlid fishes in Lake Tanganyika

Virginie Ricci, Fabrizia Ronco, Zuzana Musilova & Walter Salzburger

Table of Contents:

FIGURE S1 Barplot showing the number of nucleotide/amino acid differences of species with intraspecific variation in rhodopsin. For each species, the bar on the left represents the number of nucleotide differences, whereas the bar on the right shows the number of amino acid differences. Differences due to ambiguous nucleotides/amino acids (at heterozygous sites) are shown in white. Note that nucleotide differences do not always result in amino acid changes and that only two individuals per most species are included in this study. Species names are color-coded according to tribe (as in Ronco et al. 2021).

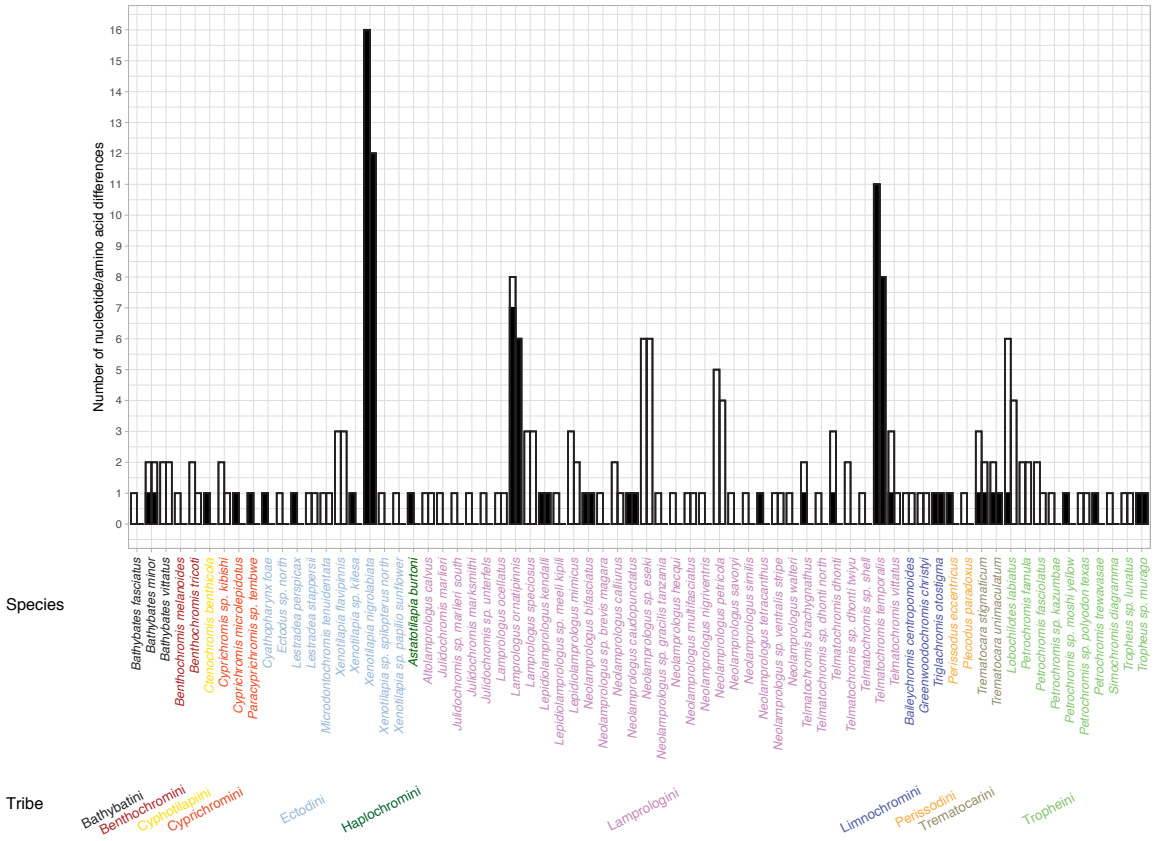

FIGURE S2 Codon and amino acid diversity along the rhodopsin (RH1) protein sequence. **(A)** Barplot showing the number of codon and amino acid variants along the RH1 protein sequence. The number of amino acids variants is represented in dark grey, and the number of codon variants is shown in light grey. Ambiguous sites are marked in red below the bars (arrows: variable sites with heterozygosity; vertical rectangles: sites with more than one amino acid variant due to heterozygosity). Variable known key tuning sites are shown within frames. The colored background shadings indicate the respective region of RH1 (from left to right): N-terminal and TM (transmembrane alpha-helix) I, II, III, IV, V, VI, and VII. **(B)** Barplots showing the percentage of variable amino acid sites in each region of RH1. For each RH1 region, the bar on the left includes variable homozygous sites (red rectangles in (A)), whereas the bar on the right shows variable homozygous sites including heterozygous sites. Variable sites located in the extra- and intracellular loops are combined under “Loops” (in grey).

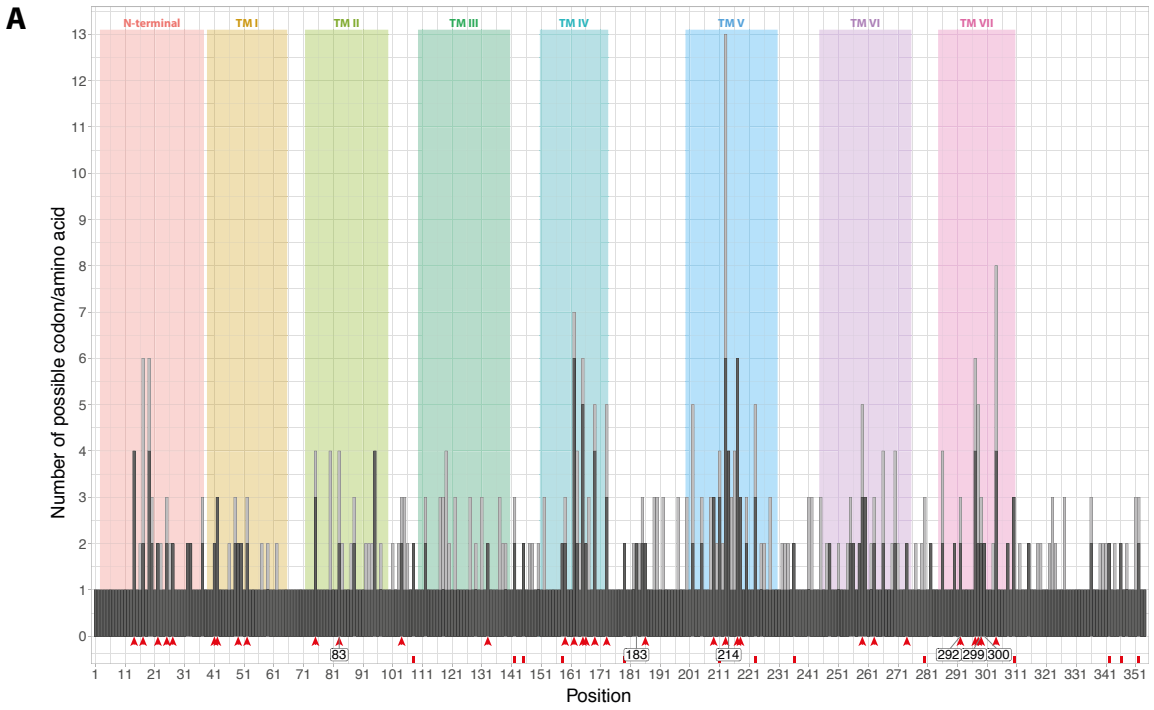
A
N-terminal
TM I
TM II
TM III
TM IV
TM V
TM VI
TM VII
Number of possible codon/amino acid
Position
83
183
214
292
299
300

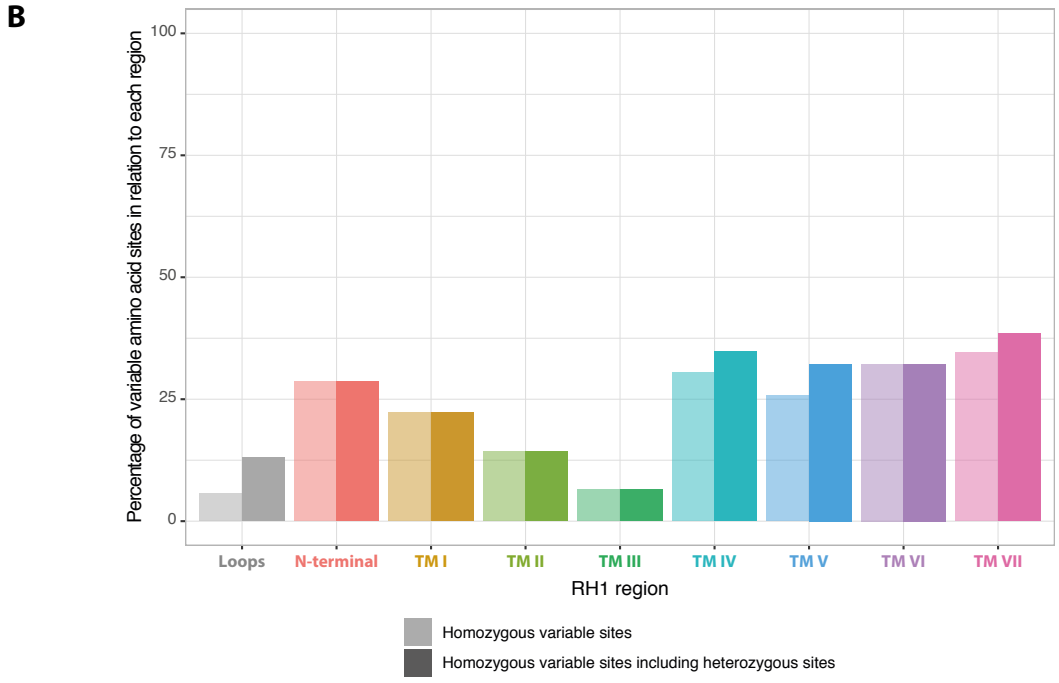
B
Percentage of variable amino acid sites in relation to each region
Loops
N-terminal
TM I
TM II
TM III
TM IV
TM V
TM VI
TM VII
RH1 region
Homozygous variable sites
Homozygous variable sites including heterozygous sites

FIGURE S3 *Rhodopsin* maximum likelihood gene tree with bootstrap support values shown in grey and amino acid changes in red (total tree length: 0.631). The tip labels are color-coded according to tribe. The number and the letter(s) next to each species names represent the number of individuals and their IDs (see Supplementary table S1 [CDS tip label]). The axis corresponds to the number of changes according to the GRT+G+I substitution model.

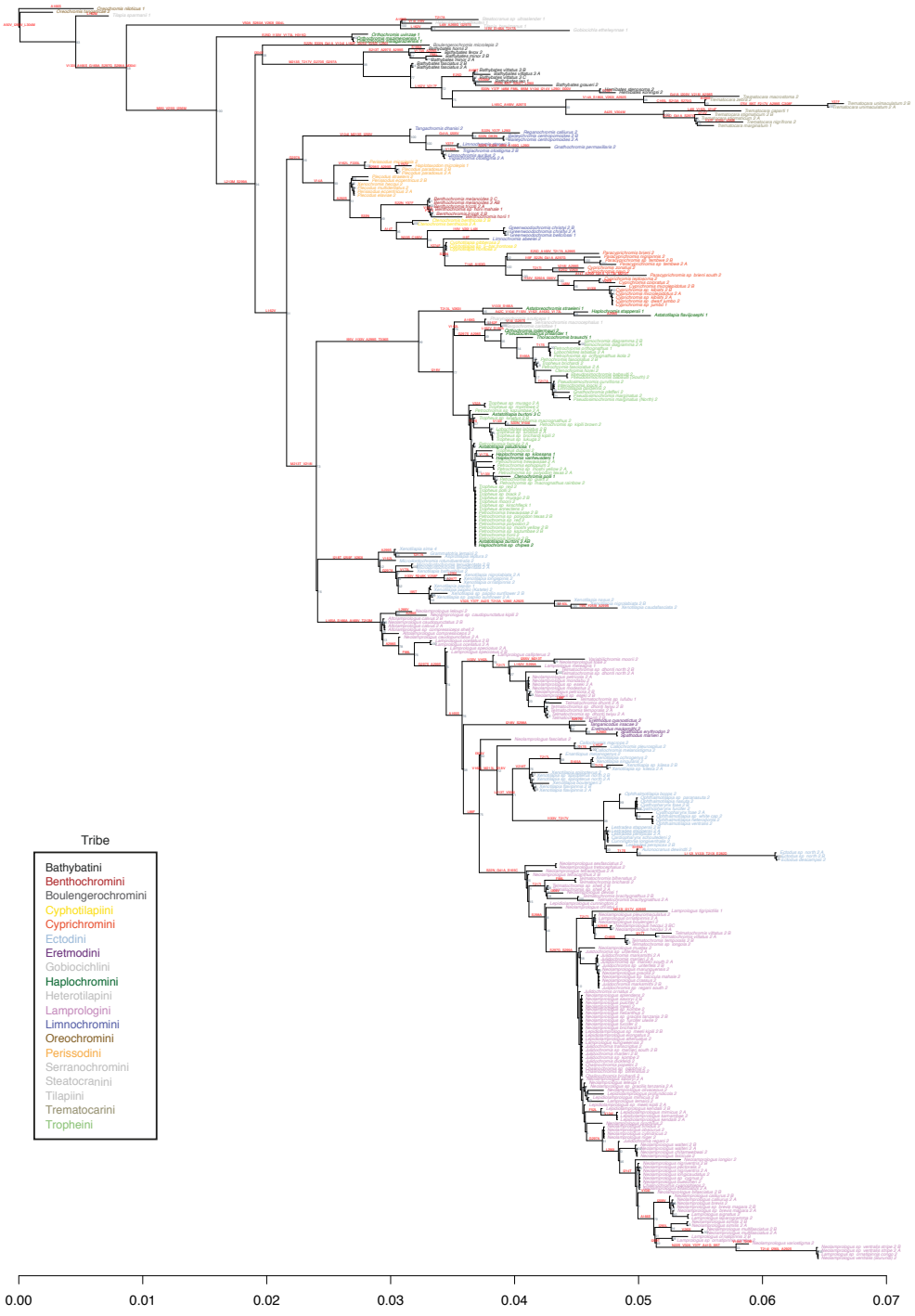

FIGURE S4 Rhodopsin Bayesian inference gene tree with posterior probabilities values shown in grey and amino acid changes in red (total tree length: 0.479). The tip labels are color-coded according to tribe. The number and the letter(s) next to each species names represent the number of individuals and their IDs (see Supplementary table S1 [CDS tip label]). The axis corresponds to the number of changes according to the GRT+G+I substitution model.

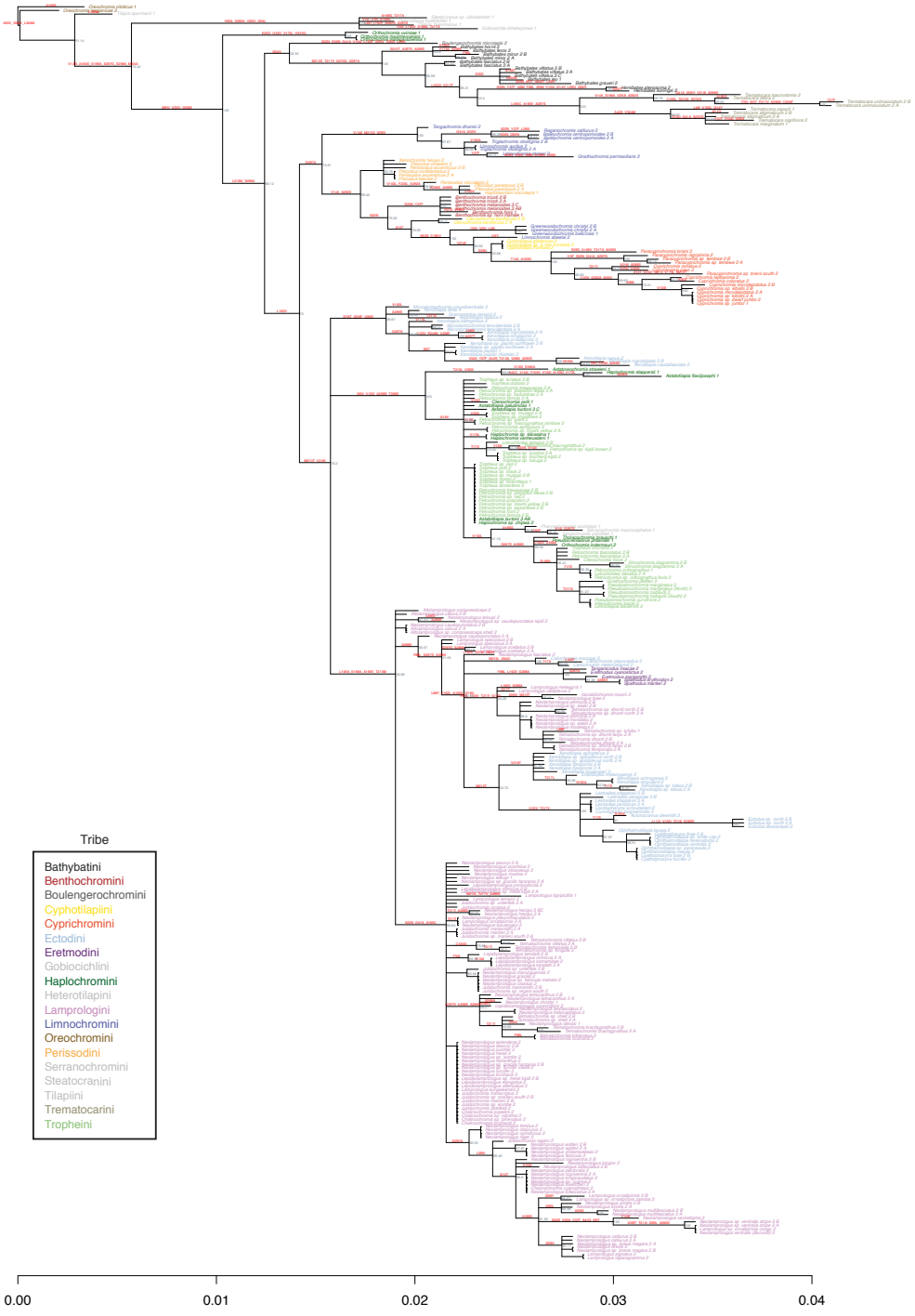

FIGURE S5 Rhodopsin maximum likelihood amino acid tree with bootstrap support values shown in grey and amino acid changes in red (total tree length: 0.139). The tip labels are color-coded according to tribe. The number and the letter(s) next to each species names represent the number of individuals and their IDs (see Supplementary table S1 [CDS tip label]). The axis corresponds to the number of changes according to the JTT+I+G+F substitution model.

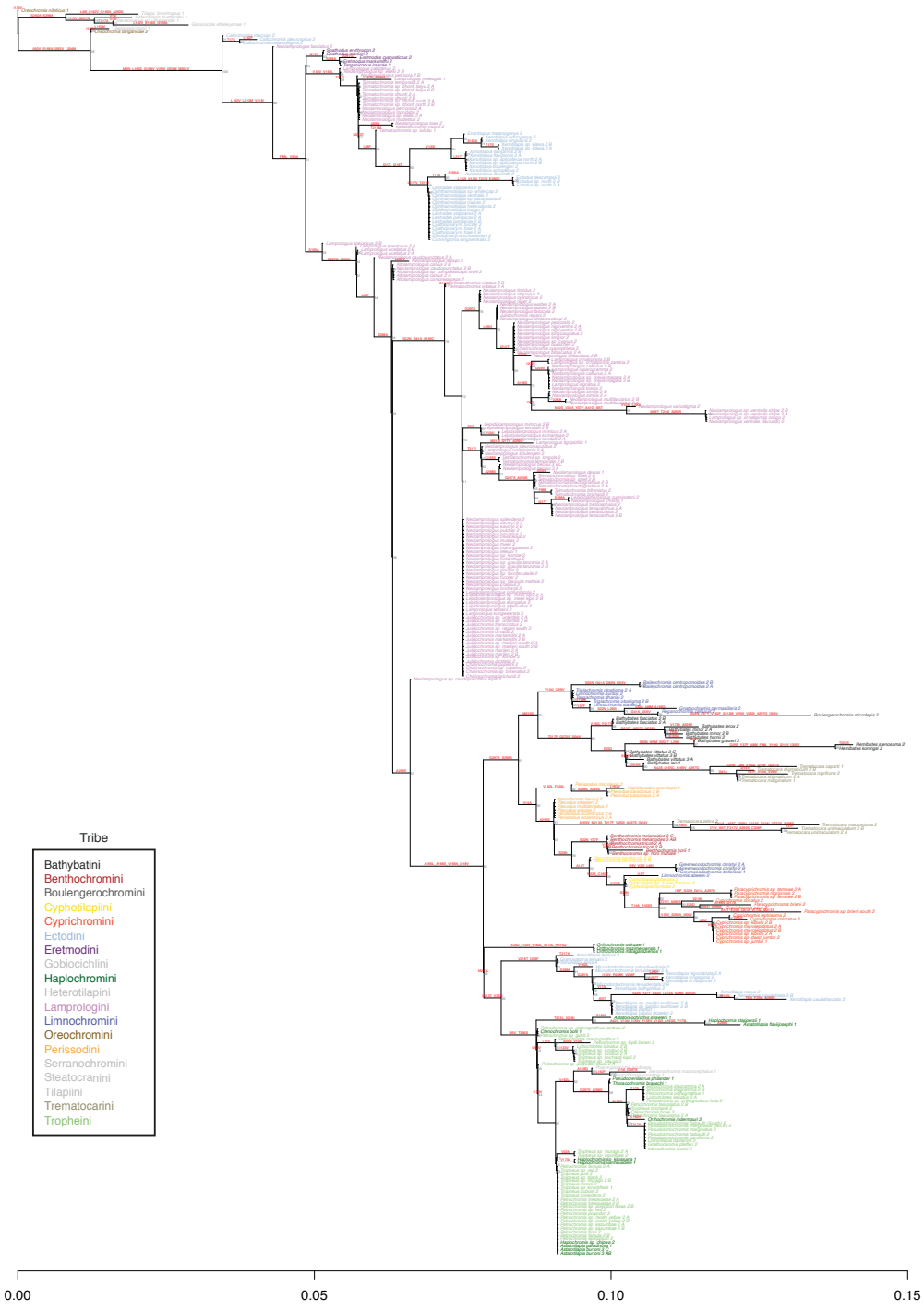

FIGURE S6 Rhodopsin Bayesian inference amino acid tree with posterior probabilities values shown in grey and amino acid changes in red (total tree length: 0.07). The tip labels are color-coded according to tribe. The number and the letter(s) next to each species names represent the number of individuals and their IDs (see Supplementary table S1 [CDS tip label]). The axis corresponds to the number of changes according to the JTT+I+G+F substitution model.

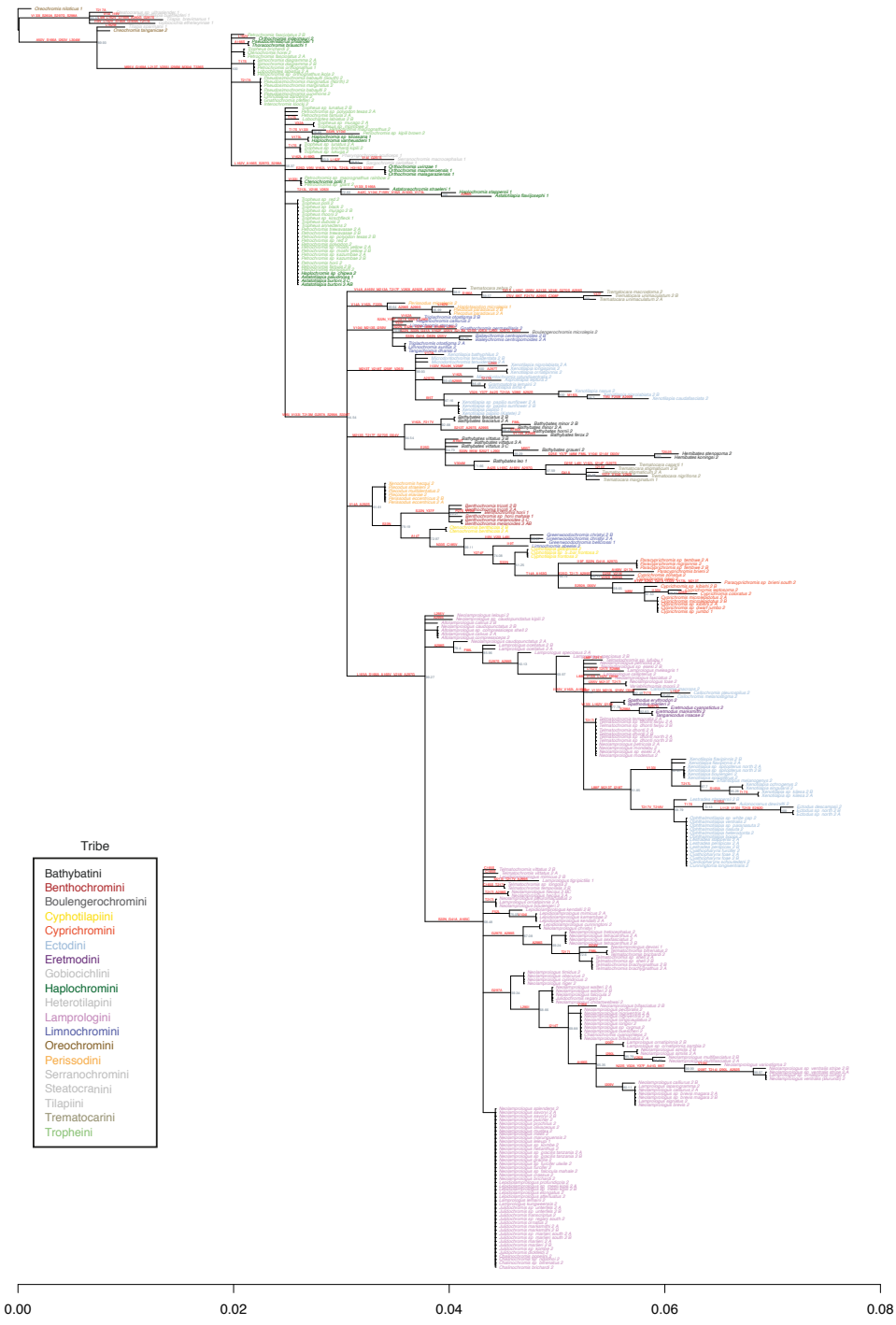

FIGURE S7 Rhodopsin amino acid substitutions at known key tuning sites (positions 83, 183, 214, 292, 299, and 300) mapped on the maximum likelihood gene tree (see Figure 3). Each colored dot corresponds to a substitution at a specific position along the rhodopsin amino acid sequence. The color of dots corresponds to the direction of the predicted shift of the peak spectral sensitivity (blue: shift toward shorter wavelength, red: shift toward longer wavelength). The colored arches around the gene tree indicate the tribe to which a species belongs to (see Figure S3 and Table S1 for full species names). The number and the letter(s) next to each abbreviated species name represent the number of individuals and their IDs (see Supplementary table S1 [CDS tip label]).

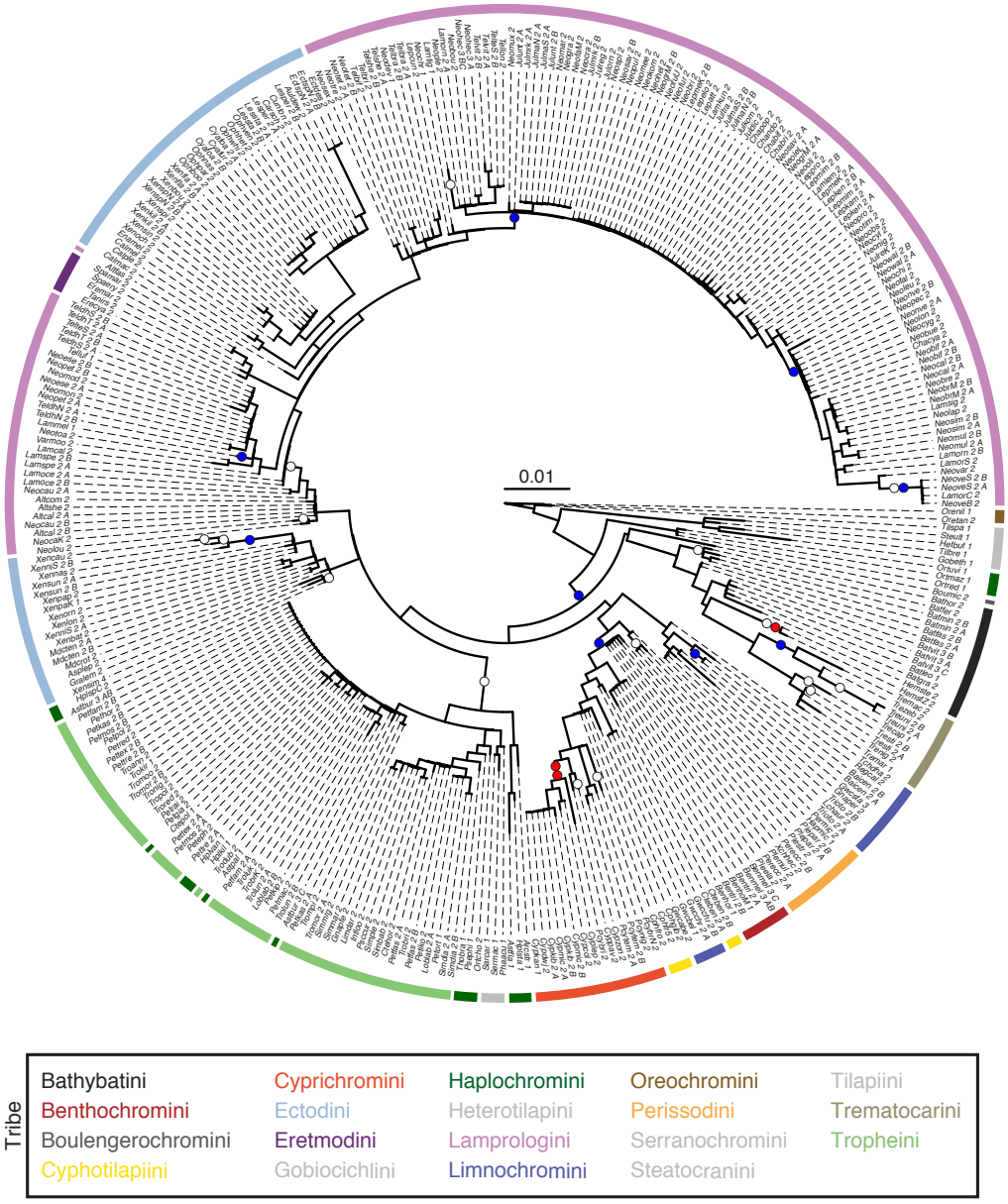

FIGURE S8 Dotplots of depth-associated amino acid substitutions in rhodopsin (RH1; BayesTraits analysis comparing only shallow- and deep-water living species). Each plot corresponds to a specific amino acid at a particular position in RH1. RH1 positions are color-coded according to regions (N-terminal and transmembrane alpha-helices [TM]). Each individual is represented by a dot and color-coded according to tribe. The x-axis represents the shallow- and deep-water living species, the y-axis indicates the absence (0) and/or presence (1) of the respective amino acid (plotted with jitter points for better visualization). Note that dotplots for a given position are not perfectly symmetrical, which is due to ambiguous amino acid sites.

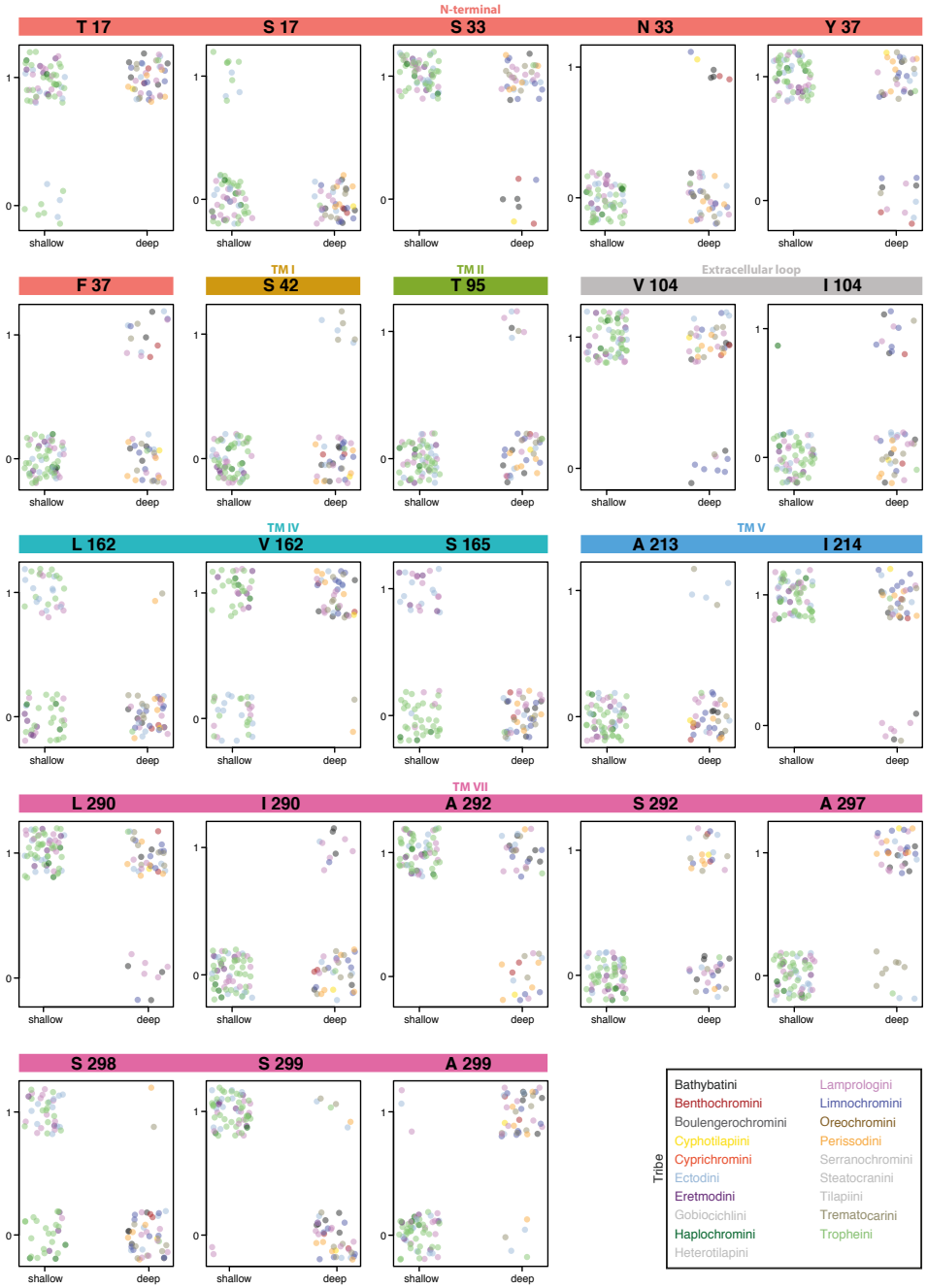
N-terminal
T 17
S 17
S 33
N 33
Y 37
TM I
TM II
Extracellular loop
F 37
S 42
T 95
V 104
I 104
TM IV
TM V
L 162
V 162
S 165
A 213
I 214
TM VII
L 290
I 290
A 292
S 292
A 297
S 298
S 299
A 299
shallow
deep
Tribe
Bathybatini
Benthochromini
Boulengerochromini
Cyphotilapiini
Cyprichromini
Ectodini
Eretmodini
Gobiocichlini
Haplochromini
Heterotilapini
Lamprologini
Limnochromini
Oreochromini
Perissodini
Serranochromini
Steatocranini
Tilapiini
Trematocarini
Tropheini

FIGURE S9 Rhodopsin amino acid (AA) diversity at key tuning sites and sites with potential depth-related substitutions (in bold), ordered by water depths at which a species occurrs and by tribes. Each color corresponds to a specific AA, with ambiguous character being shown in black. The x-axis is color-coded according to tribe. The number and the letter(s) next to each species names represent the number of individuals and their IDs (see Supplementary table S1 [CDS tip label]). The y-axis represents the AA sites in the different RH1 regions according to the reference (*O. niloticus*; TM: transmembrane alpha-helix; see Figure 4).

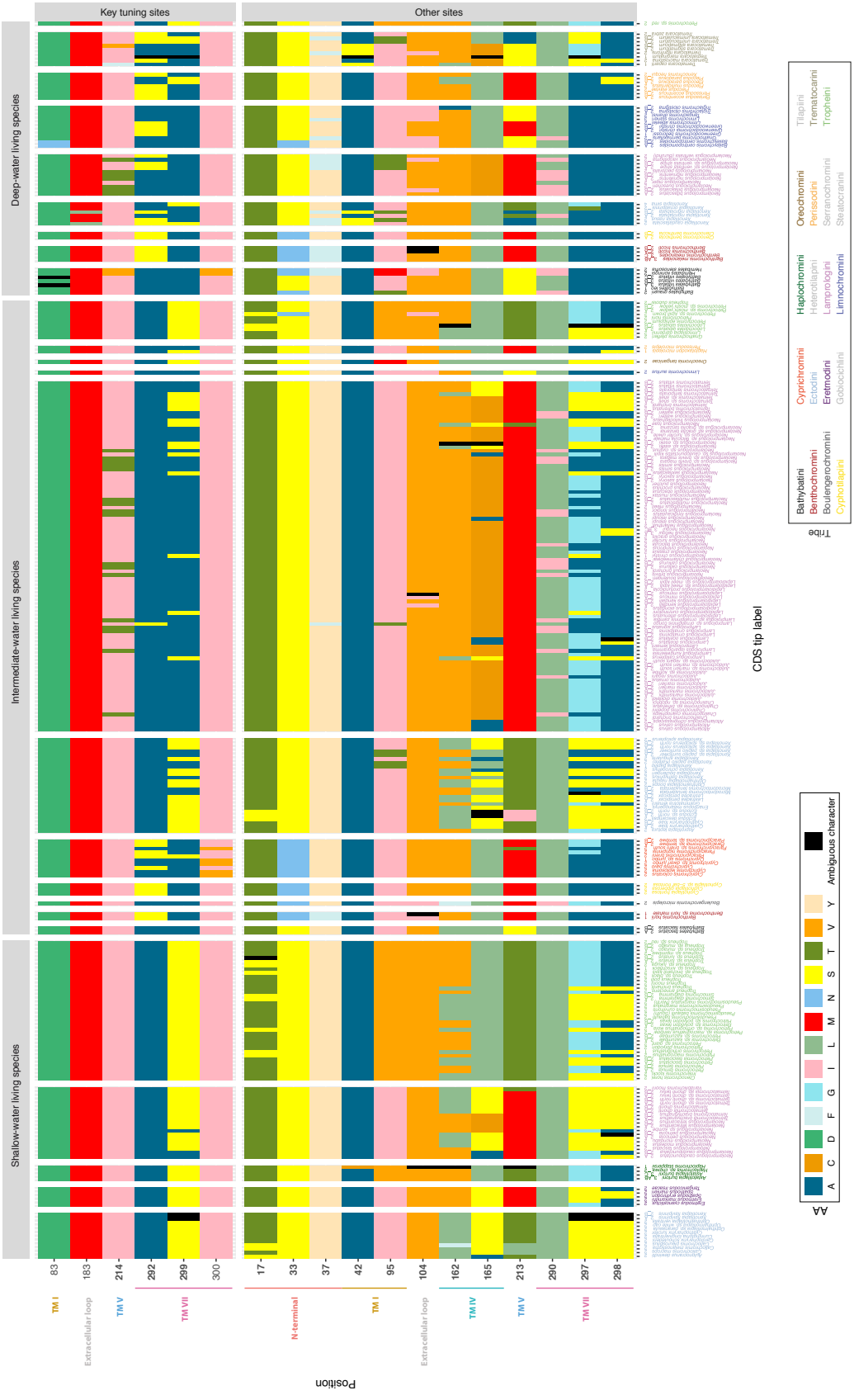
Key tuning sites
Other sites
Deep-water living species
Intermediate-water living species
Shallow-water living species
83
183
214
292
299
300
17
33
37
42
95
104
162
165
213
290
297
298
TM I
Extracellular loop
TM V
TM VII
N-terminal
TM I
Extracellular loop
TM IV
TM V
TM VII
Position
CDS tip label
Tribe
Bathybatini
Benthochromini
Boulengerochromini
Cyphotilapiini
Cyprichromini
Ectodini
Eretmodini
Gobiocichlini
Haplochromini
Heterotilapiini
Lamprologini
Limnochromini
Oreochromini
Perissodini
Serranochromini
Steatocranini
Tilapiini
Trematocarini
Tropheini
AA
A
C
D
F
G
I
L
M
N
S
T
V
Y
Ambiguous character

TABLE S1 Overview of the dataset used for this study, including taxonomic information, sex, depth, tip labels used for phylogenetic trees, and coverage of the sequence data.

Species abbr. (full name)	Tribe	Sex	ID	Depth	CDS unique ID	CDS tip label	AA unique ID	CDS reads depth after mapping to the ref. genome (mean|median)	Genome wide reads depth after mapping to the ref. genome (mean|median)	Ratio of CDS and genome wide reads depth (mean|median)
Orenil (*Oreochromis niloticus*)	Oreochromini	F	RefSeq	NA	haplo0	Orenil_1	haplo0	NA	NA	NA
Batfas (*Bathybates fasciatus*)	Bathybatini	F	GPB2	intermediate	haplo1	Batfas_2_A	haplo1	8.98|9	6.85|9	1.31|1
Batfas (*Bathybates fasciatus*)	Bathybatini	M	ITH3	intermediate	haplo2	Batfas_2_B	haplo1	13.89|14	10.25|14	1.36|1
Batfer (*Bathybates ferox*)	Bathybatini	M	LCD6	NA	haplo3	Batfer_2	haplo2	7.69|8	6.13|8	1.25|1
Batfer (*Bathybates ferox*)	Bathybatini	F	LCD7	NA	haplo3	Batfer_2	haplo2	6.35|7	5.79|7	1.1|1
Batgra (*Bathybates graueri*)	Bathybatini	M	ILG7	deep	haplo4	Batgra_2	haplo3	8.77|8	8.96|12	0.98|0.67
Batgra (*Bathybates graueri*)	Bathybatini	F	IUI8	deep	haplo4	Batgra_2	haplo3	7.42|7	6.92|9	1.07|0.78
Bathor (*Bathybates hornii*)	Bathybatini	M	JDE3	NA	haplo5	Bathor_2	haplo4	9.38|9	7.7|10	1.22|0.9
Bathor (*Bathybates hornii*)	Bathybatini	M?	JDE4	NA	haplo5	Bathor_2	haplo4	11.43|12	10.07|14	1.14|0.86
Batleo (*Bathybates leo*)	Bathybatini	F	ILF7	deep	haplo6	Batleo_1	haplo5	9.3|9	6.43|8	1.45|1.12
Batmin (*Bathybates minor*)	Bathybatini	F	IXA5	NA	haplo7	Batmin_2_A	haplo6	7.7|8	7.13|9	1.08|0.89
Batmin (*Bathybates minor*)	Bathybatini	M	JBG3	NA	haplo8	Batmin_2_B	haplo7	9.71|10	6.65|9	1.46|1.11
Batvit (*Bathybates vittatus*)	Bathybatini	M	ITD7	deep	haplo9	Batvit_3_C	haplo8	7.87|8	7.09|9	1.11|0.89
Batvit (*Bathybates vittatus*)	Bathybatini	M	JDE6	deep	haplo10	Batvit_3_A	haplo9	13.05|13	8.93|12	1.46|1.08
Batvit (*Bathybates vittatus*)	Bathybatini	F	JDE7	deep	haplo11	Batvit_3_B	haplo10	9.92|10	8.87|12	1.12|0.83
Hemste (*Hemibates stenosoma*)	Bathybatini	M	IXC2	deep	haplo13	Hemste_2	haplo12	8.1|8	6.5|8	1.25|1
Hemste (*Hemibates stenosoma*)	Bathybatini	F	IXC3	deep	haplo13	Hemste_2	haplo12	8.75|9	6.78|9	1.29|1
HemstZ (*Hemibates koningsi*)	Bathybatini		IZA5	deep	haplo12	HemstZ_2	haplo11	15.79|15	11.79|16	1.34|0.94
HemstZ (*Hemibates koningsi*)	Bathybatini	F	IJC5	deep	haplo12	HemstZ_2	haplo11	15.71|15	8.3|10	1.89|1.5
BenhoM (*Benthochromis* sp. "horii mahale")	Benthochromini	M	LEF2	intermediate	haplo14	BenhoM_1	haplo13	15.45|15	11.25|15	1.37|1
Benhor (*Benthochromis horii*)	Benthochromini	M	ILF8	intermediate	haplo15	Benhor_1	haplo14	12.21|13	8.7|11	1.4|1.18
Benmel (*Benthochromis melanoides*)	Benthochromini	F	ILG3	deep	haplo16	Benmel_3_AB	haplo15	10.8|10	8.75|12	1.23|0.83
Benmel (*Benthochromis melanoides*)	Benthochromini	M	IXB8	deep	haplo16	Benmel_3_AB	haplo15	7.42|7	7.05|9	1.05|0.78
Benmel (*Benthochromis melanoides*)	Benthochromini	F	IZA2	deep	haplo17	Benmel_3_C	haplo15	8.98|9	7.09|9	1.27|1
Bentri (*Benthochromis tricoti*)	Benthochromini	M	LDA7	deep	haplo18	Bentri_2_A	haplo16	8.78|8	7.11|9	1.23|0.89
Bentri (*Benthochromis tricoti*)	Benthochromini	F	LDA9	deep	haplo19	Bentri_2_B	haplo17	12.69|13	7.47|10	1.7|1.3
Boumic (*Boulengerochromis microlepis*)	Boulengerochromini	F	JAE7	intermediate	haplo20	Boumic_2	haplo18	16.86|17	13.85|18	1.22|0.94
Boumic (*Boulengerochromis microlepis*)	Boulengerochromini	M	JCF2	intermediate	haplo20	Boumic_2	haplo18	18.16|18	14.52|19	1.25|0.95
Cphfr5 (*Cyphotilapia* sp. "5-bar frontosa")	Cyphotilapiini	M	KAG3	intermediate	haplo21	Cphfr5_2	haplo19	10.65|11	9.73|12	1.09|0.92
Cphfr5 (*Cyphotilapia* sp. "5-bar frontosa")	Cyphotilapiini	F	KDG2	intermediate	haplo21	Cphfr5_2	haplo19	14.42|14	12.26|16	1.18|0.88
Cphfro (*Cyphotilapia frontosa*)	Cyphotilapiini	F	LEI6	intermediate	haplo21	Cphfro_2	haplo19	9.21|9	6.71|8	1.37|1.12
Cphfro (*Cyphotilapia frontosa*)	Cyphotilapiini	M	LEI9	intermediate	haplo21	Cphfro_2	haplo19	9.83|10	6.64|8	1.48|1.25
Cphgib (*Cyphotilapia gibberosa*)	Cyphotilapiini	M	INH7	intermediate	haplo21	Cphgib_2	haplo19	12.46|12	9.5|12	1.31|1
Cphgib (*Cyphotilapia gibberosa*)	Cyphotilapiini	F	INH9	intermediate	haplo21	Cphgib_2	haplo19	14.54|15	9.05|11	1.61|1.36
Cteben (*Ctenochromis benthicola*)	Cyphotilapiini	M	DMD1	deep	haplo22	Cteben_2_A	haplo20	10.41|11	7.99|10	1.3|1.1

Cteben (*Ctenochromis benthicola*)	Cyphotilapiini	F	IYA8	deep	haplo23	Cteben_2_B	haplo20	8.71|9	6.97|9	1.25|1
Cypcol (*Cyprichromis coloratus*)	Cyprichromini	M	JEC7	intermediate	haplo24	Cypcol_2	haplo21	20.25|20	14.8|21	1.37|0.95
Cypcol (*Cyprichromis coloratus*)	Cyprichromini	F	JED2	intermediate	haplo24	Cypcol_2	haplo21	20.46|20	13.6|19	1.5|1.05
Cypdwj (*Cyprichromis* sp. "dwarf jumbo")	Cyprichromini	M	KFA7	intermediate	haplo25	Cypdwj_2	haplo22	16.97|17	12.22|17	1.39|1
Cypdwj (*Cyprichromis* sp. "dwarf jumbo")	Cyprichromini	F	KFA9	intermediate	haplo25	Cypdwj_2	haplo22	14.83|15	10.16|14	1.46|1.07
Cypkan (*Cyprichromis* sp. "jumbo")	Cyprichromini	M	INH1	intermediate	haplo25	Cypkan_1	haplo22	15.27|15	9.35|13	1.63|1.15
Cypkib (*Cyprichromis* sp. "kibishi")	Cyprichromini	M	Bel16	NA	haplo26	Cypkib_2_B	haplo23	8.06|8	6.37|8	1.27|1
Cypkib (*Cyprichromis* sp. "kibishi")	Cyprichromini	F	Bel18	NA	haplo25	Cypkib_2_A	haplo22	10.07|11	6.99|9	1.44|1.22
Cyplep (*Cyprichromis leptosoma*)	Cyprichromini	M	ISI2	intermediate	haplo27	Cyplep_2	haplo24	9.95|10	8.51|11	1.17|0.91
Cyplep (*Cyprichromis leptosoma*)	Cyprichromini	F	ISI6	intermediate	haplo27	Cyplep_2	haplo24	10.18|10	7.75|10	1.31|1
Cypmic (*Cyprichromis microlepidotus*)	Cyprichromini	M	JVE1	NA	haplo25	Cypmic_2_A	haplo22	8.6|9	5.86|8	1.47|1.12
Cypmic (*Cyprichromis microlepidotus*)	Cyprichromini	F	JVF2	NA	haplo28	Cypmic_2_B	haplo22	8.35|8	6.43|8	1.3|1
Cyppav (*Cyprichromis pavo*)	Cyprichromini	M	JEB2	intermediate	haplo29	Cyppav_2	haplo25	10.26|10	8.58|11	1.2|0.91
Cyppav (*Cyprichromis pavo*)	Cyprichromini	F	JEB4	intermediate	haplo29	Cyppav_2	haplo25	10.71|10	7.32|9	1.46|1.11
Cypzon (*Cyprichromis zonatus*)	Cyprichromini	M	GPC9	NA	haplo30	Cypzon_2	haplo26	10.15|10	9.34|12	1.09|0.83
Cypzon (*Cyprichromis zonatus*)	Cyprichromini	F	GPD1	NA	haplo30	Cypzon_2	haplo26	7.42|8	6.1|8	1.22|1
Pcybri (*Paracyprichromis* sp. "brieni south")	Cyprichromini	M	IQB9	intermediate	haplo32	Pcybri_2	haplo82	12.48|12	7.88|10	1.58|1.2
Pcybri (*Paracyprichromis* sp. "brieni south")	Cyprichromini	F	IQC1	intermediate	haplo32	Pcybri_2	haplo28	7.39|7	5.75|7	1.29|1
PcybrN (*Paracyprichromis brieni*)	Cyprichromini	M	JXI2	intermediate	haplo31	PcybrN_2	haplo27	8.8|9	6.81|9	1.29|1
PcybrN (*Paracyprichromis brieni*)	Cyprichromini	F	JXI4	intermediate	haplo31	PcybrN_2	haplo27	8.34|8	5.8|8	1.44|1
Pcynig (*Paracyprichromis nigripinnis*)	Cyprichromini	M	GPC4	intermediate	haplo33	Pcynig_2	haplo29	14.23|14	12.11|16	1.18|0.88
Pcynig (*Paracyprichromis nigripinnis*)	Cyprichromini	F	GPC6	intermediate	haplo33	Pcynig_2	haplo29	7.19|7	6.15|8	1.17|0.88
Pcytem (*Paracyprichromis* sp. "tembwe")	Cyprichromini	M	JWD1	intermediate	haplo34	Pcytem_2_A	haplo29	18.3|19	15.83|22	1.16|0.86
Pcytem (*Paracyprichromis* sp. "tembwe")	Cyprichromini	F	JWD2	intermediate	haplo35	Pcytem_2_B	haplo29	24.14|25	15.05|21	1.6|1.19
Asplep (*Asprotilapia leptura*)	Ectodini	F	INF1	intermediate	haplo36	Asplep_2	haplo30	13.95|14	9.28|13	1.5|1.08
Asplep (*Asprotilapia leptura*)	Ectodini	M	INF2	intermediate	haplo36	Asplep_2	haplo30	21.5|21	13.27|19	1.62|1.11
Auldew (*Aulonocranus dewindti*)	Ectodini	F	AUA1	shallow	haplo37	Auldew_2	haplo31	10.33|10	7.57|10	1.36|1
Auldew (*Aulonocranus dewindti*)	Ectodini	F	AUA9	shallow	haplo37	Auldew_2	haplo31	10.59|11	7.44|10	1.42|1.1
Calmac (*Callochromis macrops*)	Ectodini	M	BND3	shallow	haplo38	Calmac_2	haplo32	12.25|12	7.59|10	1.61|1.2
Calmac (*Callochromis macrops*)	Ectodini	F	BND5	shallow	haplo38	Calmac_2	haplo32	13.56|13	8.19|11	1.66|1.18
Calmel (*Callochromis melanostigma*)	Ectodini	M	KAF3	shallow	haplo39	Calmel_2	haplo33	9.57|10	7.28|10	1.31|1
Calmel (*Callochromis melanostigma*)	Ectodini	F	KAF4	shallow	haplo39	Calmel_2	haplo33	9.75|9	7.3|10	1.34|0.9
Calple (*Callochromis pleurospilus*)	Ectodini	M	JZE2	shallow	haplo40	Calple_2	haplo34	10.53|10	7.68|10	1.37|1
Calple (*Callochromis pleurospilus*)	Ectodini	F	JZE4	shallow	haplo40	Calple_2	haplo34	24.28|25	14|20	1.73|1.25
Carsch (*Cardiopharynx schoutedeni*)	Ectodini	M	KAF1	shallow	haplo41	Carsch_2	haplo35	9.34|10	6.99|9	1.34|1.11
Carsch (*Cardiopharynx schoutedeni*)	Ectodini	F	KAF2	shallow	haplo41	Carsch_2	haplo35	18.11|18	11.82|17	1.53|1.06
Cunlon (*Cunningtonia longiventralis*)	Ectodini	M	IWD7	shallow	haplo41	Cunlon_2	haplo35	9.66|9	6.19|8	1.56|1.12
Cunlon (*Cunningtonia longiventralis*)	Ectodini	F	IWD8	shallow	haplo41	Cunlon_2	haplo35	11.73|11	7.32|10	1.6|1.1
Cyafoa (*Cyathopharynx foae*)	Ectodini	F	IOD4	intermediate	haplo42	Cyafoa_2_A	haplo35	8.45|9	6.58|9	1.28|1
Cyafoa (*Cyathopharynx foae*)	Ectodini	M	IOD6	intermediate	haplo43	Cyafoa_2_B	haplo35	7.46|7	5.56|7	1.34|1
Cyafur (*Cyathopharynx furcifer*)	Ectodini	M	AVH2	shallow	haplo43	Cyafur_2	haplo35	9.85|10	7.73|10	1.27|1
Cyafur (*Cyathopharynx furcifer*)	Ectodini	F	AYE5	shallow	haplo43	Cyafur_2	haplo35	10.45|10	7.82|11	1.34|0.91
Ectdes (*Ectodus descampsii*)	Ectodini	M	IRD7	intermediate	haplo44	Ectdes_2	haplo36	9.71|10	9.44|13	1.03|0.77
Ectdes (*Ectodus descampsii*)	Ectodini	F	IRD8	intermediate	haplo44	Ectdes_2	haplo36	8.44|8	6.59|9	1.28|0.89
EctspN (*Ectodus* sp. "north")	Ectodini	M	KHC4	intermediate	haplo45	EctspN_2_A	haplo37	7.1|7	6.46|9	1.1|0.78
EctspN (*Ectodus* sp. "north")	Ectodini	F	KHC5	intermediate	haplo46	EctspN_2_B	haplo37	10.45|10	6.3|8	1.66|1.25

Enamel (*Enantiopus melanogenys*)	Ectodini	M	AWC5	intermediate	haplo47	Enamel_2	haplo38	12.61|12	7.97|11	1.58|1.09
Enamel (*Enantiopus melanogenys*)	Ectodini	F	BNC5	intermediate	haplo47	Enamel_2	haplo38	11.11|11	8.63|12	1.29|0.92
Gralem (*Grammatotria lemairii*)	Ectodini	M	JDD7	intermediate	haplo48	Gralem_2	haplo39	14.85|15	12.1|17	1.23|0.88
Gralem (*Grammatotria lemairii*)	Ectodini	F	JDD8	intermediate	haplo48	Gralem_2	haplo39	7.74|7	6.75|9	1.15|0.78
Lesper (*Lestradea perspicax*)	Ectodini	M	IRA1	intermediate	haplo49	Lesper_2_B	haplo35	6.79|7	5.8|8	1.17|0.88
Lesper (*Lestradea perspicax*)	Ectodini	F	IRA2	intermediate	haplo41	Lesper_2_A	haplo35	10.9|10	7.96|11	1.37|0.91
Lessta (*Lestradea stappersii*)	Ectodini	F	JVH2	NA	haplo41	Lessta_2_A	haplo35	9.78|10	6.52|9	1.5|1.11
Lessta (*Lestradea stappersii*)	Ectodini	M	JVH3	NA	haplo50	Lessta_2_B	haplo40	5.43|5	5.34|7	1.02|0.71
Mdcrot (*Microdontochromis rotundiventralis*)	Ectodini	M	JBE6	NA	haplo51	Mdcrot_2	haplo41	13.45|13	7.11|10	1.89|1.3
Mdcrot (*Microdontochromis rotundiventralis*)	Ectodini	F	JBE7	NA	haplo51	Mdcrot_2	haplo41	15.41|15	11.73|17	1.31|0.88
Mdcten (*Microdontochromis tenuidentata*)	Ectodini	M	LHG4	intermediate	haplo52	Mdcten_2_A	haplo42	13.3|13	9.35|13	1.42|1
Mdcten (*Microdontochromis tenuidentata*)	Ectodini	F	LHG6	intermediate	haplo53	Mdcten_2_B	haplo43	12.7|13	10.66|15	1.19|0.87
Ophboo (*Ophthalmotilapia boops*)	Ectodini	M	LFI4	intermediate	haplo54	Ophboo_2	haplo35	8.2|8	7.27|10	1.13|0.8
Ophboo (*Ophthalmotilapia boops*)	Ectodini	F	LFI6	intermediate	haplo54	Ophboo_2	haplo35	9.19|9	7.06|9	1.3|1
Ophhet (*Ophthalmotilapia heterodonta*)	Ectodini	M	Bel06	NA	haplo55	Ophhet_2	haplo35	8.39|8	6.24|8	1.34|1
Ophhet (*Ophthalmotilapia heterodonta*)	Ectodini	M	Bel12	NA	haplo55	Ophhet_2	haplo35	7.45|7	6.85|9	1.09|0.78
Ophnas (*Ophthalmotilapia nasuta*)	Ectodini	M	AXH6	intermediate	haplo43	Ophnas_2	haplo35	8.46|8	7.68|10	1.1|0.8
Ophnas (*Ophthalmotilapia nasuta*)	Ectodini	F	AXH8	intermediate	haplo43	Ophnas_2	haplo35	11.46|11	7.99|11	1.43|1
Ophpar (*Ophthalmotilapia* sp. "paranasuta")	Ectodini	M	JYF7	shallow	haplo43	Ophpar_2	haplo35	14.58|15	9.38|13	1.55|1.15
Ophpar (*Ophthalmotilapia* sp. "paranasuta")	Ectodini	F	JYG5	shallow	haplo43	Ophpar_2	haplo35	10.13|10	7.61|10	1.33|1
Ophven (*Ophthalmotilapia ventralis*)	Ectodini	M	IQD3	shallow	haplo55	Ophven_2	haplo35	8.09|8	7.43|10	1.09|0.8
Ophven (*Ophthalmotilapia ventralis*)	Ectodini	F	IQE4	shallow	haplo55	Ophven_2	haplo35	6.79|6	6.82|9	1|0.67
Ophwhi (*Ophthalmotilapia* sp. "white cap")	Ectodini	M	LGH1	shallow	haplo55	Ophwhi_2	haplo35	10.71|10	7.85|11	1.36|0.91
Ophwhi (*Ophthalmotilapia* sp. "white cap")	Ectodini	F	LGH3	shallow	haplo55	Ophwhi_2	haplo35	8.91|9	7.16|10	1.24|0.9
Xenbat (*Xenotilapia bathyphilus*)	Ectodini	M	IVB4	intermediate	haplo56	Xenbat_2	haplo44	11.44|11	8.56|12	1.34|0.92
Xenbat (*Xenotilapia bathyphilus*)	Ectodini	F	IVB5	intermediate	haplo56	Xenbat_2	haplo44	7.62|7	6.85|9	1.11|0.78
Xenbou (*Xenotilapia boulengeri*)	Ectodini	M	IPE3	intermediate	haplo57	Xenbou_2	haplo45	8.8|10	7.19|9	1.22|1.11
Xenbou (*Xenotilapia boulengeri*)	Ectodini	F	IPE7	intermediate	haplo57	Xenbou_2	haplo45	8.68|9	6.99|9	1.24|1
Xencau (*Xenotilapia caudafasciata*)	Ectodini	M	IXB9	deep	haplo58	Xencau_2	haplo46	11.31|12	7.53|10	1.5|1.2
Xencau (*Xenotilapia caudafasciata*)	Ectodini	F	IXC1	deep	haplo58	Xencau_2	haplo46	8.27|8	7|9	1.18|0.89
Xenfla (*Xenotilapia flavipinnis*)	Ectodini	M	JAF7	shallow	haplo59	Xenfla_2_A	haplo47	22.89|23	14.1|20	1.62|1.15
Xenfla (*Xenotilapia flavipinnis*)	Ectodini	F	JAF9	shallow	haplo60	Xenfla_2_B	haplo48	17.2|17	12.53|18	1.37|0.94
Xenkil (*Xenotilapia* sp. "kilesa")	Ectodini	M	Bel01	NA	haplo61	Xenkil_2_A	haplo49	14.71|13	9.96|14	1.48|0.93
Xenkil (*Xenotilapia* sp. "kilesa")	Ectodini	M	Bel03	NA	haplo62	Xenkil_2_B	haplo49	9.57|10	5.77|8	1.66|1.25
Xenlon (*Xenotilapia longispinis*)	Ectodini	M	KAF5	NA	haplo63	Xenlon_2	haplo50	13.43|13	8.27|11	1.62|1.18
Xenlon (*Xenotilapia longispinis*)	Ectodini	F	KAF6	NA	haplo63	Xenlon_2	haplo50	10.44|11	9.14|12	1.14|0.92
Xennas (*Xenotilapia nasus*)	Ectodini	M	IMF7	deep	haplo64	Xennas_2	haplo51	8.69|8	6.62|9	1.31|0.89
Xennas (*Xenotilapia nasus*)	Ectodini	F	IMF8	deep	haplo64	Xennas_2	haplo51	17.28|17	10.49|14	1.65|1.21
XenniS (*Xenotilapia nigrolabiata*)	Ectodini	F	IXF4	deep	haplo65	XenniS_2_A	haplo52	21.09|20	13.27|19	1.59|1.05
XenniS (*Xenotilapia nigrolabiata*)	Ectodini	M	IZC7	deep	haplo66	XenniS_2_B	haplo53	6.21|6	7.18|9	0.86|0.67
Xenoch (*Xenotilapia ochrogenys*)	Ectodini	M	JVH4	intermediate	haplo67	Xenoch_2	haplo54	13.21|14	8.72|12	1.51|1.17
Xenoch (*Xenotilapia ochrogenys*)	Ectodini	F	JVI5	intermediate	haplo67	Xenoch_2	haplo54	15.87|16	10.21|14	1.55|1.14
Xenorn (*Xenotilapia ornatipinnis*)	Ectodini	M	JZE6	deep	haplo63	Xenorn_2	haplo50	8.65|8	8.13|11	1.06|0.73
Xenorn (*Xenotilapia ornatipinnis*)	Ectodini	F	JZE8	deep	haplo63	Xenorn_2	haplo50	8.58|9	7.57|10	1.13|0.9
XenpaK (*Xenotilapia papilio*)	Ectodini	F	A206	intermediate	haplo68	XenpaK_1	haplo55	16.87|16	9.23|12	1.83|1.33
Xenpap (*Xenotilapia papilio* (Katete))	Ectodini	M	IVF4	intermediate	haplo68	Xenpap_2	haplo55	17.27|18	10.42|14	1.66|1.29

Xenpap (*Xenotilapia papilio* (Katete))	Ectodini	F	IVF5	intermediate	haplo68	Xenpap_2	haplo55	8.23|9	6.29|8	1.31|1.12
Xensim (*Xenotilapia sima*)	Ectodini	M	IUF7	deep	haplo69	Xensim_4	haplo39	9.32|9	8.17|11	1.14|0.82
Xensim (*Xenotilapia sima*)	Ectodini	F	IUF8	deep	haplo69	Xensim_4	haplo39	10.94|11	8.23|11	1.33|1
Xensim (*Xenotilapia sima*)	Ectodini	M	LBE2	deep	haplo69	Xensim_4	haplo39	10.26|10	8.26|11	1.24|0.91
Xensim (*Xenotilapia sima*)	Ectodini	F	LBE9	deep	haplo69	Xensim_4	haplo39	8.84|9	6.48|8	1.36|1.12
Xensin (*Xenotilapia singularis*)	Ectodini	M	IRD9	intermediate	haplo67	Xensin_2	haplo54	9.24|9	7.06|10	1.31|0.9
Xensin (*Xenotilapia singularis*)	Ectodini	F	IRE3	intermediate	haplo67	Xensin_2	haplo54	8.81|8	6.52|9	1.35|0.89
Xenspi (*Xenotilapia spilopterus*)	Ectodini	M	AXB5	intermediate	haplo72	Xenspi_2	haplo45	8.99|9	7.54|10	1.19|0.9
Xenspi (*Xenotilapia spilopterus*)	Ectodini	F	AXB8	intermediate	haplo72	Xenspi_2	haplo45	13.72|14	7.52|10	1.82|1.4
XenspN (*Xenotilapia* sp. "spilopterus north")	Ectodini	M	LEA3	intermediate	haplo70	XenspN_2_A	haplo45	7.42|7	6.5|9	1.14|0.78
XenspN (*Xenotilapia* sp. "spilopterus north")	Ectodini	F	LEA4	intermediate	haplo71	XenspN_2_B	haplo45	9.21|9	6.31|8	1.46|1.12
Xensun (*Xenotilapia* sp. "papilio sunflower")	Ectodini	M	GPF8	intermediate	haplo73	Xensun_2_A	haplo55	8.15|8	6.96|9	1.17|0.89
Xensun (*Xenotilapia* sp. "papilio sunflower")	Ectodini	F	GPF9	intermediate	haplo74	Xensun_2_B	haplo55	10.63|10	7.72|10	1.38|1
Erecya (*Eretmodus cyanostictus*)	Eretmodini	M	IZH7	shallow	haplo75	Erecya_2	haplo56	27.01|26	17.51|25	1.54|1.04
Erecya (*Eretmodus cyanostictus*)	Eretmodini	F	IZI3	shallow	haplo75	Erecya_2	haplo56	16.59|17	11.41|16	1.45|1.06
Eremar (*Eretmodus marksmithi*)	Eretmodini	M	JXE9	shallow	haplo76	Eremar_2	haplo57	12.1|11	9.51|13	1.27|0.85
Eremar (*Eretmodus marksmithi*)	Eretmodini	F	JXF4	shallow	haplo76	Eremar_2	haplo57	7.95|8	6.09|8	1.31|1
Spaery (*Spathodus erythrodon*)	Eretmodini	M	JUB6	shallow	haplo77	Spaery_2	haplo58	11.72|11	6.84|9	1.71|1.22
Spaery (*Spathodus erythrodon*)	Eretmodini	F	JUB7	shallow	haplo77	Spaery_2	haplo58	11.27|11	8.08|11	1.39|1
Spamar (*Spathodus marlieri*)	Eretmodini	M	JZB7	shallow	haplo77	Spamar_2	haplo58	6.9|7	5.93|8	1.16|0.88
Spamar (*Spathodus marlieri*)	Eretmodini	F	JZD3	shallow	haplo77	Spamar_2	haplo58	13.72|14	9.7|13	1.41|1.08
Tanirs (*Tanganicodus irsacae*)	Eretmodini	M	JYH3	shallow	haplo78	Tanirs_2	haplo57	16.42|15	9.21|12	1.78|1.25
Tanirs (*Tanganicodus irsacae*)	Eretmodini	F	JYH7	shallow	haplo78	Tanirs_2	haplo57	9.19|9	6.86|9	1.34|1
Gobeth (*Gobiocichla ethelwynnae*)*	Gobiocichlini	M	JWE7 (no genome draft assembly)	NA	haplo79	Gobeth_1	haplo59	15.98|16	12.8|17	1.25|0.94
Tilbre (*Tilapia brevimanus*)*	Gobiocichlini	F	JWF9	NA	haplo80	Tilbre_1	haplo60	23.09|22	14.6|18	1.58|1.22
Arcstr (*Astatoreochromis straeleni*)*	Haplochromini	M	KAE8	NA	haplo81	Arcstr_1	haplo61	7.59|8	6.88|9	1.1|0.89
Astbur (*Astatotilapia burtoni*)*	Haplochromini	M	IZA1	shallow	haplo82	Astbur_3_AB	haplo62	8.2|8	7.63|10	1.07|0.8
Astbur (*Astatotilapia burtoni*)*	Haplochromini	F	IZC5 (no genome draft assembly)	shallow	haplo82	Astbur_3_AB	haplo62	24.08|24	14.46|20	1.67|1.2
Astbur (*Astatotilapia burtoni*)*	Haplochromini	F	JYD5	shallow	haplo83	Astbur_3_C	haplo62	4.9|5	4.94|6	0.99|0.83
Astfla (*Astatotilapia flavijosephi*)*	Haplochromini	M	LJD2	NA	haplo84	Astfla_1	haplo63	9.06|9	5.32|7	1.7|1.29
Astpal (*Astatotilapia paludinosa*)*	Haplochromini	M	KYG1	NA	haplo85	Astpal_1	haplo62	7.86|8	5.86|7	1.34|1.14
Ctepol (*Ctenochromis polli*)*	Haplochromini	M	JWG2 (no genome draft assembly)	NA	haplo86	Ctepol_1	haplo64	18|19	13.2|18	1.36|1.06
Hplkil (*Haplochromis* sp. "kilossana")*	Haplochromini	M	LJE8 (no genome draft assembly)	NA	haplo87	Hplkil_1	haplo65	27.33|27	17.26|25	1.58|1.08
HplspC (*Haplochromis* sp. "chipwa")*	Haplochromini	M	HXC4	shallow	haplo82	HplspC_2	haplo62	7.8|7	6.08|8	1.28|0.88
HplspC (*Haplochromis* sp. "chipwa")*	Haplochromini	F	HXC5	shallow	haplo82	HplspC_2	haplo62	9.03|9	8.62|11	1.05|0.82
Hplsta (*Haplochromis stappersii*)*	Haplochromini	M	JYD3	shallow	haplo88	Hplsta_1	haplo66	16.75|15	11.08|15	1.51|1
Hplvan (*Haplochromis vanheusdeni*)*	Haplochromini	M	JWG3	NA	haplo87	Hplvan_1	haplo65	9.9|10	6.53|8	1.52|1.25
Ortcho (*Orthochromis indermauri*)*	Haplochromini	F	HXC6	NA	haplo89	Ortcho_2	haplo67	18.42|18	14.35|20	1.28|0.9
Ortcho (*Orthochromis indermauri*)*	Haplochromini	M	HXC7	NA	haplo89	Ortcho_2	haplo67	7.09|7	5.97|8	1.19|0.88
Ortmaz (*Orthochromis mazimeroensis*)*	Haplochromini	M	KDC6	NA	haplo90	Ortmaz_1	haplo68	7.79|8	6.34|8	1.23|1
Ortred (*Orthochromis malagaraziensis*)*	Haplochromini	M	KYE2	NA	haplo90	Ortred_1	haplo68	11.17|11	6.46|8	1.73|1.38

Ortuvi (*Orthochromis uvinzae*)*	Haplochromini	M	KYE7	NA	haplo91	Ortuvi_1	haplo68	7.95|8	6.36|8	1.25|1
Psephi (*Pseudocrenilabrus philander*)*	Haplochromini	M	JWG1 (no genome draft assembly)	NA	haplo92	Psephi_1	haplo69	21.39|21	15.01|21	1.43|1
Thobra (*Thoracochromis brauschi*)*	Haplochromini	M	JWF8	NA	haplo93	Thobra_1	haplo69	18.25|18	13.83|19	1.32|0.95
Hetbut (*Heterotilapia buettikoferi*)*	Heterotilapini		JWE3	NA	haplo94	Hetbut_1	haplo70	10.89|11	7.57|9	1.44|1.22
Altcal (*Altolamprologus calvus*)	Lamprologini	M	IOE2	intermediate	haplo95	Altcal_2_A	haplo71	10.03|10	7.55|10	1.33|1
Altcal (*Altolamprologus calvus*)	Lamprologini	F	IOE3	intermediate	haplo96	Altcal_2_B	haplo72	10.4|11	8.88|12	1.17|0.92
Altcom (*Altolamprologus compressiceps*)	Lamprologini	M	ISB1	intermediate	haplo97	Altcom_2	haplo71	9.61|10	7.88|11	1.22|0.91
Altcom (*Altolamprologus compressiceps*)	Lamprologini	F	ISC9	intermediate	haplo97	Altcom_2	haplo71	13.39|14	8.82|12	1.52|1.17
Altfas (*Neolamprologus fasciatus*)	Lamprologini	M	AUE7	shallow	haplo98	Altfas_2	haplo73	14.17|14	9.63|13	1.47|1.08
Altfas (*Neolamprologus fasciatus*)	Lamprologini	F	AXD5	shallow	haplo98	Altfas_2	haplo73	7.96|7	7.73|11	1.03|0.64
Altshe (*Altolamprologus* sp. "compressiceps shell")	Lamprologini	M	IRH2	NA	haplo95	Altshe_2	haplo71	6.49|7	5.51|7	1.18|1
Altshe (*Altolamprologus* sp. "compressiceps shell")	Lamprologini	F	IRH4	NA	haplo95	Altshe_2	haplo71	8.29|8	5.77|7	1.44|1.14
Chabif (*Chalinochromis* sp. "bifrenatus")	Lamprologini	F	LDD9	intermediate	haplo99	Chabif_2	haplo74	10.01|10	7.23|10	1.38|1
Chabif (*Chalinochromis* sp. "bifrenatus")	Lamprologini	M	LDE1	intermediate	haplo99	Chabif_2	haplo74	10.74|11	7.29|10	1.47|1.1
Chabri (*Chalinochromis brichardi*)	Lamprologini	F	AVA9	intermediate	haplo99	Chabri_2	haplo74	8.66|8	7.45|10	1.16|0.8
Chabri (*Chalinochromis brichardi*)	Lamprologini	M	AVB2	intermediate	haplo99	Chabri_2	haplo74	9.62|10	7.22|10	1.33|1
Chacya (*Chalinochromis cyanophleps*)	Lamprologini	M	LGG6	intermediate	haplo100	Chacya_2	haplo75	12.22|12	7.75|10	1.58|1.2
Chacya (*Chalinochromis cyanophleps*)	Lamprologini	F	LGG7	intermediate	haplo100	Chacya_2	haplo75	14.38|14	7.39|10	1.95|1.4
Chando (*Chalinochromis* sp. "ndobhoi")	Lamprologini	M	KEE9	intermediate	haplo99	Chando_2	haplo74	9.42|10	6.88|9	1.37|1.11
Chando (*Chalinochromis* sp. "ndobhoi")	Lamprologini	F	KEF1	intermediate	haplo99	Chando_2	haplo74	10.83|11	7.1|9	1.53|1.22
Chapop (*Chalinochromis popelini*)	Lamprologini	M	Bel07	intermediate	haplo99	Chapop_2	haplo74	12.16|10	7.38|10	1.65|1
Chapop (*Chalinochromis popelini*)	Lamprologini	F	Bel09	intermediate	haplo99	Chapop_2	haplo74	8.95|8	6.65|9	1.35|0.89
Juldic (*Julidochromis dickfeldi*)	Lamprologini	M	IRC4	intermediate	haplo99	Juldic_2	haplo74	14.53|14	9.53|13	1.52|1.08
Juldic (*Julidochromis dickfeldi*)	Lamprologini	F	IRC5	intermediate	haplo99	Juldic_2	haplo74	12.41|12	7.01|9	1.77|1.33
Julkom (*Julidochromis* sp. "kombe")	Lamprologini	M	ILD9	intermediate	haplo99	Julkom_2	haplo74	9.1|9	6.9|9	1.32|1
Julkom (*Julidochromis* sp. "kombe")	Lamprologini	F	INA6	intermediate	haplo99	Julkom_2	haplo74	7.16|7	6.38|8	1.12|0.88
JulmaN (*Julidochromis marlieri*)	Lamprologini	M	JXB5	intermediate	haplo101	JulmaN_2_A	haplo74	16.96|16	8.77|12	1.93|1.33
JulmaN (*Julidochromis marlieri*)	Lamprologini	F	JXC1	intermediate	haplo99	JulmaN_2_B	haplo74	12.8|12	8.48|11	1.51|1.09
JulmaS (*Julidochromis* sp. "marlieri south")	Lamprologini	F	LBA1	intermediate	haplo101	JulmaS_2_A	haplo74	8.75|8	7.89|11	1.11|0.73
JulmaS (*Julidochromis* sp. "marlieri south")	Lamprologini	M	LBF3	intermediate	haplo99	JulmaS_2_B	haplo74	11.47|12	8.35|11	1.37|1.09
Julmrk (*Julidochromis marksmithi*)	Lamprologini	M	LFG8	intermediate	haplo101	Julmrk_2_A	haplo74	7.13|7	6.53|9	1.09|0.78
Julmrk (*Julidochromis marksmithi*)	Lamprologini	F	LFH1	intermediate	haplo102	Julmrk_2_B	haplo74	10.27|10	8.31|11	1.24|0.91
Julorn (*Julidochromis ornatus*)	Lamprologini	M	ISB7	intermediate	haplo103	Julorn_2	haplo74	9.09|9	6.34|8	1.43|1.12
Julorn (*Julidochromis ornatus*)	Lamprologini	F	ISC1	intermediate	haplo103	Julorn_2	haplo74	11.81|12	8.15|11	1.45|1.09
Julreg (*Julidochromis* sp. "regani south")	Lamprologini	F	IRB2	intermediate	haplo102	Julreg_2	haplo74	11.61|12	6.4|8	1.81|1.5
Julreg (*Julidochromis* sp. "regani south")	Lamprologini	M	IRB8	intermediate	haplo102	Julreg_2	haplo74	8.64|8	7.36|10	1.17|0.8
JulreK (*Julidochromis regani*)	Lamprologini	F	KFF4	intermediate	haplo104	JulreK_2	haplo76	9.41|9	7.2|10	1.31|0.9
JulreK (*Julidochromis regani*)	Lamprologini	M	KHE6	intermediate	haplo104	JulreK_2	haplo76	7.11|7	6.76|9	1.05|0.78
Jultra (*Julidochromis transcriptus*)	Lamprologini	M	HFG1287	NA	haplo99	Jultra_2	haplo74	14.12|14	10.48|14	1.35|1
Jultra (*Julidochromis transcriptus*)	Lamprologini	F	LJC2	NA	haplo99	Jultra_2	haplo74	13.84|14	9.46|13	1.46|1.08
Julunt (*Julidochromis* sp. "unterfels")	Lamprologini	M	JWA1	NA	haplo105	Julunt_2_A	haplo74	20.71|21	13.56|19	1.53|1.11
Julunt (*Julidochromis* sp. "unterfels")	Lamprologini	F	JWA2	NA	haplo106	Julunt_2_B	haplo74	20.4|21	15.12|22	1.35|0.95
Lamcal (*Lamprologus callipterus*)	Lamprologini	M	IPH2	intermediate	haplo107	Lamcal_2	haplo77	16.17|17	9.64|13	1.68|1.31
Lamcal (*Lamprologus callipterus*)	Lamprologini	F	JAB1	intermediate	haplo107	Lamcal_2	haplo77	9.2|9	7.48|10	1.23|0.9
Lamkun (*Lamprologus kungweensis*)	Lamprologini	M	JXG8	intermediate	haplo99	Lamkun_2	haplo74	14.97|15	12.18|17	1.23|0.88

Lamkun (*Lamprologus kungweensis*)	Lamprologini	F	JXH2	intermediate	haplo99	Lamkun_2	haplo74	19.56|19	12.23|17	1.6|1.12
Lamlem (*Lamprologus lemairii*)	Lamprologini	F	IPD6	intermediate	haplo108	Lamlem_2	haplo74	7.18|7	6.18|8	1.16|0.88
Lamlem (*Lamprologus lemairii*)	Lamprologini	M	IZI7	intermediate	haplo108	Lamlem_2	haplo74	9.78|10	7.55|10	1.3|1
Lammel (*Lamprologus meleagris*)	Lamprologini	M	JWA8	NA	NA	NA	NA	5.37|5	5.44|7	0.99|0.71
Lammel (*Lamprologus meleagris*)	Lamprologini	F	JWA9	NA	haplo109	Lammel_1	haplo78	9.45|9	10.36|14	0.91|0.64
Lamoce (*Lamprologus ocellatus*)	Lamprologini	M	ILC1	intermediate	haplo110	Lamoce_2_A	haplo79	8.17|8	6.6|9	1.24|0.89
Lamoce (*Lamprologus ocellatus*)	Lamprologini	F	ILD3	intermediate	haplo111	Lamoce_2_B	haplo80	11.2|11	7.66|10	1.46|1.1
LamorC (*Lamprologus* sp. "ornatipinnis congo")	Lamprologini	M	JWA3	intermediate	haplo112	LamorC_2	haplo81	9.97|10	6.5|9	1.53|1.11
LamorC (*Lamprologus* sp. "ornatipinnis congo")	Lamprologini	F	JWA4	intermediate	haplo112	LamorC_2	haplo81	6.91|7	6.3|8	1.1|0.88
Lamorn (*Lamprologus ornatipinnis*)	Lamprologini	M	JZF3	intermediate	haplo114	Lamorn_2_A	haplo83	20.09|21	13.7|19	1.47|1.11
Lamorn (*Lamprologus ornatipinnis*)	Lamprologini	F	JZF4	intermediate	haplo115	Lamorn_2_B	haplo82	17.31|18	11.29|16	1.53|1.12
LamorS (*Lamprologus* sp. "ornatipinnis zambia")	Lamprologini	M	JDF5	intermediate	haplo113	LamorS_2	haplo82	12.5|13	7.69|10	1.63|1.3
LamorS (*Lamprologus* sp. "ornatipinnis zambia")	Lamprologini	F	JDG4	intermediate	haplo113	LamorS_2	haplo82	8.25|8	6.17|8	1.34|1
Lamsig (*Lamprologus signatus*)	Lamprologini	M	IWD5	intermediate	haplo116	Lamsig_2	haplo84	9.68|9	7.8|11	1.24|0.82
Lamsig (*Lamprologus signatus*)	Lamprologini	F	IWD6	intermediate	haplo116	Lamsig_2	haplo84	14.02|14	8.94|12	1.57|1.17
Lamspe (*Lamprologus speciosus*)	Lamprologini	M	KCG2	NA	haplo117	Lamspe_2_A	haplo85	10.6|11	9.24|13	1.15|0.85
Lamspe (*Lamprologus speciosus*)	Lamprologini	F	KCG3	NA	haplo118	Lamspe_2_B	haplo86	15.97|15	12.69|18	1.26|0.83
Lamtig (*Lamprologus tigripictilis*)	Lamprologini	F	JWF6	NA	haplo119	Lamtig_1	haplo87	21.11|20	13.31|19	1.59|1.05
Lepatt (*Lepidiolamprologus attenuatus*)	Lamprologini	M	AVD4	intermediate	haplo99	Lepatt_2	haplo74	9.03|9	7.05|9	1.28|1
Lepatt (*Lepidiolamprologus attenuatus*)	Lamprologini	F	AVG5	intermediate	haplo99	Lepatt_2	haplo74	9.76|10	7.72|10	1.26|1
Lepcun (*Lepidiolamprologus cunningtoni*)	Lamprologini	F	IOH4	intermediate	haplo120	Lepcun_2	haplo88	9.14|9	7.8|10	1.17|0.9
Lepcun (*Lepidiolamprologus cunningtoni*)	Lamprologini	M	IOH5	intermediate	haplo120	Lepcun_2	haplo88	20.36|20	12.52|17	1.63|1.18
Lepelo (*Lepidiolamprologus elongatus*)	Lamprologini	M	AUE6	intermediate	haplo99	Lepelo_2	haplo74	10.7|10	6.92|9	1.55|1.11
Lepelo (*Lepidiolamprologus elongatus*)	Lamprologini	F	AUG8	intermediate	haplo99	Lepelo_2	haplo74	11.01|11	7.24|10	1.52|1.1
Lepkam (*Lepidiolamprologus kamambae*)	Lamprologini	M	LFF7	NA	haplo121	Lepkam_2	haplo89	9.37|9	5.65|7	1.66|1.29
Lepkam (*Lepidiolamprologus kamambae*)	Lamprologini	F	LFF8	NA	haplo121	Lepkam_2	haplo89	11.93|12	7.9|11	1.51|1.09
Lepken (*Lepidiolamprologus kendalli*)	Lamprologini	M	IMD1	intermediate	haplo121	Lepken_2_A	haplo89	19.49|20	12.71|18	1.53|1.11
Lepken (*Lepidiolamprologus kendalli*)	Lamprologini	F	IMD2	intermediate	haplo122	Lepken_2_B	haplo90	11.03|11	7.36|10	1.5|1.1
LepmeK (*Lepidiolamprologus* sp. "meeli kipili")	Lamprologini	F	LHA2	intermediate	haplo99	LepmeK_2_B	haplo74	9.04|9	7.11|9	1.27|1
LepmeK (*Lepidiolamprologus* sp. "meeli kipili")	Lamprologini	M	LHA5	intermediate	haplo123	LepmeK_2_A	haplo74	12.9|13	7.56|10	1.71|1.3
Lepmim (*Lepidiolamprologus mimicus*)	Lamprologini	M	LDD1	intermediate	haplo121	Lepmim_2_A	haplo89	9.26|9	7.26|10	1.28|0.9
Lepmim (*Lepidiolamprologus mimicus*)	Lamprologini	F	LDD6	intermediate	haplo124	Lepmim_2_B	haplo91	13.16|13	7.24|10	1.82|1.3
Leppro (*Lepidiolamprologus profundicola*)	Lamprologini	M	KAD2	intermediate	haplo125	Leppro_2	haplo74	10.71|10	8.17|11	1.31|0.91
Leppro (*Lepidiolamprologus profundicola*)	Lamprologini	F	KEB8	intermediate	haplo125	Leppro_2	haplo74	12.76|12	8.21|11	1.55|1.09
Neobif (*Neolamprologus bifasciatus*)	Lamprologini	M	LHF6	deep	haplo100	Neobif_2_A	haplo75	5.77|5	6.93|9	0.83|0.56
Neobif (*Neolamprologus bifasciatus*)	Lamprologini	F	LHF7	deep	haplo126	Neobif_2_B	haplo92	10.99|11	6.9|9	1.59|1.22
Neobou (*Neolamprologus boulengeri*)	Lamprologini	F	KCE5	intermediate	haplo114	Neobou_2	haplo83	9.56|9	6.61|9	1.45|1
Neobou (*Neolamprologus boulengeri*)	Lamprologini	M	KYB9	intermediate	haplo114	Neobou_2	haplo83	12.54|12	7.33|10	1.71|1.2
Neobre (*Neolamprologus brevis*)	Lamprologini	M	ILB6	intermediate	haplo128	Neobre_2	haplo84	8.35|8	6.21|8	1.34|1
Neobre (*Neolamprologus brevis*)	Lamprologini	F	ILB7	intermediate	haplo128	Neobre_2	haplo84	7.24|7	6.48|8	1.12|0.88
Neobri (*Neolamprologus brichardi*)	Lamprologini	F	JUH9	intermediate	haplo99	Neobri_2	haplo74	12.08|12	8.02|11	1.51|1.09
Neobri (*Neolamprologus brichardi*)	Lamprologini	M	JUI1	intermediate	haplo99	Neobri_2	haplo74	7.46|8	5.93|8	1.26|1
NeobrM (*Neolamprologus* sp. "brevis magara")	Lamprologini	M	KCI6	intermediate	haplo127	NeobrM_2_A	haplo84	16.25|16	12.96|18	1.25|0.89
NeobrM (*Neolamprologus* sp. "brevis magara")	Lamprologini	F	KCI7	intermediate	haplo128	NeobrM_2_B	haplo84	10.82|10	7.05|9	1.53|1.11
Neobue (*Neolamprologus buescheri*)	Lamprologini	M	JEI4	deep	haplo100	Neobue_2	haplo75	5.25|5	6.88|9	0.76|0.56
Neobue (*Neolamprologus buescheri*)	Lamprologini	F	JEI5	deep	haplo100	Neobue_2	haplo75	9.28|9	7|9	1.33|1

NeocaK (*Neolamprologus* sp. "caudopunctatus kipili")	Lamprologini	M	LDG2	intermediate	haplo129	NeocaK_2	haplo93	10.54|10	6.81|9	1.55|1.11
NeocaK (*Neolamprologus* sp. "caudopunctatus kipili")	Lamprologini	F	LDG3	intermediate	haplo129	NeocaK_2	haplo93	9.81|9	7.69|10	1.28|0.9
Neocal (*Neolamprologus calliurus*)	Lamprologini	M	ILA7	intermediate	haplo130	Neocal_2_A	haplo84	10.88|10	9.27|13	1.17|0.77
Neocal (*Neolamprologus calliurus*)	Lamprologini	F	INC7	intermediate	haplo131	Neocal_2_B	haplo94	7.57|7	7.81|10	0.97|0.7
Neocau (*Neolamprologus caudopunctatus*)	Lamprologini	M	IQA3	shallow	haplo95	Neocau_2_B	haplo71	18.78|19	13.82|20	1.36|0.95
Neocau (*Neolamprologus caudopunctatus*)	Lamprologini	F	IQA4	shallow	haplo132	Neocau_2_A	haplo95	11.76|11	7.31|10	1.61|1.1
Neochi (*Neolamprologus chitamwebwai*)	Lamprologini	M	KHA7	intermediate	haplo133	Neochi_2	haplo76	10.05|10	6.74|9	1.49|1.11
Neochi (*Neolamprologus chitamwebwai*)	Lamprologini	F	KHA9	intermediate	haplo133	Neochi_2	haplo76	8.67|8	5.71|7	1.52|1.14
Neochr (*Neolamprologus christyi*)	Lamprologini	F	ITG2	intermediate	haplo134	Neochr_1	haplo88	10.67|11	7.98|11	1.34|1
Neochr (*Neolamprologus christyi*)	Lamprologini	M	IZI8	intermediate	NA	NA	NA	6.05|6	6.42|8	0.94|0.75
Neocra (*Neolamprologus crassus*)	Lamprologini	M	IVE8	intermediate	haplo102	Neocra_2	haplo74	13|13	8.44|11	1.54|1.18
Neocra (*Neolamprologus crassus*)	Lamprologini	F	IVF1	intermediate	haplo102	Neocra_2	haplo74	10.15|10	8.39|11	1.21|0.91
Neocyg (*Neolamprologus* sp. "cygnus")	Lamprologini	M	LFD2	intermediate	haplo100	Neocyg_2	haplo75	12.31|13	7.89|10	1.56|1.3
Neocyg (*Neolamprologus* sp. "cygnus")	Lamprologini	F	LFD4	intermediate	haplo100	Neocyg_2	haplo75	12.57|13	7.7|10	1.63|1.3
Neocyl (*Neolamprologus cylindricus*)	Lamprologini	M	GPH1	intermediate	haplo135	Neocyl_2	haplo96	18.27|18	12.85|18	1.42|1
Neocyl (*Neolamprologus cylindricus*)	Lamprologini	F	GPH2	intermediate	haplo135	Neocyl_2	haplo96	11.75|12	9.15|12	1.28|1
Neodev (*Neolamprologus devosi*)*	Lamprologini	M	LEH2	NA	haplo136	Neodev_1	haplo97	16.1|17	9.38|13	1.72|1.31
Neoese (*Neolamprologus* sp. "eseki")	Lamprologini	M	LFB7	intermediate	haplo137	Neoese_2_A	haplo98	11.76|12	5.88|8	2|1.5
Neoese (*Neolamprologus* sp. "eseki")	Lamprologini	F	LFB9	intermediate	haplo138	Neoese_2_B	haplo99	10.8|10	7.87|11	1.37|0.91
Neofal (*Neolamprologus falcicula*)	Lamprologini	M	JXD4	intermediate	haplo133	Neofal_2	haplo76	13.69|13	8.68|12	1.58|1.08
Neofal (*Neolamprologus falcicula*)	Lamprologini	F	JXD7	intermediate	haplo133	Neofal_2	haplo76	15.98|16	10.56|14	1.51|1.14
NeofaM (*Neolamprologus* sp. "falcicula mahale")	Lamprologini	F	LCB5	intermediate	haplo102	NeofaM_2	haplo74	6.98|7	6|8	1.16|0.88
NeofaM (*Neolamprologus* sp. "falcicula mahale")	Lamprologini	M	LCC2	intermediate	haplo102	NeofaM_2	haplo74	9.75|9	5.88|8	1.66|1.12
Neofur (*Neolamprologus furcifer*)	Lamprologini	M	JEI6	intermediate	haplo99	Neofur_2	haplo74	10.79|11	9.72|13	1.11|0.85
Neofur (*Neolamprologus furcifer*)	Lamprologini	F	JEI8	intermediate	haplo99	Neofur_2	haplo74	21.36|21	12.25|17	1.74|1.24
NeofuU (*Neolamprologus* sp. "furcifer ulwile")	Lamprologini	F	LDF4	intermediate	haplo99	NeofuU_2	haplo74	9.06|9	7.31|10	1.24|0.9
NeofuU (*Neolamprologus* sp. "furcifer ulwile")	Lamprologini	M	LDF5	intermediate	haplo99	NeofuU_2	haplo74	11.83|12	7.39|10	1.6|1.2
Neogra (*Neolamprologus gracilis*)	Lamprologini	F	JWH1	intermediate	haplo102	Neogra_2	haplo74	12.95|12	10.85|15	1.19|0.8
Neogra (*Neolamprologus gracilis*)	Lamprologini	M	JWH2	intermediate	haplo102	Neogra_2	haplo74	19.1|20	12.3|17	1.55|1.18
NeogrM (*Neolamprologus* sp. "gracilis tanzania")	Lamprologini	M	LCB4	intermediate	haplo99	NeogrM_2_B	haplo74	8.16|8	6.4|8	1.27|1
NeogrM (*Neolamprologus* sp. "gracilis tanzania")	Lamprologini	F	LCC6	intermediate	haplo139	NeogrM_2_A	haplo74	11.09|11	6.58|9	1.69|1.22
Neohec (*Neolamprologus hecqui*)	Lamprologini	M	A142	intermediate	haplo140	Neohec_3_A	haplo100	17.02|16	10.86|15	1.57|1.07
Neohec (*Neolamprologus hecqui*)	Lamprologini		Bel13	intermediate	haplo141	Neohec_3_BC	haplo100	6.75|7	6.18|8	1.09|0.88
Neohec (*Neolamprologus hecqui*)	Lamprologini		Bel14	intermediate	haplo141	Neohec_3_BC	haplo100	9.02|9	6.56|9	1.38|1
Neohel (*Neolamprologus helianthus*)	Lamprologini	F	JWG8	intermediate	haplo99	Neohel_2	haplo74	8.96|9	5.3|7	1.69|1.29
Neohel (*Neolamprologus helianthus*)	Lamprologini	M	JWG9	intermediate	haplo99	Neohel_2	haplo74	13.45|13	10.1|14	1.33|0.93
Neokom (*Neolamprologus* sp. "kombe")	Lamprologini	M	ILE5	shallow	haplo99	Neokom_2	haplo74	6.41|6	5.53|7	1.16|0.86
Neokom (*Neolamprologus* sp. "kombe")	Lamprologini	F	ILE6	shallow	haplo99	Neokom_2	haplo74	10.19|10	7.77|10	1.31|1
Neolap (*Lamprologus laparogramma*)	Lamprologini	F	JDI1	intermediate	haplo116	Neolap_2	haplo84	9.09|8	7.38|10	1.23|0.8
Neolap (*Lamprologus laparogramma*)	Lamprologini	M	JDI2	intermediate	haplo116	Neolap_2	haplo84	13.43|13	9.06|12	1.48|1.08
NeoleL (*Neolamprologus leleupi*)	Lamprologini		JWH9	intermediate	haplo142	NeoleL_1	haplo74	13.26|13	10.12|14	1.31|0.93
Neoleu (*Neolamprologus longior*)	Lamprologini	M	KEH3	intermediate	haplo143	Neoleu_2	haplo75	17.34|17	11.97|17	1.45|1
Neoleu (*Neolamprologus longior*)	Lamprologini	F	LEE1	intermediate	haplo143	Neoleu_2	haplo75	8.27|8	6.7|9	1.23|0.89
Neolon (*Neolamprologus longicaudatus*)	Lamprologini	M	JWI2	intermediate	haplo100	Neolon_2	haplo75	12.61|12	7.77|10	1.62|1.2
Neolon (*Neolamprologus longicaudatus*)	Lamprologini	F	JWI3	intermediate	haplo100	Neolon_2	haplo75	13.28|13	10.14|14	1.31|0.93

Neolou (*Neolamprologus leloupi*)	Lamprologini	M	LCA1	intermediate	haplo144	Neolou_2	haplo101	12.08|12	7.02|9	1.72|1.33
Neolou (*Neolamprologus leloupi*)	Lamprologini	F	LCA2	intermediate	haplo144	Neolou_2	haplo101	11.47|11	7.8|11	1.47|1
Neomar (*Neolamprologus marunguensis*)	Lamprologini	M	JWH3	NA	haplo102	Neomar_2	haplo74	15.94|16	10.37|14	1.54|1.14
Neomar (*Neolamprologus marunguensis*)	Lamprologini	F	JWH4	NA	haplo102	Neomar_2	haplo74	15.76|16	10.71|15	1.47|1.07
Neomee (*Neolamprologus meeli*)	Lamprologini	M	JDF3	intermediate	haplo99	Neomee_2	haplo74	9.99|10	6.46|8	1.55|1.25
Neomee (*Neolamprologus meeli*)	Lamprologini	F	JDF4	intermediate	haplo99	Neomee_2	haplo74	16.66|16	12.99|18	1.28|0.89
Neomod (*Neolamprologus modestus*)	Lamprologini	M	IMG9	shallow	haplo137	Neomod_2	haplo98	12.38|12	7.99|11	1.55|1.09
Neomod (*Neolamprologus modestus*)	Lamprologini	F	IMH3	shallow	haplo137	Neomod_2	haplo98	12.89|13	9.33|13	1.38|1
Neomon (*Neolamprologus mondabu*)	Lamprologini	M	JVB4	shallow	haplo137	Neomon_2	haplo98	11.01|11	10.27|14	1.07|0.79
Neomon (*Neolamprologus mondabu*)	Lamprologini	F	JVB8	shallow	haplo137	Neomon_2	haplo98	9.73|10	8.67|12	1.12|0.83
Neomul (*Neolamprologus multifasciatus*)	Lamprologini	M	IRF6 (no genome draft assembly)	intermediate	haplo145	Neomul_2_A	haplo102	10.26|9	6.6|9	1.55|1
Neomul (*Neolamprologus multifasciatus*)	Lamprologini	F	IRF8	intermediate	haplo146	Neomul_2_B	haplo103	8.01|8	5.95|8	1.35|1
Neomux (*Neolamprologus mustax*)	Lamprologini	F	ILB4	intermediate	haplo147	Neomux_2	haplo74	11.3|11	8.11|11	1.39|1
Neomux (*Neolamprologus mustax*)	Lamprologini	M	ILH1	intermediate	haplo147	Neomux_2	haplo74	9.43|9	6.16|8	1.53|1.12
Neonig (*Neolamprologus niger*)	Lamprologini	M	KYA1	deep	haplo135	Neonig_2	haplo96	8.79|9	6.09|8	1.44|1.12
Neonig (*Neolamprologus niger*)	Lamprologini	F	KYA5	deep	haplo135	Neonig_2	haplo96	9.1|9	6.47|8	1.41|1.12
Neonve (*Neolamprologus nigriventris*)	Lamprologini	F	A108	deep	haplo100	Neonve_2_A	haplo75	12.87|13	9.24|12	1.39|1.08
Neonve (*Neolamprologus nigriventris*)	Lamprologini	M	LJC3	deep	haplo148	Neonve_2_B	haplo75	15.23|14	10.29|14	1.48|1
Neoobs (*Neolamprologus obscurus*)	Lamprologini	F	IMA1	intermediate	haplo135	Neoobs_2	haplo96	10.83|11	7.05|9	1.54|1.22
Neoobs (*Neolamprologus obscurus*)	Lamprologini	M	IMA2	intermediate	haplo135	Neoobs_2	haplo96	9.26|9	6.26|8	1.48|1.12
Neooli (*Neolamprologus olivaceous*)	Lamprologini	F	JWH5	NA	haplo149	Neooli_2	haplo74	17.33|17	10.27|14	1.69|1.21
Neooli (*Neolamprologus olivaceous*)	Lamprologini	M	JWH6	NA	haplo149	Neooli_2	haplo74	10.55|11	11.04|15	0.96|0.73
Neopec (*Neolamprologus pectoralis*)	Lamprologini	M	JWA7	deep	haplo100	Neopec_2	haplo75	14.72|14	10.65|15	1.38|0.93
Neopec (*Neolamprologus pectoralis*)	Lamprologini	F	JWI6	deep	haplo100	Neopec_2	haplo75	13.43|14	10.62|14	1.26|1
Neopet (*Neolamprologus petricola*)	Lamprologini	M	LGH8	shallow	haplo150	Neopet_2_B	haplo104	12.22|12	7.4|10	1.65|1.2
Neopet (*Neolamprologus petricola*)	Lamprologini	F	LGI1	shallow	haplo137	Neopet_2_A	haplo98	10.83|11	7.68|10	1.41|1.1
Neople (*Neolamprologus pleuromaculatus*)	Lamprologini	M	JZF1	NA	haplo114	Neople_2	haplo83	12.4|12	7.75|10	1.6|1.2
Neople (*Neolamprologus pleuromaculatus*)	Lamprologini	F	JZF2	NA	haplo114	Neople_2	haplo83	20.46|21	13.53|19	1.51|1.11
Neopro (*Neolamprologus prochilus*)	Lamprologini	M	IVH1	intermediate	haplo151	Neopro_2	haplo74	8.57|8	7.57|10	1.13|0.8
Neopro (*Neolamprologus prochilus*)	Lamprologini	F	IVH2	intermediate	haplo151	Neopro_2	haplo74	9.72|9	7.08|9	1.37|1
Neopul (*Neolamprologus pulcher*)	Lamprologini	M	ISA6	intermediate	haplo99	Neopul_2	haplo774	8.15|8	6.57|9	1.24|0.89
Neopul (*Neolamprologus pulcher*)	Lamprologini	F	ISB3	intermediate	haplo99	Neopul_2	haplo74	11.3|11	7.44|10	1.52|1.1
Neosav (*Neolamprologus savoryi*)	Lamprologini	M	ISA8	intermediate	haplo99	Neosav_2_B	haplo74	11.88|12	8.35|11	1.42|1.09
Neosav (*Neolamprologus savoryi*)	Lamprologini	F	IYA4	intermediate	haplo152	Neosav_2_A	haplo74	8.93|8	6.36|8	1.4|1
Neosex (*Neolamprologus sexfasciatus*)	Lamprologini	M	IND7	intermediate	haplo153	Neosex_2	haplo105	8.33|8	7.7|10	1.08|0.8
Neosex (*Neolamprologus sexfasciatus*)	Lamprologini	F	IND8	intermediate	haplo153	Neosex_2	haplo105	9.38|8	7.26|10	1.29|0.8
Neosim (*Neolamprologus similis*)	Lamprologini	M	KEC1	intermediate	haplo154	Neosim_2_A	haplo106	12.46|12	8.22|11	1.52|1.09
Neosim (*Neolamprologus similis*)	Lamprologini	F	KEC2	intermediate	haplo155	Neosim_2_B	haplo106	12.8|12	7.27|10	1.76|1.2
Neospl (*Neolamprologus splendens*)	Lamprologini	M	A188 (no genome draft assembly)	NA	haplo99	Neospl_2	haplo74	16.46|16	6.63|7	2.48|2.29
Neospl (*Neolamprologus splendens*)	Lamprologini	M	LJD3 (no genome draft assembly)	NA	haplo99	Neospl_2	haplo74	22.51|22	8.07|9	2.79|2.44
Neotet (*Neolamprologus tetracanthus*)	Lamprologini	M	IPF7	shallow	haplo156	Neotet_2_A	haplo105	7.98|8	6.65|9	1.2|0.89
Neotet (*Neolamprologus tetracanthus*)	Lamprologini	F	IPG3	shallow	haplo157	Neotet_2_B	haplo105	13.64|14	9.95|14	1.37|1
Neotim (*Neolamprologus timidus*)	Lamprologini	M	LGE2	NA	haplo135	Neotim_2	haplo96	8.6|8	7.36|10	1.17|0.8
Neotim (*Neolamprologus timidus*)	Lamprologini	F	LGE3	NA	haplo135	Neotim_2	haplo96	7.78|8	6.05|8	1.29|1

Neotoa (*Neolamprologus toae*)	Lamprologini	M	JZD5	intermediate	haplo158	Neotoa_2	haplo107	13.36|14	8.15|11	1.64|1.27
Neotoa (*Neolamprologus toae*)	Lamprologini	F	JZD6	intermediate	haplo158	Neotoa_2	haplo107	10.01|10	8.9|12	1.12|0.83
Neotre (*Neolamprologus tretocephalus*)	Lamprologini	M	KFH4	intermediate	haplo153	Neotre_2	haplo105	12.09|12	7.35|10	1.64|1.2
Neotre (*Neolamprologus tretocephalus*)	Lamprologini	F	KFH5	intermediate	haplo153	Neotre_2	haplo105	11.66|12	7.34|10	1.59|1.2
Neovar (*Neolamprologus variostigma*)	Lamprologini	M	JWA5	deep	haplo159	Neovar_2	haplo108	19.57|19	13.78|19	1.42|1
Neovar (*Neolamprologus variostigma*)	Lamprologini	F	JWA6	deep	haplo159	Neovar_2	haplo108	20.86|20	15.23|22	1.37|0.91
NeoveB (*Neolamprologus ventralis* (Burundi))	Lamprologini	M	KAG7	deep	haplo112	NeoveB_2	haplo81	19.82|19	13.73|19	1.44|1
NeoveB (*Neolamprologus ventralis* (Burundi))	Lamprologini	F	KAG8	deep	haplo112	NeoveB_2	haplo81	23.74|23	14.75|21	1.61|1.1
NeoveS (*Neolamprologus* sp. "ventralis stripe")	Lamprologini	M	JED4	deep	haplo160	NeoveS_2_B	haplo109	10.34|10	7.71|10	1.34|1
NeoveS (*Neolamprologus* sp. "ventralis stripe")	Lamprologini	F	JED5	deep	haplo112	NeoveS_2_A	haplo81	20.67|21	13.26|18	1.56|1.17
Neowal (*Neolamprologus walteri*)	Lamprologini	F	KFD2	intermediate	haplo133	Neowal_2_A	haplo76	6.84|7	7.12|9	0.96|0.78
Neowal (*Neolamprologus walteri*)	Lamprologini	M	KFD4	intermediate	haplo161	Neowal_2_B	haplo76	7.9|8	6.99|9	1.13|0.89
Telbif (*Telmatochromis bifrenatus*)	Lamprologini	M	KYB7	intermediate	haplo162	Telbif_2	haplo110	8.99|9	6.86|9	1.31|1
Telbif (*Telmatochromis bifrenatus*)	Lamprologini	F	KYB8	intermediate	haplo162	Telbif_2	haplo110	9.88|10	7.04|9	1.4|1.11
Telbra (*Telmatochromis brachygnathus*)	Lamprologini	M	JBE8	shallow	haplo163	Telbra_2_A	haplo111	9.83|9	6.45|8	1.52|1.12
Telbra (*Telmatochromis brachygnathus*)	Lamprologini	F	JBE9	shallow	haplo164	Telbra_2_B	haplo111	7.29|7	6.75|9	1.08|0.78
Telbri (*Telmatochromis brichardi*)	Lamprologini	M	JVI9	intermediate	haplo162	Telbri_2	haplo110	14.42|15	7.92|11	1.82|1.36
Telbri (*Telmatochromis brichardi*)	Lamprologini	F	JXA4	intermediate	haplo162	Telbri_2	haplo110	8.4|8	7.77|10	1.08|0.8
TeldhN (*Telmatochromis* sp. "dhonti north")	Lamprologini	M	JUD4	shallow	haplo165	TeldhN_2_A	haplo98	7.68|8	5.9|8	1.3|1
TeldhN (*Telmatochromis* sp. "dhonti north")	Lamprologini	F	JUD5	shallow	haplo166	TeldhN_2_B	haplo98	17|17	11.58|16	1.47|1.06
TeldhS (*Telmatochromis dhonti*)	Lamprologini	F	LBF7	shallow	haplo167	TeldhS_2_A	haplo98	11.28|11	6.63|9	1.7|1.22
TeldhS (*Telmatochromis dhonti*)	Lamprologini	M	LBF8	shallow	haplo168	TeldhS_2_B	haplo98	10.54|10	6.3|8	1.67|1.25
TeldhT (*Telmatochromis* sp. "dhonti twiyu")	Lamprologini	M	LHC1	shallow	haplo169	TeldhT_2_A	haplo98	20.7|20	12.37|17	1.67|1.18
TeldhT (*Telmatochromis* sp. "dhonti twiyu")	Lamprologini	F	LHF2	shallow	haplo170	TeldhT_2_B	haplo98	17.21|17	11.15|15	1.54|1.13
Tellon (*Telmatochromis* sp. "longola")	Lamprologini	M	JWC8	NA	haplo171	Tellon_2	haplo112	10.72|10	6.74|9	1.59|1.11
Tellon (*Telmatochromis* sp. "longola")	Lamprologini	F	JWC9	NA	haplo171	Tellon_2	haplo112	19.21|20	11.94|17	1.61|1.18
Telluf (*Telmatochromis* sp. "lufubu")*	Lamprologini	M	HXC8	NA	haplo172	Telluf_1	haplo113	10.27|10	7.75|10	1.33|1
Telshe (*Telmatochromis* sp. "shell")	Lamprologini	M	IRI8	intermediate	haplo173	Telshe_2_A	haplo111	11.83|11	8.07|11	1.47|1
Telshe (*Telmatochromis* sp. "shell")	Lamprologini	F	IRI9	intermediate	haplo174	Telshe_2_B	haplo111	10.59|11	6.61|9	1.6|1.22
TelteS (*Telmatochromis temporalis*)	Lamprologini	M	IMB3	intermediate	haplo175	TelteS_2_B	haplo112	8.43|8	5.64|7	1.49|1.14
TelteS (*Telmatochromis temporalis*)	Lamprologini	F	IMB4	intermediate	haplo170	TelteS_2_A	haplo98	10.42|10	8.08|11	1.29|0.91
Telvit (*Telmatochromis vittatus*)	Lamprologini	M	JBD5	intermediate	haplo176	Telvit_2_A	haplo114	9.53|10	6.85|9	1.39|1.11
Telvit (*Telmatochromis vittatus*)	Lamprologini	F	JBD6	intermediate	haplo177	Telvit_2_B	haplo115	9.7|10	7.29|10	1.33|1
Varmoo (*Variabilichromis moorii*)	Lamprologini	F	AUC3	shallow	haplo178	Varmoo_2	haplo107	10.04|10	9.06|12	1.11|0.83
Varmoo (*Variabilichromis moorii*)	Lamprologini	M	AUC4	shallow	haplo178	Varmoo_2	haplo197	10.27|10	7.34|10	1.4|1
Baicen (*Baileychromis centropomoides*)	Limnochromini	M	JAB7	deep	haplo179	Baicen_2_A	haplo116	8.04|9	6.68|8	1.2|1.12
Baicen (*Baileychromis centropomoides*)	Limnochromini	F	JAE9	deep	haplo180	Baicen_2_B	haplo117	10.57|11	9.59|13	1.1|0.85
Gnaper (*Gnathochromis permaxillaris*)	Limnochromini	F	ITA4	deep	haplo181	Gnaper_2	haplo118	13.28|13	8.57|11	1.55|1.18
Gnaper (*Gnathochromis permaxillaris*)	Limnochromini	M	IUI5	deep	haplo181	Gnaper_2	haplo118	10.49|10	8.1|10	1.3|1
Gwcabe (*Limnochromis abeelei*)	Limnochromini	F	ITB3	deep	haplo182	Gwcabe_2	haplo119	11.24|12	8.04|10	1.4|1.2
Gwcabe (*Limnochromis abeelei*)	Limnochromini	M	ITB4	deep	haplo182	Gwcabe_2	haplo119	9.53|9	6.99|9	1.36|1
Gwcbel (*Greenwoodochromis bellcrossi*)	Limnochromini	F	IXB5	deep	haplo183	Gwcbel_1	haplo120	14.2|14	9.5|12	1.49|1.17
Gwcchr (*Greenwoodochromis christyi*)	Limnochromini	M	IZE4	deep	haplo184	Gwcchr_2_A	haplo121	13.65|14	9.34|12	1.46|1.17
Gwcchr (*Greenwoodochromis christyi*)	Limnochromini	F	IZF1	deep	haplo185	Gwcchr_2_B	haplo122	6.86|6	7|9	0.98|0.67
Gwcsta (*Limnochromis staneri*)	Limnochromini	F	ITA6	deep	haplo186	Gwcsta_3	haplo123	20.07|21	13.94|19	1.44|1.11
Gwcsta (*Limnochromis staneri*)	Limnochromini	M	ITC2	deep	haplo186	Gwcsta_3	haplo123	9.43|9	6.72|8	1.4|1.12

Gwcsta (*Limnochromis staneri*)	Limnochromini	M	IXB6	deep	haplo186	Gwcsta_3	haplo123	11.71|11	7.19|9	1.63|1.22
Lchaur (*Limnochromis auritus*)	Limnochromini	F	ITB1	intermediate	haplo187	Lchaur_2	haplo124	10.2|10	7.62|10	1.34|1
Lchaur (*Limnochromis auritus*)	Limnochromini	M	JAF5	intermediate	haplo187	Lchaur_2	haplo124	10.54|10	7.84|10	1.34|1
Regcal (*Reganochromis calliurus*)	Limnochromini	M	IUI1	NA	haplo188	Regcal_2	haplo125	8.71|8	6.39|8	1.36|1
Regcal (*Reganochromis calliurus*)	Limnochromini	F	IUI4	NA	haplo188	Regcal_2	haplo125	8.46|8	7.25|9	1.17|0.89
Tchdha (*Tangachromis dhanisi*)	Limnochromini	M	LJA7	deep	haplo189	Tchdha_2	haplo124	7.32|7	5.96|8	1.23|0.88
Tchdha (*Tangachromis dhanisi*)	Limnochromini	F	LJA8	deep	haplo189	Tchdha_2	haplo124	15.33|15	11.76|16	1.3|0.94
Trioto (*Triglachromis otostigma*)	Limnochromini	F	JEG5	deep	haplo187	Trioto_2_A	haplo124	11.81|12	8.68|11	1.36|1.09
Trioto (*Triglachromis otostigma*)	Limnochromini	M	JEG6	deep	haplo190	Trioto_2_B	haplo126	9.48|9	6.58|8	1.44|1.12
Oretan (*Oreochromis tanganicae*)*	Oreochromini	M	JAB6	intermediate	haplo191	Oretan_2	haplo127	16.8|17	16.93|19	0.99|0.89
Oretan (*Oreochromis tanganicae*)*	Oreochromini	F	JAC7	intermediate	haplo191	Oretan_2	haplo127	17.41|17	16.12|18	1.08|0.94
Hapmic (*Haplotaxodon microlepis*)	Perissodini	M	IQB8	intermediate	haplo192	Hapmic_1	haplo128	18.69|17	12.37|17	1.51|1
Perecc (*Perissodus eccentricus*)	Perissodini	M	IXA4	deep	haplo193	Perecc_2_A	haplo129	12.02|12	8.07|11	1.49|1.09
Perecc (*Perissodus eccentricus*)	Perissodini	M	IZB2	deep	haplo194	Perecc_2_B	haplo129	17.74|16	11.76|16	1.51|1
Permic (*Perissodus microlepis*)	Perissodini	M	IQC4	intermediate	haplo195	Permic_2	haplo130	12.09|12	8.82|12	1.37|1
Permic (*Perissodus microlepis*)	Perissodini	F	IQI4	intermediate	haplo195	Permic_2	haplo130	9.19|9	6.73|9	1.37|1
Pleela (*Plecodus elaviae*)	Perissodini	M	LHI4	deep	haplo193	Pleela_2	haplo129	10.92|10	7.5|10	1.46|1
Pleela (*Plecodus elaviae*)	Perissodini	F	LHI6	deep	haplo193	Pleela_2	haplo129	12.37|12	7.72|10	1.6|1.2
Plemul (*Plecodus multidentatus*)	Perissodini	F	IZA8	deep	haplo193	Plemul_2	haplo129	18.18|19	13.1|18	1.39|1.06
Plemul (*Plecodus multidentatus*)	Perissodini	M	IZA9	deep	haplo193	Plemul_2	haplo129	11.01|11	9.41|12	1.17|0.92
Plepar (*Plecodus paradoxus*)	Perissodini	M	JDI4	deep	haplo196	Plepar_2_A	haplo131	11.67|12	8.3|11	1.41|1.09
Plepar (*Plecodus paradoxus*)	Perissodini	F	LEC7	deep	haplo197	Plepar_2_B	haplo131	8.88|9	6.63|8	1.34|1.12
Plestr (*Plecodus straeleni*)	Perissodini	F	INE8	NA	haplo198	Plestr_2	haplo129	19.56|20	13.66|19	1.43|1.05
Plestr (*Plecodus straeleni*)	Perissodini	M	INE9	NA	haplo198	Plestr_2	haplo129	14.63|15	8.83|12	1.66|1.25
Xchhec (*Xenochromis hecqui*)	Perissodini	M	IUI7	deep	haplo199	Xchhec_2	haplo129	7.15|7	6.54|8	1.09|0.88
Xchhec (*Xenochromis hecqui*)	Perissodini	F	JAH7	deep	haplo199	Xchhec_2	haplo129	14.71|15	9.18|12	1.6|1.25
Phaacu (*Pharyngochromis acuticeps*)*	Serranochromini	M	JWF3	NA	haplo200	Phaacu_1	haplo132	17.54|18	13.53|18	1.3|1
Sarcar (*Sargochromis carlottae*)*	Serranochromini	Juv.	JWF4	NA	haplo201	Sarcar_1	haplo133	18.14|18	12.9|17	1.41|1.06
Sermac (*Serranochromis macrocephalus*)*	Serranochromini	M	JWF5	NA	haplo202	Sermac_1	haplo134	22.39|23	16|22	1.4|1.05
Steult (*Steatocranus* sp. "ultraslender")*	Steatocranini	M	JWE8	NA	haplo203	Steult_1	haplo135	14.41|15	11.21|15	1.29|1
Tilspa (*Tilapia sparmanii*)*	Tilapiini	M	JWF7	NA	haplo204	Tilspa_1	haplo136	19.26|18	15.35|20	1.25|0.9
Trecap (*Trematocara caparti*)	Trematocarini		LJC8	deep	haplo205	Trecap_1	haplo137	11.42|10	6.51|8	1.75|1.25
Tremac (*Trematocara macrostoma*)	Trematocarini	M	IUD8	deep	haplo206	Tremac_2	haplo138	13.39|14	9.99|14	1.34|1
Tremac (*Trematocara macrostoma*)	Trematocarini	F	IUD9	deep	haplo206	Tremac_2	haplo138	12.92|12	9.09|13	1.42|0.92
Tremar (*Trematocara marginatum*)	Trematocarini	M	ISA1	deep	NA	NA	NA	7.49|7	5.92|8	1.27|0.88
Tremar (*Trematocara marginatum*)	Trematocarini	F	ISA3	deep	haplo207	Tremar_1	haplo139	17.43|18	10.94|16	1.59|1.12
Trenig (*Trematocara nigrifrons*)	Trematocarini	F	GPA1	deep	haplo208	Trenig_2	haplo140	6.83|6	5.95|8	1.15|0.75
Trenig (*Trematocara nigrifrons*)	Trematocarini	M	IUE5	deep	haplo208	Trenig_2	haplo140	18.57|19	10.92|15	1.7|1.27
Tresti (*Trematocara stigmaticum*)	Trematocarini	M	IUE7	deep	haplo209	Tresti_2_A	haplo141	17.02|17	8.24|11	2.07|1.55
Tresti (*Trematocara stigmaticum*)	Trematocarini	M	IZE1	deep	haplo210	Tresti_2_B	haplo412	10.56|11	8.33|12	1.27|0.92
Treuni (*Trematocara unimaculatum*)	Trematocarini	M	IXA3	deep	haplo211	Treuni_2_A	haplo413	10.54|10	8.86|12	1.19|0.83
Treuni (*Trematocara unimaculatum*)	Trematocarini	F	IXA6	deep	haplo212	Treuni_2_B	haplo144	6.86|7	8.64|12	0.79|0.58
Trezeb (*Trematocara zebra*)	Trematocarini	M	LFC9	deep	haplo213	Trezeb_2	haplo145	5.43|5	5.55|7	0.98|0.71
Trezeb (*Trematocara zebra*)	Trematocarini	F	LFE4	deep	haplo213	Trezeb_2	haplo145	8.11|7	5.77|8	1.41|0.88
Ctehor (*Ctenochromis horei*)	Tropheini	M	AVA8	shallow	haplo214	Ctehor_2	haplo146	8.52|8	7.61|10	1.12|0.8
Ctehor (*Ctenochromis horei*)	Tropheini	F	AXA7	shallow	haplo214	Ctehor_2	haplo146	10.52|11	7.93|10	1.33|1.1

Gnapfe (*Gnathochromis pfefferi*)	Tropheini	M	AWB7	intermediate	haplo215	Gnapfe_2	haplo147	11.24|12	7.22|10	1.56|1.2
Gnapfe (*Gnathochromis pfefferi*)	Tropheini	F	AWE2	intermediate	haplo215	Gnapfe_2	haplo147	8.92|8	7|9	1.27|0.89
Intloo (*Interochromis loocki*)	Tropheini	F	IPB6	shallow	haplo216	Intloo_2	haplo147	11.95|12	8.64|11	1.38|1.09
Intloo (*Interochromis loocki*)	Tropheini	M	IPF3	shallow	haplo216	Intloo_2	haplo147	6.69|7	6.92|9	0.97|0.78
Limdar (*Limnotilapia dardennii*)	Tropheini	F	AWI5	intermediate	haplo216	Limdar_2	haplo147	9.64|9	7.49|10	1.29|0.9
Limdar (*Limnotilapia dardennii*)	Tropheini	M	AWI6	intermediate	haplo216	Limdar_2	haplo147	9.76|10	7.61|10	1.28|1
Loblab (*Lobochilotes labiatus*)	Tropheini	M	ISD8	intermediate	haplo217	Loblab_2_A	haplo148	10.6|11	7.24|9	1.46|1.22
Loblab (*Lobochilotes labiatus*)	Tropheini	F	ISE5	intermediate	haplo218	Loblab_2_B	haplo149	10.62|11	6.3|8	1.69|1.38
Peteph (*Petrochromis ephippium*)	Tropheini	F	IPC1	intermediate	haplo219	Peteph_2	haplo62	7.28|7	7.12|9	1.02|0.78
Peteph (*Petrochromis ephippium*)	Tropheini	M	IYA5	intermediate	haplo219	Peteph_2	haplo62	6.68|7	5.72|7	1.17|1
Petfam (*Petrochromis famula*)	Tropheini	F	IYA6	shallow	haplo82	Petfam_2_B	haplo62	5.55|6	5.66|7	0.98|0.86
Petfam (*Petrochromis famula*)	Tropheini	M	IYA7	shallow	haplo220	Petfam_2_A	haplo150	7.39|7	7.8|10	0.95|0.7
Petfas (*Petrochromis fasciolatus*)	Tropheini	M	GPH7	shallow	haplo221	Petfas_2_A	haplo146	9.15|9	7.69|10	1.19|0.9
Petfas (*Petrochromis fasciolatus*)	Tropheini	F	JAE1	shallow	haplo222	Petfas_2_B	haplo151	11.59|12	7.58|10	1.53|1.2
Petgia (*Petrochromis* sp. "giant")	Tropheini	M	LDC6	shallow	haplo223	Petgia_2	haplo64	12.13|12	7.86|10	1.54|1.2
Petgia (*Petrochromis* sp. "giant")	Tropheini	F	LHD2	shallow	haplo223	Petgia_2	haplo64	11.81|12	7.27|9	1.62|1.33
Pethor (*Petrochromis horii*)	Tropheini	M	IWB5	intermediate	haplo82	Pethor_2	haplo62	9.14|9	7.09|9	1.29|1
Pethor (*Petrochromis horii*)	Tropheini	F	IWB6	intermediate	haplo82	Pethor_2	haplo62	10.73|10	9.24|12	1.16|0.83
Petiko (*Petrochromis* sp. "orthognathus ikola")	Tropheini	M	LFA6	shallow	haplo217	Petiko_2	haplo148	8.6|9	7.06|9	1.22|1
Petiko (*Petrochromis* sp. "orthognathus ikola")	Tropheini	F	LFA8	shallow	haplo217	Petiko_2	haplo148	8.98|9	7.33|9	1.23|1
Petkas (*Petrochromis* sp. "kazumbae")	Tropheini	F	KEA4	shallow	haplo82	Petkas_2_B	haplo62	8.94|9	7.97|10	1.12|0.9
Petkas (*Petrochromis* sp. "kazumbae")	Tropheini	M	KEB4	shallow	haplo224	Petkas_2_A	haplo62	9.28|9	8.21|11	1.13|0.82
Petkip (*Petrochromis* sp. "kipili brown")	Tropheini	M	LDE3	intermediate	haplo225	Petkip_2	haplo152	6.67|6	6.24|8	1.07|0.75
Petkip (*Petrochromis* sp. "kipili brown")	Tropheini	F	LDE4	intermediate	haplo225	Petkip_2	haplo152	11.15|11	7.13|9	1.56|1.22
Petmac (*Petrochromis macrognathus*)	Tropheini	M	LDA4	shallow	haplo226	Petmac_2	haplo153	8.6|8	6.8|9	1.26|0.89
Petmac (*Petrochromis macrognathus*)	Tropheini	F	LJB1	shallow	haplo226	Petmac_2	haplo153	8.54|9	6.11|8	1.4|1.12
Petmos (*Petrochromis* sp. "moshi yellow")	Tropheini	M	LCF6	intermediate	haplo219	Petmos_2_A	haplo62	11.32|11	7.47|10	1.52|1.1
Petmos (*Petrochromis* sp. "moshi yellow")	Tropheini	F	LCF8	intermediate	haplo82	Petmos_2_B	haplo62	11.08|10	6.94|9	1.6|1.11
Petort (*Petrochromis orthognathus*)	Tropheini	F	JXH4	shallow	NA	NA	NA	2.57|2	4.03|5	0.64|0.4
Petort (*Petrochromis orthognathus*)	Tropheini	M	JXH5	shallow	haplo217	Petort_1	haplo148	18.7|19	11.88|16	1.57|1.19
Petpol (*Petrochromis polyodon*)	Tropheini	M	AWB9	shallow	haplo82	Petpol_2	haplo62	9|8	7.41|9	1.21|0.89
Petpol (*Petrochromis polyodon*)	Tropheini	F	AWI4	shallow	haplo82	Petpol_2	haplo62	10.8|10	7.47|10	1.45|1
Petrai (*Petrochromis* sp. "macrognathus rainbow")	Tropheini	M	LGB5	shallow	haplo223	Petrai_2	haplo64	10.77|11	7.16|9	1.5|1.22
Petrai (*Petrochromis* sp. "macrognathus rainbow")	Tropheini	F	LGB8	shallow	haplo223	Petrai_2	haplo64	9.42|9	7.24|9	1.3|1
Petred (*Petrochromis* sp. "red")	Tropheini	M	LCD1	deep	haplo82	Petred_2	haplo62	10.02|10	6.25|8	1.6|1.25
Petred (*Petrochromis* sp. "red")	Tropheini	F	LCD5	deep	haplo82	Petred_2	haplo62	8.5|9	6.26|8	1.36|1.12
Pettex (*Petrochromis* sp. "polyodon texas")	Tropheini	M	LHB1	shallow	haplo227	Pettex_2_A	haplo154	10.41|11	7.75|10	1.34|1.1
Pettex (*Petrochromis* sp. "polyodont texas")	Tropheini	F	LHB3	shallow	haplo82	Pettex_2_B	haplo62	13.56|14	9.46|12	1.43|1.17
Pettre (*Petrochromis trewavasae*)	Tropheini	M	IWC9	NA	haplo228	Pettre_2_A	haplo62	16.65|17	13.55|18	1.23|0.94
Pettre (*Petrochromis trewavasae*)	Tropheini	F	IWD4	NA	haplo82	Pettre_2_B	haplo62	9.36|9	7.97|10	1.17|0.9
Psccur (*Pseudosimochromis curvifrons*)	Tropheini	F	AXF8	shallow	haplo216	Psccur_2	haplo147	11.65|12	8.66|11	1.35|1.09
Psccur (*Pseudosimochromis curvifrons*)	Tropheini	M	AYC7	shallow	haplo216	Psccur_2	haplo147	13.55|13	9.44|13	1.44|1
Simbab (*Pseudosimochromis babaulti*)	Tropheini	M	JUA3	shallow	haplo229	Simbab_2	haplo147	11.13|11	7.94|10	1.4|1.1
Simbab (*Pseudosimochromis babaulti*)	Tropheini	F	JUA4	shallow	haplo229	Simbab_2	haplo147	11.68|11	12.04|16	0.97|0.69
Simdia (*Simochromis diagramma*)	Tropheini	F	AUD8	shallow	haplo230	Simdia_2_A	haplo148	15.32|15	9.73|13	1.57|1.15
Simdia (*Simochromis diagramma*)	Tropheini	M	AUE1	shallow	haplo231	Simdia_2_B	haplo148	10.19|11	9.15|12	1.11|0.92

Simmar (*Pseudosimochromis marginatus*)	Tropheini	M	KCE7	shallow	haplo232	Simmar_2	haplo147	14.17|14	9.52|13	1.49|1.08
Simmar (*Pseudosimochromis marginatus*)	Tropheini	F	KCF3	shallow	haplo232	Simmar_2	haplo147	22.03|22	14.43|20	1.53|1.1
Simmrg (*Pseudosimochromis marginatus* (North))	Tropheini	M	KFE8	shallow	haplo232	Simmrg_2	haplo147	10.44|10	7.03|9	1.49|1.11
Simmrg (*Pseudosimochromis marginatus* (North))	Tropheini	F	KFF1	shallow	haplo232	Simmrg_2	haplo147	12.83|12	7.42|10	1.73|1.2
Simple (*Pseudosimochromis babaulti* (South))	Tropheini	M	AUB6	shallow	haplo229	Simple_2	haplo147	12.71|13	9.26|12	1.37|1.08
Simple (*Pseudosimochromis babaulti* (South))	Tropheini	F	AVB6	shallow	haplo229	Simple_2	haplo147	11|12	9.21|12	1.19|1
Troann (*Tropheus annectens*)	Tropheini	M	JWG4	shallow	haplo82	Troann_2	haplo62	16.98|17	13.3|18	1.28|0.94
Troann (*Tropheus annectens*)	Tropheini	F	JWG5	shallow	haplo82	Troann_2	haplo62	9.71|9	7.6|10	1.28|0.9
Trobri (*Tropheus brichardi*)	Tropheini	M	JYI8	shallow	haplo234	Trobri_2	haplo146	12.15|12	8.33|11	1.46|1.09
Trobri (*Tropheus brichardi*)	Tropheini	F	JZA3	shallow	haplo234	Trobri_2	haplo146	10.15|10	8.31|11	1.22|0.91
TrobrK (*Tropheus* sp. "brichardi kipili")	Tropheini	M	LGA5	shallow	haplo233	TrobrK_2	haplo155	6.81|6	7.09|9	0.96|0.67
TrobrK (*Tropheus* sp. "brichardi kipili")	Tropheini	F	LGA6	shallow	haplo233	TrobrK_2	haplo155	12.12|12	7.61|10	1.59|1.2
Trodub (*Tropheus duboisi*)	Tropheini	M	KHA4	intermediate	haplo235	Trodub_2	haplo62	14.37|14	7.34|9	1.96|1.56
Trodub (*Tropheus duboisi*)	Tropheini	F	KHA5	intermediate	haplo235	Trodub_2	haplo62	8.6|8	7.83|10	1.1|0.8
Trokir (*Tropheus* sp. "kirschfleck")	Tropheini	M	LCF1	shallow	haplo82	Trokir_1	haplo62	8.23|7	7.08|9	1.16|0.78
Trokir (*Tropheus* sp. "kirschfleck")	Tropheini	F	LCF3	shallow	NA	NA	NA	7.28|7	6.47|8	1.13|0.88
Troluk (*Tropheus* sp. "lukuga")	Tropheini	M	KEF2	shallow	haplo233	Troluk_2	haplo155	16.95|17	11.25|15	1.51|1.13
Troluk (*Tropheus* sp. "lukuga")	Tropheini	F	KEF3	shallow	haplo233	Troluk_2	haplo155	9.91|10	7.08|9	1.4|1.11
Trolun (*Tropheus* sp. "lunatus")	Tropheini	M	KED6	shallow	haplo236	Trolun_2_B	haplo156	8.25|7	7.18|9	1.15|0.78
Trolun (*Tropheus* sp. "lunatus")	Tropheini	F	KED7	shallow	haplo233	Trolun_2_A	haplo155	10.61|11	7.65|10	1.39|1.1
Tromoo (*Tropheus moorii*)	Tropheini	M	JBH4	shallow	haplo82	Tromoo_2	haplo62	8.09|8	6.57|8	1.23|1
Tromoo (*Tropheus moorii*)	Tropheini	F	JBH5	shallow	haplo82	Tromoo_2	haplo62	7.77|7	7.53|10	1.03|0.7
Tromor (*Tropheus* sp. "murago")	Tropheini	M	LHD9	shallow	haplo82	Tromor_2_B	haplo62	10.04|10	7.38|9	1.36|1.11
Tromor (*Tropheus* sp. "murago")	Tropheini	F	LHE3	shallow	haplo237	Tromor_2_A	haplo157	10.05|9	7.1|9	1.42|1
Trompi (*Tropheus* sp. "mpimbwe")	Tropheini	M	LDI5	shallow	haplo237	Trompi_2	haplo157	9.53|9	6.87|9	1.39|1
Trompi (*Tropheus* sp. "mpimbwe")	Tropheini	F	LDI7	shallow	haplo237	Trompi_2	haplo157	8.1|8	6.17|8	1.31|1
Tronig (*Tropheus* sp. "black")	Tropheini	F	JVC3	shallow	haplo82	Tronig_2	haplo62	16.54|17	10.01|13	1.65|1.31
Tronig (*Tropheus* sp. "black")	Tropheini	M	JVC9	shallow	haplo82	Tronig_2	haplo62	9.14|9	8.12|11	1.13|0.82
Tropol (*Tropheus polli*)	Tropheini	M	LEF8	shallow	haplo82	Tropol_2	haplo62	13.05|13	11.33|15	1.15|0.87
Tropol (*Tropheus polli*)	Tropheini	F	LEF9	shallow	haplo82	Tropol_2	haplo62	16.95|17	11.24|15	1.51|1.13
Trored (*Tropheus* sp. "red")	Tropheini	M	IOD9	shallow	haplo82	Trored_2	haplo62	11.17|11	8.7|11	1.28|1
Trored (*Tropheus* sp. "red")	Tropheini	F	IOE1	shallow	haplo82	Trored_2	haplo62	10.79|11	7.35|9	1.47|1.22

Species which are not part of the Lake Tanganyika radiation (outgroup species or species nested with the radiation) are marked with an asterik (*). The first entry of the table is the reference genome.

TABLE S2 Character diagnostics table calculated with PAUP* based on the rhodopsin maximum likelihood gene tree (on the left) and the Bayesian inference gene tree (on the right). Amino acid positions refer to the RH1 protein of the reference (*O. niloticus*).

Maximum likelihood gene tree									
Position	Range	Min. steps	Tree steps	Max. steps	CI	RI	RC	HI	G-fit
14	3	3	7	46	0.429	0.907	0.389	0.571	0.429
17	1	1	5	19	0.2	0.778	0.156	0.8	0.429
19	3	3	5	9	0.6	0.667	0.4	0.4	0.6
20	1	1	1	3	1	1	1	0	1
22	1	1	7	116	0.143	0.948	0.135	0.857	0.333
25	1	1	6	14	0.167	0.615	0.103	0.833	0.375
27	1	1	1	1	1	0/0	0/0	0	1
32	1	1	4	11	0.25	0.7	0.175	0.75	0.5
33	1	1	8	33	0.125	0.781	0.098	0.875	0.3
37	1	1	8	21	0.125	0.65	0.081	0.875	0.3
41	1	1	8	116	0.125	0.939	0.117	0.875	0.3
42	2	2	3	9	0.667	0.857	0.571	0.333	0.75
48	1	1	3	11	0.333	0.8	0.267	0.667	0.6
49	1	1	3	3	0.333	0	0	0.667	0.6
50	1	1	2	5	0.5	0.75	0.375	0.5	0.75
52	1	1	1	4	1	1	1	0	1
75	1	1	1	2	1	1	1	0	1
83	1	1	1	2	1	1	1	0	1
88	1	1	6	31	0.167	0.833	0.139	0.833	0.375
95	3	3	8	89	0.375	0.942	0.353	0.625	0.375
104	1	1	10	21	0.1	0.55	0.055	0.9	0.25
112	1	1	1	3	1	1	1	0	1
133	1	1	12	104	0.083	0.893	0.074	0.917	0.214
159	1	1	1	1	1	0/0	0/0	0	1
162	5	5	18	93	0.278	0.852	0.237	0.722	0.188
163	1	1	2	17	0.5	0.938	0.469	0.5	0.75
165	3	3	8	183	0.375	0.972	0.365	0.625	0.375
166	1	1	9	159	0.111	0.949	0.105	0.889	0.273
169	3	3	8	155	0.375	0.967	0.363	0.625	0.375
173	2	2	6	9	0.333	0.429	0.143	0.667	0.429
183	1	1	1	2	1	1	1	0	1
185	1	1	1	22	1	1	1	0	1
186	1	1	2	3	0.5	0.5	0.25	0.5	0.75
202	1	1	2	2	0.5	0	0	0.5	0.75
205	1	1	3	6	0.333	0.6	0.2	0.667	0.6

Bayesian gene tree									
Position	Range	Min. steps	Tree steps	Max. steps	CI	RI	RC	HI	G-fit
14	3	3	7	46	0.429	0.907	0.389	0.571	0.429
17	1	1	5	19	0.2	0.778	0.156	0.8	0.429
19	3	3	5	9	0.6	0.667	0.4	0.4	0.6
20	1	1	1	3	1	1	1	0	1
22	1	1	7	116	0.143	0.948	0.135	0.857	0.333
25	1	1	6	14	0.167	0.615	0.103	0.833	0.375
27	1	1	1	1	1	0/0	0/0	0	1
32	1	1	4	11	0.25	0.7	0.175	0.75	0.5
33	1	1	8	33	0.125	0.781	0.098	0.875	0.3
37	1	1	8	21	0.125	0.65	0.081	0.875	0.3
41	1	1	8	116	0.125	0.939	0.117	0.875	0.3
42	2	2	3	9	0.667	0.857	0.571	0.333	0.75
48	1	1	3	11	0.333	0.8	0.267	0.667	0.6
49	1	1	3	3	0.333	0	0	0.667	0.6
50	1	1	2	5	0.5	0.75	0.375	0.5	0.75
52	1	1	1	4	1	1	1	0	1
75	1	1	1	2	1	1	1	0	1
83	1	1	1	2	1	1	1	0	1
88	1	1	8	31	0.125	0.767	0.096	0.875	0.3
95	3	3	8	89	0.375	0.942	0.353	0.625	0.375
104	1	1	10	21	0.1	0.55	0.055	0.9	0.25
112	1	1	1	3	1	1	1	0	1
133	1	1	13	104	0.077	0.883	0.068	0.923	0.2
159	1	1	1	1	1	0/0	0/0	0	1
162	5	5	20	93	0.25	0.83	0.207	0.75	0.167
163	1	1	2	17	0.5	0.938	0.469	0.5	0.75
165	3	3	8	183	0.375	0.972	0.365	0.625	0.375
166	1	1	9	159	0.111	0.949	0.105	0.889	0.273
169	3	3	9	155	0.333	0.961	0.32	0.667	0.333
173	2	2	6	9	0.333	0.429	0.143	0.667	0.429
183	1	1	1	2	1	1	1	0	1
185	1	1	1	22	1	1	1	0	1
186	1	1	2	3	0.5	0.5	0.25	0.5	0.75
202	1	1	2	2	0.5	0	0	0.5	0.75
205	1	1	3	6	0.333	0.6	0.2	0.667	0.6

209	2	2	4	14	0.5	0.833	0.417	0.5	0.6
213	5	5	15	161	0.333	0.936	0.312	0.667	0.231
214	3	3	5	28	0.6	0.92	0.552	0.4	0.6
217	5	5	16	90	0.312	0.871	0.272	0.688	0.214
218	2	2	8	172	0.25	0.965	0.241	0.75	0.333
220	1	1	1	4	1	1	1	0	1
248	1	1	1	3	1	1	1	0	1
255	1	1	1	7	1	1	1	0	1
256	1	1	1	7	1	1	1	0	1
258	1	1	1	3	1	1	1	0	1
259	2	2	3	25	0.667	0.957	0.638	0.333	0.75
260	2	2	2	4	1	1	1	0	1
263	1	1	10	35	0.1	0.735	0.074	0.9	0.25
266	1	1	1	1	1	0/0	0/0	0	1
270	1	1	2	19	0.5	0.944	0.472	0.5	0.75
274	1	1	1	18	1	1	1	0	1
282	1	1	1	3	1	1	1	0	1
286	1	1	1	3	1	1	1	0	1
290	1	1	9	32	0.111	0.742	0.082	0.889	0.273
292	1	1	5	38	0.2	0.892	0.178	0.8	0.429
297	3	3	16	206	0.188	0.936	0.175	0.812	0.188
298	1	1	11	96	0.091	0.895	0.081	0.909	0.231
299	1	1	14	161	0.071	0.919	0.066	0.929	0.188
300	1	1	2	11	0.5	0.9	0.45	0.5	0.75
304	3	3	9	34	0.333	0.806	0.269	0.667	0.333
308	1	1	1	2	1	1	1	0	1
315	1	1	1	3	1	1	1	0	1
336	1	1	1	66	1	1	1	0	1

209	2	2	4	14	0.5	0.833	0.417	0.5	0.6
213	5	5	15	161	0.333	0.936	0.312	0.667	0.231
214	3	3	5	28	0.6	0.92	0.552	0.4	0.6
217	5	5	18	90	0.278	0.847	0.235	0.722	0.188
218	2	2	9	172	0.222	0.959	0.213	0.778	0.3
220	1	1	1	4	1	1	1	0	1
248	1	1	1	3	1	1	1	0	1
255	1	1	1	7	1	1	1	0	1
256	1	1	1	7	1	1	1	0	1
258	1	1	1	3	1	1	1	0	1
259	2	2	3	25	0.667	0.957	0.638	0.333	0.75
260	2	2	2	4	1	1	1	0	1
263	1	1	10	35	0.1	0.735	0.074	0.9	0.25
266	1	1	1	1	1	0/0	0/0	0	1
270	1	1	2	19	0.5	0.944	0.472	0.5	0.75
274	1	1	1	18	1	1	1	0	1
282	1	1	1	3	1	1	1	0	1
286	1	1	1	3	1	1	1	0	1
290	1	1	9	32	0.111	0.742	0.082	0.889	0.273
292	1	1	6	38	0.167	0.865	0.144	0.833	0.375
297	3	3	17	206	0.176	0.931	0.164	0.824	0.176
298	1	1	13	96	0.077	0.874	0.067	0.923	0.2
299	1	1	15	161	0.067	0.912	0.061	0.933	0.176
300	1	1	2	11	0.5	0.9	0.45	0.5	0.75
304	3	3	9	34	0.333	0.806	0.269	0.667	0.333
308	1	1	1	2	1	1	1	0	1
315	1	1	1	3	1	1	1	0	1
336	1	1	1	66	1	1	1	0	1

CI: Consistency Index; RI: Retention Index; RC: Rescaled CI; HI: Homoplasy Index; G-fit: Goodness-of-fit statistic.

TABLE S3 Rhodopsin positive selection results based on a CodeML random-site model comparison (M1a vs. M2a and M7 vs. M8a) and the Bayesian inference gene tree. The pairs of models were tested using a Likelihood Ratio Test (LRT) following a χ2 distribution. Values of each site class ω_0, ω_1, ω_2 are specified for models M1a and M2a. The shape parameters *p* and *q* are specified for models M7 and M8. The value ω_p corresponds to the positively selected site class for M8. The proportion of each site class is reported in parenthesis.

				Parameters						
Model	**np**	**ln*L***	**κ**	***ω*$_0$/*p***	***ω*$_1$/*q***	***ω*$_2$/*ω*$_p$**	**Null**	**LRT**	**df**	***P***
M1a	3	-5531	2.090	0 (92.8%)	1 (7.2%)					
M2a	5	-5184	2.743	0.009 (90.5%)	1 (8.4%)	12.664 (1%)	M1a	695	2	< 0.0001
M7	3	-5593	2.363	0.008	0.024					
M8	5	-5191	2.766	0.028	0.206	12.373 (1.2%)	M7	806	2	< 0.0001

np: number of parameters; ln*L*: *ln* likelihood; kappa: transition/transversion ratio; Null: null model; df: degrees of freedom.

TABLE S4 Rhodopsin (RH1) positively selected sites of random site models M2a and M8 using the maximum likelihood gene tree. Significant results are shown in bold (*: Pr>95%; **: Pr>99%). Amino acid positions refer to the RH1 protein of the reference genome (*O. niloticus*).

Site model M2a: Bayes Empirical Bayes (BEB) analysis					
Location	**Position**	**Amino acid**	**Pr(w>1)**	**Post. mean +- SE for w**	
N-terminal	**14**	**V**	**1.000****	**10.177**	**0.498**
N-terminal	17	T	0.934	9.561	2.332
N-terminal	19	I	0.863	8.9	3.187
N-terminal	**22**	**S**	**0.999****	**10.172**	**0.541**
N-terminal	**25**	**E**	**0.999****	**10.172**	**0.537**
N-terminal	32	V	0.563	6.125	4.535
N-terminal	**33**	**S**	**1.000****	**10.177**	**0.497**
N-terminal	**37**	**Y**	**1.000****	**10.177**	**0.501**
TM I	**41**	**G**	**1.000****	**10.177**	**0.495**
TM I	42	A	0.59	6.38	4.499
TM II	**88**	**F**	**0.996****	**10.139**	**0.767**
TM II	**95**	**M**	**1.000****	**10.176**	**0.507**
Extracellular loop	**104**	**V**	**1.000****	**10.178**	**0.493**
TM III	**133**	**V**	**1.000****	**10.178**	**0.493**
TM IV	**162**	**L**	**1.000****	**10.178**	**0.493**
TM IV	**165**	**L**	**1.000****	**10.178**	**0.493**
TM IV	**166**	**S**	**1.000****	**10.177**	**0.495**
TM IV	**169**	**G**	**1.000****	**10.177**	**0.493**
TM IV	**173**	**V**	**0.992****	**10.104**	**0.949**
TM V	**213**	**L**	**1.000****	**10.178**	**0.493**
TM V	214	I	0.852	8.805	3.28
TM V	**217**	**T**	**1.000****	**10.178**	**0.493**
TM V	**218**	**V**	**1.000****	**10.177**	**0.494**
TM VI	**263**	**I**	**1.000****	**10.178**	**0.493**
TM VI	**270**	**G**	**0.983***	**10.022**	**1.278**
TM VII	**290**	**L**	**1.000****	**10.177**	**0.495**

Site model M8: Bayes Empirical Bayes (BEB) analysis					
Location	**Position**	**Amino acid**	**Pr(w>1)**	**Post. mean +- SE for w**	
N-terminal	**14**	**V**	**1.000****	**9.714**	**0.632**
N-terminal	**17**	**T**	**0.997****	**9.687**	**0.796**
N-terminal	**19**	**I**	**0.994****	**9.655**	**0.952**
N-terminal	**22**	**S**	**1.000****	**9.714**	**0.633**
N-terminal	**25**	**E**	**1.000****	**9.714**	**0.633**
N-terminal	**32**	**V**	**0.955***	**9.303**	**1.954**
N-terminal	**33**	**S**	**1.000****	**9.714**	**0.632**
N-terminal	**37**	**Y**	**1.000****	**9.714**	**0.632**
TM I	**41**	**G**	**1.000****	**9.714**	**0.632**
TM I	**42**	**A**	**0.960***	**9.346**	**1.865**
TM I	48	I	0.508	5.212	4.459
TM II	**88**	**F**	**1.000****	**9.713**	**0.637**
TM II	**95**	**M**	**1.000****	**9.714**	**0.632**
Extracellular loop	**104**	**V**	**1.000****	**9.714**	**0.632**
TM III	**133**	**V**	**1.000****	**9.714**	**0.632**
TM IV	**162**	**L**	**1.000****	**9.714**	**0.632**
TM IV	**165**	**L**	**1.000****	**9.714**	**0.632**
TM IV	**166**	**S**	**1.000****	**9.714**	**0.632**
TM IV	**169**	**G**	**1.000****	**9.714**	**0.632**
TM IV	**173**	**V**	**1.000****	**9.712**	**0.648**
Extracellular loop	186	S	0.635	6.364	4.349
TM V	205	I	0.518	5.297	4.459
TM V	209	I	0.931	9.076	2.356
TM V	**213**	**L**	**1.000****	**9.714**	**0.632**
TM V	**214**	**I**	**0.993****	**9.651**	**0.973**
TM V	**217**	**T**	**1.000****	**9.714**	**0.632**
TM V	**218**	**V**	**1.000****	**9.714**	**0.632**
TM VI	**263**	**I**	**1.000****	**9.714**	**0.632**
TM VI	**270**	**G**	**0.999****	**9.704**	**0.699**
TM VII	**290**	**L**	**1.000****	**9.714**	**0.632**

TM VII	292	A	0.92	9.438	2.526
TM VII	**297**	**S**	**1.000****	**10.178**	**0.493**
TM VII	**298**	**S**	**1.000****	**10.178**	**0.493**
TM VII	**299**	**S**	**1.000****	**10.178**	**0.493**
TM VII	**304**	**L**	**1.000****	**10.178**	**0.493**

TM VII	**292**	**A**	**0.996****	**9.681**	**0.827**
TM VII	**297**	**S**	**1.000****	**9.714**	**0.632**
TM VII	**298**	**S**	**1.000****	**9.714**	**0.632**
TM VII	**299**	**S**	**1.000****	**9.714**	**0.632**
TM VII	**304**	**L**	**1.000****	**9.714**	**0.632**

TM: transmembrane alpha-helix.

TABLE S5 Rhodopsin (RH1) positively selected sites of random site models M2a and M8 using the Bayesian inference gene tree. Significant results are shown in bold (*: Pr>95%; **: Pr>99%). Amino acid positions refer to the RH1 protein of the reference genome (*O. niloticus*).

Site model M2a: Bayes Empirical Bayes (BEB) analysis					
Location	**Position**	**Amino acid**	**Pr(w>1)**	**Post. mean +- SE for w**	
N-terminal	**14**	**V**	**1.000****	**10.498**	**0.062**
N-terminal	**17**	**T**	**0.985***	**10.356**	**1.153**
N-terminal	**19**	**I**	**0.969***	**10.207**	**1.638**
N-terminal	**22**	**S**	**1.000****	**10.497**	**0.114**
N-terminal	**25**	**E**	**1.000****	**10.496**	**0.132**
N-terminal	32	V	0.847	9.044	3.42
N-terminal	**33**	**S**	**1.000****	**10.498**	**0.056**
N-terminal	**37**	**Y**	**1.000****	**10.498**	**0.062**
TM I	**41**	**G**	**1.000****	**10.498**	**0.053**
TM I	42	A	0.857	9.136	3.328
TM II	**88**	**F**	**1.000****	**10.498**	**0.051**
TM II	**95**	**M**	**1.000****	**10.497**	**0.069**
Extracellular loop	**104**	**V**	**1.000****	**10.498**	**0.048**
TM III	**133**	**V**	**1.000****	**10.498**	**0.047**
TM IV	**162**	**L**	**1.000****	**10.498**	**0.047**
TM IV	**165**	**L**	**1.000****	**10.498**	**0.047**
TM IV	**166**	**S**	**1.000****	**10.498**	**0.051**
TM IV	**169**	**G**	**1.000****	**10.498**	**0.048**
TM IV	**173**	**V**	**0.998****	**10.482**	**0.387**
TM V	209	I	0.789	8.492	3.877
TM V	**213**	**L**	**1.000****	**10.498**	**0.047**
TM V	**214**	**I**	**0.969***	**10.2**	**1.655**
TM V	**217**	**T**	**1.000****	**10.498**	**0.047**

Site model M8: Bayes Empirical Bayes (BEB) analysis					
Location	**Position**	**Amino acid**	**Pr(w>1)**	**Post. mean +- SE for w**	
N-terminal	**14**	**V**	**1.000****	**10.489**	**0.103**
N-terminal	**17**	**T**	**0.999****	**10.484**	**0.255**
N-terminal	**19**	**I**	**0.999****	**10.478**	**0.35**
N-terminal	**22**	**S**	**1.000****	**10.489**	**0.104**
N-terminal	**25**	**E**	**1.000****	**10.489**	**0.105**
N-terminal	**32**	**V**	**0.991****	**10.397**	**0.951**
N-terminal	**33**	**S**	**1.000****	**10.489**	**0.103**
N-terminal	**37**	**Y**	**1.000****	**10.489**	**0.103**
TM I	**41**	**G**	**1.000****	**10.489**	**0.103**
TM I	**42**	**A**	**0.991****	**10.404**	**0.916**
TM I	48	I	0.82	8.729	3.759
TM I	49	L	0.651	7.071	4.666
TM II	**88**	**F**	**1.000****	**10.489**	**0.103**
TM II	**95**	**M**	**1.000****	**10.489**	**0.103**
Extracellular loop	**104**	**V**	**1.000****	**10.489**	**0.103**
TM III	112	L	0.625	6.813	4.745
TM III	**133**	**V**	**1.000****	**10.489**	**0.103**
TM IV	**162**	**L**	**1.000****	**10.489**	**0.103**
TM IV	163	A	0.691	7.457	4.536
TM IV	**165**	**L**	**1.000****	**10.489**	**0.103**
TM IV	**166**	**S**	**1.000****	**10.489**	**0.103**
TM IV	**169**	**G**	**1.000****	**10.489**	**0.103**
TM IV	**173**	**V**	**1.000****	**10.489**	**0.123**
Extracellular loop	186	S	0.832	8.845	3.666
TM V	202	S	0.592	6.485	4.825
TM V	205	I	0.826	8.789	3.709
TM V	**209**	**I**	**0.986***	**10.352**	**1.154**
TM V	**213**	**L**	**1.000****	**10.489**	**0.103**
TM V	**214**	**I**	**0.999****	**10.477**	**0.354**
TM V	**217**	**T**	**1.000****	**10.489**	**0.103**

TM V	**218**	**V**	**1.000****	**10.498**	**0.049**
TM VI	**263**	**I**	**1.000****	**10.498**	**0.047**
TM VI	**270**	**G**	**0.993****	**10.433**	**0.783**
TM VII	**290**	**L**	**1.000****	**10.498**	**0.051**
TM VII	**292**	**A**	**0.998****	**10.481**	**0.4**
TM VII	**297**	**S**	**1.000****	**10.498**	**0.047**
TM VII	**298**	**S**	**1.000****	**10.498**	**0.047**
TM VII	**299**	**S**	**1.000****	**10.498**	**0.047**
TM VII	**304**	**L**	**1.000****	**10.498**	**0.048**

TM V	**218**	**V**	**1.000****	**10.489**	**0.103**
TM VI	259	I	0.773	8.271	4.098
TM VI	**263**	**I**	**1.000****	**10.489**	**0.103**
TM VI	**270**	**G**	**1.000****	**10.486**	**0.213**
TM VII	**290**	**L**	**1.000****	**10.489**	**0.103**
TM VII	**292**	**A**	**1.000****	**10.489**	**0.124**
TM VII	**297**	**S**	**1.000****	**10.489**	**0.103**
TM VII	**298**	**S**	**1.000****	**10.489**	**0.103**
TM VII	**299**	**S**	**1.000****	**10.489**	**0.103**
TM VII	**304**	**L**	**1.000****	**10.489**	**0.103**

TM: transmembrane alpha-helix.

TABLE S6 Rhodopsin positive selection results (CodeML) of the branch-site (BrS) model H0 and HA using the maximum likelihood (ML) and Bayesian inference gene trees. The background (B) branches include shallow-water living species and the foreground (F) branches comprise deep-water living species. The pair models are tested using the Likelihood Ratio Test (LRT) following a χ2 distribution. Values of each site class ω_0, ω_1, ω_{2a}, ω_{2b} are specified for each branch (F and B). The proportion of each site class is written in parenthesis.

					Parameters							
	Model	**np**	**ln*L***	**κ**	ω_0	ω_1	ω_{2a}	ω_{2b}	**Null**	**LRT**	**df**	***P***
ML gene tree	**BrS H0**	4	-3426	2.091	**B**: 0 **F**: 0 (87.2%)	**B**: 1 **F**: 1 (12.8%)	**B**: 0 **F**: 1 (0%)	**B**: 1 **F**: 1 (0%)				
	BrS HA	5	-3426	2.091	**B**: 0 **F**: 0 (87.2%)	**B**: 1 **F**: 1 (12.8%)	**B**: 0 **F**: 1 (0%)	**B**: 1 F: 1 (0%)	BrS H0	0	1	-
Bayesian gene tree	**BrS H0**	4	-3515	2.022	**B**: 0 **F**: 0 (88.5%)	**B**: 1 **F**: 1 (11.5%)	**B**: 0 **F**: 1 (0%)	**B**: 1 **F**: 1 (0%)				
	BrS HA	5	-3515	2.022	**B**: 0 **F**: 0 (88.5%)	**B**: 1 **F**: 1 (11.5%)	**B**: 0 **F**: 1 (0%)	**B**: 1 **F**: 1 (0%)	BrS H0	0	1	-

np: number of parameters; ln*L*: *ln* likelihood; kappa: transition/transversion ratio; Null: null model; df: degrees of freedom.

TABLE S7 Results of the rhodopsin (RH1) positive selection analyses (HyPhy) of pervasive site-level selection tests FUBAR and FEL using the maximum likelihood gene tree. FUBAR identifies positively selected sites while FEL identifies both positively and negatively selected sites. Amino acid positions refer to the RH1 protein of the reference genome (*O. niloticus*).

FUBAR				
Location	**Position**	**alpha**	**beta**	**Post. prob. for positive selection**
N-terminal	14	0.553	7.175	0.9951
N-terminal	22	0.614	5.837	0.9824
N-terminal	25	0.658	6.267	0.98
N-terminal	32	0.607	3.767	0.9325
N-terminal	33	0.724	6.686	0.9782
N-terminal	37	1.734	9.352	0.9213
TM I	41	0.542	6.995	0.9959
TM I	42	0.608	3.741	0.9317
TM II	88	0.698	7.87	0.983
TM II	95	0.613	7.141	0.9911
Extracellular loop	104	1.745	10.05	0.9288
TM III	133	0.592	11.761	0.9976
TM IV	162	1.345	25.329	0.9987
TM IV	165	0.573	15.196	0.9997
TM IV	166	0.55	10.039	0.9981
TM IV	169	1.248	7.724	0.9564
TM V	209	0.67	3.379	0.9112
TM V	213	2.765	16.96	0.9511
TM V	214	0.581	4.836	0.9699

FEL						
Location	**Position**	**alpha**	**beta**	**LRT**	**Selection detected**	**P value < 0.05**
N-terminal	14	0	4.656	5.68	Positive	0.0172
TM I	41	0	4.313	5.428	Positive	0.0198
TM I	46	6.451	0	8.632	Negative	0.0033
TM II	80	4.994	0	8.646	Negative	0.0033
TM II	94	4.882	0	8.364	Negative	0.0038
TM II	95	0	4.665	4.166	Positive	0.0412
TM III	119	7.952	0	9.768	Negative	0.0018
TM III	122	6.262	0	7.643	Negative	0.0057
TM III	133	0	7.472	7.528	Positive	0.0061
TM III	138	3.916	0	5.571	Negative	0.0183
Extracellular loop	142	3.72	0	4.751	Negative	0.0293
TM IV	152	6.127	0	6.773	Negative	0.0093
TM IV	162	1.557	15.709	9.318	Positive	0.0023
TM IV	163	7.49	1.256	5.711	Negative	0.0169
TM IV	165	0	10.07	11.264	Positive	0.0008
TM IV	166	0	6.92	8.172	Positive	0.0043
TM IV	167	19.188	0	22.657	Negative	0
Extracellular loop	197	3.913	0	6.338	Negative	0.0118
TM V	200	12.782	0	14.933	Negative	0.0001
TM V	202	10.033	1.726	6.368	Negative	0.0116
TM V	208	8.876	0	9.869	Negative	0.0017
TM V	215	2.678	0	3.892	Negative	0.0485

TM V	217	0.569	17.989	1
TM V	218	0.558	8.482	0.9969
TM VI	263	1.444	9.146	0.9476
TM VII	290	0.636	11.621	0.9957
TM VII	292	0.613	5.491	0.9742
TM VII	297	1.778	15.48	0.9889
TM VII	299	1.667	15.487	0.9897

TM V	216	4.477	0	5.916	Negative	0.015
TM V	217	0	13.117	14.862	Positive	0.0001
TM V	218	0	5.925	6.759	Positive	0.0093
TM V	223	12.61	0	12.916	Negative	0.0003
TM V	228	4.218	0	6.394	Negative	0.0114
Extracellular loop	232	6.447	0	7.745	Negative	0.0054
TM VI	245	5.089	0	7.747	Negative	0.0054
TM VI	254	2.685	0	4.499	Negative	0.0339
TM VI	269	3.838	0	5.541	Negative	0.0186
TM VII	290	0	7.792	6.484	Positive	0.0109
TM VII	299	1.951	10.458	4.207	Positive	0.0402
Extracellular loop	323	9.238	0	11.237	Negative	0.0008
Extracellular loop	339	5.873	0	7.419	Negative	0.0065
Extracellular loop	340	6.285	0	7.787	Negative	0.0053
Extracellular loop	341	8.727	0	11.705	Negative	0.0006
Extracellular loop	348	5.896	0	7.435	Negative	0.0064
Extracellular loop	351	2.429	0	4.234	Negative	0.0396

TM: transmembrane alpha-helix.

CHAPTER 2

Visual opsin gene expression evolution in the adaptive radiation of cichlid fishes of Lake Tanganyika

Virginie Ricci, Fabrizia Ronco, Nicolas Boileau & Walter Salzburger

Science Advances (2023)


Science
Advances
8 SEPTEMBER 2023
AAAS

SCIENCE ADVANCES | RESEARCH ARTICLE

EVOLUTIONARY BIOLOGY

Visual opsin gene expression evolution in the adaptive radiation of cichlid fishes of Lake Tanganyika

Virginie Ricci[1]*, Fabrizia Ronco[1,2], Nicolas Boileau[1], Walter Salzburger[1]*

Tuning the visual sensory system to the ambient light is essential for survival in many animal species. This is often achieved through duplication, functional diversification, and/or differential expression of visual opsin genes. Here, we examined 753 new retinal transcriptomes from 112 species of cichlid fishes from Lake Tanganyika to unravel adaptive changes in gene expression at the macro-evolutionary and ecosystem level of one of the largest vertebrate adaptive radiations. We found that, across the radiation, all seven cone opsins—but not the rhodopsin—rank among the most differentially expressed genes in the retina, together with other vision-, circadian rhythm–, and hemoglobin-related genes. We propose two visual palettes characteristic of very shallow- and deep-water living species, respectively, and show that visual system adaptations along two major ecological axes, macro-habitat and diet, occur primarily via gene expression variation in a subset of cone opsin genes.

INTRODUCTION

Animals perceive a range of abiotic and biotic environmental cues through one or several of their sensory systems (*1*–*3*). This ability to monitor—and to situationally respond to—their surroundings is key to animal survival, which in turn exposes the different components of sensory systems, and hence the genes and genetic networks underlying them, to strong selection (*4*–*7*).

In many animal species, the visual sensory system is central to a number of vital tasks including orientation, navigation, foraging, predator avoidance, communication, mate choice, and circadian rhythm adjustment (*8*–*10*). The primary sensory organ of the visual system is the eye, which is present—in varying forms and levels of complexity—in almost all animal phyla (*11*–*13*). Eyes convert visual stimuli into neuronal signals. This "phototransduction cascade" is initiated through the light-induced isomerization of a photon-sensitive nonprotein chromophore (retinal) that is covalently bound to a visual opsin protein to form the visual pigment contained in the photoreceptor cells in the retina, the multilayered neural tissue lining the eye's inner surface (*10*, *14*–*17*). The specific waveband of light absorbed by a visual pigment—typically indicated by the maximal spectral sensitivity (λ_{max})—is mainly determined by the type of visual opsin protein (*18*–*20*).

In the vertebrate eye, two basic kinds of photoreceptor cells are present in the retina, the cone photoreceptor cells responsible for photopic (color) vision under bright-light conditions and the rod photoreceptors accounting for scotopic vision in dim light (*14*). At the molecular level, vertebrates are equipped with an ancestral set of five types of visual opsin genes: four cone opsins that form visual pigments sensitive to the ultraviolet (UV) (*SWS1*), the violet-blue (*SWS2*), the green (*RH2*), and the red (*LWS*) wavebands of the light spectrum, plus typically a single rod opsin (*RH1*) [(*10*, *14*, *18*, *19*, *21*, *22*), but see (*23*)]. The evolution of visual opsin genes has been more dynamic in teleost fishes than in other vertebrate clades, which is evident—among other things—from the expansion of the visual opsin gene repertoire to a median number of six cone opsins in teleosts (compared to two to four in most tetrapods) and a record number of 38 rod opsins in the deep-sea silver spinyfin (*10*, *23*–*25*). The greater diversity and complexity of the visual opsin gene repertoire is likely a response to the greater diversity of light environments that fishes are exposed to.

In aquatic environments, light is absorbed and scattered in the water column as a function of wavelength and depth, which is due to the optical properties of water in combination with other factors such as phytoplankton content, dissolved organic matter, and silt (*26*–*28*). In general, a broad-spectral waveband ranging from UV to red light is available in shallow waters, whereas in deeper waters a narrower spectrum remains, with a prevalence of blue and blue-green hues (*27*–*29*). In line with this, many organisms living in the aquatic realm feature specific adaptations of their visual systems that function to better match the ambient light conditions (*10*, *14*, *21*, *23*, *30*–*38*). With respect to teleost fishes, a variety of scenarios have been documented on how they can maximize their visual performance in a given environmental context (*10*, *23*, *32*, *39*). These include adaptive modifications in eye size and/or morphology, lens structure, photoreceptor compositions, and layering of the retina (*40*, *41*); adaptive changes in visual opsin gene sequences (*30*, *37*, *42*); the expansion of the visual opsin gene repertoire coupled with functional diversification (*23*, *24*, *43*–*45*); and changes in expression levels of the different visual opsin genes (*46*–*49*).

Here, we scrutinized the nature of visual adaptations across one of the most notable examples of adaptive radiation and explosive diversification, the cichlid fishes of African Lake Tanganyika (*50*–*53*). Approximately 240 cichlid species have evolved in this lake from a common ancestor in less than 10 million years, occupying a wide range of habitat and feeding niches and varying greatly in species-specific morphological, behavioral, and life-history traits. Cichlids rely, in principle, on a dichromatic to tetrachromatic color vision system and have seven cone opsins plus one rod opsin (Nile tilapia: *SWS1*, λ_{max} = 360 nm; *SWS2B*, λ_{max} = 425 nm; *SWS2A*[α], λ_{max} = 456 nm; *RH2B*, λ_{max} = 472 nm; *RH2A*β, λ_{max} = 517 nm; *RH2A*α, λ_{max} = 528 nm; *LWS*, λ_{max} = 560 nm; *RH1*, λ_{max} = 516 nm) (*10*, *23*, *32*, *54*, *55*). The arrangement of photoreceptor cells in the retina was further shown to vary between

[1]Zoological Institute, Department of Environmental Sciences, University of Basel, Basel, Switzerland. [2]Natural History Museum, University of Oslo, Oslo, Norway.
*Corresponding author. Email: virginie.ricci@unibas.ch (V.R.); walter.salzburger@unibas.ch (W.S.)

cichlid species, resulting in different mosaic arrangements of rods, single and double cones (two joined single cones), with single cones typically expressing short wavelength–sensitive opsins (*SWS1*, *SWS2A*, and *SWS2B*) and double cones expressing medium to long wavelength–sensitive ones (*RH2A*α, *RH2A*β, *RH2B*, and *LWS*) (*10*, *32*, *36*). Among the available visual opsin genes, usually only a subset—often referred to as visual palette—is expressed at a given life stage (*31*, *36*, *39*, *47*, *48*, *54*, *56*, *57*). Since the reinspection of whole-genome data from virtually all cichlid species in Lake Tanganyika (*52*) did not reveal evidence for gene duplications or strong signals of positive selection [$d_N/d_S < 1$, but see (*58*)] in any of the visual opsin genes (see below), we here focused on gene expression dynamics and produced 753 retinal transcriptomes in a phylogenetically, ecologically, and phenotypically representative set of 112 cichlid species endemic to Lake Tanganyika (that is, close to half of the lake's cichlid fauna) to (i) identify likely adaptive changes in the expression of vision-related genes, (ii) define putative visual palettes on the basis of cone opsin expression profiles and reconstruct their evolution, and (iii) test for an association between opsin expression levels and the species' macrohabitat, feeding ecology, as well as a vision-related phenotype, eye size.

RESULTS

To investigate visual opsin and overall retinal gene expression dynamics in the adaptive radiation of cichlid fishes of Lake Tanganyika, we generated 753 transcriptome profiles from retinal tissue of 112 species covering all 12 cichlid tribes endemic to that lake plus one Haplochromini species from the Lake Tanganyika drainage, and one representative each of the more widespread tribes Oreochromini and Tylochromini that are not part of the in situ radiation but colonized the lake secondarily (see table S1 for details on specimens) (*52*). To account for sex and intraspecific differences, we collected at least three males and three females per species, whereby samples were taken at roughly the same time of the day whenever possible. For each specimen, total RNA extracted from the retina of a single eye was sequenced on Illumina NovaSeq 6000 [TruSeq standard protocol with 100 base pairs (bp) paired end; median number of sequenced reads per sample = 19,537,332; fig. S1A and table S2] after RiboZero Gold ribosomal RNA (rRNA) depletion (Illumina). As in our previous work (*59*), the individual RNA reads of every library were mapped to the phylogenetically equidistant—with respect to the ingroup taxa—*Oreochromis niloticus* reference genome (RefSeq accession GCF_001858045.2; female) to infer which genes were expressed and at which levels. After selection of protein-coding and long noncoding RNA (lncRNA) features and removal of lowly expressed genes, the total read count in exonic features ranged from 32,854 to 7,643,707 per library (median = 2,383,349; fig. S1B and table S2), and the number of expressed genes varied from 7952 (27.42%) to 28,068 (96.78%) (median = 22,087, total of 29,002 RNA features; fig. S1C and table S2). The variation in read counts and numbers of expressed genes between samples was mainly explained by differences in the number of sequenced reads and the rRNA contents (fig. S2).

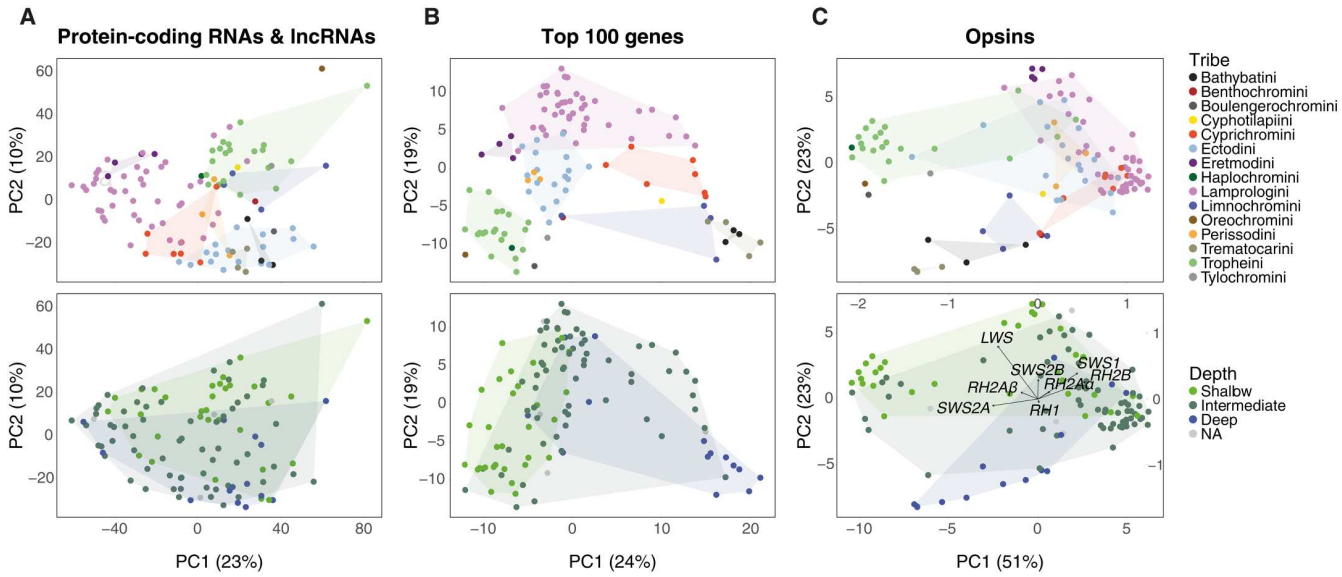

Fig. 1. Retinal gene expression patterns in Lake Tanganyika cichlid fishes. PCAs of (**A**) overall gene expression levels (protein-coding RNAs and lncRNAs combined), (**B**) gene expression levels of the top 100 genes with the greatest variance in gene expression, and (**C**) visual opsin gene expression levels. Each dot represents the weighted mean value of a given species and is color-coded according to the tribe that a species belongs to (top) or the depth category at which a species occurs (bottom; NA indicates that the depth of occurrence is unknown for the species in question, or that the three depth categories do not adequately capture the ecology of a given species). Tribal assignments and tribe color-coding follow (*52*). Tribal and depth ranges are indicated with convex hulls (except for NAs). The loadings of PC1 and PC2 are indicated in the PCA plot of visual opsins color-coded by depth in (C). The variance explained by each principal component is reported in parenthesis. PCA plots of protein-coding RNAs and lncRNAs combined and visual opsins at the individual level are available on Dryad (https://datadryad.org/stash/dataset/doi:10.5061/dryad.r2280gbj2).

The visual opsin gene repertoire of Lake Tanganyika cichlids

Before investigating the expression of visual opsin genes, we confirmed the presence of seven cone opsins (*SWS1*, *SWS2B*, *SWS2A*, *RH2B*, *RH2A*β, *RH2A*α, and *LWS*) and one rhodopsin (*RH1*) in the genomes of Tanganyikan cichlids. A reexamination of the results of our previous gene duplication analysis based on 488 genomes (246 taxa) (*52*) revealed no evidence that any particular visual opsin gene was duplicated in any of the studied cichlid species. When applying our cichlid-tailored opsin raw read mapping approach [results are available on Dryad: https://datadryad.org/stash/dataset/doi:10.5061/dryad.r2280gbj2; for results involving *RH1*, see (*30*)] to the cone opsins, we confirmed the presence of a single copy of each cone opsin gene—complete or "degenerated"—in 517 Lake Tanganyika cichlid genomes (271 species including outgroups). We also reinspected the results of our previous positive selection analysis based on 471 genomes (243 taxa) (*52*) and found no clear signs of positive selection ($d_N/d_S < 1$) in any of the cone opsins across the radiation [for results involving *RH1*, see (*30*)].

Gene expression patterns in the retina of Lake Tanganyika cichlids

To visualize transcriptome-wide patterns of gene expression differentiation in the retinal tissue of Lake Tanganyika cichlids, we performed a principal components analysis (PCA) on the basis of weighted species mean values measured as normalized read counts using the variance stabilizing transformation method (VST; Fig. 1 and fig. S3) (PCA plots at the individual level are available on Dryad: https://datadryad.org/stash/dataset/doi:10.5061/dryad.r2280gbj2). Like in all other tissues investigated so far across the adaptive radiation of cichlid fishes in Lake Tanganyika (*59*), a strong phylogenetic signal was recovered in the retinal gene expression profiles, with species mainly clustering according to tribes and only to a moderate degree according to water depth of occurrence (Fig. 1A). The only representative of the Haplochromini (*Astatotilapia burtoni*) clustered with members of the Tropheini, with whom it shares a common ancestor (*60*). *Oreochromis tanganicae* (Oreochromini) and *Interochromis loocki* (Tropheini) appeared separate from the rest of the species, which was, however, not the case for the phylogenetically most distant species (*Tylochromis polylepis*; Tylochromini), which clustered with Tropheini representatives. The PCA based on protein-coding RNAs alone (25,335 features; fig. S3A) largely recovered the global gene expression patterns, which is not surprising given that protein-coding RNAs accounted for 87.36% of the expressed genes in our dataset. The PCA based on lncRNAs (3667 features; 12.64% of the expressed genes; fig. S3B) recovered an even stronger phylogenetic signal with very little overlap between tribes.

To focus on the most differentially expressed genes in our dataset, we performed PCAs based on the top 100 (Fig. 1B and table S4) and the top 500 genes (fig. S3C) with the greatest variance in gene expression. In both PCAs, species generally clustered by tribe with little (top 100 genes) to moderate (top 500 genes) overlap between tribes. At the same time, we found a clear separation between species with respect to the water depth at which they occur, with little overlap between shallow- and deep-water living species, except for one deep-water species (*Plecodus paradoxus*, Perissodini) that clustered with shallow-water representatives (along PC1 accounting for 24% of the variance in the top 100 genes, Fig. 1B, and PC2 accounting for 16% of the variance in the top 500 genes, fig. S3C). All seven cone opsin genes (but not the rod opsin, *RH1*; table S3) ranked within the top 37 genes with the greatest variance in expression (five of the cone opsins were in the top 12 genes; table S4), with the red-sensitive opsin (*LWS*) being the single-most differentially expressed gene in the retina of Lake Tanganyika cichlids overall. In addition to visual opsins, 14 of the top 100 genes have a known function related to vision, including retinal phosphodiesterase subunit genes and rhodopsin kinases (table S4). Moreover, there were eight hemoglobin subunit genes among the top 18 genes (table S4), indicating that in Tanganyikan cichlids, hemoglobin genes are differentially expressed along the depth gradient. This result is compatible with the finding that hemoglobin genes in Lake Malawi cichlids have experienced divergent selection with respect to depth (*61*, *62*). Since the retinal tissue is avascular in most vertebrates (*63*, *64*), we suspect that the hemoglobin genes are not expressed in the retina itself, but in the blood vessels nourishing it (*65*). Last, five genes with a putative function in circadian rhythm regulation, which also depends on light detection in (cichlid) fishes (*10*, *66*, *67*), ranked among the top 80 genes (table S4).

In a third step, we focused exclusively on the visual opsin gene expression profiles and performed a PCA based on the expression information from the seven cone and the single rod opsins (Fig. 1C) (PCA plots at the individual level are available on Dryad: https://datadryad.org/stash/dataset/doi:10.5061/dryad.r2280gbj2). In the same way as in the PCAs of the top 100 (Fig. 1B) and top 500 (fig. S3C) genes with the greatest variance in gene expression, species clustered according to tribes with overlap between some of the tribes, but also with respect to depth of occurrence (in this case mainly represented by PC2 accounting for 23% of the variance; Fig. 1C).

Opsin expression profiles and visual palettes

To examine interspecific differences in the expression of visual opsin genes, as well as to discriminate between rod and cone and between single and double cone opsin expression profiles, we calculated the relative proportion that each individual opsin gene contributed to the total pool of visual opsin genes expressed in a given species [as weighted species means based on TPM (transcripts per million)]. This proportion was calculated twice, once correcting the *RH2A*α/*RH2A*β proportion to account for the high degree of exonic sequence identity between these genes (Fig. 2 and table S3) and once without such a correction, leading to very similar results (fig. S4). Overall, very little variation in visual opsin gene expression profiles was found between specimens of the same species (barplots at the individual level are available on Dryad: https://datadryad.org/stash/dataset/doi:10.5061/dryad.r2280gbj2). Between species, however, our analyses revealed substantial differences with respect to the relative amount of rod versus cone opsin expression, and the number and relative proportion of visual opsin genes expressed in single and double cones (Fig. 2, figs. S4 and S5, and table S5): In all but two Eretmodini species (*Tanganicodus irsacae* and *Spathodus erythrodon*), the rod opsin (*RH1*) contributed to more than half of the total opsin expression in the retina (minimum, 42.90%; median, 82.55%; mean, 81.91%; maximum, 98.05%). The species expressing *RH1* the most (>90%) belonged mainly to the tribes Bathybatini, Boulengerochromini, Ectodini, and Trematocarini, which mostly occur at intermediate to greater water depths. Among the cone opsins, we found that double cone opsins

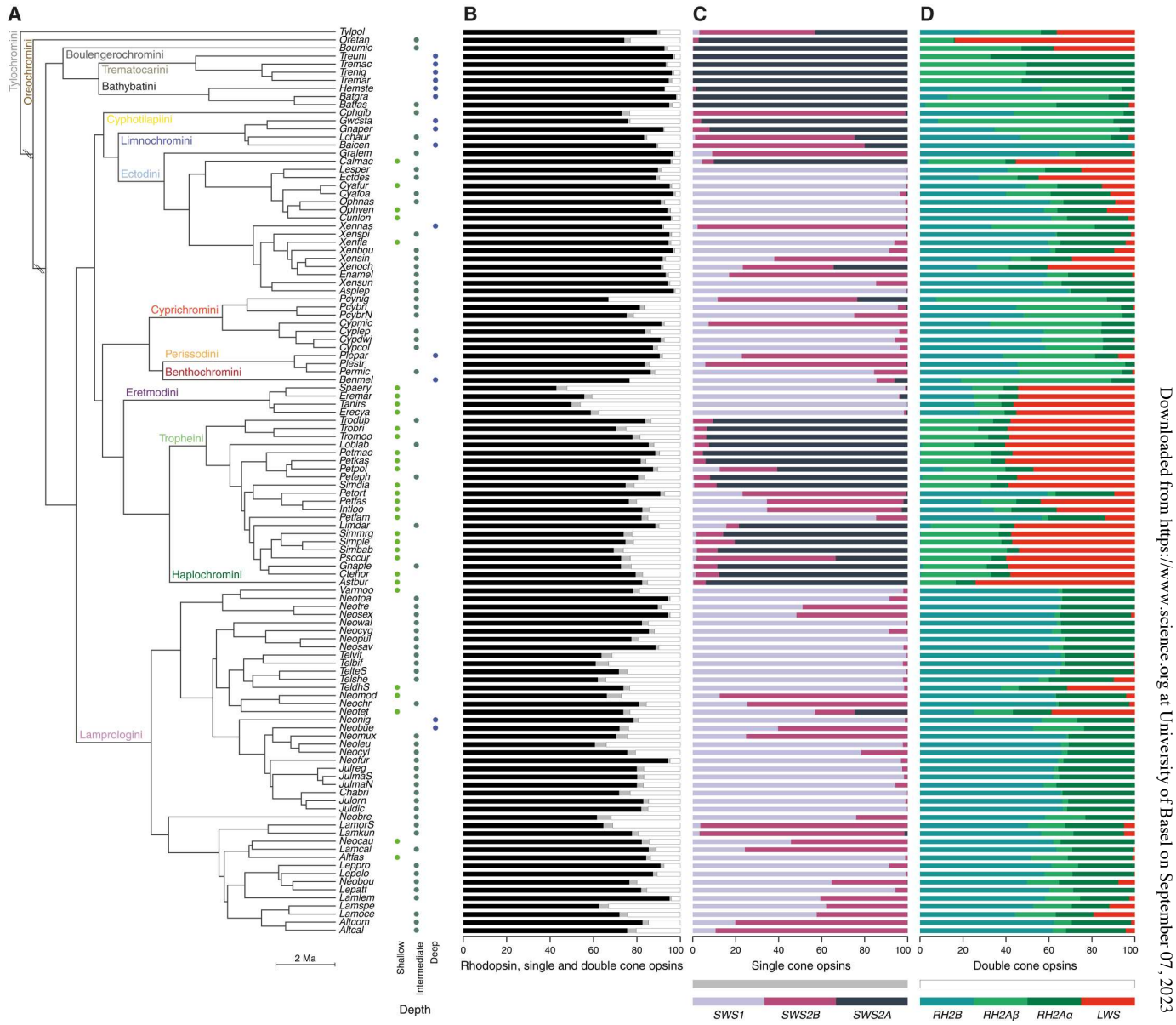

Fig. 2. Visual opsin gene expression profiles along the species tree of Lake Tanganyika cichlids. (**A**) Time-calibrated species tree of the cichlid fishes of Lake Tanganyika [taken from (*52*)], pruned to the focal taxa of this study (see table S1 for full species names, branches indicated with "\\" are not drawn to scale). For each species, the depth of occurrence—in three depth categories—is indicated and color-coded (absence of a dot indicates that the depth of occurrence is unknown for the species in question, or that the three depth categories do not adequately capture the ecology of a given species). (**B**) Relative proportions of rhodopsin versus cone opsin expression per species. (**C**) Relative proportions of single cone opsin expression per species. (**D**) Relative proportions of double cone opsin expression per species. Cone opsins are color-coded according to their spectral sensitivity. Single cone opsins include the UV-sensitive *SWS1*, the violet-sensitive *SWS2B*, and the blue-sensitive *SWS2A*. Double cone opsins comprise the green-sensitive *RH2B*, *RH2Aα*, and *RH2Aβ*, as well as the red-sensitive *LWS*.

(minimum, 1.63%; median, 14.63%; mean, 15.62%; maximum, 52.27%) were, on average, expressed 6.7 times (median, 6.5) more than single cone opsins (minimum, 0.001%; median, 2.42%; mean, 2.47%; maximum, 6.67%). This number comes close to the ratio of single to double cone photoreceptor cells previously reported for cichlid retinas [retinal mosaic of 1:4; (*10*, *68*), but see (*36*)]. However, high-resolution retinal images [e.g., fluorescent in situ hybridization of the retina (*69*)] would be required to confirm that the proportion of expressed single and double cone opsins reflects the number of single and double cone photoreceptor cells. The majority of species expressed predominantly one of the three single cone opsin genes (≥80% *SWS1* expression, N = 47 species; ≥80% *SWS2A*, N = 26; ≥80% *SWS2B*, N = 11), and typically two double cone opsins were expressed to a much greater extent [≥80% *RH2B* + *RH2As*, N = 78; ≥80% *RH2As* + *LWS*, N = 21; ≥80% *RH2B* + *LWS*, N = 2; note that for analytical reasons and just like in previous studies

(*47*, *48*, *56*), *RH2Aα* and *RH2Aβ* were combined here and denoted as *RH2As*]. *Paracyprichromis nigripinnis* (Cyprichromini) and *Benthochromis melanoides* (Benthochromini) were the only two species with close to zero single cone opsin expression (TPM of single cone opsins smaller than 2.5 for both species), and the four Trematocarini species as well as *Baileychromis centropomoides* (Limnochromini) were the only species with one cone opsin representing more than 99% of the double cone opsin expression (*RH2As* and *RH2B*, respectively).

To examine patterns of expression correlation among the visual opsin genes, we tested for pairwise (evolutionary) correlations of gene expression levels across the radiation [Spearman's *r* of TPMs and on phylogenetically independent contrasts (PICs) thereof; figs. S6 with *RH2As* and S7 with *RH2Aα* and *RH2Aβ*]. We detected numerous positive and negative correlations in gene expression levels across the visual opsin genes (out of 28 tests, 18 were significantly correlated based on TPMs and 15 based on PICs). For example, the expression of *SWS1* is positively correlated with that of *RH2B*, and the expression of *RH1* is negatively correlated with that of *RH2As* (fig. S6). We further observed that species tend to express a given opsin at the expense of one or more other opsins (e.g., *SWS1* versus *SWS2A* and *SWS2A* versus *RH2B*) and that this tendency is mainly driven by the distinct subset of expressed single cone opsin genes between species belonging to the tribes Bathybatini, Trematocarini, and Tropheini and the species of the remaining tribes (Fig. 2 and figs. S6 and S7).

Next, we used the cone opsin expression information to delineate visual palettes in cichlid fishes in Lake Tanganyika with two methods: (i) using the respective combinations of the most highly expressed single cone opsin and the two most highly expressed double cone opsins ("SDD majority-rule clustering") and (ii) using hierarchical clustering with a number of clusters (*k*) ranging from three to eight (fig. S8). Overall, our results revealed that most of the Tanganyikan cichlids express one of the three common visual palettes previously identified in cichlids (*31*, *47*, *56*, *70*), a short- (*SWS1* + *RH2B* + *RH2As*; present in 49 species with the SDD majority-rule clustering and in 50 species with $k = 3$ in the hierarchical clustering analysis), a middle- (*SWS2B* + *RH2B* + *RH2As*, 22 species with SDD; 34 species with $k = 3$), or a long-wavelength palette (*SWS2A* + *RH2As* + *LWS*, 18 species; 25 species with $k = 3$; Fig. 3 and figs. S8B and S9). When compared to previous findings (*47*), we were only able to reaffirm the visual palettes of 7 (using the hierarchical clustering with $k = 3$) out of 19 commonly studied species with our more sensitive detection method (RNA sequencing versus real-time quantitative polymerase chain reaction), our approximately twice as large sample size per species, and our exclusive use of specimens from the wild.

According to the SDD majority-rule clustering, there is evidence for the presence of five additional discrete visual palettes in Tanganyikan cichlids, including a shallow-water visual palette (*SWS1* + *RH2B* + *LWS*) that is exclusive to *Telmatochromis dhonti* (Lamprologini) and the four Eretmodini species investigated in our study, and a deep-water visual palette (*SWS2A* + *RH2B* + *RH2As*) exclusively expressed in eight species of the tribes Bathybatini, Limnochromini, and Trematocarini (Fig. 3 and fig. S8). Further, we found that the shallow- and deep-water visual palettes include three combinations of most highly expressed genes each (based on the majority-rule clustering of the complete set of single and double cone opsins; fig. S10). In addition, six other such combinations were depth-specific (*SWS2B* + *RH2B* + *RH2As*, two; *SWS2B* + *RH2B* + *LWS*, two; *SWS2A* + *RH2As* + *LWS*, two; fig. S10). The eight putative visual palettes suggested by the SDD majority-rule clustering are supported by a PCA based on the expression information of the cone opsin genes, which separated the different palettes, in particular along PC1 and PC3 (Fig. 3B and fig. S11, A to C). Future research, for example, using high-resolution imaging or single-cell gene expression information, would be necessary to validate the visual palettes.

We then performed ancestral state reconstructions on the basis of the visual palettes defined in this study and the time-calibrated species tree [taken from (*52*)] to investigate and compare turnovers between visual palettes. This was done once with the eight visual palettes identified with the SDD clustering (Fig. 3C) and once using the three visual palettes identified with the hierarchical clustering at $k = 3$ (fig. S9C). We found that at least three (when considering a total of eight visual palettes; Fig. 3, A and C) to five (when considering three visual palettes; fig. S9, A and C) transitions from another state to the short-wavelength palette occurred in the course of the cichlid radiation in Lake Tanganyika. According to these analyses, the long-wavelength visual palette emerged at least four times (Fig. 3, A and C, and fig. S9, A and C). The middle-wavelength palette arose at least 16 to 17 times, and from the short-wavelength palette in all but one case with the SDD clustering (in the Tropheini clade: *Petrochromis orthognathus*) and three cases with the hierarchical clustering at $k = 3$ (in the Tropheini clade: *P. polyodon*; *P. orthognathus*, *P. fasciolatus*, and *I. loocki*, and *Pseudosimochromis curvifrons*) (Fig. 3, A and C, and fig. S9, A and C). The shallow- and deep-water palettes are likely to have evolved twice each (Fig. 3C). An ancestral state reconstruction (phylomorphospace) based on a PCA of the expression information of the cone opsin genes and the species tree (*52*) supported the repeated evolution of the visual palettes within different clades (fig. S11, D to F), most clearly visible when PC1 and PC3 are compared (fig. S11E).

Ecological and morphological correlates of visual opsin gene expression

To test whether, at the macroevolutionary scale of an adaptive radiation, there is an association between the expression of visual opsin genes and ecological and morphological parameters, we performed linear regression (lm) and phylogenetic generalized least squares (pGLS) analyses, using available ecological and morphological data from the different Tanganyikan cichlid species and the time-calibrated species tree (*52*). Specifically, we tested for an association between individual visual opsin gene expression profiles and the stable carbon (C) and nitrogen (N) isotope composition as approximations for the relative position of a species along the benthic(littoral)–(deep)pelagic (from therein benthic-pelagic) macrohabitat axis ($\delta^{13}C$ value) (fig. S12) and the relative trophic level ($\delta^{15}N$ value) (fig. S13), respectively, as well as the relative eye size (fig. S14) as a putatively adaptive morphological trait in the context of vision [eye size data were extracted from morphometric analyses based on x-ray images from (*52*)]. In addition, to account for the multicollinearity of the expression profiles (see figs. S6 and S7), we fitted a phylogenetic partial least square regression (pPLS) for each of the eco/morphological proxies with all cone opsin expression profiles together. Our results showed that the expression of *RH2As* is positively associated with the benthic-pelagic trajectory ($\delta^{13}C$; see Fig. 4A for the pPLS analysis; pGLS: $R^2 = 0.084$, $P =$

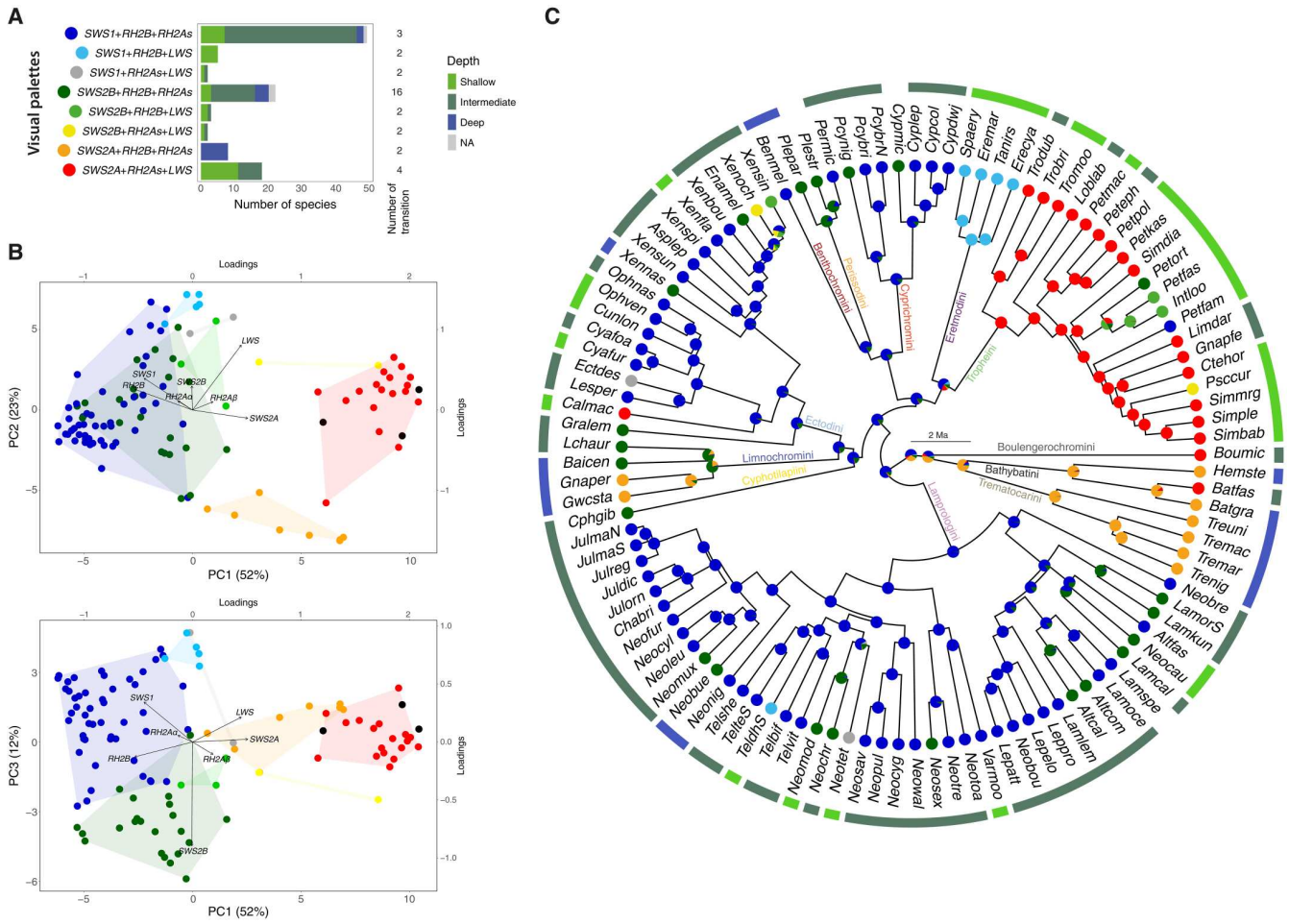

Fig. 3. Visual palette evolution in Lake Tanganyika cichlid fishes. (**A**) Barplot showing the number of species sharing one of the eight visual palettes identified based on the species-specific combinations of the most highly expressed single cone opsin and the two most highly expressed double cone opsins (SDD majority-rule clustering). Barplots are color-coded according to the respective proportion of species in the three depth categories at which the species occur. The number of evolutionary transitions into the respective visual palette according the ancestral state reconstruction shown in (C) is indicated on the right margin. (**B**) PCAs of the visual cone opsin gene expression levels. Each dot represents the weighted mean value of a given species and is color-coded according to the visual palettes defined in (A). The range of the visual palettes across the PCAs is indicated with convex hulls (except for *A. burtoni*, *O. tanganicae*, and *T. polylepis*). The loadings for PC1 and PC2 are represented with a black arrow. The variance explained by each principal component (PC) is reported in parenthesis. (**C**) Ancestral state reconstruction of visual palettes along the time-calibrated species tree [taken from (*52*) and pruned to the species included in this study (see table S1 for full species names]. Pie charts at the internal nodes indicate the relative posterior probability that the ancestor expressed each of the eight visual palettes and are color-coded according to the visual palettes shown in (A). Note that, just like in previous studies (*47*, *48*, *56*), *RH2A*α and *RH2A*β were combined under the category *RH2As*, and that the primarily riverine haplochromine *A. burtoni* as well as the more distantly related species *O. tanganicae* and *T. polylepis* were excluded from this analysis.

0.0022, λ = 0.85, fig. S12). Hence, species living in more shallow-water habitats express proportionally less *RH2As*, whereas species living in more pelagic and/or more deeper-water habitats express more *RH2As*. Further, we found that the negatively correlated single cone opsins *SWS1* and *SWS2A* (see Fig. 1C and fig. S6) are associated with the feeding ecology of the species (δ^{15}N; see Fig. 4B for the pPLS and fig. S13 for the pGLS analyses). More specifically, *SWS1* is proportionally overexpressed at lower trophic levels (pGLS: $R^2 = 0.09$, $P = 0.0014$, λ = 0.99; fig. S13) and *SWS2A* is proportionally overexpressed at higher trophic levels (pGLS: $R^2 = 0.09$, $P = 0.0015$, λ = 1; fig. S13). Last, our analyses uncovered a positive association between *RH1* expression and relative eye size (see Fig. 4C and fig. S14; pGLS: $R^2 = 0.09$, $P = 0.0015$, λ = 0.76).

DISCUSSION

The fine-tuning of the visual sensory system to better match the ambient light conditions is essential for the survival of many animal species and can be achieved through a number of molecular mechanisms including the duplication, functional diversification, and differential expression of visual opsin genes (*6*, *7*, *10*, *32*). In the present study, we report the sequencing and in-depth examination of 753 retinal transcriptomes from 112 endemic species of cichlid fishes from Lake Tanganyika with the aim to provide an understanding of (visual opsin) gene expression evolution in the macro-evolutionary context of a massive adaptive radiation.

At the whole retinal transcriptome level—that is, all protein-coding RNAs and lncRNAs combined, but also when protein-

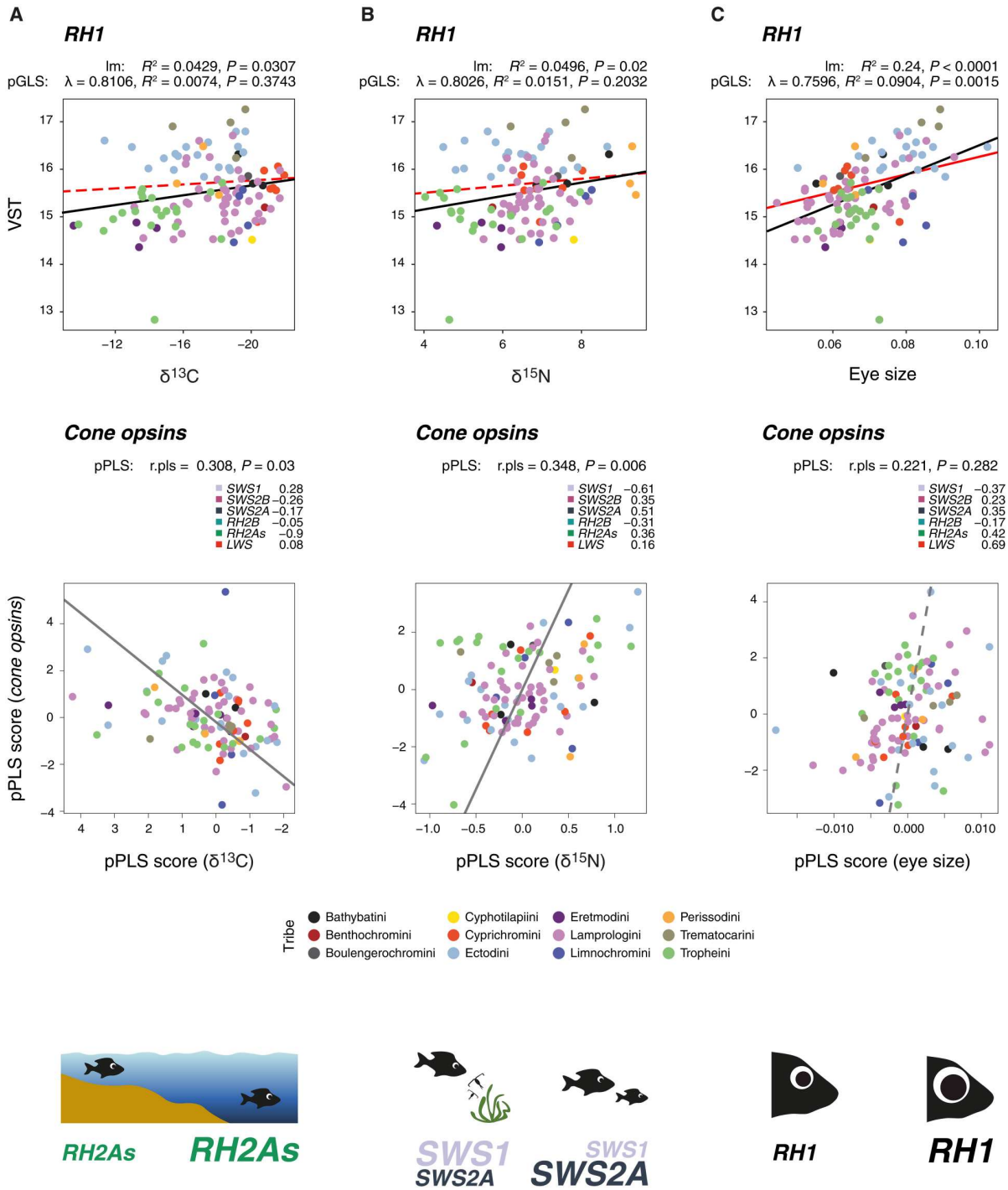

Fig. 4. Visual opsin gene expression and its association with macrohabitat, feeding ecology, and eye size. lm, pGLS, and pPLS analyses showing the associations between visual opsin gene expression (VST-normalized count) and (**A**) $\delta^{13}C$ values as habitat proxy for a species' position along the benthic-pelagic axis, (**B**) $\delta^{15}N$ values as proxy for the relative trophic level of a species, and (**C**) relative eye size. The top three panels show the association of rhodopsin (*RH1*) with the respective traits. The lm-fit is depicted in black, and the pGLS-fit is depicted in red (at $P < 0.05$ with a solid line). For each test, the *P* value (*P*) and the R-squared (R^2) are indicated, as well as the parameter lambda (λ) for the pGLS. The bottom three panels show scatter plots of the pPLS of the cone opsins and the ecological and morphological traits. The pPLS-fit is depicted as a gray line (at $P < 0.05$ with a solid line). The corresponding pPLS coefficient (r-PLS) and the *P* value (*P*) along with the PLS loadings are indicated above each plot. Each dot represents a species and is color-coded according to tribe. The tests for an association of individual cone opsin expression level and each ecological/morphological trait are provided in the Supplementary Materials as figs. S12 to S14. The primarily riverine haplochromine *A. burtoni* as well as the more distantly related species *O. tanganicae* and *T. polylepis* were excluded from this analysis.

coding features and lncRNAs are considered individually (Fig. 1 and fig. S3)—our results confirm the general trend in vertebrates (*71*), including in cichlids (*59*), that the transcriptome-wide patterns of gene expression differentiation in a given tissue mirror phylogeny. However, unlike in the other tissues that have been investigated in such a detail and with a similar taxonomic coverage across the adaptive radiation of cichlid fishes in Lake Tanganyika (brain, gills, liver, ovary/testis, and lower pharyngeal jaw bone) (*59*), there is no such clear separation in global gene expression patterns in retinal tissue between the Lamprologini—the most species-rich cichlid tribe in Lake Tanganyika—and the rest of the radiation.

In aquatic ecosystems of sufficient depth, the light environment changes most along the depth gradient, which is due to the optical properties of water (*27*, *28*). While a water depth–related pattern is not apparent from the PCA of overall gene expression levels in the cichlid assemblage of Lake Tanganyika (Fig. 1A), there is an obvious separation between shallow- and deep-water living species when only the top 100 (Fig. 1B) or the top 500 genes (fig. S3C) with the greatest variance in our dataset, or only the visual opsin genes (Fig. 1C), are considered. All seven cone opsins rank among the top 100 most differentially expressed genes in the retina, with *LWS* being the single-most differentially expressed gene overall and all cone opsin genes ranking in the top 37 genes (table S4). In addition to the cone opsins, we also found 14 other vision-related genes, plus 5 genes with a known function in circadian rhythm regulation, and 8 hemoglobin subunit genes (likely expressed in the retinal vasculature) among top 100 most differentially expressed genes. Together, this suggests that in cichlids from Lake Tanganyika, gene-regulatory processes may have played a crucial role in the repeated (Fig. 3) and rapid (in less than 10 million years) adaptations of the retina to deep-water conditions characterized by light of a narrower spectral waveband and reduced levels of dissolved oxygen.

In contrast to the cone opsins that mediate color discrimination, the rod opsin (*RH1*) responsible for scotopic vision is not in the top 100 most differentially expressed retinal genes across the Tanganyikan cichlid fauna (it ranks at position 849). *RH1* is by far the most highly expressed visual opsin gene in Tanganyikan cichlids (>50% of the total visual opsin expression levels in all species except for two Eretmodini representatives; median, 82.55%; mean, 81.91%; Fig. 2 and table S5), which is most likely due to the comparatively larger number of rod photoreceptor cells compared to cones in the cichlid retina (*10*, *68*). We also found that *RH1* expression levels are associated with relative eye size (Fig. 4C), suggesting that bigger eyes either contain proportionally more rods expressing *RH1* at similar levels as in smaller eyes or contain rods that express proportionally more *RH1*. In any case, relative *RH1* expression levels do not significantly scale with our proxy for the benthic-pelagic axis (the stable carbon isotope signature; Fig. 4A), nor is there an obvious association with species-specific water depth categories (Fig. 2 and fig. S5). Instead, it has previously been shown that specific amino acid substitutions in *RH1*, often at so-called key tuning sites, correlate strongly with water depth in cichlids from lakes Malawi and Tanganyika (*30*, *72*, *73*). This suggests that the fine-tuning of scotopic vision along the depth gradient—for which in Tanganyikan cichlids (*30*), just as in most other vertebrate species (*14*, *21*), only one single opsin (*RH1*) is responsible—is primarily achieved via adaptive modifications of the *RH1* coding sequence, whereas the fine-tuning of photopic vision, which involves up to seven cone opsin genes in cichlids (*47*, *48*), seems to involve changes in their expression levels. Future studies should examine the cone opsin coding sequences in more detail in Lake Tanganyika cichlids, also with respect to adaptive changes at putative key tuning sites.

Overall, we found that all studied cichlid species from Lake Tanganyika expressed *RH1* as well as the cone opsins *SWS2B*, *RH2B*, *RH2Aα*, and *RH2Aβ* (Fig. 2 and table S5), which cover, together with *SWS2A*, the central waveband of the visible light spectrum. On the other hand, six species did not express *SWS1* (Bathybatini: *Bathybates fasciatus*, *Hemibates stenosoma*; Boulengerochromini: *Boulengerochromis microlepis*; Limnochromini: *Gnathochromis permaxillaris*, *Limnochromis staneri*; Trematocarini: *Trematocara nigrifrons*), of which only *B. microlepis* is not strictly living in deeper waters and *T. nigrifrons* lives in the depth and migrates during the night into shallower zone of the lake; for three species living at intermediate water depths, we did not find an expression signal for *SWS2A* (Ectodini: *Lestradea perspicax*, *Xenotilapia boulengeri*; Lamprologini: *Neolamprologus savoryi*), and four species had no *LWS* expression (Bathybatini: *H. stenosoma*; Lamprologini: *Neolamprologus pulcher*; Limnochromini: *G. permaxillaris*; Trematocarini: *Trematocara macrostoma*), which are all deep-water species except for *N. pulcher* living at intermediate depths. Two deep-water species (*G. permaxillaris* and *H. stenosoma*) thus lack expression of both the shortest- (*SWS1*) and the longest-wavelength sensitive (*LWS*) cone opsins. In one intermediate- and two deep-water species, we could further attribute the lack of expression to the pseudogenization of a particular cone opsin gene (*SWS2A* in *X. boulengeri*; *SWS1* in *T. nigrifrons*; *LWS* in *T. macrostoma*), suggesting that these species have transitioned from zero expression ("non-usage") of a cone opsin gene, as observed in a number of primarily deep-water living cichlid species in Lake Tanganyika (see above), to cone opsin loss ("degeneration"), as seen in many marine fish living at greater water depths (*23*, *25*).

A second major axis of expression differentiation in visual opsin genes in fishes occurs in response to differences in feeding ecology (*10*). By and large, we confirm previous results in Lake Malawi cichlids, where expression levels of the UV-sensitive *SWS1* correlate with food type, and algae and plankton eaters feature higher *SWS1* expression levels possibly enhancing UV vision (*47*, *48*, *74*, *75*). In our analysis of 112 Tanganyikan cichlid species, we found that *SWS1* shows a significant association with our proxy for trophic ecology, the stable nitrogen isotope signature, but we also found that *SWS2A* is associated with feeding ecology (Fig. 4B), with species at lower trophic levels expressing proportionally more *SWS1* and less *SWS2A*, and vice versa. Cichlid species at the lower end of the trophic chain (algae and plankton eaters) express more *SWS1*, confirming the increase of UV sensitivity to better detect the UV-absorbing zooplankton against a bright UV background (*47*, *48*, *75*). On the other hand, algae- and plankton-eating species express less *SWS2A*. Species express either *SWS1* or *SWS2A* (Fig. 4 and figs. S5 to S7), suggesting that these two single cone opsin genes might have a similar function (better detection of feeding items against the background).

In African cichlid fishes, visual opsin gene expression is typically categorized in the form of visual palettes, defined by the dominating single and the two most highly expressed double cone opsins (*31*, *36*, *47*, *48*, *56*). Three main visual palettes have so far been identified in cichlids: a short- (dominated by *SWS1* + *RH2B* + *RH2As*), a middle- (*SWS2B* + *RH2B* + *RH2As*), and a long-wavelength visual

palette (*SWS2A* + *RH2As* + *LWS*). In the present study, we confirm that most cichlid species from Lake Tanganyika express one of these three visual palettes (Fig. 3 and figs. S8 and S9). However, we provide evidence for at least two additional visual palettes that are associated with a particular light environment: (i) a visual palette dominated by the cone opsins having their peak spectral sensitivities at both ends of the visible light spectrum (*SWS1* + *RH2B* + *LWS*) characteristic of one Lamprologini and four Eretmodini species, which are all among the most shallow-water living cichlid species that occur in Lake Tanganyika, and (ii) a visual palette dominated by the cone opsins sensitive to the most central waveband of the spectrum (*SWS2A* + *RH2B* + *RH2As*) exclusive to deep-water living species of the tribes Bathybatini, Limnochromini, and Trematocarini (Fig. 3). Our ancestral state reconstruction of visual palettes along the time-calibrated species tree showed that numerous evolutionary transitions occurred between visual palettes in the course of the adaptive radiation of cichlid fishes in Lake Tanganyika (Fig. 3C and fig. S9C). The visual sensory system thus emerges as yet another highly dynamic trait complex in Lake Tanganyika cichlids, in addition to body shape (*52*), trophic morphology (*52*, *76*), body pigmentation (*52*), and sex determination systems (*77*).

Overall, we found that, at the macroevolutionary and ecosystem level of a massive adaptive radiation of cichlid fishes, changes in the expression of core components of the visual sensory system, the visual opsin genes, play a major role in visual adaptation. Through the examination of 753 retinal expression profiles in 112 closely related cichlid species from Lake Tanganyika, we identified three main axes of visual system tuning: (i) The visual system of shallow-water and more benthic cichlid species is characterized by proportionally lower expression levels of the green-sensitive *RH2A*s, whereas deeper living and more pelagic species express more *RH2A*s (Fig. 4A); (ii) cichlid species at the lower end of the trophic chain (algae and plankton eaters) express proportionally more of the UV-sensitive *SWS1* and less of the blue-sensitive *SWS2A,* whereas the opposite is true for more predatorial cichlids including the scale-eaters of the tribe Perissodini (Fig. 4B); and (iii) species with larger eyes express proportionally more *RH1* and vice versa (Fig. 4C). This suggests that, when the entire adaptive radiation of cichlid fishes in Lake Tanganyika is considered, adaptations to a particular light environment involve a trade-off in the relative levels of visual opsin gene expression between a subset of cone opsin genes [*RH2As* along the depth gradient, *SWS1* and *SWS2A* along the trophic level; Fig. 4]. Together, our in-depth examination of hundreds of retinal transcriptomes sheds light on the dynamics and the changes in the expression of visual opsin genes in the adaptive radiation of cichlid fishes in Lake Tanganyika.

MATERIALS AND METHODS

Experimental design

In this study, we sequenced 753 new retinal transcriptomes of 112 cichlid species from African Lake Tanganyika to (i) identify adaptive changes in the expression of rod and cone visual opsin genes, (ii) define and reconstruct the evolution of visual palettes on the basis of cone opsin expression levels, and (iii) examine rod and cone opsin expression levels in relation to macrohabitat, diet, and relative eye size.

Sampling and dataset

Sampling of fish eyes was performed between 2014 and 2020 at 44 locations at Lake Tanganyika covering the entire north-south axis of this approximately 670-km-long lake. Sampling and sample exportation were performed in accordance to the relevant permits issued by the (i) Ministère de l'Eau, de l'Environnement, de l'Aménagement du Territoire et de l'Urbanisme, Republic of Burundi (nr. 770 06/62710), the Université du Burundi (Cabinet du Recteur and Directeur de la Recherche et de l'Innovation; nr. 2014/R991), and the Permanent Mission of the Republic of Burundi to the United Nations, Geneva (work permits 544-547/GE/2014), for the Republic of Burundi; (ii) the Tanzania Commission for Science and Technology (COSTECH; research permits 2015-176-NA-2015 and 2016-373-NA-2015-96), the Tanzania National Parks Authority (TANAPA; research permits TNP/HQ/C.10/13/2015 and TNP/HQ/C.10/13/2017), the Tanzania Wildlife Research Institute (TAWIRI; permit 13300), the Department of Immigration (permits CTA0329016 and RPC11100834), and the Tanzanian Fisheries Research Institute (TAFIRI; permits TAF/KGM/R/VOL.V/236 and TAF/KGM/R.1/VOL.V/121) for the United Republic of Tanzania; and (iii) the Department of Immigration (study permits SP000627, SP001995, SP004273, SP005937, and SP226456) and the Department of Fisheries for the Republic of Zambia. Sampling and all further experiments were approved by the appropriate ethics committees.

Fish were caught with barrier nets while snorkeling or scuba diving or purchased from local fishermen, covering a depth range of <1 to >100 m (note that in Lake Tanganyika fish occur down to the oxycline at 150 to 200 m). Eyes were dissected in the field from freshly caught specimens after the fish had been euthanized and photographed, measured, and weighted. Both eyes from a given specimen were stored in RNAlater (Ambion) until further steps in the laboratory (see below). Our final dataset included eyes of 753 adult specimens, representing at least three male and three female individuals of 112 species covering all 12 Tanganyikan cichlid tribes (Bathybatini, Benthochromini, Boulengerochromini, Cyphotilapiini, Cyprichromini, Ectodini, Eretmodini, Lamprologini, Limnochromini, Perissodini, Trematocarini, and Tropheini) and one representative each of the tribes Haplochromini, Oreochromini, and Tylochromini (see table S1 for details on samples, sampling dates and localities, and sex).

The following additional data from our previous work were included in this study: The time-calibrated species tree based on genome-wide data, raw sequencing data [National Center for Biotechnology Information (NCBI) BioProject accession no. PRJNA550295], gene duplication and positive selection analyses, stable carbon (C) and nitrogen (N) isotope signatures, and relative eye size data were taken from Ronco *et al.* (*52*) (data available on Dryad: https://datadryad.org/stash/dataset/doi:10.5061/dryad.9w0vt4bbf), and habitat categories (shallow water depth of 0 to 10 m, intermediate water depth of 10 to 20 m, and deep water depth of >20 m) were taken from Ricci *et al.* (*30*) (data available on Dryad: https://datadryad.org/stash/dataset/doi:10.5061/dryad.4mw6m90c7).

Dissection, extraction, library preparation, and Illumina sequencing

For each specimen, the retina of a single eye was dissected and homogenized (FastPrep-24; MP Biomedicals), and the total RNA was

extracted using the Direct-zol RNA kit (Zymo) according to the manufacturer's protocol. Individual libraries were constructed using the Illumina TruSeq stranded protocol including RiboZero Gold rRNA depletion (Illumina) and sequenced on Illumina NovaSeq 6000 in PE 100-bp mode. Library construction and sequencing were conducted at the Genomics Facility Basel, which is jointly operated by the University of Basel and the Department of Biosystems Science and Engineering (D-BSSE) of ETH Zurich. Samples were randomized with respect to species and sex for both the dissection/extraction and the sequencing steps. Library preparations of 84 samples failed in a first attempt but could successfully be repeated in a second round. If two sequencing runs were performed for a given sample, the runs were combined for downstream analyses. The raw read data from all 753 samples are available from NCBI under the BioProject accession number PRJNA913112.

Quality filtering, mapping, and read counting

Quality filtering and adapter removal of Illumina strand-specific paired-end sequences were performed using Trimmomatic [v. 0.39; (*78*)] with a 4-bp window size, a required window quality of 15, and 80 bp as minimum read length. As in our previous work (*59*), cleaned reads were mapped against the Nile tilapia reference genome (*O. niloticus*; RefSeq accession GCF_001858045.2, female), which is phylogenetically equidistant to all members of the cichlid adaptive radiation in Lake Tanganyika (that is, all species in our dataset except *O. tanganicae* and *T. polylepis*), using STAR [v. 2.7.3a; (*79*)] with --outFilterMultimapNmax 1 --outFilterMatchNminOverLread 0.4 --outFilterScoreMinOverLread 0.4. To obtain a reasonable estimate of mapped reads to exonic features, we filtered out mapped singletons and then assigned and counted read pairs within exons using the HTSeq-count script from the HTSeq framework [v. 0.11.2; (*80*)]. Because of the high gene sequence similarity between *RH2A*α and *RH2A*β (percent sequence identity of exons between 94.81 and 99.40%; table S5), we retrieved all read pairs exactly mapping to both features and corrected the read count by assigning the remaining read pairs to *RH2A*α and *RH2A*β according to their original ratio. The total number of exonic features retrieved by HTSeq-count was 41,945 (out of 42,622 annotated genes; see data S1). We filtered the read count dataset to retain both protein-coding RNAs and lncRNAs (*59*, *81*). This resulted in 38,228 RNAs, from which we excluded 9226 lowly expressed genes (≤5 counts in less than three samples). The final read count dataset used for the subsequent analyses included 29,002 RNAs, from which 25,335 were protein-coding RNAs (out of 29,532 exonic feature) and 3667 were lncRNAs (out of 8696 exonic features).

Principal components analysis

Before PCA, we normalized the final read count dataset using the R package DESeq2 [v. 1.34.0; (*82*)]. We set the experimental design formula to "~ species + sex" and converted the data using VST [with parameter blind = FALSE; see (*59*)]. We then calculated the weighted species mean of VST values per gene to rely on samples with higher number of sequenced reads. PCAs were performed with the prcomb function in R (*83*) for the overall dataset containing both protein-coding RNAs and lncRNAs, for protein-coding RNAs and lncRNAs individually, for the top 500 and the top 100 genes with the greatest variance in gene expression, and for the visual opsin genes. In addition, we performed a PCA based on the expression information of the cone opsin genes to validate the visual palettes delineated using the clustering methods (see below) and reconstructed ancestral states along the time-calibrated species of (*52*) with the phylomorphospace function of the R package phytools (v. 0.7-90) (*84*).

Opsin expression profiles and visual palette identification

To account for variation in sequencing depth and visual opsin gene length, we converted the final read count dataset to TPM and calculated the weighted species means of TPM per gene to rely on samples with higher numbers of sequenced reads. We then calculated the percent of weighted species mean TPM of each visual opsin gene relative to the total visual opsin pool and to opsin categories (single cone opsins: *SWS1*, *SWS2B*, and *SWS2A*; double cone opsins: *RH2B*, *RH2A*α, *RH2A*β, and *LWS*; in addition to the rhodopsin *RH1* and cone opsins).

To examine the pattern of expression correlation of visual opsin genes, we tested for correlations (Spearman's correlation coefficients) between all pairs of opsins using the percent weighted species mean TPM of each visual opsin gene relative to the total visual opsin pool. We further calculated PICs [pic function of the R package ape; v. 5.5; (*85*)] along the species tree and inferred Spearman's correlation coefficients for PICs (i.e., through the origin) using the cor.table function of the R package picante [v. 1.8.1, (*86*)]. *P* values were adjusted for multiple testing using the Benjamini and Hochberg method.

To characterize visual palettes in the cichlid fish fauna of Lake Tanganyika, we applied two strategies: (i) defining visual palettes according to the single-most highly expressed single cone opsin and the two most highly expressed double cone opsins applying a majority-rule criterion (SDD majority-rule clustering) and (ii) performing a hierarchical clustering analysis with the number of clusters (*k*) ranging from three to eight and using the R function hclust with the Ward's method [see (*48*)], cross-validated with the *k*-nearest neighbor (knn) classification method. We opted for the SDD majority-rule clustering method to account for the predominant expression level (≥80%) of a unique single cone opsin and two double cone opsins and confirmed our findings by applying the majority-rule clustering method on the complete set of single and double cone opsins. For these analyses, we combined *RH2A*α and *RH2A*β into the category *RH2As*, as it has been done in previous studies (*48*, *54*, *56*, *87*), and we also included species with close to zero cone opsin expression or with a predominant expression of one double cone opsin. For the SDD majority-rule and the hierarchical clustering methods, we then reconstructed the ancestral states of visual palettes along the species tree using make.simmap function of the R package phytools (*84*) [with 10,000 simulations, an equal-rates model, the maximum likelihood method, and a Bayesian Markov-Chain Monte-Carlo (MCMC) strategy]. As this part of our study focused exclusively on the adaptive radiation of cichlid fishes in Lake Tanganyika as defined in (*52*), we excluded the primarily riverine haplochromine species *A. burtoni* (Haplochromini) and the two distantly related species of the tribes Oreochromini and Tylochromini.

Regression analyses

We then examined whether, at the level of the entire adaptive radiation, there is an association between visual opsin gene expression levels and ecological and morphological traits. Using lm and pGLS

analyses [pgls function of the R package caper; v. 1.0.1; (*88*)], we thus analyzed the relationship between weighted species mean VST-normalized count of visual opsins and (i) $\delta^{13}C$ values as macrohabitat proxy, (ii) $\delta^{15}N$ values as proxy for relative trophic level, and (iii) relative eye size (as ratio of square root of the eye area and centroid size). Furthermore, to account for the multicollinearity of the expression profiles (see figs. S6 and S7), we fitted a pPLS for each of the eco/morphological traits and all cone opsin expression profiles [phylo.integration function of the R package geomorph; v. 4.0.4; (*89*)]. Again, we combined *RH2Aα* and *RH2Aβ* into *RH2As*. For the same reasons as mentioned above, we again excluded the single representatives each of Haplochromini, Oreochromini, and Tylochromini. Last, to highlight the relationships among the ecological and morphological traits, we performed lm and pGLS analyses between the species' $\delta^{13}C$ values, $\delta^{15}N$ values, and relative eye size (fig. S15A), plus a phylogenetic analysis of variance (ANOVA) between the species' depth of occurrence and each ecological and morphological trait (fig. S15B and table S6) using the phylANOVA function of the R package phytools (*84*) (with 1000 simulations and "BH" as method).

Genomic analyses

To screen for possible duplications of particular visual opsin genes in Tanganyikan cichlids, we reinspected the gene duplication estimates of 488 genomes (246 taxa) from Ronco *et al.* (*52*). Furthermore, we used the cichlid-tailored opsin raw read mapping approach of Ricci *et al.* (*30*) to confirm the presence of a single copy per cone opsin gene [*RH1* results in (*30*)] and to retrieve the protein-coding sequences in 517 genomes (271 species, including outgroups and nonendemic species nested in the radiation). We further examined the completeness of the protein-coding sequence of the visual opsins with no gene expression. Last, we reinspected signals of positive selection in the cone opsin genes [no data available for *RH2Aα* and *RH2Aβ*; *RH1* results in (*30*)] by extracting the d_N/d_S ratio per opsin in 471 genomes (243 taxa) from the positive selection analysis of (*52*). Note that we did not test for positive selection across sites [see (*58*)] but instead used the available data of (*52*).

Statistical analysis

All statistical tests and parameters are reported in Materials and Methods and in the figure legends. Statistical analyses were performed using R (v. 4.1.2 and 4.2.2).

Supplementary Materials

This PDF file includes:
Figs. S1 to S15
Tables S1 to S6
Legend for data S1

Other Supplementary Material for this manuscript includes the following:
Data S1

REFERENCES AND NOTES

1. A. J. Hudspeth, N. K. Logothetis, Sensory systems. *Curr. Opin. Neurobiol.* **10**, 631–641 (2000).
2. M. F. Land, Biology of sensory systems. *Trends Neurosci.* **23**, 588–589 (2000).
3. T. J. Ness, T. J. Brennan, Sensory systems, in *Foundations of Anesthesia: Basic Sciences for Clinical Practice* (Elsevier, 2006), pp. 257–266.
4. D. M. Hunt, M. W. Hankins, S. P. Collin, N. J. Marshall, The evolution of photoreceptors and visual photopigments in vertebrates, in *Evolution of Visual and Non-Visual Pigments* (Springer-Verlag, 2014), pp. 163–217.
5. M. Inoue-Murayama, S. Kawamura, A. Weiss, *From Genes to Animal Behavior: Social Structures, Personalities, Communication by Color* (Springer, 2011).
6. P. Oteiza, M. W. Baldwin, Evolution of sensory systems. *Curr. Opin. Neurobiol.* **71**, 52–59 (2021).
7. M. W. Baldwin, M. C. Ko, Functional evolution of vertebrate sensory receptors. *Horm. Behav.* **124**, 104771 (2020).
8. T. W. Cronin, S. Johnsen, N. J. Marshall, E. J. Warrant, *Visual Ecology* (Princeton Univ. Press, 2014).
9. J. N. Lythgoe, *The Ecology of Vision* (Clarendon Press, 1979).
10. Z. Musilova, W. Salzburger, F. Cortesi, The visual opsin gene repertoires of teleost fishes: Evolution, ecology, and function. *Annu. Rev. Cell Dev. Biol.* **37**, 441–468 (2021).
11. M. F. Land, D.-E. Nilsson, Animal eyes. *Zool. J. Linn. Soc.* **166**, 912 (2012).
12. T. H. Oakley, D. I. Speiser, How complexity originates: The evolution of animal eyes. *Annu. Rev. Ecol. Evol. Syst.* **46**, 237–260 (2015).
13. M. F. Land, The optical structures of animal eyes. *Curr. Biol.* **15**, R319–R323 (2005).
14. J. K. Bowmaker, Evolution of vertebrate visual pigments. *Vision Res.* **48**, 2022–2041 (2008).
15. K. Palczewski, T. Kumasaka, T. Hori, C. A. Behnke, H. Motoshima, B. A. Fox, I. Le Trong, D. C. Teller, T. Okada, R. E. Stenkamp, M. Yamamoto, M. Miyano, Crystal structure of rhodopsin: A G protein-coupled receptor. *Science* **289**, 739–745 (2000).
16. G. Wald, The molecular basis of visual excitation. *Nature* **219**, 800–807 (1968).
17. D. C. Teller, R. E. Stenkamp, K. Palczewski, Evolutionary analysis of rhodopsin and cone pigments: Connecting the three-dimensional structure with spectral tuning and signal transfery. *FEBS Lett.* **555**, 151–159 (2003).
18. S. Yokoyama, Molecular evolution of vertebrate visual pigments. *Prog. Retin. Eye Res.* **19**, 385–419 (2000).
19. S. Yokoyama, Evolution of dim-light and color vision pigments. *Annu. Rev. Genomics Hum. Genet.* **9**, 259–282 (2008).
20. W. Wang, J. H. Geiger, B. Borhan, The photochemical determinants of color vision. *Bioessays* **36**, 65–74 (2014).
21. W. I. L. Davies, S. P. Collin, D. M. Hunt, Molecular ecology and adaptation of visual photopigments in craniates. *Mol. Ecol.* **21**, 3121–3158 (2012).
22. T. D. Lamb, S. P. Collin, N. P. J. Edward, Evolution of the vertebrate eye: Opsins, photoreceptors, retina and eye cup. *Nat. Rev. Neurosci.* **8**, 960–976 (2007).
23. Z. Musilova, F. Cortesi, M. Matschiner, W. I. L. Davies, J. S. Patel, S. M. Stieb, F. De Busserolles, M. Malmstrøm, O. K. Tørresen, C. J. Brown, J. K. Mountford, R. Hanel, D. L. Stenkamp, K. S. Jakobsen, K. L. Carleton, S. Jentoft, J. Marshall, W. Salzburger, Vision using multiple distinct rod opsins in deep-sea fishes. *Science* **364**, 588–592 (2019).
24. F. Cortesi, Z. Musilová, S. M. Stieb, N. S. Hart, U. E. Siebeck, M. Malmstrøm, O. K. Tørresen, S. Jentoft, K. L. Cheney, N. J. Marshall, K. L. Carleton, W. Salzburger, Ancestral duplications and highly dynamic opsin gene evolution in percomorph fishes. *Proc. Natl. Acad. Sci. U.S.A.* **112**, 1493–1498 (2015).
25. J. J. Lin, F. Y. Wang, W. H. Li, T. Y. Wang, The rises and falls of opsin genes in 59 ray-finned fish genomes and their implications for environmental adaptation. *Sci. Rep.* **7**, 15568 (2017).
26. J. T. O. Kirk, *Light and Photosynthesis in Aquatic Ecosystems* (Cambridge Univ. Press, 1983).
27. E. J. Warrant, N. A. Locket, Vision in the deep sea. *Biol. Rev. Camb. Philos. Soc.* **79**, 671–712 (2004).
28. F. W. Munz, W. N. McFarland, Evolutionary adaptations of fishes to the photic environment, in *The Visual System in Vertebrates*, F. Crescitelli, Ed. (Springer-Verlag, 1977), pp. 193–274.
29. S. Yokoyama, R. Yokoyama, Adaptive evolution of photoreceptors and visual pigments in vertebrates. *Annu. Rev. Ecol. Syst.* **27**, 543–567 (1996).
30. V. Ricci, F. Ronco, Z. Musilova, W. Salzburger, Molecular evolution and depth-related adaptations of rhodopsin in the adaptive radiation of cichlid fishes in Lake Tanganyika. *Mol. Ecol.* **31**, 2882–2897 (2022).
31. K. Carleton, Cichlid fish visual systems: Mechanisms of spectral tuning. *Integr. Zool.* **4**, 75–86 (2009).
32. K. L. Carleton, D. Escobar-Camacho, S. M. Stieb, F. Cortesi, N. J. Marshall, Seeing the rainbow: Mechanisms underlying spectral sensitivity in teleost fishes. *J. Exp. Biol.* **223**, jeb193334 (2020).
33. F. E. Hauser, B. S. Chang, Insights into visual pigment adaptation and diversity from model ecological and evolutionary systems. *Curr. Opin. Genet. Dev.* **47**, 110–120 (2017).
34. F. E. Hauser, K. L. Ilves, R. K. Schott, E. Alvi, H. López-Fernández, B. S. W. Chang, Evolution, inactivation and loss of short wavelength-sensitive opsin genes during the diversification of Neotropical cichlids. *Mol. Ecol.* **30**, 1688–1703 (2021).

35. N. J. Marshall, F. Cortesi, F. de Busserolles, U. E. Siebeck, K. L. Cheney, Colours and colour vision in reef fishes: Past, present and future research directions. *J. Fish Biol.* **95**, 5–38 (2019).
36. Z. Musilova, A. Indermaur, A. R. Bitja-Nyom, D. Omelchenko, M. Kłodawska, L. Albergati, K. Remišová, W. Salzburger, Evolution of the visual sensory system in cichlid fishes from crater lake Barombi Mbo in Cameroon. *Mol. Ecol.* **28**, 5010–5031 (2019).
37. R. K. Schott, S. P. Refvik, F. E. Hauser, H. López-Fernández, B. S. W. Chang, Divergent positive selection in rhodopsin from lake and riverine cichlid fishes. *Mol. Biol. Evol.* **31**, 1149–1165 (2014).
38. Y. Terai, R. Miyagi, M. Aibara, S. Mizoiri, H. Imai, T. Okitsu, A. Wada, S. Takahashi-Kariyazono, A. Sato, H. Tichy, H. D. J. Mrosso, S. I. Mzighani, N. Okada, Visual adaptation in Lake Victoria cichlid fishes: Depth-related variation of color and scotopic opsins in species from sand/mud bottoms. *BMC Evol. Biol.* **17**, 200 (2017).
39. K. L. Carleton, M. R. Yourick, Axes of visual adaptation in the ecologically diverse family Cichlidae. *Semin. Cell Dev. Biol.* **106**, 43–52 (2020).
40. F. de Busserolles, L. Fogg, F. Cortesi, J. Marshall, The exceptional diversity of visual adaptations in deep-sea teleost fishes. *Semin. Cell Dev. Biol.* **106**, 20–30 (2020).
41. W. R. A. Muntz, Yellow filters and the absorption of light by the visual pigments of some amazonian fishes. *Vision Res.* **13**, 2235–2254 (1973).
42. J. Torres-Dowdall, F. Henning, K. R. Elmer, A. Meyer, Ecological and lineage-specific factors drive the molecular evolution of rhodopsin in cichlid fishes. *Mol. Biol. Evol.* **32**, 2876–2882 (2015).
43. D. J. Rennison, G. L. Owens, J. S. Taylor, Opsin gene duplication and divergence in ray-finned fish. *Mol. Phylogenet. Evol.* **62**, 986–1008 (2012).
44. G. L. Owens, D. J. Rennison, Evolutionary ecology of opsin gene sequence, expression and repertoire. *Mol. Ecol.* **26**, 1207–1210 (2017).
45. C. J. Weadick, B. S. W. Chang, Complex patterns of divergence among green-sensitive (RH2a) African cichlid opsins revealed by Clade model analyses. *BMC Evol. Biol.* **12**, (2012).
46. L. G. Fogg, F. Cortesi, D. Lecchini, C. Gache, N. J. Marshall, F. de Busserolles, Development of dim-light vision in the nocturnal reef fish family Holocentridae I: Retinal gene expression. *J. Exp. Biol.* **225**, jeb244513 (2022).
47. K. E. O'Quin, C. M. Hofmann, H. A. Hofmann, K. L. Carleton, K. E. O'Quin, C. M. Hofmann, H. A. Hofmann, K. L. Carleton, Parallel evolution of opsin gene expression in african cichlid fishes. *Mol. Biol. Evol.* **27**, 2839–2854 (2010).
48. C. M. Hofmann, K. E. O'Quin, N. J. Marshall, T. W. Cronin, O. Seehausen, K. L. Carleton, The eyes have it: Regulatory and structural changes both underlie cichlid visual pigment diversity. *PLOS Biol.* **7**, e1000266 (2009).
49. M. Tobler, S. W. Coleman, B. D. Perkins, G. G. Rosenthal, Reduced opsin gene expression in a cave-dwelling fish. *Biol. Lett.* **6**, 98–101 (2010).
50. G. Fryer, T. D. Iles, *The Cichlid Fishes of the Great Lakes of Africa. Their Biology and Evolution* (Oliver and Boyd, 1972).
51. W. Salzburger, Understanding explosive diversification through cichlid fish genomics. *Nat. Rev. Genet.* **19**, 705–717 (2018).
52. F. Ronco, M. Matschiner, A. Böhne, A. Boila, H. H. Büscher, A. El Taher, A. Indermaur, M. Malinsky, V. Ricci, A. Kahmen, S. Jentoft, W. Salzburger, Drivers and dynamics of a massive adaptive radiation in cichlid fishes. *Nature* **589**, 76–81 (2021).
53. F. Ronco, H. H. Büscher, A. Indermaur, W. Salzburger, The taxonomic diversity of the cichlid fish fauna of ancient Lake Tanganyika, East Africa. *J. Great Lakes Res.* **46**, 1067–1078 (2020).
54. T. C. Spady, J. W. L. Parry, P. R. Robinson, D. M. Hunt, J. K. Bowmaker, K. L. Carleton, Evolution of the cichlid visual palette through ontogenetic subfunctionalization of the opsin gene arrays. *Mol. Biol. Evol.* **23**, 1538–1547 (2006).
55. V. I. Govardovskii, N. Fyhrquist, T. Reuter, D. G. Kuzmin, K. Donner, In search of the visual pigment template. *Vis. Neurosci.* **17**, 509–528 (2000).
56. K. L. Carleton, C. M. Hofmann, C. Klisz, Z. Patel, L. M. Chircus, L. H. Simenauer, N. Soodoo, R. C. Albertson, J. R. Ser, Genetic basis of differential opsin gene expression in cichlid fishes. *J. Evol. Biol.* **23**, 840–853 (2010).
57. J. Torres-Dowdall, N. Karagic, A. Härer, A. Meyer, Diversity in visual sensitivity across Neotropical cichlid fishes via.pdf. *Mol. Ecol.* **30**, 1180–1891 (2021).
58. I. Irisarri, P. Singh, S. Koblmüller, J. Torres-Dowdall, F. Henning, P. Franchini, C. Fischer, A. R. Lemmon, E. M. Lemmon, G. G. Thallinger, C. Sturmbauer, A. Meyer, Phylogenomics uncovers early hybridization and adaptive loci shaping the radiation of Lake Tanganyika cichlid fishes. *Nat. Commun.* **9**, 3159 (2018).
59. A. El Taher, A. Böhne, N. Boileau, F. Ronco, A. Indermaur, L. Widmer, W. Salzburger, Gene expression dynamics during rapid organismal diversification in African cichlid fishes. *Nat. Ecol. Evol.* **5**, 243–250 (2021).
60. W. Salzburger, T. Mack, E. Verheyen, A. Meyer, Out of Tanganyika: Genesis, explosive speciation, key-innovations and phylogeography of the haplochromine cichlid fishes. *BMC Evol. Biol.* **5**, 17 (2005).
61. C. Hahn, M. J. Genner, G. F. Turner, D. A. Joyce, The genomic basis of cichlid fish adaptation within the deepwater "twilight zone" of Lake Malawi. *Evol. Lett.* **1**, 184–198 (2017).
62. M. Malinsky, H. Svardal, A. M. Tyers, E. A. Miska, M. J. Genner, G. F. Turner, R. Durbin, Whole-genome sequences of Malawi cichlids reveal multiple radiations interconnected by gene flow. *Nat. Ecol. Evol.* **2**, 1940–1955 (2018).
63. C. Damsgaard, H. Lauridsen, A. M. D. Funder, J. S. Thomsen, T. Desvignes, D. A. Crossley, P. R. Møller, D. T. T. Huong, N. T. Phuong, H. W. Detrich, A. Brüel, H. Wilkens, E. Warrant, T. Wang, J. R. Nyengaard, M. Berenbrink, M. Bayley, Retinal oxygen supply shaped the functional evolution of the vertebrate eye. *eLife* **8**, e52153 (2019).
64. C. Damsgaard, H. Lauridsen, T. S. Harter, G. T. Kwan, J. S. Thomsen, A. M. D. Funder, C. T. Supuran, M. Tresguerres, P. G. D. Matthews, C. J. Brauner, A novel acidification mechanism for greatly enhanced oxygen supply to the fish retina. *eLife* **9**, e58995 (2020).
65. Y. Alvarez, M. L. Cederlund, D. C. Cottell, B. R. Bill, S. C. Ekker, J. Torres-Vazquez, B. M. Weinstein, D. R. Hyde, T. S. Vihtelic, B. N. Kennedy, Genetic determinants of hyaloid and retinal vasculature in zebrafish. *BMC Dev. Biol.* **7**, 114 (2007).
66. I. A. Frøland Steindal, D. Whitmore, Circadian clocks in fish-what have we learned so far? *Biology (Basel).* **8**, 17 (2019).
67. R. Feuda, A. K. Menon, M. C. Göpfert, Rethinking opsins. *Mol. Biol. Evol.* **39**, msac033 (2022).
68. K. L. Carleton, B. E. Dalton, D. Escobar-Camacho, S. P. Nandamuri, Proximate and ultimate causes of variable visual sensitivities: Insights from cichlid fish radiations. *Genesis* **54**, 299–325 (2016).
69. B. E. Dalton, E. R. Loew, T. W. Cronin, K. L. Carleton, Spectral tuning by opsin coexpression in retinal regions that view different parts of the visual field. *Proc. R. Soc. B Biol. Sci.* **281**, 20141980 (2014).
70. C. M. Hofmann, K. L. Carleton, Gene duplication and differential gene expression play an important role in the diversification of visual pigments in fish. *Integr. Comp. Biol.* **49**, 630–643 (2009).
71. D. Brawand, M. Soumillon, A. Necsulea, P. Julien, G. Csárdi, P. Harrigan, M. Weier, A. Liechti, A. Aximu-Petri, M. Kircher, F. W. Albert, U. Zeller, P. Khaitovich, F. Grützner, S. Bergmann, R. Nielsen, S. Pääbo, H. Kaessmann, The evolution of gene expression levels in mammalian organs. *Nature* **478**, 343–348 (2011).
72. M. Malinsky, R. J. Challis, A. M. Tyers, S. Schiffels, Y. Terai, B. P. Ngatunga, E. A. Miska, R. Durbin, M. J. Genner, G. F. Turner, Genomic islands of speciation separate cichlid ecomorphs in an East African crater lake. *Science* **350**, 1493–1498 (2015).
73. H. Nagai, Y. Terai, T. Sugawara, H. Imai, H. Nishihara, M. Hori, N. Okada, Reverse evolution in RH1 for adaptation of cichlids to water depth in Lake Tanganyika. *Mol. Biol. Evol.* **28**, 1769–1776 (2011).
74. R. Jordan, D. Howe, F. Juanes, J. J. Stauffer Jr., E. Loew, Ultraviolet radiation enhances zooplanktivory rate in ultraviolet sensitive cichlids. *Afr. J. Ecol.* **42**, 228–231 (2004).
75. H. I. Browman, I. Novales-Flamarique, C. W. Hawryshyn, Ultraviolet photoreception contributes to prey search behaviour in two species of zooplanktivorous fishes. *J. Exp. Biol.* **186**, 187–198 (1994).
76. F. Ronco, W. Salzburger, Tracing evolutionary decoupling of oral and pharyngeal jaws in cichlid fishes. *Evol. Lett.* **5**, 625–635 (2021).
77. A. El Taher, F. Ronco, M. Matschiner, W. Salzburger, A. Böhne, Dynamics of sex chromosome evolution in a rapid radiation of cichlid fishes. *Sci. Adv.* **7**, eabe8215 (2021).
78. A. M. Bolger, M. Lohse, B. Usadel, Trimmomatic: A flexible trimmer for Illumina sequence data. *Bioinformatics* **30**, 2114–2120 (2014).
79. A. Dobin, C. A. Davis, F. Schlesinger, J. Drenkow, C. Zaleski, S. Jha, P. Batut, M. Chaisson, T. R. Gingeras, STAR: Ultrafast universal RNA-seq aligner. *Bioinformatics* **29**, 15–21 (2013).
80. S. Anders, P. T. Pyl, W. Huber, HTSeq-A Python framework to work with high-throughput sequencing data. *Bioinformatics* **31**, 166–169 (2015).
81. A. Necsulea, H. Kaessmann, Evolutionary dynamics of coding and non-coding transcriptomes. *Nat. Rev. Genet.* **15**, 734–748 (2014).
82. M. I. Love, W. Huber, S. Anders, Moderated estimation of fold change and dispersion for RNA-seq data with DESeq2. *Genome Biol.* **15**, 550 (2014).
83. R Core Team, *R: A Language and Environment for Statistical Computing* (R Foundation for Statistical Computing, 2022).
84. L. J. Revell, phytools: An R package for phylogenetic comparative biology (and other things). *Methods Ecol. Evol.* **3**, 217–223 (2012).
85. E. Paradis, J. Claude, K. Strimmer, APE: Analyses of phylogenetics and evolution in R language. *Bioinformatics* **20**, 289–290 (2004).
86. S. W. Kembel, P. D. Cowan, M. R. Helmus, W. K. Cornwell, H. Morlon, D. D. Ackerly, S. P. Blomberg, C. O. Webb, Picante: R tools for integrating phylogenies and ecology. *Bioinformatics* **26**, 1463–1464 (2010).
87. K. L. Carleton, T. C. Spady, J. T. Streelman, M. R. Kidd, W. N. McFarland, E. R. Loew, Visual sensitivities tuned by heterochronic shifts in opsin gene expression. *BMC Biol.* **6**, 22 (2008).
88. D. Orme, The caper package: Comparative analysis of phylogenetics and evolution in R. R Package version 0.5, 2 (2013).

89. D. C. Adams, E. Otárola-Castillo, Geomorph: An R package for the collection and analysis of geometric morphometric shape data. *Methods Ecol. Evol.* **4**, 393–399 (2013).

Acknowledgments: We thank A. El Taher, A. Indermaur, and L. Widmer for assistance in the field; A. Irakoze, G. Katai, G. Kazumbe, D. Mwanakulya, J. Sichilima, and H. D. Sichilima Jr. for help and support during field work; G. Banyankimbona (Burundi), L. Makasa (Zambia), and M. Mukuli (Tanzania) for help with obtaining researcher permits; F. Cortesi, A. El Taher, A. Fages, L. Fogg, Z. Musilova, M. Policarpo, and P. Tschopp for valuable feedback and/or discussions; S. Stieb for the demonstration of retina dissection; C. Huyghe for help with retina dissection; and the Genomics Facility Basel (ETH Zurich) for sequencing our RNA samples. Calculations were performed at sciCORE (https://scicore.unibas.ch/), the Center for Scientific Computing at the University of Basel, with support by the Swiss Institute of Bioinformatics (SIB). **Funding:** This work was funded by grants from the European Research Council (ERC, CoG number 617585 "CICHLID~X") and the Swiss National Science Foundation (SNSF) to W.S. (numbers 176039 and 208002) and F.R. (number 206869). **Author contributions:** Experimental design: V.R. and W.S. Sampling and field work: V.R., N.B., F.R., and W.S. Retina dissection and RNA extraction: V.R. and N.B. Gene expression analyses: V.R. Comparative analyses: V.R. and F.R. Supervision: F.R. and W.S. Writing—original draft: V.R. and W.S. Writing—review and editing: V.R., W.S., F.R., and N.B.

Competing interests: The authors declare that they have no competing interests. **Data and materials availability:** The raw read data are available from NCBI under the BioProject accession number PRJNA913112. The raw read count table has been uploaded in the Supplementary Materials (data S1). Data and custom scripts have been deposited on Dryad (https://datadryad.org/stash/dataset/doi:10.5061/dryad.r2280gbj2) and on GitHub (https://github.com/Ninet93/RNASeq_Ricci_et_al.git). The time-calibrated species tree, raw genome sequencing data (NCBI BioProject accession no. PRJNA550295), gene duplication and positive selection analyses, stable carbon (C) and nitrogen (N) isotope signatures, and relative eye size data were taken from Ronco *et al.* (*52*) (data available on Dryad: https://datadryad.org/stash/dataset/doi:10.5061/dryad.9w0vt4bbf). The habitat categories were taken from Ricci *et al.* (*30*) (data available on Dryad: https://datadryad.org/stash/dataset/doi:10.5061/dryad.4mw6m90c7). All data needed to evaluate the conclusions in the paper are present in the paper and/or the Supplementary Materials.

Submitted 17 January 2023
Accepted 7 August 2023
Published 6 September 2023
10.1126/sciadv.adg6568

ScienceAdvances

Visual opsin gene expression evolution in the adaptive radiation of cichlid fishes of Lake Tanganyika

Virginie Ricci, Fabrizia Ronco, Nicolas Boileau, and Walter Salzburger

Sci. Adv., **9** (36), eadg6568.
DOI: 10.1126/sciadv.adg6568

Science Advances (ISSN) is published by the American Association for the Advancement of Science. 1200 New York Avenue NW, Washington, DC 20005. The title *Science Advances* is a registered trademark of AAAS.

Science Advances
AAAS

Supplementary Materials for

Visual opsin gene expression evolution in the adaptive radiation of cichlid fishes of Lake Tanganyika

Virginie Ricci *et al.*

Corresponding author: Virginie Ricci, virginie.ricci@unibas.ch; Walter Salzburger, walter.salzburger@unibas.ch

Sci. Adv. **9**, eadg6568 (2023)
DOI: 10.1126/sciadv.adg6568

The PDF file includes:

Figs. S1 to S15
Tables S1 to S6
Legend for data S1

Other Supplementary Material for this manuscript includes the following:

Data S1

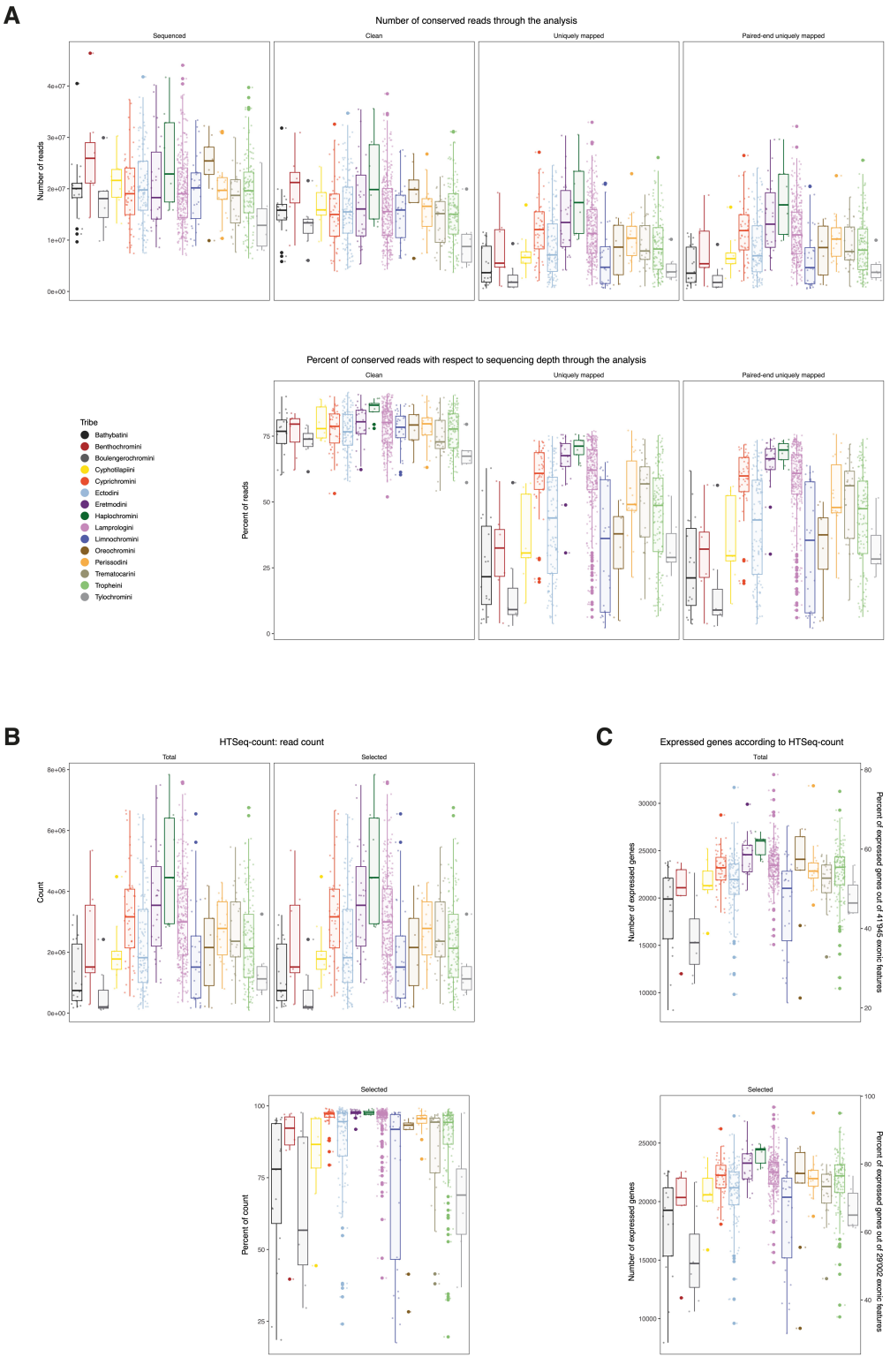
A
Number of conserved reads through the analysis
Sequenced
Clean
Uniquely mapped
Paired-end uniquely mapped
Number of reads
Percent of conserved reads with respect to sequencing depth through the analysis
Percent of reads
Tribe
Bathybatini
Benthochromini
Boulengerochromini
Cyphotilapiini
Cyprichromini
Ectodini
Eretmodini
Haplochromini
Lamprologini
Limnochromini
Oreochromini
Perissodini
Trematocarini
Tropheini
Tylochromini
B
HTSeq-count: read count
Total
Selected
Count
Percent of count
C
Expressed genes according to HTSeq-count
Number of expressed genes
Percent of expressed genes out of 41945 exonic features
Percent of expressed genes out of 29002 exonic features

Fig. S1. Summary statistics of RNA sequencing and filtering. (**A**) Boxplot showing the number and proportion of reads sequenced and retained at the different analytical steps per tribe. (**B**) Barplot showing the number and proportion of read counts before and after selecting protein-coding RNAs and lncRNAs. (**C**) Barplot showing the number of expressed genes before and after selection of protein-coding RNAs and lncRNAs. Barplots and boxplots are colour-coded according to tribes. Tribal assignments and tribe colour-coding follow Ronco et al. (2021) (*52*). Sequencing runs were combined if two sequencing runs were performed for a given sample.

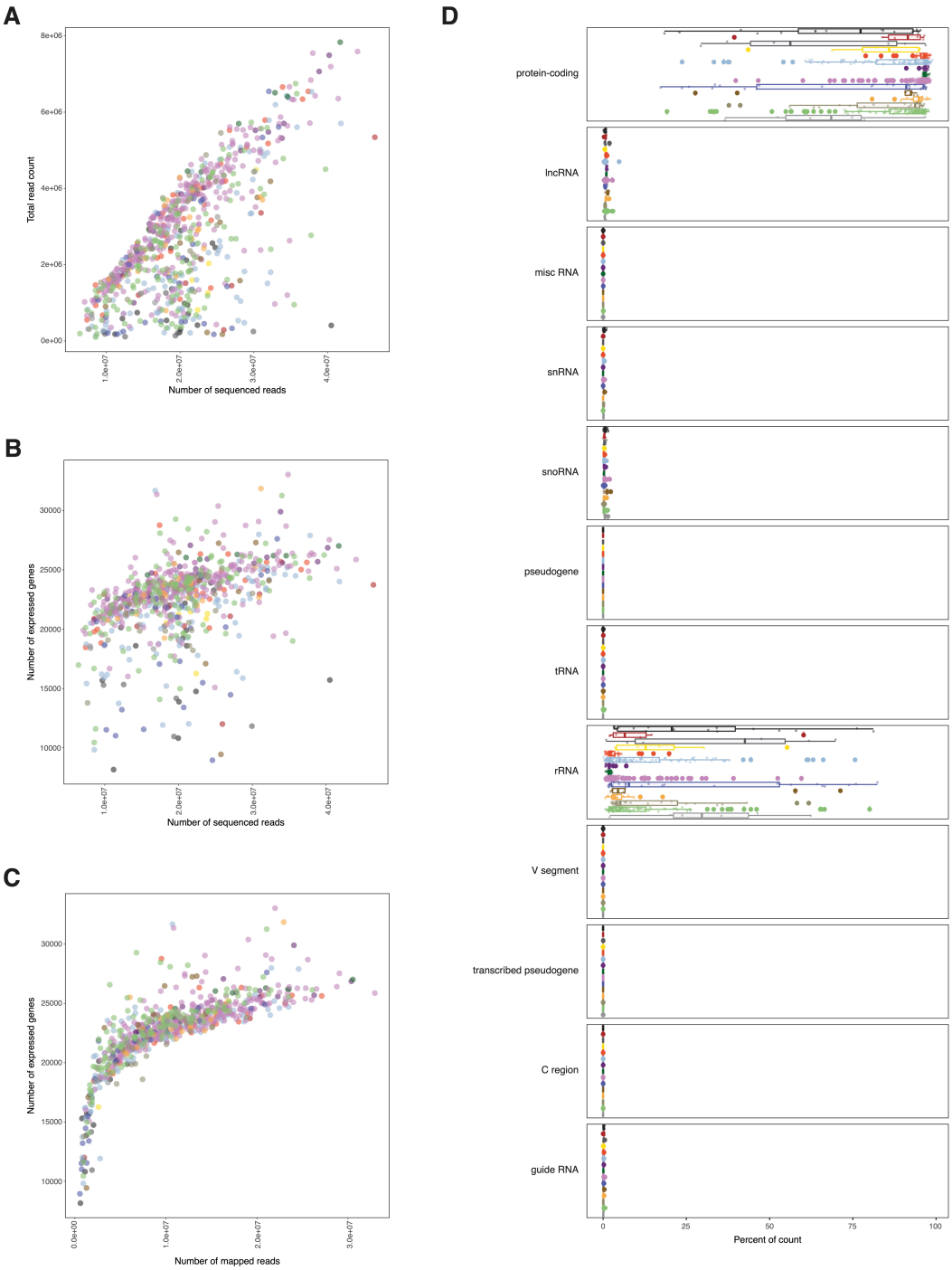
A
Total read count
Number of sequenced reads
B
Number of expressed genes
Number of sequenced reads
C
Number of expressed genes
Number of mapped reads
D
protein-coding
lncRNA
misc RNA
snRNA
snoRNA
pseudogene
tRNA
rRNA
V segment
transcribed pseudogene
C region
guide RNA
Percent of count

Fig. S2. Summary statistics of read mapping. Scatter plot of (**A**) the number of sequenced reads and total read counts in genomic features, (**B**) the number of sequenced reads and the number of expressed genes detected, and (**C**) the number of mapped reads and the number of expressed genes detected. (**D**) Barplot showing the proportion of read counts per genomic feature for each tribe. Tribal assignments and tribe colour-coding follow Ronco et al. (2021) (*52*) (see fig. S1).

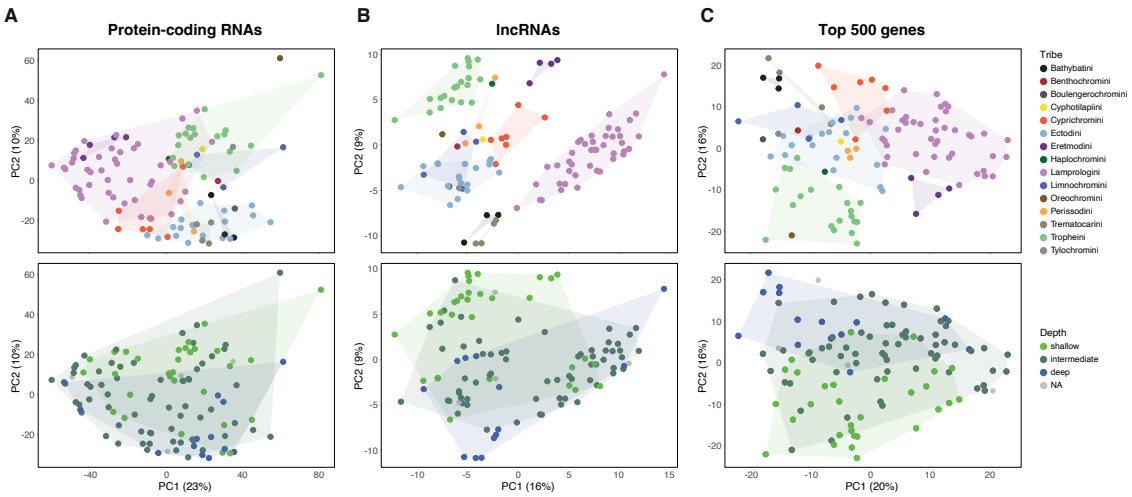

Fig. S3. Retinal gene expression patterns by biotypes and for the top 500 genes. PCAs of (**A**) protein-coding expression levels, (**B**) lncRNAs expression levels and (**C**) gene expression levels of the top 500 genes with the greatest variance in gene expression. Each dot represents the weighted mean value of a given species and is colour-coded according to the tribe that a species belongs to (top panels), or the depth-category at which a species occurs (bottom panels). Tribal and depth ranges are indicated with convex hulls. Tribal assignments and tribe colour-coding follow Ronco et al. (2021) (*52*). The depth of occurrence – in three depth-categories – is indicated and colour-coded per species (NA indicates that the depth of occurrence is unknown for the species in question, or that the three depth categories do not adequately capture the ecology of a given species). Tribal and depth ranges are indicated with convex hulls (except for NA as depth). The variance explained by each principal component (PC) is reported in parenthesis.

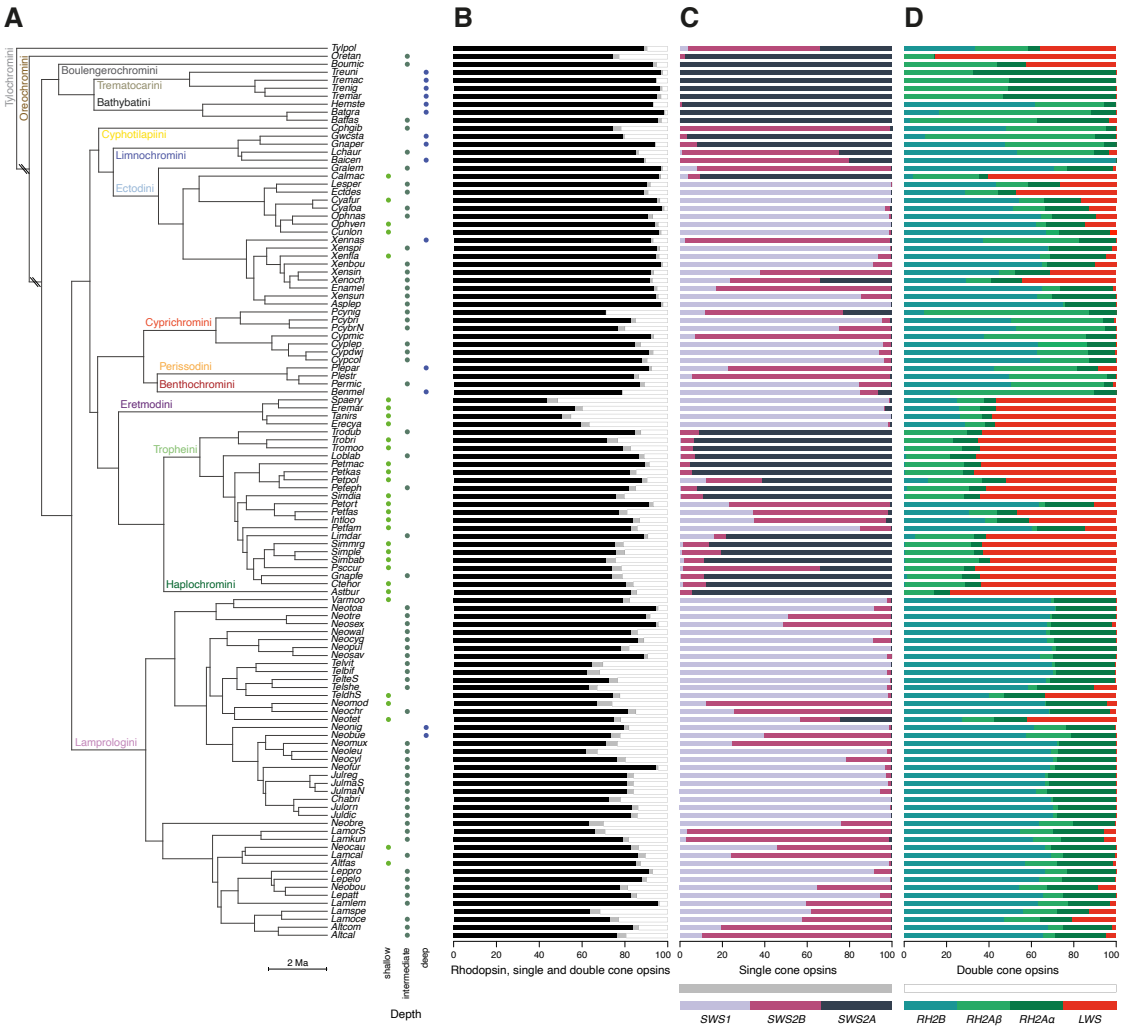

Fig. S4. Visual opsin gene expression profiles along the species tree of Lake Tanganyika cichlids before the correction of the *RH2Aα*/*RH2Aβ* proportion. (**A**) Time-calibrated species tree of the cichlid fishes of Lake Tanganyika (taken from Ronco et al. 2021) (*52*), pruned to the focal taxa of this study (see table S1 for full species names, branches indicated with '\\' are not drawn to scale). The depth of occurrence – in three depth-categories – is indicated and colour-coded per species (absence of a dot indicates that the depth of occurrence is unknown for the species in question, or that the three depth categories do not adequately capture the ecology of a given species). (**B**) Relative proportions of rhodopsin *versus* cone opsins expression per species. (**C**) Relative proportions of single cone opsins expression per species. (**D**) Relative proportions of double cone opsins expression per species. Cone opsins are colour-coded according to their spectral sensitivity. Single cone opsins include the UV-sensitive *SWS1*, the violet-sensitive *SWS2B*, and the blue-sensitive SWS2A. Double cone opsins comprise the green-sensitive *RH2B*, *RH2Aα*, and *RH2Aβ*, as well as the red-sensitive *LWS*.

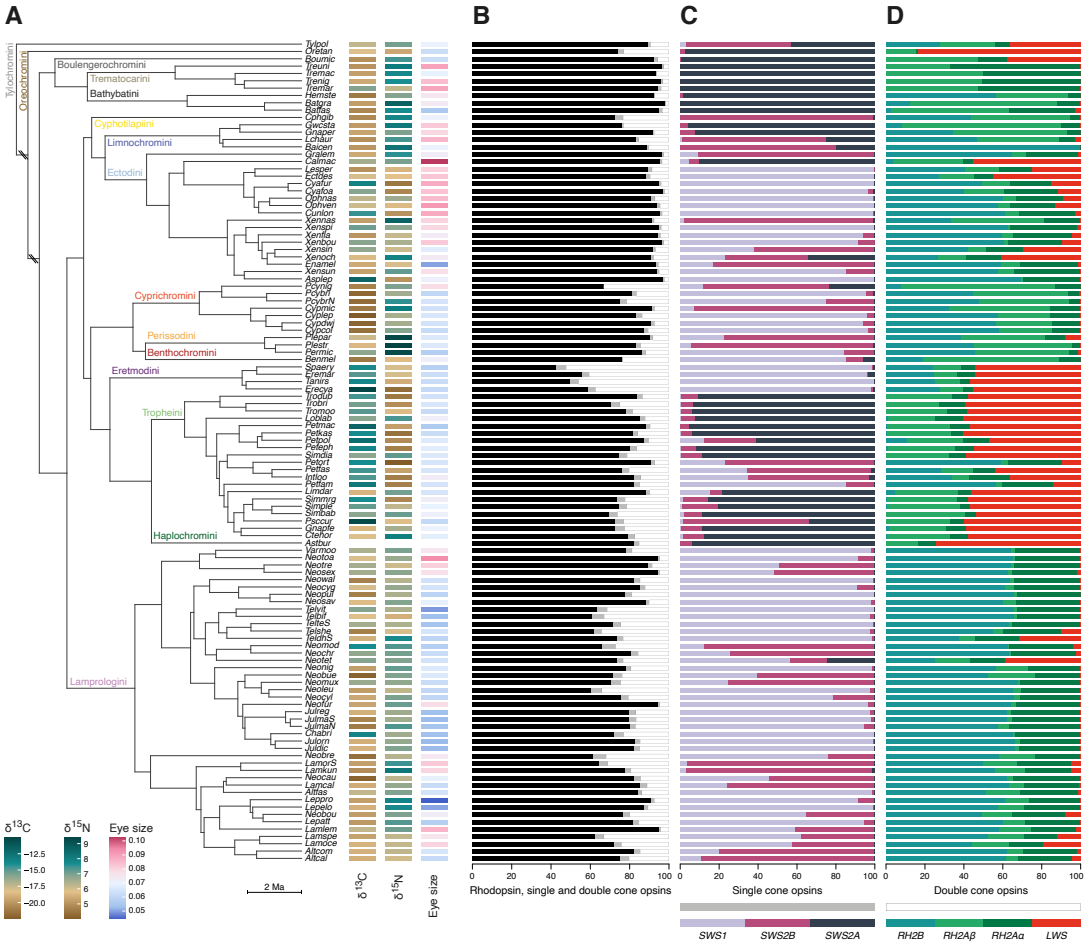

Fig. S5. Visual opsin gene expression profiles along the species tree of Lake Tanganyika cichlids. (**A**) Time-calibrated species tree of the cichlid fishes of Lake Tanganyika (taken from Ronco et al. 2021) (*52*), pruned to the focal taxa of this study (see table S1 for full species names, branches indicated with '\\' are not drawn to scale). The relative position along the benthic-pelagic axis (based on the carbon stable isotope composition $\delta^{13}C$), the relative trophic level (based on the nitrogen stable isotope composition $\delta^{15}N$), and the relative eye size are indicated and colour-coded per species (absence of rectangle indicates missing data; data taken from Ronco et al. 2021) (*52*). (**B**) Relative proportions of rhodopsin *versus* cone opsins expression per species. (**C**) Relative proportions of single cone opsins expression per species. (**D**) Relative proportions of double cone opsins expression per species. Cone opsins are colour-coded according to their spectral sensitivity. Single cone opsins include the UV-sensitive *SWS1*, the violet-sensitive *SWS2B*, and the blue-sensitive *SWS2A*. Double cone opsins comprise the green-sensitive *RH2B*, *RH2Aα*, and *RH2Aβ*, as well as the red-sensitive *LWS*.

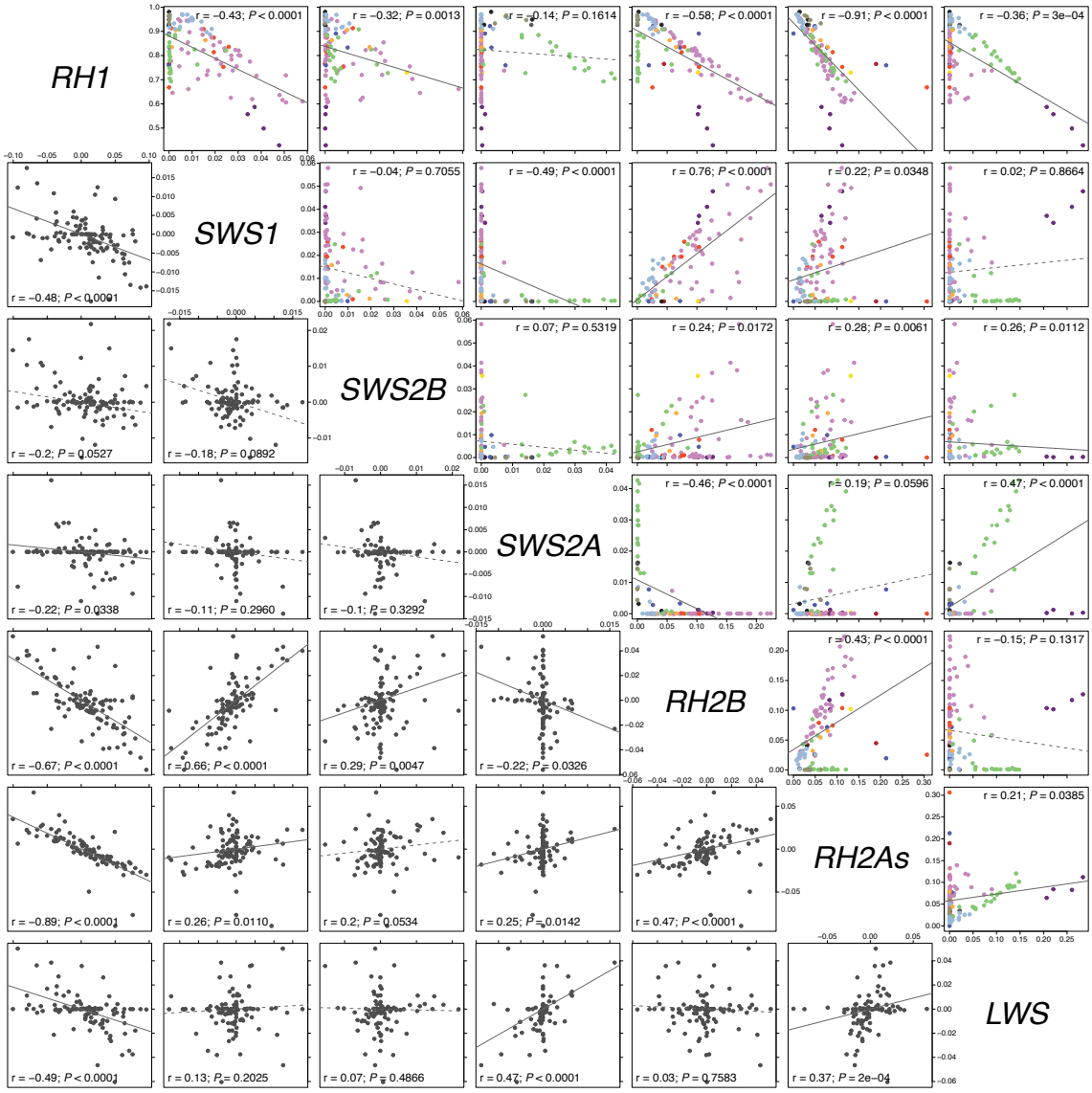

Fig. S6. Expression correlation of visual opsin genes (*RH2Aα* and *RH2Aβ* combined as *RH2As*). The panels show scatter plots for each pair of opsins. The upper part of the matrix displays the correlation based on TPM values (%TPM relative to the complete set of opsins) and the lower part of the matrix shows the phylogenetic independent contrast thereof. Significant (evolutionary) correlations are highlighted with a solid line at $P < 0.05$ (adjusted for multiple testing using the Benjamini & Hochberg method). Each dot represents a species and is colour-coded according to tribe (upper matrix). Note that, just like in previous studies (*47*, *48*, *56*), *RH2Aα* and *RH2Aβ* were combined under the category RH2As (see Supplementary Materials Fig. S7 for results with *RH2Aα* and *RH2Aβ*), and that the primarily riverine haplochromine *A. burtoni* as well as the more distantly related species *O. tanganicae* and *T. polylepis* were excluded from this analysis.

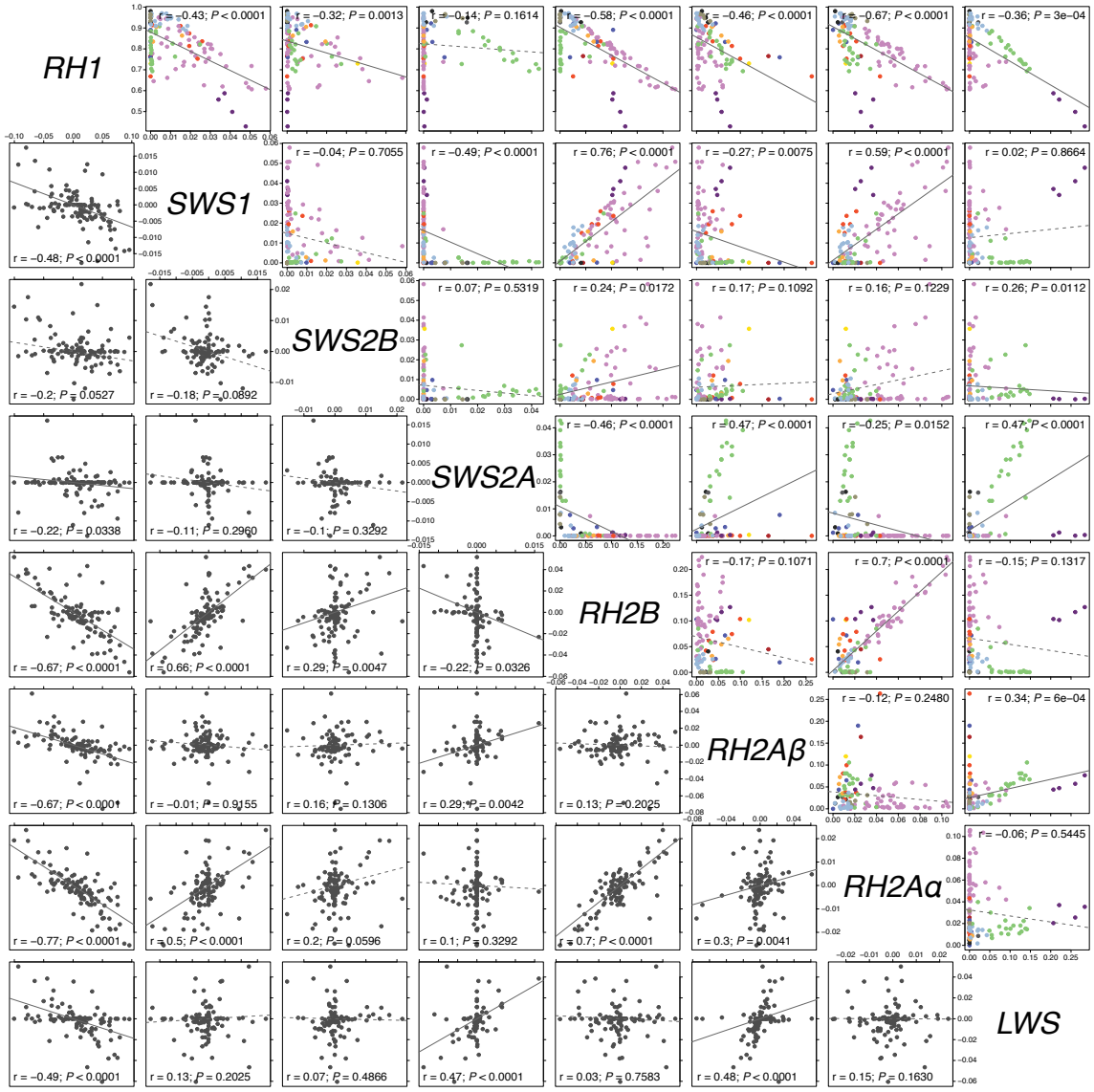

Fig. S7. Expression correlation of visual opsin genes with *RH2Aα* and *RH2Aβ*. The panels show scatter plots for each pair of opsins. The upper part of the matrix displays the correlation based on TPM values (%TPM relative to the complete set of opsins) and the lower part of the matrix shows the phylogenetic independent contrast thereof. Significant (evolutionary) correlations are highlighted with a solid line at $P < 0.05$ (adjusted for multiple testing using the Benjamini & Hochberg method). Each dot represents a species and is colour-coded according to tribe (upper matrix). Note that the primarily riverine haplochromine *A. burtoni* as well as the more distantly related species *O. tanganicae* and *T. polylepis* were excluded from this analysis.

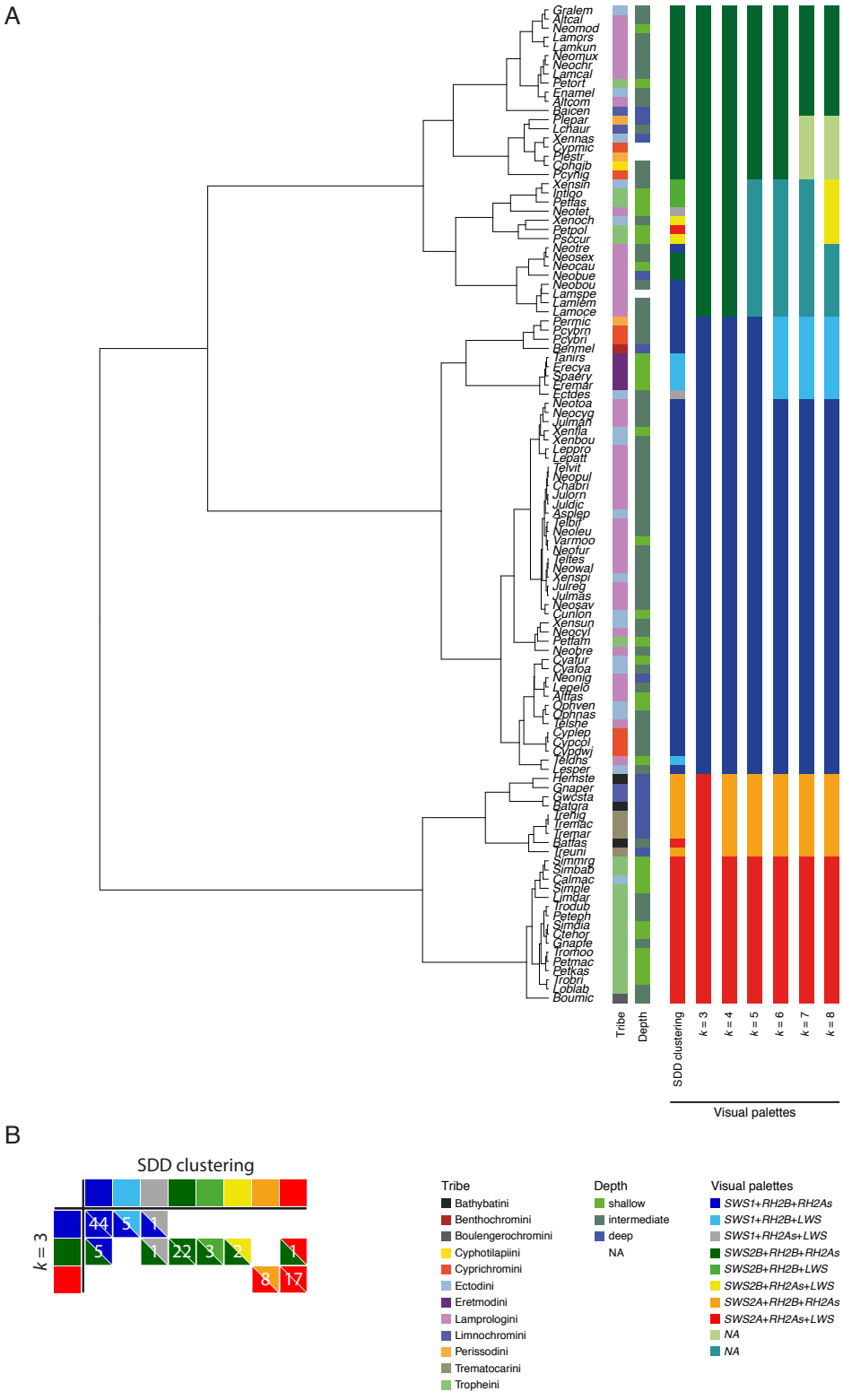
A
Gralem
Altcal
Neomod
Lamors
Lamkun
Neomux
Neochr
Lamcal
Petort
Enamel
Altcom
Baicen
Plepar
Lchaur
Xennas
Cyprnic
Plestr
Cphgib
Pcyhig
Xensin
Intligo
Petfas
Neotet
Xenoch
Petpol
Pscour
Neotre
Neosex
Neocau
Neobue
Neobou
Lamspe
Lamlem
Lamoce
Permic
Pcybrn
Pcybri
Behmel
Tanirs
Erecya
Spaery
Eremar
Ectdes
Neotoa
Neocyg
Julmar
Xenfla
Xenbou
Leppro
Lepatt
Telvit
Neopul
Chabri
Julorn
Juldic
Asplep
Telbil
Neoleu
Varmoo
Neofur
Telfes
Neowal
Xenspi
Julreg
Julmas
Neosav
Cunlon
Xensun
Negcyl
Petfam
Neobre
Cyatur
Cyafoa
Neonig
Lepel6
Altfas
Ophven
Ophnas
Telshe
Cyplep
Cypcol
Cyptwi
Telchs
Lesper
Hemste
Gnaper
Gwcsta
Batgra
Trehig
Tremac
Tremar
Batfas
Treuni
Simmrg
Simbab
Calmac
Simple
Limdar
Trodub
Peteph
Simdia
Ctehor
Gnaple
Tromoo
Petmac
Petkas
Trobri
Loblab
Boumic
Tribe
Depth
SDD clustering
k = 3
k = 4
k = 5
k = 6
k = 7
k = 8
Visual palettes
B
SDD clustering
k = 3
44
5
1
5
1
22
3
2
1
8
17
Tribe
Bathybatini
Benthochromini
Boulengerochromini
Cyphotilapiini
Cyprichromini
Ectodini
Eretmodini
Lamprologini
Limnochromini
Perissodini
Trematocarini
Tropheini
Depth
shallow
intermediate
deep
NA
Visual palettes
SWS1+RH2B+RH2As
SWS1+RH2B+LWS
SWS1+RH2As+LWS
SWS2B+RH2B+RH2As
SWS2B+RH2B+LWS
SWS2B+RH2As+LWS
SWS2A+RH2B+RH2As
SWS2A+RH2As+LWS
NA
NA

Fig. S8. Visual palette characterization in Lake Tanganyika cichlid fishes. (**A**) Dendrogram based on the hierarchical clustering analysis. Tribal, depth and visual palette assignments are indicated next to each abbreviated species name. The eight visual palettes identified based on the species-specific combinations of the most highly expressed single cone opsin and the two most highly expressed double cone opsins (SDD) (see Fig. 3), as well as the visual palettes with a number of clusters (*k*) ranging from three to eight are shown. Tribal assignments and tribe colour-coding follow Ronco et al. (2021) (*52*). The depth of occurrence – in three depth-categories – is indicated and colour-coded per species (NA or absence of rectangle indicates that the depth of occurrence is unknown for the species in question, or that the three depth categories do not adequately capture the ecology of a given species). (**B**) Table showing the number of species that express a given visual palette according to the SDD and the hierarchical methods. Note that, just like in previous studies (*47*, *48*, *56*), *RH2Aα* and *RH2Aβ* were combined under the category *RH2As*, and that the primarily riverine haplochromine *A. burtoni* as well as the more distantly related species *O. tanganicae* and *T. polylepis* were excluded from this analysis.

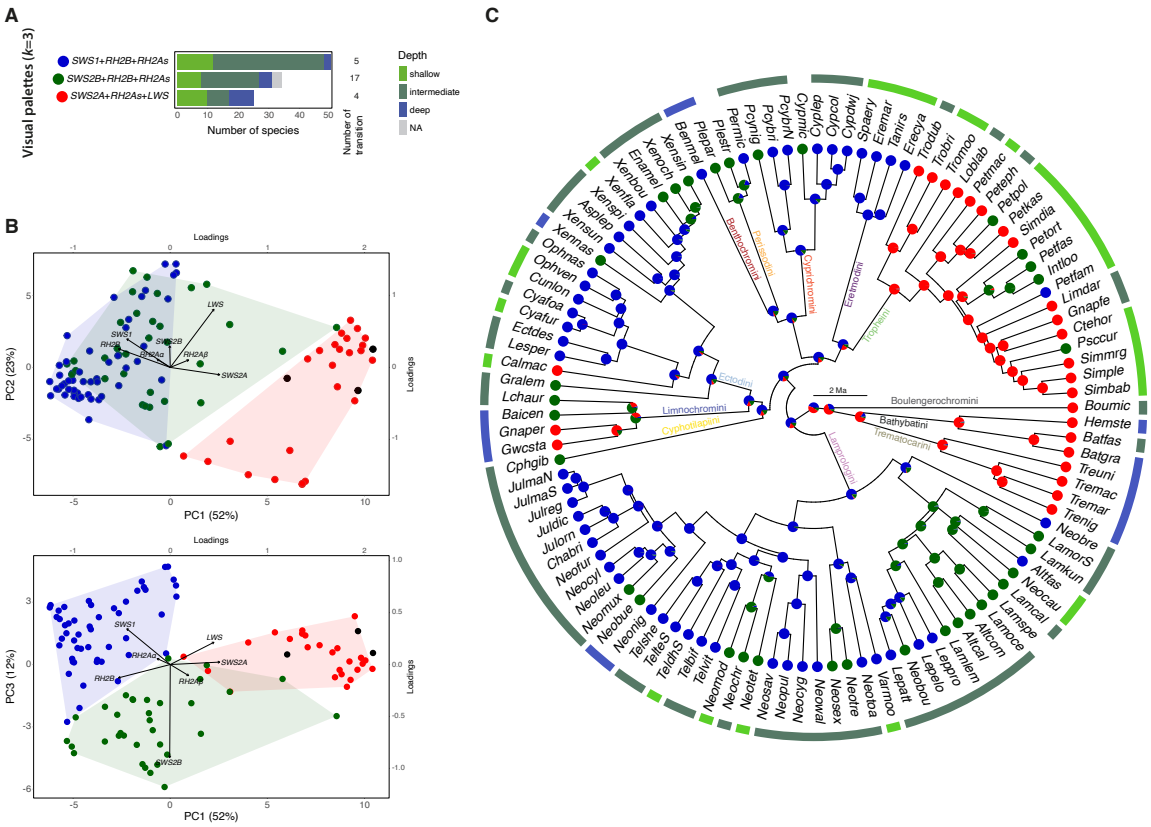

Fig. S9. Visual palette evolution in Lake Tanganyika cichlid fishes. (**A**) Barplot showing the number of species sharing one of the three visual palettes identified based on the hierarchical clustering analysis (*k*=3). Barplots are colour-coded according to the respective proportion of species in the three depth-categories at which the species occur. The number of evolutionary transitions into the respective visual palette according the ancestral state reconstruction shown in (**C**) is indicated on the right margin. (**B**) PCAs of the visual cone opsin gene expression levels. Each dot represents the weighted mean value of a given species and is colour-coded according to the visual palettes defined in (**A**). Visual palettes are indicated with convex hulls (except for *A. burtoni*, *O. tanganicae* and *T. polylepis*). The loadings of each PCA axis are indicated as black arrows. The variance explained by each principal component (PC) is reported in parenthesis. (**C**) Ancestral state reconstruction of visual palettes along the time-calibrated species tree (taken from Ronco et al. 2021 (*52*) and pruned to the species included in this study (see table S1 for full species names). Pie charts at the internal nodes indicate the relative posterior probability that the ancestor expressed each of the three visual palettes and are colour-coded according to the visual palettes shown in (**A**). Note that, just like in previous studies (*47*, *48*, *56*), *RH2Aα* and *RH2Aβ* were combined under the category *RH2As*, and that the primarily riverine haplochromine *A. burtoni* as well as the more distantly related species *O. tanganicae* and *T. polylepis* were excluded from this analysis.

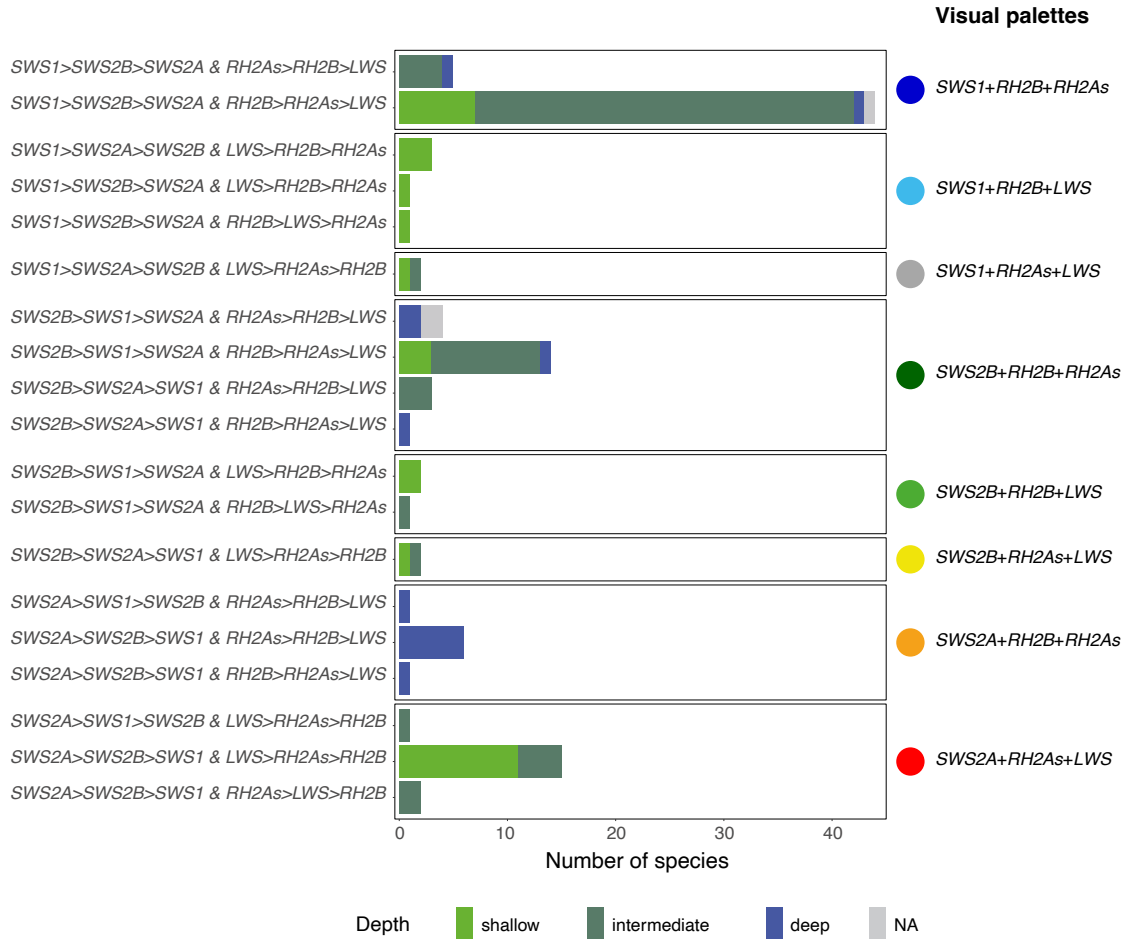

Fig. S10. Visual palette identification based on the expression level of single and double cone opsins in Lake Tanganyika cichlid fishes. Barplot showing the number of species sharing one of the 19 visual palettes identified based on the species-specific combinations of expressed single cone opsins and expressed double cone opsins using the majority-rule clustering method. Barplots are colour-coded according to the respective proportion of species in the three depth-categories at which the species occur. Barplots are grouped into the eight visual palettes identified based on the species-specific combinations of the most highly expressed single cone opsin and the two most highly expressed double cone opsins (SDD) (see Fig. 3). Note that, just like in previous studies (*47*, *48*, *56*), *RH2Aα* and *RH2Aβ* were combined under the category *RH2As*, and that the primarily riverine haplochromine *A. burtoni* as well as the more distantly related species *O. tanganicae* and *T. polylepis* were excluded from this analysis.

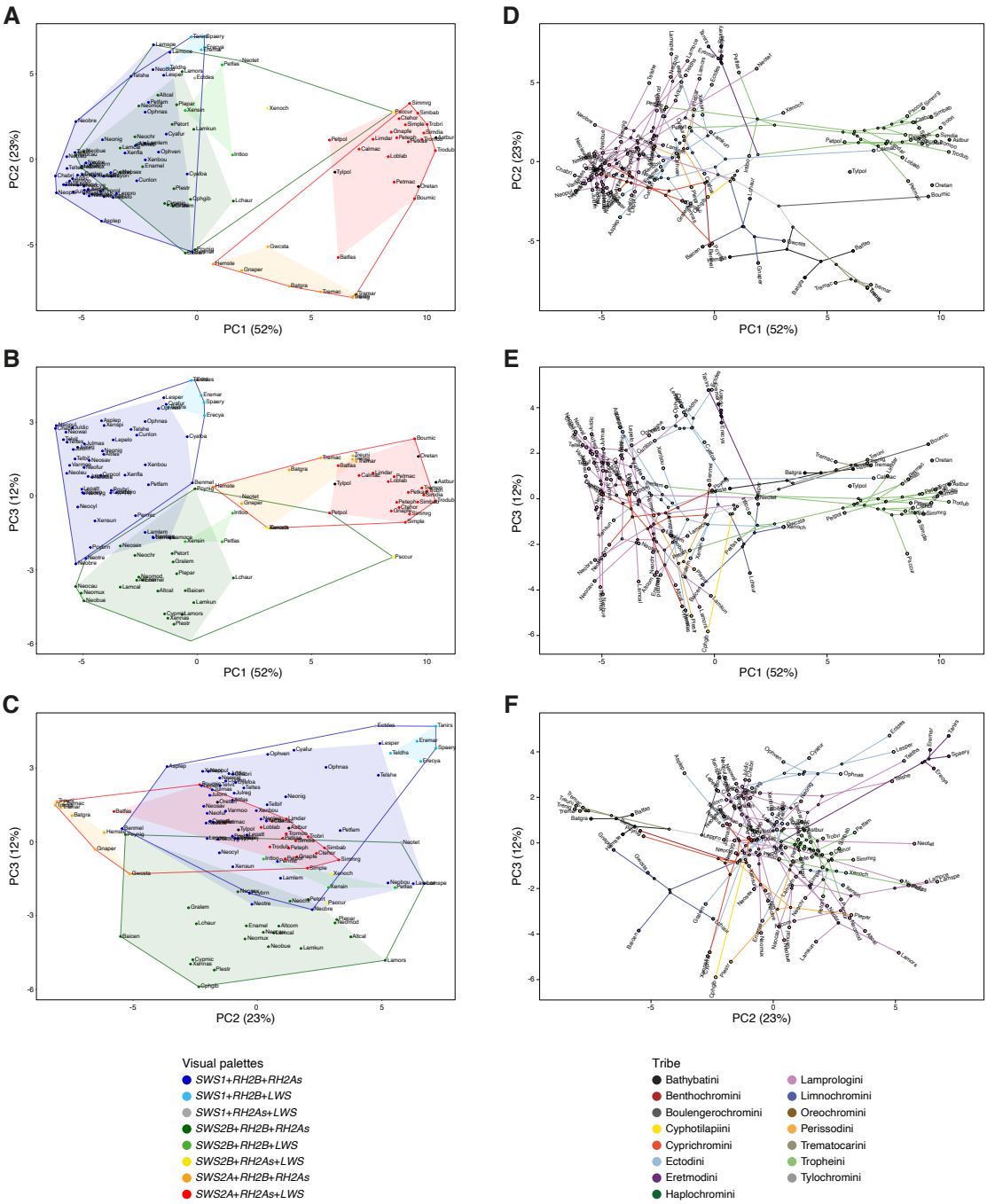
A
B
C
D
E
F
PC1 (52%)
PC2 (23%)
PC3 (12%)
Visual palettes
SWS1+RH2B+RH2As
SWS1+RH2B+LWS
SWS1+RH2As+LWS
SWS2B+RH2B+RH2As
SWS2B+RH2B+LWS
SWS2B+RH2As+LWS
SWS2A+RH2B+RH2As
SWS2A+RH2As+LWS
Tribe
Bathybatini
Benthochromini
Boulengerochromini
Cyphotilapiini
Cyprichromini
Ectodini
Eretmodini
Haplochromini
Lamprologini
Limnochromini
Oreochromini
Perissodini
Trematocarini
Tropheini
Tylochromini

Fig. S11. Visual palettes validation and phylomorphospace. PCAs of the visual cone opsin gene expression levels. (**A-C**) Each dot represents the weighted mean value of a given species and is colour-coded according to the eight visual palettes identified based on the species-specific combinations of the most highly expressed single cone opsin and the two most highly expressed double cone opsins (SDD) (see Fig. 3). The ranges of the visual palettes are indicated with convex hulls (coloured background shadings for the eight visual palettes based on the SDD clustering method and coloured delineations for the visual palettes identified using the hierarchical clustering method with k=3). (**D-F**) Each dot represents the weighted mean value of a given species and is colour-coded according to tribe. The ancestral state reconstruction (phylomorphospace) is based on the time-calibrated species tree (taken from Ronco et al. 2021 (*52*)). The species' relationship is represented by connective lines and colour-coded according to tribe. The variance explained by each principal component (PC) is reported in parenthesis. Note that *A. burtoni*, *O. tanganicae* and *T. polylepis* are present on the PCA (as in Fig. 1 and S3), but excluded from the visual palette clustering.

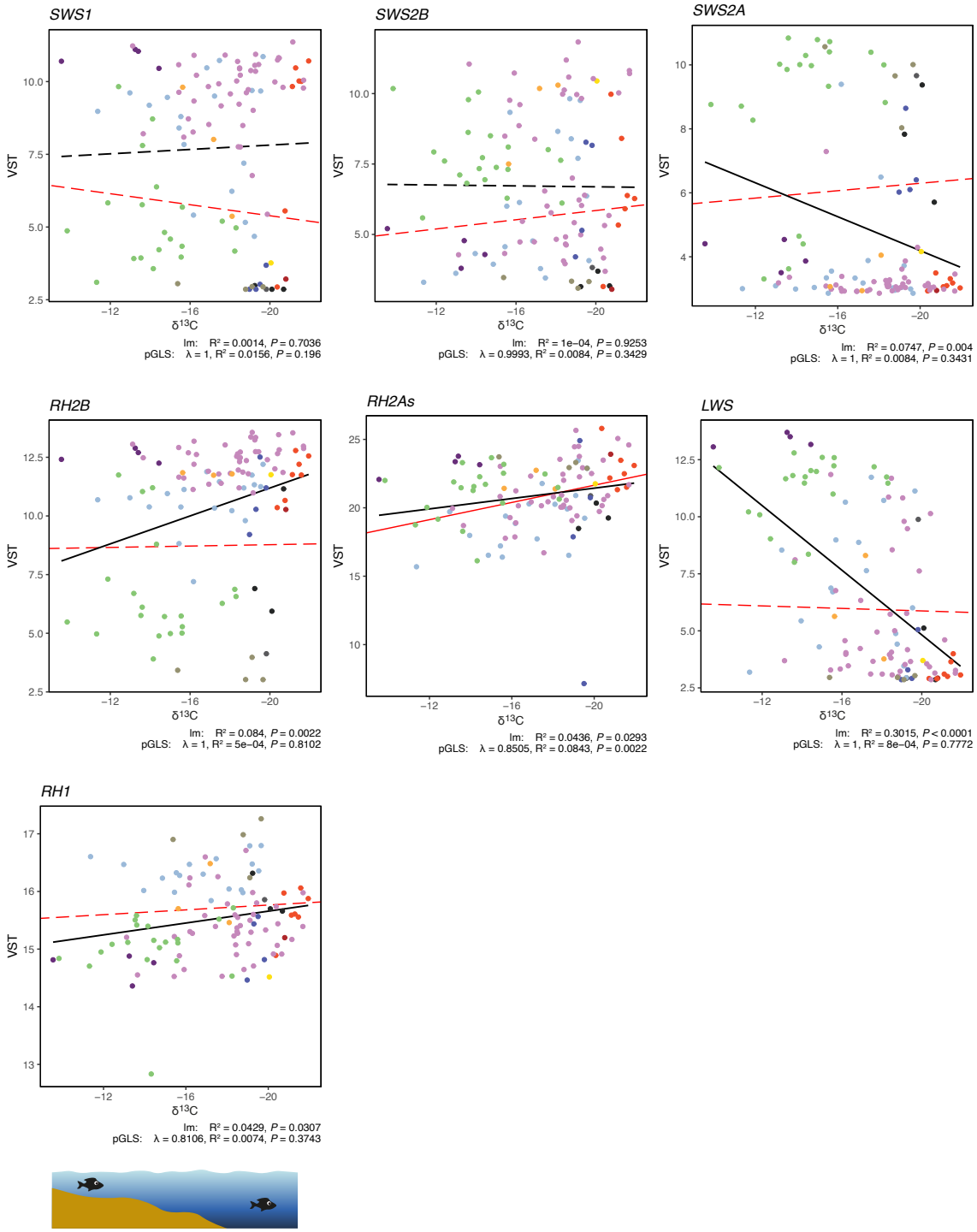
SWS1
VST
δ13C
lm: R² = 0.0014, P = 0.7036
pGLS: λ = 1, R² = 0.0156, P = 0.196
SWS2B
VST
δ13C
lm: R² = 1e−04, P = 0.9253
pGLS: λ = 0.9993, R² = 0.0084, P = 0.3429
SWS2A
VST
δ13C
lm: R² = 0.0747, P = 0.004
pGLS: λ = 1, R² = 0.0084, P = 0.3431
RH2B
VST
δ13C
lm: R² = 0.084, P = 0.0022
pGLS: λ = 1, R² = 5e−04, P = 0.8102
RH2As
VST
δ13C
lm: R² = 0.0436, P = 0.0293
pGLS: λ = 0.8505, R² = 0.0843, P = 0.0022
LWS
VST
δ13C
lm: R² = 0.3015, P < 0.0001
pGLS: λ = 1, R² = 8e−04, P = 0.7772
RH1
VST
δ13C
lm: R² = 0.0429, P = 0.0307
pGLS: λ = 0.8106, R² = 0.0074, P = 0.3743

Fig. S12. Visual opsin gene expression and its association with habitat. Linear regression (lm) and phylogenetic generalized least squares (pGLS) analyses showing the associations between visual opsin gene expression (VST normalized count) and $\delta^{13}C$-values as habitat proxy for a species' position along the benthic-pelagic axis. The panels show scatter plots for each visual opsin gene. For each test, the R-squared (R^2) and the p-value (P) are indicated, as well as the parameter lambda (λ) for the pGLS. The lm-fit is depicted in black and the pGLS-fit in red (at $P < 0.05$ with a solid line). Each dot represents a species and is colour-coded according to tribe. The primarily riverine haplochromine *A. burtoni* as well as the more distantly related species *O. tanganicae* and *T. polylepis* were excluded from this analysis.

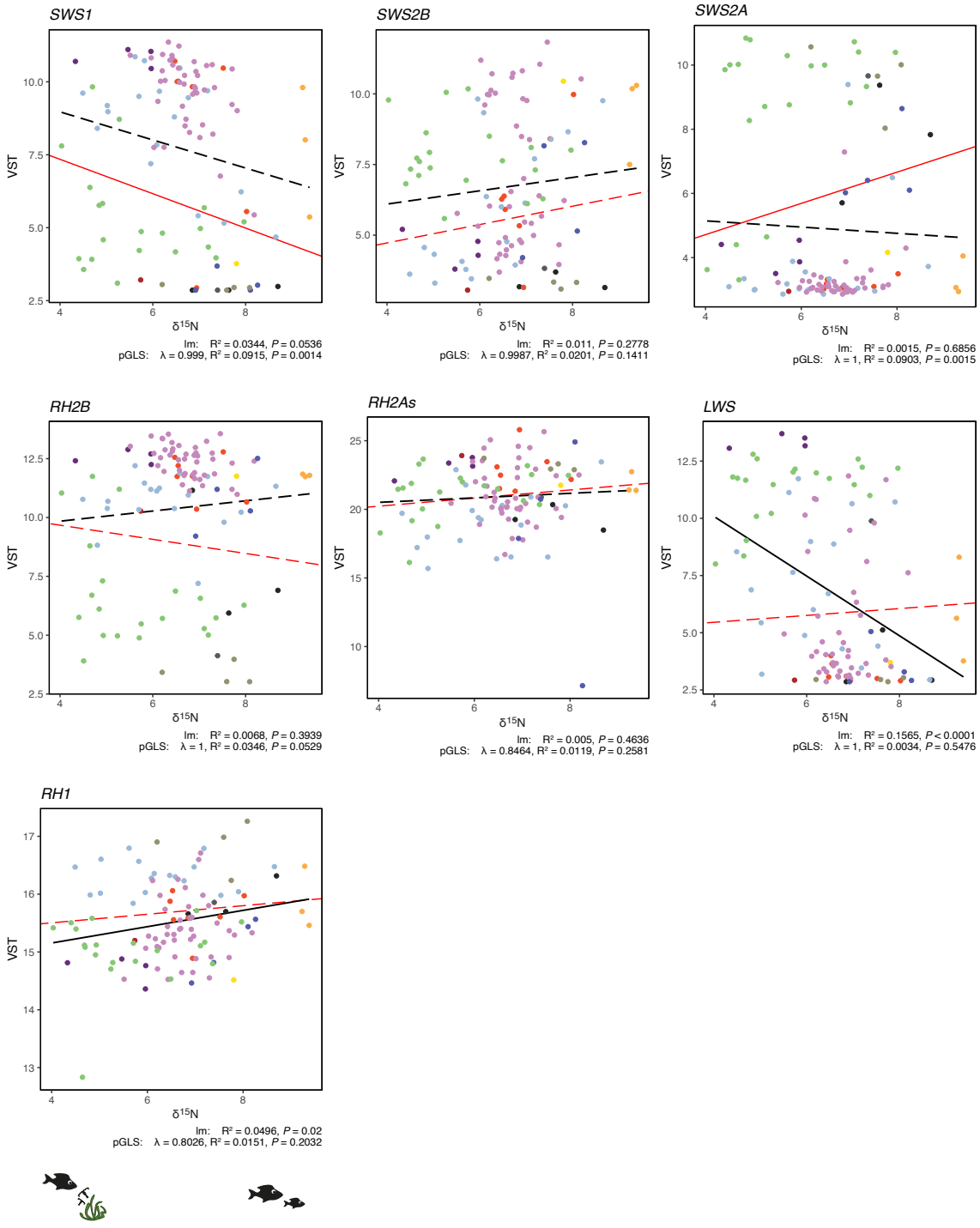
SWS1
VST
δ15N
lm: R² = 0.0344, P = 0.0536
pGLS: λ = 0.999, R² = 0.0915, P = 0.0014
SWS2B
VST
δ15N
lm: R² = 0.011, P = 0.2778
pGLS: λ = 0.9987, R² = 0.0201, P = 0.1411
SWS2A
VST
δ15N
lm: R² = 0.0015, P = 0.6856
pGLS: λ = 1, R² = 0.0903, P = 0.0015
RH2B
VST
δ15N
lm: R² = 0.0068, P = 0.3939
pGLS: λ = 1, R² = 0.0346, P = 0.0529
RH2As
VST
δ15N
lm: R² = 0.005, P = 0.4636
pGLS: λ = 0.8464, R² = 0.0119, P = 0.2581
LWS
VST
δ15N
lm: R² = 0.1565, P < 0.0001
pGLS: λ = 1, R² = 0.0034, P = 0.5476
RH1
VST
δ15N
lm: R² = 0.0496, P = 0.02
pGLS: λ = 0.8026, R² = 0.0151, P = 0.2032

Fig. S13. Visual opsin gene expression and its association with trophic level. Linear regression (lm) and phylogenetic generalized least squares (pGLS) analyses showing the associations between visual opsin gene expression (VST normalized count) and $\delta^{15}N$-values as proxy for the relative trophic level of a species. The panels show scatter plots for each visual opsin gene. For each test, the R-squared (R^2) and the p-value (P) are indicated, as well as the parameter lambda (λ) for the pGLS. The lm-fit is depicted in black and the pGLS-fit in red (at $P < 0.05$ with a solid line). Each dot represents a species and is colour-coded according to tribe. The primarily riverine haplochromine *A. burtoni* as well as the more distantly related species *O. tanganicae* and *T. polylepis* were excluded from this analysis.

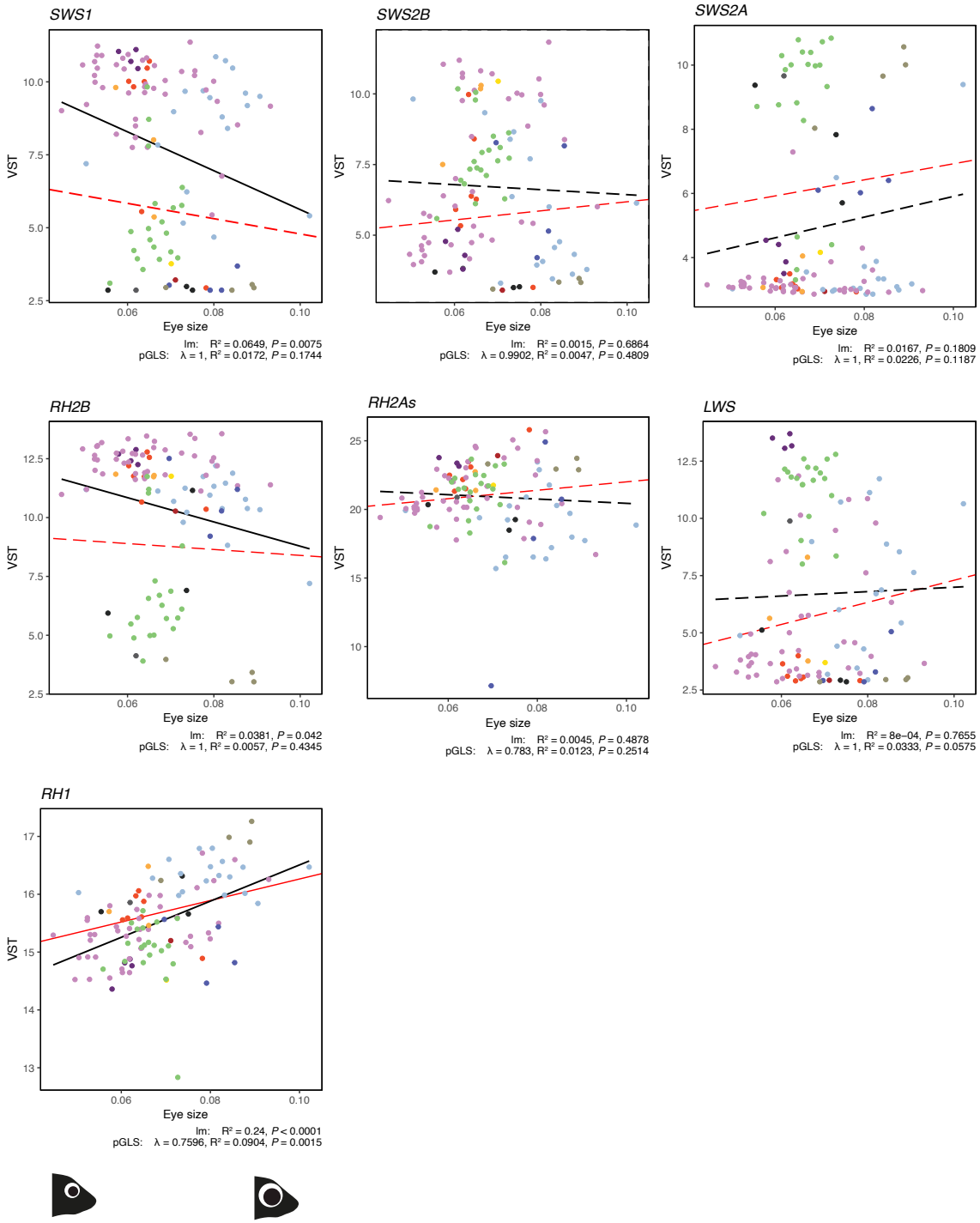
SWS1
VST
Eye size
lm: R² = 0.0649, P = 0.0075
pGLS: λ = 1, R² = 0.0172, P = 0.1744
SWS2B
VST
Eye size
lm: R² = 0.0015, P = 0.6864
pGLS: λ = 0.9902, R² = 0.0047, P = 0.4809
SWS2A
VST
Eye size
lm: R² = 0.0167, P = 0.1809
pGLS: λ = 1, R² = 0.0226, P = 0.1187
RH2B
VST
Eye size
lm: R² = 0.0381, P = 0.042
pGLS: λ = 1, R² = 0.0057, P = 0.4345
RH2As
VST
Eye size
lm: R² = 0.0045, P = 0.4878
pGLS: λ = 0.783, R² = 0.0123, P = 0.2514
LWS
VST
Eye size
lm: R² = 8e−04, P = 0.7655
pGLS: λ = 1, R² = 0.0333, P = 0.0575
RH1
VST
Eye size
lm: R² = 0.24, P < 0.0001
pGLS: λ = 0.7596, R² = 0.0904, P = 0.0015

Fig. S14. Visual opsin gene expression and its association with eye size. Linear regression (lm) and phylogenetic generalized least squares (pGLS) analyses showing the associations between visual opsin gene expression (VST normalized count) and relative eye size. The panels show scatter plots for each visual opsin gene. For each test, the R-squared (R^2) and the p-value (P) are indicated, as well as the parameter lambda (λ) for the pGLS. The lm-fit is depicted in black and the pGLS-fit in red (at $P < 0.05$ with a solid line). Each dot represents a species and is colour-coded according to tribe. The primarily riverine haplochromine *A. burtoni* as well as the more distantly related species *O. tanganicae* and *T. polylepis* were excluded from this analysis.

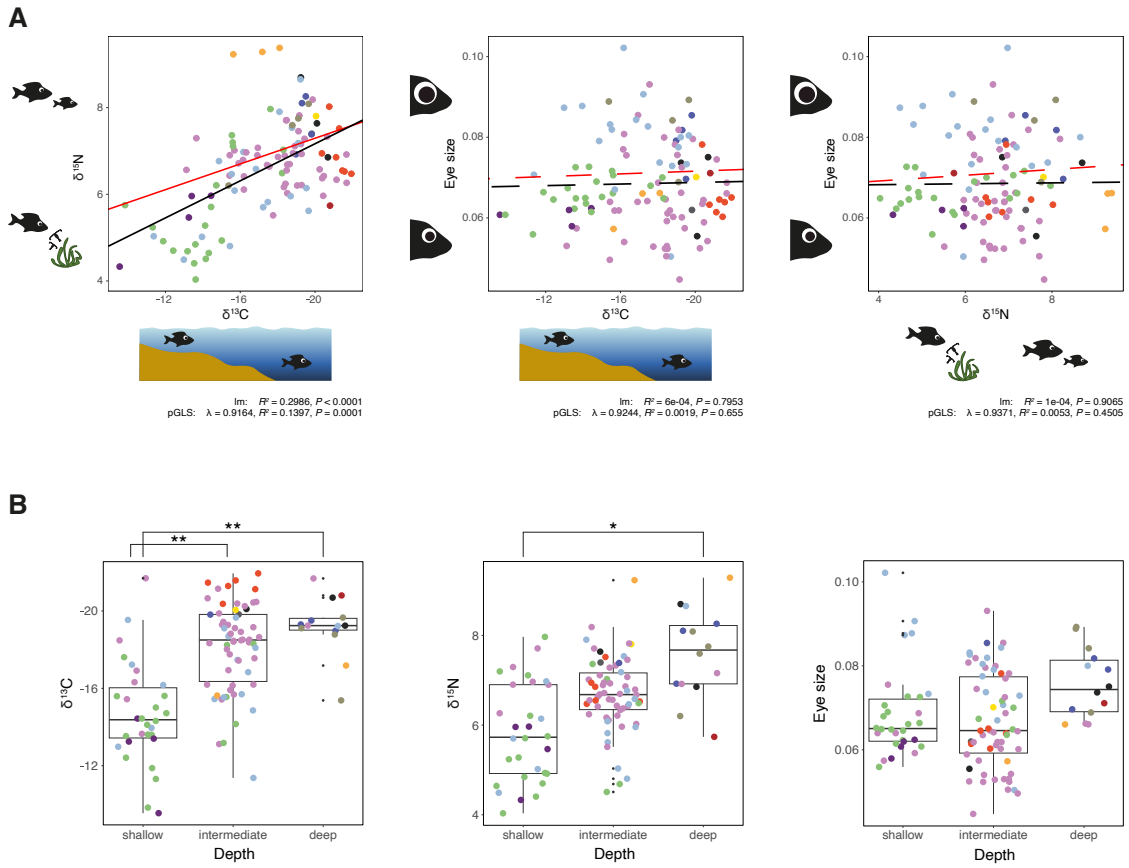

Fig. S15. Relationship between the eco-morphological traits. (**A**) Linear regression (lm) and phylogenetic generalized least squares (pGLS) analyses showing the associations between $\delta^{13}C$-values (habitat proxy for a species' position along the benthic-pelagic axis), $\delta^{15}N$-values (proxy for the relative trophic level of a species), and relative eye size. The panels show scatter plots for each test. The lm-fit is depicted in black and the pGLS-fit in red (at $P < 0.05$ with a solid line). Each dot represents a species and is colour-coded according to tribe. For each test, the R-squared (R^2) and the p-value (P) are indicated, as well as the parameter lambda (λ) for the pGLS. (**B**) Scattered boxplots showing the species distribution of $\delta^{13}C$-values, $\delta^{15}N$-values, and relative eye size relative to the depth category. Each scattered dot represents a species and is colour-coded according to tribe. The significant results based on the phylogenetic ANOVA test are depicted with asterisk (**: $P < 0.01$; *: $P < 0.05$; complete results in table S6). The primarily riverine haplochromine *A. burtoni* as well as the more distantly related species *O. tanganicae* and *T. polylepis* were excluded from this analysis.

Table S1. Overview of the dataset used for this study, including taxonomic, sample, and sampling information. Species which are not part of the Lake Tanganyika radiation ("outgroup" species or non-endemic species nested with the radiation) are marked with an asterisk (*).

Tribe	Species abbr. (full name)	Specimen ID	Sample ID	Sex	Sampling date	Location	GPS	Country
Bathybatini	Batfas (*Bathybates fasciatus*)	ITH3	JRA8	M	2014.07.24	Chipwa Fishermen	8°36'22.2"S 31°11'10.0"E	Zambia
Bathybatini	Batfas (*Bathybates fasciatus*)	ITH5	JRD1	M	2014.07.24	Chipwa Fishermen	8°36'22.2"S 31°11'10.0"E	Zambia
Bathybatini	Batfas (*Bathybates fasciatus*)	LNB1	MAH1	M	2016.08.22	Toby's Place	8°37'23.6"S 31°12'01.6"E	Zambia
Bathybatini	Batfas (*Bathybates fasciatus*)	LNI8	MZE8	F	2016.08.23	Chipwa Fishermen	8°36'22.2"S 31°11'10.0"E	Zambia
Bathybatini	Batfas (*Bathybates fasciatus*)	OME5	QDH1	F	2017.02.02	Nganja	06°10'24"S 029°44'25"E	Tanzania
Bathybatini	Batfas (*Bathybates fasciatus*)	OME6	QDI2	F	2017.02.02	Nganja	06°10'24"S 029°44'25"E	Tanzania
Bathybatini	Batfas (*Bathybates fasciatus*)	OME7	QFA4	M	2017.02.02	Nganja	06°10'24"S 029°44'25"E	Tanzania
Bathybatini	Batgra (*Bathybates grauer*i)	ILG7	DWC5	M	2014.08.16	Kombe Fishermen	8°47'36"S 31°01'06"E	Zambia
Bathybatini	Batgra (*Bathybates grauer*i)	LNB2	MAI3	M	2016.08.22	Toby's Place	8°37'23.6"S 31°12'01.6"E	Zambia
Bathybatini	Batgra (*Bathybates grauer*i)	LNB4	MBB3	F	2016.08.22	Toby's Place	8°37'23.6"S 31°12'01.6"E	Zambia
Bathybatini	Batgra (*Bathybates grauer*i)	LNB5	MBC6	M	2016.08.22	Toby's Place	8°37'23.6"S 31°12'01.6"E	Zambia
Bathybatini	Batgra (*Bathybates grauer*i)	LNB6	MBD7	F	2016.08.22	Toby's Place	8°37'23.6"S 31°12'01.6"E	Zambia
Bathybatini	Batgra (*Bathybates grauer*i)	SME7	SME7	F	2020.11.03	Chipwa Fishermen	8°36'22.2"S 31°11'10.0"E	Zambia
Bathybatini	Hemste (*Hemibates stenosoma*)	LOD8	NLD7	M	2016.08.26	Chipwa Fishermen	8°36'22.2"S 31°11'10.0"E	Zambia
Bathybatini	Hemste (*Hemibates stenosoma*)	LOD9	NLE8	M	2016.08.26	Chipwa Fishermen	8°36'22.2"S 31°11'10.0"E	Zambia
Bathybatini	Hemste (*Hemibates stenosoma*)	LPG3	NFC6	M	2016.08.25	Chipwa Fishermen	8°36'22.2"S 31°11'10.0"E	Zambia
Bathybatini	Hemste (*Hemibates stenosoma*)	RYD7	RCB2	F	2019.08.16	Chipwa Fishermen	8°36'22.2"S 31°11'10.0"E	Zambia
Bathybatini	Hemste (*Hemibates stenosoma*)	RYE1	RCE5	F	2019.08.17	Chipwa Fishermen	8°36'22.2"S 31°11'10.0"E	Zambia
Bathybatini	Hemste (*Hemibates stenosoma*)	RYE2	RCF6	F	2019.08.17	Chipwa Fishermen	8°36'22.2"S 31°11'10.0"E	Zambia
Benthochromini	Benmel (*Benthochromis melanoides*)	ILG5	DWB3	F	2014.08.16	Kombe Fishermen	8°47'36"S 31°01'06"E	Zambia
Benthochromini	Benmel (*Benthochromis melanoides*)	LNI9	MZF9	F	2016.08.23	Chipwa Fishermen	8°36'22.2"S 31°11'10.0"E	Zambia
Benthochromini	Benmel (*Benthochromis melanoides*)	LPA2	MZI2	F	2016.08.23	Chipwa Fishermen	8°36'22.2"S 31°11'10.0"E	Zambia
Benthochromini	Benmel (*Benthochromis melanoides*)	RYA2	QYB2	F	2019.08.13	Toby's Place	8°37'23.6"S 31°12'01.6"E	Zambia
Benthochromini	Benmel (*Benthochromis melanoides*)	RYB8	QZG7	M	2019.08.14	Chipwa Fishermen	8°36'22.2"S 31°11'10.0"E	Zambia
Benthochromini	Benmel (*Benthochromis melanoides*)	RYB9	RAB2	M	2019.08.14	Chipwa Fishermen	8°36'22.2"S 31°11'10.0"E	Zambia
Benthochromini	Benmel (*Benthochromis melanoides*)	RYC1	RAC3	M	2019.08.14	Chipwa Fishermen	8°36'22.2"S 31°11'10.0"E	Zambia
Boulengerochromini	Boumic (*Boulengerochromis microlepis*)	JAE6	GYC5	F	2014.07.31	Chipwa Fishermen	8°36'22.2"S 31°11'10.0"E	Zambia
Boulengerochromini	Boumic (*Boulengerochromis microlepis*)	MOF1	NUB5	M	2016.09.06	Kasenga West Fishermen	8°34'00.1"S 30°45'23.2"E	Zambia
Boulengerochromini	Boumic (*Boulengerochromis microlepis*)	MOF2	NUC6	M	2016.09.06	Chimba	08°25'34"S 30°27'24"E	Zambia
Boulengerochromini	Boumic (*Boulengerochromis microlepis*)	MPD5	OCB5	F	2016.09.09	Kachese	8°29'25.9"S 30°28'39.0"E	Zambia
Boulengerochromini	Boumic (*Boulengerochromis microlepis*)	MPG4	QKA4	F	2016.09.11	Mpende Fisheries	8°28'56.8"S 30°28'00.5"E	Zambia
Boulengerochromini	Boumic (*Boulengerochromis microlepis*)	RYH8	SPD4	F	2019.08.22	Toby's Place	8°37'23.6"S 31°12'01.6"E	Zambia
Boulengerochromini	Boumic (*Boulengerochromis microlepis*)	SNI1	SNI1	M	2020.11.04	Chipwa Fishermen	8°36'22.2"S 31°11'10.0"E	Zambia
Cyphotilapiini	Cphgib (*Cyphotilapia gibberosa*)	INH9	DWE7	F	2014.08.17	Kanfonki	8° 42' 10"S 30° 55' 21"E	Zambia
Cyphotilapiini	Cphgib (*Cyphotilapia gibberosa*)	MOA9	NRB5	F	2016.08.30	Chituta	8°43'25"S 31°09'00"E	Zambia
Cyphotilapiini	Cphgib (*Cyphotilapia gibberosa*)	MPE8	ODD7	F	2016.09.10	Mpende Fisheries	8°28'56.8"S 30°28'00.5"E	Zambia
Cyphotilapiini	Cphgib (*Cyphotilapia gibberosa*)	MPE9	ODE8	M	2016.09.10	Mpende Fisheries	8°28'56.8"S 30°28'00.5"E	Zambia
Cyphotilapiini	Cphgib (*Cyphotilapia gibberosa*)	MPF1	ODF9	M	2016.09.10	Mpende Fisheries	8°28'56.8"S 30°28'00.5"E	Zambia
Cyphotilapiini	Cphgib (*Cyphotilapia gibberosa*)	MPF2	ODH1	M	2016.09.10	Mpende Fisheries	8°28'56.8"S 30°28'00.5"E	Zambia
Cyphotilapiini	Cphgib (*Cyphotilapia gibberosa*)	RKI4	QUF2	M	2017.08.27	Chituta	8°43'25"S 31°09'00"E	Zambia
Cyphotilapiini	Cphgib (*Cyphotilapia gibberosa*)	RLA8	QVE1	F	2017.08.27	Chituta	8°43'25"S 31°09'00"E	Zambia
Cyphotilapiini	Cphgib (*Cyphotilapia gibberosa*)	RLB3	QVI5	F	2017.08.27	Chituta	8°43'25"S 31°09'00"E	Zambia
Cyprichromini	Cypcol (*Cyprichromis coloratus*)	IQC6	JJE8	M	2014.07.22	Toby's Place	8°37'23.6"S 31°12'01.6"E	Zambia
Cyprichromini	Cypcol (*Cyprichromis coloratus*)	IQC7	JJF9	M	2014.07.22	Toby's Place	8°37'23.6"S 31°12'01.6"E	Zambia
Cyprichromini	Cypcol (*Cyprichromis coloratus*)	IUA6	JSE1	F	2014.07.25	Isanga	8°39'16.4"S 31°11'30.6"E	Zambia
Cyprichromini	Cypcol (*Cyprichromis coloratus*)	LNF1	MSA4	M	2016.08.22	Toby's Place	8°37'23.6"S 31°12'01.6"E	Zambia
Cyprichromini	Cypcol (*Cyprichromis coloratus*)	LNF2	MSB5	M	2016.08.22	Toby's Place	8°37'23.6"S 31°12'01.6"E	Zambia
Cyprichromini	Cypcol (*Cyprichromis coloratus*)	LNF3	MSC6	M	2016.08.22	Toby's Place	8°37'23.6"S 31°12'01.6"E	Zambia
Cyprichromini	Cypcol (*Cyprichromis coloratus*)	RYA9	QZA1	F	2019.08.14	Toby's Place	8°37'23.6"S 31°12'01.6"E	Zambia
Cyprichromini	Cypcol (*Cyprichromis coloratus*)	RYC2	RAD4	F	2019.08.14	Toby's Place	8°37'23.6"S 31°12'01.6"E	Zambia
Cyprichromini	Cypcol (*Cyprichromis coloratus*)	RYC3	RAE5	F	2019.08.14	Toby's Place	8°37'23.6"S 31°12'01.6"E	Zambia
Cyprichromini	Cypdwj (*Cyprichromis* sp. "dwarf jumbo")	MVC5	OHH1	M	2017.01.18	Nondwa Point	04°51'51"S 029°36'26"E	Tanzania
Cyprichromini	Cypdwj (*Cyprichromis* sp. "dwarf jumbo")	MVC6	OHI2	M	2017.01.18	Nondwa Point	04°51'51"S 029°36'26"E	Tanzania
Cyprichromini	Cypdwj (*Cyprichromis* sp. "dwarf jumbo")	MVC7	OIA4	M	2017.01.18	Nondwa Point	04°51'51"S 029°36'26"E	Tanzania
Cyprichromini	Cypdwj (*Cyprichromis* sp. "dwarf jumbo")	MVC8	OIB5	F	2017.01.18	Nondwa Point	04°51'51"S 029°36'26"E	Tanzania
Cyprichromini	Cypdwj (*Cyprichromis* sp. "dwarf jumbo")	MVC9	OIC6	F	2017.01.18	Nondwa Point	04°51'51"S 029°36'26"E	Tanzania
Cyprichromini	Cypdwj (*Cyprichromis* sp. "dwarf jumbo")	MVD1	OID7	F	2017.01.18	Nondwa Point	04°51'51"S 029°36'26"E	Tanzania
Cyprichromini	Cyplep (*Cyprichromis leptosoma*)	LNE5	MRF9	F	2016.08.22	Toby's Place	8°37'23.6"S 31°12'01.6"E	Zambia
Cyprichromini	Cyplep (*Cyprichromis leptosoma*)	LPC5	MYA4	F	2016.08.24	Toby's Place	8°37'23.6"S 31°12'01.6"E	Zambia
Cyprichromini	Cyplep (*Cyprichromis leptosoma*)	MUG5	LTG8	M	2016.08.21	Toby's Place	8°37'23.6"S 31°12'01.6"E	Zambia
Cyprichromini	Cyplep (*Cyprichromis leptosoma*)	MUG6	LTI2	M	2016.08.21	Toby's Place	8°37'23.6"S 31°12'01.6"E	Zambia
Cyprichromini	Cyplep (*Cyprichromis leptosoma*)	MUG7	LUA2	F	2016.08.21	Toby's Place	8°37'23.6"S 31°12'01.6"E	Zambia
Cyprichromini	Cyplep (*Cyprichromis leptosoma*)	MUG8	LUB5	M	2016.08.21	Toby's Place	8°37'23.6"S 31°12'01.6"E	Zambia
Cyprichromini	Cypmic (*Cyprichromis microlepidotus*)	ONF2	PZH1	M	2017.01.23	Mabilibili	6°26'50.6"S 29°54'40.0"E	Tanzania
Cyprichromini	Cypmic (*Cyprichromis microlepidotus*)	ONF3	PZI2	M	2017.01.23	Mabilibili	6°26'50.6"S 29°54'40.0"E	Tanzania
Cyprichromini	Cypmic (*Cyprichromis microlepidotus*)	ONF4	QAA4	M	2017.01.23	Mabilibili	6°26'50.6"S 29°54'40.0"E	Tanzania
Cyprichromini	Cypmic (*Cyprichromis microlepidotus*)	ONF5	QAB5	F	2017.01.23	Mabilibili	6°26'50.6"S 29°54'40.0"E	Tanzania
Cyprichromini	Cypmic (*Cyprichromis microlepidotus*)	ONF6	QAC6	F	2017.01.23	Mabilibili	6°26'50.6"S 29°54'40.0"E	Tanzania
Cyprichromini	Cypmic (*Cyprichromis microlepidotus*)	ONF7	QAD7	F	2017.01.23	Mabilibili	6°26'50.6"S 29°54'40.0"E	Tanzania
Cyprichromini	Pcybri (*Paracyprichromis* sp. "brieni south")	IQB9	JII3	M	2014.07.22	Toby's Place	8°37'23.6"S 31°12'01.6"E	Zambia
Cyprichromini	Pcybri (*Paracyprichromis* sp. "brieni south")	IQC1	JJA4	F	2014.07.22	Toby's Place	8°37'23.6"S 31°12'01.6"E	Zambia
Cyprichromini	Pcybri (*Paracyprichromis* sp. "brieni south")	IQC2	JJB5	M	2014.07.22	Toby's Place	8°37'23.6"S 31°12'01.6"E	Zambia
Cyprichromini	Pcybri (*Paracyprichromis* sp. "brieni south")	IQC3	JJC6	F	2014.07.22	Toby's Place	8°37'23.6"S 31°12'01.6"E	Zambia
Cyprichromini	Pcybri (*Paracyprichromis* sp. "brieni south")	MUG2	LTD5	F	2016.08.21	Toby's Place	8°37'23.6"S 31°12'01.6"E	Zambia
Cyprichromini	Pcybri (*Paracyprichromis* sp. "brieni south")	MUG3	LTE8	M	2016.08.21	Toby's Place	8°37'23.6"S 31°12'01.6"E	Zambia
Cyprichromini	Pcybri (*Paracyprichromis* sp. "brieni south")	MUG4	LTF7	F	2016.08.21	Toby's Place	8°37'23.6"S 31°12'01.6"E	Zambia
Cyprichromini	Pcybri (*Paracyprichromis* sp. "brieni south")	RYB1	QZB2	F	2019.08.14	Toby's Place	8°37'23.6"S 31°12'01.6"E	Zambia
Cyprichromini	PcybrN (*Paracyprichromis brieni*)	JXI2	KPD5	M	2015.01.09	Nyaruhongoka 2	3°41'55.00"S 29°19'12.30"E	Burundi
Cyprichromini	PcybrN (*Paracyprichromis brieni*)	JXI3	KPE6	M	2015.01.09	Nyaruhongoka 2	3°41'55.00"S 29°19'12.30"E	Burundi
Cyprichromini	PcybrN (*Paracyprichromis brieni*)	JXI4	KPF7	F	2015.01.09	Nyaruhongoka 2	3°41'55.00"S 29°19'12.30"E	Burundi
Cyprichromini	PcybrN (*Paracyprichromis brieni*)	JXI5	KPG8	F	2015.01.09	Nyaruhongoka 2	3°41'55.00"S 29°19'12.30"E	Burundi
Cyprichromini	PcybrN (*Paracyprichromis brieni*)	MVD2	OIE8	M	2017.01.18	Nondwa Point	04°51'51"S 029°36'26"E	Tanzania

Cyprichromini	PcybrN (*Paracyprichromis brieni*)	MVD3	OIF9	F	2017.01.18	Nondwa Point	04°51'51"S 029°36'26"E	Tanzania
Cyprichromini	Pcynig (*Paracyprichromis nigripinnis*)	MOA1	NQB5	M	2016.08.30	Chituta	8°43'25"S 31°09'00"E	Zambia
Cyprichromini	Pcynig (*Paracyprichromis nigripinnis*)	MOA2	NQC9	M	2016.08.30	Chituta	8°43'25"S 31°09'00"E	Zambia
Cyprichromini	Pcynig (*Paracyprichromis nigripinnis*)	MOA3	NQD7	M	2016.08.30	Chituta	8°43'25"S 31°09'00"E	Zambia
Cyprichromini	Pcynig (*Paracyprichromis nigripinnis*)	MOA4	NQE8	F	2016.08.30	Chituta	8°43'25"S 31°09'00"E	Zambia
Cyprichromini	Pcynig (*Paracyprichromis nigripinnis*)	MOA5	NQF9	F	2016.08.30	Chituta	8°43'25"S 31°09'00"E	Zambia
Cyprichromini	Pcynig (*Paracyprichromis nigripinnis*)	MOA6	NQH1	F	2016.08.30	Chituta	8°43'25"S 31°09'00"E	Zambia
Ectodini	Asplep (*Asprotilapia leptura*)	LOA1	MXA4	F	2016.08.23	Isanga	8°39'16.4"S 31°11'30.6"E	Zambia
Ectodini	Asplep (*Asprotilapia leptura*)	LPB9	NBD7	M	2016.08.24	Toby's Place	8°37'23.6"S 31°12'01.6"E	Zambia
Ectodini	Asplep (*Asprotilapia leptura*)	LPC1	NBE8	M	2016.08.24	Toby's Place	8°37'23.6"S 31°12'01.6"E	Zambia
Ectodini	Asplep (*Asprotilapia leptura*)	LPC2	NBF9	F	2016.08.24	Toby's Place	8°37'23.6"S 31°12'01.6"E	Zambia
Ectodini	Asplep (*Asprotilapia leptura*)	LPC3	NBH1	F	2016.08.24	Toby's Place	8°37'23.6"S 31°12'01.6"E	Zambia
Ectodini	Asplep (*Asprotilapia leptura*)	RYC4	RAF6	M	2019.08.14	Toby's Place	8°37'23.6"S 31°12'01.6"E	Zambia
Ectodini	Calmac (*Callochromis macrops*)	LPF1	NDI2	M	2016.08.25	Toby's Place	8°37'23.6"S 31°12'01.6"E	Zambia
Ectodini	Calmac (*Callochromis macrops*)	LPI2	NHD7	M	2016.08.25	Toby's Place	8°37'23.6"S 31°12'01.6"E	Zambia
Ectodini	Calmac (*Callochromis macrops*)	MOH5	NWH1	F	2016.09.07	Ndole bay harbor	8°28'34.1"S 30°26'57.6"E	Zambia
Ectodini	Calmac (*Callochromis macrops*)	MOH6	NWI2	F	2016.09.07	Ndole bay harbor	8°28'34.1"S 30°26'57.6"E	Zambia
Ectodini	Calmac (*Callochromis macrops*)	MOH7	NXA4	F	2016.09.07	Ndole bay harbor	8°28'34.1"S 30°26'57.6"E	Zambia
Ectodini	Calmac (*Callochromis macrops*)	MUC5	LYD7	M	2016.08.20	Toby's Place	8°37'23.6"S 31°12'01.6"E	Zambia
Ectodini	Cunlon (*Cunningtonia longiventralis*)	IQH5	JLB4	M	2014.07.22	Toby's Place	8°37'23.6"S 31°12'01.6"E	Zambia
Ectodini	Cunlon (*Cunningtonia longiventralis*)	LPC7	MYC6	F	2016.08.24	Toby's Place	8°37'23.6"S 31°12'01.6"E	Zambia
Ectodini	Cunlon (*Cunningtonia longiventralis*)	LPC8	MYD7	M	2016.08.24	Toby's Place	8°37'23.6"S 31°12'01.6"E	Zambia
Ectodini	Cunlon (*Cunningtonia longiventralis*)	LPC9	MYE8	M	2016.08.24	Toby's Place	8°37'23.6"S 31°12'01.6"E	Zambia
Ectodini	Cunlon (*Cunningtonia longiventralis*)	LPD1	MYF9	F	2016.08.24	Toby's Place	8°37'23.6"S 31°12'01.6"E	Zambia
Ectodini	Cunlon (*Cunningtonia longiventralis*)	LPF5	NED7	F	2016.08.25	Toby's Place	8°37'23.6"S 31°12'01.6"E	Zambia
Ectodini	Cyafoa (*Cyathopharynx foae*)	IPF1	JGE1	M	2014.07.21	Toby's Place	8°37'23.6"S 31°12'01.6"E	Zambia
Ectodini	Cyafoa (*Cyathopharynx foae*)	IUB6	JSG4	M	2014.07.25	Isanga	8°39'16.4"S 31°11'30.6"E	Zambia
Ectodini	Cyafoa (*Cyathopharynx foae*)	MOF3	NUD7	M	2016.09.06	Chimba	08°25'34"S 30°27'24"E	Zambia
Ectodini	Cyafoa (*Cyathopharynx foae*)	MOF4	NUE8	F	2016.09.06	Chimba	08°25'34"S 30°27'24"E	Zambia
Ectodini	Cyafoa (*Cyathopharynx foae*)	MPG6	QKC6	F	2016.09.11	Mpende Fisheries	8°28'56.8"S 30°28'00.5"E	Zambia
Ectodini	Cyafoa (*Cyathopharynx foae*)	MPG7	QKD7	F	2016.09.11	Mpende Fisheries	8°28'56.8"S 30°28'00.5"E	Zambia
Ectodini	Cyafur (*Cyathopharynx furcifer*)	LPD3	MYI2	M	2016.08.24	Toby's Place	8°37'23.6"S 31°12'01.6"E	Zambia
Ectodini	Cyafur (*Cyathopharynx furcifer*)	LPF2	NEA4	M	2016.08.25	Toby's Place	8°37'23.6"S 31°12'01.6"E	Zambia
Ectodini	Cyafur (*Cyathopharynx furcifer*)	LPF3	NEB5	M	2016.08.25	Toby's Place	8°37'23.6"S 31°12'01.6"E	Zambia
Ectodini	Cyafur (*Cyathopharynx furcifer*)	MOF5	NUF9	F	2016.09.06	Chimba	08°25'34"S 30°27'24"E	Zambia
Ectodini	Cyafur (*Cyathopharynx furcifer*)	MPD3	OBI2	F	2016.09.09	Kachese	8°29'25.9"S 30°28'39.0"E	Zambia
Ectodini	Cyafur (*Cyathopharynx furcifer*)	MPD4	OCA4	F	2016.09.09	Kachese	8°29'25.9"S 30°28'39.0"E	Zambia
Ectodini	Ectdes (*Ectodus descampsii*)	ITA1	JPB1	F	2014.07.24	Toby's Place	8°37'23.6"S 31°12'01.6"E	Zambia
Ectodini	Ectdes (*Ectodus descampsii*)	LOG2	NNF9	M	2016.08.26	Toby's Place	8°37'23.6"S 31°12'01.6"E	Zambia
Ectodini	Ectdes (*Ectodus descampsii*)	MPD9	OCE8	F	2016.09.10	Ndole bay harbor	8°28'34.1"S 30°26'57.6"E	Zambia
Ectodini	Ectdes (*Ectodus descampsii*)	RKF5	QTG3	F	2017.08.26	Toby's Place	8°37'23.6"S 31°12'01.6"E	Zambia
Ectodini	Ectdes (*Ectodus descampsii*)	RKF6	QTH4	M	2017.08.26	Toby's Place	8°37'23.6"S 31°12'01.6"E	Zambia
Ectodini	Ectdes (*Ectodus descampsii*)	RKF7	QTI5	M	2017.08.26	Toby's Place	8°37'23.6"S 31°12'01.6"E	Zambia
Ectodini	Ectdes (*Ectodus descampsii*)	RKF8	QUA7	F	2017.08.26	Toby's Place	8°37'23.6"S 31°12'01.6"E	Zambia
Ectodini	Ectdes (*Ectodus descampsii*)	RKF9	QUB8	M	2017.08.26	Toby's Place	8°37'23.6"S 31°12'01.6"E	Zambia
Ectodini	Ectdes (*Ectodus descampsii*)	RKG1	QUC9	F	2017.08.26	Toby's Place	8°37'23.6"S 31°12'01.6"E	Zambia
Ectodini	Enamel (*Enantiopus melanogenys*)	OMA1	QCC6	M	2017.01.27	Mwamahunga	04°54'43"S 029°35'54"E	Tanzania
Ectodini	Enamel (*Enantiopus melanogenys*)	OMA2	QCD7	M	2017.01.27	Mwamahunga	04°54'43"S 029°35'54"E	Tanzania
Ectodini	Enamel (*Enantiopus melanogenys*)	OMA3	QCE8	F	2017.01.27	Mwamahunga	04°54'43"S 029°35'54"E	Tanzania
Ectodini	Enamel (*Enantiopus melanogenys*)	OMA4	QCF9	F	2017.01.27	Mwamahunga	04°54'43"S 029°35'54"E	Tanzania
Ectodini	Enamel (*Enantiopus melanogenys*)	OMA5	QCH1	F	2017.01.27	Mwamahunga	04°54'43"S 029°35'54"E	Tanzania
Ectodini	Enamel (*Enantiopus melanogenys*)	ONI9	QCB5	M	2017.01.27	Mwamahunga	04°54'43"S 029°35'54"E	Tanzania
Ectodini	Gralem (*Grammatotria lemairii*)	IUA7	JSF3	M	2014.07.25	Toby's Place	8°37'23.6"S 31°12'01.6"E	Zambia
Ectodini	Gralem (*Grammatotria lemairii*)	LOB6	NII3	F	2016.08.26	Chipwa Fishermen	8°36'22.2"S 31°11'10.0"E	Zambia
Ectodini	Gralem (*Grammatotria lemairii*)	LPF4	NEC6	M	2016.08.25	Chipwa Fishermen	8°36'22.2"S 31°11'10.0"E	Zambia
Ectodini	Gralem (*Grammatotria lemairii*)	LPF7	NEF9	F	2016.08.25	Chipwa Fishermen	8°36'22.2"S 31°11'10.0"E	Zambia
Ectodini	Gralem (*Grammatotria lemairii*)	LPG1	NFA4	M	2016.08.25	Chipwa Fishermen	8°36'22.2"S 31°11'10.0"E	Zambia
Ectodini	Gralem (*Grammatotria lemairii*)	MPB8	OAD7	F	2016.09.08	Katete 3	08° 20' 16"S 30° 30' 40"E	Zambia
Ectodini	Lesper (*Lestradea perspicax*)	MVF8	OLA4	M	2017.01.19	George's place	04°53'06"S 029°37'15"E	Tanzania
Ectodini	Lesper (*Lestradea perspicax*)	MVF9	OLB5	M	2017.01.19	George's place	04°53'06"S 029°37'15"E	Tanzania
Ectodini	Lesper (*Lestradea perspicax*)	MVG1	OLC6	M	2017.01.19	George's place	04°53'06"S 029°37'15"E	Tanzania
Ectodini	Lesper (*Lestradea perspicax*)	MVG2	OLD7	F	2017.01.19	George's place	04°53'06"S 029°37'15"E	Tanzania
Ectodini	Lesper (*Lestradea perspicax*)	MVG4	OLF9	F	2017.01.19	George's place	04°53'06"S 029°37'15"E	Tanzania
Ectodini	Lesper (*Lestradea perspicax*)	MVG6	OLI2	F	2017.01.19	George's place	04°53'06"S 029°37'15"E	Tanzania
Ectodini	Ophnas (*Ophthalmotilapia nasuta*)	LNE2	MRC6	F	2016.08.22	Toby's Place	8°37'23.6"S 31°12'01.6"E	Zambia
Ectodini	Ophnas (*Ophthalmotilapia nasuta*)	LNE3	MRD6	M	2016.08.22	Toby's Place	8°37'23.6"S 31°12'01.6"E	Zambia
Ectodini	Ophnas (*Ophthalmotilapia nasuta*)	LNE4	MRE8	F	2016.08.22	Toby's Place	8°37'23.6"S 31°12'01.6"E	Zambia
Ectodini	Ophnas (*Ophthalmotilapia nasuta*)	LNE8	MRH1	M	2016.08.22	Toby's Place	8°37'23.6"S 31°12'01.6"E	Zambia
Ectodini	Ophnas (*Ophthalmotilapia nasuta*)	LNE9	MRI2	M	2016.08.22	Toby's Place	8°37'23.6"S 31°12'01.6"E	Zambia
Ectodini	Ophnas (*Ophthalmotilapia nasuta*)	LNG6	MTE8	F	2016.08.22	Toby's Place	8°37'23.6"S 31°12'01.6"E	Zambia
Ectodini	Ophven (*Ophthalmotilapia ventralis*)	IQD3	JKC5	M	2014.07.22	Toby's Place	8°37'23.6"S 31°12'01.6"E	Zambia
Ectodini	Ophven (*Ophthalmotilapia ventralis*)	IQE4	JKE8	F	2014.07.22	Toby's Place	8°37'23.6"S 31°12'01.6"E	Zambia
Ectodini	Ophven (*Ophthalmotilapia ventralis*)	IQE8	JKF8	F	2014.07.22	Toby's Place	8°37'23.6"S 31°12'01.6"E	Zambia
Ectodini	Ophven (*Ophthalmotilapia ventralis*)	LNB7	MBE6	M	2016.08.22	Toby's Place	8°37'23.6"S 31°12'01.6"E	Zambia
Ectodini	Ophven (*Ophthalmotilapia ventralis*)	MUC1	LXG8	M	2016.08.20	Toby's Place	8°37'23.6"S 31°12'01.6"E	Zambia
Ectodini	Ophven (*Ophthalmotilapia ventralis*)	MUH6	LVA4	F	2016.08.21	Toby's Place	8°37'23.6"S 31°12'01.6"E	Zambia
Ectodini	Ophven (*Ophthalmotilapia ventralis*)	MUI8	LWD5	M	2016.08.21	Toby's Place	8°37'23.6"S 31°12'01.6"E	Zambia
Ectodini	Xenbou (*Xenotilapia boulengeri*)	IPC4	JFH4	M	2014.07.20	Toby's Place	8°37'23.6"S 31°12'01.6"E	Zambia
Ectodini	Xenbou (*Xenotilapia boulengeri*)	IPE7	JGC9	F	2014.07.21	Toby's Place	8°37'23.6"S 31°12'01.6"E	Zambia
Ectodini	Xenbou (*Xenotilapia boulengeri*)	LOB7	NJA4	M	2016.08.26	Toby's Place	8°37'23.6"S 31°12'01.6"E	Zambia
Ectodini	Xenbou (*Xenotilapia boulengeri*)	LOB8	NJB5	M	2016.08.26	Toby's Place	8°37'23.6"S 31°12'01.6"E	Zambia
Ectodini	Xenbou (*Xenotilapia boulengeri*)	LOB9	NJC6	F	2016.08.26	Toby's Place	8°37'23.6"S 31°12'01.6"E	Zambia
Ectodini	Xenbou (*Xenotilapia boulengeri*)	MUF4	LSE6	F	2016.08.20	Toby's Place	8°37'23.6"S 31°12'01.6"E	Zambia
Ectodini	Xenfla (*Xenotilapia flavipinnis*)	LPG5	NFE8	F	2016.08.25	Toby's Place	8°37'23.6"S 31°12'01.6"E	Zambia
Ectodini	Xenfla (*Xenotilapia flavipinnis*)	LPG6	NFF9	M	2016.08.25	Toby's Place	8°37'23.6"S 31°12'01.6"E	Zambia
Ectodini	Xenfla (*Xenotilapia flavipinnis*)	LPG7	NFH1	F	2016.08.25	Toby's Place	8°37'23.6"S 31°12'01.6"E	Zambia
Ectodini	Xenfla (*Xenotilapia flavipinnis*)	LPG8	NFI2	M	2016.08.25	Toby's Place	8°37'23.6"S 31°12'01.6"E	Zambia
Ectodini	Xenfla (*Xenotilapia flavipinnis*)	LPH1	NGB5	F	2016.08.25	Toby's Place	8°37'23.6"S 31°12'01.6"E	Zambia
Ectodini	Xenfla (*Xenotilapia flavipinnis*)	LPH4	NGE8	M	2016.08.25	Toby's Place	8°37'23.6"S 31°12'01.6"E	Zambia
Ectodini	Xennas (*Xenotilapia nasus*)	MOB5	NRF9	F	2016.08.30	Chituta	8°43'25"S 31°09'00"E	Zambia
Ectodini	Xennas (*Xenotilapia nasus*)	MOB6	NRH1	M	2016.08.30	Chituta	8°43'25"S 31°09'00"E	Zambia
Ectodini	Xennas (*Xenotilapia nasus*)	MOC7	NTA4	F	2016.08.31	Chituta	8°43'25"S 31°09'00"E	Zambia
Ectodini	Xennas (*Xenotilapia nasus*)	MOC8	NTB5	M	2016.08.31	Chituta	8°43'25"S 31°09'00"E	Zambia
Ectodini	Xennas (*Xenotilapia nasus*)	MOC9	NTC6	F	2016.08.31	Chituta	8°43'25"S 31°09'00"E	Zambia

Ectodini	Xennas (*Xenotilapia nasus*)	MOD3	NTF9	M	2016.08.31	Chituta	8°43'25"S 31°09'00"E	Zambia
Ectodini	Xenoch (*Xenotilapia ochrogenys*)	JVH4	KNF7	M	2015.01.07	Mireille fishermen	3°24'12.10"S 29°21'33.30"E	Burundi
Ectodini	Xenoch (*Xenotilapia ochrogenys*)	JVH8	KNG8	F	2015.01.07	Mireille fishermen	3°24'12.10"S 29°21'33.30"E	Burundi
Ectodini	Xenoch (*Xenotilapia ochrogenys*)	JVI2	KNH9	M	2015.01.07	Mireille fishermen	3°24'12.10"S 29°21'33.30"E	Burundi
Ectodini	Xenoch (*Xenotilapia ochrogenys*)	JVI5	KMA2	F	2015.01.07	Mireille fishermen	3°24'12.10"S 29°21'33.30"E	Burundi
Ectodini	Xenoch (*Xenotilapia ochrogenys*)	MVE5	OKA4	M	2017.01.19	George's place	04°53'06"S 029°37'15"E	Tanzania
Ectodini	Xenoch (*Xenotilapia ochrogenys*)	MVE6	OKB5	F	2017.01.19	George's place	04°53'06"S 029°37'15"E	Tanzania
Ectodini	Xensin (*Xenotilapia singularis*)	LOF8	NND7	F	2016.08.26	Toby's Place	8°37'23.6"S 31°12'01.6"E	Zambia
Ectodini	Xensin (*Xenotilapia singularis*)	LOF9	NNE8	F	2016.08.26	Toby's Place	8°37'23.6"S 31°12'01.6"E	Zambia
Ectodini	Xensin (*Xenotilapia singularis*)	MPE3	OCH1	M	2016.09.10	Ndole bay harbor	8°28'34.1"S 30°26'57.6"E	Zambia
Ectodini	Xensin (*Xenotilapia singularis*)	MPE4	OCI2	M	2016.09.10	Ndole bay harbor	8°28'34.1"S 30°26'57.6"E	Zambia
Ectodini	Xensin (*Xenotilapia singularis*)	MPE5	ODA4	M	2016.09.10	Ndole bay harbor	8°28'34.1"S 30°26'57.6"E	Zambia
Ectodini	Xensin (*Xenotilapia singularis*)	MPE6	ODB6	F	2016.09.10	Ndole bay harbor	8°28'34.1"S 30°26'57.6"E	Zambia
Ectodini	Xensin (*Xenotilapia singularis*)	MPG8	QKE8	F	2016.09.11	Ndole bay harbor	8°28'34.1"S 30°26'57.6"E	Zambia
Ectodini	Xenspi (*Xenotilapia spilopterus*)	LNH2	MWB5	M	2016.08.23	Toby's Place	8°37'23.6"S 31°12'01.6"E	Zambia
Ectodini	Xenspi (*Xenotilapia spilopterus*)	LNH4	MWC6	F	2016.08.23	Toby's Place	8°37'23.6"S 31°12'01.6"E	Zambia
Ectodini	Xenspi (*Xenotilapia spilopterus*)	LNH6	MWD7	M	2016.08.23	Toby's Place	8°37'23.6"S 31°12'01.6"E	Zambia
Ectodini	Xenspi (*Xenotilapia spilopterus*)	LNH8	MWE8	M	2016.08.23	Toby's Place	8°37'23.6"S 31°12'01.6"E	Zambia
Ectodini	Xenspi (*Xenotilapia spilopterus*)	LNI3	MWI2	F	2016.08.23	Toby's Place	8°37'23.6"S 31°12'01.6"E	Zambia
Ectodini	Xenspi (*Xenotilapia spilopterus*)	LPA3	MXF9	F	2016.08.23	Toby's Place	8°37'23.6"S 31°12'01.6"E	Zambia
Ectodini	Xenspi (*Xenotilapia spilopterus*)	MUF6	LSH1	M	2016.08.21	Toby's Place	8°37'23.6"S 31°12'01.6"E	Zambia
Ectodini	Xensun (*Xenotilapia* sp. "papilio sunflower")	IUD1	JSI6	F	2014.07.25	Isanga	8°39'16.4"S 31°11'30.6"E	Zambia
Ectodini	Xensun (*Xenotilapia* sp. "papilio sunflower")	RYE9	RDE5	M	2019.08.19	Isanga	8°39'16.4"S 31°11'30.6"E	Zambia
Ectodini	Xensun (*Xenotilapia* sp. "papilio sunflower")	RYF1	RDF6	M	2019.08.19	Isanga	8°39'16.4"S 31°11'30.6"E	Zambia
Ectodini	Xensun (*Xenotilapia* sp. "papilio sunflower")	RYF2	RDG7	F	2019.08.19	Isanga	8°39'16.4"S 31°11'30.6"E	Zambia
Ectodini	Xensun (*Xenotilapia* sp. "papilio sunflower")	RYF3	RDH8	F	2019.08.19	Isanga	8°39'16.4"S 31°11'30.6"E	Zambia
Ectodini	Xensun (*Xenotilapia* sp. "papilio sunflower")	RYF4	REI9	F	2019.08.19	Isanga	8°39'16.4"S 31°11'30.6"E	Zambia
Ectodini	Xensun (*Xenotilapia* sp. "papilio sunflower")	RYF5	REB2	M	2019.08.19	Isanga	8°39'16.4"S 31°11'30.6"E	Zambia
Eretmodini	Erecya (*Eretmodus cyanostictus*)	ISG1	JOD3	F	2014.07.23	Toby's Place	8°37'23.6"S 31°12'01.6"E	Zambia
Eretmodini	Erecya (*Eretmodus cyanostictus*)	LNA3	LWH9	M	2016.08.21	Toby's Place	8°37'23.6"S 31°12'01.6"E	Zambia
Eretmodini	Erecya (*Eretmodus cyanostictus*)	MUD5	LZD5	F	2016.08.20	Toby's Place	8°37'23.6"S 31°12'01.6"E	Zambia
Eretmodini	Erecya (*Eretmodus cyanostictus*)	MUE2	LRC1	F	2016.08.20	Toby's Place	8°37'23.6"S 31°12'01.6"E	Zambia
Eretmodini	Erecya (*Eretmodus cyanostictus*)	MUI3	LVG8	M	2016.08.21	Toby's Place	8°37'23.6"S 31°12'01.6"E	Zambia
Eretmodini	Erecya (*Eretmodus cyanostictus*)	MUI5	LWA2	M	2016.08.21	Toby's Place	8°37'23.6"S 31°12'01.6"E	Zambia
Eretmodini	Eremar (*Eretmodus marksmithi*)	JXE9	KOF7	M	2015.01.08	Nyaruhongoka 2	3°41'55.00"S 29°19'12.30"E	Burundi
Eretmodini	Eremar (*Eretmodus marksmithi*)	JXF4	KOG8	F	2015.01.08	Nyaruhongoka 2	3°41'55.00"S 29°19'12.30"E	Burundi
Eretmodini	Eremar (*Eretmodus marksmithi*)	JXF8	KOH9	M	2015.01.08	Nyaruhongoka 2	3°41'55.00"S 29°19'12.30"E	Burundi
Eretmodini	Eremar (*Eretmodus marksmithi*)	MUB6	LXC6	M	2016.08.08	Pemba DRC	S03°36'39.1" S29°09'02.5"E	DRC
Eretmodini	Eremar (*Eretmodus marksmithi*)	ONA8	PVE8	F	2017.01.20	Mwamahunga	04°54'43"S 029°35'54"E	Tanzania
Eretmodini	Eremar (*Eretmodus marksmithi*)	ONA9	PVF9	F	2017.01.20	Mwamahunga	04°54'43"S 029°35'54"E	Tanzania
Eretmodini	Eremar (*Eretmodus marksmithi*)	ONB1	PVH1	F	2017.01.20	Mwamahunga	04°54'43"S 029°35'54"E	Tanzania
Eretmodini	Eremar (*Eretmodus marksmithi*)	ONB2	PVI2	M	2017.01.20	Mwamahunga	04°54'43"S 029°35'54"E	Tanzania
Eretmodini	Spaery (*Spathodus erythrodon*)	JUG8	KJG7	M	2015.01.05	Kitaza south	3°37'32.5"S 29°20'32.6"E	Burundi
Eretmodini	Spaery (*Spathodus erythrodon*)	JUG9	KJH8	F	2015.01.05	Kitaza south	3°37'32.5"S 29°20'32.6"E	Burundi
Eretmodini	Spaery (*Spathodus erythrodon*)	JUH1	KKA1	M	2015.01.05	Kitaza south	3°37'32.5"S 29°20'32.6"E	Burundi
Eretmodini	Spaery (*Spathodus erythrodon*)	JUH2	KKB2	M	2015.01.05	Kitaza south	3°37'32.5"S 29°20'32.6"E	Burundi
Eretmodini	Spaery (*Spathodus erythrodon*)	JUH3	KKC3	F	2015.01.05	Kitaza south	3°37'32.5"S 29°20'32.6"E	Burundi
Eretmodini	Spaery (*Spathodus erythrodon*)	JUH4	KKD4	F	2015.01.05	Kitaza south	3°37'32.5"S 29°20'32.6"E	Burundi
Eretmodini	Tanirs (*Tanganicodus irsacae*)	JYH3	KQD5	M	2015.01.11	Nyanza Lac	4°14'26.80"S 29°33'0.40"E	Burundi
Eretmodini	Tanirs (*Tanganicodus irsacae*)	JYH7	KQE6	F	2015.01.11	Nyanza Lac	4°14'26.80"S 29°33'0.40"E	Burundi
Eretmodini	Tanirs (*Tanganicodus irsacae*)	JYI2	KQF7	M	2015.01.11	Nyanza Lac	4°14'26.80"S 29°33'0.40"E	Burundi
Eretmodini	Tanirs (*Tanganicodus irsacae*)	JYI7	KQG8	F	2015.01.11	Nyanza Lac	4°14'26.80"S 29°33'0.40"E	Burundi
Eretmodini	Tanirs (*Tanganicodus irsacae*)	OMF1	QFC6	F	2017.02.02	Nganja	06°10'24"S 029°44'25"E	Tanzania
Eretmodini	Tanirs (*Tanganicodus irsacae*)	OMF2	QFD7	M	2017.02.02	Nganja	06°10'24"S 029°44'25"E	Tanzania
Haplochromini	Astbur (*Astatotilapia burtoni*)*	JYD7	KRD5	M	2015.01.10	Bujumbura Creek	03°23'30.9"S 029°20'57.9"E	Burundi
Haplochromini	Astbur (*Astatotilapia burtoni*)*	JYD8	KRE6	M	2015.01.10	Bujumbura Creek	03°23'30.9"S 029°20'57.9"E	Burundi
Haplochromini	Astbur (*Astatotilapia burtoni*)*	JYD9	KRF7	F	2015.01.10	Bujumbura Creek	03°23'30.9"S 029°20'57.9"E	Burundi
Haplochromini	Astbur (*Astatotilapia burtoni*)*	JYE1	KRG8	F	2015.01.10	Bujumbura Creek	03°23'30.9"S 029°20'57.9"E	Burundi
Haplochromini	Astbur (*Astatotilapia burtoni*)*	RYC6	RAH8	M	2019.08.15	Kalambo Lake / Chipwa	8°36'6.27"S 31°11'13.24"E	Zambia
Haplochromini	Astbur (*Astatotilapia burtoni*)*	RYC7	RBA1	M	2019.08.15	Kalambo Lake / Chipwa	8°36'6.27"S 31°11'13.24"E	Zambia
Haplochromini	Astbur (*Astatotilapia burtoni*)*	RYC8	RBB2	M	2019.08.15	Kalambo Lake / Chipwa	8°36'6.27"S 31°11'13.24"E	Zambia
Haplochromini	Astbur (*Astatotilapia burtoni*)*	RYC9	RBC3	F	2019.08.15	Kalambo Lake / Chipwa	8°36'6.27"S 31°11'13.24"E	Zambia
Haplochromini	Astbur (*Astatotilapia burtoni*)*	RYD1	RBD4	F	2019.08.15	Kalambo Lake / Chipwa	8°36'6.27"S 31°11'13.24"E	Zambia
Lamprologini	Altcal (*Altolamprologus calvus*)	MPB9	OAE8	M	2016.09.08	Katete 2	08°19'41"S 30°31'36"E	Zambia
Lamprologini	Altcal (*Altolamprologus calvus*)	MPC1	OAF9	M	2016.09.08	Katete 2	08°19'41"S 30°31'36"E	Zambia
Lamprologini	Altcal (*Altolamprologus calvus*)	MPC2	OAH1	M	2016.09.08	Katete 2	08°19'41"S 30°31'36"E	Zambia
Lamprologini	Altcal (*Altolamprologus calvus*)	MPD1	OBF9	F	2016.09.09	Kachese	8°29'25.9"S 30°28'39.0"E	Zambia
Lamprologini	Altcal (*Altolamprologus calvus*)	MPD2	OBH1	F	2016.09.09	Kachese	8°29'25.9"S 30°28'39.0"E	Zambia
Lamprologini	Altcal (*Altolamprologus calvus*)	MPD7	OCD7	F	2016.09.09	Kachese	8°29'25.9"S 30°28'39.0"E	Zambia
Lamprologini	Altcom (*Altolamprologus compressiceps*)	ISB1	JMD5	M	2014.07.23	Toby's Place	8°37'23.6"S 31°12'01.6"E	Zambia
Lamprologini	Altcom (*Altolamprologus compressiceps*)	ISB5	JMG8	M	2014.07.23	Toby's Place	8°37'23.6"S 31°12'01.6"E	Zambia
Lamprologini	Altcom (*Altolamprologus compressiceps*)	ISC9	JNG7	F	2014.07.23	Toby's Place	8°37'23.6"S 31°12'01.6"E	Zambia
Lamprologini	Altcom (*Altolamprologus compressiceps*)	ISD2	JNH8	F	2014.07.23	Toby's Place	8°37'23.6"S 31°12'01.6"E	Zambia
Lamprologini	Altcom (*Altolamprologus compressiceps*)	MUF7	LSI2	M	2016.08.21	Toby's Place	8°37'23.6"S 31°12'01.6"E	Zambia
Lamprologini	Altcom (*Altolamprologus compressiceps*)	MUF8	LTA4	F	2016.08.21	Toby's Place	8°37'23.6"S 31°12'01.6"E	Zambia
Lamprologini	Altfas (*Neolamprologus fasciatus*)	LNC3	MCB3	M	2016.08.22	Toby's Place	8°37'23.6"S 31°12'01.6"E	Zambia
Lamprologini	Altfas (*Neolamprologus fasciatus*)	LNC4	MCC4	M	2016.08.22	Toby's Place	8°37'23.6"S 31°12'01.6"E	Zambia
Lamprologini	Altfas (*Neolamprologus fasciatus*)	LNC5	MCD7	M	2016.08.22	Toby's Place	8°37'23.6"S 31°12'01.6"E	Zambia
Lamprologini	Altfas (*Neolamprologus fasciatus*)	LOH5	NPB5	F	2016.08.27	Toby's Place	8°37'23.6"S 31°12'01.6"E	Zambia
Lamprologini	Altfas (*Neolamprologus fasciatus*)	LPH9	NHB5	F	2016.08.25	Toby's Place	8°37'23.6"S 31°12'01.6"E	Zambia
Lamprologini	Altfas (*Neolamprologus fasciatus*)	MUB9	LXF7	M	2016.08.20	Toby's Place	8°37'23.6"S 31°12'01.6"E	Zambia
Lamprologini	Altfas (*Neolamprologus fasciatus*)	TWI8	TWI8	F	2020.11.01	Toby's Place	8°37'23.6"S 31°12'01.6"E	Zambia
Lamprologini	Chabri (*Chalinochromis brichardi*)	LPB8	NBC6	F	2016.08.23	Toby's Place	8°37'23.6"S 31°12'01.6"E	Zambia
Lamprologini	Chabri (*Chalinochromis brichardi*)	MUD6	LZF4	M	2016.08.20	Toby's Place	8°37'23.6"S 31°12'01.6"E	Zambia
Lamprologini	Chabri (*Chalinochromis brichardi*)	MUD7	LZF7	F	2016.08.20	Toby's Place	8°37'23.6"S 31°12'01.6"E	Zambia
Lamprologini	Chabri (*Chalinochromis brichardi*)	MUD8	LZG8	M	2016.08.20	Toby's Place	8°37'23.6"S 31°12'01.6"E	Zambia
Lamprologini	Chabri (*Chalinochromis brichardi*)	MUD9	LZI2	M	2016.08.20	Toby's Place	8°37'23.6"S 31°12'01.6"E	Zambia
Lamprologini	Chabri (*Chalinochromis brichardi*)	MUE1	LRA2	F	2016.08.20	Toby's Place	8°37'23.6"S 31°12'01.6"E	Zambia
Lamprologini	Juldic (*Julidochromis dickfeldi*)	MOG6	NVI2	F	2016.09.06	Chimba	08°25'34"S 30°27'24"E	Zambia
Lamprologini	Juldic (*Julidochromis dickfeldi*)	MOG7	NWA4	M	2016.09.06	Chimba	08°25'34"S 30°27'24"E	Zambia
Lamprologini	Juldic (*Julidochromis dickfeldi*)	MOG8	NWB5	F	2016.09.06	Chimba	08°25'34"S 30°27'24"E	Zambia
Lamprologini	Juldic (*Julidochromis dickfeldi*)	MOG9	NWC6	M	2016.09.06	Chimba	08°25'34"S 30°27'24"E	Zambia
Lamprologini	Juldic (*Julidochromis dickfeldi*)	MOH1	NWD7	M	2016.09.06	Chimba	08°25'34"S 30°27'24"E	Zambia
Lamprologini	Juldic (*Julidochromis dickfeldi*)	MOH2	NWE8	F	2016.09.06	Chimba	08°25'34"S 30°27'24"E	Zambia

Lamprologini	JulmaN (*Julidochromis marlieri*)	JXB5	KMF7	M	2015.01.07	Nyaruhongoka 2	3°41'55.00"S 29°19'12.30"E	Burundi
Lamprologini	JulmaN (*Julidochromis marlieri*)	JXC1	KMG8	F	2015.01.07	Nyaruhongoka 2	3°41'55.00"S 29°19'12.30"E	Burundi
Lamprologini	JulmaN (*Julidochromis marlieri*)	JXC5	KMH9	F	2015.01.07	Nyaruhongoka 2	3°41'55.00"S 29°19'12.30"E	Burundi
Lamprologini	JulmaN (*Julidochromis marlieri*)	JXC8	KOA2	M	2015.01.07	Nyaruhongoka 2	3°41'55.00"S 29°19'12.30"E	Burundi
Lamprologini	JulmaN (*Julidochromis marlieri*)	MVD9	OJD7	F	2017.01.18	Nondwa Point	04°51'51"S 029°36'26"E	Tanzania
Lamprologini	JulmaN (*Julidochromis marlieri*)	MVE1	OJE8	F	2017.01.18	Nondwa Point	04°51'51"S 029°36'26"E	Tanzania
Lamprologini	JulmaN (*Julidochromis marlieri*)	ONB7	PWE8	M	2017.01.20	Mwamahunga	04°54'43"S 029°35'54"E	Tanzania
Lamprologini	JulmaS (*Julidochromis* sp. "marlieri south")	MUH1	LUD7	F	2016.08.21	Toby's Place	8°37'23.6"S 31°12'01.6"E	Zambia
Lamprologini	JulmaS (*Julidochromis* sp. "marlieri south")	RYD4	RBG7	F	2019.08.15	Toby's Place	8°37'23.6"S 31°12'01.6"E	Zambia
Lamprologini	JulmaS (*Julidochromis* sp. "marlieri south")	RYE3	RCG7	F	2019.08.17	Toby's Place	8°37'23.6"S 31°12'01.6"E	Zambia
Lamprologini	JulmaS (*Julidochromis* sp. "marlieri south")	RYE4	RCH8	M	2019.08.17	Toby's Place	8°37'23.6"S 31°12'01.6"E	Zambia
Lamprologini	JulmaS (*Julidochromis* sp. "marlieri south")	RYE5	RDA1	F	2019.08.17	Toby's Place	8°37'23.6"S 31°12'01.6"E	Zambia
Lamprologini	JulmaS (*Julidochromis* sp. "marlieri south")	RYE7	RDC3	M	2019.08.17	Toby's Place	8°37'23.6"S 31°12'01.6"E	Zambia
Lamprologini	JulmaS (*Julidochromis* sp. "marlieri south")	RYE8	RDD4	M	2019.08.17	Toby's Place	8°37'23.6"S 31°12'01.6"E	Zambia
Lamprologini	Julorn (*Julidochromis ornatus*)	ISB7	JMH9	M	2014.07.23	Toby's Place	8°37'23.6"S 31°12'01.6"E	Zambia
Lamprologini	Julorn (*Julidochromis ornatus*)	ISC4	JND4	F	2014.07.23	Toby's Place	8°37'23.6"S 31°12'01.6"E	Zambia
Lamprologini	Julorn (*Julidochromis ornatus*)	ISC7	JNF6	M	2014.07.23	Toby's Place	8°37'23.6"S 31°12'01.6"E	Zambia
Lamprologini	Julorn (*Julidochromis ornatus*)	LPA8	NAB5	M	2016.08.23	Toby's Place	8°37'23.6"S 31°12'01.6"E	Zambia
Lamprologini	Julorn (*Julidochromis ornatus*)	MUB8	LXE6	F	2016.08.20	Toby's Place	8°37'23.6"S 31°12'01.6"E	Zambia
Lamprologini	Julorn (*Julidochromis ornatus*)	MUD4	LZC4	F	2016.08.20	Toby's Place	8°37'23.6"S 31°12'01.6"E	Zambia
Lamprologini	Julreg (*Julidochromis* sp. "regani south")	MOF7	NUH1	M	2016.09.06	Chimba	08°25'34"S 30°27'24"E	Zambia
Lamprologini	Julreg (*Julidochromis* sp. "regani south")	MOF8	NVA4	M	2016.09.06	Chimba	08°25'34"S 30°27'24"E	Zambia
Lamprologini	Julreg (*Julidochromis* sp. "regani south")	MOF9	NVB5	F	2016.09.06	Chimba	08°25'34"S 30°27'24"E	Zambia
Lamprologini	Julreg (*Julidochromis* sp. "regani south")	MOG2	NVD7	F	2016.09.06	Chimba	08°25'34"S 30°27'24"E	Zambia
Lamprologini	Julreg (*Julidochromis* sp. "regani south")	MOG3	NVE8	M	2016.09.06	Chimba	08°25'34"S 30°27'24"E	Zambia
Lamprologini	Julreg (*Julidochromis* sp. "regani south")	MOG5	NVH1	F	2016.09.06	Chimba	08°25'34"S 30°27'24"E	Zambia
Lamprologini	Lamcal (*Lamprologus callipterus*)	IPH2	JHD9	M	2014.07.21	Toby's Place	8°37'23.6"S 31°12'01.6"E	Zambia
Lamprologini	Lamcal (*Lamprologus callipterus*)	JAB1	HAI2	F	2014.07.30	Toby's Place	8°37'23.6"S 31°12'01.6"E	Zambia
Lamprologini	Lamcal (*Lamprologus callipterus*)	LPH2	NGC6	F	2016.08.25	Toby's Place	8°37'23.6"S 31°12'01.6"E	Zambia
Lamprologini	Lamcal (*Lamprologus callipterus*)	LPH3	NGD7	F	2016.08.25	Toby's Place	8°37'23.6"S 31°12'01.6"E	Zambia
Lamprologini	Lamcal (*Lamprologus callipterus*)	LPH5	NGF9	F	2016.08.25	Toby's Place	8°37'23.6"S 31°12'01.6"E	Zambia
Lamprologini	Lamcal (*Lamprologus callipterus*)	LPH7	NGI2	M	2016.08.25	Toby's Place	8°37'23.6"S 31°12'01.6"E	Zambia
Lamprologini	Lamcal (*Lamprologus callipterus*)	LPH8	NHA4	M	2016.08.25	Toby's Place	8°37'23.6"S 31°12'01.6"E	Zambia
Lamprologini	Lamkun (*Lamprologus kungweensis*)	JXG8	KPB3	M	2015.01.08	Nyaruhongoka 2	3°41'55.00"S 29°19'12.30"E	Burundi
Lamprologini	Lamkun (*Lamprologus kungweensis*)	JXH2	KPC4	F	2015.01.08	Nyaruhongoka 2	3°41'55.00"S 29°19'12.30"E	Burundi
Lamprologini	Lamkun (*Lamprologus kungweensis*)	ONC9	PXI2	M	2017.01.21	Kalalangabo	04°50'37"S 029°36'34"E	Tanzania
Lamprologini	Lamkun (*Lamprologus kungweensis*)	OND1	PYA4	M	2017.01.21	Kalalangabo	04°50'37"S 029°36'34"E	Tanzania
Lamprologini	Lamkun (*Lamprologus kungweensis*)	ONE4	PZD7	F	2017.01.21	Kalalangabo	04°50'37"S 029°36'34"E	Tanzania
Lamprologini	Lamkun (*Lamprologus kungweensis*)	ONE5	PZE8	F	2017.01.21	Kalalangabo	04°50'37"S 029°36'34"E	Tanzania
Lamprologini	Lamlem (*Lamprologus lemairii*)	LNF9	MSH1	F	2016.08.22	Toby's Place	8°37'23.6"S 31°12'01.6"E	Zambia
Lamprologini	Lamlem (*Lamprologus lemairii*)	LNG2	MTA4	M	2016.08.22	Toby's Place	8°37'23.6"S 31°12'01.6"E	Zambia
Lamprologini	Lamlem (*Lamprologus lemairii*)	RKA9	QQA7	M	2017.08.09	Toby's Place	8°37'23.6"S 31°12'01.6"E	Zambia
Lamprologini	Lamlem (*Lamprologus lemairii*)	RKB7	QQG3	F	2017.08.10	Toby's Place	8°37'23.6"S 31°12'01.6"E	Zambia
Lamprologini	Lamlem (*Lamprologus lemairii*)	RKB8	QQH4	F	2017.08.10	Toby's Place	8°37'23.6"S 31°12'01.6"E	Zambia
Lamprologini	Lamlem (*Lamprologus lemairii*)	RKB9	QQI5	F	2017.08.10	Toby's Place	8°37'23.6"S 31°12'01.6"E	Zambia
Lamprologini	Lamlem (*Lamprologus lemairii*)	RKF3	QTE1	M	2017.08.26	Toby's Place	8°37'23.6"S 31°12'01.6"E	Zambia
Lamprologini	Lamlem (*Lamprologus lemairii*)	RKF4	QTF2	M	2017.08.26	Toby's Place	8°37'23.6"S 31°12'01.6"E	Zambia
Lamprologini	Lamoce (*Lamprologus ocellatus*)	LPI3	NHE8	M	2016.08.25	Toby's Place	8°37'23.6"S 31°12'01.6"E	Zambia
Lamprologini	Lamoce (*Lamprologus ocellatus*)	MOI4	NXH1	M	2016.09.07	Chibwensolo	08°26'34"S 30°27'17"E	Zambia
Lamprologini	Lamoce (*Lamprologus ocellatus*)	MOI5	NXI2	F	2016.09.07	Chibwensolo	08°26'34"S 30°27'17"E	Zambia
Lamprologini	Lamoce (*Lamprologus ocellatus*)	MPA2	NYF9	F	2016.09.07	Chibwensolo	08°26'34"S 30°27'17"E	Zambia
Lamprologini	Lamoce (*Lamprologus ocellatus*)	MPA3	NYH1	F	2016.09.07	Chibwensolo	08°26'34"S 30°27'17"E	Zambia
Lamprologini	Lamoce (*Lamprologus ocellatus*)	MPA4	NYI2	M	2016.09.07	Chibwensolo	08°26'34"S 30°27'17"E	Zambia
Lamprologini	LamorS (*Lamprologus* sp. "ornatipinnis zambia")	MPF4	ODI2	M	2016.09.10	Ndole bay harbor	8°28'34.1"S 30°26'57.6"E	Zambia
Lamprologini	LamorS (*Lamprologus* sp. "ornatipinnis zambia")	MPF6	OEB5	M	2016.09.10	Ndole bay harbor	8°28'34.1"S 30°26'57.6"E	Zambia
Lamprologini	LamorS (*Lamprologus* sp. "ornatipinnis zambia")	MPF7	OEC6	F	2016.09.10	Ndole bay harbor	8°28'34.1"S 30°26'57.6"E	Zambia
Lamprologini	LamorS (*Lamprologus* sp. "ornatipinnis zambia")	MPF8	OED7	F	2016.09.10	Ndole bay harbor	8°28'34.1"S 30°26'57.6"E	Zambia
Lamprologini	LamorS (*Lamprologus* sp. "ornatipinnis zambia")	MPF9	OEE8	F	2016.09.10	Ndole bay harbor	8°28'34.1"S 30°26'57.6"E	Zambia
Lamprologini	LamorS (*Lamprologus* sp. "ornatipinnis zambia")	MPG1	OEF9	M	2016.09.10	Ndole bay harbor	8°28'34.1"S 30°26'57.6"E	Zambia
Lamprologini	Lamspe (*Lamprologus speciosus*)	KCG2	KUC4	M	2015.01.16	Nyanza Lac	4°14'26.80"S 29°33'0.40"E	Burundi
Lamprologini	Lamspe (*Lamprologus speciosus*)	KCG3	KUD5	F	2015.01.16	Nyanza Lac	4°14'26.80"S 29°33'0.40"E	Burundi
Lamprologini	Lamspe (*Lamprologus speciosus*)	MVH9	PTE1	M	2017.01.19	George's place	04°53'06"S 029°37'15"E	Tanzania
Lamprologini	Lamspe (*Lamprologus speciosus*)	MVI1	PTE8	F	2017.01.19	George's place	04°53'06"S 029°37'15"E	Tanzania
Lamprologini	Lamspe (*Lamprologus speciosus*)	MVI2	PTF9	F	2017.01.19	George's place	04°53'06"S 029°37'15"E	Tanzania
Lamprologini	Lamspe (*Lamprologus speciosus*)	MVI3	PTH1	M	2017.01.19	George's place	04°53'06"S 029°37'15"E	Tanzania
Lamprologini	Lepatt (*Lepidiolamprologus attenuatus*)	LNF4	MSD7	M	2016.08.22	Toby's Place	8°37'23.6"S 31°12'01.6"E	Zambia
Lamprologini	Lepatt (*Lepidiolamprologus attenuatus*)	LNF7	MSE8	F	2016.08.22	Toby's Place	8°37'23.6"S 31°12'01.6"E	Zambia
Lamprologini	Lepatt (*Lepidiolamprologus attenuatus*)	LNF8	MSF9	M	2016.08.22	Toby's Place	8°37'23.6"S 31°12'01.6"E	Zambia
Lamprologini	Lepatt (*Lepidiolamprologus attenuatus*)	LNG1	MSI2	F	2016.08.22	Toby's Place	8°37'23.6"S 31°12'01.6"E	Zambia
Lamprologini	Lepatt (*Lepidiolamprologus attenuatus*)	LNG5	MTD7	M	2016.08.22	Toby's Place	8°37'23.6"S 31°12'01.6"E	Zambia
Lamprologini	Lepatt (*Lepidiolamprologus attenuatus*)	LPD2	MYH1	F	2016.08.24	Toby's Place	8°37'23.6"S 31°12'01.6"E	Zambia
Lamprologini	Lepelo (*Lepidiolamprologus elongatus*)	LNC2	MCA4	M	2016.08.22	Toby's Place	8°37'23.6"S 31°12'01.6"E	Zambia
Lamprologini	Lepelo (*Lepidiolamprologus elongatus*)	LNG3	MTB5	F	2016.08.22	Toby's Place	8°37'23.6"S 31°12'01.6"E	Zambia
Lamprologini	Lepelo (*Lepidiolamprologus elongatus*)	LNG4	MTC6	F	2016.08.22	Toby's Place	8°37'23.6"S 31°12'01.6"E	Zambia
Lamprologini	Lepelo (*Lepidiolamprologus elongatus*)	LNG7	MTF9	M	2016.08.22	Toby's Place	8°37'23.6"S 31°12'01.6"E	Zambia
Lamprologini	Lepelo (*Lepidiolamprologus elongatus*)	LOA9	NIC6	F	2016.08.25	Chipwa Fishermen	8°36'22.2"S 31°11'10.0"E	Zambia
Lamprologini	Lepelo (*Lepidiolamprologus elongatus*)	LPG2	NFB5	M	2016.08.25	Toby's Place	8°37'23.6"S 31°12'01.6"E	Zambia
Lamprologini	Lepelo (*Lepidiolamprologus elongatus*)	MUF5	LSF9	M	2016.08.20	Toby's Place	8°37'23.6"S 31°12'01.6"E	Zambia
Lamprologini	Leppro (*Lepidiolamprologus profundicola*)	OMI2	QHB5	M	2017.02.05	Myako	6°05'16.8"S 29°43'40.6"E	Tanzania
Lamprologini	Leppro (*Lepidiolamprologus profundicola*)	OMI3	QHC6	F	2017.02.05	Myako	6°05'16.8"S 29°43'40.6"E	Tanzania
Lamprologini	Leppro (*Lepidiolamprologus profundicola*)	OMI4	QHD7	F	2017.02.05	Myako	6°05'16.8"S 29°43'40.6"E	Tanzania
Lamprologini	Leppro (*Lepidiolamprologus profundicola*)	OND8	PYI2	M	2017.01.21	Kalalangabo	04°50'37"S 029°36'34"E	Tanzania
Lamprologini	Leppro (*Lepidiolamprologus profundicola*)	ONE3	PZC6	M	2017.01.21	Kalalangabo	04°50'37"S 029°36'34"E	Tanzania
Lamprologini	Leppro (*Lepidiolamprologus profundicola*)	ONF9	QAF9	F	2017.01.23	Mabilibili	6°26'50.6"S 29°54'40.0"E	Tanzania
Lamprologini	Leppro (*Lepidiolamprologus profundicola*)	QJC6	QHH1	M	2017.02.08	Lubugwe River	6°14'37.8"S 29°44'08.3"E	Tanzania
Lamprologini	Leppro (*Lepidiolamprologus profundicola*)	QJC7	QHI2	F	2017.02.08	Msilambula	6°25'18.00"S 29°51'58.00"E	Tanzania
Lamprologini	Neobou (*Neolamprologus boulengeri*)	KCD6	KTE6	M	2015.01.16	Nyanza Lac	4°14'26.80"S 29°33'0.40"E	Burundi
Lamprologini	Neobou (*Neolamprologus boulengeri*)	MVG5	OLH1	M	2017.01.19	George's place	04°53'06"S 029°37'15"E	Tanzania
Lamprologini	Neobou (*Neolamprologus boulengeri*)	MVG7	PSA4	F	2017.01.19	George's place	04°53'06"S 029°37'15"E	Tanzania
Lamprologini	Neobou (*Neolamprologus boulengeri*)	MVG8	PSB5	M	2017.01.19	George's place	04°53'06"S 029°37'15"E	Tanzania
Lamprologini	Neobou (*Neolamprologus boulengeri*)	MVG9	PSC6	M	2017.01.19	George's place	04°53'06"S 029°37'15"E	Tanzania
Lamprologini	Neobou (*Neolamprologus boulengeri*)	MVH1	PSD7	F	2017.01.19	George's place	04°53'06"S 029°37'15"E	Tanzania
Lamprologini	Neobou (*Neolamprologus boulengeri*)	MVH2	PSE8	F	2017.01.19	George's place	04°53'06"S 029°37'15"E	Tanzania
Lamprologini	Neobre (*Neolamprologus brevis*)	MVH3	PSF9	F	2017.01.19	George's place	04°53'06"S 029°37'15"E	Tanzania

Lamprologini	Neobre (*Neolamprologus brevis*)	MVH4	PSH1	M	2017.01.19	George's place	04°53'06"S 029°37'15"E	Tanzania
Lamprologini	Neobre (*Neolamprologus brevis*)	MVH5	PSI2	M	2017.01.19	George's place	04°53'06"S 029°37'15"E	Tanzania
Lamprologini	Neobre (*Neolamprologus brevis*)	MVH6	PTA4	M	2017.01.19	George's place	04°53'06"S 029°37'15"E	Tanzania
Lamprologini	Neobre (*Neolamprologus brevis*)	MVH7	PTB5	F	2017.01.19	George's place	04°53'06"S 029°37'15"E	Tanzania
Lamprologini	Neobre (*Neolamprologus brevis*)	MVH8	PTC6	F	2017.01.19	George's place	04°53'06"S 029°37'15"E	Tanzania
Lamprologini	Neobue (*Neolamprologus buescheri*)	MPC4	OAI2	M	2016.09.09	Kachese	8°29'25.9"S 30°28'39.0"E	Zambia
Lamprologini	Neobue (*Neolamprologus buescheri*)	MPC5	OBA4	M	2016.09.09	Kachese	8°29'25.9"S 30°28'39.0"E	Zambia
Lamprologini	Neobue (*Neolamprologus buescheri*)	MPC6	OBB5	M	2016.09.09	Kachese	8°29'25.9"S 30°28'39.0"E	Zambia
Lamprologini	Neobue (*Neolamprologus buescheri*)	MPC7	OBC6	F	2016.09.09	Kachese	8°29'25.9"S 30°28'39.0"E	Zambia
Lamprologini	Neobue (*Neolamprologus buescheri*)	MPC8	OBD7	F	2016.09.09	Kachese	8°29'25.9"S 30°28'39.0"E	Zambia
Lamprologini	Neobue (*Neolamprologus buescheri*)	MPC9	OBE8	F	2016.09.09	Kachese	8°29'25.9"S 30°28'39.0"E	Zambia
Lamprologini	Neocau (*Neolamprologus caudopunctatus*)	IQA3	JIA5	M	2014.07.21	Toby's Place	8°37'23.6"S 31°12'01.6"E	Zambia
Lamprologini	Neocau (*Neolamprologus caudopunctatus*)	IQA4	JIB6	F	2014.07.21	Toby's Place	8°37'23.6"S 31°12'01.6"E	Zambia
Lamprologini	Neocau (*Neolamprologus caudopunctatus*)	IQA5	JIC7	M	2014.07.21	Toby's Place	8°37'23.6"S 31°12'01.6"E	Zambia
Lamprologini	Neocau (*Neolamprologus caudopunctatus*)	IQA8	JID8	F	2014.07.21	Toby's Place	8°37'23.6"S 31°12'01.6"E	Zambia
Lamprologini	Neocau (*Neolamprologus caudopunctatus*)	MUH2	LUE6	M	2016.08.21	Toby's Place	8°37'23.6"S 31°12'01.6"E	Zambia
Lamprologini	Neocau (*Neolamprologus caudopunctatus*)	MUH3	LUF7	F	2016.08.21	Toby's Place	8°37'23.6"S 31°12'01.6"E	Zambia
Lamprologini	Neochr (*Neolamprologus christyi*)	ITG2	JQG5	F	2014.07.24	Chipwa Fishermen	8°36'22.2"S 31°11'10.0"E	Zambia
Lamprologini	Neochr (*Neolamprologus christyi*)	IUF5	JTE1	M	2014.07.25	Isanga	8°39'16.4"S 31°11'30.6"E	Zambia
Lamprologini	Neochr (*Neolamprologus christyi*)	LOE2	NLF9	M	2016.08.26	Chipwa Fishermen	8°36'22.2"S 31°11'10.0"E	Zambia
Lamprologini	Neochr (*Neolamprologus christyi*)	LOE3	NLH1	F	2016.08.26	Chipwa Fishermen	8°36'22.2"S 31°11'10.0"E	Zambia
Lamprologini	Neochr (*Neolamprologus christyi*)	LOH4	NPA3	F	2016.08.27	Toby's Place	8°37'23.6"S 31°12'01.6"E	Zambia
Lamprologini	Neochr (*Neolamprologus christyi*)	LPI8	NIB5	M	2016.08.25	Toby's Place	8°37'23.6"S 31°12'01.6"E	Zambia
Lamprologini	Neocyg (*Neolamprologus* sp. "cygnus")	LFD9	KXA3	M	2015.08.15	Korongwe	7°08'13"S 30°30'28"E	Tanzania
Lamprologini	Neocyg (*Neolamprologus* sp. "cygnus")	LFE1	KXB4	F	2015.08.15	Korongwe	7°08'13"S 30°30'28"E	Tanzania
Lamprologini	Neocyg (*Neolamprologus* sp. "cygnus")	LFE2	KXC5	F	2015.08.15	Korongwe	7°08'13"S 30°30'28"E	Tanzania
Lamprologini	Neocyg (*Neolamprologus* sp. "cygnus")	LFE3	KXD6	F	2015.08.15	Korongwe	7°08'13"S 30°30'28"E	Tanzania
Lamprologini	Neocyg (*Neolamprologus* sp. "cygnus")	LGC6	KXE7	M	2015.08.18	Mvuna Island	7°26'39.0"S 30°32'38.0"E	Tanzania
Lamprologini	Neocyg (*Neolamprologus* sp. "cygnus")	LGG3	KXF8	M	2015.08.19	Ulwile Musi Point	7°28'44"S 30°34'35"E	Tanzania
Lamprologini	Neocyg (*Neolamprologus* sp. "cygnus")	RKC7	QSA7	F	2017.08.22	Twiyu	7° 34' 55"S 30° 37' 42"E	Tanzania
Lamprologini	Neocyg (*Neolamprologus* sp. "cygnus")	RKC8	QSB8	M	2017.08.22	Twiyu	7° 34' 55"S 30° 37' 42"E	Tanzania
Lamprologini	Neocyg (*Neolamprologus* sp. "cygnus")	RKC9	QSC9	M	2017.08.22	Twiyu	7° 34' 55"S 30° 37' 42"E	Tanzania
Lamprologini	Neocyg (*Neolamprologus* sp. "cygnus")	RKD1	QSE1	M	2017.08.22	Twiyu	7° 34' 55"S 30° 37' 42"E	Tanzania
Lamprologini	Neocyg (*Neolamprologus* sp. "cygnus")	RKD2	QSF2	F	2017.08.22	Twiyu	7° 34' 55"S 30° 37' 42"E	Tanzania
Lamprologini	Neocyg (*Neolamprologus* sp. "cygnus")	RKD3	QSG3	F	2017.08.22	Twiyu	7° 34' 55"S 30° 37' 42"E	Tanzania
Lamprologini	Neocyl (*Neolamprologus cylindricus*)	LOA2	MXB5	F	2016.08.23	Isanga	8°39'16.4"S 31°11'30.6"E	Zambia
Lamprologini	Neocyl (*Neolamprologus cylindricus*)	LOA3	MXC6	M	2016.08.23	Isanga	8°39'16.4"S 31°11'30.6"E	Zambia
Lamprologini	Neocyl (*Neolamprologus cylindricus*)	LPD4	NCA4	F	2016.08.24	Toby's Place	8°37'23.6"S 31°12'01.6"E	Zambia
Lamprologini	Neocyl (*Neolamprologus cylindricus*)	LPD5	NCB5	F	2016.08.24	Toby's Place	8°37'23.6"S 31°12'01.6"E	Zambia
Lamprologini	Neocyl (*Neolamprologus cylindricus*)	LPD6	NCC6	M	2016.08.24	Toby's Place	8°37'23.6"S 31°12'01.6"E	Zambia
Lamprologini	Neocyl (*Neolamprologus cylindricus*)	LPG4	NFD7	M	2016.08.25	Toby's Place	8°37'23.6"S 31°12'01.6"E	Zambia
Lamprologini	Neocyl (*Neolamprologus cylindricus*)	RYE6	RDB2	F	2019.08.17	Toby's Place	8°37'23.6"S 31°12'01.6"E	Zambia
Lamprologini	Neofur (*Neolamprologus furcifer*)	IPF4	JGG3	F	2014.07.21	Toby's Place	8°37'23.6"S 31°12'01.6"E	Zambia
Lamprologini	Neofur (*Neolamprologus furcifer*)	LOH1	NOF9	F	2016.08.27	Toby's Place	8°37'23.6"S 31°12'01.6"E	Zambia
Lamprologini	Neofur (*Neolamprologus furcifer*)	LOH2	NOH4	F	2016.08.27	Toby's Place	8°37'23.6"S 31°12'01.6"E	Zambia
Lamprologini	Neofur (*Neolamprologus furcifer*)	LOH8	NPE8	M	2016.08.27	Toby's Place	8°37'23.6"S 31°12'01.6"E	Zambia
Lamprologini	Neofur (*Neolamprologus furcifer*)	LPC6	MYB5	M	2016.08.24	Toby's Place	8°37'23.6"S 31°12'01.6"E	Zambia
Lamprologini	Neofur (*Neolamprologus furcifer*)	MUF9	LTB5	M	2016.08.21	Toby's Place	8°37'23.6"S 31°12'01.6"E	Zambia
Lamprologini	Neoleu (*Neolamprologus longior*)	LED9	KVG7	F	2015.06.29	Storo bay	06° 01' 01"S 029° 44' 58"E	Tanzania
Lamprologini	Neoleu (*Neolamprologus longior*)	OMF3	QGA1	M	2017.02.02	Nganja	06°10'24"S 029°44'25"E	Tanzania
Lamprologini	Neoleu (*Neolamprologus longior*)	OMF4	QGA4	M	2017.02.02	Nganja	06°10'24"S 029°44'25"E	Tanzania
Lamprologini	Neoleu (*Neolamprologus longior*)	OMI8	QGB1	F	2017.02.05	Myako	6°05'16.8"S 29°43'40.6"E	Tanzania
Lamprologini	Neoleu (*Neolamprologus longior*)	QJA1	QGB4	F	2017.02.05	Myako	6°05'16.8"S 29°43'40.6"E	Tanzania
Lamprologini	Neoleu (*Neolamprologus longior*)	QJA2	QGB7	F	2017.02.05	Myako	6°05'16.8"S 29°43'40.6"E	Tanzania
Lamprologini	Neoleu (*Neolamprologus longior*)	QJA3	QGC1	F	2017.02.05	Myako	6°05'16.8"S 29°43'40.6"E	Tanzania
Lamprologini	Neoleu (*Neolamprologus longior*)	QJA4	QGC4	M	2017.02.05	Myako	6°05'16.8"S 29°43'40.6"E	Tanzania
Lamprologini	Neoleu (*Neolamprologus longior*)	QJA5	QGC7	M	2017.02.05	Myako	6°05'16.8"S 29°43'40.6"E	Tanzania
Lamprologini	Neoleu (*Neolamprologus longior*)	QJB2	QGE7	M	2017.02.06	Bulu Point	06° 00' 58"S 029° 44' 47"E	Tanzania
Lamprologini	Neoleu (*Neolamprologus longior*)	QJB3	QGF1	M	2017.02.06	Bulu Point	06° 00' 58"S 029° 44' 47"E	Tanzania
Lamprologini	Neoleu (*Neolamprologus longior*)	QJB6	QGG1	F	2017.02.06	Bulu Point	06° 00' 58"S 029° 44' 47"E	Tanzania
Lamprologini	Neoleu (*Neolamprologus longior*)	QJC8	QGG4	M	2017.02.08	Msilambula	6°25'18.00"S 29°51'58.00"E	Tanzania
Lamprologini	Neomod (*Neolamprologus modestus*)	IQA1	JHH3	M	2014.07.21	Toby's Place	8°37'23.6"S 31°12'01.6"E	Zambia
Lamprologini	Neomod (*Neolamprologus modestus*)	IQA2	JHI4	M	2014.07.21	Toby's Place	8°37'23.6"S 31°12'01.6"E	Zambia
Lamprologini	Neomod (*Neolamprologus modestus*)	LND4	MDD7	F	2016.08.22	Toby's Place	8°37'23.6"S 31°12'01.6"E	Zambia
Lamprologini	Neomod (*Neolamprologus modestus*)	LND5	MDE8	F	2016.08.22	Toby's Place	8°37'23.6"S 31°12'01.6"E	Zambia
Lamprologini	Neomod (*Neolamprologus modestus*)	MUC4	LYB3	M	2016.08.20	Toby's Place	8°37'23.6"S 31°12'01.6"E	Zambia
Lamprologini	Neomod (*Neolamprologus modestus*)	MUE3	LRC4	F	2016.08.20	Toby's Place	8°37'23.6"S 31°12'01.6"E	Zambia
Lamprologini	Neomux (*Neolamprologus mustax*)	MOB8	NSA4	M	2016.08.30	Chituta	8°43'25"S 31°09'00"E	Zambia
Lamprologini	Neomux (*Neolamprologus mustax*)	MOC4	NSF9	M	2016.08.30	Chituta	8°43'25"S 31°09'00"E	Zambia
Lamprologini	Neomux (*Neolamprologus mustax*)	MOD1	NTD7	F	2016.08.31	Chituta	8°43'25"S 31°09'00"E	Zambia
Lamprologini	Neomux (*Neolamprologus mustax*)	MOD2	NTE8	F	2016.08.31	Chituta	8°43'25"S 31°09'00"E	Zambia
Lamprologini	Neomux (*Neolamprologus mustax*)	RKI8	QUG3	M	2017.08.27	Chituta	8°43'25"S 31°09'00"E	Zambia
Lamprologini	Neomux (*Neolamprologus mustax*)	RKI9	QUH4	M	2017.08.27	Chituta	8°43'25"S 31°09'00"E	Zambia
Lamprologini	Neomux (*Neolamprologus mustax*)	RLA2	QUI5	F	2017.08.27	Chituta	8°43'25"S 31°09'00"E	Zambia
Lamprologini	Neomux (*Neolamprologus mustax*)	RLA6	QVB8	M	2017.08.27	Chituta	8°43'25"S 31°09'00"E	Zambia
Lamprologini	Neomux (*Neolamprologus mustax*)	RLA7	QVC9	F	2017.08.27	Chituta	8°43'25"S 31°09'00"E	Zambia
Lamprologini	Neonig (*Neolamprologus niger*)	ONG9	QBA4	M	2017.01.25	Kananiye	04°47'39"S 029°35'58"E	Tanzania
Lamprologini	Neonig (*Neolamprologus niger*)	ONH1	QBB5	M	2017.01.25	Kananiye	04°47'39"S 029°35'58"E	Tanzania
Lamprologini	Neonig (*Neolamprologus niger*)	ONH2	QBC6	M	2017.01.25	Kananiye	04°47'39"S 029°35'58"E	Tanzania
Lamprologini	Neonig (*Neolamprologus niger*)	ONH3	QBD7	F	2017.01.25	Kananiye	04°47'39"S 029°35'58"E	Tanzania
Lamprologini	Neonig (*Neolamprologus niger*)	ONH4	QBE8	F	2017.01.25	Kananiye	04°47'39"S 029°35'58"E	Tanzania
Lamprologini	Neonig (*Neolamprologus niger*)	ONH5	QBF9	F	2017.01.25	Kananiye	04°47'39"S 029°35'58"E	Tanzania
Lamprologini	Neopul (*Neolamprologus pulcher*)	ISA7	JMA2	M	2014.07.23	Toby's Place	8°37'23.6"S 31°12'01.6"E	Zambia
Lamprologini	Neopul (*Neolamprologus pulcher*)	ISB3	JMF7	F	2014.07.23	Toby's Place	8°37'23.6"S 31°12'01.6"E	Zambia
Lamprologini	Neopul (*Neolamprologus pulcher*)	ISB4	JME6	F	2014.07.23	Toby's Place	8°37'23.6"S 31°12'01.6"E	Zambia
Lamprologini	Neopul (*Neolamprologus pulcher*)	LOE4	NLI2	F	2016.08.26	Chipwa Fishermen	8°36'22.2"S 31°11'10.0"E	Zambia
Lamprologini	Neopul (*Neolamprologus pulcher*)	MUH4	LUH1	M	2016.08.21	Toby's Place	8°37'23.6"S 31°12'01.6"E	Zambia
Lamprologini	Neopul (*Neolamprologus pulcher*)	MUH5	LUH9	M	2016.08.21	Toby's Place	8°37'23.6"S 31°12'01.6"E	Zambia
Lamprologini	Neosav (*Neolamprologus savoryi*)	ISA8	JMB3	M	2014.07.23	Toby's Place	8°37'23.6"S 31°12'01.6"E	Zambia
Lamprologini	Neosav (*Neolamprologus savoryi*)	ISA9	JMC4	M	2014.07.23	Toby's Place	8°37'23.6"S 31°12'01.6"E	Zambia
Lamprologini	Neosav (*Neolamprologus savoryi*)	LOC2	NJE8	M	2016.08.26	Toby's Place	8°37'23.6"S 31°12'01.6"E	Zambia
Lamprologini	Neosav (*Neolamprologus savoryi*)	LOC3	NJF9	M	2016.08.26	Toby's Place	8°37'23.6"S 31°12'01.6"E	Zambia
Lamprologini	Neosav (*Neolamprologus savoryi*)	LOC4	NJH1	M	2016.08.26	Toby's Place	8°37'23.6"S 31°12'01.6"E	Zambia
Lamprologini	Neosav (*Neolamprologus savoryi*)	LOC7	NKB5	F	2016.08.26	Toby's Place	8°37'23.6"S 31°12'01.6"E	Zambia

Lamprologini	Neosav (*Neolamprologus savoryi*)	LOC8	NKC6	F	2016.08.26	Toby's Place	8°37'23.6"S 31°12'01.6"E	Zambia
Lamprologini	Neosav (*Neolamprologus savoryi*)	LOC9	NKD7	F	2016.08.26	Toby's Place	8°37'23.6"S 31°12'01.6"E	Zambia
Lamprologini	Neosex (*Neolamprologus sexfasciatus*)	MOG1	NVC6	F	2016.09.06	Chimba	08°25'34"S 30°27'24"E	Zambia
Lamprologini	Neosex (*Neolamprologus sexfasciatus*)	RKB6	QQF2	M	2017.08.10	Toby's Place	8°37'23.6"S 31°12'01.6"E	Zambia
Lamprologini	Neosex (*Neolamprologus sexfasciatus*)	RKE7	QSH4	M	2017.08.24	Malasa Island	8° 12' 43"S 30° 56' 47"E	Tanzania
Lamprologini	Neosex (*Neolamprologus sexfasciatus*)	RKE8	QSI5	F	2017.08.24	Malasa Island	8° 12' 43"S 30° 56' 47"E	Tanzania
Lamprologini	Neosex (*Neolamprologus sexfasciatus*)	RKE9	QTA7	M	2017.08.24	Malasa Island	8° 12' 43"S 30° 56' 47"E	Tanzania
Lamprologini	Neosex (*Neolamprologus sexfasciatus*)	RKF1	QTB8	F	2017.08.24	Malasa Island	8° 12' 43"S 30° 56' 47"E	Tanzania
Lamprologini	Neosex (*Neolamprologus sexfasciatus*)	RKF2	QTC9	F	2017.08.24	Malasa Island	8° 12' 43"S 30° 56' 47"E	Tanzania
Lamprologini	Neotet (*Neolamprologus tetracanthus*)	IPF7	JHA6	M	2014.07.21	Toby's Place	8°37'23.6"S 31°12'01.6"E	Zambia
Lamprologini	Neotet (*Neolamprologus tetracanthus*)	IPG3	JHB7	F	2014.07.21	Toby's Place	8°37'23.6"S 31°12'01.6"E	Zambia
Lamprologini	Neotet (*Neolamprologus tetracanthus*)	IPG6	JHC8	M	2014.07.21	Toby's Place	8°37'23.6"S 31°12'01.6"E	Zambia
Lamprologini	Neotet (*Neolamprologus tetracanthus*)	IPH9	JHG2	F	2014.07.21	Toby's Place	8°37'23.6"S 31°12'01.6"E	Zambia
Lamprologini	Neotet (*Neolamprologus tetracanthus*)	MUC9	LYG8	F	2016.08.20	Toby's Place	8°37'23.6"S 31°12'01.6"E	Zambia
Lamprologini	Neotet (*Neolamprologus tetracanthus*)	MUD2	LZA2	M	2016.08.20	Toby's Place	8°37'23.6"S 31°12'01.6"E	Zambia
Lamprologini	Neotoa (*Neolamprologus toae*)	JZD5	KSH9	M	2015.01.11	Nyanza Lac	4°14'26.80"S 29°33'0.40"E	Burundi
Lamprologini	Neotoa (*Neolamprologus toae*)	JZD6	KTA2	F	2015.01.11	Nyanza Lac	4°14'26.80"S 29°33'0.40"E	Burundi
Lamprologini	Neotoa (*Neolamprologus toae*)	KCD9	KTF7	F	2015.01.16	Nyanza Lac	4°14'26.80"S 29°33'0.40"E	Burundi
Lamprologini	Neotoa (*Neolamprologus toae*)	KCE6	KTG8	M	2015.01.16	Nyanza Lac	4°14'26.80"S 29°33'0.40"E	Burundi
Lamprologini	Neotoa (*Neolamprologus toae*)	MUB1	LXA4	F	2016.08.08	Pemba DRC	S03°36'39.1" S29°09'02.5"E	DRC
Lamprologini	Neotoa (*Neolamprologus toae*)	MUB2	LXB5	M	2016.08.08	Pemba DRC	S03°36'39.1" S29°09'02.5"E	DRC
Lamprologini	Neotoa (*Neolamprologus toae*)	MVA1	OFA4	F	2017.01.17	Kaku	04°53'47"S 029°36'42"E	Tanzania
Lamprologini	Neotoa (*Neolamprologus toae*)	MVA2	OFB5	M	2017.01.17	Kaku	04°53'47"S 029°36'42"E	Tanzania
Lamprologini	Neotoa (*Neolamprologus toae*)	MVA3	OFC6	M	2017.01.17	Kaku	04°53'47"S 029°36'42"E	Tanzania
Lamprologini	Neotre (*Neolamprologus tretocephalus*)	MVA4	OFD7	F	2017.01.17	Kaku	04°53'47"S 029°36'42"E	Tanzania
Lamprologini	Neotre (*Neolamprologus tretocephalus*)	MVA5	OFE8	F	2017.01.17	Kaku	04°53'47"S 029°36'42"E	Tanzania
Lamprologini	Neotre (*Neolamprologus tretocephalus*)	MVA6	OFF9	F	2017.01.17	Kaku	04°53'47"S 029°36'42"E	Tanzania
Lamprologini	Neotre (*Neolamprologus tretocephalus*)	MVB5	OGF9	M	2017.01.17	Kaku	04°53'47"S 029°36'42"E	Tanzania
Lamprologini	Neotre (*Neolamprologus tretocephalus*)	MVB6	OGH1	M	2017.01.17	Kaku	04°53'47"S 029°36'42"E	Tanzania
Lamprologini	Neotre (*Neolamprologus tretocephalus*)	MVB7	OGI2	M	2017.01.17	Kaku	04°53'47"S 029°36'42"E	Tanzania
Lamprologini	Neowal (*Neolamprologus walteri*)	MVA8	OFI2	M	2017.01.17	Kaku	04°53'47"S 029°36'42"E	Tanzania
Lamprologini	Neowal (*Neolamprologus walteri*)	MVA9	OGA4	F	2017.01.17	Kaku	04°53'47"S 029°36'42"E	Tanzania
Lamprologini	Neowal (*Neolamprologus walteri*)	MVB1	OGB5	F	2017.01.17	Kaku	04°53'47"S 029°36'42"E	Tanzania
Lamprologini	Neowal (*Neolamprologus walteri*)	MVB2	OGC6	M	2017.01.17	Kaku	04°53'47"S 029°36'42"E	Tanzania
Lamprologini	Neowal (*Neolamprologus walteri*)	MVB3	OGD7	F	2017.01.17	Kaku	04°53'47"S 029°36'42"E	Tanzania
Lamprologini	Neowal (*Neolamprologus walteri*)	MVB8	OHA4	M	2017.01.17	Kaku	04°53'47"S 029°36'42"E	Tanzania
Lamprologini	Telbif (*Telmatochromis bifrenatus*)	ONB4	PWB5	M	2017.01.20	Mwamahunga	04°54'43"S 029°35'54"E	Tanzania
Lamprologini	Telbif (*Telmatochromis bifrenatus*)	ONB5	PWC6	M	2017.01.20	Mwamahunga	04°54'43"S 029°35'54"E	Tanzania
Lamprologini	Telbif (*Telmatochromis bifrenatus*)	ONB6	PWD7	M	2017.01.20	Mwamahunga	04°54'43"S 029°35'54"E	Tanzania
Lamprologini	Telbif (*Telmatochromis bifrenatus*)	ONE6	PZF9	F	2017.01.21	Kalalangabo	04°50'37"S 029°36'34"E	Tanzania
Lamprologini	Telbif (*Telmatochromis bifrenatus*)	ONG1	QAH1	F	2017.01.23	Mabilibili	6°26'50.6"S 29°54'40.0"E	Tanzania
Lamprologini	Telbif (*Telmatochromis bifrenatus*)	ONG8	QAI2	F	2017.01.24	Nondwa Bay	4°51'50.8"S 29°36'34.7"E	Tanzania
Lamprologini	TeldhS (*Telmatochromis dhonti*)	IZE3	BLD8	M	2014.07.28	Kalambo Lake / Chipwa	8°36'6.27"S 31°11'13.24"E	Zambia
Lamprologini	TeldhS (*Telmatochromis dhonti*)	IZF8	BLE9	M	2014.07.28	Kalambo Lake / Chipwa	8°36'6.27"S 31°11'13.24"E	Zambia
Lamprologini	TeldhS (*Telmatochromis dhonti*)	LOE5	NMA4	F	2016.08.26	Chipwa Fishermen	8°36'22.2"S 31°11'10.0"E	Zambia
Lamprologini	TeldhS (*Telmatochromis dhonti*)	LOE6	NMB5	F	2016.08.26	Chipwa Fishermen	8°36'22.2"S 31°11'10.0"E	Zambia
Lamprologini	TeldhS (*Telmatochromis dhonti*)	LOE7	NMC6	F	2016.08.26	Chipwa Fishermen	8°36'22.2"S 31°11'10.0"E	Zambia
Lamprologini	TeldhS (*Telmatochromis dhonti*)	LOE8	NMD7	M	2016.08.26	Chipwa Fishermen	8°36'22.2"S 31°11'10.0"E	Zambia
Lamprologini	Telshe (*Telmatochromis* sp. "shell")	MPA5	NZA4	M	2016.09.07	Chibwensolo	08°26'34"S 30°27'17"E	Zambia
Lamprologini	Telshe (*Telmatochromis* sp. "shell")	MPA6	NZB5	M	2016.09.07	Chibwensolo	08°26'34"S 30°27'17"E	Zambia
Lamprologini	Telshe (*Telmatochromis* sp. "shell")	MPA7	NZC6	M	2016.09.07	Chibwensolo	08°26'34"S 30°27'17"E	Zambia
Lamprologini	Telshe (*Telmatochromis* sp. "shell")	MPA8	NZD7	F	2016.09.07	Chibwensolo	08°26'34"S 30°27'17"E	Zambia
Lamprologini	Telshe (*Telmatochromis* sp. "shell")	MPA9	NZE8	F	2016.09.07	Chibwensolo	08°26'34"S 30°27'17"E	Zambia
Lamprologini	Telshe (*Telmatochromis* sp. "shell")	MPB1	NZF9	F	2016.09.07	Chibwensolo	08°26'34"S 30°27'17"E	Zambia
Lamprologini	TelteS (*Telmatochromis temporalis*)	IPA7	JFC6	M	2014.07.20	Toby's Place	8°37'23.6"S 31°12'01.6"E	Zambia
Lamprologini	TelteS (*Telmatochromis temporalis*)	LND7	MDH1	F	2016.08.22	Toby's Place	8°37'23.6"S 31°12'01.6"E	Zambia
Lamprologini	TelteS (*Telmatochromis temporalis*)	LPB2	NAE8	F	2016.08.23	Toby's Place	8°37'23.6"S 31°12'01.6"E	Zambia
Lamprologini	TelteS (*Telmatochromis temporalis*)	MUF1	LSB3	M	2016.08.20	Toby's Place	8°37'23.6"S 31°12'01.6"E	Zambia
Lamprologini	TelteS (*Telmatochromis temporalis*)	MUI6	LWB5	F	2016.08.21	Toby's Place	8°37'23.6"S 31°12'01.6"E	Zambia
Lamprologini	TelteS (*Telmatochromis temporalis*)	MUI7	LWC4	M	2016.08.21	Toby's Place	8°37'23.6"S 31°12'01.6"E	Zambia
Lamprologini	Telvit (*Telmatochromis vittatus*)	IPA5	JFB3	M	2014.07.20	Toby's Place	8°37'23.6"S 31°12'01.6"E	Zambia
Lamprologini	Telvit (*Telmatochromis vittatus*)	ISG9	JOE4	M	2014.07.23	Toby's Place	8°37'23.6"S 31°12'01.6"E	Zambia
Lamprologini	Telvit (*Telmatochromis vittatus*)	LOH6	NPC6	F	2016.08.27	Toby's Place	8°37'23.6"S 31°12'01.6"E	Zambia
Lamprologini	Telvit (*Telmatochromis vittatus*)	LPI1	NHC6	F	2016.08.25	Toby's Place	8°37'23.6"S 31°12'01.6"E	Zambia
Lamprologini	Telvit (*Telmatochromis vittatus*)	LPI4	NHF9	F	2016.08.25	Toby's Place	8°37'23.6"S 31°12'01.6"E	Zambia
Lamprologini	Telvit (*Telmatochromis vittatus*)	MUC3	LYA2	M	2016.08.20	Toby's Place	8°37'23.6"S 31°12'01.6"E	Zambia
Lamprologini	Telvit (*Telmatochromis vittatus*)	RYC5	RAG7	F	2019.08.14	Toby's Place	8°37'23.6"S 31°12'01.6"E	Zambia
Lamprologini	Varmoo (*Variabilichromis moorii*)	LNA2	LWH1	M	2016.08.21	Toby's Place	8°37'23.6"S 31°12'01.6"E	Zambia
Lamprologini	Varmoo (*Variabilichromis moorii*)	LNA4	MAA4	F	2016.08.21	Toby's Place	8°37'23.6"S 31°12'01.6"E	Zambia
Lamprologini	Varmoo (*Variabilichromis moorii*)	LNC6	MCE8	M	2016.08.22	Toby's Place	8°37'23.6"S 31°12'01.6"E	Zambia
Lamprologini	Varmoo (*Variabilichromis moorii*)	LPE4	NDB5	F	2016.08.24	Toby's Place	8°37'23.6"S 31°12'01.6"E	Zambia
Lamprologini	Varmoo (*Variabilichromis moorii*)	MUH9	LVD7	F	2016.08.21	Toby's Place	8°37'23.6"S 31°12'01.6"E	Zambia
Lamprologini	Varmoo (*Variabilichromis moorii*)	MUI1	LVE6	M	2016.08.21	Toby's Place	8°37'23.6"S 31°12'01.6"E	Zambia
Lamprologini	Varmoo (*Variabilichromis moorii*)	MUI4	LVI2	M	2016.08.21	Toby's Place	8°37'23.6"S 31°12'01.6"E	Zambia
Limnochromini	Baicen (*Baileychromis centropomoides*)	IXH9	HQH3	M	2014.07.28	Chipwa Fishermen	8°36'22.2"S 31°11'10.0"E	Zambia
Limnochromini	Baicen (*Baileychromis centropomoides*)	JAE9	GYD6	F	2014.07.31	Chipwa Fishermen	8°36'22.2"S 31°11'10.0"E	Zambia
Limnochromini	Baicen (*Baileychromis centropomoides*)	LOD2	NKF9	F	2016.08.26	Chipwa Fishermen	8°36'22.2"S 31°11'10.0"E	Zambia
Limnochromini	Baicen (*Baileychromis centropomoides*)	LPE7	NDE8	F	2016.08.25	Chipwa Fishermen	8°36'22.2"S 31°11'10.0"E	Zambia
Limnochromini	Baicen (*Baileychromis centropomoides*)	RYB6	QZH8	M	2019.08.14	Chipwa Fishermen	8°36'22.2"S 31°11'10.0"E	Zambia
Limnochromini	Baicen (*Baileychromis centropomoides*)	RYD5	RBH8	M	2019.08.16	Chipwa Fishermen	8°36'22.2"S 31°11'10.0"E	Zambia
Limnochromini	Baicen (*Baileychromis centropomoides*)	RYD6	RCA1	F	2019.08.16	Chipwa Fishermen	8°36'22.2"S 31°11'10.0"E	Zambia
Limnochromini	Gnaper (*Gnathochromis permaxillaris*)	IUI5	HQA6	M	2014.07.27	Chipwa Fishermen	8°36'22.2"S 31°11'10.0"E	Zambia
Limnochromini	Gnaper (*Gnathochromis permaxillaris*)	IXA1	HQD9	M	2014.07.27	Chipwa Fishermen	8°36'22.2"S 31°11'10.0"E	Zambia
Limnochromini	Gnaper (*Gnathochromis permaxillaris*)	IXA8	HQF1	F	2014.07.27	Chipwa Fishermen	8°36'22.2"S 31°11'10.0"E	Zambia
Limnochromini	Gnaper (*Gnathochromis permaxillaris*)	LNA9	MAF9	F	2016.08.22	Toby's Place	8°37'23.6"S 31°12'01.6"E	Zambia
Limnochromini	Gnaper (*Gnathochromis permaxillaris*)	LNC9	MCI2	M	2016.08.22	Toby's Place	8°37'23.6"S 31°12'01.6"E	Zambia
Limnochromini	Gnaper (*Gnathochromis permaxillaris*)	LND3	MDC4	F	2016.08.22	Toby's Place	8°37'23.6"S 31°12'01.6"E	Zambia
Limnochromini	Gwesta (*Limnochromis staneri*)	ITA6	JPE4	F	2014.07.24	Chipwa Fishermen	8°36'22.2"S 31°11'10.0"E	Zambia
Limnochromini	Gwesta (*Limnochromis staneri*)	ITA8	JPF5	F	2014.07.24	Chipwa Fishermen	8°36'22.2"S 31°11'10.0"E	Zambia
Limnochromini	Gwesta (*Limnochromis staneri*)	ITC2	JQA9	M	2014.07.24	Chipwa Fishermen	8°36'22.2"S 31°11'10.0"E	Zambia
Limnochromini	Gwesta (*Limnochromis staneri*)	IXB3	HQG2	M	2014.07.27	Chipwa Fishermen	8°36'22.2"S 31°11'10.0"E	Zambia
Limnochromini	Gwesta (*Limnochromis staneri*)	LND2	MDB5	M	2016.08.22	Toby's Place	8°37'23.6"S 31°12'01.6"E	Zambia
Limnochromini	Gwesta (*Limnochromis staneri*)	LNI7	MZD7	F	2016.08.23	Chipwa Fishermen	8°36'22.2"S 31°11'10.0"E	Zambia
Limnochromini	Gwesta (*Limnochromis staneri*)	SAF1	SPH8	M	2019.08.24	Chipwa Fishermen	8°36'22.2"S 31°11'10.0"E	Zambia

Limnochromini	Gwcsta (*Limnochromis staneri*)	SAF5	SQA1	F	2019.08.24	Chipwa Fishermen	8°36'22.2"S 31°11'10.0"E	Zambia
Limnochromini	Lchaur (*Limnochromis auritus*)	ITB1	JPG6	F	2014.07.24	Chipwa Fishermen	8°36'22.2"S 31°11'10.0"E	Zambia
Limnochromini	Lchaur (*Limnochromis auritus*)	LNI2	MWH1	M	2016.08.23	Chipwa Fishermen	8°36'22.2"S 31°11'10.0"E	Zambia
Limnochromini	Lchaur (*Limnochromis auritus*)	LNI4	MZA4	F	2016.08.23	Chipwa Fishermen	8°36'22.2"S 31°11'10.0"E	Zambia
Limnochromini	Lchaur (*Limnochromis auritus*)	LNI5	MZB5	M	2016.08.23	Chipwa Fishermen	8°36'22.2"S 31°11'10.0"E	Zambia
Limnochromini	Lchaur (*Limnochromis auritus*)	LNI6	MZC6	M	2016.08.23	Chipwa Fishermen	8°36'22.2"S 31°11'10.0"E	Zambia
Limnochromini	Lchaur (*Limnochromis auritus*)	RKI2	QUE1	F	2017.08.27	Chituta	8°43'25"S 31°09'00"E	Zambia
Limnochromini	Lchaur (*Limnochromis auritus*)	RLC3	QWH4	M	2017.08.28	Chipwa Fishermen	8°36'22.2"S 31°11'10.0"E	Zambia
Limnochromini	Lchaur (*Limnochromis auritus*)	RLC5	QIB8	F	2017.08.28	Chipwa Fishermen	8°36'22.2"S 31°11'10.0"E	Zambia
Oreochromini	Oretan (*Oreochromis tanganicae*)*	JAB5	GYA3	M	2014.07.30	Chipwa Fishermen	8°36'22.2"S 31°11'10.0"E	Zambia
Oreochromini	Oretan (*Oreochromis tanganicae*)*	JCA3	GYG9	F	2014.07.31	Chipwa Fishermen	8°36'22.2"S 31°11'10.0"E	Zambia
Oreochromini	Oretan (*Oreochromis tanganicae*)*	MOE9	NUA4	M	2016.09.05	Kabyolwe	08° 34' 09"S 30° 45' 02"E	Zambia
Oreochromini	Oretan (*Oreochromis tanganicae*)*	MPG2	OEH1	F	2016.09.10	Ndole bay harbor	8°28'34.1"S 30°26'57.6"E	Zambia
Oreochromini	Oretan (*Oreochromis tanganicae*)*	RLB6	QWA7	F	2017.08.27	Chipwa Fishermen	8°36'22.2"S 31°11'10.0"E	Zambia
Oreochromini	Oretan (*Oreochromis tanganicae*)*	RLB7	QWB8	F	2017.08.27	Chipwa Fishermen	8°36'22.2"S 31°11'10.0"E	Zambia
Oreochromini	Oretan (*Oreochromis tanganicae*)*	RLB8	QWC9	M	2017.08.27	Chipwa Fishermen	8°36'22.2"S 31°11'10.0"E	Zambia
Oreochromini	Oretan (*Oreochromis tanganicae*)*	RLB9	QWE1	F	2017.08.27	Chipwa Fishermen	8°36'22.2"S 31°11'10.0"E	Zambia
Oreochromini	Oretan (*Oreochromis tanganicae*)*	RLC1	QWF2	M	2017.08.27	Chipwa Fishermen	8°36'22.2"S 31°11'10.0"E	Zambia
Perissodini	Permic (*Perissodus microlepis*)	LPD7	NCD7	M	2016.08.24	Toby's Place	8°37'23.6"S 31°12'01.6"E	Zambia
Perissodini	Permic (*Perissodus microlepis*)	MUC6	LYC4	M	2016.08.20	Toby's Place	8°37'23.6"S 31°12'01.6"E	Zambia
Perissodini	Permic (*Perissodus microlepis*)	MUC7	LYE8	F	2016.08.20	Toby's Place	8°37'23.6"S 31°12'01.6"E	Zambia
Perissodini	Permic (*Perissodus microlepis*)	MUC8	LYF7	F	2016.08.20	Toby's Place	8°37'23.6"S 31°12'01.6"E	Zambia
Perissodini	Permic (*Perissodus microlepis*)	MUD1	LYI2	M	2016.08.20	Toby's Place	8°37'23.6"S 31°12'01.6"E	Zambia
Perissodini	Permic (*Perissodus microlepis*)	MUG9	LUC4	F	2016.08.21	Toby's Place	8°37'23.6"S 31°12'01.6"E	Zambia
Perissodini	Plepar (*Plecodus paradoxus*)	OMG8	QFF9	M	2017.02.04	Kalila Nkwasi	06°15'38"S 029°44'12"E	Tanzania
Perissodini	Plepar (*Plecodus paradoxus*)	OMG9	QFH1	M	2017.02.04	Kalila Nkwasi	06°15'38"S 029°44'12"E	Tanzania
Perissodini	Plepar (*Plecodus paradoxus*)	OMH1	QFI2	F	2017.02.04	Kalila Nkwasi	06°15'38"S 029°44'12"E	Tanzania
Perissodini	Plepar (*Plecodus paradoxus*)	OMH2	QHA4	F	2017.02.04	Kalila Nkwasi	06°15'38"S 029°44'12"E	Tanzania
Perissodini	Plepar (*Plecodus paradoxus*)	OMI5	QHE8	F	2017.02.05	Myako	6°05'16.8"S 29°43'40.6"E	Tanzania
Perissodini	Plepar (*Plecodus paradoxus*)	OMI7	QHF9	M	2017.02.05	Myako	6°05'16.8"S 29°43'40.6"E	Tanzania
Perissodini	Plestr (*Plecodus straeleni*)	MOA7	NQI2	M	2016.08.30	Chituta	8°43'25"S 31°09'00"E	Zambia
Perissodini	Plestr (*Plecodus straeleni*)	MOA8	NRA4	M	2016.08.30	Chituta	8°43'25"S 31°09'00"E	Zambia
Perissodini	Plestr (*Plecodus straeleni*)	MPB7	OAC6	M	2016.09.08	Katete 2	08°19'41"S 30°31'36"E	Zambia
Perissodini	Plestr (*Plecodus straeleni*)	MPD6	OCC6	F	2016.09.09	Kachese	8°29'25.9"S 30°28'39.0"E	Zambia
Perissodini	Plestr (*Plecodus straeleni*)	MPE7	ODC6	F	2016.09.10	Mpende Fisheries	8°28'56.8"S 30°28'00.5"E	Zambia
Perissodini	Plestr (*Plecodus straeleni*)	MPG5	QKB5	F	2016.09.11	Mpende Fisheries	8°28'56.8"S 30°28'00.5"E	Zambia
Trematocarini	Tremac (*Trematocara macrostoma*)	IUC4	JSH5	M	2014.07.25	Toby's Place	8°37'23.6"S 31°12'01.6"E	Zambia
Trematocarini	Tremac (*Trematocara macrostoma*)	IUD7	JTA7	F	2014.07.25	Toby's Place	8°37'23.6"S 31°12'01.6"E	Zambia
Trematocarini	Tremac (*Trematocara macrostoma*)	LOD5	NLA4	F	2016.08.26	Chipwa Fishermen	8°36'22.2"S 31°11'10.0"E	Zambia
Trematocarini	Tremac (*Trematocara macrostoma*)	LOD6	NLB5	M	2016.08.26	Chipwa Fishermen	8°36'22.2"S 31°11'10.0"E	Zambia
Trematocarini	Tremac (*Trematocara macrostoma*)	RYB7	RAA1	M	2019.08.14	Chipwa Fishermen	8°36'22.2"S 31°11'10.0"E	Zambia
Trematocarini	Tremac (*Trematocara macrostoma*)	SAE5	SPE5	F	2019.08.24	Chipwa Fishermen	8°36'22.2"S 31°11'10.0"E	Zambia
Trematocarini	Tremar (*Trematocara marginatum*)	ISA1	JLD6	M	2014.07.22	Toby's Place	8°37'23.6"S 31°12'01.6"E	Zambia
Trematocarini	Tremar (*Trematocara marginatum*)	ISA3	JLE7	F	2014.07.22	Toby's Place	8°37'23.6"S 31°12'01.6"E	Zambia
Trematocarini	Tremar (*Trematocara marginatum*)	ITI7	JRF3	M	2014.07.25	Chipwa Fishermen	8°36'22.2"S 31°11'10.0"E	Zambia
Trematocarini	Tremar (*Trematocara marginatum*)	ITI8	JRG4	M	2014.07.25	Chipwa Fishermen	8°36'22.2"S 31°11'10.0"E	Zambia
Trematocarini	Tremar (*Trematocara marginatum*)	IUA1	JRH5	F	2014.07.25	Toby's Place	8°37'23.6"S 31°12'01.6"E	Zambia
Trematocarini	Tremar (*Trematocara marginatum*)	LOG3	NNH1	M	2016.08.26	Toby's Place	8°37'23.6"S 31°12'01.6"E	Zambia
Trematocarini	Tremar (*Trematocara marginatum*)	LOG4	NNI2	M	2016.08.26	Toby's Place	8°37'23.6"S 31°12'01.6"E	Zambia
Trematocarini	Tremar (*Trematocara marginatum*)	LOG5	NOA4	M	2016.08.26	Toby's Place	8°37'23.6"S 31°12'01.6"E	Zambia
Trematocarini	Tremar (*Trematocara marginatum*)	LOG7	NOC6	F	2016.08.26	Toby's Place	8°37'23.6"S 31°12'01.6"E	Zambia
Trematocarini	Tremar (*Trematocara marginatum*)	LOG8	NOD7	F	2016.08.26	Toby's Place	8°37'23.6"S 31°12'01.6"E	Zambia
Trematocarini	Tremar (*Trematocara marginatum*)	LOG9	NOE8	F	2016.08.26	Toby's Place	8°37'23.6"S 31°12'01.6"E	Zambia
Trematocarini	Trenig (*Trematocara nigrifrons*)	ITH1	JQH6	M	2014.07.24	Chipwa Fishermen	8°36'22.2"S 31°11'10.0"E	Zambia
Trematocarini	Trenig (*Trematocara nigrifrons*)	ITH2	JQI7	M	2014.07.24	Chipwa Fishermen	8°36'22.2"S 31°11'10.0"E	Zambia
Trematocarini	Trenig (*Trematocara nigrifrons*)	ITH9	JRE2	F	2014.07.24	Chipwa Fishermen	8°36'22.2"S 31°11'10.0"E	Zambia
Trematocarini	Trenig (*Trematocara nigrifrons*)	IUA4	JSB8	F	2014.07.25	Toby's Place	8°37'23.6"S 31°12'01.6"E	Zambia
Trematocarini	Trenig (*Trematocara nigrifrons*)	IUA5	JSC9	F	2014.07.25	Toby's Place	8°37'23.6"S 31°12'01.6"E	Zambia
Trematocarini	Trenig (*Trematocara nigrifrons*)	IUE5	JTB8	M	2014.07.25	Toby's Place	8°37'23.6"S 31°12'01.6"E	Zambia
Trematocarini	Treuni (*Trematocara unimaculatum*)	LNA7	MAD5	F	2016.08.22	Toby's Place	8°37'23.6"S 31°12'01.6"E	Zambia
Trematocarini	Treuni (*Trematocara unimaculatum*)	LNA8	MAE6	F	2016.08.22	Toby's Place	8°37'23.6"S 31°12'01.6"E	Zambia
Trematocarini	Treuni (*Trematocara unimaculatum*)	LNB3	MBA4	F	2016.08.22	Toby's Place	8°37'23.6"S 31°12'01.6"E	Zambia
Trematocarini	Treuni (*Trematocara unimaculatum*)	LPF6	NEE8	M	2016.08.25	Chipwa Fishermen	8°36'22.2"S 31°11'10.0"E	Zambia
Trematocarini	Treuni (*Trematocara unimaculatum*)	RYD8	RCC3	M	2019.08.17	Chipwa Fishermen	8°36'22.2"S 31°11'10.0"E	Zambia
Trematocarini	Treuni (*Trematocara unimaculatum*)	RYD9	RCD4	M	2019.08.17	Chipwa Fishermen	8°36'22.2"S 31°11'10.0"E	Zambia
Tropheini	Ctehor (*Ctenochromis horei*)	LNB8	MBF9	F	2016.08.22	Toby's Place	8°37'23.6"S 31°12'01.6"E	Zambia
Tropheini	Ctehor (*Ctenochromis horei*)	LNB9	MBG8	F	2016.08.22	Toby's Place	8°37'23.6"S 31°12'01.6"E	Zambia
Tropheini	Ctehor (*Ctenochromis horei*)	LNC7	MCF7	M	2016.08.22	Toby's Place	8°37'23.6"S 31°12'01.6"E	Zambia
Tropheini	Ctehor (*Ctenochromis horei*)	LNC8	MCH1	M	2016.08.22	Toby's Place	8°37'23.6"S 31°12'01.6"E	Zambia
Tropheini	Ctehor (*Ctenochromis horei*)	LND6	MDF9	M	2016.08.22	Toby's Place	8°37'23.6"S 31°12'01.6"E	Zambia
Tropheini	Ctehor (*Ctenochromis horei*)	LND9	MRA4	F	2016.08.22	Toby's Place	8°37'23.6"S 31°12'01.6"E	Zambia
Tropheini	Gnapfe (*Gnathochromis pfefferi*)	LNC1	MBH9	M	2016.08.22	Toby's Place	8°37'23.6"S 31°12'01.6"E	Zambia
Tropheini	Gnapfe (*Gnathochromis pfefferi*)	LNE1	MRB5	F	2016.08.22	Toby's Place	8°37'23.6"S 31°12'01.6"E	Zambia
Tropheini	Gnapfe (*Gnathochromis pfefferi*)	LPB5	NAI2	F	2016.08.23	Toby's Place	8°37'23.6"S 31°12'01.6"E	Zambia
Tropheini	Gnapfe (*Gnathochromis pfefferi*)	MUD3	LZB5	M	2016.08.20	Toby's Place	8°37'23.6"S 31°12'01.6"E	Zambia
Tropheini	Gnapfe (*Gnathochromis pfefferi*)	MUF2	LSC4	M	2016.08.20	Toby's Place	8°37'23.6"S 31°12'01.6"E	Zambia
Tropheini	Gnapfe (*Gnathochromis pfefferi*)	MUF3	LSD7	F	2016.08.20	Toby's Place	8°37'23.6"S 31°12'01.6"E	Zambia
Tropheini	Intloo (*Interochromis loocki*)	IPB2	JFD8	F	2014.07.20	Toby's Place	8°37'23.6"S 31°12'01.6"E	Zambia
Tropheini	Intloo (*Interochromis loocki*)	IPB6	JFE9	F	2014.07.20	Toby's Place	8°37'23.6"S 31°12'01.6"E	Zambia
Tropheini	Intloo (*Interochromis loocki*)	IPF3	JGF2	M	2014.07.21	Toby's Place	8°37'23.6"S 31°12'01.6"E	Zambia
Tropheini	Intloo (*Interochromis loocki*)	IZI5	HAA4	M	2014.07.29	Toby's Place	8°37'23.6"S 31°12'01.6"E	Zambia
Tropheini	Intloo (*Interochromis loocki*)	MUH7	LVB3	M	2016.08.21	Toby's Place	8°37'23.6"S 31°12'01.6"E	Zambia
Tropheini	Intloo (*Interochromis loocki*)	MUH8	LVC4	F	2016.08.21	Toby's Place	8°37'23.6"S 31°12'01.6"E	Zambia
Tropheini	Limdar (*Limnotilapia dardennii*)	ISA5	JLG9	F	2014.07.22	Toby's Place	8°37'23.6"S 31°12'01.6"E	Zambia
Tropheini	Limdar (*Limnotilapia dardennii*)	LOD1	NKE8	F	2016.08.26	Toby's Place	8°37'23.6"S 31°12'01.6"E	Zambia
Tropheini	Limdar (*Limnotilapia dardennii*)	LOH3	NOI2	M	2016.08.27	Toby's Place	8°37'23.6"S 31°12'01.6"E	Zambia
Tropheini	Limdar (*Limnotilapia dardennii*)	LPF9	NEI2	M	2016.08.25	Chipwa Fishermen	8°36'22.2"S 31°11'10.0"E	Zambia
Tropheini	Limdar (*Limnotilapia dardennii*)	MVE4	OJI2	M	2017.01.18	Nondwa Point	04°51'51"S 029°36'26"E	Tanzania
Tropheini	Limdar (*Limnotilapia dardennii*)	OMA6	QCI2	M	2017.01.28	Kananiye	04°47'39"S 029°35'58"E	Tanzania
Tropheini	Limdar (*Limnotilapia dardennii*)	OMA7	QEH1	M	2017.01.28	Kananiye	04°47'39"S 029°35'58"E	Tanzania
Tropheini	Limdar (*Limnotilapia dardennii*)	ONC8	PXH1	F	2017.01.21	Kalalangabo	04°50'37"S 029°36'34"E	Tanzania
Tropheini	Limdar (*Limnotilapia dardennii*)	ONF8	QAE8	F	2017.01.23	Mabilibili	6°26'50.6"S 29°54'40.0"E	Tanzania
Tropheini	Loblab (*Lobochilotes labiatus*)	ISD8	JNI9	M	2014.07.23	Toby's Place	8°37'23.6"S 31°12'01.6"E	Zambia
Tropheini	Loblab (*Lobochilotes labiatus*)	ISF2	JOC2	M	2014.07.23	Toby's Place	8°37'23.6"S 31°12'01.6"E	Zambia

Tropheini	Loblab (*Lobochilotes labiatus*)	LOH7	NPD7	F	2016.08.27	Toby's Place	8°37'23.6"S 31°12'01.6"E	Zambia
Tropheini	Loblab (*Lobochilotes labiatus*)	LPE2	NCI2	F	2016.08.24	Toby's Place	8°37'23.6"S 31°12'01.6"E	Zambia
Tropheini	Loblab (*Lobochilotes labiatus*)	LPE3	NDA4	F	2016.08.24	Toby's Place	8°37'23.6"S 31°12'01.6"E	Zambia
Tropheini	Loblab (*Lobochilotes labiatus*)	MUC2	LXI2	M	2016.08.20	Toby's Place	8°37'23.6"S 31°12'01.6"E	Zambia
Tropheini	Peteph (*Petrochromis ephippium*)	IPC1	JFG3	F	2014.07.20	Toby's Place	8°37'23.6"S 31°12'01.6"E	Zambia
Tropheini	Peteph (*Petrochromis ephippium*)	IPC7	JFI6	F	2014.07.21	Toby's Place	8°37'23.6"S 31°12'01.6"E	Zambia
Tropheini	Peteph (*Petrochromis ephippium*)	LOB3	NIF9	F	2016.08.25	Chipwa Fishermen	8°36'22.2"S 31°11'10.0"E	Zambia
Tropheini	Peteph (*Petrochromis ephippium*)	LOB4	NIH1	M	2016.08.25	Chipwa Fishermen	8°36'22.2"S 31°11'10.0"E	Zambia
Tropheini	Peteph (*Petrochromis ephippium*)	LPE5	NDC6	M	2016.08.24	Toby's Place	8°37'23.6"S 31°12'01.6"E	Zambia
Tropheini	Peteph (*Petrochromis ephippium*)	LPI6	NHI2	M	2016.08.25	Toby's Place	8°37'23.6"S 31°12'01.6"E	Zambia
Tropheini	Petfam (*Petrochromis famula*)	IYA6	HAD7	F	2014.07.29	Toby's Place	8°37'23.6"S 31°12'01.6"E	Zambia
Tropheini	Petfam (*Petrochromis famula*)	IYA7	HAE8	M	2014.07.29	Toby's Place	8°37'23.6"S 31°12'01.6"E	Zambia
Tropheini	Petfam (*Petrochromis famula*)	LNG8	MTH1	F	2016.08.22	Toby's Place	8°37'23.6"S 31°12'01.6"E	Zambia
Tropheini	Petfam (*Petrochromis famula*)	LNG9	MTI2	M	2016.08.22	Toby's Place	8°37'23.6"S 31°12'01.6"E	Zambia
Tropheini	Petfam (*Petrochromis famula*)	LNH1	MWA4	F	2016.08.22	Toby's Place	8°37'23.6"S 31°12'01.6"E	Zambia
Tropheini	Petfam (*Petrochromis famula*)	LPA5	MXH1	M	2016.08.23	Toby's Place	8°37'23.6"S 31°12'01.6"E	Zambia
Tropheini	Petfas (*Petrochromis fasciolatus*)	LNA5	MAB3	F	2016.08.21	Toby's Place	8°37'23.6"S 31°12'01.6"E	Zambia
Tropheini	Petfas (*Petrochromis fasciolatus*)	LPA9	NAC6	F	2016.08.23	Toby's Place	8°37'23.6"S 31°12'01.6"E	Zambia
Tropheini	Petfas (*Petrochromis fasciolatus*)	LPB1	NAD7	M	2016.08.23	Toby's Place	8°37'23.6"S 31°12'01.6"E	Zambia
Tropheini	Petfas (*Petrochromis fasciolatus*)	LPB3	NAG5	F	2016.08.23	Toby's Place	8°37'23.6"S 31°12'01.6"E	Zambia
Tropheini	Petfas (*Petrochromis fasciolatus*)	LPB4	NAH1	M	2016.08.23	Toby's Place	8°37'23.6"S 31°12'01.6"E	Zambia
Tropheini	Petfas (*Petrochromis fasciolatus*)	LPB6	NBA4	M	2016.08.23	Toby's Place	8°37'23.6"S 31°12'01.6"E	Zambia
Tropheini	Petkas (*Petrochromis* sp. "kazumbae")	KEA4	KVB2	F	2015.06.24	Kaku	04°53'47"S 029°36'42"E	Tanzania
Tropheini	Petkas (*Petrochromis* sp. "kazumbae")	KEA8	KVC3	F	2015.06.24	Kaku	04°53'47"S 029°36'42"E	Tanzania
Tropheini	Petkas (*Petrochromis* sp. "kazumbae")	KEB4	KVD4	M	2015.06.24	Kaku	04°53'47"S 029°36'42"E	Tanzania
Tropheini	Petkas (*Petrochromis* sp. "kazumbae")	KHI8	KVA1	M	2015.06.24	Kaku	04°53'47"S 029°36'42"E	Tanzania
Tropheini	Petkas (*Petrochromis* sp. "kazumbae")	ONH6	QBH1	F	2017.01.25	Kananiye	04°47'39"S 029°35'58"E	Tanzania
Tropheini	Petkas (*Petrochromis* sp. "kazumbae")	ONH7	QBI2	M	2017.01.25	Kananiye	04°47'39"S 029°35'58"E	Tanzania
Tropheini	Petmac (*Petrochromis macrognathus*)	LOH9	NPF9	F	2016.08.27	Toby's Place	8°37'23.6"S 31°12'01.6"E	Zambia
Tropheini	Petmac (*Petrochromis macrognathus*)	LOI1	NPH1	M	2016.08.27	Toby's Place	8°37'23.6"S 31°12'01.6"E	Zambia
Tropheini	Petmac (*Petrochromis macrognathus*)	LOI2	NPI2	M	2016.08.27	Toby's Place	8°37'23.6"S 31°12'01.6"E	Zambia
Tropheini	Petmac (*Petrochromis macrognathus*)	LOI3	NQA4	M	2016.08.27	Toby's Place	8°37'23.6"S 31°12'01.6"E	Zambia
Tropheini	Petmac (*Petrochromis macrognathus*)	MOF6	NUI2	F	2016.09.06	Chimba	08°25'34"S 30°27'24"E	Zambia
Tropheini	Petmac (*Petrochromis macrognathus*)	MOH4	NWF9	F	2016.09.06	Chimba	08°25'34"S 30°27'24"E	Zambia
Tropheini	Petort (*Petrochromis orthognathus*)	OND2	PYB5	F	2017.01.21	Kalalangabo	04°50'37"S 029°36'34"E	Tanzania
Tropheini	Petort (*Petrochromis orthognathus*)	OND3	PYC6	F	2017.01.21	Kalalangabo	04°50'37"S 029°36'34"E	Tanzania
Tropheini	Petort (*Petrochromis orthognathus*)	OND4	PYD7	F	2017.01.21	Kalalangabo	04°50'37"S 029°36'34"E	Tanzania
Tropheini	Petort (*Petrochromis orthognathus*)	OND5	PYE8	M	2017.01.21	Kalalangabo	04°50'37"S 029°36'34"E	Tanzania
Tropheini	Petort (*Petrochromis orthognathus*)	OND6	PYF9	M	2017.01.21	Kalalangabo	04°50'37"S 029°36'34"E	Tanzania
Tropheini	Petort (*Petrochromis orthognathus*)	OND7	PYH1	M	2017.01.21	Kalalangabo	04°50'37"S 029°36'34"E	Tanzania
Tropheini	Petpol (*Petrochromis polyodon*)	IQG2	JKI2	M	2014.07.22	Toby's Place	8°37'23.6"S 31°12'01.6"E	Zambia
Tropheini	Petpol (*Petrochromis polyodon*)	LOB2	NIE8	F	2016.08.25	Chipwa Fishermen	8°36'22.2"S 31°11'10.0"E	Zambia
Tropheini	Petpol (*Petrochromis polyodon*)	RKB3	QQB8	F	2017.08.10	Toby's Place	8°37'23.6"S 31°12'01.6"E	Zambia
Tropheini	Petpol (*Petrochromis polyodon*)	RKB4	QQC9	F	2017.08.10	Toby's Place	8°37'23.6"S 31°12'01.6"E	Zambia
Tropheini	Petpol (*Petrochromis polyodon*)	RKB5	QQE1	F	2017.08.10	Toby's Place	8°37'23.6"S 31°12'01.6"E	Zambia
Tropheini	Petpol (*Petrochromis polyodon*)	RKC1	QRA7	M	2017.08.11	Toby's Place	8°37'23.6"S 31°12'01.6"E	Zambia
Tropheini	Petpol (*Petrochromis polyodon*)	RKC2	QRB8	M	2017.08.11	Toby's Place	8°37'23.6"S 31°12'01.6"E	Zambia
Tropheini	Petpol (*Petrochromis polyodon*)	RKC3	QRC9	M	2017.08.11	Toby's Place	8°37'23.6"S 31°12'01.6"E	Zambia
Tropheini	Psccur (*Pseudosimochromis curvifrons*)	IPA2	JFA1	M	2014.07.20	Toby's Place	8°37'23.6"S 31°12'01.6"E	Zambia
Tropheini	Psccur (*Pseudosimochromis curvifrons*)	ISC6	JNE5	M	2014.07.23	Toby's Place	8°37'23.6"S 31°12'01.6"E	Zambia
Tropheini	Psccur (*Pseudosimochromis curvifrons*)	LPD8	NCE8	M	2016.08.24	Toby's Place	8°37'23.6"S 31°12'01.6"E	Zambia
Tropheini	Psccur (*Pseudosimochromis curvifrons*)	LPE1	NCH1	F	2016.08.24	Toby's Place	8°37'23.6"S 31°12'01.6"E	Zambia
Tropheini	Psccur (*Pseudosimochromis curvifrons*)	MUE9	LSA4	F	2016.08.20	Toby's Place	8°37'23.6"S 31°12'01.6"E	Zambia
Tropheini	Psccur (*Pseudosimochromis curvifrons*)	ONH8	QCA4	F	2017.01.25	Kananiye	04°47'39"S 029°35'58"E	Tanzania
Tropheini	Simbab (*Pseudosimochromis babaulti*)	JUG2	KJB2	M	2015.01.05	Kitaza south	3°37'32.5"S 29°20'32.6"E	Burundi
Tropheini	Simbab (*Pseudosimochromis babaulti*)	JUG3	KJA1	M	2015.01.05	Kitaza south	3°37'32.5"S 29°20'32.6"E	Burundi
Tropheini	Simbab (*Pseudosimochromis babaulti*)	JUG4	KJC3	M	2015.01.05	Kitaza south	3°37'32.5"S 29°20'32.6"E	Burundi
Tropheini	Simbab (*Pseudosimochromis babaulti*)	JUG5	KJD4	F	2015.01.05	Kitaza south	3°37'32.5"S 29°20'32.6"E	Burundi
Tropheini	Simbab (*Pseudosimochromis babaulti*)	JUG6	KJE5	F	2015.01.05	Kitaza south	3°37'32.5"S 29°20'32.6"E	Burundi
Tropheini	Simbab (*Pseudosimochromis babaulti*)	JUG7	KJF6	F	2015.01.05	Kitaza south	3°37'32.5"S 29°20'32.6"E	Burundi
Tropheini	Simdia (*Simochromis diagramma*)	IPH6	JHF1	M	2014.07.21	Toby's Place	8°37'23.6"S 31°12'01.6"E	Zambia
Tropheini	Simdia (*Simochromis diagramma*)	IQC9	JJI2	M	2014.07.22	Toby's Place	8°37'23.6"S 31°12'01.6"E	Zambia
Tropheini	Simdia (*Simochromis diagramma*)	LOF6	NNB5	F	2016.08.26	Toby's Place	8°37'23.6"S 31°12'01.6"E	Zambia
Tropheini	Simdia (*Simochromis diagramma*)	LPA6	MXI2	M	2016.08.23	Toby's Place	8°37'23.6"S 31°12'01.6"E	Zambia
Tropheini	Simdia (*Simochromis diagramma*)	LPA7	NAA4	F	2016.08.23	Toby's Place	8°37'23.6"S 31°12'01.6"E	Zambia
Tropheini	Simdia (*Simochromis diagramma*)	LPB7	NBB5	F	2016.08.23	Toby's Place	8°37'23.6"S 31°12'01.6"E	Zambia
Tropheini	Simdia (*Simochromis diagramma*)	LPD9	NCF9	F	2016.08.24	Toby's Place	8°37'23.6"S 31°12'01.6"E	Zambia
Tropheini	Simmrg (*Pseudosimochromis marginatus* (North))	ONA5	PVB5	M	2017.01.20	Mwamahunga	04°54'43"S 029°35'54"E	Tanzania
Tropheini	Simmrg (*Pseudosimochromis marginatus* (North))	ONA6	PVC6	M	2017.01.20	Mwamahunga	04°54'43"S 029°35'54"E	Tanzania
Tropheini	Simmrg (*Pseudosimochromis marginatus* (North))	ONA7	PVD7	F	2017.01.20	Mwamahunga	04°54'43"S 029°35'54"E	Tanzania
Tropheini	Simmrg (*Pseudosimochromis marginatus* (North))	ONB8	PWF9	M	2017.01.20	Mwamahunga	04°54'43"S 029°35'54"E	Tanzania
Tropheini	Simmrg (*Pseudosimochromis marginatus* (North))	ONB9	PWH1	F	2017.01.20	Mwamahunga	04°54'43"S 029°35'54"E	Tanzania
Tropheini	Simmrg (*Pseudosimochromis marginatus* (North))	ONC1	PWI2	F	2017.01.20	Mwamahunga	04°54'43"S 029°35'54"E	Tanzania
Tropheini	Simple (*Pseudosimochromis babaulti* (South))	ISB9	JNB2	M	2014.07.23	Toby's Place	8°37'23.6"S 31°12'01.6"E	Zambia
Tropheini	Simple (*Pseudosimochromis babaulti* (South))	ISC3	JNC3	F	2014.07.23	Toby's Place	8°37'23.6"S 31°12'01.6"E	Zambia
Tropheini	Simple (*Pseudosimochromis babaulti* (South))	MUE5	LRE6	M	2016.08.20	Toby's Place	8°37'23.6"S 31°12'01.6"E	Zambia
Tropheini	Simple (*Pseudosimochromis babaulti* (South))	MUE6	LRF7	F	2016.08.20	Toby's Place	8°37'23.6"S 31°12'01.6"E	Zambia
Tropheini	Simple (*Pseudosimochromis babaulti* (South))	MUE7	LRH1	M	2016.08.20	Toby's Place	8°37'23.6"S 31°12'01.6"E	Zambia
Tropheini	Simple (*Pseudosimochromis babaulti* (South))	MUE8	LRH9	F	2016.08.20	Toby's Place	8°37'23.6"S 31°12'01.6"E	Zambia
Tropheini	Trobri (*Tropheus brichardi*)	JYI8	KQH9	M	2015.01.11	Nyanza Lac	4°14'26.80"S 29°33'0.40"E	Burundi
Tropheini	Trobri (*Tropheus brichardi*)	JZA3	KSA2	F	2015.01.11	Nyanza Lac	4°14'26.80"S 29°33'0.40"E	Burundi
Tropheini	Trobri (*Tropheus brichardi*)	JZA7	KSB3	M	2015.01.11	Nyanza Lac	4°14'26.80"S 29°33'0.40"E	Burundi
Tropheini	Trobri (*Tropheus brichardi*)	JZB3	KSC4	F	2015.01.11	Nyanza Lac	4°14'26.80"S 29°33'0.40"E	Burundi
Tropheini	Trobri (*Tropheus brichardi*)	ONB3	PWA4	F	2017.01.20	Mwamahunga	04°54'43"S 029°35'54"E	Tanzania
Tropheini	Trobri (*Tropheus brichardi*)	ONC2	PXA4	F	2017.01.20	Mwamahunga	04°54'43"S 029°35'54"E	Tanzania
Tropheini	Trobri (*Tropheus brichardi*)	ONC3	PXB5	M	2017.01.20	Mwamahunga	04°54'43"S 029°35'54"E	Tanzania
Tropheini	Trobri (*Tropheus brichardi*)	ONC5	PXD7	M	2017.01.20	Mwamahunga	04°54'43"S 029°35'54"E	Tanzania
Tropheini	Trobri (*Tropheus brichardi*)	ONC6	PXE8	F	2017.01.20	Mwamahunga	04°54'43"S 029°35'54"E	Tanzania
Tropheini	Trodub (*Tropheus duboisi*)	MVE2	OJF9	F	2017.01.18	Nondwa Point	04°51'51"S 029°36'26"E	Tanzania
Tropheini	Trodub (*Tropheus duboisi*)	MVE3	OJH1	F	2017.01.18	Nondwa Point	04°51'51"S 029°36'26"E	Tanzania
Tropheini	Trodub (*Tropheus duboisi*)	ONA1	PUF8	F	2017.01.20	Mwamahunga	04°54'43"S 029°35'54"E	Tanzania
Tropheini	Trodub (*Tropheus duboisi*)	ONA2	PUH1	M	2017.01.20	Mwamahunga	04°54'43"S 029°35'54"E	Tanzania
Tropheini	Trodub (*Tropheus duboisi*)	ONA3	PUI2	M	2017.01.20	Mwamahunga	04°54'43"S 029°35'54"E	Tanzania
Tropheini	Trodub (*Tropheus duboisi*)	ONA4	PVA4	M	2017.01.20	Mwamahunga	04°54'43"S 029°35'54"E	Tanzania

Tropheini	Tromoo (*Tropheus moorii*)	LOA4	MXD7	M	2016.08.23	Isanga	8°39'16.4"S 31°11'30.6"E	Zambia
Tropheini	Tromoo (*Tropheus moorii*)	LOA5	MXE8	F	2016.08.23	Isanga	8°39'16.4"S 31°11'30.6"E	Zambia
Tropheini	Tromoo (*Tropheus moorii*)	LOE9	NME8	M	2016.08.26	Isanga	8°39'16.4"S 31°11'30.6"E	Zambia
Tropheini	Tromoo (*Tropheus moorii*)	LOF2	NMF9	M	2016.08.26	Isanga	8°39'16.4"S 31°11'30.6"E	Zambia
Tropheini	Tromoo (*Tropheus moorii*)	LOF3	NMH1	M	2016.08.26	Isanga	8°39'16.4"S 31°11'30.6"E	Zambia
Tropheini	Tromoo (*Tropheus moorii*)	LOF4	NMI2	F	2016.08.26	Isanga	8°39'16.4"S 31°11'30.6"E	Zambia
Tropheini	Tromoo (*Tropheus moorii*)	LOF5	NNA4	F	2016.08.26	Isanga	8°39'16.4"S 31°11'30.6"E	Zambia
Tylochromini	Tylpol (*Tylochromis polylepis*)*	ONG2	QEA4	F	2017.01.24	Katanga Fishmarket	4°54'53.5"S 29°36'46.5"E	Tanzania
Tylochromini	Tylpol (*Tylochromis polylepis*)*	ONG3	QEB5	F	2017.01.24	Katanga Fishmarket	4°54'53.5"S 29°36'46.5"E	Tanzania
Tylochromini	Tylpol (*Tylochromis polylepis*)*	ONG4	QEC6	F	2017.01.24	Katanga Fishmarket	4°54'53.5"S 29°36'46.5"E	Tanzania
Tylochromini	Tylpol (*Tylochromis polylepis*)*	ONG5	QED7	M	2017.01.24	Katanga Fishmarket	4°54'53.5"S 29°36'46.5"E	Tanzania
Tylochromini	Tylpol (*Tylochromis polylepis*)*	ONG6	QEE8	M	2017.01.24	Katanga Fishmarket	4°54'53.5"S 29°36'46.5"E	Tanzania

Table S2. General sequencing and read mapping summary statistics. Sequencing runs were combined if two sequencing runs were performed for a given sample.

	Minimum	1st quartile	Median	Mean	3rd quartile	Maximum
RIN	0.00	3.10	5.30	5.04	6.80	10.00
Sequenced reads	6'426'710.00	14'682'946.00	19'537'332.00	20'041'240.36	23'887'882.00	46'398'252.00
Clean reads	3'729'746.00	11'003'988.00	15'534'866.00	15'878'684.82	19'766'060.00	38'500'788.00
Uniquely mapped reads (including singletons)	548'008.00	5'704'354.00	9'504'434.00	10'389'813.16	14'489'124.00	32'945'752.00
Uniquely mapped reads (including reads that map to both RH2Aα and RH2Aβ)	524'602.00	5'609'510.00	9'296'646.00	10'155'775.84	14'142'998.00	32'148'590.00
Read count	99'545.00	1'469'533.00	2'475'695.00	2'702'347.07	3'810'049.00	7'835'692.00
Read count of protein-coding RNAs and lncRNAs (lowly expressed genes removed)	32'854.00	1'337'511.00	2'383'349.00	2'570'621.62	3'687'395.00	7'643'707.00
Expressed genes (out of 41'945 exonic features)	8'155.00 (19.44%)	21'368.00 (50.94%)	23'017.00 (54.87%)	22'545.16 (53.75%)	24'320.00 (57.98%)	33'038.00 (78.77%)
Expressed genes (out of 29'002 protein-coding RNAs and lncRNAs, lowly expressed genes removed)	7'952.00 (27.42%)	20'713.00 (71.42%)	22'087.00 (76.16%)	21'554.01 (74.32%)	23'132.00 (79.76%)	28'068.00 (96.78%)

Table S3. Visual opsins annotated in the genome assembly of *Oreochromis niloticus* and sequence identity between *RH2Aα* and *RH2Aβ* (in *O. niloticus*).

Summary of *Oreochromis niloticus* opsin annotation											
Opsin	**Product ID**	**Opsin type**	**Gene ID**	**Transcript ID**	**Protein ID**	**Exonic length**	**Scaffold**	**Strand**	**Start (mRNA)**	**End (mRNA)**	**Number exons**
SWS1	short-wave-sensitive opsin 1	single cone	opn1sw	XM_003448756.3	XP_003448804.1	1441	NC_031981.2	+	23259248	23261101	5
SWS2B	blue-sensitive opsin	single cone	LOC100695018	XM_003442630.3	XP_003442678.1	1955	NC_031970.2	+	31297075	31300426	5
SWS2A	blue-sensitive opsin	single cone	LOC100695287	XM_003442631.4	XP_003442679.1	1339	NC_031970.2	+	31290787	31293150	5
RH2B	green-sensitive opsin	double cone	LOC100711209	XM_003448346.5	XP_003448394.1	1721	NC_031970.2	+	16262397	16266219	5
RH2Aβ	green-sensitive opsin	double cone	LOC100710676	XM_003448344.3	XP_003448392.1	1603	NC_031970.2	+	16286976	16289027	5
RH2Aα	green-sensitive opsin	double cone	LOC100710942	XM_005453560.4	XP_005453617.1	3639	NC_031970.2	-	16285535	16275172	8
RH2Aα	green-sensitive opsin	double cone	LOC100710942	XM_025907202.1	XP_025762987.1	3639	NC_031970.2	-	16285535	16275172	8
LWS	red-sensitive opsin	double cone	LOC100694761	XM_003442629.4	XP_003442677.1	1353	NC_031970.2	+	31305600	31308046	6
RH1	rhodopsin	rod	LOC100691236	XM_003439005.3	XP_003439053.1	1607	NC_031984.2	+	14827754	14829360	1

Percent identity between *RH2Aα* and *RH2Aβ*	
Exon	**Percent identity**
exons 1	94.81%
exons 2	97.04%
exons 3	99.40%
exons 4	97.50%
exons 5	98.99%

Table S4. Top 100 genes with the greatest variance in gene expression based on the PCA (see Fig. 1B). Gene information are based on *O. niloticus* genome annotation. Functional category assignment is based on g:Profiler and UniProt annotations. Visual opsin genes and other vision-related genes are indicated in bold.

	Gene ID	Scaffold	Gene product	Variance	PC1 loading	PC2 loading	PC3 loading	Functional category
1	**LOC100694761**	**NC_031970.2**	**red-sensitive opsin (LWS)**	**13.451**	**-0.296**	**-0.166**	**-0.227**	**vision-related**
2	LOC100704125	NC_031973.2	hemoglobin subunit alpha	12.419	0.384	-0.096	-0.153	oxygen-related
3	LOC100704040	NC_031973.2	hemoglobin subunit beta-1	11.876	0.372	-0.098	-0.149	oxygen-related
4	**LOC100711209**	**NC_031970.2**	**green-sensitive opsin (RH2B)**	**9.079**	**0.023**	**0.354**	**0.068**	**vision-related**
5	**opn1sw**	**NC_031981.2**	**short-wave-sensitive opsin 1 (SWS1)**	**8.436**	**-0.074**	**0.341**	**0.040**	**vision-related**
6	LOC109201892	NC_031969.2	hemoglobin subunit alpha-A	8.277	-0.320	-0.003	0.146	oxygen-related
7	**LOC100695287**	**NC_031970.2**	**blue-sensitive opsin (SWS2A)**	**7.688**	**-0.033**	**-0.295**	**-0.142**	**vision-related**
8	LOC102080222	NC_031969.2	hemoglobin subunit alpha-B	7.213	-0.168	-0.039	0.117	oxygen-related
9	LOC109201893	NC_031969.2	hemoglobin subunit beta-A-like	7.084	-0.297	-0.015	0.127	oxygen-related
10	LOC102078435	NC_031967.2	lncRNA	6.999	-0.167	-0.139	-0.038	
11	LOC109201896	NC_031969.2	hemoglobin subunit alpha-A	6.819	-0.282	0.038	0.142	oxygen-related
12	**LOC100695018**	**NC_031970.2**	**blue-sensitive opsin (SWS2B)**	**6.030**	**-0.057**	**0.043**	**-0.027**	**vision-related**
13	LOC100694067	NC_031982.2	serine/threonine-protein kinase NIM1	5.074	-0.053	0.057	-0.301	
14	LOC100704059	NC_031969.2	hemoglobin subunit beta-A	4.768	-0.219	-0.061	0.115	oxygen-related
15	LOC112841672	NC_031967.2	uncharacterized protein LOC112841672	4.507	-0.130	-0.113	-0.029	
16	LOC109201189	NC_031967.2	hepatitis A virus cellular receptor 2 homolog	3.984	-0.034	-0.144	-0.073	
17	**LOC100691394**	**NC_031965.2**	**retinal cone rhodopsin-sensitive cGMP 3',5'-cyclic phosphodiesterase subunit gamma**	**3.981**	**-0.061**	**0.063**	**0.079**	**vision-related**
18	LOC100701987	NC_031969.2	hemoglobin subunit beta-A	3.728	-0.172	0.006	0.127	oxygen-related
19	**LOC100690212**	**NC_031976.2**	**protein NDRG1**	**3.608**	**-0.037**	**0.075**	**-0.246**	**vision-related**
20	LOC100704359	NC_031976.2	kell blood group glycoprotein	3.600	-0.052	-0.169	-0.059	
21	**arr3**	**NC_031966.2**	**arrestin-C**	**3.221**	**0.023**	**0.174**	**0.152**	**vision-related**
22	**LOC100694101**	**NC_031975.2**	**rhodopsin kinase**	**3.168**	**-0.012**	**0.054**	**-0.143**	**vision-related**
23	LOC100698998	NC_031972.2	myosin heavy chain, fast skeletal muscle	3.164	0.011	0.153	0.000	
24	LOC100705805	NC_031986.2	adenylate cyclase type 8	2.785	-0.063	0.111	-0.203	
25	LOC100695208	NC_031972.2	transcription factor 12	2.724	-0.057	0.093	-0.210	
26	palb2	NC_031971.2	partner and localizer of BRCA2	2.645	0.025	0.121	0.055	
27	LOC100700828	NC_031985.2	PR domain zinc finger protein 1	2.506	-0.063	0.096	-0.135	
28	LOC100700677	NC_031976.2	G protein-activated inward rectifier potassium channel 3	2.357	-0.107	0.066	0.024	
29	LOC102076239	NW_020327503.1	uncharacterized protein LOC102076239	2.341	-0.089	-0.111	-0.003	
30	**LOC100697435**	**NC_031969.2**	**retinal cone rhodopsin-sensitive cGMP 3',5'-cyclic phosphodiesterase subunit gamma**	**2.331**	**0.125**	**-0.058**	**0.076**	**vision-related**
31	LOC109202003	NC_031969.2	ferritin, middle subunit-like	2.317	-0.015	-0.169	0.002	
32	LOC100710422	NC_031970.2	inhibin beta B chain	2.222	-0.040	0.086	-0.003	
33	**grk7**	**NC_031982.2**	**rhodopsin kinase**	**2.210**	**0.087**	**-0.010**	**0.151**	**vision-related**
34	LOC100707699	NC_031970.2	nuclear receptor subfamily 1 group D member 1	2.132	-0.030	0.017	-0.205	
35	**LOC100705221**	**NC_031966.2**	**protein RD3**	**2.089**	**0.063**	**-0.120**	**0.106**	**vision-related**
36	**LOC100710676**	**NC_031970.2**	**green-sensitive opsin (RH2Aβ)**	**2.028**	**0.008**	**-0.013**	**-0.093**	**vision-related**
37	**LOC100710942**	**NC_031970.2**	**green-sensitive opsin (RH2Aα)**	**2.022**	**0.000**	**0.136**	**-0.037**	**vision-related**
38	LOC100700801	NC_031986.2	obscurin	2.012	-0.055	-0.097	-0.020	
39	LOC100698791	NC_031981.2	aryl hydrocarbon receptor nuclear translocator-like protein 2	1.918	-0.025	0.068	-0.188	circadian-related
40	LOC102077300	NC_031967.2	hemicentin-2	1.916	-0.062	-0.085	-0.002	
41	LOC100696748	NC_031979.2	heat shock cognate 71 kDa protein	1.903	0.006	-0.001	-0.027	
42	rsrp1	NC_031983.2	arginine/serine-rich protein 1	1.877	-0.053	0.048	0.026	
43	LOC100705039	NC_031970.2	tubulin monoglycylase TTLL3	1.819	0.016	0.025	0.118	
44	LOC100702396	NC_031987.2	titin	1.794	0.015	0.077	0.022	
45	LOC100704234	NC_031969.2	coenzyme Q-binding protein COQ10 homolog, mitochondrial	1.785	0.041	0.018	0.147	oxygen-related
46	LOC100703692	NC_031970.2	class E basic helix-loop-helix protein 40	1.781	0.048	-0.034	0.178	circadian-related
47	LOC100706607	NC_031973.2	sarcoplasmic/endoplasmic reticulum calcium ATPase 1	1.756	0.028	0.092	0.013	
48	LOC100698477	NC_031972.2	cytosolic purine 5'-nucleotidase	1.745	-0.036	-0.063	0.013	
49	**LOC100697897**	**NC_031985.2**	**recoverin**	**1.737**	**-0.014**	**0.111**	**0.063**	**vision-related**
50	syne2	NC_031983.2	nesprin-2	1.730	-0.057	0.096	-0.154	
51	LOC100711794	NC_031974.2	NACHT, LRR and PYD domains-containing protein 3-like	1.676	-0.005	-0.105	-0.027	
52	LOC100705152	NC_031987.2	WD repeat, SAM and U-box domain-containing protein 1	1.659	-0.047	-0.107	-0.012	
53	LOC109203836	NC_031975.2	mastermind-like protein 1	1.659	-0.012	0.048	-0.018	
54	LOC102078900	NC_031981.2	serine/threonine-protein kinase pim-2	1.613	0.005	-0.025	0.051	
55	guca1a	NC_031981.2	guanylyl cyclase-activating protein 1	1.607	-0.052	0.046	-0.133	
56	LOC112842060	NC_031979.2	lncRNA	1.591	-0.066	-0.114	-0.003	
57	LOC100701380	NC_031975.2	creatine kinase M-type	1.583	0.027	0.100	0.013	
58	LOC106097280	NW_020327404.1	uncharacterized protein LOC106097280	1.571	-0.077	-0.082	-0.002	
59	LOC102078920	NW_020327203.1	lncRNA	1.564	-0.051	-0.056	0.002	
60	LOC100702315	NC_031985.2	uncharacterized protein LOC100702315	1.564	-0.025	0.034	-0.008	
61	LOC100698069	NC_031979.2	guanylyl cyclase-activating protein 1	1.540	-0.006	0.087	0.081	
62	LOC100696371	NC_031971.2	sodium/potassium/calcium exchanger 2	1.517	0.075	0.018	0.100	
63	LOC100694340	NC_031982.2	uncharacterized protein LOC100694340	1.515	-0.013	0.052	-0.139	
64	mylpf	NC_031969.2	myosin regulatory light chain 2, skeletal muscle	1.505	0.025	0.103	0.011	
65	LOC102077385	NC_031987.2	myelin-oligodendrocyte glycoprotein/sodium channel subunit beta-3	1.493	-0.006	-0.016	-0.019	
66	LOC100698934	NC_031972.2	poly [ADP-ribose] polymerase 6	1.492	-0.031	0.111	-0.117	
67	**LOC100695749**	**NC_031971.2**	**retinal cone rhodopsin-sensitive cGMP 3',5'-cyclic phosphodiesterase subunit gamma**	**1.488**	**0.072**	**0.016**	**0.087**	**vision-related**
68	LOC106098072	NC_031969.2	lncRNA	1.485	-0.023	0.093	-0.100	
69	xdh	NC_031986.2	xanthine dehydrogenase/oxidase	1.478	-0.057	0.039	-0.126	
70	**LOC100696010**	**NC_031971.2**	**retinal cone rhodopsin-sensitive cGMP 3',5'-cyclic phosphodiesterase subunit gamma**	**1.473**	**0.040**	**-0.006**	**0.136**	**vision-related**
71	**LOC102077467**	**NC_031974.2**	**cyclic nucleotide-gated cation channel beta-3**	**1.435**	**0.092**	**-0.012**	**-0.016**	**vision-related**
72	bhlhe40	NC_031970.2	class E basic helix-loop-helix protein 40	1.430	0.075	-0.062	0.125	
73	LOC102079244	NW_020328614.1	uncharacterized protein LOC102079244	1.430	-0.056	-0.091	0.012	
74	LOC100695257	NC_031987.2	titin	1.419	-0.006	0.063	-0.025	
75	LOC100690808	NC_031970.2	period circadian protein homolog 3	1.403	0.050	-0.062	0.149	circadian-related
76	LOC102076719	NC_031967.2	barrier-to-autointegration factor-like protein	1.403	0.009	0.068	-0.032	
77	LOC100695408	NC_031967.2	LOW QUALITY PROTEIN: period circadian protein homolog 1	1.384	0.055	-0.095	0.068	circadian-related
78	znf277	NC_031972.2	zinc finger protein 277	1.370	0.003	-0.053	0.010	
79	LOC100702088	NC_031986.2	NLR family CARD domain-containing protein 3	1.368	-0.001	-0.123	0.000	
80	LOC100690310	NC_031979.2	protein phosphatase 1A	1.350	0.074	-0.037	0.117	circadian-related
81	LOC109195069	NC_031981.2	lncRNA	1.343	0.018	-0.106	0.035	
82	LOC102081276	NC_031969.2	nuclear GTPase SLIP-GC	1.338	-0.057	-0.051	0.001	
83	LOC100702938	NC_031979.2	creatine kinase M-type	1.335	0.027	0.086	0.026	
84	LOC109204658	NC_031977.2	lncRNA	1.333	-0.008	0.091	-0.015	
85	hsd11b2	NC_031965.2	corticosteroid 11-beta-dehydrogenase isozyme 2	1.325	0.011	0.057	-0.037	
86	hsd17b3	NC_031977.2	testosterone 17-beta-dehydrogenase 3	1.325	-0.025	0.038	-0.005	

87	**LOC100699863**	**NC_031965.2**	**photoreceptor-specific nuclear receptor**	**1.324**	**0.072**	**-0.065**	**0.087**	**vision-related**
88	LOC100712429	NC_031981.2	histone H4	1.319	-0.040	0.061	0.023	
89	tfr2	NC_031967.2	transferrin receptor protein 2	1.316	-0.010	0.104	0.013	
90	LOC100692640	NC_031969.2	parvalbumin beta	1.310	0.015	0.107	0.014	
91	LOC100691580	NW_020328805.1	NACHT, LRR and PYD domains-containing protein 12	1.310	-0.059	0.076	0.011	
92	LOC109202915	NC_031972.2	lncRNA	1.300	-0.039	-0.068	-0.022	
93	pde6c	NC_031973.2	cone cGMP-specific 3',5'-cyclic phosphodiesterase subunit alpha'	1.298	0.079	0.016	0.099	
94	**LOC100693336**	**NC_031986.2**	**retinol dehydrogenase 8**	**1.293**	**0.028**	**-0.015**	**0.140**	**vision-related**
95	focad	NC_031967.2	focadhesin	1.290	0.005	0.122	0.004	
96	cyp1a	NC_031965.2	cytochrome P450 1A	1.286	-0.020	0.056	-0.035	
97	**LOC102078384**	**NC_031980.2**	**retinitis pigmentosa 1-like 1 protein**	**1.284**	**0.086**	**0.016**	**0.073**	**vision-related**
98	LOC112847094	NC_031971.2	lncRNA	1.274	0.007	0.054	0.001	
99	LOC100696691	NC_031986.2	phospholipid hydroperoxide glutathione peroxidase	1.274	-0.067	0.069	-0.021	
100	gapdh	NC_031976.2	glyceraldehyde-3-phosphate dehydrogenase	1.270	0.018	0.075	0.001	

Table S5. Summary statistics of the visual opsin gene expression profiles (see Fig. 2).

Opsin expression relative to all opsins						
Opsin	**Minimum**	**1st quartile**	**Median**	**Mean**	**3rd quartile**	**Maximum**
SWS1	0%	0.0405%	0.8333%	1.2952%	2.1889%	5.7913%
SWS2B	0.0003%	0.0226%	0.1332%	0.6357%	0.7309%	5.8249%
SWS2A	0%	0.0008%	0.0025%	0.5388%	0.3958%	4.2659%
RH2B	0.0002%	1.6441%	4.3993%	6.1273%	10.0190%	22.4120%
RH2Aβ	0.0017%	0.4762%	1.7785%	3.1813%	4.6059%	26.3142%
RH2Aα	0.0035%	1.1644%	1.8134%	3.0179%	4.4552%	10.5913%
LWS	0%	0.0041%	0.1319%	3.2895%	4.0075%	28.3877%
RH1	42.8958%	74.7822%	82.5519%	81.9142%	91.1066%	98.0490%

Single and double cone opsin expression relative to all opsins						
Opsin type	**Minimum**	**1st quartile**	**Median**	**Mean**	**3rd quartile**	**Maximum**
Single cones	0.0010%	1.2485%	2.4164%	2.4697%	3.5341%	6.6666%
Double cones	1.6336%	7.4449%	14.6261%	15.6160%	22.3591%	52.2654%

Opsin expression relative to single cone opsins						
Opsin	**Minimum**	**1st quartile**	**Median**	**Mean**	**3rd quartile**	**Maximum**
SWS1	0%	1.9269%	49.6986%	50.4429%	97.5503%	99.8632%
SWS2B	0.0615%	1.1589%	6.5087%	24.5122%	43.9162%	98.6571%
SWS2A	0%	0.0352%	0.1254%	25.0450%	47.4953%	99.9152%

Opsin expression relative to double cone opsins						
Opsin	**Minimum**	**1st quartile**	**Median**	**Mean**	**3rd quartile**	**Maximum**
RH2B	0.0065%	17.5146%	49.9724%	40.3411%	61.4649%	99.9473%
RH2Aβ	0.0167%	4.5924%	15.9413%	21.1992%	32.8135%	81.7016%
RH2Aα	0.0337%	9.8159%	22.9199%	21.4667%	31.0411%	67.1772%
LWS	0%	0.0432%	1.8039%	16.9930%	36.6980%	84.1273%

Table S6. Phylogenetic ANOVA statistics of the eco-morphological traits with the species' depth of occurrence (see fig. S15).

Traits	*F* or *t* value	*P* value
δ13C-values	28.33317	0.00100
shallow vs. deep	6.05271	0.00450
shallow vs. intermediate	6.76963	0.00300
intermediate vs. deep	1.53262	0.44300
δ15N-values	18.06541	0.01200
shallow vs. deep	-5.78800	0.02400
shallow vs. intermediate	-4.11756	0.08550
intermediate vs. deep	-3.23637	0.09100
Relative eye size	3.82417	0.42200
shallow vs. deep	-2.02978	0.52050
shallow vs. intermediate	0.72494	0.75500
intermediate vs. deep	-2.76513	0.35700

Data S1. (separate file)

Raw read count table in exonic features generated using the HTSeq-count script from the HTSeq framework (v. 0.11.2; (*80*)) with the correction of *RH2Aα*/*RH2Aβ* proportion. Each row is a cichlid individual (named according to the abbreviated species name, specimen ID and sample ID; see table S1) and each column is a gene (based on *Oreochromis niloticus* genome annotation; RefSeq accession GCF_001858045.2).

CHAPTER 3

Drivers and dynamics of a massive adaptive radiation in cichlid fishes

Fabrizia Ronco, Michael Matschiner, Astrid Böhne, Anna Boila, Heinz H. Büscher, Athimed El Taher, Adrian Indermaur, Milan Malinsky, **Virginie Ricci**, Ansgar Kahmen, Sissel Jentoft & Walter Salzburger

Nature (2021)

Article

Drivers and dynamics of a massive adaptive radiation in cichlid fishes

https://doi.org/10.1038/s41586-020-2930-4

Received: 4 February 2020

Accepted: 20 August 2020

Published online: 18 November 2020

Check for updates

Fabrizia Ronco[1]✉, Michael Matschiner[1,2,3], Astrid Böhne[1,4], Anna Boila[1], Heinz H. Büscher[1], Athimed El Taher[1], Adrian Indermaur[1], Milan Malinsky[1], Virginie Ricci[1], Ansgar Kahmen[5], Sissel Jentoft[3] & Walter Salzburger[1,3]✉

Adaptive radiation is the likely source of much of the ecological and morphological diversity of life[1–4]. How adaptive radiations proceed and what determines their extent remains unclear in most cases[1,4]. Here we report the in-depth examination of the spectacular adaptive radiation of cichlid fishes in Lake Tanganyika. On the basis of whole-genome phylogenetic analyses, multivariate morphological measurements of three ecologically relevant trait complexes (body shape, upper oral jaw morphology and lower pharyngeal jaw shape), scoring of pigmentation patterns and approximations of the ecology of nearly all of the approximately 240 cichlid species endemic to Lake Tanganyika, we show that the radiation occurred within the confines of the lake and that morphological diversification proceeded in consecutive trait-specific pulses of rapid morphospace expansion. We provide empirical support for two theoretical predictions of how adaptive radiations proceed, the 'early-burst' scenario[1,5] (for body shape) and the stages model[1,6,7] (for all traits investigated). Through the analysis of two genomes per species and by taking advantage of the uneven distribution of species in subclades of the radiation, we further show that species richness scales positively with per-individual heterozygosity, but is not correlated with transposable element content, number of gene duplications or genome-wide levels of selection in coding sequences.

At the macroevolutionary level, the diversity of life has been shaped mainly by two antagonistic processes: evolutionary radiations increase, and extinction events decrease, organismal diversity over time[5,8,9]. Evolutionary radiations are referred to as adaptive radiations if new lifeforms evolve rapidly through adaptive diversification into a variety of ecological niches, which typically presupposes ecological opportunity[1–3,10]. Whether or not an adaptive radiation occurs depends on a variety of extrinsic and intrinsic factors as well as on contingency, whereas the magnitude of an adaptive radiation is determined by the interplay between its main components, speciation (minus extinction) and adaptation to distinct ecological niches[1,2,4,11]. Despite considerable scientific interest in the phenomenon of adaptive radiation as the cradle of organismal diversity[1,2,10,12,13], many predictions regarding its drivers and dynamics remain untested, particularly in exceptionally species-rich instances. Here, we examine what some consider as the "most outstanding example of adaptive radiation"[14], the species flock of cichlid fishes in Lake Tanganyika. This cichlid assemblage comprises about 240 species[15], which together feature an extraordinary degree of morphological, ecological and behavioural diversity[14–17]. We construct a species tree of Lake Tanganyika's cichlid fauna on the basis of genome-wide data, demonstrate the adaptive nature of the radiation, reconstruct eco-morphological diversification along the species tree, and test general and cichlid-specific predictions related to adaptive radiation.

In situ radiation in Lake Tanganyika

To establish the phylogenetic context of cichlid evolution in Lake Tanganyika, we estimated the age of the radiation through divergence time analyses based on cichlid and other teleost fossils[18], and constructed time-calibrated species trees using 547 newly sequenced cichlid genomes (Supplementary Table 1). Our new phylogenetic hypotheses (Fig. 1, Extended Data Figs. 1–4, Supplementary Figs. 1, 2) support the assignment of the Tanganyikan cichlid fauna into 16 subclades—corresponding to the taxonomic grouping of species into tribes[15]—and confirm that the Tanganyikan representatives of the tribes Coptodonini, Oreochromini and Tylochromini belong to more ancestral and widespread lineages that have colonized the lake secondarily[12,15,19] (Supplementary Discussion). It has been under debate whether all endemic Tanganyikan cichlid tribes evolved within the confines of Lake Tanganyika or whether some of them evolved elsewhere before the formation of the lake[20–22]. Our time calibrations establish that the most recent common ancestor of the cichlid radiation in Lake Tanganyika lived around 9.7 million years ago (Ma) (95% highest-posterior-density

[1]Zoological Institute, Department of Environmental Sciences, University of Basel, Basel, Switzerland. [2]Palaeontological Institute and Museum, University of Zurich, Zurich, Switzerland. [3]Centre for Ecological and Evolutionary Synthesis (CEES), Department of Biosciences, University of Oslo, Oslo, Norway. [4]Centre for Molecular Biodiversity Research (ZMB), Zoological Research Museum Alexander Koenig, Bonn, Germany. [5]Botany, Department of Environmental Sciences, University of Basel, Basel, Switzerland. ✉e-mail: fabrizia.ronco@unibas.ch; walter.salzburger@unibas.ch

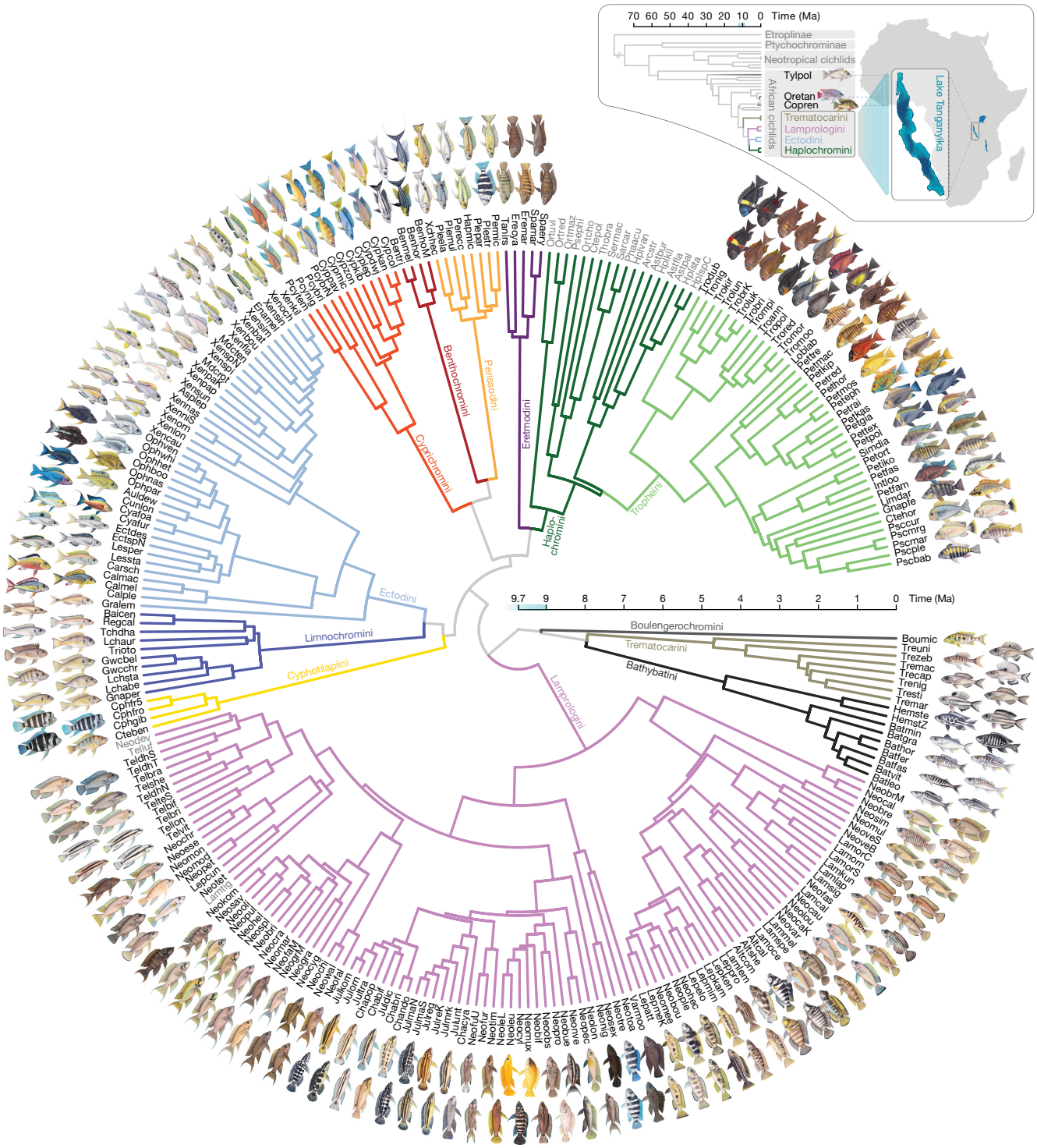

Fig. 1 | Time-calibrated species tree of the cichlid fishes of African Lake Tanganyika. The species tree was time calibrated with a relaxed-clock model and is based on a maximum-likelihood topology inferred from genome-wide SNPs. Species names are abbreviated using a six-letter code, whereby the first three letters represent the genus and the last three letters the species name (Supplementary Table 1; see Extended Data Fig. 2 for the phylogeny with full species names). Branches are coloured according to tribes, and for all lake species an illustration is shown. Representatives of riverine cichlids (grey font) are nested within the radiation. The inset shows the time-calibrated phylogeny of more ancestral cichlid lineages (estimated under the multi-species coalescent model, Extended Data Fig. 1), highlighting the phylogenetic positions of the Tanganyikan representatives of the tribes Coptodonini (*Coptodon rendalli* (Copren)), Oreochromini (*Oreochromis tanganicae* (Oretan)) and Tylochromini (*Tylochromis polylepis* (Tylpol)), which colonized the lake secondarily. The schematic map of the African continent shows the position of the three Great Lakes Victoria, Malawi and Tanganyika, with a magnified section of Lake Tanganyika. The presumed age of Lake Tanganyika[23] (9–12 Myr) is indicated in blue along the time axes. Species trees based on alternative topologies are presented in Extended Data Figs. 2–4, and uncalibrated nuclear and mitochondrial phylogenies on the specimen level are shown in Supplementary Figs. 1, 2.

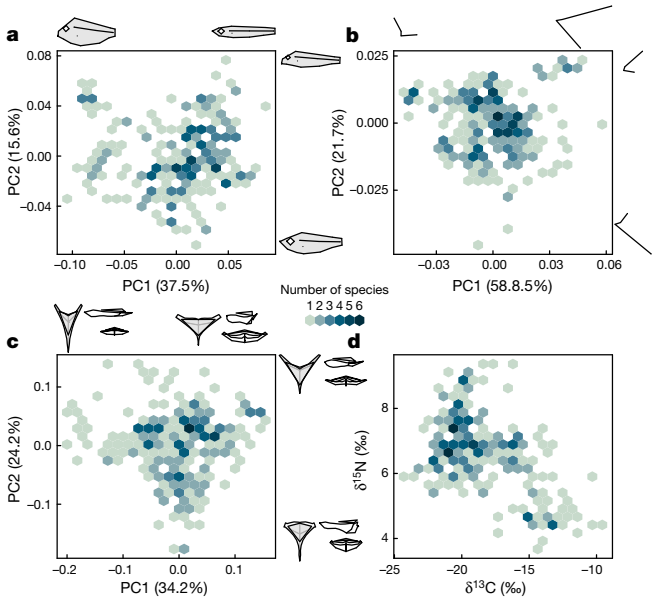

Fig. 2 | Morphospace and ecospace occupation of the cichlid fishes of Lake Tanganyika. a–**c**, PCA of body shape (**a**, $n = 242$ taxa; 2,197 specimens), upper oral jaw morphology (**b**, $n = 242$ taxa; 2,197 specimens) and lower pharyngeal jaw shape (**c**, $n = 239$ taxa, 1,168 specimens) along with the associated shape changes. **d**, Ecospace spanned by the stable C and N isotope composition ($\delta^{13}C$ and $\delta^{15}N$ values; $n = 236$ taxa; 2,259 specimens). The colour scale indicates the number of species in 20 by 20 bins across the trait space (see Extended Data Figs. 6, 7 for PCA and stable-isotope biplots with a focus on morpho- and ecospace occupation per tribe).

age interval: 10.1–9.1 Ma) (Fig. 1), which coincides with the appearance of lacustrine conditions in the Tanganyikan Rift[23]. This suggests that the radiation commenced shortly after the lake had formed and that all endemic cichlid tribes have evolved and diversified in situ, that is, within the temporal and geographical context of Lake Tanganyika.

Phenotypes correlate with environments

Because—in the case of adaptive radiation—diversification occurs via niche specialization, a strong association is expected in the extant fauna between the environment occupied by a species and the specific morphological features used to exploit it[2,3]. To quantify eco-morphological diversification across the radiation, we investigated three trait complexes through landmark-based morphometric analyses. Specifically, we quantified body shape and upper oral jaw morphology using 2D landmarks acquired from X-ray images and the shape of the lower pharyngeal jaw bone based on 3D landmarks derived from micro-computed tomography (μCT) scans (Extended Data Fig. 5). To approximate the ecological niche of each species, we used the carbon and nitrogen stable-isotope composition of muscle tissue, which provides information about the relative position along the benthic–pelagic axis ($\delta^{13}C$ value) and the relative trophic level ($\delta^{15}N$ value), respectively[16,24]—a pattern that we corroborate here for Lake Tanganyika (Extended Data Fig. 6a, Supplementary Discussion). The major axes of shape variation for each trait complex were identified through a principal component analysis (PCA). To test for phenotype–environment correlations and to identify the ecologically most relevant components of each of these trait complexes, we performed a two-block partial least-square analysis (PLS) with the stable-isotope measurements, and applied a phylogenetic generalized least-square analysis (pGLS) to account for phylogenetic dependence.

The quantification of variation in body shape revealed that principal component 1 (PC1) represented mainly differences in aspect ratio, whereas PC2 was loaded with changes in head morphology (Fig. 2a). The changes in aspect ratio (comparable to PC1) were correlated with the $\delta^{13}C$ and $\delta^{15}N$ values (PLS: Pearson's $r = 0.69$, $R^2 = 0.48$, $P = 0.001$; pGLS: $R^2 = 0.12$, $P < 0.001$, $\lambda_{pGLS} = 1.007$). PC1 of upper oral jaw morphology mainly represented changes in the orientation and relative size of the premaxilla, which was also the main correlate to the stable C and N isotope composition (PLS: Pearson's $r = 0.62$, $R^2 = 0.38$, $P = 0.001$; pGLS: $R^2 = 0.09$, $P < 0.001$, $\lambda_{pGLS} = 1.023$), whereas PC2 was defined by changes in the ratio of the rostral versus the lateral part of the bone (Fig. 2b). For lower pharyngeal jaw shape, we found that PC1 reflected mainly changes in the aspect ratio of the jaw bone in combination with an increased posterior thickness, whereas PC2 involved similar shifts in thickness, yet in this case in combination with changes in the lengths of the postero-lateral horns that act as muscle-attachment structures[25] (Fig. 2c). The PLS revealed that shape changes similar to PC2 are best associated with stable-isotope values (PLS: Pearson's $r = 0.67$, $R^2 = 0.45$, $P = 0.001$; pGLS: $R^2 = 0.16$, $P < 0.001$, $\lambda_{pGLS} = 1.018$). The PCAs further revealed that the occupied area of the morphospace and ecospace scales with the number of species in the tribes (Extended Data Figs. 6, 7; ecospace: Pearson's $r = 0.88$, d.f. = 9, $P < 0.001$; body shape: Pearson's $r = 0.91$, d.f. = 9, $P < 0.001$; upper oral jaw morphology: Pearson's $r = 0.88$, d.f. = 9, $P < 0.001$; lower pharyngeal jaw shape: Pearson's $r = 0.83$, d.f. = 9, $P = 0.002$), a pattern that is not driven by sample size only (Supplementary Discussion).

Overall, the significant association between each of the three traits and the stable C and N isotope composition underpins their adaptive value (Extended Data Fig. 8a–c). A joint consideration points out that deep-bodied cichlids with inferior mouths and thick lower pharyngeal jaws with short horns are associated with higher stable-isotope projections (high $\delta^{13}C$ and low $\delta^{15}N$ values), indicating that such fishes occur predominantly in the benthic/littoral zone of the lake and feed on plants and algae, whereas more elongated species with more superior mouths and longer and thinner lower pharyngeal jaws are generally associated with lower stable-isotope projections (low $\delta^{13}C$ and high $\delta^{15}N$ values), suggesting a more pelagic lifestyle and a higher position in the food chain.

Pulses of morphological diversification

Next, we investigated the temporal dynamics of how the observed eco-morphological disparity emerged over the course of the radiation. In addition to the three eco-morphological traits, we also scored male pigmentation patterns to approximate disparity along the signalling axis—another potentially important component of diversification in adaptive radiations[1,6,7,26]. For all four traits, we estimated morphospace expansion through time using ancestral-state reconstructions along the time-calibrated species tree and applying a variable-rates model of trait evolution[27,28] (Extended Data Fig. 8d, e). We calculated morphological disparity as the extent of occupied morphospace in time intervals of 0.15 million years (Myr) in comparison to a null model that assumes Brownian motion. Likewise, evolutionary rates through time were calculated as mean evolutionary rates derived from the variable-rates model, sampled at the same time points along the phylogeny.

Our analyses uncovered a pattern of discrete pulses in morphospace expansion, which were followed, in most cases, by morphospace packing (Fig. 3). The timing of these pulses differed among the traits. For body shape, we found a pulse of rapid morphospace expansion early in the radiation, alongside the first pulse of lower pharyngeal jaw shape diversification (Fig. 3b, c); this early phase of the radiation also features the highest evolutionary rates for body shape (Fig. 3d). The pulse in upper oral jaw diversification occurred in the middle phase of the radiation. Evolutionary rates were increased during this period, and were even higher at a later phase that was dominated by packing of the upper oral jaw morphospace rather than its expansion (Fig. 3b–d). This

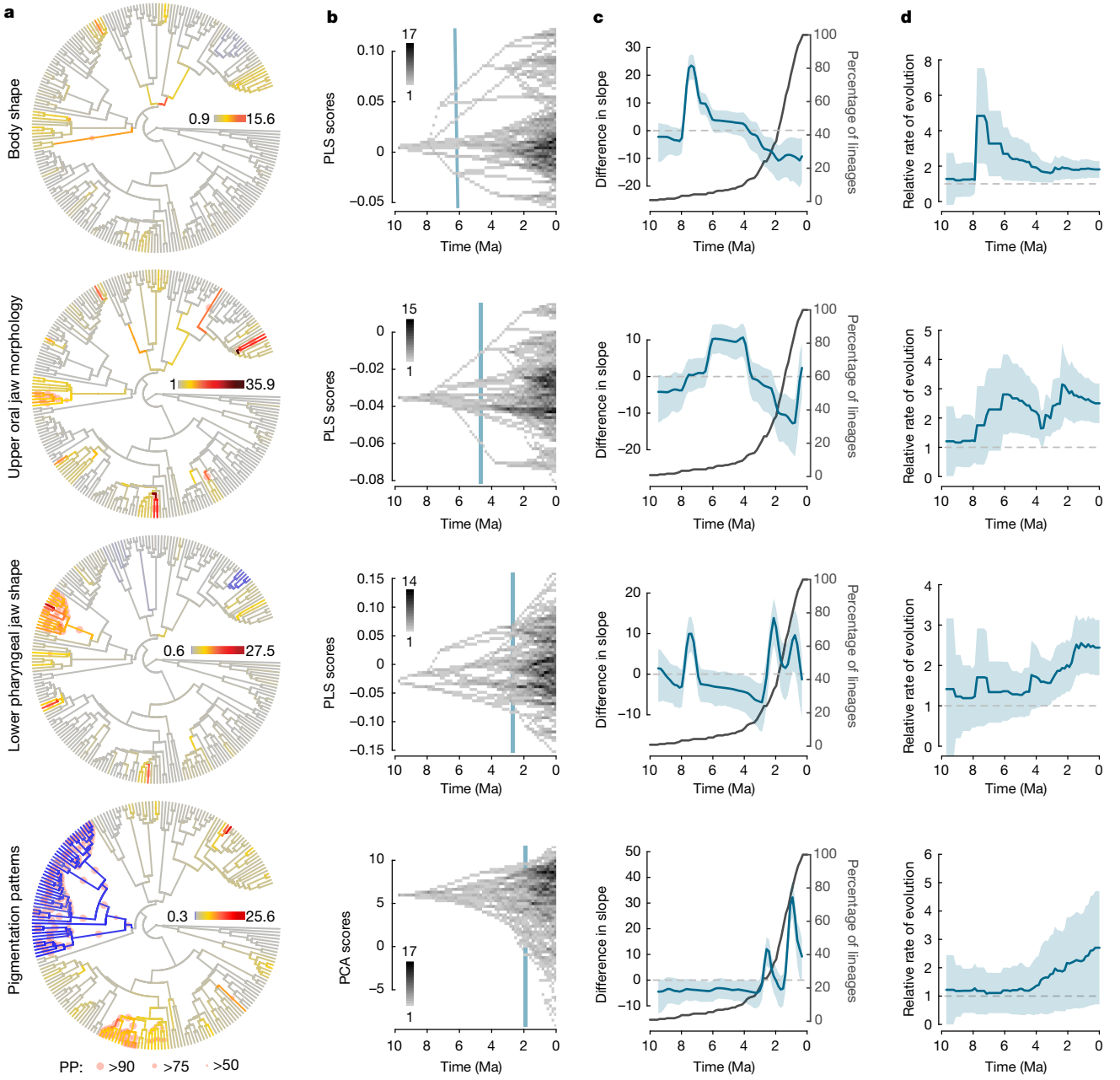

Fig. 3 | Temporal dynamics of morphological diversification in the adaptive radiation of cichlid fishes in Lake Tanganyika. a–d, First row: body shape, $n = 232$ taxa, 2,164 specimens; second row: upper oral jaw morphology, $n = 232$ taxa, 2,164 specimens; third row: lower pharyngeal jaw shape, $n = 232$ taxa, 1,148 specimens; fourth row: pigmentation patterns, $n = 218$ taxa, 1,016 specimens. **a**, Species tree (Fig. 1) with branches coloured according to the mean relative rates of trait evolution for each trait. PP, posterior probability for rate shift. **b**, Morphospace densities (number of lineages) through time for each trait. Blue lines indicate the point in time when 50% of the extant morphospace had become occupied. **c**, Comparison of slopes (blue) of morphospace expansion over time between the observed data and the Brownian motion null model of trait evolution (mean across 500 Brownian motion simulations with 95% quantiles). A difference in slopes above zero represents morphospace expansion and values below zero indicate morphospace packing relative to the null model. Lineage accumulation through time derived from the species tree is shown in dark grey. **d**, Mean relative rates of trait evolution over time with standard deviation (blue).

suggests that, in that later phase, rapidly evolving lineages diverged into pre-occupied regions of the morphospace, ultimately resulting in convergent forms[16]. The second pulse in lower pharyngeal jaw morphospace expansion happened late in the radiation when evolutionary rates were also highest for this trait (Fig. 3b–d). Thus, the theoretical prediction that eco-morphological diversification is rapid early in an adaptive radiation and slows down through time as the available niche space becomes filled[1,5] applies only to body shape. Yet, this early burst in body shape diversification was not connected to a substantial increase in lineage accumulation (Fig. 3c).

Pigmentation patterns showed a single pulse of diversification and increased evolutionary rates late in the radiation—a signature unlikely to be caused by a high turnover rate in this trait (Supplementary Discussion). This late pulse of diversification in pigmentation patterns, together with the consecutive pulses of morphospace expansion in the eco-morphological traits, is in agreement with the prediction that

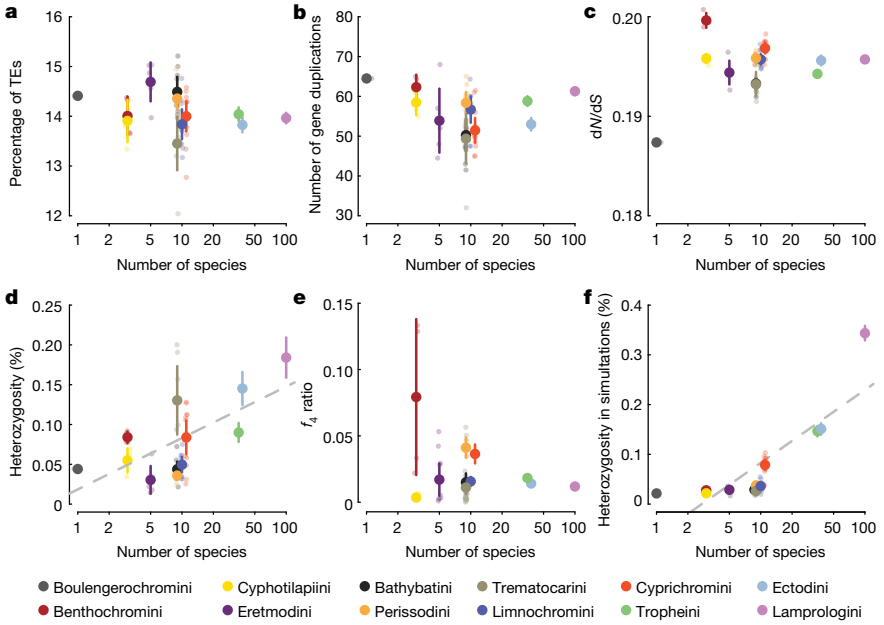

Fig. 4 | Association between genomic features and species richness across the cichlid tribes in Lake Tanganyika. Each genomic summary statistic was tested for a correlation with species richness per tribe (log transformed). To account for phylogenetic structure in the data, we calculated phylogenetic independent contrasts for each variable. Data points are coloured according to tribes; large points are tribe means shown with 95% confidence intervals, small points represent species means and are only shown for group sizes <40. **a**, Percentage of the genome identified as transposable elements (TEs) (Pearson's $r = -0.31$, d.f. = 10, $P = 0.33$; tribe means are based on one genome per species; Extended Data Fig. 9a). **b**, Number of duplicated genes (Pearson's $r = -0.27$, d.f. = 10, $P = 0.40$; tribe means are based on species means). **c**, Genome-wide d*N*/d*S* ratios as a measure of selection on coding sequences (Pearson's $r = 0.26$, d.f. = 10, $P = 0.42$; tribe means are based on species means across a set of 15,294 genes per genome; Extended Data Fig. 9b). **d**, Percentage of heterozygous sites per genome (Pearson's $r = 0.70$, d.f. = 10, $P = 0.012$; tribe means are based on species means). **e**, f_4-ratio statistics as a measure of gene flow among species within each tribe (Pearson's $r = -0.35$, d.f. = 9, $P = 0.29$; tribe means are based on all species triplets within each tribe; see Extended Data Fig. 10 for a summary of the f_4-ratio statistics for all species comparisons). **f**, Mean percentage of heterozygous sites in simulations with within-tribe migration rates sampled from the observed f_4-ratio statistics (Pearson's $r = 0.84$, d.f. = 10, $P = 0.00067$; tribe means are based on species means across 20 simulations; Extended Data Fig. 9c).

diversification in an adaptive radiation proceeds in discrete temporal stages—first in macrohabitat use, then by trophic specialization, followed by a final stage of divergence along the signalling axes[1,6,7]. However, in contrast to the conventional stages model, the most recent stage of the cichlid adaptive radiation in Lake Tanganyika, which coincides with a large number of speciation events (Fig. 3c), is characterized by temporally overlapping pulses of diversification in both a putative signalling trait and in an ecologically relevant trait. The lower pharyngeal jaw shape is the only trait complex showing two discrete pulses of morphospace expansion—one early in the radiation and one late when niche space already became limited. This later pulse suggests that diversification in the pharyngeal jaw apparatus facilitated fine-scaled resource partitioning after body shape and upper oral jaw morphospaces had been explored, resulting in the densely packed niche space observed today (Figs. 2, 3b).

Genomic features and species richness

Finally, we examined whether the diversity patterns arising over the course of the radiation are linked with particular genomic features. It has previously been suggested—on the basis of five reference cichlid genomes—that the radiating African cichlid lineages are characterized by increased transposable element counts, increased levels of gene duplications, and genome-wide accelerated coding-sequence evolution[13]. Because of the phylogenetic substructure of Lake Tanganyika's cichlid fauna and the widely differing species numbers among tribes, our data offered the opportunity to examine genomic features for an association with per-tribe species richness within a large-scale radiation. We did not find evidence that members of species-rich tribes exhibit greater numbers of transposable elements (Fig. 4a) or more duplicated genes in their genomes (Fig. 4b), nor do they feature elevated genome-wide signatures of selection in coding sequences (Fig. 4c) (see also Extended Data Fig. 9). However, we found that a tribe's species richness scales positively with a common measure of genetic diversity: genome-wide heterozygosity (Fig. 4d). That genetic diversity is linked to species richness has been previously suspected, although the nature of this relationship and the determinants of genetic diversity are under debate[29,30].

Elevated levels of heterozygosity could potentially result from hybridization[31], which has itself been suggested as a trigger of cichlid radiations[22,32,33]. In Tanganyikan cichlids, the level of gene flow within tribes (estimated using f_4-ratio values[34]) does not correlate with a tribe's species richness (Fig. 4e, Extended Data Fig. 10). Nevertheless, much of the variation in heterozygosity as well as its correlation with species richness can be explained by the observed levels of gene flow within tribes in combination with the reduced gene flow among them: through coalescent simulations of genome evolution along the species tree we show that variation in migration rates, sampled from the empirical f_4-ratio estimates, can produce levels of heterozygosity that are similar to the ones observed in nature (Fig. 4f). Hence, the correlation between species richness and heterozygosity can be explained by gene flow and phylogenetic structure, which is consistent with the expectation that the effect of gene flow scales positively with the number of hybridizing species and the divergence among these. In the cichlid radiation in Lake Malawi, which is an order of magnitude younger than the one in Lake Tanganyika, heterozygosity levels vary much less among lineages and

do not scale with species richness, which—according to our findings—can be explained by the much lower levels of genetic differentiation between the hybridizing species[33].

Conclusion

On the basis of a comprehensive dataset on cichlid fishes from African Lake Tanganyika, we tested predictions related to the phenomenon of adaptive radiation. We establish that the Tanganyikan cichlid radiation unfolded within the temporal and spatial confines of the lake, giving rise to an endemic fauna consisting of about 240 species in 52 genera and 13 tribes in less than 10 Myr. Although the ancestors of these tribes initially found comparable ecological opportunity, present-day species numbers differ by two orders of magnitude among these phylogenetic sublineages. Our analyses of morphological, ecological and genomic information revealed that, taken as a whole, species-rich tribes occupy larger fractions of the morphospace and ecospace and contain species that are, at the per-genome level, genetically more diverse, which appears to be linked to gene flow. We demonstrate a phenotype–environment association in three trait complexes (body shape, upper oral jaw morphology and lower pharyngeal jaw shape) and pinpoint their most relevant adaptive components. We show that eco-morphological diversification was not gradual over the course of the radiation. Instead, we identified trait-specific pulses of accelerated phenotypic evolution, whereby only diversification in body shape shows an early burst[1,5]. The sequence of the trait-specific pulses essentially follows the pattern postulated in the stages model of adaptive radiation[1,6,7], with the extension that the most recent stage of the cichlid adaptive radiation in Lake Tanganyika, which is characterized by a large number of speciation events, is defined by increased diversification in both an ecological (lower pharyngeal jaw) and a signalling (pigmentation) trait. To what extent the observed diversity and disparity patterns were shaped by past environmental fluctuations and extinction dynamics cannot be answered conclusively through the investigation of the extant fauna alone.

Online content

Any methods, additional references, Nature Research reporting summaries, source data, extended data, supplementary information, acknowledgements, peer review information; details of author contributions and competing interests; and statements of data and code availability are available at https://doi.org/10.1038/s41586-020-2930-4.

1. Gavrilets, S. & Losos, J. B. Adaptive radiation: contrasting theory with data. *Science* **323**, 732–737 (2009).
2. Schluter, D. *The Ecology of Adaptive Radiation* (Oxford Univ. Press, 2000).
3. Simpson, G. G. *The Major Features of Evolution* (Columbia Univ. Press, 1953).
4. Glor, R. E. Phylogenetic insights on adaptive radiation. *Annu. Rev. Ecol. Evol. Syst.* **41**, 251–270 (2010).
5. Foote, M. The evolution of morphological diversity. *Annu. Rev. Ecol. Syst.* **28**, 129–152 (1997).
6. Danley, P. D. & Kocher, T. D. Speciation in rapidly diverging systems: lessons from Lake Malawi. *Mol. Ecol.* **10**, 1075–1086 (2001).
7. Streelman, J. T. & Danley, P. D. The stages of vertebrate evolutionary radiation. *Trends Ecol. Evol.* **18**, 126–131 (2003).
8. Benton, M. J. Diversification and extinction in the history of life. *Science* **268**, 52–58 (1995).
9. Sepkoski, J. J., Jr. Rates of speciation in the fossil record. *Phil. Trans. R. Soc. Lond. B* **353**, 315–326 (1998).
10. Berner, D. & Salzburger, W. The genomics of organismal diversification illuminated by adaptive radiations. *Trends Genet.* **31**, 491–499 (2015).
11. Wagner, C. E., Harmon, L. J. & Seehausen, O. Ecological opportunity and sexual selection together predict adaptive radiation. *Nature* **487**, 366–369 (2012).
12. Salzburger, W. Understanding explosive diversification through cichlid fish genomics. *Nat. Rev. Genet.* **19**, 705–717 (2018).
13. Brawand, D. et al. The genomic substrate for adaptive radiation in African cichlid fish. *Nature* **513**, 375–381 (2014).
14. Fryer, G. & Iles, T. D. *The Cichlid Fishes of the Great Lakes of Africa* (T.F.H. Publications, 1972).
15. Ronco, F., Büscher, H. H., Indermaur, A. & Salzburger, W. The taxonomic diversity of the cichlid fish fauna of ancient Lake Tanganyika, East Africa. *J. Gt. Lakes Res.* **46**, 1067–1078 (2020).
16. Muschick, M., Indermaur, A. & Salzburger, W. Convergent evolution within an adaptive radiation of cichlid fishes. *Curr. Biol.* **22**, 2362–2368 (2012).
17. Salzburger, W., Van Bocxlaer, B. & Cohen, A. S. Ecology and evolution of the African Great Lakes and their faunas. *Annu. Rev. Ecol. Evol. Syst.* **45**, 519–545 (2014).
18. Matschiner, M., Böhne, A., Ronco, F. & Salzburger, W. The genomic timeline of cichlid diversification across continents. *Nat. Commun.* https://doi.org/10.1038/s41467-020-17827-9 (2020).
19. Koch, M. et al. Evolutionary history of the endemic Lake Tanganyika cichlid fish *Tylochromis polylepis*: A recent intruder to a mature adaptive radiation. *J. Zool. Syst. Evol. Res.* **45**, 64–71 (2007).
20. Salzburger, W., Meyer, A., Baric, S., Verheyen, E. & Sturmbauer, C. Phylogeny of the Lake Tanganyika cichlid species flock and its relationship to the Central and East African haplochromine cichlid fish faunas. *Syst. Biol.* **51**, 113–135 (2002).
21. Schedel, F. D. B., Musilova, Z. & Schliewen, U. K. East African cichlid lineages (Teleostei: Cichlidae) might be older than their ancient host lakes: new divergence estimates for the east African cichlid radiation. *BMC Evol. Biol.* **19**, 94 (2019).
22. Irisarri, I. et al. Phylogenomics uncovers early hybridization and adaptive loci shaping the radiation of Lake Tanganyika cichlid fishes. *Nat. Commun.* **9**, 3159 (2018).
23. Cohen, A. S., Soreghan, M. J. & Scholz, C. A. Estimating the age of formation of lakes: an example from Lake Tanganyika, East African Rift system. *Geology* **21**, 511–514 (1993).
24. Post, D. M. Using stable isotopes to estimate trophic position: models, methods, and assumptions. *Ecology* **83**, 703–718 (2002).
25. Liem, K. F. Evolutionary strategies and morphological innovations: cichlid pharyngeal jaws. *Syst. Zool.* **22**, 425–441 (1973).
26. Salzburger, W. The interaction of sexually and naturally selected traits in the adaptive radiations of cichlid fishes. *Mol. Ecol.* **18**, 169–185 (2009).
27. Venditti, C., Meade, A. & Pagel, M. Multiple routes to mammalian diversity. *Nature* **479**, 393–396 (2011).
28. Cooney, C. R. et al. Mega-evolutionary dynamics of the adaptive radiation of birds. *Nature* **542**, 344–347 (2017).
29. Ellegren, H. & Galtier, N. Determinants of genetic diversity. *Nat. Rev. Genet.* **17**, 422–433 (2016).
30. Schluter, D. & Pennell, M. W. Speciation gradients and the distribution of biodiversity. *Nature* **546**, 48–55 (2017).
31. Grant, P. R. & Grant, B. R. *40 Years of Evolution: Darwin's Finches on Daphne Major Island* (Princeton Univ. Press, 2014).
32. Meier, J. I. et al. Ancient hybridization fuels rapid cichlid fish adaptive radiations. *Nat. Commun.* **8**, 14363 (2017).
33. Malinsky, M. et al. Whole-genome sequences of Malawi cichlids reveal multiple radiations interconnected by gene flow. *Nat. Ecol. Evol.* **2**, 1940–1955 (2018).
34. Patterson, N. et al. Ancient admixture in human history. *Genetics* **192**, 1065–1093 (2012).

Article

Methods

No statistical methods were used to predetermine sample size. The experiments were not randomized. The investigators were not blinded to allocation during experiments and outcome assessment.

Sampling

Sampling was conducted between 2014 and 2017 at 130 locations at Lake Tanganyika. To maximise taxon coverage, we included additional specimens from previous expeditions (4.9% of the samples) as well as from other collections (0.8%). The final dataset (301 taxa; $n = 2{,}723$ specimens) contained an almost complete taxon sampling of the cichlid fauna of Lake Tanganyika, as well as 18 representative cichlid species from nearby waterbodies, and 32 outgroup species. All analyses described below are based on the same set of typically 10 specimens per species, or subsets thereof (Supplementary Tables 1, 2, Supplementary Methods).

Whole-genome sequencing

Genomic DNA of typically one male and one female specimen per species ($n = 547$) was extracted from fin clips preserved in ethanol using the E.Z.N.A. Tissue DNA Kit (Omega Bio-Tek) and sheared on a Covaris E220 (60 µl with 10% duty factor, 175 W, 200 cycles for 65 s). Individual libraries were prepared using TruSeq DNA PCR-Free Sample Preparation kit (Illumina; low sample protocol) for 350-bp insert size, pooled (six per lane), and sequenced at 126-bp paired-end on an Illumina HiSeq 2500 (Supplementary Table 1 contains information on read depths).

Assessing genomic variation

After adaptor removal with Trimmomatic[35] (v.0.36), reads of 528 genomes (all species belonging to the cichlid radiation in Lake Tanganyika plus additional species nested within this radiation and some selected outgroup species; Supplementary Table 1) were mapped to the Nile tilapia reference genome (RefSeq accession GCF_001858045.1[36]) using BWA-MEM[37] (v.0.7.12). Variant calling was performed with HaplotypeCaller and GenotypeGVCF tools[38] (v.3.7) (GATK), applying a minimum base quality score of 30. Variant calls were filtered with BCFtools[39] (v.1.6; FS < 20, QD > 2, MQ > 20, DP > 4,000, DP < 8,000, ReadPosRankSum > −0.5, MQRankSum > −0.5). We applied a filter to sites in proximity to indels with a minor allele count greater than 2, depending on the size of the indel. With SNPable (http://lh3lh3.users.sourceforge.net/snpable.shtml), we determined all sites within regions of the Nile tilapia reference genome in which read mapping could be ambiguous and masked these sites. Using VCFtools[40] (v.0.1.14) we further masked, per individual, genotypes with a read depth below 4 or a genotype quality below 20. Sites that were no longer polymorphic after the filtering steps were excluded, resulting in a dataset of 57,751,375 SNPs. Called variants were phased with the software beagle[41] (v.4.1). The phasing of *Neolamprologus cancellatus*, which appeared to be F_1 hybrids, was further improved with a custom script. Further details are provided in the Supplementary Methods.

De novo genome assemblies

De novo genome assemblies were generated from the raw-read data for each individual following an approach described previously[42,43], using CeleraAssembler[44] (v.8.3) and FLASH[45] (v.1.2.11). Eight genomes repeatedly failed to assemble and were therefore excluded from further analyses (specimen vouchers: A188, IRF6, IZC5, JWE7, JWG1, JWG2, LJD3 and LJE8). Assembly quality was assessed with QUAST[46] (v.4.5) and completeness was determined with BUSCO[47] (v.3). Assembly statistics summarized with MultiQC[48] (v.1.7) are available on Dryad.

Determining the age of the radiation

To determine the age of the cichlid radiation in Lake Tanganyika, we applied phylogenomic molecular-clock analyses for representatives of all cichlid subfamilies and the most divergent tribes, together with non-cichlid outgroups (44 species; Extended Data Fig. 1). Following Matschiner et al.[18] we identified and filtered orthologue sequences from genome assemblies and compiled 'strict' and 'permissive' datasets that contained alignments for 510 and 1,161 genes and had total alignment lengths of 542,922 and 1,353,747 bp, respectively. We first analysed the topology of the species with the multi-species coalescent model implemented in ASTRAL[49] (v.5.6.3), based on gene trees that we estimated for both datasets with BEAST2[50] (v.2.5.0). As undetected past introgression can influence divergence-time estimates in molecular clock analyses, we further tested for signals of introgression in the form of asymmetric species relationship in gene trees and excluded five species (*Fundulus heteroclitus*, *Tilapia brevimanus*, *Pelmatolapia mariae*, *Tilapia sparrmanii*, and *Steatocranus* sp. 'ultraslender') potentially affected by introgression from all subsequent molecular-clock analyses. We then estimated divergence times among the most divergent cichlid tribes and the age of the cichlid radiation in Lake Tanganyika with the multi-species coalescent model in StarBEAST2[51] (v.0.15.5), using the 'strict' set of gene alignments (Extended Data Fig. 1). Further details are provided in the Supplementary Methods.

Phylogenetic inference

To infer a complete phylogeny of the cichlid radiation in Lake Tanganyika (the Tanganyikan representatives of the more ancestral tribes Coptodonini, Oreochromini and Tylochromini were excluded) from genome-wide SNPs we applied additional filters, retaining only SNPs with <40% missing data and between-SNP distances of at least 100 bp. The remaining 3,630,997 SNPs were used to infer a maximum-likelihood phylogeny with RAxML[52] (v.8.2.4; Fig. 1, Extended Data Fig. 2, Supplementary Fig. 1). The species-tree topology was further estimated under the multi-species coalescent model from a set of local phylogenies with ASTRAL (Extended Data Fig. 3); these local phylogenies were inferred with IQ-TREE[53] (v.1.7-beta7) from alignments for 1,272 genomic regions determined to be particularly suitable for phylogenetic analysis (see Supplementary Methods). We also applied the multi-species coalescent model implemented in SNAPP[54] (v.1.4.2) to the dataset of genome-wide SNPs (Extended Data Fig. 4). Species-level phylogenies resulting from these different approaches were used as topological constraints in subsequent relaxed-clock analyses of divergence times (see below). In addition, we estimated the mitochondrial phylogeny based on maximum-likelihood with RAxML (Supplementary Fig. 2). Further details are provided in the Supplementary Methods.

Divergence time estimates within the radiation

For relaxed-clock analyses, the 1,272 alignments were further filtered by applying stricter thresholds on the proportion of missing data and the strength of recombination signals. Ten remaining alignments with a length greater than 2,500 bp and less than 130 hemiplasies (total length: 30,738 bp; completeness: 95.8%), were then used jointly to estimate divergence times with the uncorrelated-lognormal relaxed-clock model implemented in BEAST2. To account for phylogenetic uncertainty in downstream phylogenetic comparative analyses, we performed three separate sets of relaxed clock analyses, in which the topology was either fixed to the species-level phylogeny inferred with RAxML (Fig. 1, Extended Data Fig. 2), the species tree inferred with ASTRAL (Extended Data Fig. 3) or the Bayesian species tree inferred with SNAPP (Extended Data Fig. 4). Further details are provided in the Supplementary Methods.

Morphometrics

To quantify body shape and upper oral jaw morphology, we applied a landmark-based geometric morphometric approach to digital X-ray images (for the full set of 10 specimens per species whenever possible; $n = 2{,}197$). We selected 21 landmarks, of which 17 were distributed across the skeleton and four defined the premaxilla (Extended Data Fig. 5a).

Landmark coordinates were digitized using FIJI[55] (v2.0.0-rc-68/1.521i). To extract overall body shape information, we excluded landmark 16, which marks the lateral end of the premaxilla, hence minimizing the impact of the orientation of the upper oral jaw. We then applied a Procrustes superimposition to remove the effect of size, orientation, and translational position of the coordinates.

For upper oral jaw morphology, we used a subset of four landmarks. A crucial feature of the oral jaw morphology is the orientation of the mouth relative to the body axes. However, this component of the upper oral jaw morphology would be lost in a classical geometric morphometric analysis, in which only pure shape information is retained. To overcome this, we extracted the premaxilla-specific landmarks (1, 2, 16 and 21) after Procrustes superimposition of the entire set of landmarks and subsequently recentred the landmarks to align the specimens without rotation. Thus, the resulting landmark coordinates do not represent the pure shape of the premaxilla but additionally contain information on its orientation and size in relation to body axes and body size, respectively.

To quantify lower pharyngeal jaw bone shape in 3D, a landmark-based geometric morphometric approach was applied on µCT scans of the head region of five specimens per species (n = 1,168). To capture all potential functionally important structures of the lower pharyngeal jaw bone, we selected a set of 27 landmarks (10 true landmarks and 17 sliding semi-landmarks) well distributed across the left side of the bone (Extended Data Fig. 5b). Landmark coordinates were acquired using TINA[56] (v.6.0). To retain the lateral symmetric properties of the shape data during superimposition, we reconstructed the right side of the lower pharyngeal jaw bone by mirroring the landmark coordinates across the plane of bilateral symmetry fitted through all landmarks theoretically lying on this plane. We then superimposed the resulting 42 landmarks while sliding the semi-landmarks along the curves by minimizing Procrustes distances and retained the symmetric component only.

To identify the major axes of shape variation across the multivariate datasets we performed a PCA for each trait. We also calculated morphospace size per tribe as the square root of the convex hull area spanned by species means of the PC1 and PC2 scores. We then tested for a correlation between morphospace size and estimated species richness of a tribe[15] (log-transformed to obtain normal distribution). To account for phylogenetic non-independence, we calculated phylogenetic independent contrasts with the R package ape[57] (v.5.2) using the species tree (Fig. 1) pruned to the tribe level. We then calculated Pearson's correlation coefficients for independent contrasts using the function cor.table of the R package picante[58] (v.1.8).

All landmark coordinates for geometric morphometric analyses were processed and analysed in R[59] (v.3.5.2) using the packages geomorph[60] (v.3.0.7) and Morpho[61] (v.2.6). Further details are provided in the Supplementary Methods.

Stable-isotope analysis

To approximate ecology for each species, we measured the stable carbon (C) and nitrogen (N) isotope composition of all available specimens from Lake Tanganyika (n = 2,259). We analysed a small (0.5–1 mg) dried muscle sample of each specimen with a Flash 2000 elemental analyser coupled to a Delta Plus XP continuous-flow isotope ratio mass spectrometer (IRMS) via a Conflo IV interface (Thermo Fisher Scientific). Carbon and nitrogen isotope data were normalized to the VPDB (Vienna Pee Dee Belemnite) and Air-N_2 scales, respectively, using laboratory standards which were calibrated against international standards. Values are reported in standard per-mil notation (‰), and long-term analytical precision was 0.2‰ for $\delta^{13}C$ values and 0.1‰ for $\delta^{15}N$ values. Note that we have used some of these stable-isotope values in a previous study[62].

To confirm interpretability of the $\delta^{13}C$ and $\delta^{15}N$ values, we additionally collected and analysed baseline samples covering several trophic levels from the northern and the southern basin of Lake Tanganyika (Supplementary Methods, Supplementary Discussion).

To test for a correlation of ecospace size with species richness of the tribes, we applied the same approach as described above to the $\delta^{13}C$ and $\delta^{15}N$ values.

Phenotype–environment association

For each trait (body shape, upper oral jaw, lower pharyngeal jaw) we performed a two-block PLS analysis based on species means of the Procrustes aligned landmark coordinates and the stable C and N isotope compositions using the function two.b.pls in geomorph. To account for phylogenetic dependence of the data we applied a pGLS as implemented in the R package caper[63] (v.1.0.1) across the two sets of PLS scores (each morphological axis and the stable-isotope projection) using the time-calibrated species tree based on the maximum-likelihood topology. The strength of phylogenetic signal in the data was accounted for by optimising the branch length transformation parameter lambda using a maximum-likelihood approach.

Scoring pigmentation patterns

To quantify a putative signalling trait in cichlids, we scored the pigmentation patterns in typically five male specimens per species (n = 1,016), on the basis of standardized images taken in the field after capture of the specimens (see Supplementary Methods). Following the strategy described in Seehausen et al.[64], the presence or absence of 20 pigmentation features was recorded, whereby we extended number of scored features to include additional body and fin pigmentation patterns (Extended Data Fig. 5c). We then applied a logistic PCA implemented in the R package logisticPCA[65] (v.0.2) and used the PC1 scores as univariate proxy for differentiation along the signalling axes for further analyses.

Trait evolution modelling and disparity estimates

To investigate the temporal dynamics of morphological diversification over the course of the radiation we essentially followed the strategy of Cooney et al.[28] (which is based on measurements on extant taxa and assumes constant niche space and no or constant extinction over the course of the radiation), using the PLS scores of body shape, upper oral jaw morphology, and lower pharyngeal jaw shape and the PC1 scores of pigmentation patterns as well as the time-calibrated maximum-likelihood species tree topology. For each trait we assessed the phylogenetic signal in the data by calculating Pagel's lambda and Blomberg's K with the R package phytools[66] (v.0.6-60). We then tested the fit of four models of trait evolution for each of the four traits. We applied a white noise model, a Brownian motion model, a single-optimum Ornstein–Uhlenbeck model and an early burst model of trait evolution using the function fitContinuous of the R package geiger[67] (v.2.0.6.1). Additionally, we fitted a variable-rates model (a Brownian motion model which allows for rate shift on branches and nodes) using the software BayesTrait (http://www.evolution.rdg.ac.uk/; v.3) with uniform prior distributions adjusted to our dataset (alpha: −1–1, sigma: 0–0.001 for morphometric traits; alpha: 0–10, sigma: 0–10 for pigmentation pattern) and applying single-chain Markov-chain Monte Carlo runs with one billion iterations. We sampled parameters every 100,000th iteration, after a pre-set burnin of 10,000,000 iterations. We then tested for each trait for convergence of the chain using a Cramer–von Mises statistic implemented in the R package coda[68] (v.0.19-3). The models were compared by calculating their log-likelihood and Akaike information criterion (AIC) difference (Extended Data Fig. 8d). Based on differences in AIC, the variable-rates model was best supported for all traits but body shape, which showed a strong signal of an early burst of trait evolution (Extended Data Fig. 8d, note that the variable-rates model has the highest log-likelihood for body shape as well). We nevertheless focused on the variable-rates model for further analyses of all traits to be able to compare temporal patterns of trait evolution among the traits.

Article

To estimate morphospace expansion through time we used a maximum-likelihood ancestral-state reconstruction implemented in phytools. To account for differences in the rate of trait evolution along the phylogeny, we reconstructed ancestral states using the mean rate-transformed tree derived from the variable-rates model. We then projected the ancestral states onto the original species tree and calculated the morphospace extent (that is, the range of trait values) in time intervals of 0.15 million years (note that this is an arbitrary value; however, differently sized time intervals had no effect on the interpretation of the results). For each time point we extracted the branches existing at that time and predicted the trait value linearly between nodes. We then compared the resulting morphospace expansion over time relative to a null model of trait evolution. We therefore simulated 500 datasets (PLS and PC1 scores) under Brownian motion given the original species tree with parameters derived from the Brownian motion model fit to the original data. For each simulated dataset we produced morphospace-expansion curves using the same approach as described above. We then compared the slopes of our observed data with each of the null models by calculating the difference of slopes through time (Fig. 3) using linear models fitted for each time interval with the two subsequent time intervals. Note that for body shape we also estimated morphospace expansion through time using the early burst model for ancestral-state reconstruction, which resulted in a very similar pattern of trait diversification.

Unlike other metrics of disparity (for example, variance or mean pairwise distances) morphospace extent is not sensitive to the density distribution of measurements within the morphospace and captures its full range[69]. Hence, comparing the extent of morphospace between observed data and the null model directly unveils the contribution of morphospace expansion relative to the null model; and because the increase in lineages over time is identical in the observed and the simulated data, this comparison also provides an estimate for morphospace packing.

To summarize evolutionary rates we calculated the mean rate of trait evolution inferred by the variable-rates model in the same 0.15 million years intervals along the phylogeny.

To account for phylogenetic uncertainty in the tree topology we repeated the analyses of trait evolution using the time-calibrated trees based on tree topologies estimated with ASTRAL and SNAPP (Extended Data Figs. 3, 4; Supplementary Methods; Supplementary Discussion). Furthermore, to also account for uncertainty in branch lengths, we repeated the analysis on 100 trees from the Bayesian posterior distribution for each of the three trees (Extended Data Fig. 8d, e, results are provided on Dryad).

Further details can be found in the Supplementary Methods.

Characterization of repeat content

For the repeat content analysis, we randomly selected one de novo genome assembly per species of the radiation (n = 245). We performed a de novo identification of repeat families using RepeatModeler (v.1.0.11; http://www.repeatmasker.org). We then combined the RepeatModeler output library with the available cichlid-specific libraries (Dfam and RepBase; v.27.01.2017; http://www.repeatmasker.org; 258 ancestral and ubiquitous sequences, 161 cichlid-specific repeats, and 6 lineage-specific sequences; 65,118, 273,530 and 6,667 bp in total, respectively) and used the software RepeatMasker (v.4.0.7; http://www.repeatmasker.org) (-xsmall -s -e ncbi -lib combined_libraries.fa) to identify and soft-mask interspersed repeats and low complexity DNA sequences in each assembly. The reported summary statistics were obtained using RepeatMasker's buildSummary.pl script (Fig. 4a, Extended Data Fig. 9a, results per genome are provided on Dryad).

Gene duplication estimates

Per genome, gene duplication events were identified with the structural variant identification pipeline smoove (population calling method; https://github.com/brentp/smoove, docker image cloned 20/12/2018), which builds upon lumpy[70], svtyper[71] and svtools (https://github.com/hall-lab/svtools). Variants were called per sample (n = 488 genomes, 246 taxa of the Tanganyika radiation) from the initial mapping files against the Nile tilapia reference genome with the function 'call'. The union of sites across all samples was obtained with the function 'merge', then all samples were genotyped at those sites with the function 'genotype', and depth information was added with --duphold. Genotypes were combined with the function 'paste' and annotated with 'annotate' and the reference genome annotation file. The obtained VCF file was filtered with BCFtools to keep only duplications longer than 1 kb and of high quality (MSHQ >3 or MSHQ = −1, FMT/DHFFC[0] > 1.3, QUAL >100). The resulting file was loaded into R (v.3.6.0) with vcfR[72] (v.1.8.0) and filtered to keep only duplications with less than 20% missing genotypes. Next, we removed duplication events with a length outside 1.5 times the interquartile range above the upper quartile of all duplication length, resulting in a final dataset of 476 duplications (Fig. 4b).

Analyses of selection on coding sequence

To predict genes within the de novo genome assemblies, we used AUGUSTUS[73] (v.3.2.3) with default parameters and 'zebrafish' as species parameter (n = 485 genomes, 245 taxa). For each prediction we inferred orthology to Nile tilapia genes (GCF_001858045.1_ASM185804v2) with GMAP (GMAP-GSNAP[74]; v.2017-08-15) applying a minimum trimmed coverage of 0.5 and a minimum identity of 0.8. We excluded specimens with less than 18,000 tilapia orthologous genes detected (resulting in n = 471 genomes, 243 taxa). Next, we kept only those tilapia protein coding sequences that had at least one of their exons present in at least 80% of the assemblies (260,335 exons were retained, representing 34,793 protein coding sequences). Based on the Nile tilapia reference genome annotation file, we reconstructed for each assembly the orthologous coding sequences. Missing exon sequences were set to Ns. We then kept a single protein coding sequence per gene (the one being present in the maximum number of species with the highest percentage of sequence length), resulting in 15,294 protein coding sequences. Per gene, a multiple sequence alignment was then produced using MACSE[75] (v.2.01). We calculated for each specimen and each gene the number of synonymous (S) and non-synonymous (N) substitutions by pairwise comparison to the orthologue tilapia sequence using codeml with runmode −2 within PAML[76] (v.4.9e). To obtain an estimate of the genome-wide sequence evolution rate that is independent of filtering thresholds, we calculated the genome-wide dN/dS ratio for each specimen based on the sum of dS and dN across all genes (Fig. 4c, Extended Data Fig. 9b).

Signals of past introgression

We used the f_4-ratio statistic[34] to assess genomic evidence for interspecific gene exchange. We calculated the f_4-ratio for all combinations of trios of species on the filtered VCF files using the software Dsuite[77] (v.0.2 r20), with *T. sparrmanii* as outgroup species (we excluded *N. cancellatus* as all specimens of this species appeared to be F_1 hybrids; Supplementary Methods). The f_4-ratio statistic estimates the admixture proportion, that is, the proportion of the genome affected by gene flow. The results presented in this study (Fig. 4e, Extended Data Fig. 10) are based on the 'tree' output of the Dsuite function Dtrios, with each trio arranged according to the species tree on the basis of the maximum-likelihood topology. The per-tribe analyses (Fig. 4e) were based only on comparisons where all species within a trio belong to the same tribe (n = 243 taxa).

In addition to the f_4-ratio we also identified signals of past introgression among species using a phylogenetic approach by testing for asymmetry in the relationships of species trios in 1,272 local maximum-likelihood trees generated using IQ-TREE (Supplementary Methods; Extended Data Fig. 10).

Heterozygosity

We calculated the number of heterozygous sites per genome ($n = 488$ genomes, 246 taxa from the Tanganyika radiation) from the VCF files using the BCFtools function stats and then quantified the percentage of heterozygous sites among the number of callable sites per genome (see above) (Fig. 4d).

To explore if the observed levels of heterozygosity per tribe can be explained by the levels of gene flow within tribes we performed coalescent simulations with msprime[78] (v.0.7.4). We simulated genome evolution of all species of the radiation following the time-calibrated species tree (Fig. 1), assuming a generation time of 3 years[79] and a constant effective population size of 20,000 individuals. Species divergences were implemented as mass migration events and introgression within tribes as migration between species pairs with rates set according to their introgression (f_4-ratio) signals inferred with Dsuite. To convert the f_4-ratio values into migration rates, we applied a scaling factor of 5×10^{-6}, which results in a close correspondence in magnitude of the simulated introgression signals to those observed empirically (Fig. 4, Extended Data Fig. 9c). In each of 20 separate simulations, we randomly sampled one pairwise f_4-ratio value for each pair of species (there are many f_4 ratios per species pair—one for each possible third species added to the test trio; the maximum values per pair are shown in Extended Data Fig. 10). The simulated data consisted of one chromosome of 100 kb (mutation rate: 3.5×10^{-9} per bp per generation[33], recombination rate: 2.2×10^{-8} per bp per generation; see Supplementary Methods). Levels of heterozygosity were calculated for all simulated datasets as described for the empirical data.

To account for between-tribe gene flow we further performed simulations in which migration between tribes was also sampled from the empirical f_4-ratio distribution. For simplicity in setting up the simulation model, we assume that gene flow between tribes is ongoing until present day, which is clearly an overestimate (see Supplementary Discussion). Nevertheless, the results of these simulations support our hypothesized scenario, confirming that much of the variation in heterozygosity as well as its correlation with species richness can be explained by the observed levels of gene flow.

Correlation of genome-wide statistics with species richness

We tested for a correlation between tribe means (based on species means) of each genomic summary statistics (transposable element counts, number of gene duplications, genome-wide d*N*/d*S* ratio, per-genome heterozygosity, and f_4-ratio, as well as the heterozygosity and f_4-ratio statistics derived from simulated genome evolution) and species richness of the tribes, applying the same approach as described above for tests of correlation between morpho- and ecospace size and species richness.

Reporting summary

Further information on research design is available in the Nature Research Reporting Summary linked to this paper.

Data availability

All newly sequenced genomes for this study and their raw reads are available from NCBI under the BioProject accession number PRJNA550295 (https://www.ncbi.nlm.nih.gov/bioproject/). The VCF file, tree files, summary statistics of the assembled genomes and phenotypic datasets generated and analysed during this study are available as downloadable files on Dryad (https://doi.org/10.5061/dryad.9w0vt4bbf). The Nile tilapia reference genome used is available under RefSeq accession GCF_001858045.1. All X-ray data are available on MorphoSource under the project number P1093. Source data are provided with this paper.

Code availability

Code used to analyse the data is available on GitHub (https://github.com/cichlidx/ronco_et_al), except for analyses where single commands from publicly available software were used and where all settings are fully reported in the Methods and/or Supplementary Methods.

35. Bolger, A. M., Lohse, M. & Usadel, B. Trimmomatic: a flexible trimmer for Illumina sequence data. *Bioinformatics* **30**, 2114–2120 (2014).
36. Conte, M. A., Gammerdinger, W. J., Bartie, K. L., Penman, D. J. & Kocher, T. D. A high quality assembly of the Nile Tilapia (*Oreochromis niloticus*) genome reveals the structure of two sex determination regions. *BMC Genomics* **18**, 341 (2017).
37. Li, H. & Durbin, R. Fast and accurate short read alignment with Burrows–Wheeler transform. *Bioinformatics* **25**, 1754–1760 (2009).
38. McKenna, A. et al. The Genome Analysis Toolkit: a MapReduce framework for analyzing next-generation DNA sequencing data. *Genome Res.* **20**, 1297–1303 (2010).
39. Li, H. A statistical framework for SNP calling, mutation discovery, association mapping and population genetical parameter estimation from sequencing data. *Bioinformatics* **27**, 2987–2993 (2011).
40. Danecek, P. et al. The variant call format and VCFtools. *Bioinformatics* **27**, 2156–2158 (2011).
41. Browning, S. R. & Browning, B. L. Rapid and accurate haplotype phasing and missing-data inference for whole-genome association studies by use of localized haplotype clustering. *Am. J. Hum. Genet.* **81**, 1084–1097 (2007).
42. Böhne, A. et al. Repeated evolution versus common ancestry: Sex chromosome evolution in the haplochromine *Pseudocrenilabrus philander*. *Genome Biol. Evol.* **11**, 439–458 (2019).
43. Malmstrøm, M., Matschiner, M., Tørresen, O. K., Jakobsen, K. S. & Jentoft, S. Data descriptor: Whole genome sequencing data and de novo draft assemblies for 66 teleost species. *Sci. Data* **4**, 1–13 (2017).
44. Myers, E. W. et al. A whole-genome assembly of *Drosophila*. *Science* **287**, 2196–2204 (2000).
45. Magoč, T. & Salzberg, S. L. FLASH: fast length adjustment of short reads to improve genome assemblies. *Bioinformatics* **27**, 2957–2963 (2011).
46. Gurevich, A., Saveliev, V., Vyahhi, N. & Tesler, G. QUAST: quality assessment tool for genome assemblies. *Bioinformatics* **29**, 1072–1075 (2013).
47. Simão, F. A., Waterhouse, R. M., Ioannidis, P., Kriventseva, E. V. & Zdobnov, E. M. BUSCO: assessing genome assembly and annotation completeness with single-copy orthologs. *Bioinformatics* **31**, 3210–3212 (2015).
48. Ewels, P., Magnusson, M., Lundin, S., Käller, M. & Multi, Q. C. MultiQC: summarize analysis results for multiple tools and samples in a single report. *Bioinformatics* **32**, 3047–3048 (2016).
49. Zhang, C., Rabiee, M., Sayyari, E. & Mirarab, S. ASTRAL-III: polynomial time species tree reconstruction from partially resolved gene trees. *BMC Bioinformatics* **19** (Suppl 6), 153 (2018).
50. Bouckaert, R. et al. BEAST 2.5: An advanced software platform for Bayesian evolutionary analysis. *PLOS Comput. Biol.* **15**, e1006650 (2019).
51. Ogilvie, H. A., Bouckaert, R. R. & Drummond, A. J. StarBEAST2 brings faster species tree inference and accurate estimates of substitution rates. *Mol. Biol. Evol.* **34**, 2101–2114 (2017).
52. Stamatakis, A. RAxML version 8: a tool for phylogenetic analysis and post-analysis of large phylogenies. *Bioinformatics* **30**, 1312–1313 (2014).
53. Nguyen, L.-T., Schmidt, H. A., von Haeseler, A. & Minh, B. Q. IQ-TREE: a fast and effective stochastic algorithm for estimating maximum-likelihood phylogenies. *Mol. Biol. Evol.* **32**, 268–274 (2015).
54. Bryant, D., Bouckaert, R., Felsenstein, J., Rosenberg, N. A. & RoyChoudhury, A. Inferring species trees directly from biallelic genetic markers: bypassing gene trees in a full coalescent analysis. *Mol. Biol. Evol.* **29**, 1917–1932 (2012).
55. Schindelin, J. et al. Fiji: an open-source platform for biological-image analysis. *Nat. Methods* **9**, 676–682 (2012).
56. Schunke, A. C., Bromiley, P. A., Tautz, D. & Thacker, N. A. TINA manual landmarking tool: software for the precise digitization of 3D landmarks. *Front. Zool.* **9**, 6 (2012).
57. Paradis, E., Claude, J. & Strimmer, K. APE: Analyses of phylogenetics and evolution in R language. *Bioinformatics* **20**, 289–290 (2004).
58. Kembel, S. W. et al. Picante: R tools for integrating phylogenies and ecology. *Bioinformatics* **26**, 1463–1464 (2010).
59. R Development Core Team. R: A language and environment for statistical computing. *R Foundation for Statistical Computing* (2018).
60. Adams, D. C. & Otárola-Castillo, E. Geomorph: An R package for the collection and analysis of geometric morphometric shape data. *Methods Ecol. Evol.* **4**, 393–399 (2013).
61. Schlager, S. in *Statistical Shape and Deformation Analysis* (eds Zheng, G., Li, S. & Szekely, G.) 217–256 (Academic Press, 2017).
62. Ronco, F., Roesti, M. & Salzburger, W. A functional trade-off between trophic adaptation and parental care predicts sexual dimorphism in cichlid fish. *Proc. R. Soc. Lond. B* **286**, 20191050 (2019).
63. Orme, D. *The Caper Package: Comparative Analysis of Phylogenetics and Evolution in R* https://cran.r-project.org/web/packages/caper/vignettes/caper.pdf (2018).
64. Seehausen, O., Mayhew, P. J. & Van Alphen, J. J. M. Evolution of colour patterns in East African cichlid fish. *J. Evol. Biol.* **12**, 514–534 (1999).
65. Landgraf, A. J. & Lee, Y. Dimensionality reduction for binary data through the projection of natural parameters. *J. Multivar. Anal.* 104668 (2020).
66. Revell, L. J. phytools: An R package for phylogenetic comparative biology (and other things). *Methods Ecol. Evol.* **3**, 217–223 (2012).

Article

67. Harmon, L. J., Weir, J. T., Brock, C. D., Glor, R. E. & Challenger, W. GEIGER: investigating evolutionary radiations. *Bioinformatics* **24**, 129–131 (2008).
68. Plummer, M., Best, N., Cowles, K. & Vines, K. CODA: convergence diagnosis and output analysis for MCMC. *R News* **6**, 7–11 (2005).
69. Ciampaglio, C. N., Kemp, M. & McShea, D. W. Detecting changes in morphospace occupation patterns in the fossil record: characterization and analysis of measures of disparity. *Paleobiology* **27**, 695–715 (2001).
70. Layer, R. M., Chiang, C., Quinlan, A. R. & Hall, I. M. LUMPY: a probabilistic framework for structural variant discovery. *Genome Biol*. **15**, R84 (2014).
71. Chiang, C. et al. SpeedSeq: ultra-fast personal genome analysis and interpretation. *Nat. Methods* **12**, 966–968 (2015).
72. Knaus, B. J. & Grünwald, N. J. vcfr: a package to manipulate and visualize variant call format data in R. *Mol. Ecol. Resour*. **17**, 44–53 (2017).
73. Stanke, M., Schöffmann, O., Morgenstern, B. & Waack, S. Gene prediction in eukaryotes with a generalized hidden Markov model that uses hints from external sources. *BMC Bioinformatics* **7**, 62 (2006).
74. Wu, T. D. & Watanabe, C. K. GMAP: a genomic mapping and alignment program for mRNA and EST sequences. *Bioinformatics* **21**, 1859–1875 (2005).
75. Ranwez, V., Douzery, E. J. P., Cambon, C., Chantret, N. & Delsuc, F. MACSE v2: Toolkit for the alignment of coding sequences accounting for frameshifts and stop codons. *Mol. Biol. Evol*. **35**, 2582–2584 (2018).
76. Yang, Z. PAML 4: phylogenetic analysis by maximum likelihood. *Mol. Biol. Evol*. **24**, 1586–1591 (2007).
77. Malinsky, M., Matschiner, M. & Svardal, H. Dsuite–fast *D*-statistics and related admixture evidence from VCF files. *Methods Ecol. Evol*. https://doi.org/10.1111/1755-0998.13265 (2020).
78. Kelleher, J., Etheridge, A. M. & McVean, G. Efficient coalescent simulation and genealogical analysis for large sample sizes. *PLOS Comput. Biol*. **12**, e1004842 (2016).
79. Malinsky, M. et al. Genomic islands of speciation separate cichlid ecomorphs in an East African crater lake. *Science* **350**, 1493–1498 (2015).

Acknowledgements We thank the University of Burundi, the Ministère de l'Eau, de l'Environnement, de l'Amenagement du Territoire et de l'Urbanisme, Republic of Burundi, the Centre de Recherche en Hydrobiologie (CRH), Uvira, DR Congo, the Tanzania Commission for Science and Technology (COSTECH), the Tanzania Fisheries Research Institute (TAFIRI), the Tanzania National Parks Authority (TANAPA), the Tanzania Wildlife Research Institute (TAWIRI), the Lake Tanganyika Research Unit, Department of Fisheries, Republic of Zambia, and the Zambian Department for Immigration for research permits; G. Banyankimbona, H. Mwima, G. Hakizimana, N. Muderhwa, P. Masilya, I. Kimirei, M. Mukuli Wa-Teba, G. Moshi, A. Mwakatobe, C. Katongo, T. Banda and L. Makasa for assistance with obtaining research permits; the boat crews of the *Chomba* (D. Mwanakulya, J. Sichilima, H. D. Sichilima Jr and G. Katai) and the *Maji Makubwa II* (G. Kazumbe and family) for navigation, guidance and company; the boat drivers M. Katumba and T. Musisha; the car drivers A. Irakoze and J. Leonard; M. Schreyen-Brichard, M. Mukuli Wa-Teba, G. Kazumbe, I. Kimirei, D. Schlatter, R. Schlatter, M. K. Dominico, H. Sichilima Sr, C. Zytkow, P. Lassen and V. Huwiler for logistic support; G. Banyankimbona, N. Boileau, B. Egger, Y. Fermon, G. Kazumbe, G. Katai, R. Lusoma, K. Smailus, L. Widmer and numerous fishermen at Lake Tanganyika for help during sampling; V. Huwiler, Charity, O. Mangwangwa and the Zytkow family for lodging; people of innumerable villages on the shores of Lake Tanganyika for providing workspace, shelter for night-camps and access to village infrastructure; M. Barluenga, H. Gante, Z. Musilová, F. Schedel, J. Snoeks, M. Stiassny, H. Tanaka, G. Turner and M. Van Steenberge for providing additional samples and/or specimens; M. Sánchez, A. Schweizer and A. Wegmann for assistance with the µCT scanning of large specimens; C. Moes for help with radiographs; V. Evrard for help with stable isotopes; I. Nissen and E. Burcklen for assistance with DNA shearing; M. Conte and T. D. Kocher for sharing the RepeatMasker annotations for Nile tilapia; C. Klingenberg and M. Sánchez for discussions on the morphometric approach; A. Tooming-Klunderud and team at the Norwegian Sequencing Centre and C. Beisel and team at the Genomics Facility Basel at the ETH Zurich Department of Biosystems Science and Engineering (D-BSSE), Basel, for assistance with next-generation sequencing; M. Jacquot, E. Pujades and T. Sengstag for the setup and assistance with the collection database system (LabKey); and J. Johnson and A. Viertler for fish illustrations in Fig. 1 and Extended Data Fig. 5, respectively. Calculations were performed at sciCORE (http://scicore.unibas.ch/) scientific computing centre at University of Basel (with support by the SIB/Swiss Institute of Bioinformatics) and the Abel computer cluster, University of Oslo. This work was funded by the European Research Council (ERC, Consolidator Grant Nr. 617585 'CICHLID-X' jointly hosted by the University of Basel and the University of Oslo) and the Swiss National Science Foundation (SNSF, grants 156405 and 176039) to W.S. A. Böhne was supported by the SNSF (Ambizione grant 161462).

Author contributions F.R., A.I. and W.S. designed this study (with input from H.H.B., A.K. and S.J.). F.R., A.I., H.H.B. and W.S. collected the specimens in the field. F.R. and A. Böhne extracted DNA and prepared the libraries for sequencing. S.J. coordinated sequencing. M. Matschiner performed the mapping, variant calling, phylogenetic analyses and coalescent simulations. M. Malinsky contributed to the variant calling pipelines and performed the f_4-ratio statistics. A. Böhne assembled the genomes and quantified gene duplications, A.E.T. conducted the d*N*/d*S* analyses and V.R. analysed transposable elements. A. Boila assessed stable-isotope compositions, H.H.B. radiographed the specimens and W.S. scored pigmentation patterns. F.R. curated the samples and performed µCT scanning, geometric morphometric analyses, and all analyses incorporating morphological and ecological data as well as correlations with species richness. F.R. and W.S. wrote the manuscript with contributions and/or feedback from all authors. All authors read and approved the final version of the manuscript.

Competing interests The authors declare no competing interests.

Additional information
Supplementary information is available for this paper at https://doi.org/10.1038/s41586-020-2930-4.
Correspondence and requests for materials should be addressed to F.R. or W.S.
Peer review information *Nature* thanks the anonymous reviewer(s) for their contribution to the peer review of this work.
Reprints and permissions information is available at http://www.nature.com/reprints.

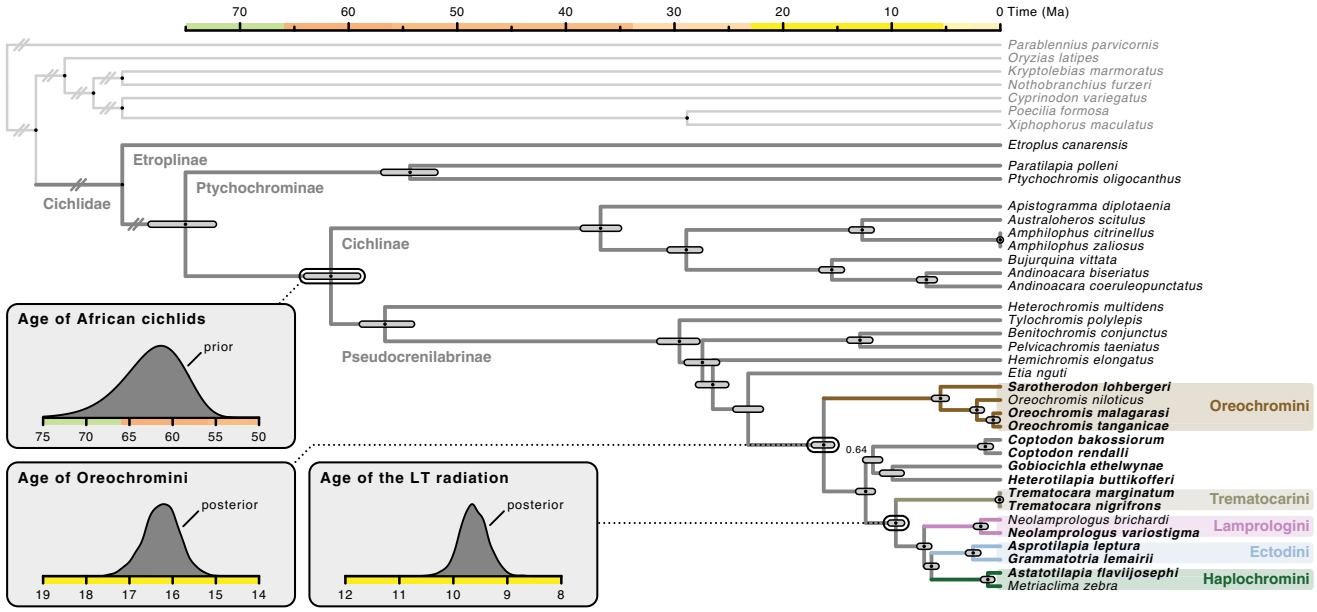

Extended Data Fig. 1 | Age of the adaptive radiation of cichlid fishes in African Lake Tanganyika. Time-calibrated species tree of species representing divergent tribes and subfamilies within cichlids as well as closely-related non-cichlid outgroups, generated with the multi-species coalescent model in StarBEAST2. Nodes marked with a black dot were constrained according to species-tree analyses with ASTRAL. Node bars indicate 95% highest-posterior density age intervals. Outgroup divergence times are not drawn to scale. Insets visualize the prior distribution applied for the age of African cichlids according to Matschiner et al.[18], as well as posterior age estimates for Oreochromini and the cichlid adaptive radiation in Lake Tanganyika (LT).

Article

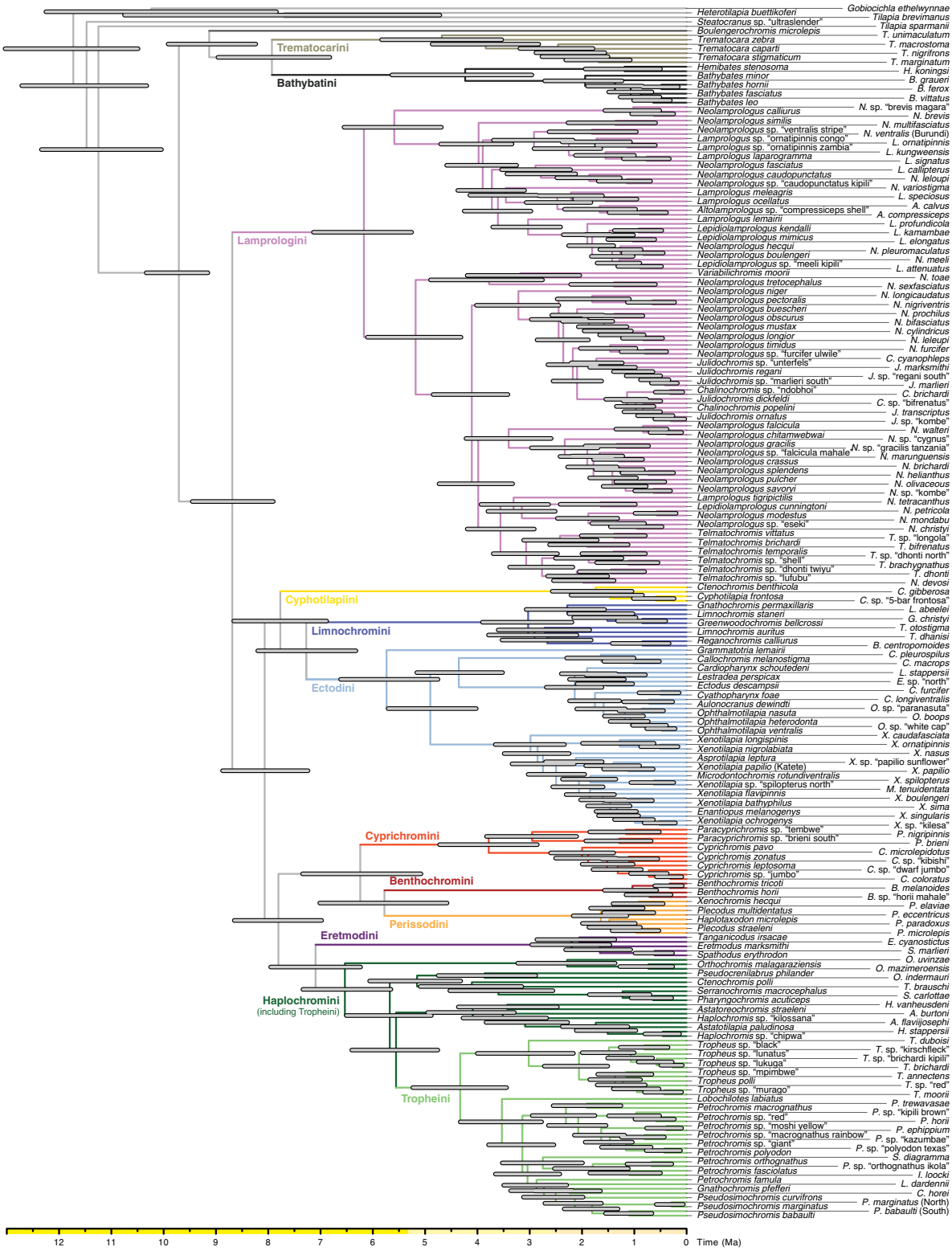

Extended Data Fig. 2 | Time-calibrated species tree of the cichlid adaptive radiation in Lake Tanganyika. The species tree is based on the maximum-likelihood topology estimated with RAxML (Fig. 1) and was time-calibrated using a relaxed-clock model in BEAST2, applied to a selected set of alignments.

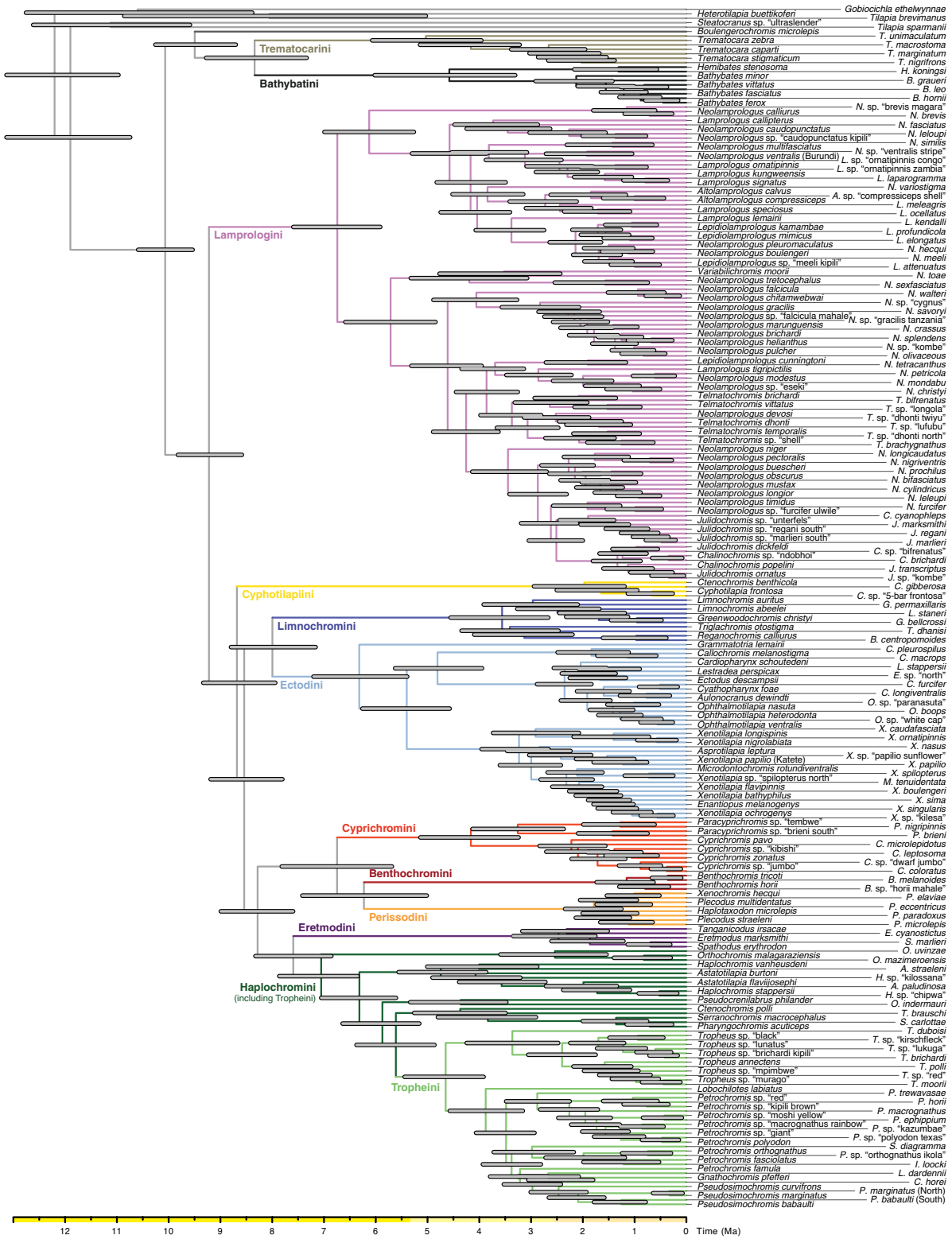

Extended Data Fig. 3 | Alternative time-calibrated species tree of the cichlid adaptive radiation in Lake Tanganyika. The species tree is based on the topology estimated with ASTRAL and was time-calibrated using a relaxed-clock model in BEAST2, applied to a selected set of alignments.

Article

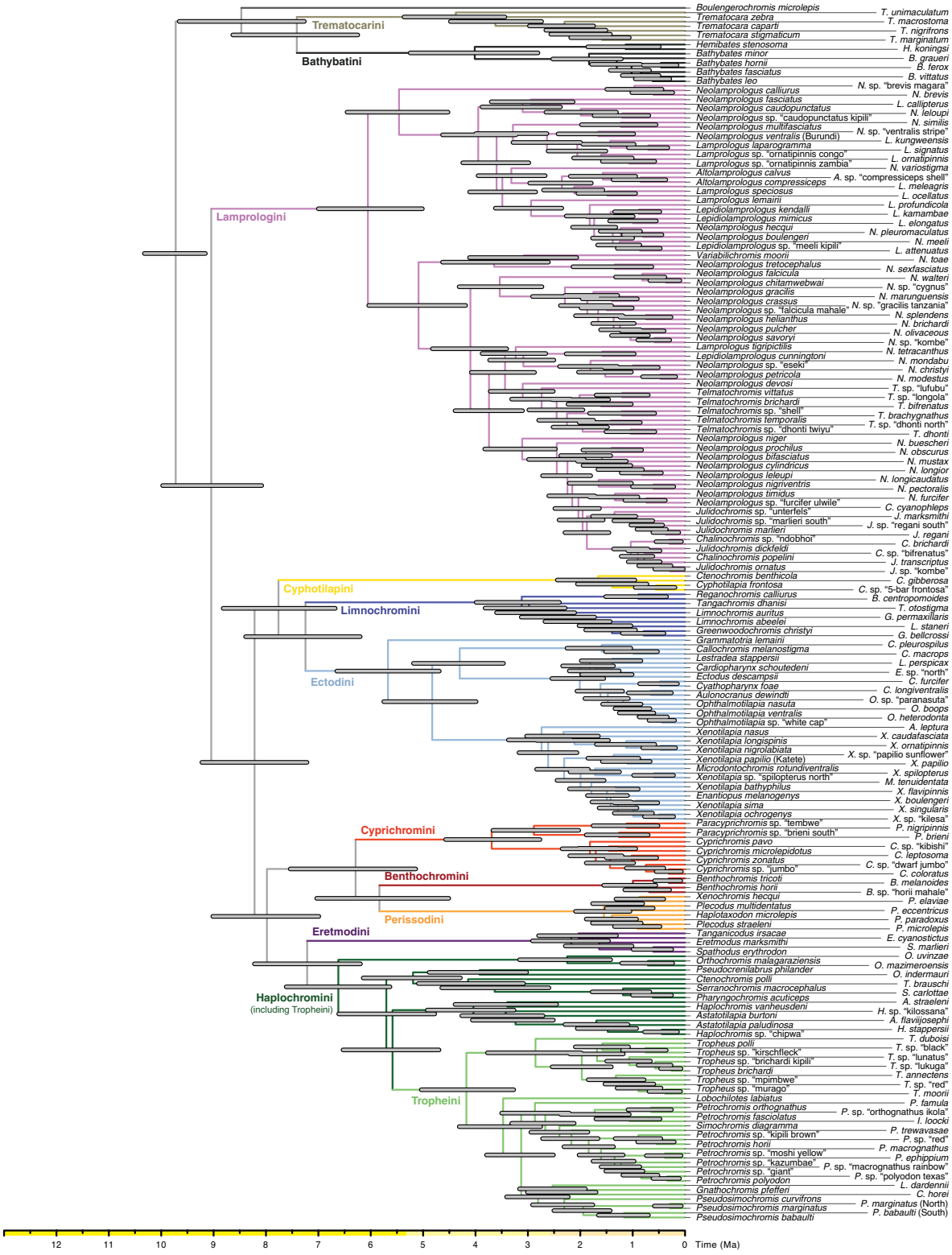

Extended Data Fig. 4 | Alternative time-calibrated species tree of the cichlid adaptive radiation in Lake Tanganyika. The species tree is based on the topology estimated with SNAPP and was time-calibrated using a relaxed-clock model in BEAST2, applied to a selected set of alignments.

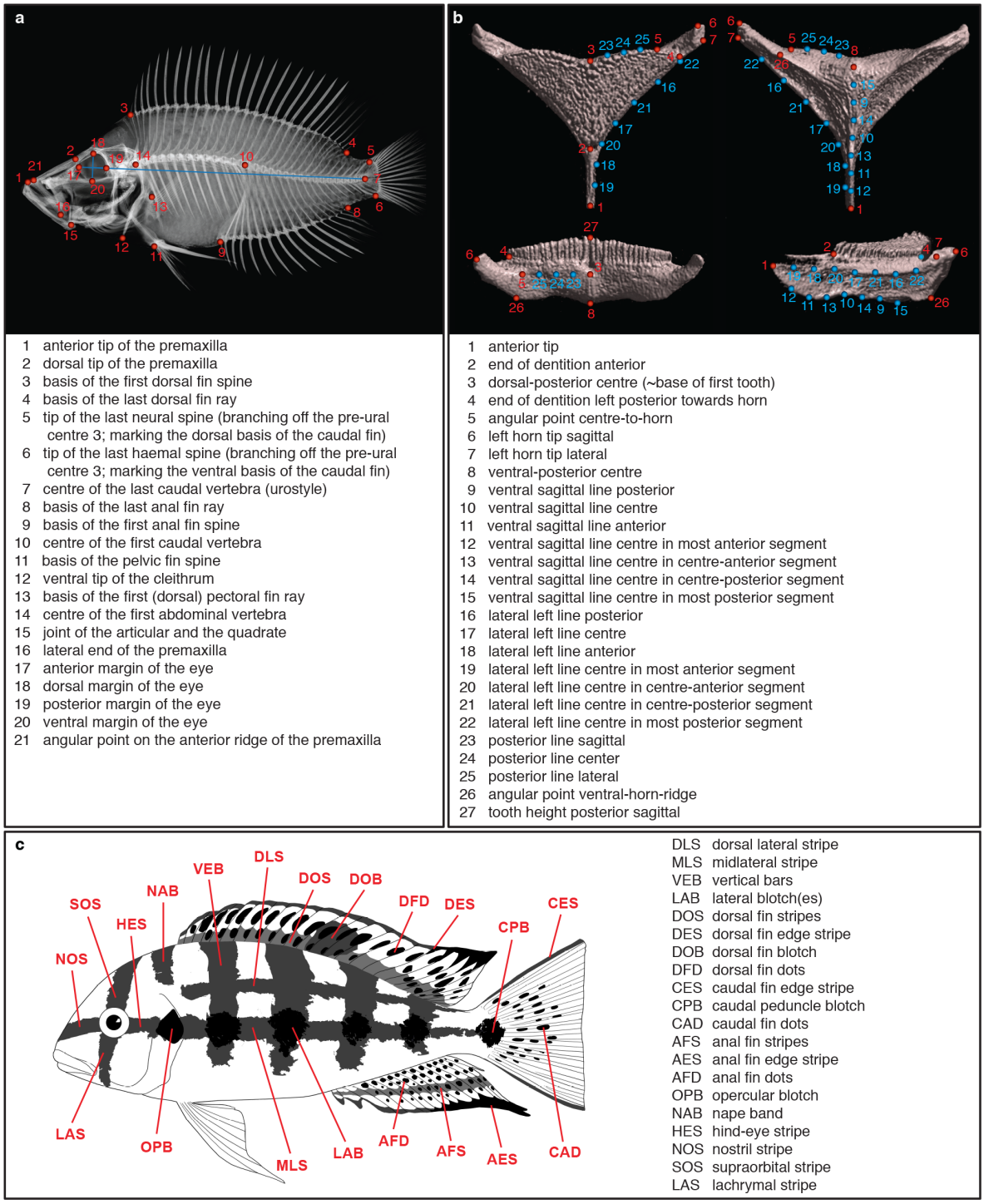

1	anterior tip of the premaxilla
2	dorsal tip of the premaxilla
3	basis of the first dorsal fin spine
4	basis of the last dorsal fin ray
5	tip of the last neural spine (branching off the pre-ural centre 3; marking the dorsal basis of the caudal fin)
6	tip of the last haemal spine (branching off the pre-ural centre 3; marking the ventral basis of the caudal fin)
7	centre of the last caudal vertebra (urostyle)
8	basis of the last anal fin ray
9	basis of the first anal fin spine
10	centre of the first caudal vertebra
11	basis of the pelvic fin spine
12	ventral tip of the cleithrum
13	basis of the first (dorsal) pectoral fin ray
14	centre of the first abdominal vertebra
15	joint of the articular and the quadrate
16	lateral end of the premaxilla
17	anterior margin of the eye
18	dorsal margin of the eye
19	posterior margin of the eye
20	ventral margin of the eye
21	angular point on the anterior ridge of the premaxilla

1	anterior tip
2	end of dentition anterior
3	dorsal-posterior centre (~base of first tooth)
4	end of dentition left posterior towards horn
5	angular point centre-to-horn
6	left horn tip sagittal
7	left horn tip lateral
8	ventral-posterior centre
9	ventral sagittal line posterior
10	ventral sagittal line centre
11	ventral sagittal line anterior
12	ventral sagittal line centre in most anterior segment
13	ventral sagittal line centre in centre-anterior segment
14	ventral sagittal line centre in centre-posterior segment
15	ventral sagittal line centre in most posterior segment
16	lateral left line posterior
17	lateral left line centre
18	lateral left line anterior
19	lateral left line centre in most anterior segment
20	lateral left line centre in centre-anterior segment
21	lateral left line centre in centre-posterior segment
22	lateral left line centre in most posterior segment
23	posterior line sagittal
24	posterior line center
25	posterior line lateral
26	angular point ventral-horn-ridge
27	tooth height posterior sagittal

DLS	dorsal lateral stripe
MLS	midlateral stripe
VEB	vertical bars
LAB	lateral blotch(es)
DOS	dorsal fin stripes
DES	dorsal fin edge stripe
DOB	dorsal fin blotch
DFD	dorsal fin dots
CES	caudal fin edge stripe
CPB	caudal peduncle blotch
CAD	caudal fin dots
AFS	anal fin stripes
AES	anal fin edge stripe
AFD	anal fin dots
OPB	opercular blotch
NAB	nape band
HES	hind-eye stripe
NOS	nostril stripe
SOS	supraorbital stripe
LAS	lachrymal stripe

Extended Data Fig. 5 | Phenotyping of the specimens. a, Two-dimensional landmarks placed on X-ray images of the specimens. To quantify overall body shape we excluded landmark 16 (to minimise the effect of the orientation of the oral jaw). To analyse upper oral jaw morphology we used landmarks 1, 2, 16 and 21. **b**, Three-dimensional landmarks used to analyse lower pharyngeal jaw shape on µCT scans of the heads. True landmarks are indicated in red, sliding semi-landmarks are indicated in blue. **c**, Body regions scored for presence/absence of pigmentation patterns.

Article

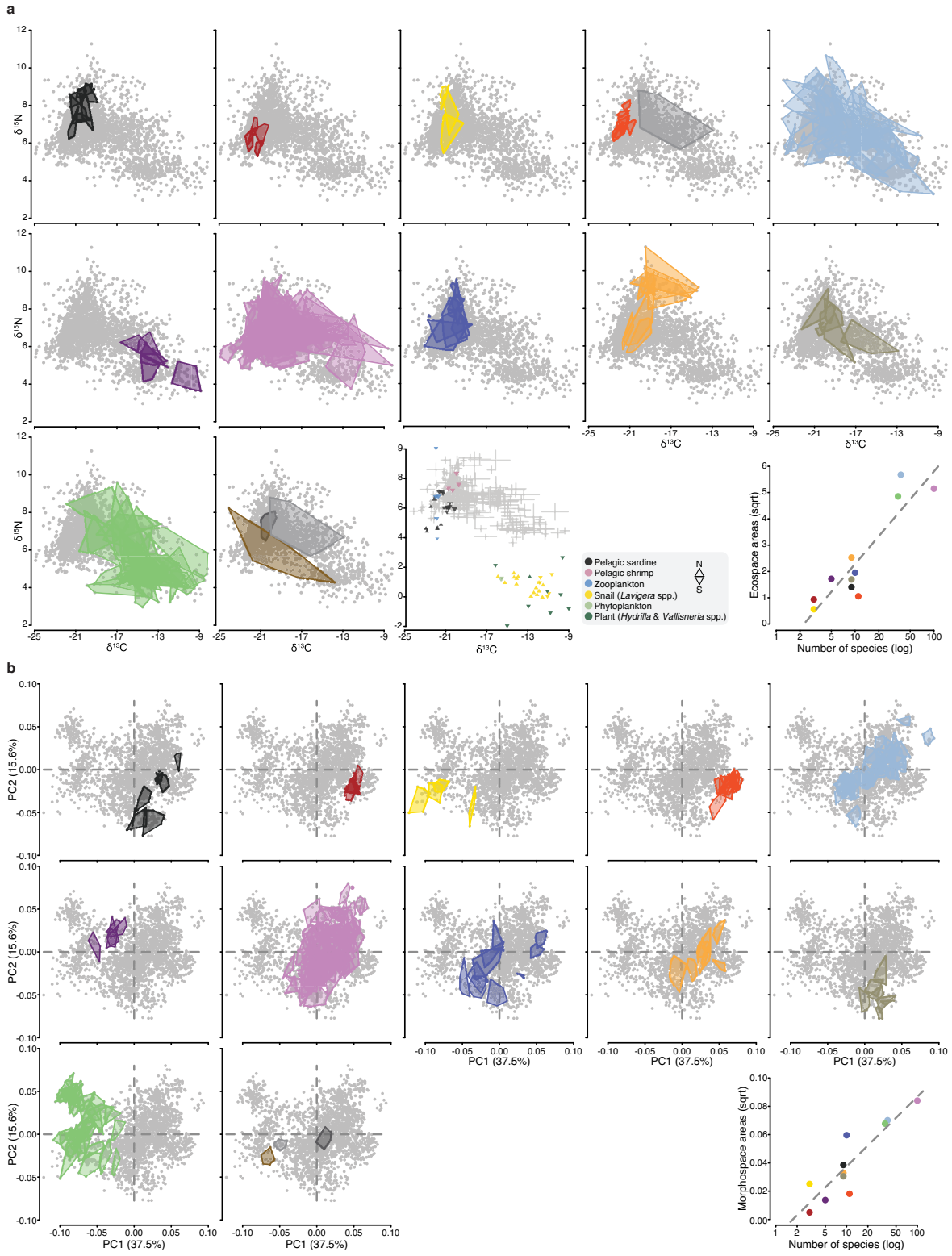

Extended Data Fig. 6 | Ecospace and morphospace occupation of the cichlid adaptive radiation in Lake Tanganyika. Scatter plots for each focal tribe (indicated with colours, see Fig. 1 for colour key) against the total eco-and morphospace (grey). Species ranges are indicated with convex hulls. **a**, Stable N and C isotope compositions ($\delta^{15}N$ and $\delta^{13}C$ values). The additional plot shows $\delta^{15}N$ and $\delta^{13}C$ values of a baseline dataset which confirms the interpretability of the stable N and C isotope composition in Lake Tanganyika (see Supplementary Methods and Discussion). **b**, PC1 and PC2 of body shape (for shape changes associated with the PC axes see Fig. 2). The last plot for each trait shows the size of the traitspace per tribe in relation to species numbers (stable isotopes: Pearson's $r = 0.88$, d.f. = 9, $P = 0.0004$; body shape: Pearson's $r = 0.91$, d.f. = 9, $P = 0.0001$). Traitspace size was calculated as the square root of the convex hull area spanned by species means.

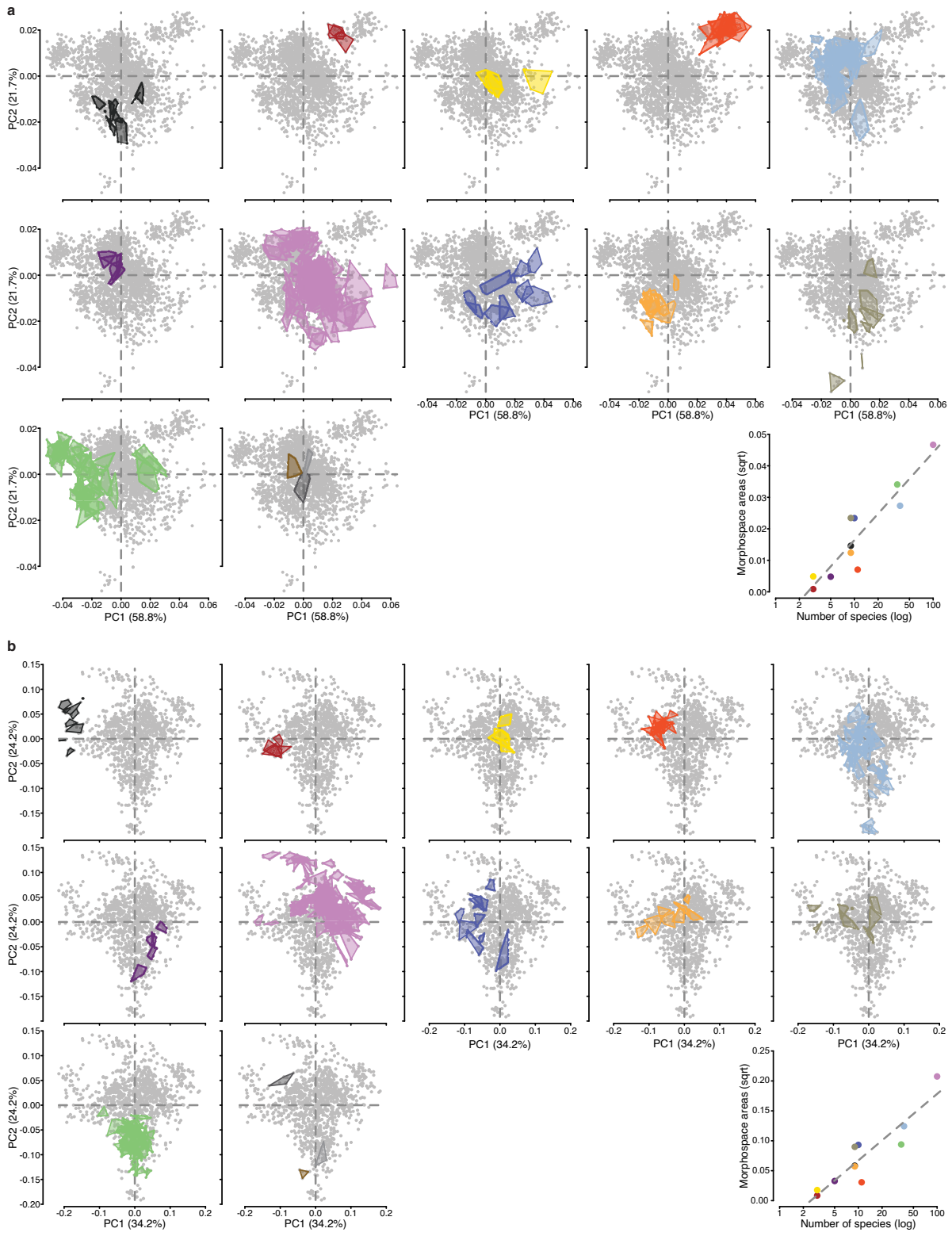

Extended Data Fig. 7 | Morphospace occupation of the cichlid adaptive radiation in Lake Tanganyika. a, **b**, Scatter plots of PC1 and PC2 for upper oral jaw morphology (**a**) and lower pharyngeal jaw shape per tribe (**b**) (indicated with colours, see Fig. 1 for colour key) against the total morphospace (grey). Species ranges are indicated with convex hulls. For shape changes associated with the respective PC-axis see Fig. 2. The last plot for each trait shows the size of the morphospace per tribe in relation to species numbers (upper oral jaw morphology: Pearson's $r = 0.88$, d.f. = 9, $P = 0.0003$; lower pharyngeal jaw shape: Pearson's $r = 0.83$, d.f. = 9, $P = 0.0017$). Morphospace size was calculated as the square root of the convex hull area spanned by species means.

Article

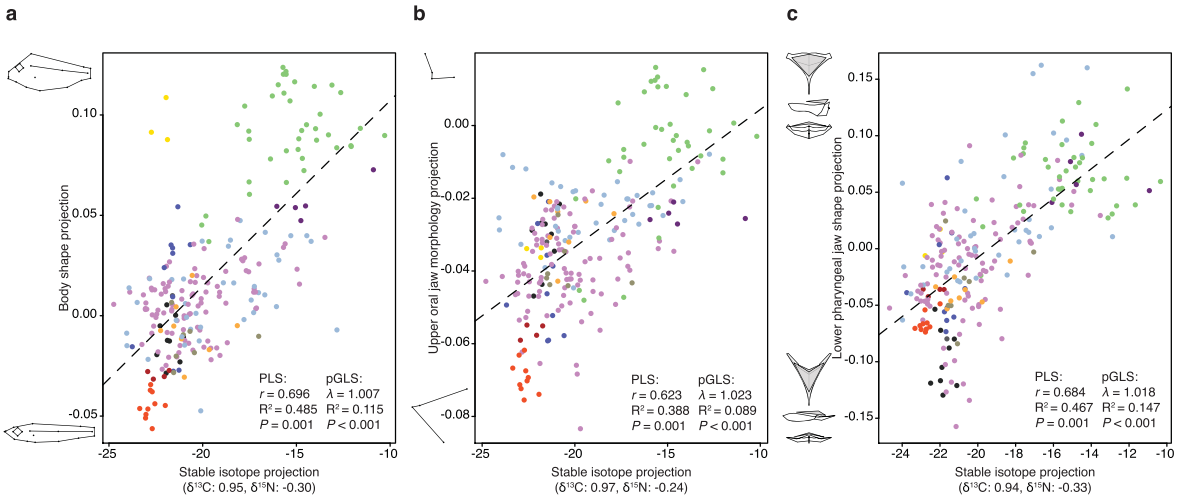

d

Tree topology	Trait	Model comparison log-likelihood difference (AIC difference) White noise	Brownian motion	Ornstein-Uhlenbeck	Early burst	Variable rates	Phylogenetic signal λ	K
Maximum-likelihood (RAxML)	Body shape	256 (477)	21 (8)	21 (10)	16 (**0**)	**0** (22)	*1.01*	*2.14*
	Upper oral jaw morphology	228 (390)	53 (40)	53 (42)	49 (35)	**0** (**0**)	*1.02*	*1.34*
	Lower pharyngeal jaw shape	193 (330)	44 (32)	44 (34)	44 (34)	**0** (**0**)	*1.02*	*1.13*
	Pigmentation pattern	101 (146)	53 (49)	45 (36)	53 (51)	**0** (**0**)	*0.94*	*0.44*
Multi-species coalescent (ASTRAL)	Body shape	258 (483)	23 (11)	23 (13)	16 (**0**)	**0** (21)	*1.02*	*2.28*
	Upper oral jaw morphology	228 (390)	54 (41)	54 (43)	50 (36)	**0** (**0**)	*1.03*	*1.42*
	Lower pharyngeal jaw shape	191 (325)	46 (35)	46 (37)	46 (37)	**0** (**0**)	*1.03*	*1.14*
	Pigmentation pattern	99 (143)	49 (43)	42 (32)	49 (45)	**0** (**0**)	*0.94*	*0.47*
Multi-species coalescent (SNAPP)	Body shape	259 (487)	19 (9)	19 (11)	14 (**0**)	**0** (25)	*1.01*	*2.12*
	Upper oral jaw morphology	225 (386)	48 (31)	48 (33)	44 (26)	**0** (**0**)	*1.02*	*1.32*
	Lower pharyngeal jaw shape	190 (324)	42 (28)	42 (30)	42 (30)	**0** (**0**)	*1.02*	*1.04*
	Pigmentation pattern	101 (147)	50 (44)	43 (32)	50 (46)	**0** (**0**)	*0.94*	*0.43*

e

Tree topology	Trait	Model comparison (AIC difference) White noise	Brownian motion	Ornstein-Uhlenbeck	Early burst	Variable rates	Phylogenetic signal λ	K	Root age
Maximum-likelihood (RAxML)	Body shape	453-486	2-11	4-13	**0**	5-30	*1-1*	*1.8-2.3*	8.8 - 10.4
	Upper oral jaw morphology	373-398	23-54	25-56	20-55	**0**	*1-1*	*1.1-1.5*	
	Lower pharyngeal jaw shape	319-337	14-65	16-63	16-67	**0**	*0.9-1*	*0.9-1.2*	
	Pigmentation pattern	133-158	37-85	27-59	39-87	**0**	*0.9-1*	*0.3-0.5*	
Multi-species coalescent (ASTRAL)	Body shape	461-494	4-13	6-15	**0**	10-28	*1-1*	*2-2.4*	9.4 - 10.9
	Upper oral jaw morphology	377-397	24-53	26-55	19-52	**0**	*1-1*	*1.2-1.5*	
	Lower pharyngeal jaw shape	316-330	13-60	15-60	15-62	**0**	*1-1*	*0.9-1.3*	
	Pigmentation pattern	130-149	30-83	24-54	32-85	**0**	*0.9-1*	*0.3-0.5*	
Multi-species coalescent (SNAPP)	Body shape	467-498	3-10	5-12	**0**	13-35	*1-1*	*1.9-2.2*	9.0 - 10.5
	Upper oral jaw morphology	371-392	14-43	16-45	10-43	**0**	*1-1*	*1.1-1.4*	
	Lower pharyngeal jaw shape	316-330	10-64	12-61	12-66	**0**	*1-1*	*0.8-1.1*	
	Pigmentation pattern	136-154	35-119	24-71	37-121	**0**	*0.9-1*	*0.3-0.5*	

Extended Data Fig. 8 | PLS fit for each multivariate trait against the stable N and C isotope compositions ($\delta^{15}N$ and $\delta^{13}C$ values) and models of trait evolution. a–**c**, PLS fits for body shape (**a**), upper oral jaw morphology (**b**) and lower pharyngeal jaw shape (**c**). Associated shape changes and loadings of the respective stable isotope projection are indicated next to the axes. Data points represent species means and are coloured according to tribe. **d**, Comparison of model fits for different models of trait evolution and phylogenetic signal for each trait complex using three time-calibrated species trees with alternative topologies. **e**, Overview of the model fits and phylogenetic signal inferred using 100 trees sampled from the posterior distributions of the time calibrations for each of the three alternative tree topologies.

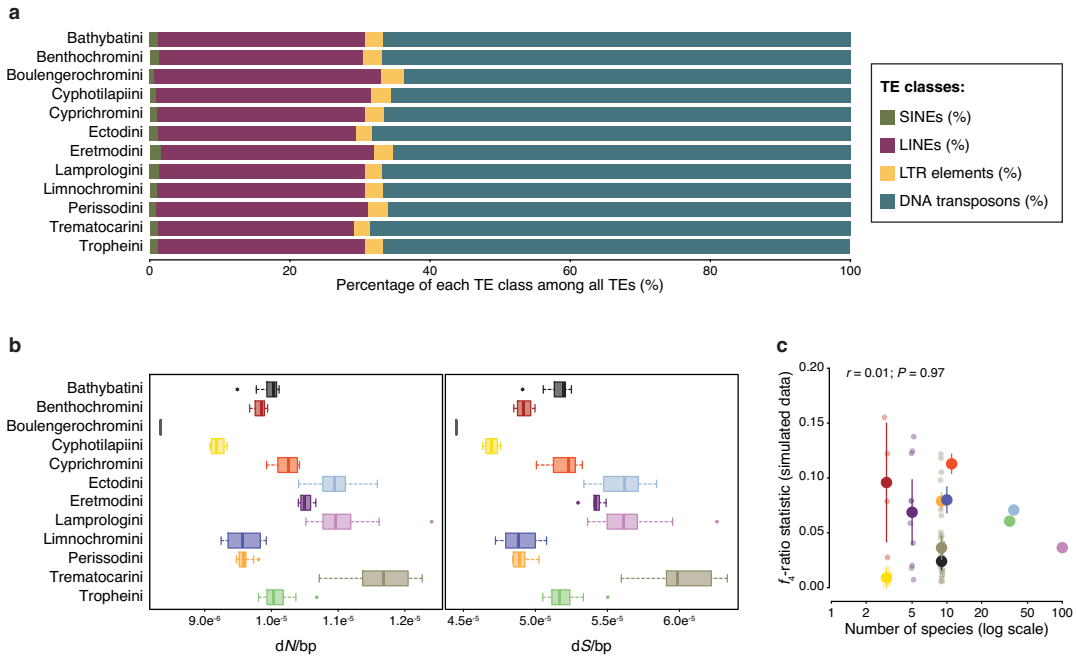

Extended Data Fig. 9 | Genome-wide statistical analyses. a, Proportion of the different classes of transposable elements (TE) among all TE for each tribe (one genome per species, $n = 245$). **b**, Species means of dN (left) and dS (right) values over alignment length for each tribe ($n = 243$ taxa, 471 genomes). The boxes' centre lines show median, box limits show first and third quartiles, and whiskers show the 1.5 × interquartile ranges. **c**, f_4-ratio statistics among species within each tribe in simulated data (tribe means are based on the mean across 20 simulations of each species triplet). Data points are coloured according to tribes; large points are tribe means shown with 95% confidence intervals, small points represent species means and are only shown for group sizes <40 species. To test for a correlation with species richness per tribe (log-transformed), we calculated phylogenetic independent contrasts for each variable and inferred Pearson's r through the origin.

Article

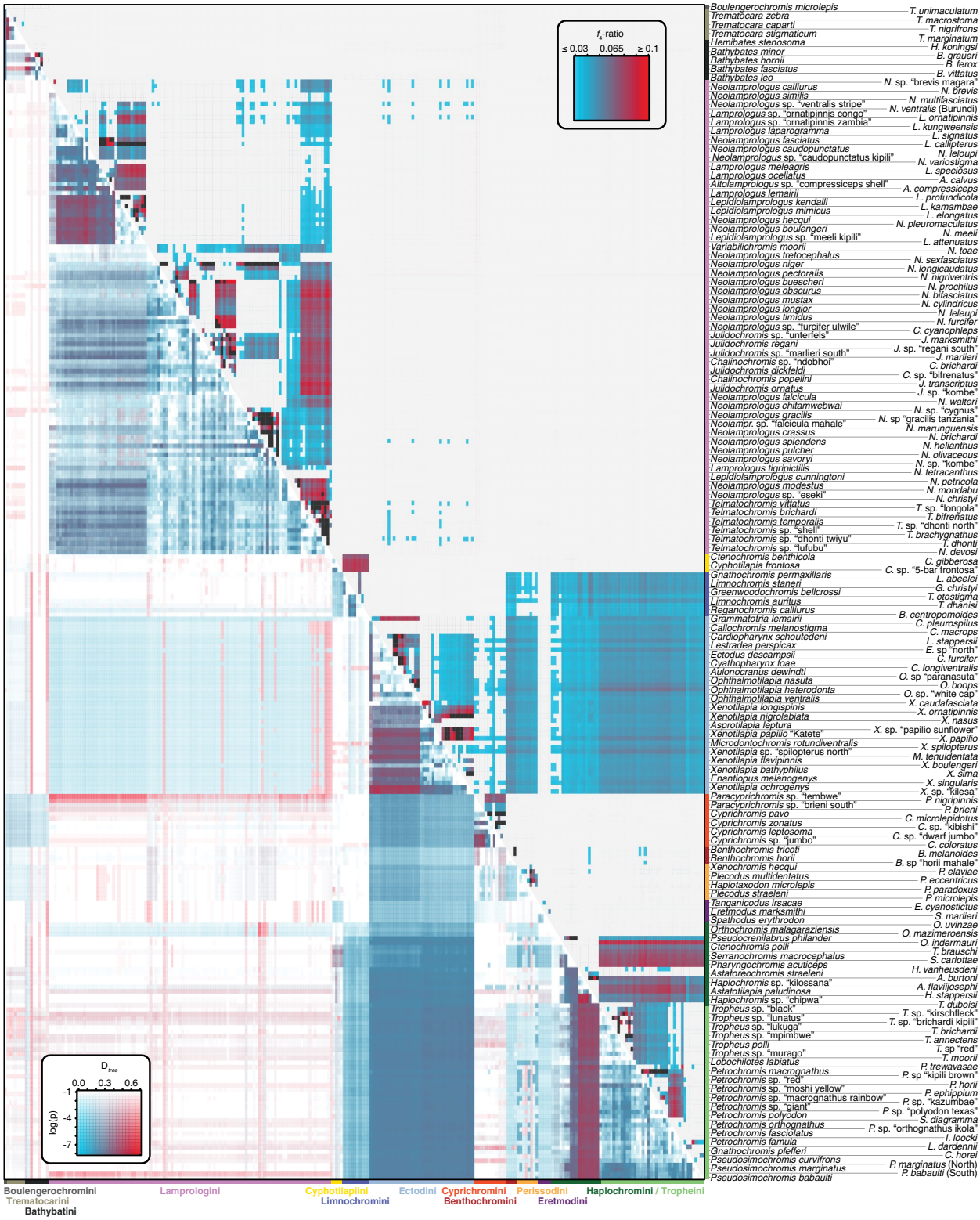

Extended Data Fig. 10 | Signals of introgression among Lake Tanganyika cichlid species. Upper matrix: maximum values of the f_4-ratio statistics between all pairs of species, derived from calculations across all combinations of species trios with *T. sparrmanii* fixed as the outgroup. The f_4-ratio estimates the proportion of the genome affected by gene flow, all presented values are statistically significant (one-sided block-jackknife tests: $P < 5 \times 10^{-5}$ after Benjamini–Hochberg correction for multiple testing). Lower matrix: D_{tree}-statistics (hue) with corresponding P-value (two-tailed binomial test, not adjusted for multiple testing; log-transformed; saturation) based on a phylogenetic approach testing for asymmetry in the relationships of species trios in 1,272 local maximum-likelihood trees (see Supplementary Methods). The two different approaches uncovered little gene flow among the tribes (see Supplementary Discussion).

nature research

Corresponding author(s): Fabrizia Ronco
Walter Salzburger

Last updated by author(s): Aug 7, 2020

Reporting Summary

Nature Research wishes to improve the reproducibility of the work that we publish. This form provides structure for consistency and transparency in reporting. For further information on Nature Research policies, see Authors & Referees and the Editorial Policy Checklist.

Statistics

For all statistical analyses, confirm that the following items are present in the figure legend, table legend, main text, or Methods section.

n/a	Confirmed	
☐	☒	The exact sample size (*n*) for each experimental group/condition, given as a discrete number and unit of measurement
☐	☒	A statement on whether measurements were taken from distinct samples or whether the same sample was measured repeatedly
☐	☒	The statistical test(s) used AND whether they are one- or two-sided *Only common tests should be described solely by name; describe more complex techniques in the Methods section.*
☒	☐	A description of all covariates tested
☐	☒	A description of any assumptions or corrections, such as tests of normality and adjustment for multiple comparisons
☐	☒	A full description of the statistical parameters including central tendency (e.g. means) or other basic estimates (e.g. regression coefficient) AND variation (e.g. standard deviation) or associated estimates of uncertainty (e.g. confidence intervals)
☐	☒	For null hypothesis testing, the test statistic (e.g. *F*, *t*, *r*) with confidence intervals, effect sizes, degrees of freedom and *P* value noted *Give P values as exact values whenever suitable.*
☐	☒	For Bayesian analysis, information on the choice of priors and Markov chain Monte Carlo settings
☒	☐	For hierarchical and complex designs, identification of the appropriate level for tests and full reporting of outcomes
☐	☒	Estimates of effect sizes (e.g. Cohen's *d*, Pearson's *r*), indicating how they were calculated

Our web collection on statistics for biologists contains articles on many of the points above.

Software and code

Policy information about availability of computer code

Data collection	FIJI (v2.0.0-rc-68/1.521i), TINA (v.6.0)
Data analysis	ASTRAL (v.5.6.3), aTRAM (v.2.0.alpha.5), AUGUSTUS (v.3.2.3), BayesTrait (http://www.evolution.rdg.ac.uk/, v.3), bcftools (v.1.6), beagle (v.4.1), BEAST 2 (v.2.5.0; packages: bModelTest (v.1.1.2), SNAPP (v.1.4.2), StarBEAST2 (v.0.15.5), TreeAnnotator (v.2.5.0)), BEDtools (v.2.21.0), BMGE (v.1.1), BUSCO (v.3), BWA-MEM (v.0.7.12), CeleraAssembler (v.8.3), Concaterpillar (v.1.7.2), Dsuite (v.0.2 r20), CT Pro 3D (V5.1.6054.18526), FLASH (v.1.2.11), GATK (v.3.6 and v.3.7), GMAP (GMAP-GSNAP, v.2017-08-15), IQ-TREE (v.1.6.8 and v.1.7-beta7), Kollector (v.1.0.1), MACSE (v.2.01, MAFFT (v.7.300), MIRA (v.4.0.2), MITObim (v.1.8), MultiQC (v.1.7), NRecon (v.1.6.10.2), msprime (v.0.7.4), PAML (v.4.9e and v.4.6), Picard-tools (v.2.7.1), PartitionFinder (v.2.1.1), PAUP* (v.4.0a164, v.4.0a163, and v.4.0a161), Python (v.2.7.10; packages: ete3 (v.3.1.1)), QUAST (v.4.5), R (v.3.5.2 and v.3.6.0; packages: ape (v.5.2), coda (v.0.19-3), Geiger (v.2.0.6.1), Geomorph (v.3.0.7), logisticPCA (v.0.2), phytools (v.0.6-60), vcfR (v.1.8.0), picante (v.1.8), ape (v.5.2), caper (v.1.0.1)), RAxML (v.8.2.4), RepeatModeler (v.1.0.11), RepeatMasker (v.4.0.7), samtools (v.1.3.1), smoove (https://github.com/brentp/smoove, docker image cloned 20/12/2018), lumpy (https://github.com/brentp/smoove, docker image cloned 20/12/2018), svtyper (https://github.com/brentp/smoove, docker image cloned 20/12/2018), svtools (https://github.com/hall-lab/svtools as part of https://github.com/brentp/smoove, docker image cloned 20/12/2018), "snapp_prep.rb" (github.com/mmatschiner/snapp_prep), SNPable (http://lh3lh3.users.sourceforge.net/snpable.shtml), TBLASTN, Tracer (v.1.7.1), Trimmomatic (v.0.36), vcftools (v.0.1.14), Identification of first-generation hybrid samples following github.com/mmatschiner/tutorials/tree/master/analysis_of_introgression_with_snp_data Code used to analyse the data is available on GitHub (https://github.com/cichlidx/ronco_et_al), except for analyses where single commands from publicly available software were used and where all settings are fully reported in the Methods and/or Supplementary Methods sections.

For manuscripts utilizing custom algorithms or software that are central to the research but not yet described in published literature, software must be made available to editors/reviewers. We strongly encourage code deposition in a community repository (e.g. GitHub). See the Nature Research guidelines for submitting code & software for further information.

Data

Policy information about availability of data

All manuscripts must include a data availability statement. This statement should provide the following information, where applicable:

- Accession codes, unique identifiers, or web links for publicly available datasets
- A list of figures that have associated raw data
- A description of any restrictions on data availability

All newly sequenced genomes for this study and their raw reads are available from NCBI under the BioProject accession number PRJNA550295 (https://www.ncbi.nlm.nih.gov/bioproject/). The VCF file, tree files, summary statistics of the assembled genomes, and phenotypic datasets generated and analysed during this study are available as downloadable files on Dryad (https://doi.org/10.5061/dryad.9w0vt4bbf). The Nile tilapia reference genome used is available under RefSeq accession GCF_001858045.1. All X-ray data are available on MorphoSource under the project number P1093.

Field-specific reporting

Please select the one below that is the best fit for your research. If you are not sure, read the appropriate sections before making your selection.

☐ Life sciences ☐ Behavioural & social sciences ☒ Ecological, evolutionary & environmental sciences

For a reference copy of the document with all sections, see nature.com/documents/nr-reporting-summary-flat.pdf

Ecological, evolutionary & environmental sciences study design

All studies must disclose on these points even when the disclosure is negative.

Study description	For the purpose of a comprehensive exploration of the evolution of cichlid fishes in Lake Tanganyika, we collected ten specimens of nearly all cichlid species occurring in that lake; sequenced the genome of one male and one female specimen per species (plus one genome of some outgroups and riverine sister taxa); assessed eco-morphological divergence by quantifying body shape (10 per species), oral jaw morphology (10 per species), lower pharyngeal jaw shape (5 per species) and stable carbon and nitrogen isotope compositions (10 per species); and quantified divergence in pigmentation patterns (5 per species).
Research sample	Our set of samples consists of ten specimens of nearly all cichlid fish species occurring in Lake Tanganyika, a set of selected outgroup species and a set of riverine species nested within the radiation. This sample was selected to maximally represent the cichlid fauna in the Lake Tanganyika drainage and the phylogenetic spectrum of East African cichlids. A comprehensive list of taxa (n=297) and specimens (n= 2'723; typically 5 males and 5 females per species) including information on the sex of the specimens is provided as Supplementary Tables 1 and 2. The ages are unknown for all specimens, but all specimens were adults. No manipulations were performed.
Sampling strategy	We collected specimens of cichlid fishes at African Lake Tanganyika that were either caught with barrier nets while snorkeling or Scuba diving, or purchased from local fishermen. After euthanasia with clove oil, we measured, weighted and photographed each specimen and took a fin clip for later DNA extraction. Specimen were formalin fixed and in a standardized way. Sampling was performed under research permits issued by the relevant authorities in the Republic of Burundi, the United Republic of Tanzania, and the Republic of Zambia. To maximize taxon sampling we included additional specimens from previous expeditions (4.9% of the samples) as well as from other collections (0.8%). The final dataset (297 taxa; n = 2'723 specimens) contained an almost complete taxon sampling of the cichlid fauna of Lake Tanganyika, 18 non-Tanganyikan cichlids nested within the radiation, and 28 outgroup species (see Supplementary Tables 1 and 2 for details). No sample size calculations were performed a priori. We sampled 10 adult specimens per species, which is sufficient to quantify eco-morphological disparity and estimate representative species means for comparative analyses. For genome sequencing we selected, whenever available, one male and one female individual per species to have both sexes represented.
Data collection	Digitalisation of Landmarks for body shape and upper oral jaw morphology: Data recorded by Fabrizia Ronco using the Software FIJI (v2.0.0-rc-68/1.521i) based on X-ray Images of the specimens. Digitalisation of Landmarks for lower pharyngeal jaw morphology: Data recorded by Fabrizia Ronco using the Software TINA (v.6.0) based on CT-scans of the specimens. Scoring pigmentation pattern: Data recorded by Walter Salzburger, scored by eye based on photographs of the specimens. Genome sequencing: DNA extraction and library preparation was performed by Fabrizia Ronco and Astrid Böhne. Sequencing was performed at the Norwegian Sequencing Centre (NSC), Oslo, and the Genomics Facility Basel (GFB) at the ETH Zurich Department of Biosystems Science and Engineering (D-BSSE), Basel, on Illumina HiSeq 2500 devices. Stable carbon (C) and nitrogen (N) isotope composition: Sample preparation was performed by Anna Boila with the help of Fabrizia Ronco. Samples were analysed by Anna Boila and Ansgar Kahmen on a Flash 2000 elemental analyser coupled to a Delta Plus XP continuous-flow isotope ratio mass spectrometer (IRMS) via a Conflo IV interface (Thermo Fisher Scientific, Bremen, Germany).
Timing and spatial scale	Sampling was conducted between 2014 and 2017 at 130 locations around Lake Tanganyika, followed by sample processing in Basel and Oslo, which required the following work packages and durations: DNA extraction and genome sequencing: April 2014 – February 2017 (Basel and Oslo).

Digitalisation of landmarks for body shape and upper oral jaw morphology: January 2018 – March 2018 (Basel).
Digitalisation of landmarks for lower pharyngeal jaw morphology: June 2016 – November 2017 (Basel).
Scoring pigmentation pattern: September 2019 (Basel).
Stable carbon (C) and nitrogen (N) isotope composition: March 2016 – October 2017 (Basel).

Data exclusions

Based on preestablished exclusion criteria for morphological analyses, specimens with broken jaws or bended bodies were excluded.
We excluded one of the sequenced genomes based on signs of contamination or DNA degradation.

Reproducibility

Due to the rather long time period for the digitalisation of landmarks for lower pharyngeal jaw morphology, we repeated (at the end of the data collection period) the data collection for the first 100 specimens scored. Biological interpretation remained unchanged.
No other data collection process was repeated, replicated or performed independently. All data collection steps which are potentially influenced by the observer (landmark digitalization, pigmentation scoring) were performed by a single person (experienced in the task) each to avoid investigator bias.

Randomization

Library pooling for Illumina sequencing was not specifically randomised, however, samples were allocated to pools based on suitable adapter combinations (according to the Illumina pooling guidelines).
Sample allocation into experimental groups is not relevant to this study, as no experimental groups were used.

Blinding

The possibility of blinding of the specimens was very limited. Although we labeled images and CT-scans only with specimen voucher IDs, species identification based on the image itself cannot be ruled out.
For all other data collection steps (data sets: stable isotope analyses and genome sequencing) blinding was not relevant as an investigator biased can be ruled out.
No blinding was applied for data analyses as taxonomic information was relevant for the analyses.

Did the study involve field work? ☒ Yes ☐ No

Field work, collection and transport

Field conditions

No field conditions are relevant to this study because we were exclusively interested in the biological specimens.

Location

Specimens were collected at Lake Tanganyika between 2014 and 2017 at 130 locations in the Republic of Burundi, the United Republic of Tanzania and the Republic of Zambia. GPS coordinates of the sampling location for each specimen are provided as downloadable file on dryad; https://doi.org/10.5061/dryad.9w0vt4bbf.

Access and import/export

All samples were collected and exported in agreement with local authorities with the following permits issued:

Republic of Burundi:

Sampling Permit, issued by the Ministère de l'Eau, de l'Environnement, de l'Amenagement du Territoire et de l'Urbanisme, Republic of Burundi
770 06/62710, issued 27/12/2014

Research permit issued by the Universite du Burundi (Cabinet du Recteur and Directeur de la Recherche et de l'Innovation)
2014/R991/Invitation (Heinz Büscher, Adrian Indermaur, Fabrizia Ronco, Walter Salzburger), issued 17/12/2014
Order de mission 35/2015 (Heinz Büscher, Adrian Indermaur, Fabrizia Ronco, Walter Salzburger), issued 19/01/2015

Work permit (Mission de travail), issued by the Permanent Mission of the Republic of Burundi to the United Nations, Geneva:
544/GE/2014/N.M.A (Heinz Büscher), valid 29/12/2014 to 28/01/2015
545/GE/2014/N.M.A (Fabrizia Ronco), valid 29/12/2014 to 28/01/2015
546/GE/2014/N.M.A (Adrian Indermaur), valid 29/12/2014 to 28/01/2015
547/GE/2014/N.M.A (Walter Salzburger), valid 29/12/2014 to 28/01/2015

Export permits, issued by the Universite du Burundi (Cabinet du Recteur and Directeur de la Recherche et de l'Innovation) and the Ministère de l'Eau, de l'Environnement, de l'Amenagement du Territoire et de l'Urbanisme:
Export/transport permit, issued 21/01/2105

The United Republic of Tanzania:

Research permits, issued by the Tanzania Commission for Science and Technology (COSTECH):
2015-173-NA-2015-96 (Adrian Indermaur), valid 29/05/2015 to 18/05/2016
2015-174-NA-2015-96 (Fabrizia Ronco), valid 29/05/2015 to 18/05/2016
2015-175-NA-2015-96 (Heinz Büscher), valid 29/05/2015 to 18/05/2016
2015-176-NA-2015-96 (Walter Salzburger), valid 29/05/2015 to 18/05/2016
2016-373-NA-2015-96 (Walter Salzburger), valid 12/12/2016 to 11/12/2017
2016-376-NA-2015-96 (Fabrizia Ronco), valid 12/12/2016 to 11/12/2017
2016-377-NA-2015-96 (Adrian Indermaur), valid 12/12/2016 to 11/12/2017
2016-378-NA-2015-96 (Heinz Büscher), valid 12/12/2016 to 11/12/2017

Research permits, issued by the Tanzania National Parks Authority (TANAPA):
TNP/HQ/C.10/13/2015 (Heinz Büscher, Adrian Indermaur, Fabrizia Ronco, Walter Salzburger), valid 30/6/15 to 29/09/16
TNP/HQ/C.10/13/2017 (Heinz Büscher, Adrian Indermaur, Fabrizia Ronco, Walter Salzburger), valid 12/12/16 to 11/12/17

Research Clearance, issued by the Tanzania Wildlife Research Institute (TAWIRI):
13300 (Heinz Büscher, Adrian Indermaur, Fabrizia Ronco, Walter Salzburger), dated 09/01/2017

Residence permits, issued by the Department of Immigration:
CTA0329015 (Heinz Büscher), valid 22/06/2015 to 21/08/2016
CTA0329016 (Walter Salzburger), valid 22/06/2015 to 21/08/2016
CTA0329017 (Adrian Indermaur), valid 22/06/2015 to 21/08/2016
CTA0329018 (Fabrizia Ronco), valid 22/06/2015 to 21/08/2016
RPC11100834 (Walter Salzburger), valid 11/12/2016 to 10/12/2017
RPC11100835 (Fabrizia Ronco), valid 11/12/2016 to 10/12/2017
RPC11100836 (Heinz Büscher), valid 11/12/2016 to 10/12/2017
RPC11100836 (Adrian Indermaur), valid 11/12/2016 to 10/12/2017

Sample export and transport permits, issued by the Tanzanian Fisheries Research Institute (TAFIRI), Ministry of Livestock and Fisheries Development:
TAF/KGM/R/VOL.V/236, issued 16/07/2015
TAF/KGM/R.1/VOL.V/121, issued 10/02/2017

Republic of Zambia:

Study permits (including residence permits), issued by the Department of Immigration and the Department of Fisheries, Ministry of Agriculture and Livestock, based on a Memorandum of Understanding (MOU)
SP000627 (Fabrizia Ronco), valid 13/07/2012 to 08/08/2016
SP000710 (Adrian Indermaur), valid 13/07/2012 to 30/10/2015
SP001995 (Walter Salzburger), valid 05/07/2013 to 05/07/2015
SP002417 (Heinz Büscher), valid 05/08/2015 to 12/11/16
SP004273 (Walter Salzburger), valid 30/07/2015 to 13/07/2020
SP005937 (Fabrizia Ronco), valid 29/07/2016 to 28/07/2018
SP005943 (Adrian Indermaur), valid 27/07/2016 to 28/07/2018

Export permits, issued by the Department of Fisheries, Ministry of Agriculture and Livestock:
Export/transport permit, issued 02/08/2013
Export/transport permit, issued 23/01/2014
Export/transport permit, issued 26/08/2015
Export/transport permit, issued 13/09/2016
Export/transport permit, issued 29/08/2017
Export/transport permit, issued 10/09/2018

Schweizerische Eidgenossenschaft/Confoederatio Helvetica (CH):

CITES Approval, issued by the Bundesamt für Veterinärwesen, Eidgenössisches Departement für Inneres:
CH018 (Adrian Indermaur, Walter Salzburger, Zoological Institute, University of Basel), valid 23/01/2013 to 31/12/2020

Recognition as Scientific Institution (according to EU-directive 92/65/EWG, Annex C), issued by the Cantonal Veterinary Office Basel Stadt:
CH-I-BS017 (Walter Salzburger), valid 11/06/2012 to 31/12/2017
CH-I-BS003h (Walter Salzburger), valid 19/02/2015 to 31/12/2019

Permit for an animal facility for cichlid fishes, issued by the Cantonal Veterinary Office Basel Stadt:
1010H (Walter Salzburger), valid 01/11/2013 to 31/10/2023

Permit to conduct and supervise animal experiments, issued by the Cantonal Veterinary Office Basel Stadt:
A2015 (Walter Salzburger), issued 19/01/2010

Permit to take tissue samples from cichlid fishes, issued by the Cantonal Veterinary Office Basel Stadt:
2317_22449 (Walter Salzburger), valid 01/12/2011 to 31/12/2014
2317_25931 (Walter Salzburger), valid 01/01/2015 to 01/01/2018
2317_29387 (Walter Salzburger), valid 02/01/2018 to 31/12/2020

Disturbance

We collected specimens primarily during snorkelling and scuba diving which allows to target individual specimens with minimum bycatch.

Reporting for specific materials, systems and methods

We require information from authors about some types of materials, experimental systems and methods used in many studies. Here, indicate whether each material, system or method listed is relevant to your study. If you are not sure if a list item applies to your research, read the appropriate section before selecting a response.

Materials & experimental systems

n/a	Involved in the study
☒	☐ Antibodies
☒	☐ Eukaryotic cell lines
☒	☐ Palaeontology
☐	☒ Animals and other organisms
☒	☐ Human research participants
☒	☐ Clinical data

Methods

n/a	Involved in the study
☒	☐ ChIP-seq
☒	☐ Flow cytometry
☒	☐ MRI-based neuroimaging

Animals and other organisms

Policy information about studies involving animals; ARRIVE guidelines recommended for reporting animal research

Laboratory animals	This study did not involved laboratory animals.
Wild animals	We collected specimens of cichlid fishes at African Lake Tanganyika that were either caught with barrier nets while snorkelling or Scuba diving, or purchased from local fishermen. After euthanasia with clove oil, we measured, weighted and photographed each specimen and took a fin clip for later DNA extraction. Specimen were formalin fixed and in a standardized way. Sampling was performed under research permits issued by the relevant authorities in the Republic of Burundi, the United Republic of Tanzania, and the Republic of Zambia. A comprehensive list of taxa (n=297) and specimens (n= 2'723; typically 5 males and 5 females per species) including information on the sex of the specimens is provided as Supplementary Tables 1 and 2. No animals were transported or kept alive.
Field-collected samples	No experiments were conducted in the field as only terminal samples were collected (see above).
Ethics oversight	Republic of Burundi: Ministère de l'Eau, de l'Environnement, de l'Amenagement du Territoire et de l'Urbanisme, Universite du Burundi (Cabinet du Recteur and Directeur de la Recherche et de l'Innovation) The United Republic of Tanzania: Tanzania Commission for Science and Technology (COSTECH): Tanzanian Fisheries Research Institute (TAFIRI), Ministry of Livestock and Fisheries Development: Republic of Zambia: Department of Fisheries, Ministry of Agriculture and Livestock Schweizerische Eidgenossenschaft/Confoederatio Helvetica (CH): Cantonal Veterinary Office Basel Stadt:

Note that full information on the approval of the study protocol must also be provided in the manuscript.

nature research

https://doi.org/10.1038/s41586-020-2930-4

Supplementary information

Drivers and dynamics of a massive adaptive radiation in cichlid fishes

In the format provided by the authors and unedited

1. Supplementary Methods

Sampling

Sampling at Lake Tanganyika was conducted during a total of ca. nine months of fieldwork between 2014 and 2017 at 130 locations in the Republic of Burundi, the Republic of Zambia, and the United Republic of Tanzania. Fishes were either caught with barrier nets while snorkelling or Scuba diving, or purchased from local fishermen. After euthanasia with clove oil, each specimen was photographed using Nikon D5000 digital cameras (Nikon Corporation, Tokyo, Japan) and a fin clip was taken and preserved in 100% ethanol for later DNA extraction. For initial fixation of the specimens, we used 10-20% formalin (depending on the size of the fish). To fix the specimens in a standardized way, we placed the fish with their right body side facing down in a plane plastic container. The body was straightened and fins were erected while covering the specimen with formalin-soaked paper towels. To ensure adequate fixation, we additionally injected formalin into the body cavity. Once specimens were fully fixed (usually after 4 days) they were rinsed and placed in water (overnight), and transferred for long-term storage into 70% ethanol. All specimens were integrated into the *Ichthyological collection on Tanganyikan cichlids of the University of Basel* (https://www.unibas.ch/de/Universitaet/Administration-Services/Generalsekretariat/Archive-Sammlungen/Wissenschaftliche-Sammlungen/Alphabetisch-sortiert/Buntbarsch-Sammlung.html).

To maximize taxon sampling, we included additional specimens from previous expeditions (4.9% of the samples) as well as from other collections (0.8%). The final dataset (301 taxa; n = 2,723 specimens) contained an almost complete taxon sampling of the cichlid fauna of Lake Tanganyika including 201 of the 208 formally described species (96.6%; note that five of the missing species have never been found since description or their species status is under discussion[15]) and all undescribed species which have been reported in a recent species inventory for Lake Tanganyika cichlids[15]. Further, we included 18 representative cichlid species from nearby waterbodies and 32 outgroup species. These additional taxa were used for phylogenetic analysis only except for *Oreochromis tanganicae* and *Tylochromis polylepis*, which occur in Lake Tanganyika and were thus included in the overall characterisation of morphospace and ecospace (PCA, Fig. 2). All analyses described below are based on the same set of typically 10 preserved specimens per species, or subsets thereof (see Supplementary Table 1; a full list of individual specimen vouchers including details on sampling location is provided as Supplementary Table 2).

Whole genome sequencing

Genomic DNA of typically one male and one female specimen per species (n = 547) was extracted from fin-clips preserved in ethanol using the E.Z.N.A. Tissue DNA Kit (Omega Bio-Tek) and sheared on a Covaris E220 (60 µl with 10% duty factor, 175 W, 200 cycles for 65 sec). Individual libraries were prepared using Illumina's TruSeq DNA PCR-Free Sample Preparation kit (Low Sample Protocol) for 350 bp insert size, pooled (six libraries per lane), and sequenced at 126 bp paired-end on an Illumina HiSeq 2500 (see Supplementary Table 1 for information on read depths).

Assessing genomic variation

To obtain a dataset of genome-wide SNPs for all species of the cichlid radiation of Lake Tanganyika, species nested within the radiation, as well as selected closely-related outgroup species (n = 528; see Supplementary Table 1 for a species list and read depth), we trimmed adapters with Trimmomatic[35] (v.0.36), mapped the reads against the Nile tilapia reference genome (*Oreochromis niloticus;* RefSeq accession GCF_001858045.1[36]), and performed variant calling.

Details on mapping, variant calling, and filtering. We customised the Nile tilapia reference genome by concatenating lexicographically all unplaced scaffolds into an 'UNPLACED' super chromosome. After mapping with BWA-MEM[37] (v.0.7.12), duplicate reads were marked with Picard-tools (http://broadinstitute.github.io/picard/; v.2.7.1), indels were realigned with GATK[38] (v.3.6), and the final alignment files in BAM format were indexed with SAMtools[82] (v.1.3.1). The per-individual read coverage distribution was determined with BEDtools[83] (v.2.21.0), and variant calling was performed with GATK's HaplotypeCaller and GenotypeGVCF tools[38] (v.3.7), applying a minimum base quality score of 30.

Variant calls were filtered according to a strict pipeline to ensure high call reliability. Sites were excluded with BCFtools[39] (v.1.6) if the Phred-scaled P-value of Fisher's exact test for strand bias was greater than 20, if the quality score normalised by read depth was below 2, if the root mean square mapping quality was below 20, or if the overall read depth across all 528 samples was either below 4,000 or above 8,000. Sites were further excluded if the Mann-Whitney-Wilcoxon rank sum test produced a test statistic below -0.5 for either site position bias within reads or mapping quality bias between reference and alternative alleles. Indels were normalised with BCFtools. As the dataset contained a large number of indels, we did not remove all SNPs within a fixed distance to indels. Instead, we applied a filter to sites in proximity to indels with a minor allele count greater than 2, depending on the size of the indel: For indels with a size of 5 bp or larger, we excluded sites within 10 bp of the indel, but sites were only excluded within 5, 3, or 2 bp if the indel size was 3-4, 2, or 1 bp, respectively. To reduce the number of indels in the dataset we also excluded nine of the outgroup species (specimen vouchers: Z03, Z07, Z09, Z17, JAB6, JAC7, KYH4, JWE6, and JWF2).

We further masked sites within regions of the Nile tilapia reference genome in which read mapping was likely to be ambiguous. To determine these regions, we used the SNPable pipeline (http://lh3lh3.users.sourceforge.net/snpable.shtml). The approach implemented in this tool divides the reference genome into overlapping fragments (in our case 100 bp fragments that overlapped by 99 bp) that are then mapped back to the reference, allowing a count of how many fragments map correctly at each site. Based on the results of this approach, we excluded all sites from regions in which less than 90 out of 100 fragments mapped back correctly. For each individual independently, we masked genotypes with a read depth below 4 or a genotype quality below 20 using VCFtools[40] (v.0.1.14). Finally, sites that were no longer polymorphic after the previous filtering steps were excluded, resulting in a dataset of 57,751,375 SNPs (VCF file available on Dryad; https://doi.org/10.5061/dryad.9w0vt4bbf). We additionally generated a more strictly filtered SNP dataset with all filtering steps as described above, but applying a minimum genotype quality of 30

instead of 20 and masking all sites of the Nile tilapia genome in which less than 95 of 100 fragments mapped back correctly. This more strictly filtered dataset included 54,048,145 SNPs.

Phasing. Called variants were phased with the software beagle[41] (v.4.1). Genotypes that had been missing or masked before the imputation step of phasing with beagle were masked again after the imputation. At this step we excluded one sample from a museum collection (specimen voucher: Bel33; *Trematocara variabile*) from further analysis, due to signs of contamination and/or DNA degradation.

Identification of first-generation hybrids

On the basis of the results of an initial application of *D* statistics[84] to the SNP dataset (see below) and the previous suggestion that *Neolamprologus cancellatus* is a hybrid species involving *Telmatochromis vittatus* as one parent[85], we analysed the genotypes of the two *N. cancellatus* specimens (specimen vouchers: LJC9 and LJD1) included in our dataset at sites that are fixed for alternative alleles in pairs of candidate parental species. We found that the two *N. cancellatus* specimens were heterozygous at 5,792 out of 5,912 sites (98%) that are fixed for alternative alleles in *T. vittatus* and *Neolamprologus fasciatus*, indicating that these two species – or lineages very closely related to them – are the parents of the two *N. cancellatus* specimens and that these two specimens represent first-generation (F1) inter-specific hybrids. As the mitochondrial genomes of the two *N. cancellatus* specimens cluster with those of the two *N. fasciatus* specimens (Supplementary Fig. 2), we further conclude that the mother of both was a *Neolamprologus* (most likely *N. fasciatus*) and the father a *Telmatochromis* (most likely *T. vittatus*), which is in agreement with field observations of male *T. vittatus* spawning at the opening of shells or cavities occupied by female *N. fasciatus*[86].

We then used this information to improve the genotype phasing for the *N. cancellatus* specimens, separating all heterozygous genotypes so that one of the two resulting haplotypes approximated the nucleotide sequence of *T. vittatus* and the other one that of *N. fasciatus*.

As the inclusion of F1 hybrids between two rather distantly related species can strongly influence phylogenetic inference, we consequently excluded *N. cancellatus* from all phylogenetic analyses at the species levels (species-tree inference and all subsequent phylogenetic comparative analyses). For individual-based phylogenetic inference we used separately the phased haplotypes of *N. cancellatus* that were obtained as described above.

De novo genome assemblies

De novo genome assemblies were generated from the Illumina raw read data for each individual following an approach described previously[42,43] using CeleraAssembler[44] (v.8.3) and FLASH[45] (v.1.2.11). Eight genomes repeatedly failed to assemble and were therefore excluded from further assembly-based analyses (specimen vouchers: A188, IRF6, IZC5, JWE7, JWG1, JWG2, LJD3, and LJE8). Assembly quality was assessed with QUAST[46] (v.4.5) and completeness was determined with BUSCO[47] (v.3; -l actinopterygii_odb9, -sp zebrafish). Assembly statistics were summarised with MultiQC[48] (v.1.7). Summary statistics are available on Dryad; https://doi.org/10.5061/dryad.9w0vt4bbf: 04_genomeAssemblies_multiQC_busco.csv, 04_genomeAssemblies_multiQC_quast.csv.

Determining the age of the radiation

To determine the age of the radiation of cichlid fishes in Lake Tanganyika, we applied phylogenomic molecular-clock analyses for representatives of all cichlid subfamilies together with non-cichlid outgroups (in total 44 species, Extended Data Fig. 1).

Selection of nuclear markers for phylogenetic analyses. The selection of nuclear markers suitable for molecular-clock analyses followed the strategy described in Matschiner *et al.*[18] and was initially based on the annotated genomes of medaka (*Oryzias latipes*), midas cichlid (*Amphilophus citrinellus*), Nile tilapia (*O. niloticus*), lyretail cichlid (*Neolamprologus brichardi*), Burton's mouthbrooder (*Astatotilapia burtoni*), and zebra mbuna (*Metriaclima zebra*) in release 94 of the ENSEMBL database[87]. We identified 3,781 genes that each had no deletions or duplications among cichlids according to ENSEMBL's gene tree information and that were composed of at least three exons longer than 150 bp. In total, the 3,781 genes contained 22,251 exons with this minimum length. For each of these exons, we quantified the sequence similarity between medaka, which we used as an outgroup, and the six cichlid species by their pairwise TBLASTN[88] bitscores. Based on this quantification, we excluded all exons for which one or more of the pairwise bitscores between orthologs were below 50 or less than 20 units greater than the largest bitscores with other genomic regions (that is, potential paralogs). This ensured that true orthologs of the exons in the dataset are recognizable by their TBLASTN bitscores, a property that we exploited in the subsequent identification of orthologs from the newly assembled cichlid genome sequences. Finally, we excluded all exons if no more than one further exon of the same gene remained in the dataset, to allow tests of within-gene exon tree concordance in the subsequent ortholog identification. The resulting dataset contained 10,590 exons of 2,081 genes. For each of these exons, we retrieved the medaka amino-acid sequence together with the exon-specific TBLASTN bitscore value that we had determined as a threshold for recognition of potential orthologs from cichlid assemblies.

Selection of species for phylogenomic analyses. To enable reliable phylogenetic time calibrations based on multiple constraints on outgroup divergences, we included not just the most divergent cichlid lineages but also representatives of closely-related outgroups within Ovalentaria[89]. As in Matschiner *et al.*[18], we included the rock-pool blenny (*Parablennius parvicornis*) to represent the order Blenniiformes, medaka (*O. latipes*) to represent the order Beloniformes, and six representatives of the order Cypriniformes: mangrove rivulus (*Kryptolebias marmoratus*), sheepshead minnow (*Cyprinodon variegatus*), mummichog (*Fundulus heteroclitus*), turquoise killifish (*Nothobranchius furzeri*), Amazon molly (*Poecilia formosa*), and platyfish (*Xiphophorus maculatus*). The genome assemblies of the rock-pool blenny and turquoise killifish were taken from Malmstrøm *et al.*[90] and Reichwald *et al.*[91], respectively, all other genome assemblies were taken from ENSEMBL release 94. We further included 36 cichlid species representing all subfamilies, the most divergent lineages of African cichlids (subfamily Pseudocrenilabrinae), and four tribes of cichlids deriving from the earliest splits of the Tanganyikan cichlid radiation. The subfamilies Etroplinae, Ptychochrominae, and Cichlinae were represented by the same species as in Matschiner *et al.*[18]: *Etroplus canarensis*, *Ptychochromis oligocanthus*, *Paratilapia polleni* "Andapa", *Apistogramma diplotaenia*, *Andinoacara biseriatus*, *Bujurquina vittata*, *Andinoacara coeruleopunctatus*, *Amphilophus citrinellus*, *Amphilophus zaliosus*,

and *Australoheros scitulus*. As in Matschiner *et al.*[18], genome assemblies of *A. citrinellus* and *A. coeruleopunctatus* were taken from ENSEMBL release 94 and from the Cambridge Cichlid Browser (http://cichlid.gurdon.cam.ac.uk/Andinoacara_coeruleopunctatus_final_min1000bp_scaffolds.fa.gz), respectively; genome assemblies of the other eight species were generated by Matschiner *et al.*[18]. Within the subfamily Pseudocrenilabrinae, we included six members of the divergent West African cichlid tribes Heterochromini, Tylochromini, Chromidotilapiini, Hemichromini, and Etiini: *Heterochromis multidens*, *Tylochromis polylepis*, *Benitochromis conjunctus*, *Pelvicachromis taeniatus*, *Hemichromis elongatus*, and *Etia nguti*. The genome assemblies of these six species were taken from Matschiner *et al.*[18]. We further included *O. niloticus* as well as three additional representatives of the tribe Oreochromini: *O. tanganicae*, *O. malagarasi*, and *Sarotherodon lohbergeri*. Of these, the genome assembly of *O. niloticus* was taken from Conte *et al.*[92], while genome assemblies for the other three species were newly generated (specimen vouchers: JAB6, KYH4, and Z05, respectively). Eight more cichlid species from outside Lake Tanganyika were included, representing the tribes Tilapiini, Steatocranini, Gobiocichlini, Pelmatolapiini, Heterotilapiini, and Coptodonini: *Tilapia sparrmanii*, *Steatocranus* sp. "ultraslender", *Gobiocichla ethelwynae*, '*Tilapia' brevimanus*, *Pelmatolapia mariae*, *Heterotilapia buttikoferi*, *Coptodon bakossiorum*, and *Coptodon rendalli*. Genome assemblies of all these species were newly generated (specimen vouchers: JWF7, JWE8, JWE7, JWF9, JWF2, JWE3, JWE5, and JWE6, respectively). Finally, four tribes nested within the Tanganyikan cichlid radiation – Trematocarini, Ectodini, Lamprologini, and Haplochromini – were represented by *Trematocara marginatum*, *Trematocara nigrifrons*, *Asprotilapia leptura*, *Grammatotria lemairii*, *Neolamprologus variostigma*, *N. brichardi*, *Astatotilapia flaviijosephi*, and *Metriaclima zebra*. With the exception of *N. brichardi* and *M. zebra*, for which genome assemblies were taken from ENSEMBL release 94 and Conte *et al.*[92], respectively, the assemblies of these species were newly generated (specimen vouchers: ISA3, IUE5, INF2, JDD7, JWA5, and LJD2). The four tribes from Lake Tanganyika were selected so that their splits included the earliest divergence within the radiation (the separation of Trematocarini from the other three tribes) while avoiding tribes for which earlier studies had inferred signals of introgression (e.g. Boulengerochromini, Bathybatini, Perissodini, and Cyprichromini)[93]. The particular samples per tribe were selected based on their comparatively high read depth (see Supplementary Table 1) or isolated geographic distribution reducing the probability of hybridisation (specimen voucher: LJD2; *A. flaviijosephi* occurring in Jordan and Israel). In total, we used genome assemblies of 44 species to determine the age of the adaptive radiation of cichlid fishes in Lake Tanganyika.

Targeted assembly of potential orthologs. To improve the contiguity of potential ortholog sequences, we complemented the 17 newly generated genome assemblies used for divergence-time estimations with targeted assemblies using both Kollector[94] (v.1.0.1) and aTRAM[95] (v.2.0.alpha.5) as described in Matschiner *et al.*[18]. As targets, we used a set of 10,373 sequences from the Nile tilapia (*O. niloticus*) genome assembly[92], each of which was the most similar homolog to one of the 10,590 selected medaka exons (no sufficiently similar homologs could be identified for 217 exons). Details on these analyses are provided in Matschiner *et al.*[18]. Targeted assemblies were merged with the whole-genome assemblies of the same species prior to further analysis.

Compilation of ortholog sequences. The identification and filtering of ortholog sequences followed the workflow first established in Malmstrøm *et al.*[90] and further developed by Musilova *et al.*[96] and Matschiner *et al.*[18]. In brief, this workflow uses exon sequences of an outgroup query together with exon-specific bitscore thresholds to identify potential orthologs, which are further filtered by dN/dS ratios, proportion of missing data, alignment reliability, GC-content variation, genomic position, within-gene exon-tree discordance, and substitution-rate variation to select the most suitable orthologs for phylogenetic divergence-time estimation. Accordingly, we used the 10,590 selected medaka exon sequences as queries in TBLASTN searches to identify potential orthologs from the 44 genome assemblies listed above. Subject sequences were accepted as candidate orthologs if their bitscore was above the exon-specific threshold determined during marker selection; this was the case for a total of 448,364 sequences. Per exon, we generated alignments of nucleotide exon sequences with MAFFT[97] (v.7.300), guided by their amino-acid translation to ensure the integrity of codon triplets.

The 10,590 exon-sequence alignments were then subjected to the following filters to select the most suitable paralog-free alignments for the subsequent phylogenomic analyses:

1) Per exon, TBLASTN bitscores of all sequences were compared and those sequences with bitscores lower than 0.9 times the highest bitscore observed for any ingroup species were discarded. For exon sequences that evolve clock-like, true orthologs should all be similarly distant to outgroup sequences; thus, this filter is expected to remove sequences that are either paralogous or do not evolve in a clock-like fashion – two properties that both render the sequences unsuitable for divergence-time estimation.
2) In pairwise comparisons with the medaka exon sequences, dN/dS ratios were calculated for all ingroup sequences using *codeml* of the PAML package[78] (v.4.6) with runmode –2, and sequences with dN/dS ratios greater than 0.25 were excluded, as this could indicate positive selection on certain branches or sites, which would imply departures from clock-like evolution.
3) We excluded all exon-sequence alignments in which sequences were missing for more than 10 of the 44 species. This filter removed 2,504 alignments.
4) We used the software BMGE[98] (v.1.1) to assess local alignment reliability and removed codons if one or more sites of the codon had a proportion of missing data greater than 20% or a smoothed entropy-like score above 0.5.
5) We excluded exon alignments that had become shorter than 150 bp after the above filtering steps; this filter removed 206 of the remaining 8,086 alignments.
6) We quantified GC content per exon sequence and removed alignments with an among-sequence standard deviation in GC content greater than 0.04, as high GC-content variation has been shown to affect phylogenetic inference[99]. This filter removed 34 of the remaining 7,880 exon alignments.
7) To allow subsequent analyses of within-gene exon-tree discordance, we retained only those exons for which at least two more exons assigned to the same gene and located within 100,000 bp of each other on the same medaka chromosome remained in the dataset. This requirement removed 1,332 of the remaining 7,846 exon alignments.
8) We tested for within-gene exon-tree discordance with the software Concaterpillar[100] (v.1.7.2). Although our phylogenetic analyses of cichlid divergence times did allow for among-gene tree

discordance, we conservatively assumed that within-gene exon-tree discordance was more likely the result of paralogy than of within-gene recombination (due to incomplete lineage sorting, see below). If at least three exons of a gene had trees that were concordant with each other, these were concatenated into gene alignments; all other exon alignments were discarded. After applying this filter, 1,293 genes with a total of 6,076 exons remained in the dataset.

9) To characterize how fast and clock-like genes evolve, we estimated the mean and the standard deviation of the substitution rate across species for each gene, using the Bayesian software BEAST 2[50] (v.2.5.0) with an uncorrelated lognormal (UCLN) relaxed molecular clock model[101] and the bModelTest add-on package[102] (v.1.1.2) to average over substitution models. Each analysis was set to run for 10 million Markov chain Monte Carlo (MCMC) iterations. This produced effective sample sizes (ESS) for all parameters of at least 200 for 1,121 of the 1,293 genes and ESS values of at least 100 for all parameters for all but 80 genes.
10) Gene alignments were inspected visually for potential homology errors[103] and five alignments were excluded due to possible misalignment.
11) Finally, the remaining 1,288 gene alignments were filtered in a 'strict' and 'permissive' way to select genes with low substitution rates (reducing the probability of homoplasies), comparatively clock-like evolution, and a strong and consistent phylogenetic signal. This selection was thus based on threshold values for the estimated substitution rate, the estimated coefficient of rate variation, and the minimum ESS value resulting from the analysis (as inconsistent phylogenetic signal within a gene, potentially resulting from misalignment or paralogy, can lead to low ESS values). In the 'strict' selection of genes, we required a substitution-rate estimate below 0.0015 per site and million year, a coefficient of rate variation below 0.4, and a minimum ESS value of at least 200. In contrast, our 'permissive' selection of genes allowed substitution-rate estimates up to 0.002 per site and million year, coefficients of rate variation up to 0.6, and minimum ESS values of at least 100.

The resulting 'strict' and 'permissive' datasets contained 510 and 1,161 genes and had total alignment lengths of 542,922 and 1,353,747 bp, respectively. For subsequent analyses, we generated maximum-clade-credibility consensus trees with node heights set to mean age estimates for each gene from the posterior tree distributions estimated with BEAST 2, using the program TreeAnnotator (v.2.5.0), which is part of the BEAST 2 package[50].

Species-tree inference. As a first test of the among-species relationships supported by our datasets, we performed species-tree analyses with the multi-species coalescent model implemented in the program ASTRAL[49] (v.5.6.3), separately for the 'strict' and 'permissive' sets of maximum-clade-credibility consensus gene trees. Both sets of gene trees supported exactly the same species-tree topology that fully agreed with the monophyly of all ingroup and outgroup genera, tribes, subfamilies, families, suborders, and orders, as well as the previously established sequence of tribal divergence events within Neotropical and African cichlids[22,104]. Moreover, the species trees received very high support, with posterior probabilities of 100% for all but one node. The exception was the monophyly of the outgroup species *C. variegatus* and *F. heteroclitus*, which received 56% posterior probability with the 'strict' set of gene trees and 76% with the 'permissive' set of trees.

To verify that homoplasies did not affect the reliability of our inferred species trees, we also reconstructed species relationships based on indels as markers with low frequency of homoplasies[99]. We identified indels from exon alignments of all genes in the 'strict' and 'permissive' datasets, using the versions of the exon alignments generated by step 1) of the above-described filtering sequence as some of the filtering steps would have removed indels. We only recorded non-overlapping indels that did not change the exon's reading frame and excluded those indels for which the presence or absence could not be determined in more than five species due to missing sequences. The matrices resulting from the 'strict' and 'permissive' datasets included presence or absence for 654 and 2,253 indels, respectively, of which 191 and 707 indels were parsimony-informative. We used PAUP*[105] (v.4.0a164) to reconstruct maximum-parsimony trees for the 'strict' and 'permissive' indel matrices, which had parsimony scores of 715 and 2,467, respectively. The consensus trees for the 'strict' and 'permissive' indel matrices contained 24 and 35 bifurcating nodes that were all fully concordant with the species trees inferred with the multi-species coalescent model, except for the position of *C. variegatus*, which appeared more closely related to *P. formosa* and *X. maculatus* than to *F. heteroclitus* in the maximum-parsimony trees.

Identification of species with signals of past introgression. As undetected past introgression can influence divergence-time estimates in molecular clock analyses, we tested for signals of introgression among the species in our dataset in the form of asymmetric species relationship in exon or gene trees. For each trio of species A, B, and C, one of the three possible pairs A,B, A,C, or B,C forms a sister group in the true species tree. In the absence of introgression, the multi-species coalescent model predicts this pair to have the highest frequency in a set of local phylogenies and the other two pairs to have frequencies that are similar and reflect the amount of incomplete lineage sorting (ILS). Thus, significant differences in the frequencies of the two alternative pairs can be taken as indication that introgression may have occurred; however, those differences can also arise from other model violations[106]. We tested exhaustively for significant differences between the second-highest and third-highest pair frequencies in all possible trios among the 44 species in our dataset, and then investigated specific signals of introgression further, based on genealogy interrogation[107,108]. We performed these analyses separately for four sets of trees generated with the program IQ-TREE[53] (v.1.6.8) for all gene alignments from both the 'strict' and 'permissive' sets of markers, and for sets of the exon alignments that had been concatenated for the 'strict' and 'permissive' gene alignments. Maximum-likelihood tree inference with IQ-TREE employed the program's standard model selection and two search repetitions per analysis. In agreement with recent phylogenomic studies of teleosts[18,90,96,109], we specified the blenniiform *P. parvicornis* as the outgroup to all other species, except for markers where the *P. parvicornis* sequence was missing; in those cases, all members of Cyprinodontiformes and Beloniformes were used as the outgroup. For each generated tree, we converted nodes separated by branches shorter than 0.001 substitutions per site into polytomies with the function *di2multi* of the R package ape[57] (v.5.2). The resulting tree sets were then queried for the relationships of each possible species trio, and we quantified support for introgression in the tree by applying a statistic that we call D_{tree} to highlight that the statistic is in principle related to Patterson's D statistic[84,110], only that pairs of tips are counted in sets of trees instead of shared alleles along the genome: $D_{tree} = (f_{2nd} - f_{3rd}) / (f_{2nd} +$

f_{3rd}), where f_{2nd} is the frequency of the second-most frequent pairing of two of the three species in the tree set, and f_{3rd} is the frequency of the third-most frequent (i.e. the least frequent) pairing of two species. High values of D_{tree} support introgression between the two species involved in the pair with the second-highest frequency. For example, if species A and B are found as a pair in 900 trees, species A and C form a pair in 80 trees and B and C form a pair in 20 trees, then $f_{2nd} = 80$, $f_{3rd} = 20$, and $D_{tree} = (80 - 20) / (80 + 20) = 0.6$, supporting introgression between species A and C. The significance of the difference between f_{2nd} and f_{3rd} is calculated using a one-sided binomial test. Trees in which the three species form a polytomy are ignored.

The analyses based on the 'strict' and 'permissive' tree sets generally produced the same patterns of D_{tree} variation among trios, but as expected, those based on the larger 'permissive' tree sets were statistically more significant. From the combination of our D_{tree} analyses, we formed nine hypotheses of introgression that we then investigated further with genealogy interrogation[107,108]:

1) Introgression between *H. multidens* and members of the Neotropical cichlid subfamily Cichlinae; supported e.g. by $D_{tree} = 0.19$ ($P < 10^{-6}$) for the species trio *G. ethelwynae*, *H. multidens*, and *A. zaliosus* in the 'strict' set of exon trees.
2) Introgression between *F. heteroclitus* and Poecilidae, supported e.g. by $D_{tree} = 0.25$ ($P < 10^{-4}$) for the species trio *C. variegatus*, *F. heteroclitus*, and *X. maculatus* in the 'strict' set of gene trees or $D_{tree} = 0.10$ ($P < 10^{-8}$) for the same trio in the 'permissive' set of exon trees.
3) Introgression between the Malagasy cichlid subfamily Ptychochrominae and the African subfamily Pseudocrenilabrinae, supported e.g. by $D_{tree} = 0.42$ ($P < 10^{-8}$) for the species trio *G. ethelwynae*, *H. multidens*, and *P. oligocanthus* in the 'strict' set of exon trees.
4) Introgression between the Neotropical cichlid subfamily Cichlinae and the Indian subfamily Etroplinae or the Malagasy subfamily Ptychochrominae, supported e.g. by $D_{tree} = 0.18$ ($P < 10^{-4}$) for the species trio *G. ethelwynae*, *A. coeruleopunctatus*, and *E. canarensis* in the 'strict' set of exons.
5) Introgression between '*T.*' *brevimanus* and *P. mariae*, supported e.g. by $D_{tree} = 0.33$ ($P < 10^{-8}$) for the species trio *H. buttikoferi*, '*T.*' *brevimanus*, and *P. mariae* in the 'permissive' set of gene trees.
6) Introgression between *G. ethelwynae* and *P. mariae*, supported e.g. by $D_{tree} = 0.25$ ($P < 10^{-5}$) for the species trio *H. buttikoferi*, *P. mariae*, and *G. ethelwynae* in the 'permissive' set of gene trees.
7) Introgression between the cichlid tribe Coptodonini and a clade formed by *T. sparrmanii*, *Steatocranus* sp. "ultraslender", and all members of the Lake Tanganyika radiation, supported e.g. by $D_{tree} = 0.45$ ($P < 10^{-8}$) for the species trio *G. ethelwynae*, *M. zebra*, and *C. rendalli* in the 'permissive' set of gene trees.
8) Introgression between the Indian cichlid subfamily Etroplinae and the Malagasy subfamily Ptychochrominae, supported e.g. by $D_{tree} = 0.23$ ($P < 10^{-8}$) for the species trio *G. ethelwynae*, *P. polleni* "Andapa", and *E. canarensis* in both the 'strict' and 'permissive' sets of exon trees.
9) Introgression between a clade formed by *T. sparrmanii* and *Steatocranus* sp. "ultraslender" and a clade formed by *G. ethelwynae*, *'T.' brevimanus*, *P. mariae*, and *H. buttikoferi*, supported by e.g. $D_{tree} = 0.34$ ($P < 10^{-8}$) for the species trio *A. leptura*, *Steatocranus* sp. "ultraslender", and *G. ethelwynae* in the 'permissive' set of exon trees.

We tested each of the nine hypotheses of introgression with genealogy interrogation as described in Barth *et al.*[108]. In brief, we specified for each hypothesis three alternative topology constraints and reran IQ-TREE for each marker of each set with each of the three constraints to compare the relative likelihoods of the constrained trees. For example, to test hypothesis 1), we prepared three constraints where the first enforced monophyly of the African cichlid subfamily Pseudocrenilabrinae, the second enforced monophyly of the Neotropical subfamily Cichlinae and *H. multidens*, and the third enforced monophyly of Pseudocrenilabrinae and Cichlinae without *H. multidens*. While no or only weak and inconsistent support was found for the hypotheses 1), 3), 4), 7), and 8), the results consistently supported hypotheses 2), 5), 6), and 9):

2) With all sets of trees, a majority of markers has a higher likelihood when *F. heteroclitus* is constrained to form a monophyletic group with Poecilidae, compared to when *C. variegatus* (the sister to *F. heteroclitus* in the species trees inferred with ASTRAL) is forced into the same position.
5) With all sets of trees, a majority of markers has a higher likelihood when *'T.' brevimanus* is constrained to form a monophyletic group with *P. mariae*, compared to when *H. buttikoferi* (the sister to *'T.' brevimanus* in the species trees) is forced into the same position.
6) With all sets of trees, a majority of markers has a higher likelihood when *P. mariae* is constrained to form a monophyletic group with *G. ethelwynae*, compared to when *'T.' brevimanus* and *H. buttikoferi* (which together form the sister group to *P. mariae* in the species trees) are forced into the same position.
9) In all sets of trees, a majority of markers have a higher likelihood when *T. sparrmanii* and *Steatocranus* sp. "ultraslender" are jointly constrained to form a monophyletic group with *G. ethelwynae*, *'T.' brevimanus*, *P. mariae*, and *H. buttikoferi*, compared to when all members of the Lake Tanganyika radiation (which together form the sister group to *T. sparrmanii* and *S.* sp. "ultraslender" in the species trees) are forced into the same position.

Based on the corroborated evidence for four cases of past introgression, we excluded the species *F. heteroclitus*, *'T.' brevimanus*, *P. mariae*, *T. sparrmanii,* and *Steatocranus* sp. "ultraslender" from all subsequent molecular-clock analyses.

We repeated the introgression tests described above with further tree sets based on ortholog exons and genes identified in an entirely independent round of the orthology identification workflow that relied on Nile tilapia exon sequences as queries instead of medaka sequences. In this separate application of the ortholog identification workflow, we thus used Nile tilapia as outgroup and excluded all other members of Oreochromini as well as all species more distant to the radiation in Lake Tanganyika than the Oreochromini. Instead, we included newly generated genome assemblies for three additional representatives of the radiation: *Boulengerochromis microlepis* (voucher JCF2), *Bathybates fasciatus* (ITH3), and *Hemibates koningsi* (IZA5) to allow a better focus on possible introgression events connected to the early lineages of Lake Tanganyika. In this round of ortholog identification, the application of 'strict' filters resulted in sets of 2,381 exons and 536 genes with a total alignment length of 591,993 bp, whereas 'permissive' filters produced sets that comprised 3,466 exons and 762 genes with a total of 956,463 bp. The introgression tests confirmed the above-listed hypotheses 5), 6), and 9)

and did not produce consistent signals for further introgression events involving the three additional Lake Tanganyika species.

Phylogenetic divergence-time estimation. As we expected that ILS could have occurred among the species included in our molecular-clock analyses, we estimated divergence times among cichlid fishes and the age of the cichlid adaptive radiation in Lake Tanganyika under the multi-species coalescent model, using the StarBEAST2[51] (v.0.15.5) add-on package for BEAST 2. However, despite recent speed improvements, StarBEAST2 remains computationally demanding as it estimates all marker trees jointly with the species tree. To achieve feasible run times, we therefore had to streamline the analysis in the following ways:

- We only used the 'strict' set of genes.
- We constrained the monophyly in the species tree of 34 groups that are unambiguously supported by recent phylogenomic studies[18,22,96].
- We performed parallel analyses with different fixed population sizes (see below) instead of estimating the population size from the data.
- We applied the strict molecular clock model instead of a relaxed-clock model, assuming that substitution rates are comparable at least among the Neotropical and African cichlid subfamilies Cichlinae and Pseudocrenilabrinae and that errors that could potentially result from rate variation between cichlids and outgroups do not propagate to age estimates within the subfamilies as long as the ages of subfamilies themselves are correctly constrained.
- We used the Generalised time-reversible (GTR) substitution model with gamma-distributed among-site rate variation instead of performing Bayesian model averaging.
- Instead of estimating all parameters independently for each gene, we linked the absolute substitution rates, the GTR model's relative substitution rates and base frequencies, and the alpha parameter of the gamma-distributed among-site rate variation according to partitioning schemes estimated with the program PartitionFinder[111] (v.2.1.1). Prior to these analyses with PartitionFinder, we split all gene alignments by codon position and excluded third codon positions to avoid possible effects of alignment saturation. Data blocks of first codon positions per gene and blocks of second codon positions per gene were used in separate PartitionFinder analyses (but per gene, the block composed of first codon positions and the block composed of second codon positions were forced to share the same gene tree in the subsequent StarBEAST2 analysis). The PartitionFinder analyses were repeated twice so that data blocks were first clustered by their absolute substitution rates and then by the fitted parameters of the GTR model with gamma-distributed among-site rate variation. In all PartitionFinder analyses, we employed the 'rcluster' algorithm with clustering based on the Akaike information criterion (AIC), we assumed linked branch lengths, and we required a minimum of 10,000 sites in each partition. These settings grouped the first codon position blocks into 13 partitions when clustering was based on absolute substitution rates and into six partitions when clustering was based on the GTR model parameters. The second codon position blocks were also grouped into 13 partitions when clustering was based on absolute substitution rates and into nine partitions when GTR model parameters were considered; when generating the settings file for the

StarBEAST2 analyses, the model parameters of different data blocks were linked exactly according to these partitions.

The settings for the StarBEAST2 analysis further included the birth-death model of diversification with extinction[112] and five different age constraints to calibrate divergence times, each of which was in accordance with the timeline estimated by Matschiner *et al.*[18] and implemented through a lognormal prior distribution: The age of the root was set to 92.0 Ma (with a standard deviation in log space of 0.05), the divergence of cichlids was set to 87.5 Ma (with a standard deviation of 0.06), the divergence between Beloniformes and Cyprinodontiformes was set to 74.9 Ma (with a standard deviation of 0.09), the divergence of Etroplinae was set to 76.8 (with a standard deviation of 0.07), and the divergence of Pseudocrenilabrinae and Cichlinae was set to 62.1 Ma (with a standard deviation of 0.21). We performed 19 replicate analyses for each of four assumed effective population sizes: 83,333, 166,667, 333,333, and 666,667 (in each case also assuming a generation time of 3 years[33]). Despite our model simplifications, the analyses of our dataset, which was unusually large for StarBEAST2 analyses with 510 genes and a total alignment length of 542,922 bp, required up to 10 billion MCMC iterations and a run time (wall time) of around 50 days for each of the 76 replicates to reach convergence (ESS values above 200 for all model parameters). We removed the first 55% of each completed MCMC chain as burn-in, merged the posterior distributions of the 19 replicate analyses per assumed effective population size, and thinned each merged posterior distribution to 1,000 MCMC states. From these, we generated maximum-clade-credibility consensus trees with the program TreeAnnotator. With an assumed effective population size of 666,667, the divergence of the Neotropical cichlid subfamily Cichlinae and the African subfamily Pseudocrenilabrinae was estimated at 61.6 Ma with a 95% highest-posterior-density (HPD) interval from 63.9-56.2 Ma, in agreement with the constraint centred on 62.1 Ma that we had placed on this node according to the timeline estimated by Matschiner *et al.*[18]. The age of the adaptive radiation of cichlid fishes in Lake Tanganyika, marked by the divergence between Trematocarini and the combined Lamprologini, Ectodini, and Haplochromini, was estimated in these analyses at 9.6 Ma with a 95% HPD interval from 10.1-9.1 Ma (Extended Data Fig. 1). Thus, even though the age of Lake Tanganyika, which has long been assumed to lie between 12-9 Ma[17,23], was not used as an age constraint in our analyses, our results are fully consistent with an endemic adaptive radiation of cichlid fishes soon after the early colonization of the lake by a single lineage.

In the analyses based on smaller assumed effective population sizes, the estimated age for the divergence of Cichlinae and Pseudocrenilabrinae was younger than the constraint that we had placed on this node, namely between 49.5 and 47.5 Ma instead of around 61.6 Ma[18]. We attribute this discrepancy to a conflict with the older age constraints caused by substitution-rate variation in the outgroups that was not accounted for in our analysis. After scaling the age estimates of these alternative analyses so that the divergence between Cichlinae and Pseudocrenilabrinae matches the previously determined age of around 62.1 Ma[18], the age estimates for the Lake Tanganyika radiation were 9.6 Ma, 9.4 Ma, and 9.5 Ma with assumed effective population sizes of 83,333, 166,667, and 333,333, respectively, thus corroborating our conclusion of a radiation onset around 9.6 Ma.

Phylogenetic inference

To investigate the phylogenetic structure of the cichlid radiation of Lake Tanganyika, we performed phylogenetic analyses based on genome-wide nuclear SNPs as well as assembled mitochondrial genome sequences.

Maximum-likelihood inference of among-sample relationships from genome-wide nuclear SNPs. Nuclear SNPs were used to infer a phylogeny of 518 individuals (including both phased haplotypes for each of the two *N. cancellatus* specimens) with the software RAxML[52] (v.8.2.4), using the GTRCAT substitution model. For this phylogenetic analysis, the dataset of 57,751,375 SNPs was further filtered with BCFtools to exclude sites with more than 40% missing data, followed by thinning of the dataset with VCFtools so that no two SNPs were closer than 100 bp to each other, and by discarding the second of the phased alleles of each genotype. This resulted in a dataset of 3,630,997 SNPs. The analysis accounted for the absence of invariable sites with the ascertainment bias correction developed by Felsenstein[113] and implemented in RAxML. To apply this correction, we determined the number of omitted invariant sites as the difference between the number of all callable sites (sites that were neither masked due to potentially ambiguous read mapping nor due to proximity to indels; see above) and the number of variable sites, considering the additional filtering and thinning of the dataset. To assess reliability of the results, we performed five replicates of this analysis. The phylogeny was rooted using the outgroup taxa *S.* sp. "ultraslender", *G. ethelwynae*, '*T.' brevimanus*, *P. mariae*, and *H. buttikoferi*.

Instead of applying bootstrapping, which can lead to inflated support values when concatenated alignments are used[114], we estimated node support by dividing the dataset of sites with less than 40% missing data into 100 non-overlapping subsets that each contained 471,991 SNPs, and inferring a phylogeny separately from each of these subsets. We then quantified node support for every node in the phylogeny inferred with the dataset of 3,630,997 SNPs, as the number of subset phylogenies that supported this node (Extended Data Fig. 2; tree file available on Dryad; https://doi.org/10.5061/dryad.9w0vt4bbf: 05_RAxML.tre)

A species-level tree was generated from this sample-level phylogeny by excluding for each species all tips except the one for the sample with the lowest proportion of missing data. This species-level maximum-likelihood tree inferred with RAxML was subsequently used as the first out of three topological constraints in relaxed-clock analyses of divergence times within the radiation (see below in section "Divergence time estimates within the radiation").

Species-tree inference from selected genomic regions. From the full dataset containing 57,751,375 SNPs, we generated sequence alignments for each non-overlapping window of a length of 5,000 bp (excluding the sequences of the two *N. cancellatus* specimens). For sites that were not included in the SNP dataset, it was assumed that these were invariable and identical to the corresponding site in the Nile tilapia reference genome. However, to account for potential unidentified variation, parts of all sequences were masked according to whether variation could have been detected if it existed. Thus, all regions excluded from the SNP dataset due to potentially ambiguous mapping or proximity to indels were again masked, but in addition, we also masked regions in which the overall read depth across all samples was either below 4,000 or above 8,000, and we masked, per individual, those regions where

less than 4 reads had sufficient quality for variant calling with GATK. Window alignments were further filtered according to multiple criteria to identify the most suitable alignments for phylogenetic inference: First, alignments were discarded if the overall proportion of missing data was above 70% or if the standard deviation of the proportion of missing data across tribes was above 0.02; the latter filter was applied to exclude windows with tribe-specific deletions. Second, the local phylogeny was inferred for each alignment with RAxML based on the GTRCAT substitution model, after excluding alignment regions that had a gap rate above 0.2 or an entropy score above 0.5; these values were determined with BMGE. For each local phylogeny, the Robinson-Foulds distance[115] to the phylogeny inferred from genome-wide SNPs with RAxML was calculated with the Python (v.2.7.10) package ete3[116] (v.3.1.1), and the alignment was excluded from further analysis if the calculated distance was above 700. Third, after reducing all alignments to sequences of the one individual per species that had the lowest proportion of missing data, we calculated the number of hemiplasies per alignment, assuming that this number can serve as an indicator of within-alignment recombination[117]. The number of hemiplasies was calculated as the difference between the number of variable sites and the parsimony score, which was determined with PAUP* (v.4.0a163). Subsequently, the most suitable alignments for phylogenetic inference were selected from the ones remaining in the dataset as those characterized by an alignment length greater than 2,000 bp after filtering, a number of variable sites greater than 400, and a number of hemiplasies below 200. These criteria were met by 1,272 alignments, which had a total length of 3,219,018 bp and an overall completeness of 95.1%. For each of these 1,272 alignments, maximum-likelihood trees were generated with IQ-TREE (v.1.7-beta7), assuming the GTR substitution model with gamma-distributed among-site rate variation. The maximum-likelihood trees generated by IQ-TREE were then used as input for species-tree inference under the multi-species coalescent model with ASTRAL. This species tree inferred with ASTRAL was subsequently used as the second out of three topological constraints in relaxed-clock analyses of divergence times within the radiation (see below in section “Divergence time estimates within the radiation”).

Bayesian inference of the species tree from genome-wide nuclear SNPs. We performed Bayesian species tree inference with the SNP-based molecular-clock approach of Stange *et al.*[118], using the SNAPP[54] (v.1.4.2) add-on package for BEAST 2. However, due to the high computational demand of SNAPP analyses caused by the mathematical integration over all possible trees at each SNP, we could not analyse all species of the cichlid adaptive radiation of Lake Tanganyika in a single analysis. Instead, we performed one backbone analysis with representatives of the two most divergent lineages per tribe and then used the resulting age estimates for the first within-tribe divergences as secondary age constraints for per-tribe analyses.

We selected 27 samples for the backbone analysis, so that all tribes of the radiation, except for the monotypic Boulengerochromini, were represented by at least two species descending from opposite sides of the first within-tribe divergence according to the species-level trees inferred with RAxML and ASTRAL (see above in section “Maximum-likelihood inference of among-sample relationships from genome-wide nuclear SNPs” and “Species-tree inference from selected genomic regions”, respectively). Wherever we could opt between multiple samples, we selected the one with the highest read depth after mapping. For Boulengerochromini, we included sample JCF2. In both the RAxML and

ASTRAL trees, the first divergence within Trematocarini separated *Trematocara unimaculatum* from the remaining Trematocarini; thus, we selected the *T. unimaculatum* sample with the highest read depth (IXA6) together with the sample with the highest read depth among the remaining Trematocarini, which was a *T. marginatum* (ISA3). For Bathybatini, the RAxML and ASTRAL trees agreed that the first within-tribe divergence occurred between the genera *Hemibates* and *Bathybates*; thus, we selected the samples with the highest read depth of each of the two genera, a *Hemibates koningsi* (IZA5) and a *Bathybates fasciatus* (ITH3). For Lamprologini, both trees strongly supported the same two monophyletic subgroups that included 37 and 70 species, respectively; we selected one *N. variostigma* (JWA6) and one *Julidochromis* sp. "unterfels" (JWA2) as the samples with the highest read depths in each of the two subgroups. For Cyphotilapiini, the two trees both supported *Ctenochromis benthicola* as the sister group to three species of the genus *Cyphotilapia*; thus, we selected a *Ctenochromis benthicola* (DMD1) and a *Cyphotilapia* sp. "5-bar frontosa" (KDG2). For Limnochromini, the two trees disagreed in the composition of the two clades descending from the first within-tribe divergence; however, both trees placed *Triglachromis otostigma*, *Tangachromis dhanisi*, *Reganochromis calliurus*, and *Baileychromis centropomoides* on one side of the first within-tribe divergence and *Gnathochromis permaxillaris*, *Limnochromis abeelei*, *L. staneri*, and two species of *Greenwoodochromis* on the other side; thus, we selected a *T. dhanisi* (LJA8) and a *L. staneri* (ITA6). For Ectodini, both trees placed *G. lemairii* as the sister species to a clade formed by all other members of the tribe; thus, we selected a *G. lemairii* (JDD7) and a *Xenotilapia flavipinnis* (JAF7). For Cyprichromini, both trees agreed that the first divergence occurred between the genera *Cyprichromis* and *Paracyprichromis*; thus, we selected a *Cyprichromis coloratus* (JEC7) and a *Paracyprichromis* sp. "tembwe" (JWD1). For Benthochromini, both trees placed *Benthochromis tricoti* and *B. melanoides* on one side of the first within-tribe divergence and *B. horii* and *B*. sp. "horii mahale" on the other side; thus, we selected a *B. melanoides* (ILG3) and a *B*. sp. "horii mahale" (LEF2). For Perissodini, both trees placed the first divergence between *Xenochromis hecqui*, *Plecodus elaviae*, *Plecodus multidentatus*, and *Perissodus eccentricus* on one side and *Haplotaxodon microlepis*, *H. trifasciatus*, *Plecodus paradoxus*, *P. straeleni*, and *Perissodus microlepis* on the other side; thus, we selected a *P. multidentatus* (IZA8) and a *P. straeleni* (INE8). For Eretmodini, both trees agreed that the first divergence occurred between *Tanganicodus irsacae* and *Eretmodus cyanostictus* on the one side and *Eretmodus marksmithi*, *Spathodus marlieri*, and *S. erythrodon* on the other side; thus, we selected an *E. cyanostictus* (IZH7) and an *E. marksmithi* (JXE9). For Tropheini, both trees supported the same two subgroups composed of 13 and 27 species, respectively; we selected a *Tropheus annectens* (JWG4) and a *Petrochromis trewavasae* (IWC9) as representatives of these two subgroups. Finally, the remaining lineages traditionally assigned to Haplochromini formed four strongly supported subgroups in both trees: The first included all *Orthochromis* species except *O. indermauri*, the second included *O. indermauri* together with *Pseudocrenilabrus philander*, the third included *Ctenochromis polli*, *Thoracochromis brauschi*, *Serranochromis macrocephalus*, *Sargochromis carlottae*, and *Pharyngochromis acuticeps*, and the fourth was composed of eight species of the genera *Haplochromis*, *Astatotilapia*, and *Astatoreochromis*. We included one representative of each of these four subgroups in our backbone analyses. These were an *Orthochromis uvinzae* (KYE7), an *O. indermauri* (HXC6), a *S. macrocephalus* (JWF5), and an *A. burtoni* (IZC5).

We generated all input files for SNAPP analyses with the script 'snapp_prep.rb'[118] and constrained the divergence between the three tribes Boulengerochromini, Trematocarini, and Bathybatini and all other tribes with a normally distributed prior that was centred at 9.7 Ma and had a standard deviation of 0.3, according to our estimates of the age of the cichlid adaptive radiation in Lake Tanganyika. To achieve feasible run times with SNAPP, we limited the analysis to a maximum of 10,000 variable sites, which were randomly sampled from all sites that were variable among the 27 species included in the backbone analysis. Unlike in the other phylogenetic analyses based on SNP data described above, we used the more strictly filtered SNP dataset with a minimum genotype quality of 30 for our analyses with SNAPP. As the starting tree topology, we selected the one resulting from the RAxML analysis, pruned to include the 27 species only. We performed 10 replicate SNAPP analyses, each with a run length of 1 million MCMC iterations. Convergence of MCMC chains was assessed visually with the program Tracer[119] (v.1.7.1) by comparing parameter traces across replicate analyses, and confirmed by ESS values greater than 200. After discarding the first 10% of each MCMC chain as burn-in, we merged the posterior distributions of all replicates and used these to generate maximum-clade-credibility trees with TreeAnnotator.

The ages of the first within-tribe divergences were estimated at 3.09 Ma (95% HPD: 3.42-2.77 Ma) for Trematocarini, 4.94 Ma (95% HPD: 5.40-4.53 Ma) for Bathybatini, 4.55 Ma (95% HPD: 4.93-4.13 Ma) for Lamprologini, 2.26 Ma (95% HPD: 2.60-1.93 Ma) for Cyphotilapiini, 3.73 Ma (95% HPD: 4.14-3.34 Ma) for Limnochromini, 4.35 Ma (95% HPD: 4.76-4.01 Ma) for Ectodini, 2.79 Ma (95% HPD: 3.11-2.48 Ma) for Cyprichromini, 0.21 Ma (95% HPD: 0.29-0.13 Ma) for Benthochromini, 1.31 Ma (95% HPD: 1.52-1.11 Ma) for Perissodini, 1.20 Ma (95% HPD: 1.37-1.03 Ma) for Eretmodini, and 3.02 (95% HPD: 3.34-2.68 Ma) for Tropheini. Of the four representatives of subgroups traditionally assigned to Haplochromini, *O. uvinzae* was estimated to have diverged from all other haplochromine lineages at 5.84 Ma (95% HPD: 6.29-5.44 Ma), *O. indermauri* and *S. macrocephalus* were estimated to have diverged at 4.65 Ma (95% HPD: 5.03-4.31 Ma), and *A. burtoni* was estimated to have diverged from Tropheini at 4.39 Ma (95% HPD: 4.75-4.03 Ma).

These age estimates were subsequently used to define normally-distributed priors as age constraints on the first within-tribe divergence in tribe-specific SNAPP analyses that used the same settings as the backbone analysis. For all tribes for which the RAxML and ASTRAL trees agreed on the exact composition of the two subgroups descending from the first within-tribe divergence (thus, all tribes except Limnochromini; see above), we constrained the monophyly of each of these two subgroups. In the case of Trematocarini, where the RAxML analyses suggested the possible presence of substitution-rate variation between the lineages descending from the first within-tribe divergence, we added two species of Bathybatini, *H. koningsi* (IZA5) and *B. fasciatus* (ITH3), as outgroups, and added monophyly constraints for both the ingroup and the outgroup to ensure the correct placement of the within-tribe root position. As a consequence of the outgroup addition, the age constraint was in this case not placed on the very first divergence of the tree, but only on the first divergence within the tribe Trematocarini. We also added outgroup species in the analyses of each of the four subgroups of lineages traditionally assigned to Haplochromini, as this allowed us to constrain their divergence times based on the backbone

analysis even though the backbone analysis had only included a single representative of each of the four subgroups.

As each of the three tribes Lamprologini, Ectodini, and Tropheini were too large to allow the joint analysis of all their members with SNAPP, we divided these tribes into sets of unambiguously supported subgroups and performed another layer of backbone analyses within these tribes as well as separate analyses of each subgroup. For Lamprologini, we identified five subgroups that were strongly supported by both the RAxML and ASTRAL trees: The first of these included 8 species, of which 6 were of the genus *Lamprologus* (e.g. *L. kungweensis*) and 2 were of the genus *Neolamprologus* (e.g. *N. ventralis*). The second subgroup counted 19 species, including 3 species of the genus *Altolamprologus* (e.g. *A. compressiceps*), 4 species of the genus *Lamprologus* (e.g. *L. ocellatus*), 7 species of the genus *Lepidiolamprologus* (e.g. *L. elongatus*), and 5 species of the genus *Neolamprologus* (e.g. *N. meeli*). The third subgroup counted 16 species, all of which were of the genus *Neolamprologus* (e.g. *N. brichardi*). The fourth subgroup counted 20 species, including *Lamprologus tigripictilis*, *Lepidiolamprologus cunningtoni*, 7 species of the genus *Neolamprologus* (e.g. *N. modestus*), and all 11 species of the genus *Telmatochromis*. The fifth subgroup counted 29 species, including 14 species of the genus *Neolamprologus* (e.g. *N. buescheri*), all 5 species of the genus *Chalinochromis*, and all 10 species of the genus *Julidochromis*. In total, the five subgroups included all but 15 species of Lamprologini. For our within-tribe backbone analysis, we thus selected the 15 species that were not included in any subgroup as well as two representatives of each subgroup. Like for our overall backbone analysis, these two representatives were selected so that their divergence was the first within-subgroup divergence and their read depths were maximized. Thus, we selected one *Neolamprologus ventralis* (Burundi) (KAG8) and one *Lamprologus ornatipinnis* (JZF3) as representatives of the first subgroup, a *N. variostigma* (JWA6) and a *Neolamprologus pleuromaculatus* (JZF2) as representatives of the second subgroup, a *Neolamprologus falcicula* (JXD7) and a *Neolamprologus gracilis* (JWH2) as representatives of the third subgroup, a *Lepidiolamprologus cunningtoni* (IOH5) and a *Telmatochromis* sp. “dhonti twiyu” (LHC1) as representatives of the fourth subgroup, and a *Neolamprologus pectoralis* (JWA7) and a *Julidochromis* sp. "unterfels" (JWA2) as representatives of the fifth subgroup.

For Ectodini, we used two subgroups that were unambiguously supported by both the RAxML and ASTRAL trees. The first of these contained 15 species and included all species of the genera *Ophthalmotilapia* (6 spp.), *Ectodus* (2 spp.), *Cyathopharynx* (2 spp.), *Lestradea* (2 spp.), as well as *Cardiopharynx schoutedeni*, *Aulonocranus dewindti*, and *Cunningtonia longiventralis*. The second subset counted 21 species and included all species of the genera *Xenotilapia* (17 spp.), *Microdontochromis* (2 spp.), as well as *A. leptura* and *Enantiopus melanogenys*. *G. lemairii* and three species of the genus *Callochromis* were not included in these subsets. Thus, we used these latter four species as well as two representatives of each of the two subgroups in our within-tribe backbone analysis. As representatives, we selected *C. schoutedeni* (KAF2), *O.* sp. “paranasuta” (JYF7), *X. caudafasciata* (IXB9), and *X. flavipinnis* (JAF7), again based on the same criteria as for the other backbone analyses. To ensure correct placement of the within-tribe root position, we further added two outgroups from the tribe Limnochromini, namely a *L. staneri* (ITA6) and a *T. dhanisi* (LJA8).

We also used two unambiguously supported subgroups for Tropheini. The first of these included all 13 species of the genus *Tropheus*, while the second counted 27 species including all species of the genera *Petrochromis* (16 spp.) and *Pseudosimochromis* (5 spp.) as well as *Lobochilotes labiatus*, *Interochromis loocki*, *Limnotilapia dardennii*, *Gnathochromis pfefferi*, *Ctenochromis horei*, and *Simochromis diagramma*. As representatives of these subgroups in the within-tribe backbone analysis, we used a *Tropheus duboisi* (KHA5), a *T. annectens* (JWG4), a *L. labiatus* (ISD8), and a *Petrochromis trewavasae* (IWC9). We further added an *Astatoreochromis straeleni* (KAE8) and an *A. burtoni* (IZC5) as outgroups.

For the fifth subgroup of Lamprologini and the second subgroup of Tropheini, fewer than 1,000 sites were variable and sufficiently complete within the group, due to the requirement for SNAPP analyses that all sites must have data for at least one sample of each species. For the SNAPP analyses of these two groups, we therefore used the SNP dataset with a minimum genotype quality of 20, instead of the more strictly filtered one with a quality threshold of 30 that was used for all other SNAPP analyses. This change allowed us to use the maximum amount of 10,000 variable sites for the SNAPP analyses of the two subgroups.

We again performed ten replicate analyses per group, each of which included 1 million MCMC iterations, and we resumed these for another 1 million iterations in a few cases in which the MCMC chains had not sufficiently converged after the first million iterations. The proportion of each MCMC chain that was discarded as burn-in was again set to a minimum of 10% and increased if the visual inspection of traces indicated a longer burn-in phase. For each set of analyses, we generated a combined posterior distribution by sampling 1,000 states from the post-burn-in MCMC chains of the ten analysis replicates.

Finally, the backbone and tribe-specific trees resulting from the SNAPP analyses were combined to produce complete species trees of the Lake Tanganyika cichlid radiation. Instead of combining only summary trees from all SNAPP analyses, we combined all 1,000 trees of the posterior tree distributions of each analysis to form a distribution of 1,000 trees including all species. The tree combination was done iteratively – integrating the tribe-specific trees into the backbone trees one by one – by replacing the placeholder tips in the backbone trees with the trees (after pruning the outgroups if any were used) from tribe-specific analyses. Instead of simply integrating the n^{th} tree from the tribe-specific posterior distribution into the n^{th} tree from the backbone posterior distribution, we made the replacement under consideration of the age of the connection node in the two trees. Thus, prior to each integration of a tribe-specific tree distribution into the backbone tree distribution, we ranked both the 1,000 trees from the tribe-specific distribution and the 1,000 trees from the backbone distribution by the age of the connection node, and then integrated tribe-specific trees into the backbone trees according to this rank. For example, prior to integrating the tribe-specific trees for Bathybatini into the backbone trees, the 1,000 backbone trees were ranked by the age of the two placeholder species *Hemibates koningsi* and *Bathybates fasciatus*. Similarly, the 1,000 tribe-specific trees were ranked by the age of their root node, at which *Hemibates* and *Bathybates* diverge. The two placeholder species in the first-ranked backbone tree were then replaced with the first-ranked of the tribe-specific trees and so forth. At the end of this process, all placeholder species in the backbone trees were replaced with (pruned) tribe-specific trees,

forming 1,000 species-complete trees of Lake Tanganyika cichlid fishes. From this tree distribution, we generated a maximum-clade-credibility tree with the program TreeAnnotator.

Even though the SNAPP analysis produced age estimates for every divergence event, these were based on the strict molecular clock model (the only clock model available in SNAPP) and may therefore be misleading in the presence of substitution-rate variation. For this reason, we estimated divergence times within the radiation separately with a relaxed-clock model; however, as relaxed-clock models can so far not be applied to genome-wide SNPs, these analyses were based on selected genomic regions (see below in section "Divergence time estimates within the radiation"). Nevertheless, we used the results of the SNAPP analysis to inform the relaxed-clock analyses by providing the maximum-clade-credibility tree as the third out of three topological constraints in the divergence time analyses.

Quartet inference of the species tree from genome-wide nuclear SNPs. The thinned dataset generated for phylogenetic inference from nuclear SNPs was also used to infer the species tree of 270 species included in the SNP dataset (and with both phased haplotypes for each of the two *N. cancellatus* specimens), using the quartet approach of SVDQuartets[120] implemented in the program PAUP* (v.4.0a161). A maximum of 300 million randomly selected quartets (about a third of all possible quartets) were analysed in the inference. The support for nodes in the resulting species tree was again quantified based on the 100 subsets of the SNP data generated for phylogenetic inference from nuclear SNPs (data not shown; tree files available on Dryad; https://doi.org/10.5061/dryad.9w0vt4bbf: 05_SVDquartets.tre, 05_SVDquartets_sub1.tre, 05_SVDquartets_strictlyfiltered.tre, 05_SVDquartets_strictlyfiltered_sub1.tre).

Inference of the mitochondrial phylogeny. For each individual, reads mapping to the mitochondrial genome of Nile tilapia (NCBI accession NC_013663.1) were extracted from BAM files, converted into FASTQ format with Picard-tools, and assembled with the iterative MITObim[121] (v.1.8) approach based on the MIRA[122] (v.4.0.2) assembler. The assembled mitochondrial genome sequences of all 528 individuals (including the two *N. cancellatus* samples) were then used to generate a multiple sequence alignment with MAFFT[97] (v.7.300). The mitochondrial genome-wide alignment was divided into separate alignments for each of the 12 mitochondrial protein-coding genes except *ND6*. These alignments were further split according to codon position, and the 36 resulting alignments were used to define partitions for maximum-likelihood phylogenetic inference, performed with RAxML on the basis of the GTRCAT substitution model (Supplementary Fig. 2; tree file and mitochondrial genomes are available on Dryad; https://doi.org/10.5061/dryad.9w0vt4bbf: 03_mitochondrial_assemblies.tgz, 05_mitogenome.tre).

Divergence time estimates within the radiation

We used a selected set of the phylogenetically most suitable alignments for divergence time estimation under the relaxed-molecular-clock model. The alignments were selected from the genome-wide set of alignments described above, using the same settings as for the selection of alignments for species-tree inference with ASTRAL (see above), except that the minimum alignment length was set to 2,500 bp after filtering with BMGE, and the maximum number of hemiplasies was set to 130. These criteria were met by ten alignments, which had a total length of 30,738 bp and a completeness of 95.8%.

Divergence times were inferred with BEAST 2, and the bModelTest package was used to average over substitution models for each alignment separately. We assumed a birth-death process of diversification[112] and applied the uncorrelated lognormal relaxed-clock model[101] to account for branch-rate variation. To achieve feasible run times with the computationally demanding relaxed-clock analyses, we were forced to constrain the tree topology; however, we accounted for phylogenetic uncertainty by performing three separate sets of analyses in which the topology was either fixed to the species-level phylogeny inferred with RAxML from the dataset of genome-wide SNPs (see above in section "Maximum-likelihood inference of among-sample relationships from genome-wide nuclear SNPs", Extended Data Fig. 2), the species tree inferred with ASTRAL from selected genomic regions (see above in section "Species-tree inference from selected genomic regions"; Extended Data Fig. 3), or the Bayesian species tree inferred with SNAPP from genome-wide SNPs (see above in section "Bayesian inference of the species tree from genome-wide nuclear SNPs"; Extended Data Fig. 4). In each case, the age of the root was calibrated with a normal prior distribution centred at 9.7 Ma[18]. Ten replicate BEAST 2 analyses were performed with each tree topology, with chain lengths of 20 million MCMC iterations per replicate. Convergence of MCMC chains was supported by ESS values greater than 200 for all model parameters. The posterior distributions of all replicate analyses were merged and maximum-clade-credibility trees were produced with TreeAnnotator (Fig. 1, Extended Data Figs. 2-4, tree files available on Dryad; https://doi.org/10.5061/dryad.9w0vt4bbf: 05_BEAST_RAxML.tre, 05_BEAST_ASTRAL.tre, 05_BEAST_SNAPP.tre).

2D-Morphometrics

To quantify body shape and upper oral jaw morphology, we applied a landmark-based geometric morphometric approach to digital X-ray images (for the full set of 10 specimens per species whenever possible; n = 2,197).

X-ray imaging. We acquired X-ray images of the full body of the specimens using a Faxitron Digital Specimen Radiography System LX-60, with 35 kV tube voltage and 0.3 mA tube current. Exposure times varied between 10-20 sec depending on the size of the specimen.

Landmark placing. We selected 21 landmarks, of which 17 were distributed across the skeleton and four defined the premaxilla (see Extended Data Fig. 5a). Landmark coordinates were digitized by a single person (to avoid investigator bias) using the software FIJI[55] (v2.0.0-rc-68/1.521i).

Body shape. To extract overall body shape information, we excluded landmark 16, which marks the lateral end of the premaxilla, hence minimizing the impact of the orientation of the upper oral jaw. We then applied a Procrustes superimposition to remove the effect of size, orientation, and translational position of the coordinates, followed by a PCA. Landmark coordinates were processed and analysed in R[59] (v.3.5.2) using the package geomorph[60] (v.3.0.7).

Upper oral jaw morphology. For upper oral jaw morphology, we used a subset of four landmarks. A crucial feature of the oral jaw morphology is the orientation of the mouth relative to the body axes. However, this component of the upper oral jaw morphology would be lost in a classical geometric morphometric analysis, in which only pure shape information is retained. To overcome this, we

extracted the premaxilla-specific landmarks (1, 2, 16, and 21) *after* Procrustes superimposition of the entire set of landmarks and subsequently re-centred the landmarks to align the specimens without rotation. Thus, the resulting landmark coordinates do not represent the pure shape of the premaxilla but additionally contain information on its orientation and size in relation to body axes and body size, respectively. We then performed a PCA to identify the major axes of shape variation across the multivariate dataset. Landmark coordinates were processed and analysed in R using the package geomorph.

3D-Morphometrics

To quantify lower pharyngeal jaw bone shape in 3D, a landmark-based geometric morphometric approach was applied on μCT-scans of the head region of five specimens per species (n = 1,168).

CT-scanning. We acquired CT-scans of typically five specimens per species (n = 1,168) on a Bruker Skyscan 1174v2, at 50 kV and 800 μA. Depending on the size of the specimens, we used different filtering options ranging from no filter up to 1 mm aluminium filter; exposure time was adjusted accordingly. Voxel size ranged between 6.6 μm and 29.9 μm with typically 400 projections. Reconstruction was performed using NRecon (v.1.6.10.2), while parameter settings were adjusted to optimize each scan individually. For very large specimens (> 25 cm SL) we used a Nikon XT H 225 ST with a rotating target for scanning and CT Pro 3D (V5.1.6054.18526) for reconstruction.

Landmark placing. To capture all potential functionally important structures of the lower pharyngeal jaw bone, we selected a set of 27 landmarks (10 true landmarks and 17 sliding semi-landmarks) well distributed across the left side of the bone (see Extended Data Fig. 5b). Landmark coordinates were acquired by a single person using the TINA manual landmarking tool[56], which allows digitization of 3D landmarks directly in the volume (image stack). To place semi-landmarks equally distant along ridges (ventral sagittal ridge, lateral ridge, and posterior ridge), we used three plane points to span a grid intersecting the respective ridge.

Landmark superimposition. To retain the lateral symmetric properties of the shape data during superimposition, we reconstructed the right side of the lower pharyngeal jaw bone by mirroring the landmark coordinates across the plane of bilateral symmetry fitted through all landmarks theoretically lying on this plane. The resulting set of 42 landmarks was then superimposed while sliding the semi-landmarks along the curves by minimizing Procrustes distances. To remove the remaining asymmetric component of shape variation (produced by the deviation of the non-paired landmarks from the fitted plane of bilateral symmetry), we extracted the symmetric component using the function *bilat.symmetry*, followed by a PCA. Landmark coordinates were processed and analysed in R using the package geomorph.

Stable isotope analysis

To approximate ecology for each species, we measured the stable carbon (C) and nitrogen (N) isotope composition of all available individuals per species (n = 2,259). We analysed a small (0.5 – 1 mg) dried muscle sample of each specimen with a Flash 2000 elemental analyser coupled to a Delta Plus XP continuous-flow isotope ratio mass spectrometer (IRMS) via a Conflo IV interface (Thermo Fisher

Scientific, Bremen, Germany). Carbon and nitrogen isotope data were normalised to the VPDB (Vienna Pee Dee Belemnite) and Air-N_2 scales, respectively, using laboratory standards that were calibrated against international standards. Values are reported in standard per-mil notation (‰), and long-term analytical precision was 0.2‰ for $\delta^{13}C$ values and 0.1‰ for $\delta^{15}N$ values. Note that we have used some of these stable isotope values in a previous study[62].

Baseline data. As the carbon and nitrogen stable isotope composition can be influenced by the varying biochemistry of the local environment, we additionally collected and analysed a baseline dataset covering several trophic levels form the northern and the southern basin of the lake to assure interpretability of the measured stable isotope values in cichlids. This baseline dataset included benthic samples (plants (*Hydrilla* and *Vallisneria* spp.), snails (*Lavigeria* spp.), and phytoplankton; collected near-shore in water depths of less than 5 m) as well as pelagic samples (pelagic shrimps, lake sardines (*Stolothrissa tanganicae*), and zooplankton; collected offshore).

Further, we used the stable isotope dataset of the cichlids (n = 2,259) to test whether there is a general trend in the stable isotope data that can be explained by the latitudinal and longitudinal gradient of the sampling localities. To do so, we fitted multiple regression models with stable isotope values as response variable ($\delta^{15}N$ and $\delta^{13}C$, respectively) and longitude, latitude, and species as covariates – allowing interaction (isotope ~ latitudinal * longitudinal * species). We then applied an ANOVA on each of the fitted models to calculate for each covariate and their interactions the percentage of variance explained. Additionally, we grouped the different cichlid species into ecological categories (based on the available literature[85] as well as our own observations during specimen collection) according to their trophic level (i.e. scale eaters, piscivores, fish and invertebrate feeder, fry and plankton feeder, plankton feeder, plankton feeder and invertebrate feeder, invertebrate feeder, omnivore, aufwuchs and invertebrate feeder, aufwuchs and algae feeder, and algae scraper) and their habitat (i.e. pelagic, deep-benthic, intermediate-benthic, shallow-benthic, and littoral). We applied the same linear regression models but using trophic categories instead of the species covariate for $\delta^{15}N$ ($\delta^{15}N$ ~ latitudinal * longitudinal * trophic) and using habitat categories instead of the species covariate for $\delta^{13}C$ ($\delta^{13}C$ ~ latitudinal * longitudinal * habitat).

As an alternative test of whether N and C stable isotope data show a shift depending on the sampling location, we filtered our dataset for species with a lake-wide distribution of which we had collected specimens at different geographic locations (in the northern and southern part of the lake). This subset included species (n = 19) across all trophic levels and ecologies along the benthic-pelagic trajectory (*Plecodus multidentatus, Perissodus microlepis, Bathybates fasciatus, Bathybates minor, Bathybates leo, Lepidiolamprologus profundicola, Lepidiolamprologus elongatus, Lepidiolamprologus attenuatus, Benthochromis horii, Neolamprologus savoryi, Altolamprologus compressiceps, Limnochromis auritus, Triglachromis otostigma, Neolamprologus furcifer, Ophthalmotilapia nasuta, Xenotilapia boulengeri, Ctenochromis horei, Petrochromis famula*, and *Petrochromis polyodon*). We then tested if – across this set of species – the northern and southern samples differ in their $\delta^{15}N$ and $\delta^{13}C$ stable isotope composition using a two-sided t-test across all the per-basin species means.

All statistical analyses of the stable isotope data were conducted in R. The results of all the above tests are detailed in the Supplementary Discussion section below.

Trait space occupation per tribe

We calculated, per tribe, morpho- and ecospace size as the square root of the convex hull area spanned by species means of the PC1 and PC2-scores and $\delta^{13}C$ and $\delta^{15}N$ values, respectively. We then tested for a correlation of trait space size and estimated species richness of a tribe[15] (log-transformed to obtain normal distribution). To account for phylogenetic non-independence among the data points we calculated phylogenetic independent contrasts with the R package ape[57] (v.5.2) using the species tree presented in Fig. 1 pruned to the tribe level. We then calculated Pearson's correlation coefficients for independent contrasts using the function *cor.table* of the R package picante[58] (v.1.8).

Phenotype-environment association

For each trait complex (body shape, upper oral jaw morphology, and lower pharyngeal jaw shape) we performed a two-block PLS analysis based on species means of the Procrustes aligned landmark coordinates and the stable C and N isotope compositions using the function *two.b.pls* of the R package geomorph. Similar to a PCA, in a PLS the multivariate shape data are rotated, but in this case to identify the major axes of covariation between two blocks of multivariate data. To account for phylogenetic dependence of the data we applied a phylogenetic generalized least square analysis (pGLS) as implemented in the R package caper[63] (v.1.0.1) across the two sets of PLS scores (each morphological axis with the stable isotope projection) using the time-calibrated species tree based on the maximum-likelihood topology (Fig. 1). The strength of phylogenetic signal in the data was accounted for by optimising the branch length transformation parameter lambda using a maximum-likelihood approach.

Scoring pigmentation patterns

To quantify a putative signalling trait in cichlids, we scored the pigmentation patterns typically in five male specimens per species (n = 1,016), on the basis of standardized images taken in the field after capture of the specimens (see above). Following the strategy described in Seehausen *et al.*[64], the presence/absence of 20 pigmentation features was recorded by a single person, whereby we extended the scoring method to also include additional body and fin pigmentation patterns present in Tanganyikan cichlids (Extended Data Fig. 5c). We then applied a logistic PCA implemented in the R package logisticPCA[65] (v.0.2) and used the PC1 scores as univariate proxy for differentiation along the signalling axes for further analyses.

Trait evolution modelling and disparity estimates

To investigate the temporal dynamics of diversification over the course of the cichlid adaptive radiation in Lake Tanganyika, we analysed the four trait complexes (body shape, upper oral jaw morphology, lower pharyngeal jaw shape, and pigmentation pattern) by applying a phylogenetic comparative approach to the PLS- and the PCA-scores, respectively, using the time-calibrated species tree based on the maximum-likelihood topology (Fig. 1). We therefore compared the fit of several models of trait evolution to the four traits investigated and reconstructed morphospace dynamics and evolutionary rate patterns through time essentially following the strategy described in Cooney *et al.*[28], which is based on

measurements on extant taxa and assumes constant niche-space and no (or constant) extinction over the course of the radiation. All analyses were conducted in R, unless stated otherwise. We used PLS-scores as univariate measure for the eco-morphological traits because the PLS-fit (see above) allows to identify the shape changes associated with the ecological trajectories and thus most likely represent the adaptive components of each trait complex. However, we additionally applied the same approach using PC1-scores for all traits, yielding very similar results and biological interpretations as the PLS-based analyses (results are provided on Dryad; https://doi.org/10.5061/dryad.9w0vt4bbf: 07_Temporal_patterns_complementary_results.pdf).

Phylogenetic signal. For each trait we calculated the phylogenetic signal in the data by calculating Pagel's Lambda and Blomberg's K using the function *phylosig* of the R package phytools[66] (v.0.6-60).

Fitting models of trait evolution. We tested the fit of four models of trait evolution along the time-calibrated species tree to the PLS- and the PCA-scores, respectively, for each of the four phenotypic trait complexes. We applied a white noise model, a Brownian motion (BM) model, a single-optimum Ornstein-Uhlenbeck model, and an 'early burst' model of trait evolution using the function *fitContinuous* of the R package geiger[67] (v.2.0.6.1). Additionally, we fitted a variable rates model (a BM model of trait evolution that allows for rate shifts on branches and nodes) using the software BayesTrait (http://www.evolution.rdg.ac.uk/, v.3) with uniform prior distributions adjusted to our dataset (alpha: -1 – 1, sigma: 0 – 0.001 for morphometric traits; alpha: 0 – 10, sigma: 0 – 10 for pigmentation pattern) and applying single-chain Markov chain Monte Carlo runs with one billion iterations. We sampled parameters every 100,000th iteration, after a pre-set burnin of 10,000,000 iterations. We then tested, in each separate analysis, for convergence of the chain using a Cramer-von-Mises statistic as implemented in the R package coda[68] (v.0.19-3). As all chains passed the test, we further thinned the converged chain to 5,900 post-burnin samples and summarised the results by calculating the mean rate shift and the posterior probabilities for a shift per branch. The different models were compared by calculating their log-likelihood and Akaike Information Criterion (AIC) difference (see Extended Data Fig. 8d, e). Based on difference in AIC, the variable rates model was best supported for all traits but body shape, which showed a strong signal of an early burst of trait evolution (see Extended Data Fig. 8d, e, note that the variable rates model has the highest log-likelihood for body shape as well). We nevertheless focused on the variable rates model for further analyses of all traits to be able to compare temporal patterns of trait evolution among the traits.

Morphospace expansion through time. To estimate morphospace expansion through time we used the maximum-likelihood ancestral state reconstruction implemented in the R package phytools. To account for differences in the rate of trait evolution along the phylogeny, we reconstructed ancestral states using the mean rate-transformed tree derived from the variable rates model (see above). We then projected the ancestral states onto the original species tree and calculated the morphospace extent (i.e. the range of trait values [$value_{maximum}$ - $value_{minimum}$]) in time intervals of 0.15 million years (note that this is an arbitrary value; however, differently sized time intervals had no effect on the interpretation of the results). For each time point, we extracted the branches existing at that time and predicted the trait value linearly between nodes. We then compared the resulting morphospace expansion over time relative to a null model of trait evolution. For this, we simulated 500 datasets (PLS and PC1 scores)

under BM given the original species tree with parameters derived from the BM model fit to the original data. For each simulated dataset we produced disparity-through-time curves using the same approach as described above. We then compared the slopes of our observed data with each of the null models by calculating the difference of slopes through time (Fig. 3) using linear models fitted for each time interval with the two subsequent time intervals. Note that for body shape we also estimate morphospace expansion through time using the early burst model for ancestral state reconstruction, which resulted in a very similar pattern for trait diversification and led to the same conclusion.

Unlike other metrics of disparity (e.g. variance or mean pairwise distances) morphospace extent is not sensitive to the density distribution of measurements within the morphospace and captures its full range[69]. Hence, comparing the extent of morphospace between observed data and the null model directly unveils the contribution of morphospace expansion relative to the null model; and because the increase in lineages over time is identical in the observed and the simulated data, this comparison also provides an estimate for morphospace packing.

Evolutionary rates through time. To summarise, for each trait, how the evolutionary rates changed over the course of the radiation, we calculated the mean rate of trait evolution inferred with the variable rates model in the same 0.15 million years intervals along the phylogeny. A graphical representation of evolutionary rates per tribe are available on Dryad; https://doi.org/10.5061/dryad.9w0vt4bbf: 07_Temporal_patterns_complementary_results.pdf.

Accounting for phylogenetic uncertainty. To account for phylogenetic uncertainty in the tree topology we repeated the analyses of trait evolution using the time-calibrated species trees based on tree topologies estimated with ASTRAL and SNAPP (see above and Supplementary Discussion for a comparison of the three topologies). To also account for uncertainty in branch lengths, we repeated the analysis on 100 trees from the Bayesian posterior distributions for each of the three trees. The results based on these alternative trees are provided on Dryad; https://doi.org/10.5061/dryad.9w0vt4bbf: 07_Temporal_patterns_complementary_results.pdf).

Characterisation of repeat content

For the repeat content analysis, we randomly selected one *de novo* genome assembly per species of the radiation (n = 245). We performed a *de novo* identification of repeat families using RepeatModeler[70] (v.1.0.11). We then combined the RepeatModeler output library with the available cichlid-specific libraries[71] (Dfam and RepBase; v.27.01.2017; 258 ancestral and ubiquitous sequences, 161 cichlid-specific repeats, and 6 lineage-specific sequences; 65,118, 273,530, and 6,667 bp in total, respectively) and used the software RepeatMasker[71] (v.4.0.7) (-xsmall -s -e ncbi -lib combined_libraries.fa) to identify and soft-mask interspersed repeats and low complexity DNA sequences in each assembly. The reported summary statistics were obtained using RepeatMasker's 'buildSummary.pl' script (Fig. 4a, Extended Data Fig. 9a, results per genome are provided on Dryad; https://doi.org/10.5061/dryad.9w0vt4bbf: 08_Transposable_elements.pdf).

Gene duplication estimates

Per genome, gene duplication events were identified with the structural variant identification pipeline smoove following the population calling method (https://github.com/brentp/smoove, docker image cloned 20/12/2018), which builds upon lumpy[72], svtyper[73], and svtools (https://github.com/hall-lab/svtools). Variants were called per sample (n = 488 genomes, 246 taxa of the Tanganyika radiation) from the initial mapping files against the Nile tilapia reference genome with the function *call*. The union of sites across all samples was obtained with the function *merge,* then all samples were genotyped at those sites with the function *genotype*, and depth information was added with --duphold. Genotypes were combined with the function *paste* and annotated with *annotate* and the reference genome annotation file. The obtained VCF file was filtered with BCFtools to keep only duplications longer than 1 kb and of high quality (MSHQ > 3 or MSHQ == -1, FMT/DHFFC[0] > 1.3, QUAL > 100). The resulting file was loaded into R (v.3.6.0) with vcfR[74] (v.1.8.0) and filtered to keep only duplications with less than 20% missing genotypes. Next, we removed duplication events with a length outside 1.5 times the interquartile range above the upper quartile of all duplication length, resulting in a final dataset of 476 duplications (Fig. 4b).

Analyses of selection on coding sequence

To predict genes within the *de novo* genome assemblies, we used AUGUSTUS[75] (v.3.2.3) with default parameters and 'zebrafish' as --species parameter (n = 485 genomes, 245 taxa). For each prediction we inferred orthology to Nile tilapia genes (GCF_001858045.1_ASM185804v2) with GMAP (GMAP-GSNAP[76]; v.2017-08-15) applying a minimum trimmed coverage of 0.5 and a minimum identity of 0.8. We excluded specimens with less than 18,000 Nile tilapia orthologous genes detected (resulting in 471 genomes, 243 taxa). Next, we kept only those tilapia protein coding sequences that had at least one of their exons present in at least 80% of the assemblies (260,335 exons were retained, representing 34,793 protein coding sequences). Based on the tilapia reference genome annotation file, we reconstructed for each assembly the orthologous coding sequences. Missing exon sequences were set to 'N's. We then kept a single protein coding sequence per gene (the one being present in the maximum number of species with the highest percentage of sequence length), resulting in 15,294 protein coding sequences. Per gene, a multiple sequence alignment was then produced using MACSE[77] (v.2.01). We calculated for each specimen and each gene the number of synonymous (S) and non-synonymous (N) substitutions by pairwise comparison to the ortholog Nile tilapia sequence using *codeml* with runmode -2 within PAML[78] (v.4.9e). To obtain an estimate of the genome-wide sequence evolution rate that is independent of filtering thresholds, we calculated the genome-wide dN/dS ratio for each specimen based on the sum of dS and dN across all genes (Fig. 4c, Extended Data Fig. 9b).

Signals of past introgression

We used the f_4-ratio statistic[34] to assess genomic evidence for interspecific gene exchange. We calculated the f_4-ratio for all combinations of trios of species on the filtered VCF file using the software Dsuite[79] (v.0.2 r20), with *T. sparrmanii* as outgroup species (note that we excluded *N. cancellatus* as all specimens of this species appeared to be F1 hybrids; see above). The f_4-ratio statistic (in combination with its associated P-value) estimates the 'admixture proportion', i.e. the proportion of the genome

affected by gene flow. The results presented in this manuscript (Fig. 4e, Extended Data Fig. 10) are based on the 'tree' output of the Dsuite function *Dtrios*, with each trio arranged according to the species tree based on the maximum-likelihood topology (Fig. 1). For the per tribe analyses shown in Fig. 4e we only used comparisons where all species within the trio come from the same tribe and belong to the cichlid adaptive radiation in Lake Tanganyika (n = 243 taxa).

In addition to the f_4-ratio we also identified signals of past introgression among species using a phylogenetic approach by testing for asymmetry in the relationships of species trios in 1,272 local maximum-likelihood trees generated using IQ-TREE (see above; Extended Data Fig. 10).

Heterozygosity

Empirical data. We calculated the number of heterozygous sites per genome (n = 488 genomes, 246 taxa from the Tanganyika radiation) from the VCF files using the BCFtools function *stats*. We then calculated the percentage of heterozygous sites among the number of callable sites per genome (considering mappability, proximity to indels, overall read depth, and read depth per individual; see the description of masking in the section "Details on mapping, variant calling, and filtering") (Fig. 4d).

Simulations. To explore if the observed levels of heterozygosity per tribe can be explained by the levels of gene flow within tribes, we performed coalescent simulations with the software msprime[80] (v.0.7.4) to assess the expected levels of heterozygosity in species of the Lake Tanganyika cichlid radiation given the inferred introgression signals. We simulated the evolution of all species of the radiation following the time-calibrated species tree (based on the maximum-likelihood tree topology; Fig 1), assuming a generation time of 3 years, as in Malinsky *et al.*[81], and a constant effective population size of 20,000 individuals. Each species divergence event was implemented as a mass migration between the two descendent species where all individuals of one species migrate to the other one (when viewed backwards in time). The time points of these mass migration events were set according to the corresponding divergence times in the species tree. Migration rates between pairs of species within tribes were set according to their introgression (f_4-ratio) signals inferred with Dsuite. To convert the f_4-ratio values inferred by Dsuite into migration rates, we applied a scaling factor of 5×10^{-6}, which results in a close correspondence in magnitude of the simulated introgression signals to those observed empirically (Fig. 4f, Extended Data Fig. 9c). In each of twenty separate simulations, we randomly sampled one pairwise f_4-ratio value for each pair of species for conversion to migration rates (there are many f_4-ratios per a pair of species – one for each possible third species added to the test trio; the maximum values per pair are shown in Extended Data Fig. 10). The simulated data consisted of a single chromosome of 100 kb in length with a mutation rate of 3.5×10^{-9} per bp and generation[33]. The recombination rate was set to 2.2×10^{-8} per bp per generation, based on the genome of approximately 1 Gb consisting of 22 chromosomes. As the number of chromosome arms is an excellent predictor of the total amount of recombination events[123], assuming one recombination event per chromosome is a reasonable first order approximation. Levels of heterozygosity were calculated for all simulated datasets as described for the empirical data. To confirm appropriate scaling between the empirically observed f_4-ratios and the migration rates applied in simulations, we recalculated f_4-ratios from the simulated datasets, again using Dsuite with the same settings as for the empirical dataset.

To account for between-tribe gene flow we further performed simulations in which migration between tribes was also sampled from the empirical f_4-ratio distribution. For simplicity in setting up the simulation model, we assume that gene flow between tribes is ongoing until the present day, which is clearly an overestimate (see Supplementary Discussion). Nevertheless, the results of these simulations support our hypothesized scenario, confirming that much of the variation in heterozygosity as well as its correlation with species richness can be explained by the observed levels of gene flow.

Correlation of genome-wide statistics with species richness

We tested for a correlation between tribe means of each genomic summary statistics (TE counts, number of gene duplications, genome-wide dN/dS ratio, per-genome heterozygosity, and f_4-ratio, as well as the heterozygosity and f_4-ratio statistics derived from simulated genome evolution) and species richness of the tribes. Estimated species richness for each tribe[15] was log-transformed to obtain normal distribution. To account for phylogenetic non-independence among the data points we calculated phylogenetic independent contrasts as implemented in the R package ape[57] (v.5.2) using the species tree presented in Fig. 1 (the time-calibrated species tree based on the maximum-likelihood tree topology) pruned to the tribe level. We then calculated Pearson's correlation coefficients for independent contrasts (through the origin) using the function *cor.table* of the R package picante[58] (v.1.8). Note that accounting for clade age of the tribes did not change the conclusions on the observed associations (results not shown).

2. Supplementary Discussion

The age of the cichlid radiation in Lake Tanganyika

Our phylogenomic divergence time estimates based on cichlid and other teleost fossils and without taking into consideration biogeographic assumptions such as the presumed ages of lakes[18] revealed an age of the cichlid radiation in Lake Tanganyika of 9.7 (± 0.5) Ma (Fig. 1), which is in line with the estimated age of Lake Tanganyika itself[23]. This suggests that the tribes Bathybatini, Benthochromini, Boulengerochromini, Cyphotilapiini, Cyprichromini, Ectodini, Eretmodini, Lamprologini, Limnochromini, Perissodini, Trematocarini, and the Tropheini evolved and diversified within Lake Tanganyika. Together, these tribes make up the adaptive radiation of cichlid fishes in Lake Tanganyika.

Three cichlid species endemic to Lake Tanganyika from three different tribes (*Coptodon rendalli*, *Oreochromis tanganicae*, and *Tylochromis polylepis*) are not part of the evolutionary radiation of cichlid fishes in this lake (Fig. 1). Earlier studies[19,22,124] as well as our own time-calibrated phylogenomic analyses support the interpretation that these species are secondary colonisers to Lake Tanganyika: First, the three tribes to which these species belong (Coptodonini, Oreochromini, and Tylochromini) are not the most closely-related lineages to the cichlid radiation in Lake Tanganyika. Second, our estimations of the divergence times of these tribes are older than the age of Lake Tanganyika, ranging from 12.4 Ma (Coptodonini) to 29.5 Ma (Tylochromini) (Extended Data Fig. 1). Finally, these tribes contain 18-37 species each, of which all but one species each occur only outside of Lake Tanganyika, and the single Tanganyikan representatives are phylogenetically deeply nested within their respective tribe.

Phylogenetic inference

We applied three complementary strategies to reconstruct the phylogenetic relationships among all species belonging to the adaptive radiation of cichlid fishes in Lake Tanganyika (that is, all cichlid species occurring in the lake, except *C. rendalli*, *O. tanganicae*, and *T. polylepis*; see above) from the genome-wide data and time-calibrated the resulting phylogenetic hypotheses using a relaxed-clock model. More specifically, we (*i*) inferred a maximum-likelihood (ML) phylogeny with RAxML using 3,630,997 SNPs; (*ii*) constructed a species tree based on 1,272 genomic regions with ASTRAL; and (*iii*) applied the multi-species coalescent model implemented in SNAPP using genome-wide biallelic SNPs. In addition, we applied a quartet inference approach to the SNP data and calculated a maximum-likelihood phylogeny on the basis of the mitochondrial genomes.

The phylogenetic hypotheses based on genome-wide data (ML, Fig. 1, Extended Data Fig. 2; ASTRAL, Extended Data Fig. 3; SNAPP, Extended Data Fig. 4) were largely congruent with each other and shared a majority of the internal nodes: 217 nodes (out of 264) were shared between ML and SNAPP (>82%, Robinson-Foulds distance: 94), 222 between ML and ASTRAL (>84%, Robinson-Foulds distance: 84), and 207 between SNAPP and ASTRAL (>78%, Robinson-Foulds distance: 114). Also, the quartet inference topology was rather similar to the ML, ASTRAL, and SNAPP trees (200 shared nodes with ML, Robinson-Foulds distance: 126). The topology based on the mitochondrial genomes (Supplementary Fig. 2) was more distinct, sharing 101 nodes with ML (>38%, Robinson-Foulds distance: 324), 97 with ASTRAL (>36%, Robinson-Foulds distance: 332), and 98 with SNAPP (>36%, Robinson-Foulds distance: 330). In only six cases, the representatives of a species were not resolved as monophyletic clade in the individual-level maximum-likelihood tree inferred from nuclear SNPs (Supplementary Fig. 1).

In all phylogenetic hypotheses – be it on the basis of genome-wide or mitochondrial sequence data – the respective members of a tribe formed a monophyletic group, supporting the taxonomic assignment of the Tanganyikan cichlid fauna into tribes[15]. The hypothesised evolutionary relationships among the tribes belonging to the radiation were identical between the ML and the SNAPP topology: A clade formed by the monotypic tribe Boulengerochromini plus the Trematocarini and Bathybatini was placed as sister group to the Lamprologini and the remaining tribes, in which the Cyphotilapiini plus the Limnochromini and Ectodini were resolved as sister group to the Cyprichromini, Benthochromini, and Perissodini and the Eretmodini plus the Haplochromini/Tropheini (Extended Data Figs. 2, 4). The only difference – at the level of phylogenetic relationships among tribes – between the ML and SNAPP topologies on the one hand and the ASTRAL tree on the other hand was that, in the ASTRAL tree (Extended Data Fig. 3), the Cyphotilapiini were placed as sister group to the derived clade of mouthbrooders containing the Limnochromini+Ectodini, the Cyprichromini, Benthochromini+Perissodini, and the Eretmodini+Haplochromini/Tropheini, whereas the Cyphotilapiini were part of a clade with the Limnochromini+Ectodini in the ML and SNAPP trees.

The hypothesised evolutionary relationships within the tribes of the adaptive radiation of cichlid fishes in Lake Tanganyika were also largely congruent between the topologies obtained with ML, ASTRAL, and SNAPP (see Extended Data Figs. 2-4). Qualitative differences between the phylogenetic hypotheses typically involved the placement of individual species relative to their congeners (for

example, *Lepidiolamprologus profundicola* in the ASTRAL topology) or particular subclades in a tribe (for example, *Reganochromis calliurus* and *Baileychromis centropomoides* were resolved as sister group to the remaining Limnochromini species in the SNAPP topology; the "*Neolamprologus brichardi/pulcher* clade" was placed as sister to the clade containing *Telmatochromis* in the ML topology). The relative placement to one another of some *Xenotilapia* and *Petrochromis* species differed among the three topologies as well.

In the maximum-likelihood phylogeny on the basis of the mitochondrial genomes (Supplementary Fig. 2), the monotypic Boulengerochromini were placed as sister lineages to all remaining tribes of the radiation (albeit bootstrap node support for these remaining tribes was only 79), in which the Trematocarini+Bathybatini were resolved as sister group to all other tribes. Among these, the Eretmodini formed the sister group to the Limnochromini and a clade in which the Cyphotilapiini were placed as sister clade to the Ectodini plus a clade formed by the Cyprichromini, Perissodini, and Benthochromini, and the Haplochromini/Tropheini. Thus, the general structure of the tribal relationships was comparable between the mitochondrial phylogeny and the trees inferred from genome-wide markers, with the exception of the placement of the Eretmodini. In previous studies using smaller sets of mitochondrial markers, the Eretmodini were placed as sister lineage to the Lamprologini or as sister group to the Lamprologini and a clade of mouthbrooders (see e.g.[20,125–127]).

Taken together, the different phylogenetic hypotheses reconstructed from genome-wide data of virtually all species of the adaptive radiation of cichlid fishes in Lake Tanganyika are highly congruent, and support a common scenario of the course of the radiation as well as its timeline. All our analyses (including those involving distant outgroup species to determine the age of the radiation) support monophyly of the tribes belonging to the radiation. There is also agreement between the topologies based on genome-wide markers that 14 (out of the 57) genera of cichlid fishes in Lake Tanganyika are not monophyletic, partly reflecting convergent morphological evolution within this species flock[16], once more illustrating that taxonomic revisions are needed[15].

Stable isotopes analysis

As carbon (C) and nitrogen (N) stable isotope composition can be influenced by the varying biochemistry of the local environment, we additionally collected and analysed baseline datasets covering several trophic levels from the northern and the southern basin of the lake (see Extended Data Fig. 6a). Comparing the baseline data with the stable isotope composition of the cichlids revealed a clear trophic signal in $\delta^{15}N$ with the typical ~3‰ increase from one trophic level to the next, supporting the interpretation that $\delta^{15}N$ stable isotopes values can be used as a proxy for the trophic level in Lake Tanganyika. Likewise, the $\delta^{13}C$ stable isotope values clearly discriminate between pelagic and littoral baseline samples as well as between pelagic and littoral cichlids (see Extended Data Fig. 6a).

When testing for a general trend in stable isotope composition along the latitudinal and longitudinal gradient of the sampling locations with species as additional covariate we found a significant effect for of the sampling locality ($\delta^{15}N$: $F_{latitude} = 12.92$, $P_{latitude} < 0.001$, $F_{longitude} = 749.7$, $P_{longitude} < 0.001$; $\delta^{13}C$: $F_{latitude} = 0.087$, $P_{latitude} = 0.77$, $F_{longitude} = 328.3$, $P_{longitude} < 0.001$). Likewise, when we used the ecological categories as covariate the sampling locality showed, in most cases, a significant effect in the multiple

regression model ($\delta^{15}N$: $F_{latitude} = 4.46$, $P_{latitude} = 0.035$, $F_{longitude} = 258.86$, $P_{longitude} < 0.001$; $\delta^{13}C$: $F_{latitude} = 0.016$, $P_{latitude} = 0.9$, $F_{longitude} = 59.2$, $P_{longitude} < 0.001$). However, only very little variance was explained by the sampling locations in the models ($\delta^{15}N$: latitude = 0.07%, longitude = 4.27%; $\delta^{13}C$: latitude = 0.0003%, longitude = 1.26%). Importantly, the latitude and longitude of the sampling locality showed a significant interaction with species ($\delta^{15}N$: $F_{latitude:species} = 3.3$, $P_{latitude:species} < 0.001$, $F_{longitude:species} = 5.04$, $P_{longitude:species} < 0.001$; $\delta^{13}C$: $F_{latitude:species} = 2.67$, $P_{latitude:species} < 0.001$, $F_{longitude:species} = 3.70$, $P_{longitude:species} < 0.001$) and ecological category ($\delta^{15}N$: $F_{latitude:trophic} = 7.32$, $P_{latitude: trophic} < 0.001$, $F_{longitude:trophic} = 7.71$, $P_{longitude:trophic} < 0.001$; $\delta^{13}C$: $F_{latitude:habitat} = 4.97$, $P_{latitude:habitat} < 0.001$, $F_{longitude:habitat} = 12.92$, $P_{longitude:habitat} < 0.001$). Hence, no general correction for sampling locality over the dataset is applicable to the stable isotope compositions.

Testing for a difference in stable isotope compositions between northern and southern samples across a set of species representing all trophic levels and occurring along the entire spectrum of the benthic-pelagic axis revealed no difference ($\delta^{15}N$: t = -1.56, DF = 35.1, $P = 0.13$; $\delta^{13}C$: t = 1.61, DF = 33.5, $P = 0.12$), suggesting that across contrasting ecologies the biogeochemistry is sufficiently similar among sampling locations in Lake Tanganyika to interpret the $\delta^{15}N$ and $\delta^{13}C$ stable isotope values with respect to the trophic axis and the benthic-pelagic axis.

Taken together, we conclude that, while the biogeochemical variance across sampling locations might add some additional variance to the data, the ecological signal clearly dominates in the stable isotope data. Importantly, we confirm that, across our cichlid dataset, the $\delta^{15}N$ value informs about the relative trophic level of the species and the $\delta^{13}C$ value can be interpreted as the relative position along the benthic-pelagic axis.

Trait space occupation per tribe

When comparing the size of morpho- and ecospace per tribe, we found a strong correlation between occupied trait space and species richness of a tribe (Extended Data Figs. 6, 7). To test if this pattern is mainly driven by sample size, we repeated the per-tribe morpho- and ecospace occupation analyses using a resampling strategy. We sampled 1,000 times four species per tribe and re-calculated the trait space occupation. This confirmed the positive association of morphospace occupation and tribe size for upper oral jaw morphology (Pearson's $r = 0.64$, df = 9, $P = 0.04$) and lower pharyngeal jaw shape (Pearson's $r = 0.69$, df = 9, $P = 0.02$). For body shape, the pattern was only confirmed when excluding the Limnochromini (Pearson's $r = 0.69$, df = 9, $P = 0.03$), which occupy a very large fraction of the morphospace relative to their number of species (Extended Data Figs. 6, 7). For the ecospace occupation, the resampling procedure using four species was only possible for 10 tribes (due to missing data for one of the Cyphotilapiini), which confirms the general pattern (Pearson's $r = 0.60$, df = 8, $P = 0.06$). Overall, this supports that larger tribes occupy larger areas of the morphospace – irrespective of sample size.

Late burst in diversification of pigmentation pattern

For pigmentation pattern we detected a pulse of diversification along with increasing evolutionary rates late in the radiation. This signal could potentially also occur under a scenario of a rapid turnover in this

trait, characterised by high evolutionary rates and convergent evolution. Colour patterns are known to evolve rapidly in cichlids[26,64]. However, the Ornstein-Uhlenbeck model of trait evolution which models this scenario has very low support given the data (Extended Data Fig. 8d, e). Moreover, our analysis showed that two tribes (Ectodini and Limnochromini) stand out with constantly low rates of trait evolution in pigmentation pattern throughout – suggesting that high turnover rate in this trait is not a general feature of the cichlid radiation in Lake Tanganyika. In spite of this, a late burst emerged as the general trend of trait evolution for pigmentation pattern for the remaining tribes (Fig. 3).

Signals of past introgression

To assess the extent of genetic introgression among cichlids of the radiation in Lake Tanganyika, we calculated the f_4-ratio values as well as Patterson's *D* statistic and its associated *P*-values (based on block jack-knifing) across all combinations of trios of species within the radiation (n = 265 species), resulting in 3,066,580 values for each statistic. The outgroup was in all cases fixed (*T. sparrmanii*).

We focus on the f_4-ratios because this statistic is designed to estimate the 'admixture fraction' and therefore is a suitable measure of the level of gene flow, especially when applied within the cichlid tribes of Lake Tanganyika, where the effect of any variation in overall substitution rates is unlikely to be pronounced. The distributions of all the f_4-ratio values within tribes were therefore chosen for correlation with species richness of tribes (Fig. 4e), and also served as a basis for the simulations that show how the observed levels of gene flow might have led to elevated heterozygosity in the more species-rich tribes (Fig. 4f).

There are a number of challenges associated with an interpretation of a system of over 3 million f_4-ratio estimates and in pinpointing specific introgression events from these results[79]. First, the f_4-ratio estimates the admixture fraction between a pair of species. However, it is based on trios of species (and an outgroup), and the value of the estimate depends on which other species is included in the trio and on the assumed relationship among the species in each trio. We constrained the relationships using the maximum-likelihood tree topology (Fig. 1). Therefore, the estimates rely on this phylogeny being correct. Second, a single ancestral introgression event can be responsible for many elevated f_4-ratios between multiple taxa which share drift (i.e. branches on the true phylogeny).

In Extended Data Fig. 10 we show, for each pair of species, the maximum value of the statistic across all trios in which an estimate for the pair was obtained. Therefore, in this sense we present the upper bound of the admixture fraction estimate for each pair. We show f_4-ratio values greater than 3%; the associated *P*-values show that the imbalance in allele sharing that is the basis of these f_4-ratio values is statistically significant ($P < 5\times10^{-5}$ after Benjamini-Hochberg correction for multiple testing). The vast majority of introgression signals are within tribes, with two exceptions: 1) between Cyphotilapiini and Limnochromini (where f_4-ratio values are around 8%) and 2) between the group comprising Limnochromini+Ectodini and the tribes Haplochromini/Tropheini, Benthochromini, and Perissodini (f_4-ratios around 4 to 5%). The uniformity of these signals across all pairs of species from these groups suggests that the gene flow is likely to have happened between the common ancestors of these tribes/groups. Interestingly, the f_4-ratios do not exceed 3% between Cyphotilapiini and Tropheini, where gene flow evidence was reported previously by Irisarri *et al.*[22] on the basis of Patterson's *D* statistic. In

this context we note that at the between-tribe level, the *D* statistic is more likely to be influenced by variation in overall substitution rates[128], which we also observed in our dataset.

We also see signals of introgression between Tropheini and many of the haplochromine species sampled from rivers outside of Lake Tanganyika, with admixture fractions estimated by f_4-ratios ranging between 3 and 8%. These signals come mainly in two blocks, suggesting introgression between the common ancestor of all Tropheini and the common ancestors of two riverine haplochromine lineages.

The signatures of introgression within tribes are numerous. There are 229 pairs of species with admixture proportion estimates of more than 10% (144 in Lamprologini, 43 in Ectodini, 19 in Tropheini, 11 in Cyprichromini, two in Perissodini, two in Benthochromini, two in Bathybatini, and six among the riverine haplochromines). Some of these signals confirm previous reports (e.g. strong introgression among the 'Princess cichlid' species[129]), but many of the putative hybridisation events are new findings, which we envisage as a starting point for future, more detailed, investigations.

3. References

82. Li, H. *et al.* The Sequence Alignment/Map format and SAMtools. *Bioinformatics* **25**, 2078–2079 (2009).

83. Quinlan, A. R. & Hall, I. M. BEDTools: a flexible suite of utilities for comparing genomic features. *Bioinformatics* **26**, 841–842 (2010).

84. Durand, E. Y., Patterson, N., Reich, D. & Slatkin, M. Testing for ancient admixture between closely related populations. *Mol. Biol. Evol.* **28**, 2239–2252 (2011).

85. Konings, A. *Tanganyika Cichlids in their natural habitat*. (Cichlid Press, 2015).

86. Büscher, H. H. *Neolamprologus cancellatus*, eine Chimäre aus dem Tanganjikasee. *DCG-Informationen* **50**, 282–288 (2019).

87. Zerbino, D. R. *et al.* Ensembl 2018. *Nucleic Acids Res.* **46**, D754–D761 (2017).

88. Altschul, S. F., Gish, W., Miller, W., Myers, E. W. & Lipman, D. J. Basic local alignment search tool. *J. Mol. Biol.* **215**, 403–410 (1990).

89. Wainwright, P. C. *et al.* Evolution of pharyngognathy: a phylogenetic and functional appraisal of the pharyngeal jaw key innovation in labroid fishes and beyond. *Syst. Biol.* **61**, 1001–1027 (2012).

90. Malmstrøm, M. *et al.* Evolution of the immune system influences speciation rates in teleost fishes. *Nat. Genet.* **48**, 1204–1210 (2016).

91. Reichwald, K. *et al.* Insights into sex chromosome evolution and aging from the genome of a short-lived fish. *Cell* **163**, 1527–1538 (2015).

92. Conte, M. A. *et al.* Chromosome-scale assemblies reveal the structural evolution of African cichlid genomes. *Gigascience* **8**, 288 (2019).

93. Meyer, B. S., Matschiner, M. & Salzburger, W. Disentangling incomplete lineage sorting and introgression to refine species-tree estimates for Lake Tanganyika cichlid fishes. *Syst. Biol.* **66**, 531–550 (2017).

94. Kucuk, E. *et al.* Kollector: transcript-informed, targeted de novo assembly of gene loci. *Bioinformatics* **33**, 1782–1788 (2017).

95. Allen, J. M., LaFrance, R., Folk, R. A., Johnson, K. P. & Guralnick, R. P. aTRAM 2.0: An improved, flexible locus assembler for NGS data. *Evol. Bioinforma.* **14**, 1176934318774546 (2018).

96. Musilova, Z. *et al.* Vision using multiple distinct rod opsins in deep-sea fishes. *Science* **364**, 588–592 (2019).

97. Katoh, K. & Standley, D. M. MAFFT multiple sequence alignment software version 7: improvements in performance and usability. *Mol. Biol. Evol.* **30**, 772–780 (2013).

98. Criscuolo, A. & Gribaldo, S. BMGE (Block Mapping and Gathering with Entropy): a new software for selection of phylogenetic informative regions from multiple sequence alignments. *BMC Evol. Biol.* **10**, 210 (2010).

99. Jarvis, E. D. *et al.* Whole-genome analyses resolve early branches in the tree of life of modern birds. *Science* **346**, 1320–1331 (2014).

100. Leigh, J. W., Susko, E., Baumgartner, M. & Roger, A. J. Testing congruence in phylogenomic analysis. *Syst. Biol.* **57**, 104–115 (2008).

101. Drummond, A. J., Ho, S. Y. W., Philips, M. J. & Rambaut, A. Relaxed phylogenetics and dating with confidence. *PLOS Biol.* **4**, e88 (2006).

102. Bouckaert, R. R. & Drummond, A. J. bModelTest: Bayesian phylogenetic site model averaging and model comparison. *BMC Evol. Biol.* **17**, 42 (2017).

103. Springer, M. S. & Gatesy, J. On the importance of homology in the age of phylogenomics. *Syst. Biodivers.* **16**, 210–228 (2018).

104. López-Fernández, H., Winemiller, K. O. & Honeycutt, R. L. Multilocus phylogeny and rapid radiations in Neotropical cichlid fishes (Perciformes: Cichlidae: Cichlinae). *Mol. Phylogenet. Evol.* **55**, 1070–1086 (2010).

105. Swofford, D. L. PAUP*. Phylogenetic analysis using parsimony (*and other methods). Version 4. (2003).

106. Mailund, T., Munch, K. & Schierup, M. H. Lineage sorting in apes. *Annu. Rev. Genet.* **48**, 519–535 (2014).

107. Arcila, D. *et al.* Genome-wide interrogation advances resolution of recalcitrant groups in the tree of life. *Nat. Ecol. Evol.* **1**, 1–10 (2017).

108. Barth, J. *et al.* Stable species boundaries despite ten million years of hybridization in tropical eels. *Nat. Commun.* **11,** 1433 (2020).

109. Betancur-R, R. *et al.* Phylogenetic classification of bony fishes. *BMC Evol. Biol.* **17**, 162 (2017).

110. Green, R. E. *et al.* A draft sequence of the Neandertal genome. *Science* **328**, 710–722 (2010).

111. Lanfear, R., Frandsen, P. B., Wright, A. M., Senfeld, T. & Calcott, B. PartitionFinder 2: New methods for selecting partitioned models of evolution for molecular and morphological phylogenetic analyses. *Mol. Biol. Evol.* **34**, 772–773 (2017).

112. Gernhard, T. The conditioned reconstructed process. *J. Theor. Biol.* **253**, 769–778 (2008).

113. Felsenstein, J. Phylogenies from restriction sites: A maximum-likelihood approach. *Evolution (N. Y).* **46**, 159–173 (1992).

114. Liu, L., Xi, Z., Wu, S., Davis, C. C. & Edwards, S. V. Estimating phylogenetic trees from genome-scale data. *Ann. N. Y. Acad. Sci.* **1360**, 36–53 (2015).

115. Robinson, D. F. & Foulds, L. R. Comparison of Phylogenetic Trees. *Math. Biosci.* **51**, 131–147 (1981).

116. Huerta-Cepas, J., Serra, F. & Bork, P. ETE 3: Reconstruction, analysis, and visualization of phylogenomic data. *Mol. Biol. Evol.* **33**, 1635–1638 (2016).

117. Maynard Smith, J. & Smith, N. H. Detecting recombination from gene trees. *Mol. Biol. Evol.* **15**, 590–599 (1998).

118. Stange, M., Sánchez-Villagra, M. R., Salzburger, W. & Matschiner, M. Bayesian divergence-time estimation with genome-wide SNP data of sea catfishes (Ariidae) supports Miocene closure of the Panamanian Isthmus. *Syst. Biol.* **67**, 681–699 (2018).

119. Rambaut, A., Drummond, A. J., Xie, D., Baele, G. & Suchard, M. A. Posterior summarization in Bayesian phylogenetics using Tracer 1.7. *Syst. Biol.* **67**, 901–904 (2018).

120. Chifman, J. & Kubatko, L. S. Quartet inference from SNP data under the coalescent model. *Bioinformatics* **30**, 3317–3324 (2014).

121. Hahn, C., Bachmann, L. & Chevreux, B. Reconstructing mitochondrial genomes directly from genomic next-generation sequencing reads--a baiting and iterative mapping approach. *Nucleic Acids Res.* **41**, e129--e129 (2013).

122. Chevreux, B., Wetter, T. & Suhai, S. Genome sequence assembly using trace signals and additional sequence information. *Comput. Sci. Biol. Proc. Ger. Conf. Bioinforma.* 1–12 (1999).

123. Coop, G. & Przeworski, M. An evolutionary view of human recombination. *Nat. Rev. Genet.* **8**, 23–34 (2007).

124. Dunz, A. R. & Schliewen, U. K. Molecular phylogeny and revised classification of the haplotilapiine cichlid fishes formerly referred to as 'Tilapia'. *Mol. Phylogenet. Evol.* **68**, 64–80 (2013).

125. Kocher, T. D., Conroy, J. A., McKaye, K. R., Stauffer, J. R. & Lockwood, S. F. Evolution of NADH dehydrogenase subunit 2 in east african cichlid fish. *Molecular Phylogenetics and Evolution* vol. 4 420–432 (1995).

126. Day, J. J., Cotton, J. A. & Barraclough, T. G. Tempo and mode of diversification of Lake Tanganyika cichlid fishes. *PLoS One* **3**, e1730 (2008).

127. Meyer, B. S. *et al.* Back to Tanganyika: A case of recent trans-species-flock dispersal in East African haplochromine cichlid fishes. *R. Soc. Open Sci.* **2**, 1–5 (2015).

128. Pease, J. B. & Hahn, M. W. Detection and Polarization of Introgression in a Five-Taxon Phylogeny. *Syst. Biol.* **64**, 651–662 (2015).

129. Gante, H. F. *et al.* Genomics of speciation and introgression in Princess cichlid fishes from Lake Tanganyika. *Mol. Ecol.* **25**, 6143–6161 (2016).

4. Supplementary Figures and Tables

Supplementary Fig. 1 continues on the next page

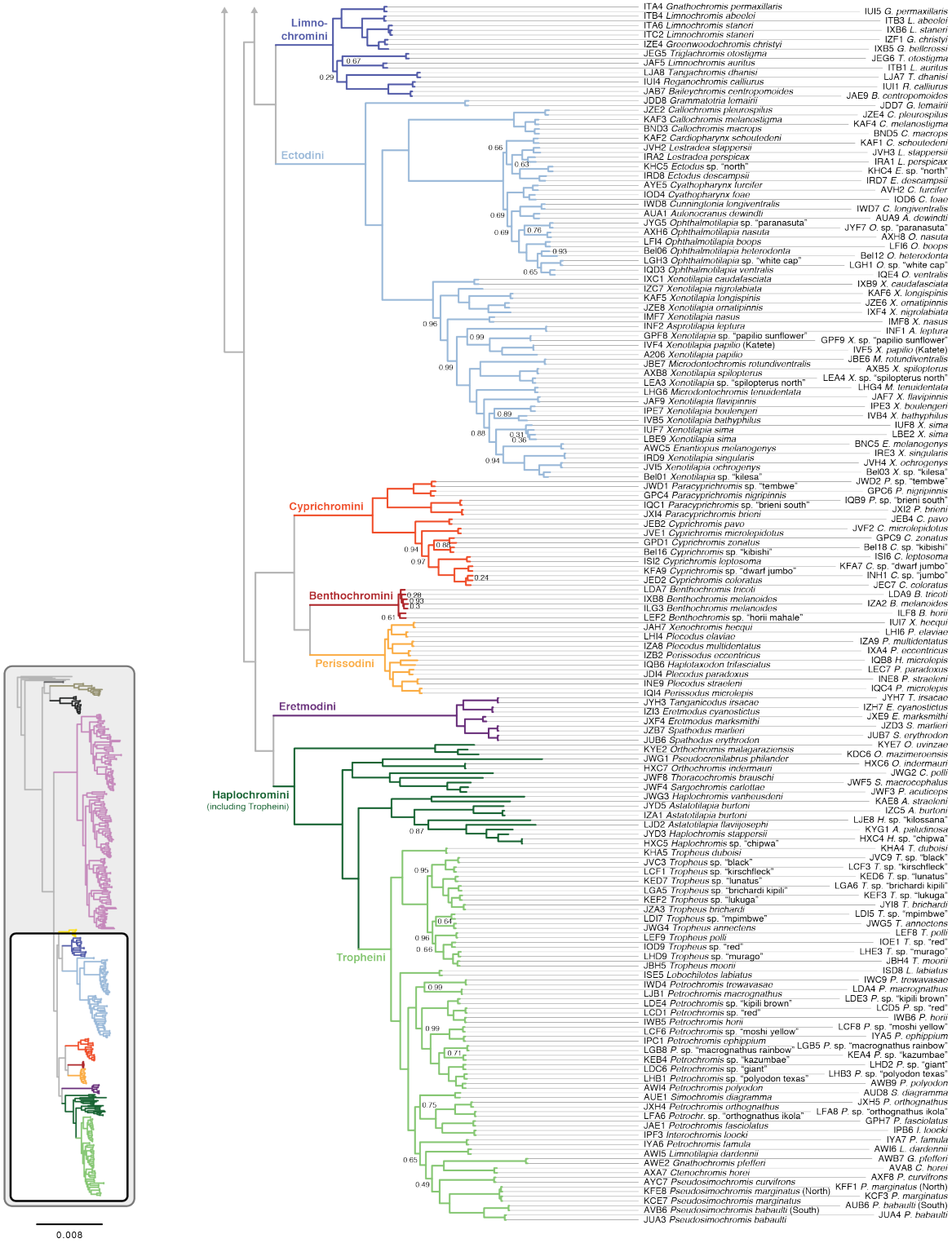

Supplementary Fig. 1 | Individual-level phylogeny for the cichlid adaptive radiation in Lake Tanganyika. Maximum-likelihood tree inferred from nuclear SNPs. Node labels indicate the proportion of data subsets supporting a clade (equal to 1 for all nodes without labels).

Supplementary Fig. 2 continues on the next page

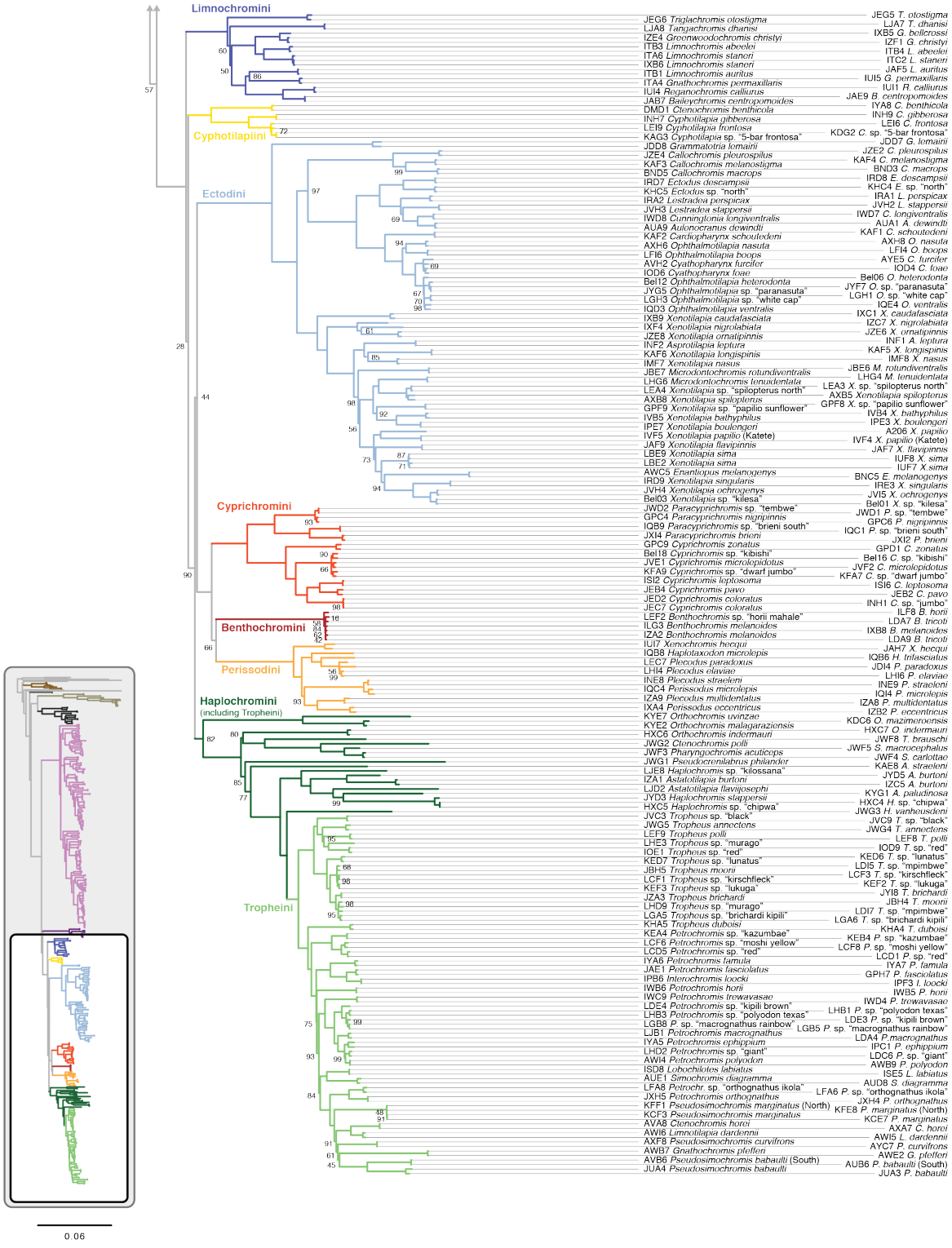

Supplementary Fig. 2 | Individual-level mitochondrial phylogeny for the cichlid adaptive radiation in Lake Tanganyika. Maximum-likelihood tree inferred from mitochondrial genomes. Node labels represent bootstrap values (100 for all nodes without labels).

Supplementary Table 1 | Sample size information per species. For each analysis the total sample size is given whereas the number in brackets indicates the number of specimens used uniquely for the respective analysis. All genomes and raw sequences are available at NCBI under the BioProject accession number PRJNA550295. A full list of individual specimen vouchers including details on sampling location is provided as Supplementary Table 2. AMNH = American Museum of Natural History (New York, USA); MRAC = Royal Museum for Central Africa (Tervuren, Belgium); HHB = Private collection of one of the authors, H.H.B.

Supplementary Table 2 | Specimen list. Overview over all cichlid specimens used in this study with taxonomic information and sampling locations.

Supplementary Tables are provided as a separate file.

Supplementary Table 1

Species abbr.	Full name	Tribe	Origin	Sample source	Stable isotope	Body & OJ morphology	LPJ shape	Pigmentation pattern	Genomes	Total specimens	Comment	Read depth after mapping to the Nile Tilapia reference genome (mean|median)
Batfas	*Bathybates fasciatus*	Bathybatini	LT	own collection	10	8	5	5	2 (1)	11	LT radiation	GPB2: 7.17|7; ITH3: 10.79|12
Batfer	*Bathybates ferox*	Bathybatini	LT	own collection	10	10	5	5	2	10	LT radiation	LCD6: 6.42|6; LCD7: 6.07|6
Batgra	*Bathybates graueri*	Bathybatini	LT	own collection	10	10	5	5	2 (2)	12	LT radiation	ILG7: 9.42|10; IUI8: 7.23|7
Bathor	*Bathybates hornii*	Bathybatini	LT	own collection	1	1	1	1	2 (2)	3	LT radiation	JDE3: 8.09|8; JDE4: 10.61|11
Batleo	*Bathybates leo*	Bathybatini	LT	own collection	10 (3)	7	5	5	1 (1)	11	LT radiation	ILF7: 6.73|7
Batmin	*Bathybates minor*	Bathybatini	LT	own collection	10	10	5	5	2 (1)	11	LT radiation	IXA5: 7.45|7; JBG3: 6.96|7
Batvit	*Bathybates vittatus*	Bathybatini	LT	own collection	10 (3)	5	5	5	3 (3)	13	LT radiation	ITD7: 7.43|7; JDE6: 9.41|10; JDE7: 9.36|9
HemstZ	*Hemibates koningsi*	Bathybatini	LT	own collection & F. Schedel	2	2	2	2	2 (1)	3	LT radiation	IZA5: 12.52|14; LJC5: 8.82|7
Hemste	*Hemibates stenosoma*	Bathybatini	LT	own collection	9	9	5	5	2 (2)	11	LT radiation	IXC2: 6.85|7; IXC3: 7.11|7
Benhor	*Benthochromis horii*	Benthochromini	LT	own collection	10	10	5	5	1 (1)	11	LT radiation	ILF8: 9.09|9
Benmel	*Benthochromis melanoides*	Benthochromini	LT	own collection	10	10	5	5	3 (3)	13	LT radiation	ILG3: 9.14|9; IXB8: 7.35|7; IZA2: 7.37|7
BenhoM	*Benthochromis* sp. "horii mahale"	Benthochromini	LT	own collection	10	10	5	5	1	10	LT radiation	LEF2: 11.86|13
Bentri	*Benthochromis tricoti*	Benthochromini	LT	own collection	10	10	5	5	2	10	LT radiation	LDA7: 7.43|7; LDA9: 7.83|8
Boumic	*Boulengerochromis microlepis*	Boulengerochromini	LT	own collection	10	10	5	5	2 (2)	12	LT radiation	JAE7: 14.67|16; JCF2: 15.43|17
Cteben	*Ctenochromis benthicola*	Cyphotilapiini	LT	own collection	0	6 (1)	5	0	2 (2)	8	LT radiation	DMD1: 8.43|8; IYA8: 7.35|7
Cphfro	*Cyphotilapia frontosa*	Cyphotilapiini	LT	own collection	10	10	5	4	2	10	LT radiation	LEI6: 7.05|7; LEI9: 6.98|7
Cphgib	*Cyphotilapia gibberosa*	Cyphotilapiini	LT	own collection	10	10	5	5	2 (2)	12	LT radiation	INH7: 10.12|10; INH9: 9.6|10
Cphfr5	*Cyphotilapia* sp. "5-bar frontosa"	Cyphotilapiini	LT	own collection	10	10	5	3	2 (2)	12	LT radiation	KAG3: 10.33|11; KDG2: 13.12|14
Cypcol	*Cyprichromis coloratus*	Cyprichromini	LT	own collection	10	10	5	5	2 (1)	11	LT radiation	JEC7: 15.66|18; JED2: 14.4|16
Cyplep	*Cyprichromis leptosoma*	Cyprichromini	LT	own collection	10	10	5	5	2 (2)	12	LT radiation	ISI2: 8.9|9; ISI6: 8.08|8
Cypmic	*Cyprichromis microlepidotus*	Cyprichromini	LT	own collection	10	10	5	5	2 (2)	12	LT radiation	JVE1: 6.1|6; JVF2: 6.7|7
Cyppav	*Cyprichromis pavo*	Cyprichromini	LT	own collection	10	10	5	5	2 (2)	12	LT radiation	JEB2: 9.01|9; JEB4: 7.66|7
Cypdwj	*Cyprichromis* sp. "dwarf jumbo"	Cyprichromini	LT	own collection	10	10	5	5	2 (2)	12	LT radiation	KFA7: 12.84|14; KFA9: 10.64|11
Cypkan	*Cyprichromis* sp. "jumbo"	Cyprichromini	LT	own collection	10	10	5	5	1	10	LT radiation	INH1: 9.78|10
Cypkib	*Cyprichromis* sp. "kibishi"	Cyprichromini	LT	MRAC	0	0	0	0	2 (2)	2	LT radiation	Bel16: 6.63|6; Bel18: 7.33|7
Cypzon	*Cyprichromis zonatus*	Cyprichromini	LT	own collection	10	10	5	5	2	10	LT radiation	GPC9: 9.79|10; GPD1: 6.35|6
PcybrN	*Paracyprichromis brieni*	Cyprichromini	LT	own collection	10	10	5	5	2 (2)	12	LT radiation	JXI2: 7.1|7; JXI4: 6.03|6
Pcynig	*Paracyprichromis nigripinnis*	Cyprichromini	LT	own collection	10	10	5	5	2 (2)	12	LT radiation	GPC4: 12.88|14; GPC6: 6.45|6
Pcybri	*Paracyprichromis* sp. "brieni south"	Cyprichromini	LT	own collection	10	10	5	5	2 (2)	12	LT radiation	IQB9: 8.27|8; IQC1: 5.99|6
Pcytem	*Paracyprichromis* sp. "tembwe"	Cyprichromini	LT	HHB	0	0	0	0	2 (2)	2	LT radiation	JWD1: 16.84|19; JWD2: 16.05|18
Asplep	*Asprotilapia leptura*	Ectodini	LT	own collection	10	10	5	5	2 (2)	12	LT radiation	INF1: 9.8|10; INF2: 14.13|16
Auldew	*Aulonocranus dewindti*	Ectodini	LT	own collection	10	10	5	5	2 (2)	12	LT radiation	AUA1: 7.93|8; AUA9: 7.81|8
Calmac	*Callochromis macrops*	Ectodini	LT	own collection	10	10	5	5	2 (2)	12	LT radiation	BND3: 7.9|8; BND5: 8.54|9
Calmel	*Callochromis melanostigma*	Ectodini	LT	own collection	10	10	5	5	2 (2)	12	LT radiation	KAF3: 7.6|8; KAF4: 7.64|8
Calple	*Callochromis pleurospilus*	Ectodini	LT	own collection	10	10	5	5	2 (2)	12	LT radiation	JZE2: 8.02|8; JZE4: 14.8|17
Carsch	*Cardiopharynx schoutedeni*	Ectodini	LT	own collection	10	10	5	2	2 (2)	12	LT radiation	KAF1: 7.3|7; KAF2: 12.46|14
Cunlon	*Cunningtonia longiventralis*	Ectodini	LT	own collection	10	10	5	5	2 (2)	12	LT radiation	IWD7: 6.48|6; IWD8: 7.71|8
Cyafoa	*Cyathopharynx foae*	Ectodini	LT	own collection	10	10	5	5	2 (2)	12	LT radiation	IOD4: 6.86|7; IOD6: 5.79|5
Cyafur	*Cyathopharynx furcifer*	Ectodini	LT	own collection	10	10	5	5	2 (2)	12	LT radiation	AVH2: 8.11|8; AYE5: 8.2|8
Ectdes	*Ectodus descampsii*	Ectodini	LT	own collection	10	10	5	3	2 (2)	12	LT radiation	IRD7: 9.87|10; IRD8: 6.84|7
EctspN	*Ectodus* sp. "north"	Ectodini	LT	own collection	10	10	5	3	2 (2)	12	LT radiation	KHC4: 6.7|7; KHC5: 6.55|6
Enamel	*Enantiopus melanogenys*	Ectodini	LT	own collection	10	10	5	5	2 (2)	12	LT radiation	AWC5: 8.35|8; BNC5: 9.07|9
Gralem	*Grammatotria lemairii*	Ectodini	LT	own collection	10 (1)	9	5	5	2 (2)	12	LT radiation	JDD7: 12.78|14; JDD8: 7.04|7
Lesper	*Lestradea perspicax*	Ectodini	LT	own collection	10	10	5	5	2 (2)	12	LT radiation	IRA1: 6.01|6; IRA2: 8.29|8
Lessta	*Lestradea stappersii*	Ectodini	LT	own collection	10	10	5	5	2 (2)	12	LT radiation	JVH2: 6.8|7; JVH3: 5.54|5
Mdcrot	*Microdontochromis rotundiventralis*	Ectodini	LT	own collection	10	10	5	5	2 (2)	12	LT radiation	JBE6: 7.4|7; JBE7: 12.3|14
Mdcten	*Microdontochromis tenuidentata*	Ectodini	LT	own collection	10	10	5	5	2 (2)	12	LT radiation	LHG4: 9.78|10; LHG6: 11.17|12
Ophboo	*Ophthalmotilapia boops*	Ectodini	LT	own collection	10	10	5	5	2	10	LT radiation	LFI4: 7.64|8; LFI6: 7.41|7
Ophhet	*Ophthalmotilapia heterodonta*	Ectodini	LT	own collection & MRAC	0	1	0	1	2 (2)	3	LT radiation	Bel06: 6.54|6; Bel12: 7.2|7
Ophnas	*Ophthalmotilapia nasuta*	Ectodini	LT	own collection	10	10	5	5	2 (2)	12	LT radiation	AXH6: 8.05|8; AXH8: 8.39|8
Ophpar	*Ophthalmotilapia* sp. "paranasuta"	Ectodini	LT	own collection	10	10	5	5	2 (2)	12	LT radiation	JYF7: 9.87|10; JYG5: 7.98|8
Ophwhi	*Ophthalmotilapia* sp. "white cap"	Ectodini	LT	own collection	10	9	5	5	2	10	LT radiation	LGH1: 8.25|8; LGH3: 7.51|7
Ophven	*Ophthalmotilapia ventralis*	Ectodini	LT	own collection	10	10	5	5	2 (2)	12	LT radiation	IQD3: 7.78|8; IQE4: 7.13|7
Xenbat	*Xenotilapia bathyphilus*	Ectodini	LT	own collection	10	10	5	5	2 (2)	12	LT radiation	IVB4: 8.98|9; IVB5: 7.15|7
Xenbou	*Xenotilapia boulengeri*	Ectodini	LT	own collection	10	10	5	5	2 (2)	12	LT radiation	IPE3: 7.56|7; IPE7: 7.34|7
Xencau	*Xenotilapia caudafasciata*	Ectodini	LT	own collection	10	9	5	5	2 (2)	12	LT radiation	IXB9: 7.85|8; IXC1: 7.27|7
Xenfla	*Xenotilapia flavipinnis*	Ectodini	LT	own collection	10	10	5	5	2 (2)	12	LT radiation	JAF7: 14.97|17; JAF9: 13.26|15
Xenlon	*Xenotilapia longispinis*	Ectodini	LT	own collection	10	10	5	5	2 (2)	12	LT radiation	KAF5: 8.69|9; KAF6: 9.6|10
Xennas	*Xenotilapia nasus*	Ectodini	LT	own collection	10	10	5	5	2 (2)	12	LT radiation	IMF7: 6.93|7; IMF8: 11.1|12
XenniS	*Xenotilapia nigrolabiata*	Ectodini	LT	own collection	10	10	5	5	2 (1)	11	LT radiation	IXF4: 14.05|16; IZC7: 7.51|7
Xenoch	*Xenotilapia ochrogenys*	Ectodini	LT	own collection	10	10	5	5	2 (2)	12	LT radiation	JVH4: 9.13|9; JVI5: 10.73|12
Xenorn	*Xenotilapia ornatipinnis*	Ectodini	LT	own collection	10	10	5	3	2 (2)	12	LT radiation	JZE6: 8.5|9; JZE8: 7.91|8
XenorS	*Xenotilapia ornatipinnis* (South)	Ectodini	LT	own collection	1	1	1	0	0	1	LT radiation	
XenpaK	*Xenotilapia papilio*	Ectodini	LT	HHB	10 (4)	4	5	0	1 (1)	11	LT radiation	A206: 9.77|9
Xenpap	*Xenotilapia papilio* (Katete)	Ectodini	LT	own collection	10	10	5	5	2 (2)	12	LT radiation	IVF4: 11|12; IVF5: 6.57|6
Xensim	*Xenotilapia sima*	Ectodini	LT	own collection	10	10	5	5	4 (2)	12	LT radiation	IUF7: 8.56|9; IUF8: 8.66|9; LBE2: 8.69|9; LBE9: 6.79|7
Xensin	*Xenotilapia singularis*	Ectodini	LT	own collection	10	10	5	5	2	10	LT radiation	IRD9: 7.34|7; IRE3: 6.79|6
Xenkil	*Xenotilapia* sp. "kilesa"	Ectodini	LT	MRAC	0	0	0	0	2 (2)	2	LT radiation	Bel01: 10.43|11; Bel03: 5.99|6
Xensun	*Xenotilapia* sp. "papilio sunflower"	Ectodini	LT	own collection	10	10	5	5	2 (2)	12	LT radiation	GPF8: 7.28|7; GPF9: 8.1|8
XenspN	*Xenotilapia* sp. "spilopterus north"	Ectodini	LT	own collection	10	10	5	0	2 (2)	12	LT radiation	LEA3: 6.78|7; LEA4: 6.59|6
Xenspi	*Xenotilapia spilopterus*	Ectodini	LT	own collection	10	10	5	5	2 (2)	12	LT radiation	AXB5: 7.89|8; AXB8: 7.87|8
Erecya	*Eretmodus cyanostictus*	Eretmodini	LT	own collection	10	10	5	4	2 (2)	12	LT radiation	IZH7: 18.76|22; IZI3: 12.02|13
Eremar	*Eretmodus marksmithi*	Eretmodini	LT	own collection	10	10	5	3	2 (2)	12	LT radiation	JXE9: 10.01|11; JXF4: 6.34|6
Spaery	*Spathodus erythrodon*	Eretmodini	LT	own collection	10	10	5	5	2 (2)	12	LT radiation	JUB6: 7.13|7; JUB7: 8.44|9
Spamar	*Spathodus marlieri*	Eretmodini	LT	own collection	10	10	5	5	2 (2)	12	LT radiation	JZB7: 6.16|6; JZD3: 10.18|11
Tanirs	*Tanganicodus irsacae*	Eretmodini	LT	own collection	10	10	5	5	2 (2)	12	LT radiation	JYH3: 9.7|10; JYH7: 7.17|7
Altcal	*Altolamprologus calvus*	Lamprologini	LT	own collection	10	10	5	5	2 (2)	12	LT radiation	IOE2: 7.92|8; IOE3: 9.38|10
Altcom	*Altolamprologus compressiceps*	Lamprologini	LT	own collection	10	10	5	5	2 (2)	12	LT radiation	ISB1: 8.29|8; ISC9: 9.3|10
Altshe	*Altolamprologus* sp. "compressiceps shell"	Lamprologini	LT	own collection	10	10	5	5	2 (2)	12	LT radiation	IRH2: 5.76|5; IRH4: 6.04|6
Chabri	*Chalinochromis brichardi*	Lamprologini	LT	own collection	10	10	5	5	2 (2)	12	LT radiation	AVA9: 7.76|8; AVB2: 7.5|8
Chacya	*Chalinochromis cyanophleps*	Lamprologini	LT	own collection	10	10	5	5	2	10	LT radiation	LGG6: 8.11|8; LGG7: 7.72|8
Chapop	*Chalinochromis popelini*	Lamprologini	LT	MRAC	0	0	0	0	2 (2)	2	LT radiation	Bel07: 7.68|7; Bel09: 6.9|7
Chabif	*Chalinochromis* sp. "bifrenatus"	Lamprologini	LT	own collection	10	10	5	5	2	10	LT radiation	LDD9: 7.53|8; LDE1: 7.59|8
Chando	*Chalinochromis* sp. "ndobhoi"	Lamprologini	LT	own collection	10	10	5	3	2 (2)	12	LT radiation	KEE9: 7.16|7; KEF1: 7.39|7
Juldic	*Julidochromis dickfeldi*	Lamprologini	LT	own collection	10	10	5	5	2 (2)	12	LT radiation	IRC4: 10|11; IRC5: 7.3|7
Julmrk	*Julidochromis marksmithi*	Lamprologini	LT	own collection	10	9	5	5	2	10	LT radiation	LFG8: 6.77|7; LFH1: 8.69|9
JulmaN	*Julidochromis marlieri*	Lamprologini	LT	own collection	10	10	5	5	2 (2)	12	LT radiation	JXB5: 9.12|10; JXC1: 8.81|9
Julorn	*Julidochromis ornatus*	Lamprologini	LT	own collection	10	10	5	5	2 (2)	12	LT radiation	ISB7: 6.61|6; ISC1: 8.51|9
JulreK	*Julidochromis regani*	Lamprologini	LT	own collection	10	10	5	1	2 (2)	12	LT radiation	KFF4: 7.47|8; KHE6: 7.01|7
Julkom	*Julidochromis* sp. "kombe"	Lamprologini	LT	own collection	10	10	5	5	2 (2)	12	LT radiation	ILD9: 7.18|7; INA6: 6.64|6
JulmaS	*Julidochromis* sp. "marlieri south"	Lamprologini	LT	own collection	10	10	5	4	2	10	LT radiation	LBA1: 8.22|8; LBF3: 8.72|9
Julreg	*Julidochromis* sp. "regani south"	Lamprologini	LT	own collection	10	10	5	5	2 (2)	12	LT radiation	IRB2: 6.63|6; IRB8: 7.63|8
Julunt	*Julidochromis* sp. "unterfels"	Lamprologini	LT	HHB	9 (3)	5	5	0	2 (2)	11	LT radiation	JWA1: 14.33|16; JWA2: 16.05|18
Jultra	*Julidochromis transcriptus*	Lamprologini	LT	H. Gante	0	0	0	0	2 (2)	2	LT radiation	HFG1287: 11|12; LJC2: 9.91|10
Lamcal	*Lamprologus callipterus*	Lamprologini	LT	own collection	10	10	5	4	2 (2)	12	LT radiation	IPH2: 10.05|11; JAB1: 7.77|8
Lamfin	*Lamprologus finalimus*	Lamprologini	LT	AMNH	0	1 (1)	0	0	0	1	LT radiation	
Lamkun	*Lamprologus kungweensis*	Lamprologini	LT	own collection	9	10 (1)	5	5	2 (2)	12	LT radiation	JXG8: 12.91|14; JXH2: 12.97|14
Lamlap	*Lamprologus laparogramma*	Lamprologini	LT	own collection	10 (1)	9	5	5	2 (2)	12	LT radiation	JDI1: 7.72|8; JDI2: 9.52|10
Lamlem	*Lamprologus lemairii*	Lamprologini	LT	own collection	10	10	5	5	2 (2)	12	LT radiation	IPD6: 6.46|6; IZI7: 7.93|8
Lammel	*Lamprologus meleagris*	Lamprologini	LT	HHB	10 (3)	8 (1)	5	0	2 (2)	13	LT radiation	JWA8: 5.66|5; JWA9: 10.88|11
Lamoce	*Lamprologus ocellatus*	Lamprologini	LT	own collection	10 (1)	9	5	5	2 (2)	12	LT radiation	ILC1: 6.88|7; ILD3: 8.02|8
Lamorn	*Lamprologus ornatipinnis*	Lamprologini	LT	own collection	10	9	5	5	2 (2)	12	LT radiation	JZF3: 14.59|16; JZF4: 12.01|13
Lamsig	*Lamprologus signatus*	Lamprologini	LT	own collection	10	10	5	5	2 (2)	12	LT radiation	IWD5: 8.15|8; IWD6: 9.37|10
LamorC	*Lamprologus* sp. "ornatipinnis congo"	Lamprologini	LT	HHB	1	5	5	0	2 (2)	7	LT radiation	JWA3: 6.8|7; JWA4: 6.58|6
LamorS	*Lamprologus* sp. "ornatipinnis zambia"	Lamprologini	LT	own collection	9	9	5	5	2 (2)	11	LT radiation	JDF5: 8.1|8; JDG4: 6.46|6
Lamspe	*Lamprologus speciosus*	Lamprologini	LT	own collection	10	10	5	5	2 (2)	12	LT radiation	KCG2: 9.72|10; KCG3: 13.48|15
Lepatt	*Lepidiolamprologus attenuatus*	Lamprologini	LT	own collection	10	10	5	5	2 (2)	12	LT radiation	AVD4: 7.38|7; AVG5: 8.1|8
Lepcun	*Lepidiolamprologus cunningtoni*	Lamprologini	LT	own collection	10	10	5	5	2	10	LT radiation	IOH4: 8.18|8; IOH5: 13.28|15
Lepelo	*Lepidiolamprologus elongatus*	Lamprologini	LT	own collection	10	10	5	5	2 (2)	12	LT radiation	AUE6: 7.25|7; AUG8: 7.6|8
Lepkam	*Lepidiolamprologus kamambae*	Lamprologini	LT	own collection	10	10	5	5	2	10	LT radiation	LFF7: 5.92|6; LFF8: 8.29|8
Lepken	*Lepidiolamprologus kendalli*	Lamprologini	LT	own collection	10	10	5	5	2 (2)	12	LT radiation	IMD1: 13.55|15; IMD2: 7.72|8
Lepmim	*Lepidiolamprologus mimicus*	Lamprologini	LT	own collection	10	10	5	5	2	10	LT radiation	LDD1: 7.63|8; LDD6: 7.6|8
Lepnka	*Lepidiolamprologus nkambae*	Lamprologini	LT	own collection	0	1 (1)	0	0	0	1	LT radiation	
Leppro	*Lepidiolamprologus profundicola*	Lamprologini	LT	own collection	10 (1)	8	5	4	2	10	LT radiation	KAD2: 8.55|9; KEB8: 8.61|9
LepmeK	*Lepidiolamprologus* sp. "meeli kipili"	Lamprologini	LT	own collection	10 (2)	7	5	5	2	10	LT radiation	LHA2: 7.43|7; LHA5: 7.94|8
Neobif	*Neolamprologus bifasciatus*	Lamprologini	LT	own collection	10	10	5	5	2	10	LT radiation	LHF6: 7.29|7; LHF7: 7.25|7
Neobou	*Neolamprologus boulengeri*	Lamprologini	LT	own collection	10	10	5	5	2 (2)	12	LT radiation	KCE5: 6.92|7; KYB9: 7.69|8
Neobre	*Neolamprologus brevis*	Lamprologini	LT	own collection	10 (1)	9	5	5	2 (2)	12	LT radiation	ILB6: 6.49|6; ILB7: 6.76|7
Neobri	*Neolamprologus brichardi*	Lamprologini	LT	own collection	10	10	5	5	2 (2)	12	LT radiation	JUH9: 8.39|9; JUI1: 6.18|6
Neobue	*Neolamprologus buescheri*	Lamprologini	LT	own collection	10	10	5	4	2 (2)	12	LT radiation	JEI4: 7.2|7; JEI5: 7.36|7
Neocal	*Neolamprologus calliurus*	Lamprologini	LT	own collection	10	10	5	5	2 (2)	12	LT radiation	ILA7: 9.77|10; INC7: 8.19|8
Neocan	*Neolamprologus cancellatus*	Lamprologini	LT	H. Tanaka & HHB	1	2	2	0	2	2	LT radiation	LJC9: 6.8|6; LJD1: 6.26|5
Neocau	*Neolamprologus caudopunctatus*	Lamprologini	LT	own collection	10	10	5	5	2 (2)	12	LT radiation	IQA3: 14.65|16; IQA4: 7.62|8
Neochi	*Neolamprologus chitamwebwai*	Lamprologini	LT	own collection	10	10	5	4	2 (2)	12	LT radiation	KHA7: 7.04|7; KHA9: 5.95|6
Neochr	*Neolamprologus christyi*	Lamprologini	LT	own collection	10	10	5	5	2 (2)	12	LT radiation	ITG2: 8.33|9; IZI8: 6.66|6
Neocra	*Neolamprologus crassus*	Lamprologini	LT	own collection	10	10	5	5	2 (2)	12	LT radiation	IVE8: 8.83|9; IVF1: 8.78|9
Neocyl	*Neolamprologus cylindricus*	Lamprologini	LT	own collection	10	10	5	5	2	10	LT radiation	GPH1: 13.67|15; GPH2: 9.64|10
Neofal	*Neolamprologus falcicula*	Lamprologini	LT	own collection	10	10	5	5	2 (2)	12	LT radiation	JXD4: 9.12|9; JXD7: 11.14|12
Neofas	*Neolamprologus fasciatus*	Lamprologini	LT	own collection	10	10	5	5	2 (2)	12	LT radiation	AUE7: 10.06|11; AXD5: 8.03|8
Neofur	*Neolamprologus furcifer*	Lamprologini	LT	own collection	10	10	5	5	2 (2)	12	LT radiation	JEI6: 10.2|11; JEI8: 12.94|14
Neogra	*Neolamprologus gracilis*	Lamprologini	LT	HHB	10 (5)	5	5	0	2 (2)	12	LT radiation	JWH1: 11.41|12; JWH2: 13|14
Neohec	*Neolamprologus hecqui*	Lamprologini	LT	HHB & MRAC	0	0	0	0	3 (3)	3	LT radiation	A142: 11.49|12; Bel13: 6.44|6; Bel14: 6.86|7
Neohel	*Neolamprologus helianthus*	Lamprologini	LT	HHB	10 (5)	5	5	0	2 (2)	12	LT radiation	JWG8: 5.51|5; JWG9: 10.62|11
NeoleL	*Neolamprologus leleupi*	Lamprologini	LT	HHB	5	3	5	0	1 (1)	6	LT radiation	JWH9: 10.69|11
Neolou	*Neolamprologus leloupi*	Lamprologini	LT	own collection	10	10	5	5	2 (2)	12	LT radiation	LCA1: 7.31|7; LCA2: 8.16|8
Neolon	*Neolamprologus longicaudatus*	Lamprologini	LT	own collection	0	0	0	0	2 (2)	2	LT radiation	JWI2: 8.17|8; JWI3: 10.71|11
Neoleu	*Neolamprologus longior*	Lamprologini	LT	own collection	10	10	5	5	2 (2)	12	LT radiation	KEH3: 12.67|14; LEE1: 7|7
Neomar	*Neolamprologus marunguensis*	Lamprologini	LT	HHB	10 (5)	5	5	0	2 (2)	12	LT radiation	JWH3: 10.92|12; JWH4: 11.28|12
Neomee	*Neolamprologus meeli*	Lamprologini	LT	own collection	10	10	5	4	2 (2)	12	LT radiation	JDF3: 6.75|6; JDF4: 13.81|15
Neomod	*Neolamprologus modestus*	Lamprologini	LT	own collection	10	10	5	5	2 (1)	11	LT radiation	IMG9: 8.35|8; IMH3: 9.78|10
Neomon	*Neolamprologus mondabu*	Lamprologini	LT	own collection	10	10	5	5	2 (2)	12	LT radiation	JVB4: 10.78|11; JVB8: 9.08|9
Neomul	*Neolamprologus multifasciatus*	Lamprologini	LT	own collection	10	10	5	5	2 (2)	12	LT radiation	IRF6: 6.96|7; IRF8: 6.26|6
Neomux	*Neolamprologus mustax*	Lamprologini	LT	own collection	10	10	5	5	2 (2)	12	LT radiation	ILB4: 8.5|9; ILH1: 6.41|6
Neonig	*Neolamprologus niger*	Lamprologini	LT	own collection	10	10	5	5	2	10	LT radiation	KYA1: 6.37|6; KYA5: 6.76|7
Neonve	*Neolamprologus nigriventris*	Lamprologini	LT	HHB	4	5	5	0	2 (2)	7	LT radiation	A108: 9.75|10; LJC3: 10.85|11
Neoobs	*Neolamprologus obscurus*	Lamprologini	LT	own collection	10	10	5	5	2 (2)	12	LT radiation	IMA1: 7.43|7; IMA2: 6.58|6
Neooli	*Neolamprologus olivaceous*	Lamprologini	LT	HHB	10 (4)	6	5	0	2 (2)	12	LT radiation	JWH5: 10.81|11; JWH6: 11.65|12
Neopec	*Neolamprologus pectoralis*	Lamprologini	LT	HHB	5	6 (1)	5	0	2 (2)	8	LT radiation	JWA7: 11.23|12; JWI6: 11.19|12
Neopet	*Neolamprologus petricola*	Lamprologini	LT	own collection	10	10	5	5	2	10	LT radiation	LGH8: 7.71|8; LGI1: 8|8
Neople	*Neolamprologus pleuromaculatus*	Lamprologini	LT	own collection	4	4	4	3	2 (2)	6	LT radiation	JZF1: 8.12|8; JZF2: 14.36|16
Neopro	*Neolamprologus prochilus*	Lamprologini	LT	own collection	10	10	5	5	2 (2)	12	LT radiation	IVH1: 7.93|8; IVH2: 7.43|7
Neopul	*Neolamprologus pulcher*	Lamprologini	LT	own collection	10	10	5	5	2 (2)	12	LT radiation	ISA6: 6.87|7; ISB3: 7.79|8
Neosav	*Neolamprologus savoryi*	Lamprologini	LT	own collection	10	10	5	5	2 (2)	12	LT radiation	ISA8: 8.78|9; IYA4: 6.64|6
Neosex	*Neolamprologus sexfasciatus*	Lamprologini	LT	own collection	10	10	5	5	2 (2)	12	LT radiation	IND7: 8.09|8; IND8: 7.6|8
Neosim	*Neolamprologus similis*	Lamprologini	LT	own collection	10	10	5	5	2 (2)	12	LT radiation	KEC1: 8.62|9; KEC2: 7.62|8
NeobrM	*Neolamprologus* sp. "brevis magara"	Lamprologini	LT	own collection	10	10	5	5	2 (2)	12	LT radiation	KCI6: 13.74|15; KCI7: 7.38|7
NeocaK	*Neolamprologus* sp. "caudopunctatus kipili"	Lamprologini	LT	own collection	10	10	5	4	2	10	LT radiation	LDG2: 7.1|7; LDG3: 8.03|8
Neocyg	*Neolamprologus* sp. "cygnus"	Lamprologini	LT	own collection	10	10	5	5	2	10	LT radiation	LFD2: 8.28|8; LFD4: 8.07|8
Neoese	*Neolamprologus* sp. "eseki"	Lamprologini	LT	own collection	10	10	5	5	2	10	LT radiation	LFB7: 6.1|6; LFB9: 8.19|8
NeofaM	*Neolamprologus* sp. "falcicula mahale"	Lamprologini	LT	own collection	11	11	5	5	2 (1)	12	LT radiation	LCB5: 6.24|6; LCC2: 6.11|6
NeofuU	*Neolamprologus* sp. "furcifer ulwile"	Lamprologini	LT	own collection	10	10	5	4	2	10	LT radiation	LDF4: 7.62|8; LDF5: 7.71|8
NeogrM	*Neolamprologus* sp. "gracilis tanzania"	Lamprologini	LT	own collection	10	10	5	5	2 (1)	11	LT radiation	LCB4: 6.67|7; LCC6: 6.87|7
Neokom	*Neolamprologus* sp. "kombe"	Lamprologini	LT	own collection	10	10	5	5	2 (2)	12	LT radiation	ILE5: 5.75|5; ILE6: 8.15|8
NeoveS	*Neolamprologus* sp. "ventralis stripe"	Lamprologini	LT	own collection	7	7	5	5	2	7	LT radiation	JED4: 8.09|8; JED5: 14.11|16
Neospl	*Neolamprologus splendens*	Lamprologini	LT	HHB	10 (5)	5	5	0	2 (2)	12	LT radiation	A188: 7.12|4; LJD3: 8.63|6
Neotet	*Neolamprologus tetracanthus*	Lamprologini	LT	own collection	10	10	5	5	2 (2)	12	LT radiation	IPF7: 6.91|7; IPG3: 10.43|11
Neotim	*Neolamprologus timidus*	Lamprologini	LT	own collection	10	10	5	2	2	10	LT radiation	LGE2: 7.67|8; LGE3: 6.29|6
Neotoa	*Neolamprologus toae*	Lamprologini	LT	own collection	10	10	5	5	2 (2)	12	LT radiation	JZD5: 8.46|9; JZD6: 9.24|10
Neotre	*Neolamprologus tretocephalus*	Lamprologini	LT	own collection	10	10	5	4	2 (2)	12	LT radiation	KFH4: 7.73|8; KFH5: 7.72|8
Neovar	*Neolamprologus variostigma*	Lamprologini	LT	HHB	0	0	0	0	2 (2)	2	LT radiation	JWA5: 14.6|16; JWA6: 16.21|19
NeoveB	*Neolamprologus ventralis* (Burundi)	Lamprologini	LT	own collection	6	6	5	0	2 (2)	8	LT radiation	KAG7: 14.64|16; KAG8: 15.74|18
Neowal	*Neolamprologus walteri*	Lamprologini	LT	own collection	10 (1)	9	5	4	2 (2)	12	LT radiation	KFD2: 7.45|7; KFD4: 7.3|7
Telbif	*Telmatochromis bifrenatus*	Lamprologini	LT	own collection	10	10	5	5	2 (2)	12	LT radiation	KYB7: 7.15|7; KYB8: 7.36|7
Telbra	*Telmatochromis brachygnathus*	Lamprologini	LT	own collection	9	9	5	5	2 (2)	11	LT radiation	JBE8: 6.74|6; JBE9: 7.03|7
Telbri	*Telmatochromis brichardi*	Lamprologini	LT	own collection	10	10	5	5	2 (2)	12	LT radiation	JVI9: 8.27|8; JXA4: 8.12|8
TeldhS	*Telmatochromis dhonti*	Lamprologini	LT	own collection	10	10	5	5	2 (2)	12	LT radiation	LBF7: 6.9|7; LBF8: 6.57|6
TeldhN	*Telmatochromis* sp. "dhonti north"	Lamprologini	LT	own collection	9	9	5	5	2 (2)	11	LT radiation	JUD4: 6.13|6; JUD5: 12.21|13

Species abbr.	Full name	Tribe	Origin	Sample source	Stable Isotope	Body & Oil morphology	LPJ shape	Pigmentation pattern	Genomes	Total specimens	Comment	Read depth after mapping to the Nile Tilapia reference genome [mean|median]
TeldhT	*Telmatochromis* sp. "dhonti twiyu"	Lamprologini	LT	own collection	10	10	5	5	2 (1)	11	LT radiation	LHC1: 13.1114; LHF2: 11.7912
Telion	*Telmatochromis* sp. "longola"	Lamprologini	LT	HHB	0	1	1	0	2 (2)	3	LT radiation	JWC8: ?/?; JWC9: 12.5814
Telshe	*Telmatochromis* sp. "shell"	Lamprologini	LT	own collection	10	10	5	5	2 (2)	12	LT radiation	IRI8: 8.469; IRI9: 6.89|7
TelteS	*Telmatochromis temporalis*	Lamprologini	LT	own collection	10	10	5	5	2 (2)	12	LT radiation	IMB3: 5.866; IMB4: 8.439
Telvit	*Telmatochromis vittatus*	Lamprologini	LT	own collection	10	10	5	5	2 (2)	12	LT radiation	JBD5: 7.1|17; JBD6: 7.598
Varmoo	*Variabilichromis moorii*	Lamprologini	LT	own collection	10	10	5	5	2 (2)	12	LT radiation	AUC3: 9.38|10; AUC4: 7.568
Baicen	*Baileychromis centropomoides*	Limnochromini	LT	own collection	10	9	5	5	2 (1)	11	LT radiation	JAB7: 7.047; JAE9: 10.15|10
Gnaper	*Gnathochromis permaxillaris*	Limnochromini	LT	own collection	10	10	5	5	2 (2)	12	LT radiation	ITA4: 9.049; IUI5: 8.539
Gwcbel	*Greenwoodochromis bellcrossi*	Limnochromini	LT	own collection	10	10	5	5	1 (1)	11	LT radiation	IXB5: 10.09|10
Gwcchr	*Greenwoodochromis christyi*	Limnochromini	LT	own collection	10	10	5	5	2 (2)	12	LT radiation	IZE4: 9.92|10; IZF1: 7.347
Lchabe	*Limnochromis abeelei*	Limnochromini	LT	own collection	10	10	5	5	2 (2)	12	LT radiation	IT83: 8.479; ITB4: 7.357
Lchaur	*Limnochromis auritus*	Limnochromini	LT	own collection	10	10	5	5	2 (2)	12	LT radiation	ITB1: 7.968; JAF5: 8.28
Lchsta	*Limnochromis staneri*	Limnochromini	LT	own collection	10	10	5	5	3 (3)	13	LT radiation	ITA6: 14.89|17; ITC2: 7.087; IXB6: 7.61|7
Regcal	*Reganochromis calliurus*	Limnochromini	LT	own collection	10	10	5	5	2 (2)	12	LT radiation	IUI1: 6.71|6; IUI4: 7.62|8
Tchdha	*Tangachromis dhanisi*	Limnochromini	LT	own collection	3	3	3	1	2	3	LT radiation	LJA7: 6.226; LJA8: 12.49|13
Tricto	*Triglachromis otostigma*	Limnochromini	LT	own collection	10	10	5	5	2	10	LT radiation	JEG5: 9.149; JEG6: 6.89|7
Hapmic	*Haplotaxodon microlepis*	Perissodini	LT	own collection	10 (2)	7	5	4	1 (1)	11	LT radiation	IQB8: 13.04|14
Haptri	*Haplotaxodon trifasciatus*	Perissodini	LT	own collection	0	0	0	0	1 (1)	1	LT radiation	IQB6: 8.17|8
Perecc	*Perissodus eccentricus*	Perissodini	LT	own collection	10 (1)	9	5	5	2 (2)	12	LT radiation	IXA4: 8.389; IZB2: 12.39|13
Permic	*Perissodus microlepis*	Perissodini	LT	own collection	8	10 (1)	5	5	2 (2)	12	LT radiation	IQC4: 9.19|10; IQI4: 6.98|7
Pleela	*Plecodus elaviae*	Perissodini	LT	own collection	10 (1)	9	5	5	2	10	LT radiation	LHI4: 7.818; LHI6: 8.05|8
Plemul	*Plecodus multidentatus*	Perissodini	LT	own collection	8	8	5	5	2 (2)	10	LT radiation	IZA8: 13.81|15; IZA9: 9.82|10
Plepar	*Plecodus paradoxus*	Perissodini	LT	own collection	10	10	5	5	2 (1)	11	LT radiation	JDI4: 8.659; LEC7: 6.88|7
Plestr	*Plecodus straeleni*	Perissodini	LT	own collection	10	10	5	5	2 (2)	12	LT radiation	INE8: 14.44|16; INE9: 9.22|10
Xchhec	*Xenochromis hecqui*	Perissodini	LT	own collection	10 (1)	9	5	5	2 (2)	12	LT radiation	IUI7: 6.75|7; JAH7: 9.58|10
Trecap	*Trematocara caparti*	Trematocarini	LT	H. Tanaka	3	3	3	0	1	3	LT radiation	LJC8: 6.945
Tremac	*Trematocara macrostoma*	Trematocarini	LT	own collection	10	10	5	5	2 (2)	12	LT radiation	IUD8: 10.72|11; IUD9: 9.76|10
Tremar	*Trematocara marginatum*	Trematocarini	LT	own collection	12 (2)	10	5	4	2 (2)	14	LT radiation	ISA1: 6.28|6; ISA3: 11.67|13
Trenig	*Trematocara nigrifrons*	Trematocarini	LT	own collection	10	10	5	2	2 (2)	12	LT radiation	GPA1: 6.31|6; IUE5: 11.73|11
Tresqn	*Trematocara* sp. "north"	Trematocarini	LT	own collection	0	1	1	0	0	1	LT radiation	
Tresti	*Trematocara stigmaticum*	Trematocarini	LT	own collection	6	6	5	5	2 (2)	8	LT radiation	IUE7: 8.82|8; IZE1: 8.83|9
Treuni	*Trematocara unimaculatum*	Trematocarini	LT	own collection	9	9	5	5	2 (2)	11	LT radiation	IXA3: 9.55|10; IXA6: 9.3|9
Trevar	*Trematocara variabile*	Trematocarini	LT	MRAC	0	0	0	0	1 (1)	1	LT radiation	Be03: 6.48|6
Trezeb	*Trematocara zebra*	Trematocarini	LT	own collection	10	10	5	2	2	10	LT radiation	LFC9: 5.96|5; LFE4: 6.23|6
Ctehor	*Ctenochromis horei*	Tropheini	LT	own collection	10	10	5	5	2 (2)	12	LT radiation	AVA8: 7.91|8; AXA7: 8.26|8
Gnapfe	*Gnathochromis pfefferi*	Tropheini	LT	own collection	10	10	5	5	2 (2)	12	LT radiation	AWB7: 7.49|8; AWE2: 7.24|7
Intlio	*Interochromis loocki*	Tropheini	LT	own collection	10	10	5	5	2 (2)	12	LT radiation	IPB6: 9.08|9; IPF3: 7.22|7
Limdar	*Limnotilapia dardennii*	Tropheini	LT	own collection	10	9	5	9	2 (2)	12	LT radiation	AWI5: 7.84|8; AWI6: 7.99|8
Loblab	*Lobochilotes labiatus*	Tropheini	LT	own collection	10	9	5	5	2 (2)	12	LT radiation	ISD8: 7.57|7; ISE5: 6.55|6
Peteph	*Petrochromis ephippium*	Tropheini	LT	own collection	10 (1)	9	5	5	2 (2)	12	LT radiation	IPC1: 7.44|7; IYA5: 5.95|6
Petfam	*Petrochromis famula*	Tropheini	LT	own collection	10	10	5	5	2 (2)	12	LT radiation	IYA6: 5.92|6; IYA7: 8.21|8
Petfas	*Petrochromis fasciolatus*	Tropheini	LT	own collection	10	10	5	5	2 (2)	12	LT radiation	GPH7: 8|8; JAE1: 7.93|8
Pethor	*Petrochromis horii*	Tropheini	LT	own collection	10	10	5	2	2 (1)	11	LT radiation	IWB5: 7.38|7; IWB6: 9.71|10
Petmac	*Petrochromis macrognathus*	Tropheini	LT	own collection	10	10	5	5	2	10	LT radiation	LDA4: 7.11|7; LJB1: 6.33|6
Petort	*Petrochromis orthognathus*	Tropheini	LT	own collection	10	10	5	3	2	10	LT radiation	JXH4: 4.17|4; JXH5: 12.62|14
Petpol	*Petrochromis polyodon*	Tropheini	LT	own collection	10	9	5	5	2 (2)	12	LT radiation	AWB9: 7.76|8; AWI4: 7.83|8
Petgia	*Petrochromis* sp. "giant"	Tropheini	LT	own collection	10 (1)	3	5	5	2	10	LT radiation	LDC8: 8.22|8; LHD2: 7.6|8
Petkas	*Petrochromis* sp. "kazumbae"	Tropheini	LT	own collection	10	10	5	5	2 (2)	12	LT radiation	KEA4: 8.39|8; KEB4: 8.63|9
Petkip	*Petrochromis* sp. "kipili brown"	Tropheini	LT	own collection	10	10	5	4	2	10	LT radiation	LDE3: 6.5|6; LDE4: 7.46|7
Petrai	*Petrochromis* sp. "macrognathus rainbow"	Tropheini	LT	own collection	10	10	5	5	2	10	LT radiation	LGB5: 7.5|7; LGB8: 7.58|8
Petmos	*Petrochromis* sp. "moshi yellow"	Tropheini	LT	own collection	10	10	5	3	2	10	LT radiation	LCF6: 7.81|8; LCF8: 7.27|7
Petiko	*Petrochromis* sp. "orthognathus ikola"	Tropheini	LT	own collection	10	10	5	5	2	10	LT radiation	LFA6: 7.4|7; LFA8: 7.69|8
Pettex	*Petrochromis* sp. "polyodon texas"	Tropheini	LT	own collection	10	10	5	5	2	10	LT radiation	LHB1: 8.12|8; LHB3: 9.99|10
Petred	*Petrochromis* sp. "red"	Tropheini	LT	own collection	10	10	5	5	2	10	LT radiation	LCD1: 6.5|6; LCD5: 6.53|6
Pettre	*Petrochromis trewavasae*	Tropheini	LT	own collection	10	10	5	5	2	10	LT radiation	IWC9: 14.43|16; IWD4: 8.34|8
Pscbab	*Pseudosimochromis babaulti*	Tropheini	LT	own collection	10	10	5	5	2 (2)	12	LT radiation	JUA3: 8.28|8; JUA4: 12.68|14
Pscpfe	*Pseudosimochromis babaulti* (South)	Tropheini	LT	own collection	10 (1)	9	5	5	2 (2)	12	LT radiation	AUB6: 9.64|10; AVB6: 9.62|10
Pscour	*Pseudosimochromis curvifrons*	Tropheini	LT	own collection	10	10	5	5	2 (2)	12	LT radiation	AXF8: 9.07|9; AYC7: 9.9|10
Pscmar	*Pseudosimochromis marginatus*	Tropheini	LT	own collection	10	10	5	5	2 (1)	11	LT radiation	KCE7: 9.91|11; KCF3: 15.2|17
Pscmrg	*Pseudosimochromis marginatus* (North)	Tropheini	LT	own collection	8 (1)	9 (1)	5	5	2 (2)	12	LT radiation	KFE8: 7.26|7; KFF1: 7.66|8
Simdia	*Simochromis diagramma*	Tropheini	LT	own collection	10	10	5	5	2 (2)	12	LT radiation	AUD8: 10.21|11; AUE1: 9.59|10
Troann	*Tropheus annectens*	Tropheini	LT	MRAC	0	0	0	0	2 (2)	2	LT radiation	JWG4: 14.12|16; JWG5: 7.94|8
Trobri	*Tropheus brichardi*	Tropheini	LT	own collection	10	10	5	5	2 (2)	12	LT radiation	JYI8: 8.73|9; JZA3: 8.69|9
Trodub	*Tropheus duboisi*	Tropheini	LT	own collection	10	10	5	3	2 (2)	12	LT radiation	KHA4: 7.66|8; KHA5: 8.19|8
Tromoo	*Tropheus moorii*	Tropheini	LT	own collection	10	10	5	5	2 (2)	12	LT radiation	JBH4: 6.83|7; JBH5: 7.86|8
Tropol	*Tropheus polli*	Tropheini	LT	own collection	10	10	5	2	2 (2)	12	LT radiation	LEF8: 11.96|13; LEF9: 11.86|13
Tronig	*Tropheus* sp. "black"	Tropheini	LT	own collection	10	10	5	5	2 (2)	12	LT radiation	JVC3: 10.56|11; JVC9: 8.5|9
TrotbK	*Tropheus* sp. "brichardi kipili"	Tropheini	LT	own collection	10	10	5	1	2	10	LT radiation	LGA5: 7.41|7; LGA6: 7.97|8
Trokir	*Tropheus* sp. "kirschfleck"	Tropheini	LT	own collection	10	10	5	5	2	10	LT radiation	LCF1: 7.38|7; LCF3: 6.73|7
Troluk	*Tropheus* sp. "lukuga"	Tropheini	LT	own collection	10	10	5	3	2 (2)	12	LT radiation	KEF2: 11.91|13; KEF3: 7.4|7
Trolun	*Tropheus* sp. "lunatus"	Tropheini	LT	own collection	10	10	5	5	2 (2)	12	LT radiation	KED6: 7.51|7; KED7: 7.99|8
Trompi	*Tropheus* sp. "mpimbwe"	Tropheini	LT	own collection	10	10	5	5	2	10	LT radiation	LDI5: 7.1|7; LDI7: 6.4|6
Tromor	*Tropheus* sp. "murago"	Tropheini	LT	own collection	10	10	5	5	2	10	LT radiation	LHD9: 7.74|8; LHE3: 7.45|7
Trored	*Tropheus* sp. "red"	Tropheini	LT	own collection	10	10	5	5	2 (2)	12	LT radiation	IDD9: 9.13|9; IQE1: 7.69|8
Arcstr	*Astatoreochromis straeleni*	Haplochromini	LT & affluent	own collection	0	0	0	0	1 (1)	1	nested within the LT radiation	KAG8: 7.28|7
Astbur	*Astatotilapia burtoni*	Haplochromini	LT & affluent	own collection	0	0	0	0	3 (3)	3	nested within the LT radiation	IZA1: 7.97|8; IZC5: 15.42|17; JYD5: 5.11|5
Astfla	*Astatotilapia flavijosephi*	Haplochromini	Jordan	Aquaria Trade	0	0	0	0	1 (1)	1	nested within the LT radiation	LJD2: 5.48|5
Astpal	*Astatotilapia paludinosus*	Haplochromini	LT affluent	own collection	0	0	0	0	1 (1)	1	nested within the LT radiation	KYG1: 6.12|6
Ctepol	*Ctenochromis polli*	Haplochromini	Congo River	Aquaria Trade	0	0	0	0	1 (1)	1	nested within the LT radiation	JWG2: 14.02|15
HplspC	*Haplochromis* sp. "chipwa"	Haplochromini	LT & affluent	own collection	0	0	0	0	2 (2)	2	nested within the LT radiation	HXC4: 6.32|6; HXC5: 9.04|9
Hplkil	*Haplochromis* sp. "kilossana"	Haplochromini	Wami River	G. Turner	0	0	0	0	1 (1)	1	nested within the LT radiation	LJE8: 18.52|22
Hplsta	*Haplochromis stappersii*	Haplochromini	LT & affluent	own collection	0	0	0	0	1 (1)	1	nested within the LT radiation	JVD3: 11.77|13
Hplvan	*Haplochromis vanheusdeni*	Haplochromini	Ruaha River	F. Schedel	0	0	0	0	1 (1)	1	nested within the LT radiation	JWG3: 6.91|7
Ortcho	*Orthochromis indermauri*	Haplochromini	LT affluent	own collection	0	0	0	0	2 (2)	2	nested within the LT radiation	HXC6: 15.22|17; HXC7: 6.26
Ortred	*Orthochromis malagaraziensis*	Haplochromini	LT affluent	own collection	0	0	0	0	1 (1)	1	nested within the LT radiation	KYE2: 6.74|7
Ortmaz	*Orthochromis mazimeroensis*	Haplochromini	LT affluent	own collection	0	0	0	0	1 (1)	1	nested within the LT radiation	KDC6: 6.63|6
Ortuvi	*Orthochromis uvinzae*	Haplochromini	LT affluent	own collection	0	0	0	0	1 (1)	1	nested within the LT radiation	KYE7: 6.61|7
Psephi	*Pseudocrenilabrus philander*	Haplochromini	LT affluent	own collection	0	0	0	0	1 (1)	1	nested within the LT radiation	JWG1: 15.96|18
Thobra	*Thoracochromis brauschi*	Haplochromini	Lake Fiwa	Aquaria Trade	0	0	0	0	1 (1)	1	nested within the LT radiation	JWF8: 14.7|16
Lamfog	*Lamprologus tigripictilis*	Lamprologini	Congo River	Aquaria Trade	0	0	0	0	1 (1)	1	nested within the LT radiation	JWF6: 14.15|16
Neodev	*Neolamprologus devosi*	Lamprologini	LT affluent	own collection	0	0	0	0	1 (1)	1	nested within the LT radiation	LEH2: 9.88|10
Telluf	*Telmatochromis* sp. "lufubu"	Lamprologini	LT affluent	own collection	0	0	0	0	1 (1)	1	nested within the LT radiation	HXG8: 8.11|8
Amptal	*Amphilophus labiatus*	Amphilophini	Lake Apoyo	M. Barluenga	0	0	0	0	1 (1)	1	outgroup	not mapped
Bencon	*Benitochromis conjunctus*	Chromidotilapiini	Cameroon	own collection	0	0	0	0	1 (1)	1	outgroup	not mapped
Peltae	*Pelvicachromis taeniatus*	Chromidotilapiini	Cameroon	own collection	0	0	0	0	2 (2)	2	outgroup	not mapped
Andbis	*Andinoacara bisertatus*	Cichlasomini	Ecuador	Z. Musilová	0	0	0	0	1 (1)	1	outgroup	not mapped
Bujvit	*Bujurquina vittata*	Cichlasomini	Paraguay	Z. Musilová	0	0	0	0	1 (1)	1	outgroup	not mapped
Copbak	*Coptodon bakossiorum*	Coptodonini	Cameroon	own collection	0	0	0	0	1 (1)	1	outgroup	not mapped
Copren	*Coptodon rendalli*	Coptodonini	LT	own collection	0	0	0	0	1 (1)	1	outgroup	JWE8: 16.07|17
Etngu	*Etia nguti*	Etini	Cameroon	own collection	0	0	0	0	1 (1)	1	outgroup	not mapped
Etrcan	*Etroplus canarensis*	Etroplini	India	Aquaria Trade	0	0	0	0	1 (1)	1	outgroup	not mapped
Apidip	*Apistogramma diplotaenia*	Geophagini	Brazil	Z. Musilová	0	0	0	0	1 (1)	1	outgroup	not mapped
Gobeth	*Gobiocichla ethelwynae*	Gobiocichlini	Cameroon	own collection	0	0	0	0	1 (1)	1	outgroup	JWE7: 13.57|15
Tillre	*Tilapia brevimanus*	Gobiocichlini	Western Africa	Aquaria Trade	0	0	0	0	1 (1)	1	outgroup	JWF9: 15.58|16
Hchelo	*Hemichromis elongatus*	Hemichromini	Cameroon	own collection	0	0	0	0	1 (1)	1	outgroup	not mapped
Aussci	*Australoheros scitulus*	Hercini	Uruguay	Aquaria Trade	0	0	0	0	1 (1)	1	outgroup	not mapped
Htcmul	*Heterochromis multidens*	Heterochromini	Cameroon	own collection	0	0	0	0	1 (1)	1	outgroup	not mapped
Hetbut	*Heterotilapia buttikoferi*	Heterotilapiini	Western Africa	Aquaria Trade	0	0	0	0	1 (1)	1	outgroup	JWE3: 7.91|8
Oremal	*Oreochromis malagarazi*	Oreochromini	LT affluent	own collection	0	0	0	0	1 (1)	1	outgroup	KYH4: 8.08|8
Oretan	*Oreochromis tanganicae*	Oreochromini	LT	own collection	10	10 (1)	5	0	2 (2)	13	outgroup	JAB6: 18.11|8; JAC7: 17.23|17
Sthcar	*Sarotherodon caroli*	Oreochromini	Lake Barombi Mbo	own collection	0	0	0	0	1 (1)	1	outgroup	Z17: 10.30|10
Sthloh	*Sarotherodon lohbergeri*	Oreochromini	Lake Barombi Mbo	own collection	0	0	0	0	2 (2)	2	outgroup	not mapped
Sthste	*Sarotherodon steinbachi*	Oreochromini	Lake Barombi Mbo	own collection	0	0	0	0	1 (1)	1	outgroup	Z07: 10.78|11
Stopin	*Stomatepia pindu*	Oreochromini	Lake Barombi Mbo	own collection	0	0	0	0	1 (1)	1	outgroup	Z09: 11.02|11
Punmac	*Pungu maclareni*	Oreochromini	Lake Barombi Mbo	own collection	0	0	0	0	1 (1)	1	outgroup	Z03: 10.84|11
Parpol	*Paratilapia polleni*	Paratilapiini	Madagascar	Zoo Zurich	0	0	0	0	1 (1)	1	outgroup	not mapped
Pelmar	*Pelmatolapia mariae*	Pelmatolapiini	Cameroon	own collection	0	0	0	0	1 (1)	1	outgroup	JWF2: 15.82|17
Phyoli	*Psychochromis oligocanthus*	Psychochromini	Madagascar	Zoo Zurich	0	0	0	0	1 (1)	1	outgroup	not mapped
Phsacu	*Pharyngochromis acuticeps*	Serranochromini	Zambezi River	own collection	0	0	0	0	1 (1)	1	outgroup	JWF3: 14.55|16
Sarcar	*Sargochromis carlottae*	Serranochromini	Zambezi River	own collection	0	0	0	0	1 (1)	1	outgroup	JWF4: 13.85|15
Sermac	*Serranochromis macrocephalus*	Serranochromini	Kafue River	own collection	0	0	0	0	1 (1)	1	outgroup	JWF5: 17.32|20
Steult	*Steatocranus* sp. "ultraslender"	Steatocranini	Congo River	Aquaria Trade	0	0	0	0	1 (1)	1	outgroup	JWE8: 12.01|13
Tilspa	*Tilapia sparmanii*	Tilapiini	Lake Chila	own collection	0	0	0	0	1 (1)	1	outgroup	JWF7: 16.58|18
Tylpol	*Tylochromis polylepis*	Tylochromini	LT	own collection	10 (1)	9	5	0	2 (2)	12	outgroup	not mapped
Total	101 taxa	33 tribes			2259 (60)	2197 (9)	1168 (0)	1016	547 (439)	2723		

Supplementary Table 2

ID	Sex	SpeciesID	Species	Tribe	CollectionDate	CollectionLocation	latitude	longitude
9689	NA	Lamfin	Lamprologus finalimus (Holotype)	Lamprologini	NA	Uvira	NA	NA
20A1	NA	Cteben	Ctenochromis benthicola	Cyphotilapiini	09.08.10	Mpulungu Fishmarket	-8.760472222	31.11219444
88-05-a	NA	Neospl	Neolamprologus splendens	Lamprologini	03.10.88	Kafitilila DRC	-7.715222	30.234139
88-05-b	NA	Neospl	Neolamprologus splendens	Lamprologini	03.10.88	Kafitilila DRC	-7.715222	30.234139
88-06	NA	Neonve	Neolamprologus nigriventris	Lamprologini	03.10.88	Kafitilila DRC	-7.715222	30.234139
88-09	NA	Tellon	Telmatochromis sp. "longola"	Lamprologini	05.10.88	Longola	-7.481944444	30.21777778
88-10	NA	Lammel	Lamprologus meleagris	Lamprologini	06.10.88	Kalubamba DRC	-7.379444444	30.18972222
88-11-a	NA	Lammel	Lamprologus meleagris	Lamprologini	06.10.88	Kalubamba DRC	-7.379444444	30.18972222
88-11-b	NA	Lammel	Lamprologus meleagris	Lamprologini	06.10.88	Kalubamba DRC	-7.379444444	30.18972222
88-19	NA	Neogra	Neolamprologus gracilis	Lamprologini	06.10.88	Kibushi	-7.666667	30.216667
89-02	NA	Neomar	Neolamprologus marunguensis	Lamprologini	26.09.89	Kafitilila DRC	-7.715222	30.234139
89-05-a	NA	Neomar	Neolamprologus marunguensis	Lamprologini	27.09.89	Kafitilila DRC	-7.715222	30.234139
89-05-b	NA	Neomar	Neolamprologus marunguensis	Lamprologini	27.09.89	Kafitilila DRC	-7.715222	30.234139
89-05-c	NA	Neomar	Neolamprologus marunguensis	Lamprologini	27.09.89	Kafitilila DRC	-7.715222	30.234139
89-07-a	NA	Neogra	Neolamprologus gracilis	Lamprologini	27.09.89	Kafitilila DRC	-7.715222	30.234139
89-07-b	NA	Neogra	Neolamprologus gracilis	Lamprologini	27.09.89	Kafitilila DRC	-7.715222	30.234139
89-07-c	NA	Neogra	Neolamprologus gracilis	Lamprologini	27.09.89	Kafitilila DRC	-7.715222	30.234139
89-07-d	NA	Neogra	Neolamprologus gracilis	Lamprologini	27.09.89	Kafitilila DRC	-7.715222	30.234139
89-15-b	NA	Neohel	Neolamprologus helianthus	Lamprologini	30.09.89	Kalo DRC	-7.795278	30.266389
89-15-c	NA	Neohel	Neolamprologus helianthus	Lamprologini	30.09.89	Kalo DRC	-7.795278	30.266389
89-15-d	NA	Neohel	Neolamprologus helianthus	Lamprologini	30.09.89	Kalo DRC	-7.795278	30.266389
89-16-a	NA	Neomar	Neolamprologus marunguensis	Lamprologini	03.10.89	Kalo DRC	-7.795278	30.266389
89-16-b	NA	Neomar	Neolamprologus marunguensis	Lamprologini	03.10.89	Kalo DRC	-7.795278	30.266389
89-17	NA	Neogra	Neolamprologus gracilis	Lamprologini	03.10.89	Kalo DRC	-7.795278	30.266389
89-28-a	NA	Lammel	Lamprologus meleagris	Lamprologini	07.10.89	Kalubamba DRC	-7.379444444	30.18972222
89-28-b	NA	Lammel	Lamprologus meleagris	Lamprologini	07.10.89	Kalubamba DRC	-7.379444444	30.18972222
89-28-c	NA	Lammel	Lamprologus meleagris	Lamprologini	07.10.89	Kalubamba DRC	-7.379444444	30.18972222
89-30-a	NA	Neospl	Neolamprologus splendens	Lamprologini	07.10.89	Kasu	-7.316667	30.15
89-30-b	NA	Neospl	Neolamprologus splendens	Lamprologini	07.10.89	Kasu	-7.316667	30.15
89-30-c	NA	Neospl	Neolamprologus splendens	Lamprologini	07.10.89	Kasu	-7.316667	30.15
89-30-d	NA	Neospl	Neolamprologus splendens	Lamprologini	07.10.89	Kasu	-7.316667	30.15
89-30-e	NA	Neospl	Neolamprologus splendens	Lamprologini	07.10.89	Kasu	-7.316667	30.15
89-31-a	NA	Neonve	Neolamprologus nigriventris	Lamprologini	01.10.89	Kalo DRC	-7.795278	30.266389
89-31-b	NA	Neonve	Neolamprologus nigriventris	Lamprologini	01.10.89	Kalo DRC	-7.795278	30.266389
89-31-c	NA	Neonve	Neolamprologus nigriventris	Lamprologini	01.10.89	Kalo DRC	-7.795278	30.266389
90-01-a	NA	XenpaK	Xenotilapia papilio	Ectodini	02.08.90	Tembwe DRC	-7.239722	30.119444
90-01-b	NA	XenpaK	Xenotilapia papilio	Ectodini	02.08.90	Tembwe DRC	-7.239722	30.119444
90-02-a	NA	XenpaK	Xenotilapia papilio	Ectodini	02.08.90	Tembwe DRC	-7.239722	30.119444
90-02-b	NA	XenpaK	Xenotilapia papilio	Ectodini	02.08.90	Tembwe DRC	-7.239722	30.119444
90-07	NA	Neospl	Neolamprologus splendens	Lamprologini	22.08.90	Tembwe DRC	-7.239722	30.119444
90-08-a	NA	Neospl	Neolamprologus splendens	Lamprologini	22.08.90	Tembwe DRC	-7.239722	30.119444
90-08-b	NA	Neospl	Neolamprologus splendens	Lamprologini	22.08.90	Tembwe DRC	-7.239722	30.119444
90-10	NA	Neopec	Neolamprologus pectoralis	Lamprologini	23.08.90	Tembwe DRC	-7.239722	30.119444
90-84	NA	Neomar	Neolamprologus marunguensis	Lamprologini	07.09.90	Myunga	-7.946111111	30.39444444
90-92-b	NA	Neonve	Neolamprologus nigriventris	Lamprologini	09.09.90	Kamakonde DRC	-7.873611111	30.30388889
91-06-a	NA	Neopec	Neolamprologus pectoralis	Lamprologini	20.04.91	Tembwe DRC	-7.239722	30.119444
91-06-b	NA	Neopec	Neolamprologus pectoralis	Lamprologini	20.04.91	Tembwe DRC	-7.239722	30.119444
91-15	NA	Neohel	Neolamprologus helianthus	Lamprologini	25.04.91	Kalo DRC	-7.795278	30.266389
91-21	NA	Neomar	Neolamprologus marunguensis	Lamprologini	26.04.91	Kamakonde DRC	-7.873611111	30.30388889
91-23-a	NA	Neohel	Neolamprologus helianthus	Lamprologini	26.04.91	Kamakonde DRC	-7.873611111	30.30388889
91-23-b	NA	Neohel	Neolamprologus helianthus	Lamprologini	26.04.91	Kamakonde DRC	-7.873611111	30.30388889
91-44-a	NA	XenpaK	Xenotilapia papilio	Ectodini	09.05.91	Tembwe DRC	-7.239722	30.119444
91-44-b	NA	XenpaK	Xenotilapia papilio	Ectodini	09.05.91	Tembwe DRC	-7.239722	30.119444
91-52-a	NA	Neogra	Neolamprologus gracilis	Lamprologini	11.05.91	Tembwe DRC	-7.239722	30.119444
91-52-b	NA	Neogra	Neolamprologus gracilis	Lamprologini	11.05.91	Tembwe DRC	-7.239722	30.119444
93-03-a	NA	Neogra	Neolamprologus gracilis	Lamprologini	25.04.93	Tembwe DRC	-7.239722	30.119444
93-03-b	NA	Neogra	Neolamprologus gracilis	Lamprologini	25.04.93	Tembwe DRC	-7.239722	30.119444
93-14	NA	LamorC	Lamprologus sp. "ornatipinnis congo"	Lamprologini	29.04.93	Kisongwa DRC	-7.233611111	30.1125
93-18-a	NA	LamorC	Lamprologus sp. "ornatipinnis congo"	Lamprologini	02.05.93	Kisongwa DRC	-7.233611111	30.1125
93-18-b	NA	LamorC	Lamprologus sp. "ornatipinnis congo"	Lamprologini	02.05.93	Kisongwa DRC	-7.233611111	30.1125
93-38-a	NA	Neohel	Neolamprologus helianthus	Lamprologini	12.05.93	Kamakonde DRC	-7.873611111	30.30388889
93-38-b	NA	Neohel	Neolamprologus helianthus	Lamprologini	12.05.93	Kamakonde DRC	-7.873611111	30.30388889
93-38-c	NA	Neohel	Neolamprologus helianthus	Lamprologini	12.05.93	Kamakonde DRC	-7.873611111	30.30388889
93-43-b	NA	Neohel	Neolamprologus helianthus	Lamprologini	13.05.93	Kamakonde DRC	-7.873611111	30.30388889
93-47-a	NA	Lammel	Lamprologus meleagris	Lamprologini	15.05.93	Kalubamba DRC	-7.379444444	30.18972222
93-47-b	NA	Lammel	Lamprologus meleagris	Lamprologini	15.05.93	Kalubamba DRC	-7.379444444	30.18972222
93-47-c	NA	Lammel	Lamprologus meleagris	Lamprologini	15.05.93	Kalubamba DRC	-7.379444444	30.18972222
93-53	NA	Neopec	Neolamprologus pectoralis	Lamprologini	17.05.93	Kisongwa DRC	-7.233611111	30.1125
93-54-a	NA	Neooli	Neolamprologus olivaceous	Lamprologini	19.05.93	Kyeso DRC	-6.816666667	29.61472222
93-54-b	NA	Neooli	Neolamprologus olivaceous	Lamprologini	19.05.93	Kyeso DRC	-6.816666667	29.61472222
93-55-a	NA	Neooli	Neolamprologus olivaceous	Lamprologini	19.05.93	Kyeso DRC	-6.816666667	29.61472222
93-55-b	NA	Neooli	Neolamprologus olivaceous	Lamprologini	19.05.93	Kyeso DRC	-6.816666667	29.61472222
93-55-c	NA	Neooli	Neolamprologus olivaceous	Lamprologini	19.05.93	Kyeso DRC	-6.816666667	29.61472222
93-60-8	NA	Neopec	Neolamprologus pectoralis	Lamprologini	26.04.93	Tembwe DRC	-7.239722	30.119444
94-18-a	NA	NeoleL	Neolamprologus leleupi	Lamprologini	24.05.94	Litimba DRC	-8.025833333	30.47888889
94-18-b	NA	NeoleL	Neolamprologus leleupi	Lamprologini	24.05.94	Litimba DRC	-8.025833333	30.47888889
94-25-a	NA	Neomar	Neolamprologus marunguensis	Lamprologini	26.05.94	Mulinde	-7.768333333	30.27166667
94-25-b	NA	Neomar	Neolamprologus marunguensis	Lamprologini	26.05.94	Mulinde	-7.768333333	30.27166667
94-51	NA	LamorC	Lamprologus sp. "ornatipinnis congo"	Lamprologini	02.06.94	Kisongwa DRC	-7.233611111	30.1125
94-60	NA	LamorC	Lamprologus sp. "ornatipinnis congo"	Lamprologini	02.06.94	Kisongwa DRC	-7.233611111	30.1125
94-77-a	NA	NeoleL	Neolamprologus leleupi	Lamprologini	09.06.94	Kitumba DRC	-6.823611111	29.62694444
94-77-b	NA	NeoleL	Neolamprologus leleupi	Lamprologini	09.06.94	Kitumba DRC	-6.823611111	29.62694444
94-78	NA	NeoleL	Neolamprologus leleupi	Lamprologini	09.06.94	Kitumba DRC	-6.823611111	29.62694444
94-85-a	NA	Neooli	Neolamprologus olivaceous	Lamprologini	11.06.94	Kyeso DRC	-6.816666667	29.61472222
94-85-b	NA	Neooli	Neolamprologus olivaceous	Lamprologini	11.06.94	Kyeso DRC	-6.816666667	29.61472222
94-86-a	NA	Neooli	Neolamprologus olivaceous	Lamprologini	11.06.94	Kyeso DRC	-6.816666667	29.61472222
94-86-b	NA	Neooli	Neolamprologus olivaceous	Lamprologini	11.06.94	Kyeso DRC	-6.816666667	29.61472222
95-04-a	NA	Neooli	Neolamprologus olivaceous	Lamprologini	29.04.95	Kyeso DRC	-6.816666667	29.61472222
95-07-a	NA	Julunt	Julidochromis sp. "unterfels"	Lamprologini	29.04.95	Kyeso DRC	-6.816666667	29.61472222
95-07-b	NA	Julunt	Julidochromis sp. "unterfels"	Lamprologini	29.04.95	Kyeso DRC	-6.816666667	29.61472222
95-07-c	NA	Julunt	Julidochromis sp. "unterfels"	Lamprologini	29.04.95	Kyeso DRC	-6.816666667	29.61472222
95-15	NA	Neopec	Neolamprologus pectoralis	Lamprologini	04.05.95	Tembwe DRC	-7.239722	30.119444
95-22-a	NA	Lammel	Lamprologus meleagris	Lamprologini	06.05.95	Kalubamba DRC	-7.379444444	30.18972222
95-22-b	NA	Lammel	Lamprologus meleagris	Lamprologini	06.05.95	Kalubamba DRC	-7.379444444	30.18972222
95-27-a	NA	XenpaK	Xenotilapia papilio	Ectodini	08.05.95	Kasenga	-8.71525	31.14186111
95-27-b	NA	XenpaK	Xenotilapia papilio	Ectodini	08.05.95	Kasenga	-8.71525	31.14186111
95-27-c	NA	XenpaK	Xenotilapia papilio	Ectodini	08.05.95	Kasenga	-8.71525	31.14186111
95-27-d	NA	XenpaK	Xenotilapia papilio	Ectodini	08.05.95	Kasenga	-8.71525	31.14186111
96-36	NA	Julunt	Julidochromis sp. "unterfels"	Lamprologini	08.10.96	Kyeso DRC	-6.816666667	29.61472222
96-37-a	NA	Julunt	Julidochromis sp. "unterfels"	Lamprologini	09.10.96	Kyeso DRC	-6.816666667	29.61472222
96-37-b	NA	Julunt	Julidochromis sp. "unterfels"	Lamprologini	09.10.96	Kyeso DRC	-6.816666667	29.61472222
96-37-c	NA	Julunt	Julidochromis sp. "unterfels"	Lamprologini	09.10.96	Kyeso DRC	-6.816666667	29.61472222
98-31-a	NA	Julunt	Julidochromis sp. "unterfels"	Lamprologini	04.05.98	Kyeso DRC	-6.816666667	29.61472222
98-31-b	NA	Julunt	Julidochromis sp. "unterfels"	Lamprologini	04.05.98	Kyeso DRC	-6.816666667	29.61472222
A108	F	Neonve	Neolamprologus nigriventris	Lamprologini	NA	NA	NA	NA
A142	M	Neohec	Neolamprologus hecqui	Lamprologini	NA	NA	NA	NA
A188	M	Neospl	Neolamprologus splendens	Lamprologini	NA	Kasu	-7.316667	30.15
A206	F	XenpaK	Xenotilapia papilio	Ectodini	NA	Tembwe DRC	-7.239722	30.119444
AUA1	F	Auldew	Aulonocranus dewindti	Ectodini	19.07.11	Toby's Place	-8.623222222	31.20044444
AUA9	F	Auldew	Aulonocranus dewindti	Ectodini	19.07.11	Toby's Place	-8.623222222	31.20044444
AUB6	M	Pscple	Pseudosimochromis babaulti (South)	Tropheini	19.07.11	Toby's Place	-8.623222222	31.20044444
AUC3	F	Varmoo	Variabilichromis moorii	Lamprologini	19.07.11	Toby's Place	-8.623222222	31.20044444
AUC4	M	Varmoo	Variabilichromis moorii	Lamprologini	19.07.11	Toby's Place	-8.623222222	31.20044444
AUD8	F	Simdia	Simochromis diagramma	Tropheini	19.07.11	Toby's Place	-8.623222222	31.20044444
AUE1	M	Simdia	Simochromis diagramma	Tropheini	19.07.11	Toby's Place	-8.623222222	31.20044444
AUE6	M	Lepelo	Lepidiolamprologus elongatus	Lamprologini	20.07.11	Toby's Place	-8.623222222	31.20044444
AUE7	M	Neofas	Neolamprologus fasciatus	Lamprologini	20.07.11	Toby's Place	-8.623222222	31.20044444
AUG8	F	Lepelo	Lepidiolamprologus elongatus	Lamprologini	20.07.11	Toby's Place	-8.623222222	31.20044444
AVA8	M	Ctehor	Ctenochromis horei	Tropheini	21.07.11	Toby's Place	-8.623222222	31.20044444
AVA9	F	Chabri	Chalinochromis brichardi	Lamprologini	21.07.11	Toby's Place	-8.623222222	31.20044444
AVB2	M	Chabri	Chalinochromis brichardi	Lamprologini	21.07.11	Toby's Place	-8.623222222	31.20044444
AVB6	F	Pscple	Pseudosimochromis babaulti (South)	Tropheini	21.07.11	Toby's Place	-8.623222222	31.20044444

AVD4	M	Lepatt	Lepidiolamprologus attenuatus	Lamprologini	23.07.11	Toby's Place	-8.623222222	31.20044444
AVG5	F	Lepatt	Lepidiolamprologus attenuatus	Lamprologini	24.07.11	Toby's Place	-8.623222222	31.20044444
AVH2	M	Cyafur	Cyathopharynx furcifer	Ectodini	24.07.11	Toby's Place	-8.623222222	31.20044444
AWB7	M	Gnapfe	Gnathochromis pfefferi	Tropheini	25.07.11	Toby's Place	-8.623222222	31.20044444
AWB9	M	Petpol	Petrochromis polyodon	Tropheini	25.07.11	Toby's Place	-8.623222222	31.20044444
AWC5	M	Enamel	Enantiopus melanogenys	Ectodini	25.07.11	Toby's Place	-8.623222222	31.20044444
AWE2	F	Gnapfe	Gnathochromis pfefferi	Tropheini	26.07.11	Toby's Place	-8.623222222	31.20044444
AWI4	F	Petpol	Petrochromis polyodon	Tropheini	26.07.11	Toby's Place	-8.623222222	31.20044444
AWI5	F	Limdar	Limnotilapia dardennii	Tropheini	26.07.11	Toby's Place	-8.623222222	31.20044444
AWI6	M	Limdar	Limnotilapia dardennii	Tropheini	26.07.11	Toby's Place	-8.623222222	31.20044444
AXA7	F	Ctehor	Ctenochromis horei	Tropheini	27.07.11	Toby's Place	-8.623222222	31.20044444
AXB5	M	Xenspi	Xenotilapia spilopterus	Ectodini	27.07.11	Toby's Place	-8.623222222	31.20044444
AXB8	F	Xenspi	Xenotilapia spilopterus	Ectodini	27.07.11	Toby's Place	-8.623222222	31.20044444
AXD5	F	Neofas	Neolamprologus fasciatus	Lamprologini	28.07.11	Toby's Place	-8.623222222	31.20044444
AXF8	F	Psccur	Pseudosimochromis curvifrons	Tropheini	28.07.11	Toby's Place	-8.623222222	31.20044444
AXH6	M	Ophnas	Ophthalmotilapia nasuta	Ectodini	29.07.11	Toby's Place	-8.623222222	31.20044444
AXH8	F	Ophnas	Ophthalmotilapia nasuta	Ectodini	29.07.11	Toby's Place	-8.623222222	31.20044444
AYC7	M	Psccur	Pseudosimochromis curvifrons	Tropheini	30.07.11	Toby's Place	-8.623222222	31.20044444
AYE5	F	Cyafur	Cyathopharynx furcifer	Ectodini	01.08.11	Toby's Place	-8.623222222	31.20044444
Bel01	M	Xenkil	Xenotilapia sp. "kilesa"	Ectodini	NA	Kilesa near Kasenga	-5.733333	29.366667
Bel03	M	Xenkil	Xenotilapia sp. "kilesa"	Ectodini	NA	Kilesa near Kasenga	-5.733333	29.366667
Bel06	M	Ophhet	Ophthalmotilapia heterodonta	Ectodini	NA	Kyanza	-7.111389	29.975833
Bel07	M	Chapop	Chalinochromis popelini	Lamprologini	NA	Mugayo	-6.778333	29.558333
Bel09	F	Chapop	Chalinochromis popelini	Lamprologini	NA	Mtoto	-6.962777778	29.73333333
Bel12	M	Ophhet	Ophthalmotilapia heterodonta	Ectodini	NA	Kitoka	-5.45	29.283333
Bel13	NA	Neohec	Neolamprologus hecqui	Lamprologini	NA	Kalemie	-5.932403	29.200324
Bel14	NA	Neohec	Neolamprologus hecqui	Lamprologini	NA	Kalemie	-5.932403	29.200324
Bel16	M	Cypkib	Cyprichromis sp. "kibishi"	Cyprichromini	NA	Milila	-5.683333	29.383333
Bel18	F	Cypkib	Cyprichromis sp. "kibishi"	Cyprichromini	NA	Milila	-5.683333	29.383333
Bel33	F	Trevar	Trematocara variabile	Trematocarini	NA	Kalemie	-5.932403	29.200324
BNC5	F	Enamel	Enantiopus melanogenys	Ectodini	05.08.11	Toby's Place	-8.623222222	31.20044444
BND3	M	Calmac	Callochromis macrops	Ectodini	05.08.11	Toby's Place	-8.623222222	31.20044444
BND5	F	Calmac	Callochromis macrops	Ectodini	05.08.11	Toby's Place	-8.623222222	31.20044444
DMC6	NA	Cteben	Ctenochromis benthicola	Cyphotilapiini	16.09.11	Mpulungu Fishmarket	-8.760472222	31.11219444
DMC7	NA	Cteben	Ctenochromis benthicola	Cyphotilapiini	16.09.11	Mpulungu Fishmarket	-8.760472222	31.11219444
DMC8	NA	Cteben	Ctenochromis benthicola	Cyphotilapiini	11.09.11	Mpulungu Fishmarket	-8.760472222	31.11219444
DMC9	NA	Cteben	Ctenochromis benthicola	Cyphotilapiini	16.09.11	Mpulungu Fishmarket	-8.760472222	31.11219444
DMD1	M	Cteben	Ctenochromis benthicola	Cyphotilapiini	16.09.11	Mpulungu Fishmarket	-8.760472222	31.11219444
DMD2	NA	Cteben	Ctenochromis benthicola	Cyphotilapiini	16.09.11	Mpulungu Fishmarket	-8.760472222	31.11219444
FPO1	M	Ptyoli	Ptychochromis oligocanthus	Ptychochromini	NA	NA	NA	NA
GPA1	F	Trenig	Trematocara nigrifrons	Trematocarini	02.09.14	Mpulungu Fishmarket	-8.760472222	31.11219444
GPA5	F	Tremar	Trematocara marginatum	Trematocarini	02.09.14	Mpulungu Fishmarket	-8.760472222	31.11219444
GPA7	M	Tremar	Trematocara marginatum	Trematocarini	02.09.14	Mpulungu Fishmarket	-8.760472222	31.11219444
GPA8	M	Tremar	Trematocara marginatum	Trematocarini	02.09.14	Mpulungu Fishmarket	-8.760472222	31.11219444
GPA9	F	Tremar	Trematocara marginatum	Trematocarini	02.09.14	Mpulungu Fishmarket	-8.760472222	31.11219444
GPB1	M	Tremar	Trematocara marginatum	Trematocarini	02.09.14	Mpulungu Fishmarket	-8.760472222	31.11219444
GPB2	F	Batfas	Bathybates fasciatus	Bathybatini	02.09.14	Mbita Island W	-8.753333333	31.08630556
GPB3	NA	Batfas	Bathybates fasciatus	Bathybatini	02.09.14	Mbita Island W	-8.753333333	31.08630556
GPB4	M	Tylpol	Tylochromis polylepis	Tylochromini	02.09.14	Mpulungu Fishmarket	-8.760472222	31.11219444
GPB5	F	Tylpol	Tylochromis polylepis	Tylochromini	02.09.14	Mpulungu Fishmarket	-8.760472222	31.11219444
GPB6	F	Limdar	Limnotilapia dardennii	Tropheini	02.09.14	Mpulungu Fishmarket	-8.760472222	31.11219444
GPB7	F	Limdar	Limnotilapia dardennii	Tropheini	02.09.14	Mpulungu Fishmarket	-8.760472222	31.11219444
GPB8	F	Limdar	Limnotilapia dardennii	Tropheini	02.09.14	Mpulungu Fishmarket	-8.760472222	31.11219444
GPB9	F	Limdar	Limnotilapia dardennii	Tropheini	02.09.14	Mpulungu Fishmarket	-8.760472222	31.11219444
GPC1	M	Limdar	Limnotilapia dardennii	Tropheini	02.09.14	Mpulungu Fishmarket	-8.760472222	31.11219444
GPC2	M	Limdar	Limnotilapia dardennii	Tropheini	02.09.14	Mpulungu Fishmarket	-8.760472222	31.11219444
GPC3	M	Limdar	Limnotilapia dardennii	Tropheini	02.09.14	Mpulungu Fishmarket	-8.760472222	31.11219444
GPC4	M	Pcynig	Paracyprichromis nigripinnis	Cyprichromini	03.09.14	Chituta	-8.723611111	31.15
GPC6	F	Pcynig	Paracyprichromis nigripinnis	Cyprichromini	03.09.14	Chituta	-8.723611111	31.15
GPC8	NA	Neopro	Neolamprologus prochilus	Lamprologini	03.09.14	Kasenga Fishermen	-8.713888889	31.14027778
GPC9	M	Cypzon	Cyprichromis zonatus	Cyprichromini	03.09.14	Chituta	-8.723611111	31.15
GPD1	F	Cypzon	Cyprichromis zonatus	Cyprichromini	03.09.14	Chituta	-8.723611111	31.15
GPD5	NA	Xensun	Xenotilapia sp. "papilio sunflower"	Ectodini	03.09.14	Chituta	-8.723611111	31.15
GPD6	NA	Xensun	Xenotilapia sp. "papilio sunflower"	Ectodini	03.09.14	Chituta	-8.723611111	31.15
GPD7	NA	Xensun	Xenotilapia sp. "papilio sunflower"	Ectodini	03.09.14	Chituta	-8.723611111	31.15
GPD8	M	Pcynig	Paracyprichromis nigripinnis	Cyprichromini	03.09.14	Chituta	-8.723611111	31.15
GPD9	M	Pcynig	Paracyprichromis nigripinnis	Cyprichromini	03.09.14	Chituta	-8.723611111	31.15
GPE1	M	Pcynig	Paracyprichromis nigripinnis	Cyprichromini	03.09.14	Chituta	-8.723611111	31.15
GPE2	NA	Pcynig	Paracyprichromis nigripinnis	Cyprichromini	03.09.14	Chituta	-8.723611111	31.15
GPE3	NA	Pcynig	Paracyprichromis nigripinnis	Cyprichromini	03.09.14	Chituta	-8.723611111	31.15
GPE4	NA	Pcynig	Paracyprichromis nigripinnis	Cyprichromini	03.09.14	Chituta	-8.723611111	31.15
GPE5	NA	Pcynig	Paracyprichromis nigripinnis	Cyprichromini	03.09.14	Chituta	-8.723611111	31.15
GPE6	F	Pcynig	Paracyprichromis nigripinnis	Cyprichromini	03.09.14	Chituta	-8.723611111	31.15
GPE7	F	Pcynig	Paracyprichromis nigripinnis	Cyprichromini	03.09.14	Chituta	-8.723611111	31.15
GPE8	F	Pcynig	Paracyprichromis nigripinnis	Cyprichromini	03.09.14	Chituta	-8.723611111	31.15
GPF2	NA	Gwcchr	Greenwoodochromis christyi	Limnochromini	03.09.14	Chituta	-8.723611111	31.15
GPF3	NA	Tromoo	Tropheus moorii	Tropheini	03.09.14	Chituta	-8.723611111	31.15
GPF4	NA	Tromoo	Tropheus moorii	Tropheini	03.09.14	Chituta	-8.723611111	31.15
GPF5	NA	Limdar	Limnotilapia dardennii	Tropheini	03.09.14	Chituta	-8.723611111	31.15
GPF6	NA	Petfas	Petrochromis fasciolatus	Tropheini	03.09.14	Chituta	-8.723611111	31.15
GPF8	M	Xensun	Xenotilapia sp. "papilio sunflower"	Ectodini	04.09.14	Isanga	-8.654555556	31.19183333
GPF9	F	Xensun	Xenotilapia sp. "papilio sunflower"	Ectodini	04.09.14	Isanga	-8.654555556	31.19183333
GPG2	NA	Xensun	Xenotilapia sp. "papilio sunflower"	Ectodini	04.09.14	Isanga	-8.654555556	31.19183333
GPG3	NA	Xensun	Xenotilapia sp. "papilio sunflower"	Ectodini	04.09.14	Isanga	-8.654555556	31.19183333
GPG4	NA	Xensun	Xenotilapia sp. "papilio sunflower"	Ectodini	04.09.14	Isanga	-8.654555556	31.19183333
GPG5	NA	Xensun	Xenotilapia sp. "papilio sunflower"	Ectodini	04.09.14	Isanga	-8.654555556	31.19183333
GPG6	NA	Xensun	Xenotilapia sp. "papilio sunflower"	Ectodini	04.09.14	Isanga	-8.654555556	31.19183333
GPG7	NA	Xensun	Xenotilapia sp. "papilio sunflower"	Ectodini	04.09.14	Isanga	-8.654555556	31.19183333
GPG8	NA	Xensun	Xenotilapia sp. "papilio sunflower"	Ectodini	04.09.14	Isanga	-8.654555556	31.19183333
GPG9	M	Neochr	Neolamprologus christyi	Lamprologini	04.09.14	Isanga	-8.654555556	31.19183333
GPH1	M	Neocyl	Neolamprologus cylindricus	Lamprologini	04.09.14	Isanga	-8.654555556	31.19183333
GPH2	F	Neocyl	Neolamprologus cylindricus	Lamprologini	04.09.14	Isanga	-8.654555556	31.19183333
GPH3	F	Neocyl	Neolamprologus cylindricus	Lamprologini	04.09.14	Isanga	-8.654555556	31.19183333
GPH4	NA	Petfas	Petrochromis fasciolatus	Tropheini	04.09.14	Isanga	-8.654555556	31.19183333
GPH6	M	JulmaS	Julidochromis sp. "marlieri south"	Lamprologini	05.09.14	Toby's Place	-8.623222222	31.20044444
GPH7	M	Petfas	Petrochromis fasciolatus	Tropheini	05.09.14	Toby's Place	-8.623222222	31.20044444
GPH8	M	Petfas	Petrochromis fasciolatus	Tropheini	05.09.14	Toby's Place	-8.623222222	31.20044444
GPH9	F	Petfas	Petrochromis fasciolatus	Tropheini	05.09.14	Toby's Place	-8.623222222	31.20044444
GPI1	NA	Petfas	Petrochromis fasciolatus	Tropheini	05.09.14	Toby's Place	-8.623222222	31.20044444
GPI2	F	Petfas	Petrochromis fasciolatus	Tropheini	05.09.14	Toby's Place	-8.623222222	31.20044444
GPI3	M	Petfas	Petrochromis fasciolatus	Tropheini	05.09.14	Toby's Place	-8.623222222	31.20044444
GPI4	NA	Pethor	Petrochromis horii	Tropheini	05.09.14	Toby's Place	-8.623222222	31.20044444
GPI5	NA	Pethor	Petrochromis horii	Tropheini	05.09.14	Toby's Place	-8.623222222	31.20044444
GPI6	NA	Petmac	Petrochromis macrognathus	Tropheini	05.09.14	Toby's Place	-8.623222222	31.20044444
HFG1287	M	Jultra	Julidochromis transcriptus	Lamprologini	NA	NA	NA	NA
HXC4	M	HplspC	Haplochromis sp. "chipwa"	Haplochromini	NA	Kalambo Lake / Chipwa	-8.601741667	31.18701111
HXC5	F	HplspC	Haplochromis sp. "chipwa"	Haplochromini	NA	Kalambo Lake / Chipwa	-8.601741667	31.18701111
HXC6	F	Ortcho	Orthochromis indermauri	Haplochromini	NA	Lufubu River 2 (Chomba)	-8.685936	30.564417
HXC7	M	Ortcho	Orthochromis indermauri	Haplochromini	NA	Lufubu River 2 (Chomba)	-8.685936	30.564417
HXC8	M	Telluf	Telmatochromis sp. "lufubu"	Lamprologini	NA	Lufubu River 2 (Chomba)	-8.685936	30.564417
ILA1	NA	Lamlem	Lamprologus lemairii	Lamprologini	15.08.14	Katoto	-8.806111111	31.02666667
ILA2	M	Neocal	Neolamprologus calliurus	Lamprologini	15.08.14	Katoto	-8.806111111	31.02666667
ILA3	M	Neocal	Neolamprologus calliurus	Lamprologini	15.08.14	Katoto	-8.806111111	31.02666667
ILA4	M	Neocal	Neolamprologus calliurus	Lamprologini	15.08.14	Katoto	-8.806111111	31.02666667
ILA5	M	Neocal	Neolamprologus calliurus	Lamprologini	15.08.14	Katoto	-8.806111111	31.02666667
ILA6	M	Neocal	Neolamprologus calliurus	Lamprologini	15.08.14	Katoto	-8.806111111	31.02666667
ILA7	M	Neocal	Neolamprologus calliurus	Lamprologini	15.08.14	Katoto	-8.806111111	31.02666667
ILA9	M	Neocal	Neolamprologus calliurus	Lamprologini	15.08.14	Katoto	-8.806111111	31.02666667
ILB1	M	Neocal	Neolamprologus calliurus	Lamprologini	15.08.14	Katoto	-8.806111111	31.02666667
ILB2	M	Lamlap	Lamprologus laparogramma	Lamprologini	15.08.14	Katoto	-8.806111111	31.02666667
ILB3	F	Lamlap	Lamprologus laparogramma	Lamprologini	15.08.14	Katoto	-8.806111111	31.02666667
ILB4	F	Neomux	Neolamprologus mustax	Lamprologini	15.08.14	Kombe	-8.793888889	31.01583333
ILB6	M	Neobre	Neolamprologus brevis	Lamprologini	15.08.14	Kombe	-8.793888889	31.01583333
ILB7	F	Neobre	Neolamprologus brevis	Lamprologini	15.08.14	Kombe	-8.793888889	31.01583333

ILC1	M	Lamoce	Lamprologus ocellatus	Lamprologini	15.08.14	Kombe	-8.793888889	31.01583333
ILC2	M	Neobre	Neolamprologus brevis	Lamprologini	15.08.14	Kombe	-8.793888889	31.01583333
ILC3	M	Neobre	Neolamprologus brevis	Lamprologini	15.08.14	Kombe	-8.793888889	31.01583333
ILC4	M	Neobre	Neolamprologus brevis	Lamprologini	15.08.14	Kombe	-8.793888889	31.01583333
ILC5	M	Neobre	Neolamprologus brevis	Lamprologini	15.08.14	Kombe	-8.793888889	31.01583333
ILC6	M	Neobre	Neolamprologus brevis	Lamprologini	15.08.14	Kombe	-8.793888889	31.01583333
ILC7	M	Neobre	Neolamprologus brevis	Lamprologini	15.08.14	Kombe	-8.793888889	31.01583333
ILC8	F	Neobre	Neolamprologus brevis	Lamprologini	15.08.14	Kombe	-8.793888889	31.01583333
ILC9	F	Neobre	Neolamprologus brevis	Lamprologini	15.08.14	Kombe	-8.793888889	31.01583333
ILD1	F	Neobre	Neolamprologus brevis	Lamprologini	15.08.14	Kombe	-8.793888889	31.01583333
ILD2	F	Neobre	Neolamprologus brevis	Lamprologini	15.08.14	Kombe	-8.793888889	31.01583333
ILD3	F	Lamoce	Lamprologus ocellatus	Lamprologini	15.08.14	Kombe	-8.793888889	31.01583333
ILD4	M	Lamoce	Lamprologus ocellatus	Lamprologini	15.08.14	Kombe	-8.793888889	31.01583333
ILD5	M	Lamoce	Lamprologus ocellatus	Lamprologini	15.08.14	Kombe	-8.793888889	31.01583333
ILD6	M	Lamoce	Lamprologus ocellatus	Lamprologini	15.08.14	Kombe	-8.793888889	31.01583333
ILD7	M	LamorS	Lamprologus sp. "ornatipinnis zambia"	Lamprologini	15.08.14	Kombe	-8.793888889	31.01583333
ILD9	M	Julkom	Julidochromis sp. "kombe"	Lamprologini	15.08.14	Kombe	-8.793888889	31.01583333
ILE4	M	Neomod	Neolamprologus modestus	Lamprologini	15.08.14	Kombe	-8.793888889	31.01583333
ILE5	M	Neokom	Neolamprologus sp. "kombe"	Lamprologini	15.08.14	Kombe	-8.793888889	31.01583333
ILE6	F	Neokom	Neolamprologus sp. "kombe"	Lamprologini	15.08.14	Kombe	-8.793888889	31.01583333
ILE7	M?	Neokom	Neolamprologus sp. "kombe"	Lamprologini	15.08.14	Kombe	-8.793888889	31.01583333
ILE8	M?	Neokom	Neolamprologus sp. "kombe"	Lamprologini	15.08.14	Kombe	-8.793888889	31.01583333
ILE9	NA	Neokom	Neolamprologus sp. "kombe"	Lamprologini	15.08.14	Kombe	-8.793888889	31.01583333
ILF1	NA	Neokom	Neolamprologus sp. "kombe"	Lamprologini	15.08.14	Kombe	-8.793888889	31.01583333
ILF2	NA	Neokom	Neolamprologus sp. "kombe"	Lamprologini	15.08.14	Kombe	-8.793888889	31.01583333
ILF3	NA	Neokom	Neolamprologus sp. "kombe"	Lamprologini	15.08.14	Kombe	-8.793888889	31.01583333
ILF4	NA	Neokom	Neolamprologus sp. "kombe"	Lamprologini	15.08.14	Kombe	-8.793888889	31.01583333
ILF5	NA	Neokom	Neolamprologus sp. "kombe"	Lamprologini	15.08.14	Kombe	-8.793888889	31.01583333
ILF6	NA	Neokom	Neolamprologus sp. "kombe"	Lamprologini	15.08.14	Kombe	-8.793888889	31.01583333
ILF7	F	Batleo	Bathybates leo	Bathybatini	16.08.14	Kombe Fishermen	-8.793333333	31.01833333
ILF8	M	Benhor	Benthochromis horii	Benthochromini	16.08.14	Kombe Fishermen	-8.793333333	31.01833333
ILG3	F	Benmel	Benthochromis melanoides	Benthochromini	16.08.14	Kombe Fishermen	-8.793333333	31.01833333
ILG7	M	Batgra	Bathybates graueri	Bathybatini	16.08.14	Kombe Fishermen	-8.793333333	31.01833333
ILH1	M	Neomux	Neolamprologus mustax	Lamprologini	16.08.14	Kombe	-8.793888889	31.01583333
ILH2	NA	Lchabe	Limnochromis abeelei	Limnochromini	16.08.14	Kombe Fishermen	-8.793333333	31.01833333
ILH3	M	Gralem	Grammatotria lemairii	Ectodini	16.08.14	Kombe Fishermen	-8.793333333	31.01833333
ILH4	M	Benhor	Benthochromis horii	Benthochromini	16.08.14	Kombe Fishermen	-8.793333333	31.01833333
ILH5	M	Benhor	Benthochromis horii	Benthochromini	16.08.14	Kombe Fishermen	-8.793333333	31.01833333
ILH6	M	Benhor	Benthochromis horii	Benthochromini	16.08.14	Kombe Fishermen	-8.793333333	31.01833333
ILH7	M	Benhor	Benthochromis horii	Benthochromini	16.08.14	Kombe Fishermen	-8.793333333	31.01833333
ILH8	M	Benhor	Benthochromis horii	Benthochromini	16.08.14	Kombe Fishermen	-8.793333333	31.01833333
ILH9	M	Benhor	Benthochromis horii	Benthochromini	16.08.14	Kombe Fishermen	-8.793333333	31.01833333
ILI1	F	Benhor	Benthochromis horii	Benthochromini	16.08.14	Kombe Fishermen	-8.793333333	31.01833333
ILI2	F	Benhor	Benthochromis horii	Benthochromini	16.08.14	Kombe Fishermen	-8.793333333	31.01833333
ILI3	F	Benhor	Benthochromis horii	Benthochromini	16.08.14	Kombe Fishermen	-8.793333333	31.01833333
ILI4	F	Benhor	Benthochromis horii	Benthochromini	16.08.14	Kombe Fishermen	-8.793333333	31.01833333
ILI5	NA	Boumic	Boulengerochromis microlepis	Boulengerochromini	16.08.14	Kombe Fishermen	-8.793333333	31.01833333
ILI6	NA	Boumic	Boulengerochromis microlepis	Boulengerochromini	16.08.14	Kombe Fishermen	-8.793333333	31.01833333
ILI7	NA	Neomux	Neolamprologus mustax	Lamprologini	16.08.14	Kombe	-8.793888889	31.01583333
ILI8	NA	Neosex	Neolamprologus sexfasciatus	Lamprologini	16.08.14	Kombe	-8.793888889	31.01583333
IMA1	F	Neoobs	Neolamprologus obscurus	Lamprologini	18.08.14	Kabwensolo	-8.609722222	30.82916667
IMA2	M	Neoobs	Neolamprologus obscurus	Lamprologini	18.08.14	Kabwensolo	-8.609722222	30.82916667
IMA3	NA	Neoobs	Neolamprologus obscurus	Lamprologini	18.08.14	Kabwensolo	-8.609722222	30.82916667
IMA4	F	Neocal	Neolamprologus calliurus	Lamprologini	18.08.14	Kabwensolo	-8.609722222	30.82916667
IMA5	M	Plestr	Plecodus straeleni	Perissodini	18.08.14	Kabwensolo	-8.609722222	30.82916667
IMA6	M	Plestr	Plecodus straeleni	Perissodini	18.08.14	Kabwensolo	-8.609722222	30.82916667
IMA7	M	Plestr	Plecodus straeleni	Perissodini	18.08.14	Kabwensolo	-8.609722222	30.82916667
IMA9	NA	Tromoo	Tropheus moorii	Tropheini	18.08.14	Kabwensolo	-8.609722222	30.82916667
IMB1	NA	Pscple	Pseudosimochromis babaulti (South)	Tropheini	18.08.14	Kabwensolo	-8.609722222	30.82916667
IMB2	NA	TelteS	Telmatochromis temporalis	Lamprologini	18.08.14	Kabwensolo	-8.609722222	30.82916667
IMB3	M	TelteS	Telmatochromis temporalis	Lamprologini	18.08.14	Kabwensolo	-8.609722222	30.82916667
IMB4	F	TelteS	Telmatochromis temporalis	Lamprologini	18.08.14	Kabwensolo	-8.609722222	30.82916667
IMB6	F	Neomux	Neolamprologus mustax	Lamprologini	18.08.14	Kabwensolo	-8.609722222	30.82916667
IMB7	M	Neomux	Neolamprologus mustax	Lamprologini	18.08.14	Kabwensolo	-8.609722222	30.82916667
IMB8	M	Neomux	Neolamprologus mustax	Lamprologini	18.08.14	Kabwensolo	-8.609722222	30.82916667
IMB9	F	Neomux	Neolamprologus mustax	Lamprologini	18.08.14	Kabwensolo	-8.609722222	30.82916667
IMC1	F	Plestr	Plecodus straeleni	Perissodini	18.08.14	Kabwensolo	-8.609722222	30.82916667
IMC2	M	Plestr	Plecodus straeleni	Perissodini	18.08.14	Kabwensolo	-8.609722222	30.82916667
IMC6	NA	Neomod	Neolamprologus modestus	Lamprologini	18.08.14	Kabwensolo	-8.609722222	30.82916667
IMD1	M	Lepken	Lepidiolamprologus kendalli	Lamprologini	19.08.14	Kabwensolo	-8.609722222	30.82916667
IMD2	F	Lepken	Lepidiolamprologus kendalli	Lamprologini	19.08.14	Kabwensolo	-8.609722222	30.82916667
IMD3	M	Lepken	Lepidiolamprologus kendalli	Lamprologini	19.08.14	Kabwensolo	-8.609722222	30.82916667
IMD4	F	Lepken	Lepidiolamprologus kendalli	Lamprologini	19.08.14	Kabwensolo	-8.609722222	30.82916667
IMD5	M	Lepken	Lepidiolamprologus kendalli	Lamprologini	19.08.14	Kabwensolo	-8.609722222	30.82916667
IMD6	F	Limdar	Limnotilapia dardennii	Tropheini	19.08.14	Kabwensolo	-8.609722222	30.82916667
IMD7	M	Neomod	Neolamprologus modestus	Lamprologini	19.08.14	Kabwensolo	-8.609722222	30.82916667
IMD8	M	Neomod	Neolamprologus modestus	Lamprologini	19.08.14	Kabwensolo	-8.609722222	30.82916667
IMD9	M	Neomod	Neolamprologus modestus	Lamprologini	19.08.14	Kabwensolo	-8.609722222	30.82916667
IME3	M	Altcal	Altolamprologus calvus	Lamprologini	19.08.14	Kabwensolo	-8.609722222	30.82916667
IME4	M	Altcal	Altolamprologus calvus	Lamprologini	19.08.14	Kabwensolo	-8.609722222	30.82916667
IME6	F	Plestr	Plecodus straeleni	Perissodini	19.08.14	Kabwensolo	-8.609722222	30.82916667
IME7	NA	Boumic	Boulengerochromis microlepis	Boulengerochromini	19.08.14	Kabwensolo Fishermen	-8.606972222	30.82980556
IME8	NA	Boumic	Boulengerochromis microlepis	Boulengerochromini	19.08.14	Kabwensolo Fishermen	-8.606972222	30.82980556
IME9	NA	Neomux	Neolamprologus mustax	Lamprologini	19.08.14	Kabwensolo	-8.609722222	30.82916667
IMF1	M	Cyafoa	Cyathopharynx foae	Ectodini	19.08.14	Kabwensolo Fishermen	-8.606972222	30.82980556
IMF2	NA	Chabri	Chalinochromis brichardi	Lamprologini	19.08.14	Kabwensolo	-8.609722222	30.82916667
IMF3	NA	Altcom	Altolamprologus compressiceps	Lamprologini	19.08.14	Kabwensolo	-8.609722222	30.82916667
IMF4	NA	Lamcal	Lamprologus callipterus	Lamprologini	19.08.14	Kabwensolo	-8.609722222	30.82916667
IMF5	NA	Tromoo	Tropheus moorii	Tropheini	19.08.14	Kabwensolo	-8.609722222	30.82916667
IMF6	NA	Neoobs	Neolamprologus obscurus	Lamprologini	19.08.14	Kabwensolo	-8.609722222	30.82916667
IMF7	M	Xenmas	Xenotilapia nasus	Ectodini	19.08.14	Chitweshiba	-8.595833333	30.8075
IMF8	F	Xenmas	Xenotilapia nasus	Ectodini	19.08.14	Chitweshiba	-8.595833333	30.8075
IMF9	M	Xenbat	Xenotilapia bathyphilus	Ectodini	19.08.14	Chitweshiba	-8.595833333	30.8075
IMG1	F	Xenmas	Xenotilapia nasus	Ectodini	19.08.14	Chitweshiba	-8.595833333	30.8075
IMG2	F	Xenmas	Xenotilapia nasus	Ectodini	19.08.14	Chitweshiba	-8.595833333	30.8075
IMG3	M	Xenmas	Xenotilapia nasus	Ectodini	19.08.14	Chitweshiba	-8.595833333	30.8075
IMG4	M	Xenmas	Xenotilapia nasus	Ectodini	19.08.14	Chitweshiba	-8.595833333	30.8075
IMG5	NA	Xenmas	Xenotilapia nasus	Ectodini	19.08.14	Chitweshiba	-8.595833333	30.8075
IMG6	NA	Tromoo	Tropheus moorii	Tropheini	19.08.14	Chitweshiba	-8.595833333	30.8075
IMG7	F	Chabri	Chalinochromis brichardi	Lamprologini	19.08.14	Chitweshiba	-8.595833333	30.8075
IMG8	M	Chabri	Chalinochromis brichardi	Lamprologini	19.08.14	Chitweshiba	-8.595833333	30.8075
IMG9	M	Neomod	Neolamprologus modestus	Lamprologini	19.08.14	Chitweshiba	-8.595833333	30.8075
IMH1	M	Neomod	Neolamprologus modestus	Lamprologini	19.08.14	Chitweshiba	-8.595833333	30.8075
IMH2	F	Neomod	Neolamprologus modestus	Lamprologini	19.08.14	Chitweshiba	-8.595833333	30.8075
IMH3	F	Neomod	Neolamprologus modestus	Lamprologini	19.08.14	Chitweshiba	-8.595833333	30.8075
IMH6	F	Xenbat	Xenotilapia bathyphilus	Ectodini	20.08.14	Chitweshiba	-8.595833333	30.8075
IMH7	F	Xenmas	Xenotilapia nasus	Ectodini	20.08.14	Chitweshiba	-8.595833333	30.8075
IMH8	M	Xenmas	Xenotilapia nasus	Ectodini	20.08.14	Chitweshiba	-8.595833333	30.8075
IMH9	M	Xenmas	Xenotilapia nasus	Ectodini	20.08.14	Chitweshiba	-8.595833333	30.8075
IMI1	NA	Xenmas	Xenotilapia nasus	Ectodini	20.08.14	Chitweshiba	-8.595833333	30.8075
IMI2	F	Lepmim	Lepidiolamprologus mimicus	Lamprologini	20.08.14	Chitweshiba	-8.595833333	30.8075
IMI3	NA	Batfas	Bathybates fasciatus	Bathybatini	20.08.14	Chitweshiba	-8.595833333	30.8075
IMI4	NA	Plestr	Plecodus straeleni	Perissodini	20.08.14	Chitweshiba	-8.595833333	30.8075
IMI5	NA	Altcal	Altolamprologus calvus	Lamprologini	20.08.14	Chitweshiba	-8.595833333	30.8075
IMI6	NA	Lepken	Lepidiolamprologus kendalli	Lamprologini	20.08.14	Chitweshiba	-8.595833333	30.8075
IMI7	NA	Lepken	Lepidiolamprologus kendalli	Lamprologini	20.08.14	Chitweshiba	-8.595833333	30.8075
IMI9	NA	Gralem	Grammatotria lemairii	Ectodini	20.08.14	Chitweshiba	-8.595833333	30.8075
INA1	NA	Plemul	Plecodus multidentatus	Perissodini	16.08.14	Kombe	-8.793888889	31.01583333
INA2	NA	Neokom	Neolamprologus sp. "kombe"	Lamprologini	16.08.14	Kombe	-8.793888889	31.01583333
INA4	M	Julkom	Julidochromis sp. "kombe"	Lamprologini	16.08.14	Kombe	-8.793888889	31.01583333
INA5	NA	Julkom	Julidochromis sp. "kombe"	Lamprologini	16.08.14	Kombe	-8.793888889	31.01583333
INA6	F	Julkom	Julidochromis sp. "kombe"	Lamprologini	16.08.14	Kombe	-8.793888889	31.01583333
INA7	M	Lamoce	Lamprologus ocellatus	Lamprologini	16.08.14	Chezi	-8.779444444	31.00555556
INA8	M	Lamoce	Lamprologus ocellatus	Lamprologini	16.08.14	Chezi	-8.779444444	31.00555556

INA9	M	Lamoce	Lamprologus ocellatus	Lamprologini	16.08.14	Chezi	-8.779444444	31.00555556
INB1	M	Lamoce	Lamprologus ocellatus	Lamprologini	16.08.14	Chezi	-8.779444444	31.00555556
INB2	F	Lamoce	Lamprologus ocellatus	Lamprologini	16.08.14	Chezi	-8.779444444	31.00555556
INB3	M	Neomux	Neolamprologus mustax	Lamprologini	16.08.14	Chezi	-8.779444444	31.00555556
INB4	F	Neomux	Neolamprologus mustax	Lamprologini	16.08.14	Chezi	-8.779444444	31.00555556
INB5	NA	Neosex	Neolamprologus sexfasciatus	Lamprologini	16.08.14	Chezi	-8.779444444	31.00555556
INB6	NA	Neosex	Neolamprologus sexfasciatus	Lamprologini	16.08.14	Chezi	-8.779444444	31.00555556
INB8	NA	Julkom	Julidochromis sp. "kombe"	Lamprologini	16.08.14	Chezi	-8.779444444	31.00555556
INB9	NA	Julkom	Julidochromis sp. "kombe"	Lamprologini	16.08.14	Chezi	-8.779444444	31.00555556
INC1	NA	Julkom	Julidochromis sp. "kombe"	Lamprologini	16.08.14	Chezi	-8.779444444	31.00555556
INC2	NA	Julkom	Julidochromis sp. "kombe"	Lamprologini	16.08.14	Chezi	-8.779444444	31.00555556
INC3	NA	Julkom	Julidochromis sp. "kombe"	Lamprologini	16.08.14	Chezi	-8.779444444	31.00555556
INC4	NA	Julkom	Julidochromis sp. "kombe"	Lamprologini	16.08.14	Chezi	-8.779444444	31.00555556
INC5	NA	Julkom	Julidochromis sp. "kombe"	Lamprologini	16.08.14	Chezi	-8.779444444	31.00555556
INC6	NA	Julkom	Julidochromis sp. "kombe"	Lamprologini	16.08.14	Chezi	-8.779444444	31.00555556
INC7	F	Neocal	Neolamprologus calliurus	Lamprologini	16.08.14	Chezi	-8.779444444	31.00555556
INC8	M	Neocal	Neolamprologus calliurus	Lamprologini	16.08.14	Chezi	-8.779444444	31.00555556
INC9	F	Neocal	Neolamprologus calliurus	Lamprologini	16.08.14	Chezi	-8.779444444	31.00555556
IND2	M	TelteS	Telmatochromis temporalis	Lamprologini	16.08.14	Chezi	-8.779444444	31.00555556
IND3	M	TelteS	Telmatochromis temporalis	Lamprologini	16.08.14	Chezi	-8.779444444	31.00555556
IND4	M	TelteS	Telmatochromis temporalis	Lamprologini	16.08.14	Chezi	-8.779444444	31.00555556
IND5	M	TelteS	Telmatochromis temporalis	Lamprologini	16.08.14	Chezi	-8.779444444	31.00555556
IND6	M	TelteS	Telmatochromis temporalis	Lamprologini	16.08.14	Chezi	-8.779444444	31.00555556
IND7	M	Neosex	Neolamprologus sexfasciatus	Lamprologini	17.08.14	Kanfonki	-8.702777778	30.9225
IND8	F	Neosex	Neolamprologus sexfasciatus	Lamprologini	17.08.14	Kanfonki	-8.702777778	30.9225
INE1	M	Neosex	Neolamprologus sexfasciatus	Lamprologini	17.08.14	Kanfonki	-8.702777778	30.9225
INE2	M	Neosex	Neolamprologus sexfasciatus	Lamprologini	17.08.14	Kanfonki	-8.702777778	30.9225
INE3	M	Neomux	Neolamprologus mustax	Lamprologini	17.08.14	Kanfonki	-8.702777778	30.9225
INE4	NA	Neomux	Neolamprologus mustax	Lamprologini	17.08.14	Kanfonki	-8.702777778	30.9225
INE5	M	Cphgib	Cyphotilapia gibberosa	Cyphotilapiini	17.08.14	Kanfonki	-8.702777778	30.9225
INE6	F	Lamlem	Lamprologus lemairii	Lamprologini	17.08.14	Kanfonki	-8.702777778	30.9225
INE7	M	Lamlem	Lamprologus lemairii	Lamprologini	17.08.14	Kanfonki	-8.702777778	30.9225
INE8	F	Plestr	Plecodus straeleni	Perissodini	17.08.14	Kanfonki	-8.702777778	30.9225
INE9	M	Plestr	Plecodus straeleni	Perissodini	17.08.14	Kanfonki	-8.702777778	30.9225
INF1	F	Asplep	Asprotilapia leptura	Ectodini	17.08.14	Kanfonki	-8.702777778	30.9225
INF2	M	Asplep	Asprotilapia leptura	Ectodini	17.08.14	Kanfonki	-8.702777778	30.9225
INF4	M	Asplep	Asprotilapia leptura	Ectodini	17.08.14	Kanfonki	-8.702777778	30.9225
INF5	M	Asplep	Asprotilapia leptura	Ectodini	17.08.14	Kanfonki	-8.702777778	30.9225
INF6	F	Asplep	Asprotilapia leptura	Ectodini	17.08.14	Kanfonki	-8.702777778	30.9225
INF7	M	Asplep	Asprotilapia leptura	Ectodini	17.08.14	Kanfonki	-8.702777778	30.9225
INF8	F	Asplep	Asprotilapia leptura	Ectodini	17.08.14	Kanfonki	-8.702777778	30.9225
INF9	F	Asplep	Asprotilapia leptura	Ectodini	17.08.14	Kanfonki	-8.702777778	30.9225
ING1	M	Asplep	Asprotilapia leptura	Ectodini	17.08.14	Kanfonki	-8.702777778	30.9225
ING2	F	Asplep	Asprotilapia leptura	Ectodini	17.08.14	Kanfonki	-8.702777778	30.9225
ING3	F	Asplep	Asprotilapia leptura	Ectodini	17.08.14	Kanfonki	-8.702777778	30.9225
ING4	NA	Permic	Perissodus microlepis	Perissodini	17.08.14	Kanfonki	-8.702777778	30.9225
ING5	NA	Permic	Perissodus microlepis	Perissodini	17.08.14	Kanfonki	-8.702777778	30.9225
ING6	M	Chabri	Chalinochromis brichardi	Lamprologini	17.08.14	Kanfonki	-8.702777778	30.9225
ING7	NA	Neomod	Neolamprologus modestus	Lamprologini	17.08.14	Kanfonki	-8.702777778	30.9225
ING8	M	Telbra	Telmatochromis brachygnathus	Lamprologini	17.08.14	Kanfonki	-8.702777778	30.9225
ING9	M	Telbra	Telmatochromis brachygnathus	Lamprologini	17.08.14	Kanfonki	-8.702777778	30.9225
INH1	M	Cypkan	Cyprichromis sp. "jumbo"	Cyprichromini	17.08.14	Kanfonki	-8.702777778	30.9225
INH2	M	Cypkan	Cyprichromis sp. "jumbo"	Cyprichromini	17.08.14	Kanfonki	-8.702777778	30.9225
INH3	M	Cypkan	Cyprichromis sp. "jumbo"	Cyprichromini	17.08.14	Kanfonki	-8.702777778	30.9225
INH4	NA	Cypkan	Cyprichromis sp. "jumbo"	Cyprichromini	17.08.14	Kanfonki	-8.702777778	30.9225
INH5	NA	Cypkan	Cyprichromis sp. "jumbo"	Cyprichromini	17.08.14	Kanfonki	-8.702777778	30.9225
INH6	NA	Cypkan	Cyprichromis sp. "jumbo"	Cyprichromini	17.08.14	Kanfonki	-8.702777778	30.9225
INH7	M	Cphgib	Cyphotilapia gibberosa	Cyphotilapiini	17.08.14	Kanfonki	-8.702777778	30.9225
INH9	F	Cphgib	Cyphotilapia gibberosa	Cyphotilapiini	17.08.14	Kanfonki	-8.702777778	30.9225
INI2	M	Neosex	Neolamprologus sexfasciatus	Lamprologini	17.08.14	Kanfonki	-8.702777778	30.9225
INI3	M	Neosex	Neolamprologus sexfasciatus	Lamprologini	17.08.14	Kanfonki	-8.702777778	30.9225
INI4	F	Neosex	Neolamprologus sexfasciatus	Lamprologini	17.08.14	Kanfonki	-8.702777778	30.9225
INI5	F	Neosex	Neolamprologus sexfasciatus	Lamprologini	17.08.14	Kanfonki	-8.702777778	30.9225
INI6	M	Neosex	Neolamprologus sexfasciatus	Lamprologini	17.08.14	Kanfonki	-8.702777778	30.9225
INI8	M	Plestr	Plecodus straeleni	Perissodini	17.08.14	Kanfonki	-8.702777778	30.9225
IOA1	M	Neobue	Neolamprologus buescheri	Lamprologini	23.08.14	Kachese	-8.490527778	30.4775
IOA2	M	Neobue	Neolamprologus buescheri	Lamprologini	23.08.14	Kachese	-8.490527778	30.4775
IOA3	F	Neobue	Neolamprologus buescheri	Lamprologini	23.08.14	Kachese	-8.490527778	30.4775
IOA4	F	Neobue	Neolamprologus buescheri	Lamprologini	23.08.14	Kachese	-8.490527778	30.4775
IOA5	M	Neobue	Neolamprologus buescheri	Lamprologini	23.08.14	Kachese	-8.490527778	30.4775
IOA6	F	Neobue	Neolamprologus buescheri	Lamprologini	23.08.14	Kachese	-8.490527778	30.4775
IOA7	NA	Neobue	Neolamprologus buescheri	Lamprologini	23.08.14	Kachese	-8.490527778	30.4775
IOA8	NA	Neobue	Neolamprologus buescheri	Lamprologini	23.08.14	Kachese	-8.490527778	30.4775
IOA9	NA	Neobue	Neolamprologus buescheri	Lamprologini	23.08.14	Kachese	-8.490527778	30.4775
IOB1	F	Julreg	Julidochromis sp. "regani south"	Lamprologini	23.08.14	Kachese	-8.490527778	30.4775
IOB2	F	Julreg	Julidochromis sp. "regani south"	Lamprologini	23.08.14	Kachese	-8.490527778	30.4775
IOB3	F	Julreg	Julidochromis sp. "regani south"	Lamprologini	23.08.14	Kachese	-8.490527778	30.4775
IOB4	M	Lamoce	Lamprologus ocellatus	Lamprologini	23.08.14	Ntingila	-8.481388889	30.46138889
IOB5	NA	Altcal	Altolamprologus calvus	Lamprologini	23.08.14	NA	NA	NA
IOB6	NA	Altcal	Altolamprologus calvus	Lamprologini	23.08.14	NA	NA	NA
IOB7	NA	Loblab	Lobochilotes labiatus	Tropheini	23.08.14	Kachese	-8.490527778	30.4775
IOB8	NA	Loblab	Lobochilotes labiatus	Tropheini	23.08.14	Kachese	-8.490527778	30.4775
IOB9	M	Neofas	Neolamprologus fasciatus	Lamprologini	23.08.14	Kachese	-8.490527778	30.4775
IOC1	M	Lepken	Lepidiolamprologus kendalli	Lamprologini	23.08.14	Kachese	-8.490527778	30.4775
IOC2	NA	Tromoo	Tropheus moorii	Tropheini	23.08.14	Kachese	-8.490527778	30.4775
IOC3	NA	Altcal	Altolamprologus calvus	Lamprologini	23.08.14	Kachese	-8.490527778	30.4775
IOC4	NA	Altcal	Altolamprologus calvus	Lamprologini	23.08.14	Kachese	-8.490527778	30.4775
IOC5	NA	Altcal	Altolamprologus calvus	Lamprologini	23.08.14	Kachese	-8.490527778	30.4775
IOC6	NA	Neoobs	Neolamprologus obscurus	Lamprologini	23.08.14	Kachese	-8.490527778	30.4775
IOC7	NA	Neoobs	Neolamprologus obscurus	Lamprologini	23.08.14	Kachese	-8.490527778	30.4775
IOC8	NA	Neoobs	Neolamprologus obscurus	Lamprologini	23.08.14	Kachese	-8.490527778	30.4775
IOC9	NA	Neoobs	Neolamprologus obscurus	Lamprologini	23.08.14	Kachese	-8.490527778	30.4775
IOD2	NA	Gralem	Grammatotria lemairii	Ectodini	23.08.14	Kachese	-8.490527778	30.4775
IOD3	NA	Gralem	Grammatotria lemairii	Ectodini	23.08.14	Kachese	-8.490527778	30.4775
IOD4	F	Cyafoa	Cyathopharynx foae	Ectodini	24.08.14	Chimba	-8.426111111	30.45666667
IOD6	M	Cyafoa	Cyathopharynx foae	Ectodini	24.08.14	Chimba	-8.426111111	30.45666667
IOD9	M	Trored	Tropheus sp. "red"	Tropheini	24.08.14	Chimba	-8.426111111	30.45666667
IOE1	F	Trored	Tropheus sp. "red"	Tropheini	24.08.14	Chimba	-8.426111111	30.45666667
IOE2	M	Altcal	Altolamprologus calvus	Lamprologini	24.08.14	Chimba	-8.426111111	30.45666667
IOE3	F	Altcal	Altolamprologus calvus	Lamprologini	24.08.14	Chimba	-8.426111111	30.45666667
IOE4	M	Altcal	Altolamprologus calvus	Lamprologini	24.08.14	Chimba	-8.426111111	30.45666667
IOE5	NA	Altcal	Altolamprologus calvus	Lamprologini	24.08.14	Chimba	-8.426111111	30.45666667
IOE6	M	Plepar	Plecodus paradoxus	Perissodini	24.08.14	Chimba	-8.426111111	30.45666667
IOE7	M	Plepar	Plecodus paradoxus	Perissodini	24.08.14	Chimba	-8.426111111	30.45666667
IOE8	NA	Trored	Tropheus sp. "red"	Tropheini	24.08.14	Chimba	-8.426111111	30.45666667
IOE9	F	Trored	Tropheus sp. "red"	Tropheini	24.08.14	Chimba	-8.426111111	30.45666667
IOF1	NA	Trored	Tropheus sp. "red"	Tropheini	24.08.14	Chimba	-8.426111111	30.45666667
IOF2	NA	Trored	Tropheus sp. "red"	Tropheini	24.08.14	Chimba	-8.426111111	30.45666667
IOF3	M	Trored	Tropheus sp. "red"	Tropheini	24.08.14	Chimba	-8.426111111	30.45666667
IOF4	M	Trored	Tropheus sp. "red"	Tropheini	24.08.14	Chimba	-8.426111111	30.45666667
IOF5	M	Trored	Tropheus sp. "red"	Tropheini	24.08.14	Chimba	-8.426111111	30.45666667
IOF6	M	Trored	Tropheus sp. "red"	Tropheini	24.08.14	Chimba	-8.426111111	30.45666667
IOF7	F	Trored	Tropheus sp. "red"	Tropheini	24.08.14	Chimba	-8.426111111	30.45666667
IOF8	M	Ophnas	Ophthalmotilapia nasuta	Ectodini	24.08.14	Chimba	-8.426111111	30.45666667
IOF9	M	Ophnas	Ophthalmotilapia nasuta	Ectodini	24.08.14	Chimba	-8.426111111	30.45666667
IOG3	M	Cyafoa	Cyathopharynx foae	Ectodini	24.08.14	Chimba	-8.426111111	30.45666667
IOG4	M	Cyafoa	Cyathopharynx foae	Ectodini	24.08.14	Chimba	-8.426111111	30.45666667
IOG5	M	Cyafoa	Cyathopharynx foae	Ectodini	24.08.14	Chimba	-8.426111111	30.45666667
IOG6	M	Cyafoa	Cyathopharynx foae	Ectodini	24.08.14	Chimba	-8.426111111	30.45666667
IOG7	M	Cyafoa	Cyathopharynx foae	Ectodini	24.08.14	Chimba	-8.426111111	30.45666667
IOG8	F	Cyafoa	Cyathopharynx foae	Ectodini	24.08.14	Chimba	-8.426111111	30.45666667
IOG9	F	Cyafoa	Cyathopharynx foae	Ectodini	24.08.14	Chimba	-8.426111111	30.45666667
IOH1	F	Cyafoa	Cyathopharynx foae	Ectodini	24.08.14	Chimba	-8.426111111	30.45666667
IOH2	F	Cyafoa	Cyathopharynx foae	Ectodini	24.08.14	Chimba	-8.426111111	30.45666667

IOH4	F	Lepcun	Lepidiolamprologus cunningtoni	Lamprologini	24.08.14	Chimba	-8.426111111	30.45666667
IOH5	M	Lepcun	Lepidiolamprologus cunningtoni	Lamprologini	24.08.14	Chimba	-8.426111111	30.45666667
IOH6	M	Regcal	Reganochromis calliurus	Limnochromini	24.08.14	Chimba	-8.426111111	30.45666667
IOH7	M	Regcal	Reganochromis calliurus	Limnochromini	24.08.14	Chimba	-8.426111111	30.45666667
IOH8	M	Lesper	Lestradea perspicax	Ectodini	24.08.14	Chimba	-8.426111111	30.45666667
IOH9	F	Lesper	Lestradea perspicax	Ectodini	24.08.14	Chimba	-8.426111111	30.45666667
IOI1	M	Lesper	Lestradea perspicax	Ectodini	24.08.14	Chimba	-8.426111111	30.45666667
IOI2	F	Lesper	Lestradea perspicax	Ectodini	24.08.14	Chimba	-8.426111111	30.45666667
IOI3	M	Lesper	Lestradea perspicax	Ectodini	24.08.14	Chimba	-8.426111111	30.45666667
IOI4	F	Lesper	Lestradea perspicax	Ectodini	24.08.14	Chimba	-8.426111111	30.45666667
IOI5	NA	Lesper	Lestradea perspicax	Ectodini	24.08.14	Chimba	-8.426111111	30.45666667
IOI6	M	Lesper	Lestradea perspicax	Ectodini	24.08.14	Chimba	-8.426111111	30.45666667
IOI7	F	Lesper	Lestradea perspicax	Ectodini	24.08.14	Chimba	-8.426111111	30.45666667
IOI8	F	Lesper	Lestradea perspicax	Ectodini	24.08.14	Chimba	-8.426111111	30.45666667
IOI9	M	Psccur	Pseudosimochromis curvifrons	Tropheini	24.08.14	Chimba	-8.426111111	30.45666667
IPA1	M	Cyafur	Cyathopharynx furcifer	Ectodini	20.07.14	Toby's Place	-8.623222222	31.20044444
IPA3	M	Chabri	Chalinochromis brichardi	Lamprologini	20.07.14	Toby's Place	-8.623222222	31.20044444
IPA4	F	Cyafur	Cyathopharynx furcifer	Ectodini	20.07.14	Toby's Place	-8.623222222	31.20044444
IPA6	F	Cyafur	Cyathopharynx furcifer	Ectodini	20.07.14	Toby's Place	-8.623222222	31.20044444
IPA8	NA	Permic	Perissodus microlepis	Perissodini	20.07.14	Toby's Place	-8.623222222	31.20044444
IPA9	NA	Xenspi	Xenotilapia spilopterus	Ectodini	20.07.14	Toby's Place	-8.623222222	31.20044444
IPB1	NA	Auldew	Aulonocranus dewindti	Ectodini	20.07.14	Toby's Place	-8.623222222	31.20044444
IPB3	M	Neosav	Neolamprologus savoryi	Lamprologini	20.07.14	Toby's Place	-8.623222222	31.20044444
IPB4	M	Lepelo	Lepidiolamprologus elongatus	Lamprologini	20.07.14	Toby's Place	-8.623222222	31.20044444
IPB5	F	Intloo	Interochromis loocki	Tropheini	20.07.14	Toby's Place	-8.623222222	31.20044444
IPB6	F	Intloo	Interochromis loocki	Tropheini	20.07.14	Toby's Place	-8.623222222	31.20044444
IPB7	M	Intloo	Interochromis loocki	Tropheini	20.07.14	Toby's Place	-8.623222222	31.20044444
IPB8	NA	Intloo	Interochromis loocki	Tropheini	20.07.14	Toby's Place	-8.623222222	31.20044444
IPB9	NA	Intloo	Interochromis loocki	Tropheini	20.07.14	Toby's Place	-8.623222222	31.20044444
IPC1	F	Peteph	Petrochromis ephippium	Tropheini	20.07.14	Toby's Place	-8.623222222	31.20044444
IPC2	NA	Xenspi	Xenotilapia spilopterus	Ectodini	20.07.14	Toby's Place	-8.623222222	31.20044444
IPC3	NA	Neotet	Neolamprologus tetracanthus	Lamprologini	20.07.14	Toby's Place	-8.623222222	31.20044444
IPC6	F	Ophnas	Ophthalmotilapia nasuta	Ectodini	20.07.14	Toby's Place	-8.623222222	31.20044444
IPC8	F	Ophnas	Ophthalmotilapia nasuta	Ectodini	21.07.14	Toby's Place	-8.623222222	31.20044444
IPC9	M	Ophnas	Ophthalmotilapia nasuta	Ectodini	21.07.14	Toby's Place	-8.623222222	31.20044444
IPD1	M	Ophnas	Ophthalmotilapia nasuta	Ectodini	21.07.14	Toby's Place	-8.623222222	31.20044444
IPD2	F	Ophnas	Ophthalmotilapia nasuta	Ectodini	21.07.14	Toby's Place	-8.623222222	31.20044444
IPD3	F	Ophnas	Ophthalmotilapia nasuta	Ectodini	21.07.14	Toby's Place	-8.623222222	31.20044444
IPD6	F	Lamlem	Lamprologus lemairii	Lamprologini	21.07.14	Toby's Place	-8.623222222	31.20044444
IPD8	NA	Neosav	Neolamprologus savoryi	Lamprologini	21.07.14	Toby's Place	-8.623222222	31.20044444
IPD9	NA	Neosav	Neolamprologus savoryi	Lamprologini	21.07.14	Toby's Place	-8.623222222	31.20044444
IPE2	NA	Neosav	Neolamprologus savoryi	Lamprologini	21.07.14	Toby's Place	-8.623222222	31.20044444
IPE3	M	Xenbou	Xenotilapia boulengeri	Ectodini	21.07.14	Toby's Place	-8.623222222	31.20044444
IPE4	NA	Lamlem	Lamprologus lemairii	Lamprologini	21.07.14	Toby's Place	-8.623222222	31.20044444
IPE5	M	Lepatt	Lepidiolamprologus attenuatus	Lamprologini	21.07.14	Toby's Place	-8.623222222	31.20044444
IPE6	F	Lepatt	Lepidiolamprologus attenuatus	Lamprologini	21.07.14	Toby's Place	-8.623222222	31.20044444
IPE7	F	Xenbou	Xenotilapia boulengeri	Ectodini	21.07.14	Toby's Place	-8.623222222	31.20044444
IPE8	M	Permic	Perissodus microlepis	Perissodini	21.07.14	Toby's Place	-8.623222222	31.20044444
IPE9	NA	Permic	Perissodus microlepis	Perissodini	21.07.14	Toby's Place	-8.623222222	31.20044444
IPF2	F	Intloo	Interochromis loocki	Tropheini	21.07.14	Toby's Place	-8.623222222	31.20044444
IPF3	M	Intloo	Interochromis loocki	Tropheini	21.07.14	Toby's Place	-8.623222222	31.20044444
IPF7	M	Neotet	Neolamprologus tetracanthus	Lamprologini	21.07.14	Toby's Place	-8.623222222	31.20044444
IPG1	NA	Permic	Perissodus microlepis	Perissodini	21.07.14	Toby's Place	-8.623222222	31.20044444
IPG2	NA	Permic	Perissodus microlepis	Perissodini	21.07.14	Toby's Place	-8.623222222	31.20044444
IPG3	F	Neotet	Neolamprologus tetracanthus	Lamprologini	21.07.14	Toby's Place	-8.623222222	31.20044444
IPG4	F	Xenspi	Xenotilapia spilopterus	Ectodini	21.07.14	Toby's Place	-8.623222222	31.20044444
IPG5	F	Lepelo	Lepidiolamprologus elongatus	Lamprologini	21.07.14	Toby's Place	-8.623222222	31.20044444
IPG7	M	Neofas	Neolamprologus fasciatus	Lamprologini	21.07.14	Toby's Place	-8.623222222	31.20044444
IPG8	F	Gnapfe	Gnathochromis pfefferi	Tropheini	21.07.14	Toby's Place	-8.623222222	31.20044444
IPG9	M	Auldew	Aulonocranus dewindti	Ectodini	21.07.14	Toby's Place	-8.623222222	31.20044444
IPH1	F	Auldew	Aulonocranus dewindti	Ectodini	21.07.14	Toby's Place	-8.623222222	31.20044444
IPH2	M	Lamcal	Lamprologus callipterus	Lamprologini	21.07.14	Toby's Place	-8.623222222	31.20044444
IPH3	F	Altcom	Altolamprologus compressiceps	Lamprologini	21.07.14	Toby's Place	-8.623222222	31.20044444
IPH4	M	Xenspi	Xenotilapia spilopterus	Ectodini	21.07.14	Toby's Place	-8.623222222	31.20044444
IPH5	M	Auldew	Aulonocranus dewindti	Ectodini	21.07.14	Toby's Place	-8.623222222	31.20044444
IPH7	F	Lepatt	Lepidiolamprologus attenuatus	Lamprologini	21.07.14	Toby's Place	-8.623222222	31.20044444
IPH8	NA	TelteS	Telmatochromis temporalis	Lamprologini	21.07.14	Toby's Place	-8.623222222	31.20044444
IPI1	M	Lamlem	Lamprologus lemairii	Lamprologini	21.07.14	Toby's Place	-8.623222222	31.20044444
IPI2	NA	Neotet	Neolamprologus tetracanthus	Lamprologini	21.07.14	Toby's Place	-8.623222222	31.20044444
IPI3	NA	Neotet	Neolamprologus tetracanthus	Lamprologini	21.07.14	Toby's Place	-8.623222222	31.20044444
IPI4	NA	Neotet	Neolamprologus tetracanthus	Lamprologini	21.07.14	Toby's Place	-8.623222222	31.20044444
IPI5	NA	Neotet	Neolamprologus tetracanthus	Lamprologini	21.07.14	Toby's Place	-8.623222222	31.20044444
IPI6	NA	Neotet	Neolamprologus tetracanthus	Lamprologini	21.07.14	Toby's Place	-8.623222222	31.20044444
IPI7	NA	Neotet	Neolamprologus tetracanthus	Lamprologini	21.07.14	Toby's Place	-8.623222222	31.20044444
IPI8	NA	Neotet	Neolamprologus tetracanthus	Lamprologini	21.07.14	Toby's Place	-8.623222222	31.20044444
IQA3	M	Neocau	Neolamprologus caudopunctatus	Lamprologini	21.07.14	Toby's Place	-8.623222222	31.20044444
IQA4	F	Neocau	Neolamprologus caudopunctatus	Lamprologini	21.07.14	Toby's Place	-8.623222222	31.20044444
IQA6	NA	Xenspi	Xenotilapia spilopterus	Ectodini	21.07.14	Toby's Place	-8.623222222	31.20044444
IQA7	M	TelteS	Telmatochromis temporalis	Lamprologini	21.07.14	Toby's Place	-8.623222222	31.20044444
IQA9	F	Neocau	Neolamprologus caudopunctatus	Lamprologini	21.07.14	Toby's Place	-8.623222222	31.20044444
IQB1	F	Neocau	Neolamprologus caudopunctatus	Lamprologini	21.07.14	Toby's Place	-8.623222222	31.20044444
IQB2	F	Neocau	Neolamprologus caudopunctatus	Lamprologini	21.07.14	Toby's Place	-8.623222222	31.20044444
IQB3	F	Neocau	Neolamprologus caudopunctatus	Lamprologini	21.07.14	Toby's Place	-8.623222222	31.20044444
IQB4	M	Neocau	Neolamprologus caudopunctatus	Lamprologini	21.07.14	Toby's Place	-8.623222222	31.20044444
IQB5	M	Neocau	Neolamprologus caudopunctatus	Lamprologini	21.07.14	Toby's Place	-8.623222222	31.20044444
IQB6	F	Haptri	Haplotaxodon trifasciatus	Perissodini	22.07.14	Toby's Place	-8.623222222	31.20044444
IQB8	M	Hapmic	Haplotaxodon microlepis	Perissodini	22.07.14	Toby's Place	-8.623222222	31.20044444
IQB9	M	Pcybri	Paracyprichromis sp. "brieni south"	Cyprichromini	22.07.14	Toby's Place	-8.623222222	31.20044444
IQC1	F	Pcybri	Paracyprichromis sp. "brieni south"	Cyprichromini	22.07.14	Toby's Place	-8.623222222	31.20044444
IQC4	M	Permic	Perissodus microlepis	Perissodini	22.07.14	Toby's Place	-8.623222222	31.20044444
IQD3	M	Ophven	Ophthalmotilapia ventralis	Ectodini	22.07.14	Toby's Place	-8.623222222	31.20044444
IQD5	M	Enamel	Enantiopus melanogenys	Ectodini	22.07.14	Toby's Place	-8.623222222	31.20044444
IQD6	M	Enamel	Enantiopus melanogenys	Ectodini	22.07.14	Toby's Place	-8.623222222	31.20044444
IQD7	NA	Lepelo	Lepidiolamprologus elongatus	Lamprologini	22.07.14	Toby's Place	-8.623222222	31.20044444
IQE1	M	Pcybri	Paracyprichromis sp. "brieni south"	Cyprichromini	22.07.14	Toby's Place	-8.623222222	31.20044444
IQE2	F	Pcybri	Paracyprichromis sp. "brieni south"	Cyprichromini	22.07.14	Toby's Place	-8.623222222	31.20044444
IQE3	M	Pcybri	Paracyprichromis sp. "brieni south"	Cyprichromini	22.07.14	Toby's Place	-8.623222222	31.20044444
IQE4	F	Ophven	Ophthalmotilapia ventralis	Ectodini	22.07.14	Toby's Place	-8.623222222	31.20044444
IQE6	F	Pcybri	Paracyprichromis sp. "brieni south"	Cyprichromini	22.07.14	Toby's Place	-8.623222222	31.20044444
IQE7	NA	Pcybri	Paracyprichromis sp. "brieni south"	Cyprichromini	22.07.14	Toby's Place	-8.623222222	31.20044444
IQF1	M	Xenbou	Xenotilapia boulengeri	Ectodini	22.07.14	Toby's Place	-8.623222222	31.20044444
IQF2	M	Cypcol	Cyprichromis coloratus	Cyprichromini	22.07.14	Toby's Place	-8.623222222	31.20044444
IQF3	M	Cypcol	Cyprichromis coloratus	Cyprichromini	22.07.14	Toby's Place	-8.623222222	31.20044444
IQF5	M	Cyafur	Cyathopharynx furcifer	Ectodini	22.07.14	Toby's Place	-8.623222222	31.20044444
IQF6	NA	Chabri	Chalinochromis brichardi	Lamprologini	22.07.14	Toby's Place	-8.623222222	31.20044444
IQF7	NA	Chabri	Chalinochromis brichardi	Lamprologini	22.07.14	Toby's Place	-8.623222222	31.20044444
IQF8	NA	Lepelo	Lepidiolamprologus elongatus	Lamprologini	22.07.14	Toby's Place	-8.623222222	31.20044444
IQF9	M	Ophven	Ophthalmotilapia ventralis	Ectodini	22.07.14	Toby's Place	-8.623222222	31.20044444
IQG1	M	Ophven	Ophthalmotilapia ventralis	Ectodini	22.07.14	Toby's Place	-8.623222222	31.20044444
IQG3	M	Ophven	Ophthalmotilapia ventralis	Ectodini	22.07.14	Toby's Place	-8.623222222	31.20044444
IQG4	M	Ophven	Ophthalmotilapia ventralis	Ectodini	22.07.14	Toby's Place	-8.623222222	31.20044444
IQG5	F	Ophven	Ophthalmotilapia ventralis	Ectodini	22.07.14	Toby's Place	-8.623222222	31.20044444
IQG6	F	Ophven	Ophthalmotilapia ventralis	Ectodini	22.07.14	Toby's Place	-8.623222222	31.20044444
IQG7	F	Ophven	Ophthalmotilapia ventralis	Ectodini	22.07.14	Toby's Place	-8.623222222	31.20044444
IQG8	M	Gnapfe	Gnathochromis pfefferi	Tropheini	22.07.14	Toby's Place	-8.623222222	31.20044444
IQH2	M	Ophven	Ophthalmotilapia ventralis	Ectodini	22.07.14	Toby's Place	-8.623222222	31.20044444
IQH3	F	Ophven	Ophthalmotilapia ventralis	Ectodini	22.07.14	Toby's Place	-8.623222222	31.20044444
IQH4	F	Ophven	Ophthalmotilapia ventralis	Ectodini	22.07.14	Toby's Place	-8.623222222	31.20044444
IQH6	M	Xenbou	Xenotilapia boulengeri	Ectodini	22.07.14	Toby's Place	-8.623222222	31.20044444
IQH7	F	Enamel	Enantiopus melanogenys	Ectodini	22.07.14	Toby's Place	-8.623222222	31.20044444
IQH8	F	Auldew	Aulonocranus dewindti	Ectodini	22.07.14	Toby's Place	-8.623222222	31.20044444
IQH9	M	Gnapfe	Gnathochromis pfefferi	Tropheini	22.07.14	Toby's Place	-8.623222222	31.20044444
IQI1	M	Cyafur	Cyathopharynx furcifer	Ectodini	22.07.14	Toby's Place	-8.623222222	31.20044444
IQI2	M	Lamlem	Lamprologus lemairii	Lamprologini	22.07.14	Toby's Place	-8.623222222	31.20044444

IQI3	NA	Neofas	Neolamprologus fasciatus	Lamprologini	22.07.14	Toby's Place	-8.623222222	31.20044444
IQI4	F	Permic	Perissodus microlepis	Perissodini	22.07.14	Toby's Place	-8.623222222	31.20044444
IQI6	M	Ctehor	Ctenochromis horei	Tropheini	22.07.14	Toby's Place	-8.623222222	31.20044444
IQI7	F	Gnapfe	Gnathochromis pfefferi	Tropheini	22.07.14	Toby's Place	-8.623222222	31.20044444
IQI8	M	Neotet	Neolamprologus tetracanthus	Lamprologini	22.07.14	Toby's Place	-8.623222222	31.20044444
IQI9	M	Neotet	Neolamprologus tetracanthus	Lamprologini	22.07.14	Toby's Place	-8.623222222	31.20044444
IRA1	M	Lesper	Lestradea perspicax	Ectodini	24.08.14	Chimba	-8.426111111	30.45666667
IRA2	F	Lesper	Lestradea perspicax	Ectodini	24.08.14	Chimba	-8.426111111	30.45666667
IRA3	F	Neofur	Neolamprologus furcifer	Lamprologini	24.08.14	Chimba	-8.426111111	30.45666667
IRA4	M	Neofur	Neolamprologus furcifer	Lamprologini	24.08.14	Chimba	-8.426111111	30.45666667
IRA5	M	Neofur	Neolamprologus furcifer	Lamprologini	24.08.14	Chimba	-8.426111111	30.45666667
IRA6	F	Neofur	Neolamprologus furcifer	Lamprologini	24.08.14	Chimba	-8.426111111	30.45666667
IRA7	M	Neofur	Neolamprologus furcifer	Lamprologini	24.08.14	Chimba	-8.426111111	30.45666667
IRA8	F	Pscple	Pseudosimochromis babaulti (South)	Tropheini	24.08.14	Chimba	-8.426111111	30.45666667
IRA9	M	Petfam	Petrochromis famula	Tropheini	24.08.14	Chimba	-8.426111111	30.45666667
IRB1	M	Petfam	Petrochromis famula	Tropheini	24.08.14	Chimba	-8.426111111	30.45666667
IRB2	F	Julreg	Julidochromis sp. "regani south"	Lamprologini	24.08.14	Chimba	-8.426111111	30.45666667
IRB3	NA	Julreg	Julidochromis sp. "regani south"	Lamprologini	24.08.14	Chimba	-8.426111111	30.45666667
IRB4	NA	Julreg	Julidochromis sp. "regani south"	Lamprologini	24.08.14	Chimba	-8.426111111	30.45666667
IRB5	NA	Julreg	Julidochromis sp. "regani south"	Lamprologini	24.08.14	Chimba	-8.426111111	30.45666667
IRB6	NA	Julreg	Julidochromis sp. "regani south"	Lamprologini	24.08.14	Chimba	-8.426111111	30.45666667
IRB7	NA	Julreg	Julidochromis sp. "regani south"	Lamprologini	24.08.14	Chimba	-8.426111111	30.45666667
IRB8	M	Julreg	Julidochromis sp. "regani south"	Lamprologini	24.08.14	Chimba	-8.426111111	30.45666667
IRB9	NA	Telvit	Telmatochromis vittatus	Lamprologini	24.08.14	Chimba	-8.426111111	30.45666667
IRC1	NA	Telvit	Telmatochromis vittatus	Lamprologini	24.08.14	Chimba	-8.426111111	30.45666667
IRC2	NA	Telvit	Telmatochromis vittatus	Lamprologini	24.08.14	Chimba	-8.426111111	30.45666667
IRC4	M	Juldic	Julidochromis dickfeldi	Lamprologini	24.08.14	Chimba	-8.426111111	30.45666667
IRC5	F	Juldic	Julidochromis dickfeldi	Lamprologini	24.08.14	Chimba	-8.426111111	30.45666667
IRC6	M	Juldic	Julidochromis dickfeldi	Lamprologini	24.08.14	Chimba	-8.426111111	30.45666667
IRC7	M	Juldic	Julidochromis dickfeldi	Lamprologini	24.08.14	Chimba	-8.426111111	30.45666667
IRC8	NA	Juldic	Julidochromis dickfeldi	Lamprologini	24.08.14	Chimba	-8.426111111	30.45666667
IRC9	M	Juldic	Julidochromis dickfeldi	Lamprologini	24.08.14	Chimba	-8.426111111	30.45666667
IRD1	M	Juldic	Julidochromis dickfeldi	Lamprologini	24.08.14	Chimba	-8.426111111	30.45666667
IRD2	NA	Xchhec	Xenochromis hecqui	Perissodini	25.08.14	Ndole Fishermen	-8.476694444	30.45566667
IRD3	NA	Xchhec	Xenochromis hecqui	Perissodini	25.08.14	Ndole Fishermen	-8.476694444	30.45566667
IRD4	F	Gralem	Grammatotria lemairii	Ectodini	25.08.14	Ndole Fishermen	-8.476694444	30.45566667
IRD5	M	Lepcun	Lepidiolamprologus cunningtoni	Lamprologini	25.08.14	Ndole Fishermen	-8.476694444	30.45566667
IRD6	NA	Lepcun	Lepidiolamprologus cunningtoni	Lamprologini	25.08.14	Ndole Fishermen	-8.476694444	30.45566667
IRD7	M	Ectdes	Ectodus descampsii	Ectodini	25.08.14	Ndole bay harbor	-8.476138889	30.44933333
IRD8	F	Ectdes	Ectodus descampsii	Ectodini	25.08.14	Ndole bay harbor	-8.476138889	30.44933333
IRD9	M	Xensin	Xenotilapia singularis	Ectodini	25.08.14	Ndole bay harbor	-8.476138889	30.44933333
IRE1	F	Xensin	Xenotilapia singularis	Ectodini	25.08.14	Ndole bay harbor	-8.476138889	30.44933333
IRE2	M	Xensin	Xenotilapia singularis	Ectodini	25.08.14	Ndole bay harbor	-8.476138889	30.44933333
IRE3	F	Xensin	Xenotilapia singularis	Ectodini	25.08.14	Ndole bay harbor	-8.476138889	30.44933333
IRE5	M	Ectdes	Ectodus descampsii	Ectodini	25.08.14	Ndole bay harbor	-8.476138889	30.44933333
IRE6	F	Ectdes	Ectodus descampsii	Ectodini	25.08.14	Ndole bay harbor	-8.476138889	30.44933333
IRE7	M	Ectdes	Ectodus descampsii	Ectodini	25.08.14	Ndole bay harbor	-8.476138889	30.44933333
IRE8	F	Ectdes	Ectodus descampsii	Ectodini	25.08.14	Ndole bay harbor	-8.476138889	30.44933333
IRE9	F	Ectdes	Ectodus descampsii	Ectodini	25.08.14	Ndole bay harbor	-8.476138889	30.44933333
IRF1	F	Ectdes	Ectodus descampsii	Ectodini	25.08.14	Ndole bay harbor	-8.476138889	30.44933333
IRF2	F	Ectdes	Ectodus descampsii	Ectodini	25.08.14	Ndole bay harbor	-8.476138889	30.44933333
IRF3	F	Ectdes	Ectodus descampsii	Ectodini	25.08.14	Ndole bay harbor	-8.476138889	30.44933333
IRF4	M	Ectdes	Ectodus descampsii	Ectodini	25.08.14	Ndole bay harbor	-8.476138889	30.44933333
IRF5	F	Ectdes	Ectodus descampsii	Ectodini	25.08.14	Ndole bay harbor	-8.476138889	30.44933333
IRF6	M	Neomul	Neolamprologus multifasciatus	Lamprologini	25.08.14	Chibwensolo	-8.442777778	30.45472222
IRF8	F	Neomul	Neolamprologus multifasciatus	Lamprologini	25.08.14	Chibwensolo	-8.442777778	30.45472222
IRG1	NA	Neomul	Neolamprologus multifasciatus	Lamprologini	25.08.14	Chibwensolo	-8.442777778	30.45472222
IRG2	NA	Neomul	Neolamprologus multifasciatus	Lamprologini	25.08.14	Chibwensolo	-8.442777778	30.45472222
IRG3	NA	Neomul	Neolamprologus multifasciatus	Lamprologini	25.08.14	Chibwensolo	-8.442777778	30.45472222
IRG4	NA	Neomul	Neolamprologus multifasciatus	Lamprologini	25.08.14	Chibwensolo	-8.442777778	30.45472222
IRG5	NA	Neomul	Neolamprologus multifasciatus	Lamprologini	25.08.14	Chibwensolo	-8.442777778	30.45472222
IRG6	NA	Neomul	Neolamprologus multifasciatus	Lamprologini	25.08.14	Chibwensolo	-8.442777778	30.45472222
IRG7	NA	Neomul	Neolamprologus multifasciatus	Lamprologini	25.08.14	Chibwensolo	-8.442777778	30.45472222
IRG8	NA	Neomul	Neolamprologus multifasciatus	Lamprologini	25.08.14	Chibwensolo	-8.442777778	30.45472222
IRG9	NA	Neomul	Neolamprologus multifasciatus	Lamprologini	25.08.14	Chibwensolo	-8.442777778	30.45472222
IRH1	NA	Neomul	Neolamprologus multifasciatus	Lamprologini	25.08.14	Chibwensolo	-8.442777778	30.45472222
IRH2	M	Altshe	Altolamprologus sp. "compressiceps shell"	Lamprologini	25.08.14	Chibwensolo	-8.442777778	30.45472222
IRH4	F	Altshe	Altolamprologus sp. "compressiceps shell"	Lamprologini	25.08.14	Chibwensolo	-8.442777778	30.45472222
IRH6	F	Altshe	Altolamprologus sp. "compressiceps shell"	Lamprologini	25.08.14	Chibwensolo	-8.442777778	30.45472222
IRH7	M	Altshe	Altolamprologus sp. "compressiceps shell"	Lamprologini	25.08.14	Chibwensolo	-8.442777778	30.45472222
IRH8	F	Altshe	Altolamprologus sp. "compressiceps shell"	Lamprologini	25.08.14	Chibwensolo	-8.442777778	30.45472222
IRH9	NA	Altshe	Altolamprologus sp. "compressiceps shell"	Lamprologini	25.08.14	Chibwensolo	-8.442777778	30.45472222
IRI1	NA	Altshe	Altolamprologus sp. "compressiceps shell"	Lamprologini	25.08.14	Chibwensolo	-8.442777778	30.45472222
IRI2	NA	Altshe	Altolamprologus sp. "compressiceps shell"	Lamprologini	25.08.14	Chibwensolo	-8.442777778	30.45472222
IRI3	NA	Altshe	Altolamprologus sp. "compressiceps shell"	Lamprologini	25.08.14	Chibwensolo	-8.442777778	30.45472222
IRI5	NA	Altshe	Altolamprologus sp. "compressiceps shell"	Lamprologini	25.08.14	Chibwensolo	-8.442777778	30.45472222
IRI6	NA	Altshe	Altolamprologus sp. "compressiceps shell"	Lamprologini	25.08.14	Chibwensolo	-8.442777778	30.45472222
IRI7	NA	Altshe	Altolamprologus sp. "compressiceps shell"	Lamprologini	25.08.14	Chibwensolo	-8.442777778	30.45472222
IRI8	M	Telshe	Telmatochromis sp. "shell"	Lamprologini	25.08.14	Chibwensolo	-8.442777778	30.45472222
IRI9	F	Telshe	Telmatochromis sp. "shell"	Lamprologini	25.08.14	Chibwensolo	-8.442777778	30.45472222
ISA1	M	Tremar	Trematocara marginatum	Trematocarini	22.07.14	Toby's Place	-8.623222222	31.20044444
ISA3	F	Tremar	Trematocara marginatum	Trematocarini	22.07.14	Toby's Place	-8.623222222	31.20044444
ISA6	M	Neopul	Neolamprologus pulcher	Lamprologini	23.07.14	Toby's Place	-8.623222222	31.20044444
ISA8	M	Neosav	Neolamprologus savoryi	Lamprologini	23.07.14	Toby's Place	-8.623222222	31.20044444
ISB1	M	Altcom	Altolamprologus compressiceps	Lamprologini	23.07.14	Toby's Place	-8.623222222	31.20044444
ISB3	F	Neopul	Neolamprologus pulcher	Lamprologini	23.07.14	Toby's Place	-8.623222222	31.20044444
ISB7	M	Julorn	Julidochromis ornatus	Lamprologini	23.07.14	Toby's Place	-8.623222222	31.20044444
ISC1	F	Julorn	Julidochromis ornatus	Lamprologini	23.07.14	Toby's Place	-8.623222222	31.20044444
ISC9	F	Altcom	Altolamprologus compressiceps	Lamprologini	23.07.14	Toby's Place	-8.623222222	31.20044444
ISD4	NA	Lamlem	Lamprologus lemairii	Lamprologini	23.07.14	Toby's Place	-8.623222222	31.20044444
ISD5	NA	Neopul	Neolamprologus pulcher	Lamprologini	23.07.14	Toby's Place	-8.623222222	31.20044444
ISD6	NA	Xenfla	Xenotilapia flavipinnis	Ectodini	23.07.14	Toby's Place	-8.623222222	31.20044444
ISD7	NA	Xenfla	Xenotilapia flavipinnis	Ectodini	23.07.14	Toby's Place	-8.623222222	31.20044444
ISD8	M	Loblab	Lobochilotes labiatus	Tropheini	23.07.14	Toby's Place	-8.623222222	31.20044444
ISE1	NA	Lepelo	Lepidiolamprologus elongatus	Lamprologini	23.07.14	Toby's Place	-8.623222222	31.20044444
ISE2	M	Pscple	Pseudosimochromis babaulti (South)	Tropheini	23.07.14	Toby's Place	-8.623222222	31.20044444
ISE3	F	Pscple	Pseudosimochromis babaulti (South)	Tropheini	23.07.14	Toby's Place	-8.623222222	31.20044444
ISE4	F	Pscple	Pseudosimochromis babaulti (South)	Tropheini	23.07.14	Toby's Place	-8.623222222	31.20044444
ISE5	F	Loblab	Lobochilotes labiatus	Tropheini	23.07.14	Toby's Place	-8.623222222	31.20044444
ISE7	NA	Altcom	Altolamprologus compressiceps	Lamprologini	23.07.14	Toby's Place	-8.623222222	31.20044444
ISE8	NA	Altcom	Altolamprologus compressiceps	Lamprologini	23.07.14	Toby's Place	-8.623222222	31.20044444
ISF1	NA	Neopul	Neolamprologus pulcher	Lamprologini	23.07.14	Toby's Place	-8.623222222	31.20044444
ISF4	F	Cyafur	Cyathopharynx furcifer	Ectodini	23.07.14	Toby's Place	-8.623222222	31.20044444
ISF5	M	Cyafur	Cyathopharynx furcifer	Ectodini	23.07.14	Toby's Place	-8.623222222	31.20044444
ISF6	NA	Lamlem	Lamprologus lemairii	Lamprologini	23.07.14	Toby's Place	-8.623222222	31.20044444
ISF7	NA	Lepatt	Lepidiolamprologus attenuatus	Lamprologini	23.07.14	Toby's Place	-8.623222222	31.20044444
ISF8	NA	Neopul	Neolamprologus pulcher	Lamprologini	23.07.14	Toby's Place	-8.623222222	31.20044444
ISF9	NA	Neopul	Neolamprologus pulcher	Lamprologini	23.07.14	Toby's Place	-8.623222222	31.20044444
ISG4	NA	Neofas	Neolamprologus fasciatus	Lamprologini	23.07.14	Toby's Place	-8.623222222	31.20044444
ISG5	NA	Neocau	Neolamprologus caudopunctatus	Lamprologini	23.07.14	Toby's Place	-8.623222222	31.20044444
ISG6	NA	Neocau	Neolamprologus caudopunctatus	Lamprologini	23.07.14	Toby's Place	-8.623222222	31.20044444
ISG7	NA	Neocau	Neolamprologus caudopunctatus	Lamprologini	23.07.14	Toby's Place	-8.623222222	31.20044444
ISG8	NA	Neocau	Neolamprologus caudopunctatus	Lamprologini	23.07.14	Toby's Place	-8.623222222	31.20044444
ISH1	NA	Lepelo	Lepidiolamprologus elongatus	Lamprologini	23.07.14	Toby's Place	-8.623222222	31.20044444
ISH2	NA	Lepelo	Lepidiolamprologus elongatus	Lamprologini	23.07.14	Toby's Place	-8.623222222	31.20044444
ISH3	NA	Lepelo	Lepidiolamprologus elongatus	Lamprologini	23.07.14	Toby's Place	-8.623222222	31.20044444
ISH4	NA	Lepelo	Lepidiolamprologus elongatus	Lamprologini	23.07.14	Toby's Place	-8.623222222	31.20044444
ISH5	NA	Gnapfe	Gnathochromis pfefferi	Tropheini	23.07.14	Toby's Place	-8.623222222	31.20044444
ISH6	NA	Gnapfe	Gnathochromis pfefferi	Tropheini	23.07.14	Toby's Place	-8.623222222	31.20044444
ISH7	NA	Neopul	Neolamprologus pulcher	Lamprologini	23.07.14	Toby's Place	-8.623222222	31.20044444
ISH8	NA	Neopul	Neolamprologus pulcher	Lamprologini	23.07.14	Toby's Place	-8.623222222	31.20044444
ISI1	NA	Varmoo	Variabilichromis moorii	Lamprologini	23.07.14	Toby's Place	-8.623222222	31.20044444
ISI2	M	Cyplep	Cyprichromis leptosoma	Cyprichromini	24.07.14	Toby's Place	-8.623222222	31.20044444
ISI6	F	Cyplep	Cyprichromis leptosoma	Cyprichromini	24.07.14	Toby's Place	-8.623222222	31.20044444

ITA4	F	Gnaper	Gnathochromis permaxillaris	Limnochromini	24.07.14	Chipwa Fishermen	-8.606166667	31.18611111
ITA6	F	Lchsta	Limnochromis staneri	Limnochromini	24.07.14	Chipwa Fishermen	-8.606166667	31.18611111
ITB1	F	Lchaur	Limnochromis auritus	Limnochromini	24.07.14	Chipwa Fishermen	-8.606166667	31.18611111
ITB3	F	Lchabe	Limnochromis abeelei	Limnochromini	24.07.14	Chipwa Fishermen	-8.606166667	31.18611111
ITB4	M	Lchabe	Limnochromis abeelei	Limnochromini	24.07.14	Chipwa Fishermen	-8.606166667	31.18611111
ITB5	NA	Lchsta	Limnochromis staneri	Limnochromini	24.07.14	Chipwa Fishermen	-8.606166667	31.18611111
ITB6	NA	Lchsta	Limnochromis staneri	Limnochromini	24.07.14	Chipwa Fishermen	-8.606166667	31.18611111
ITB7	NA	Lchsta	Limnochromis staneri	Limnochromini	24.07.14	Chipwa Fishermen	-8.606166667	31.18611111
ITB8	NA	Lchsta	Limnochromis staneri	Limnochromini	24.07.14	Chipwa Fishermen	-8.606166667	31.18611111
ITB9	NA	Lchabe	Limnochromis abeelei	Limnochromini	24.07.14	Chipwa Fishermen	-8.606166667	31.18611111
ITC1	M	Batgra	Bathybates graueri	Bathybatini	24.07.14	Chipwa Fishermen	-8.606166667	31.18611111
ITC2	M	Lchsta	Limnochromis staneri	Limnochromini	24.07.14	Chipwa Fishermen	-8.606166667	31.18611111
ITC3	F	Cyplep	Cyprichromis leptosoma	Cyprichromini	24.07.14	Chipwa Fishermen	-8.606166667	31.18611111
ITC4	F	Cyplep	Cyprichromis leptosoma	Cyprichromini	24.07.14	Chipwa Fishermen	-8.606166667	31.18611111
ITC5	M	Cyplep	Cyprichromis leptosoma	Cyprichromini	24.07.14	Chipwa Fishermen	-8.606166667	31.18611111
ITC6	M	Cyplep	Cyprichromis leptosoma	Cyprichromini	24.07.14	Chipwa Fishermen	-8.606166667	31.18611111
ITC7	M	Cyplep	Cyprichromis leptosoma	Cyprichromini	24.07.14	Chipwa Fishermen	-8.606166667	31.18611111
ITD4	NA	Cypcol	Cyprichromis coloratus	Cyprichromini	24.07.14	Toby's Place	-8.623222222	31.20044444
ITD5	NA	Batgra	Bathybates graueri	Bathybatini	24.07.14	Chipwa Fishermen	-8.606166667	31.18611111
ITD6	NA	Batgra	Bathybates graueri	Bathybatini	24.07.14	Chipwa Fishermen	-8.606166667	31.18611111
ITD7	M	Batvit	Bathybates vittatus	Bathybatini	24.07.14	Chipwa Fishermen	-8.606166667	31.18611111
ITD8	F	Pcybri	Paracyprichromis sp. "brieni south"	Cyprichromini	24.07.14	Chipwa Fishermen	-8.606166667	31.18611111
ITD9	NA	Pcybri	Paracyprichromis sp. "brieni south"	Cyprichromini	24.07.14	Chipwa Fishermen	-8.606166667	31.18611111
ITE1	M	Pcybri	Paracyprichromis sp. "brieni south"	Cyprichromini	24.07.14	Chipwa Fishermen	-8.606166667	31.18611111
ITE2	M	Pcybri	Paracyprichromis sp. "brieni south"	Cyprichromini	24.07.14	Chipwa Fishermen	-8.606166667	31.18611111
ITE3	F	Pcybri	Paracyprichromis sp. "brieni south"	Cyprichromini	24.07.14	Chipwa Fishermen	-8.606166667	31.18611111
ITE4	NA	Batleo	Bathybates leo	Bathybatini	24.07.14	Chipwa Fishermen	-8.606166667	31.18611111
ITE6	F	Cyplep	Cyprichromis leptosoma	Cyprichromini	24.07.14	Chipwa Fishermen	-8.606166667	31.18611111
ITE7	F	Cyplep	Cyprichromis leptosoma	Cyprichromini	24.07.14	Chipwa Fishermen	-8.606166667	31.18611111
ITE8	M	Cyplep	Cyprichromis leptosoma	Cyprichromini	24.07.14	Chipwa Fishermen	-8.606166667	31.18611111
ITE9	M	Cyplep	Cyprichromis leptosoma	Cyprichromini	24.07.14	Chipwa Fishermen	-8.606166667	31.18611111
ITF1	NA	Cyplep	Cyprichromis leptosoma	Cyprichromini	24.07.14	Chipwa Fishermen	-8.606166667	31.18611111
ITF2	NA	Batleo	Bathybates leo	Bathybatini	24.07.14	Chipwa Fishermen	-8.606166667	31.18611111
ITF3	M	Batvit	Bathybates vittatus	Bathybatini	24.07.14	Chipwa Fishermen	-8.606166667	31.18611111
ITF5	M	Cypcol	Cyprichromis coloratus	Cyprichromini	24.07.14	Toby's Place	-8.623222222	31.20044444
ITF6	NA	Cypcol	Cyprichromis coloratus	Cyprichromini	24.07.14	Toby's Place	-8.623222222	31.20044444
ITF7	NA	Cypcol	Cyprichromis coloratus	Cyprichromini	24.07.14	Toby's Place	-8.623222222	31.20044444
ITF8	NA	Batvit	Bathybates vittatus	Bathybatini	24.07.14	Chipwa Fishermen	-8.606166667	31.18611111
ITF9	M	Xenbou	Xenotilapia boulengeri	Ectodini	24.07.14	Chipwa Fishermen	-8.606166667	31.18611111
ITG1	NA	Petpol	Petrochromis polyodon	Tropheini	24.07.14	Chipwa Fishermen	-8.606166667	31.18611111
ITG2	F	Neochr	Neolamprologus christyi	Lamprologini	24.07.14	Chipwa Fishermen	-8.606166667	31.18611111
ITG3	M	Hapmic	Haplotaxodon microlepis	Perissodini	24.07.14	Chipwa Fishermen	-8.606166667	31.18611111
ITG4	M	Hapmic	Haplotaxodon microlepis	Perissodini	24.07.14	Chipwa Fishermen	-8.606166667	31.18611111
ITG5	M	Hapmic	Haplotaxodon microlepis	Perissodini	24.07.14	Chipwa Fishermen	-8.606166667	31.18611111
ITG6	M	Hapmic	Haplotaxodon microlepis	Perissodini	24.07.14	Chipwa Fishermen	-8.606166667	31.18611111
ITG7	F	Auldew	Aulonocranus dewindti	Ectodini	24.07.14	Toby's Place	-8.623222222	31.20044444
ITG8	NA	Petpol	Petrochromis polyodon	Tropheini	24.07.14	Toby's Place	-8.623222222	31.20044444
ITG9	NA	Petpol	Petrochromis polyodon	Tropheini	24.07.14	Toby's Place	-8.623222222	31.20044444
ITH3	M	Batfas	Bathybates fasciatus	Bathybatini	24.07.14	Chipwa Fishermen	-8.606166667	31.18611111
ITH6	NA	Boumic	Boulengerochromis microlepis	Boulengerochromini	24.07.14	Chipwa Fishermen	-8.606166667	31.18611111
ITH7	NA	Boumic	Boulengerochromis microlepis	Boulengerochromini	24.07.14	Chipwa Fishermen	-8.606166667	31.18611111
ITH8	NA	Batfas	Bathybates fasciatus	Bathybatini	24.07.14	Chipwa Fishermen	-8.606166667	31.18611111
ITI2	M	Trenig	Trematocara nigrifrons	Trematocarini	24.07.14	Chipwa Fishermen	-8.606166667	31.18611111
IUA8	F	Trenig	Trematocara nigrifrons	Trematocarini	25.07.14	Toby's Place	-8.623222222	31.20044444
IUA9	F	Trenig	Trematocara nigrifrons	Trematocarini	25.07.14	Toby's Place	-8.623222222	31.20044444
IUB1	F	Trenig	Trematocara nigrifrons	Trematocarini	25.07.14	Toby's Place	-8.623222222	31.20044444
IUB2	F	Trenig	Trematocara nigrifrons	Trematocarini	25.07.14	Toby's Place	-8.623222222	31.20044444
IUB3	F	Trenig	Trematocara nigrifrons	Trematocarini	25.07.14	Toby's Place	-8.623222222	31.20044444
IUB4	F	Trenig	Trematocara nigrifrons	Trematocarini	25.07.14	Toby's Place	-8.623222222	31.20044444
IUB5	F	Trenig	Trematocara nigrifrons	Trematocarini	25.07.14	Toby's Place	-8.623222222	31.20044444
IUC2	M	Tremar	Trematocara marginatum	Trematocarini	25.07.14	Toby's Place	-8.623222222	31.20044444
IUC3	M	Tremar	Trematocara marginatum	Trematocarini	25.07.14	Toby's Place	-8.623222222	31.20044444
IUC6	F	Tremar	Trematocara marginatum	Trematocarini	25.07.14	Toby's Place	-8.623222222	31.20044444
IUC7	F	Tremar	Trematocara marginatum	Trematocarini	25.07.14	Toby's Place	-8.623222222	31.20044444
IUD2	F	Tremar	Trematocara marginatum	Trematocarini	25.07.14	Toby's Place	-8.623222222	31.20044444
IUD3	M	Tremar	Trematocara marginatum	Trematocarini	25.07.14	Toby's Place	-8.623222222	31.20044444
IUD4	F	Tremac	Trematocara macrostoma	Trematocarini	25.07.14	Toby's Place	-8.623222222	31.20044444
IUD5	F	Tremac	Trematocara macrostoma	Trematocarini	25.07.14	Toby's Place	-8.623222222	31.20044444
IUD6	F	Tremac	Trematocara macrostoma	Trematocarini	25.07.14	Toby's Place	-8.623222222	31.20044444
IUD8	M	Tremac	Trematocara macrostoma	Trematocarini	25.07.14	Toby's Place	-8.623222222	31.20044444
IUD9	F	Tremac	Trematocara macrostoma	Trematocarini	25.07.14	Toby's Place	-8.623222222	31.20044444
IUE1	M	Tremac	Trematocara macrostoma	Trematocarini	25.07.14	Toby's Place	-8.623222222	31.20044444
IUE2	M	Tremac	Trematocara macrostoma	Trematocarini	25.07.14	Toby's Place	-8.623222222	31.20044444
IUE5	M	Trenig	Trematocara nigrifrons	Trematocarini	25.07.14	Toby's Place	-8.623222222	31.20044444
IUE7	M	Tresti	Trematocara stigmaticum	Trematocarini	25.07.14	Toby's Place	-8.623222222	31.20044444
IUF7	M	Xensim	Xenotilapia sima	Ectodini	25.07.14	Toby's Place	-8.623222222	31.20044444
IUF8	F	Xensim	Xenotilapia sima	Ectodini	25.07.14	Toby's Place	-8.623222222	31.20044444
IUG8	F	Xensim	Xenotilapia sima	Ectodini	25.07.14	Toby's Place	-8.623222222	31.20044444
IUG9	NA	Gralem	Grammatotria lemairii	Ectodini	25.07.14	Toby's Place	-8.623222222	31.20044444
IUH1	M	Cyafur	Cyathopharynx furcifer	Ectodini	25.07.14	Toby's Place	-8.623222222	31.20044444
IUH2	M	Cyafur	Cyathopharynx furcifer	Ectodini	25.07.14	Toby's Place	-8.623222222	31.20044444
IUH3	M	Cunlon	Cunningtonia longiventralis	Ectodini	25.07.14	Isanga	-8.654555556	31.19183333
IUH4	M	Neofas	Neolamprologus fasciatus	Lamprologini	25.07.14	Isanga	-8.654555556	31.19183333
IUH5	M	Batgra	Bathybates graueri	Bathybatini	25.07.14	Chipwa Fishermen	-8.606166667	31.18611111
IUH6	M	Batgra	Bathybates graueri	Bathybatini	25.07.14	Chipwa Fishermen	-8.606166667	31.18611111
IUH7	F	Batgra	Bathybates graueri	Bathybatini	25.07.14	Toby's Place	-8.623222222	31.20044444
IUH8	F	Batgra	Bathybates graueri	Bathybatini	25.07.14	Toby's Place	-8.623222222	31.20044444
IUH9	M	Batgra	Bathybates graueri	Bathybatini	25.07.14	Toby's Place	-8.623222222	31.20044444
IUI1	M	Regcal	Reganochromis calliurus	Limnochromini	25.07.14	Chipwa Fishermen	-8.606166667	31.18611111
IUI3	M	Regcal	Reganochromis calliurus	Limnochromini	26.07.14	Chipwa Fishermen	-8.606166667	31.18611111
IUI4	F	Regcal	Reganochromis calliurus	Limnochromini	26.07.14	Chipwa Fishermen	-8.606166667	31.18611111
IUI5	M	Gnaper	Gnathochromis permaxillaris	Limnochromini	27.07.14	Chipwa Fishermen	-8.606166667	31.18611111
IUI7	M	Xchhec	Xenochromis hecqui	Perissodini	27.07.14	Chipwa Fishermen	-8.606166667	31.18611111
IUI8	F	Batgra	Bathybates graueri	Bathybatini	27.07.14	Chipwa Fishermen	-8.606166667	31.18611111
IVA1	NA	Telshe	Telmatochromis sp. "shell"	Lamprologini	25.08.14	Chibwensolo	-8.442777778	30.45472222
IVA2	NA	Telshe	Telmatochromis sp. "shell"	Lamprologini	25.08.14	Chibwensolo	-8.442777778	30.45472222
IVA3	NA	Telshe	Telmatochromis sp. "shell"	Lamprologini	25.08.14	Chibwensolo	-8.442777778	30.45472222
IVA4	NA	Telshe	Telmatochromis sp. "shell"	Lamprologini	25.08.14	Chibwensolo	-8.442777778	30.45472222
IVA5	NA	Telshe	Telmatochromis sp. "shell"	Lamprologini	25.08.14	Chibwensolo	-8.442777778	30.45472222
IVA6	NA	Telshe	Telmatochromis sp. "shell"	Lamprologini	25.08.14	Chibwensolo	-8.442777778	30.45472222
IVA7	NA	Telshe	Telmatochromis sp. "shell"	Lamprologini	25.08.14	Chibwensolo	-8.442777778	30.45472222
IVA8	NA	Telshe	Telmatochromis sp. "shell"	Lamprologini	25.08.14	Chibwensolo	-8.442777778	30.45472222
IVA9	NA	Telshe	Telmatochromis sp. "shell"	Lamprologini	25.08.14	Chibwensolo	-8.442777778	30.45472222
IVB1	M	Enamel	Enantiopus melanogenys	Ectodini	25.08.14	Ntingila	-8.481388889	30.46138889
IVB2	M	Enamel	Enantiopus melanogenys	Ectodini	25.08.14	Ntingila	-8.481388889	30.46138889
IVB4	M	Xenbat	Xenotilapia bathyphilus	Ectodini	25.08.14	Ntingila	-8.481388889	30.46138889
IVB5	F	Xenbat	Xenotilapia bathyphilus	Ectodini	25.08.14	Ntingila	-8.481388889	30.46138889
IVB6	M	Xenbat	Xenotilapia bathyphilus	Ectodini	25.08.14	Ntingila	-8.481388889	30.46138889
IVB7	M	Xenbat	Xenotilapia bathyphilus	Ectodini	25.08.14	Ntingila	-8.481388889	30.46138889
IVB8	NA	Xenbat	Xenotilapia bathyphilus	Ectodini	25.08.14	Ntingila	-8.481388889	30.46138889
IVB9	NA	Xenbat	Xenotilapia bathyphilus	Ectodini	25.08.14	Ntingila	-8.481388889	30.46138889
IVC1	M	Xenbat	Xenotilapia bathyphilus	Ectodini	25.08.14	Ntingila	-8.481388889	30.46138889
IVC2	NA	Xenbat	Xenotilapia bathyphilus	Ectodini	25.08.14	Ntingila	-8.481388889	30.46138889
IVC4	F	Xenbat	Xenotilapia bathyphilus	Ectodini	25.08.14	Ntingila	-8.481388889	30.46138889
IVC7	NA	Xenbat	Xenotilapia bathyphilus	Ectodini	25.08.14	Ntingila	-8.481388889	30.46138889
IVC8	NA	Lepcun	Lepidiolamprologus cunningtoni	Lamprologini	25.08.14	Ntingila	-8.481388889	30.46138889
IVC9	NA	Lepcun	Lepidiolamprologus cunningtoni	Lamprologini	25.08.14	Ntingila	-8.481388889	30.46138889
IVD1	NA	Lepcun	Lepidiolamprologus cunningtoni	Lamprologini	25.08.14	Ntingila	-8.481388889	30.46138889
IVD2	NA	Lepcun	Lepidiolamprologus cunningtoni	Lamprologini	25.08.14	Ntingila	-8.481388889	30.46138889
IVD3	NA	Lepcun	Lepidiolamprologus cunningtoni	Lamprologini	25.08.14	Ntingila	-8.481388889	30.46138889
IVD5	NA	Julreg	Julidochromis sp. "regani south"	Lamprologini	25.08.14	Ntingila	-8.481388889	30.46138889
IVD6	NA	Julreg	Julidochromis sp. "regani south"	Lamprologini	25.08.14	Ntingila	-8.481388889	30.46138889
IVD8	NA	Juldic	Julidochromis dickfeldi	Lamprologini	25.08.14	Ntingila	-8.481388889	30.46138889
IVD9	NA	Juldic	Julidochromis dickfeldi	Lamprologini	25.08.14	Ntingila	-8.481388889	30.46138889

IVE1	NA	Juldic	Julidochromis dickfeldi	Lamprologini	25.08.14	Ntingila	-8.481388889	30.46138889
IVE2	NA	Juldic	Julidochromis dickfeldi	Lamprologini	25.08.14	Ntingila	-8.481388889	30.46138889
IVE3	NA	Juldic	Julidochromis dickfeldi	Lamprologini	25.08.14	Ntingila	-8.481388889	30.46138889
IVE5	NA	LamorS	Lamprologus sp. "ornatipinnis zambia"	Lamprologini	25.08.14	Ntingila	-8.481388889	30.46138889
IVE6	NA	LamorS	Lamprologus sp. "ornatipinnis zambia"	Lamprologini	25.08.14	Ntingila	-8.481388889	30.46138889
IVE7	NA	LamorS	Lamprologus sp. "ornatipinnis zambia"	Lamprologini	25.08.14	Ntingila	-8.481388889	30.46138889
IVE8	M	Neocra	Neolamprologus crassus	Lamprologini	26.08.14	Katete	-8.338777778	30.50794444
IVF1	F	Neocra	Neolamprologus crassus	Lamprologini	26.08.14	Katete	-8.338777778	30.50794444
IVF4	M	Xenpap	Xenotilapia papilio (Katete)	Ectodini	26.08.14	Katete 3	-8.337777778	30.51111111
IVF5	F	Xenpap	Xenotilapia papilio (Katete)	Ectodini	26.08.14	Katete 3	-8.337777778	30.51111111
IVF7	M	Neocra	Neolamprologus crassus	Lamprologini	26.08.14	Katete 2	-8.328055556	30.52666667
IVF8	NA	Neocra	Neolamprologus crassus	Lamprologini	26.08.14	Katete 2	-8.328055556	30.52666667
IVF9	NA	Neocra	Neolamprologus crassus	Lamprologini	26.08.14	Katete 2	-8.328055556	30.52666667
IVG1	M	Neocra	Neolamprologus crassus	Lamprologini	26.08.14	Katete 2	-8.328055556	30.52666667
IVG2	M	Neocra	Neolamprologus crassus	Lamprologini	26.08.14	Katete 2	-8.328055556	30.52666667
IVG3	NA	Neocra	Neolamprologus crassus	Lamprologini	26.08.14	Katete 2	-8.328055556	30.52666667
IVG4	M	Neocra	Neolamprologus crassus	Lamprologini	26.08.14	Katete 2	-8.328055556	30.52666667
IVG5	NA	Neocra	Neolamprologus crassus	Lamprologini	26.08.14	Katete 2	-8.328055556	30.52666667
IVG6	NA	Neocra	Neolamprologus crassus	Lamprologini	26.08.14	Katete 2	-8.328055556	30.52666667
IVG7	F	Neocra	Neolamprologus crassus	Lamprologini	26.08.14	Katete 2	-8.328055556	30.52666667
IVG8	NA	Loblab	Lobochilotes labiatus	Tropheini	26.08.14	Katete 2	-8.328055556	30.52666667
IVG9	NA	Loblab	Lobochilotes labiatus	Tropheini	26.08.14	Katete 2	-8.328055556	30.52666667
IVH1	M	Neopro	Neolamprologus prochilus	Lamprologini	26.08.14	Katete 2	-8.328055556	30.52666667
IVH2	F	Neopro	Neolamprologus prochilus	Lamprologini	26.08.14	Katete 2	-8.328055556	30.52666667
IVH3	NA	Neopro	Neolamprologus prochilus	Lamprologini	26.08.14	Katete 2	-8.328055556	30.52666667
IVH5	F	Xenpap	Xenotilapia papilio (Katete)	Ectodini	26.08.14	Katete 3	-8.337777778	30.51111111
IVH6	NA	Xenpap	Xenotilapia papilio (Katete)	Ectodini	26.08.14	Katete 3	-8.337777778	30.51111111
IVH7	F	Xenpap	Xenotilapia papilio (Katete)	Ectodini	26.08.14	Katete 3	-8.337777778	30.51111111
IVH8	NA	Xenpap	Xenotilapia papilio (Katete)	Ectodini	26.08.14	Katete 3	-8.337777778	30.51111111
IVH9	NA	Xenpap	Xenotilapia papilio (Katete)	Ectodini	26.08.14	Katete 3	-8.337777778	30.51111111
IVI1	NA	Xenpap	Xenotilapia papilio (Katete)	Ectodini	26.08.14	Katete 3	-8.337777778	30.51111111
IVI2	NA	Xenpap	Xenotilapia papilio (Katete)	Ectodini	26.08.14	Katete 3	-8.337777778	30.51111111
IVI3	NA	Xenpap	Xenotilapia papilio (Katete)	Ectodini	26.08.14	Katete 3	-8.337777778	30.51111111
IVI4	NA	Xenpap	Xenotilapia papilio (Katete)	Ectodini	26.08.14	Katete 3	-8.337777778	30.51111111
IVI5	NA	Xenpap	Xenotilapia papilio (Katete)	Ectodini	26.08.14	Katete 3	-8.337777778	30.51111111
IVI8	NA	Mdcrot	Microdontochromis rotundiventralis	Ectodini	26.08.14	Katete 2	-8.328055556	30.52666667
IVI9	NA	Mdcrot	Microdontochromis rotundiventralis	Ectodini	26.08.14	Katete 2	-8.328055556	30.52666667
IWA1	NA	Mdcrot	Microdontochromis rotundiventralis	Ectodini	26.08.14	Katete 2	-8.328055556	30.52666667
IWA2	NA	Mdcrot	Microdontochromis rotundiventralis	Ectodini	26.08.14	Katete 2	-8.328055556	30.52666667
IWA3	NA	Mdcrot	Microdontochromis rotundiventralis	Ectodini	26.08.14	Katete 2	-8.328055556	30.52666667
IWA4	NA	Mdcrot	Microdontochromis rotundiventralis	Ectodini	26.08.14	Katete 2	-8.328055556	30.52666667
IWA5	M	Neobue	Neolamprologus buescheri	Lamprologini	26.08.14	Katete 3	-8.337777778	30.51111111
IWA8	M	Neoobs	Neolamprologus obscurus	Lamprologini	26.08.14	Katete 2	-8.328055556	30.52666667
IWA9	M	Neoobs	Neolamprologus obscurus	Lamprologini	26.08.14	Katete 2	-8.328055556	30.52666667
IWB1	M	Neoobs	Neolamprologus obscurus	Lamprologini	26.08.14	Katete 2	-8.328055556	30.52666667
IWB2	F	Neoobs	Neolamprologus obscurus	Lamprologini	26.08.14	Katete 2	-8.328055556	30.52666667
IWB3	NA	Plestr	Plecodus straeleni	Perissodini	26.08.14	Katete 3	-8.337777778	30.51111111
IWB5	M	Pethor	Petrochromis horii	Tropheini	26.08.14	Katete 3	-8.337777778	30.51111111
IWB6	F	Pethor	Petrochromis horii	Tropheini	26.08.14	Katete 3	-8.337777778	30.51111111
IWB7	F	Pethor	Petrochromis horii	Tropheini	26.08.14	Katete 3	-8.337777778	30.51111111
IWB8	F	Pethor	Petrochromis horii	Tropheini	26.08.14	Katete 3	-8.337777778	30.51111111
IWB9	F	Pethor	Petrochromis horii	Tropheini	26.08.14	Katete 3	-8.337777778	30.51111111
IWC1	F	Pethor	Petrochromis horii	Tropheini	26.08.14	Katete 3	-8.337777778	30.51111111
IWC2	F	Pethor	Petrochromis horii	Tropheini	26.08.14	Katete 3	-8.337777778	30.51111111
IWC4	NA	Neofur	Neolamprologus furcifer	Lamprologini	26.08.14	Katete 2	-8.328055556	30.52666667
IWC5	NA	Neofur	Neolamprologus furcifer	Lamprologini	26.08.14	Katete 2	-8.328055556	30.52666667
IWC7	NA	Gnapfe	Gnathochromis pfefferi	Tropheini	26.08.14	Katete 3	-8.337777778	30.51111111
IWC9	M	Pettre	Petrochromis trewavasae	Tropheini	26.08.14	Katete 2	-8.328055556	30.52666667
IWD1	F	Pettre	Petrochromis trewavasae	Tropheini	26.08.14	Katete 2	-8.328055556	30.52666667
IWD2	F	Pettre	Petrochromis trewavasae	Tropheini	26.08.14	Katete 2	-8.328055556	30.52666667
IWD3	F	Pettre	Petrochromis trewavasae	Tropheini	26.08.14	Katete 2	-8.328055556	30.52666667
IWD4	F	Pettre	Petrochromis trewavasae	Tropheini	26.08.14	Katete 2	-8.328055556	30.52666667
IWD5	M	Lamsig	Lamprologus signatus	Lamprologini	28.08.14	Chimba	-8.426111111	30.45666667
IWD6	F	Lamsig	Lamprologus signatus	Lamprologini	28.08.14	Chimba	-8.426111111	30.45666667
IWD7	M	Cunlon	Cunningtonia longiventralis	Ectodini	27.08.14	Ntingila	-8.481388889	30.46138889
IWD8	F	Cunlon	Cunningtonia longiventralis	Ectodini	27.08.14	Ntingila	-8.481388889	30.46138889
IWE1	M	Cunlon	Cunningtonia longiventralis	Ectodini	27.08.14	Ntingila	-8.481388889	30.46138889
IWE2	M	Cunlon	Cunningtonia longiventralis	Ectodini	27.08.14	Ntingila	-8.481388889	30.46138889
IWE3	M	Cunlon	Cunningtonia longiventralis	Ectodini	27.08.14	Ntingila	-8.481388889	30.46138889
IWE4	M	Cunlon	Cunningtonia longiventralis	Ectodini	27.08.14	Ntingila	-8.481388889	30.46138889
IWE5	F	Cunlon	Cunningtonia longiventralis	Ectodini	27.08.14	Ntingila	-8.481388889	30.46138889
IWE6	F	Cunlon	Cunningtonia longiventralis	Ectodini	27.08.14	Ntingila	-8.481388889	30.46138889
IWE7	F	Cunlon	Cunningtonia longiventralis	Ectodini	27.08.14	Ntingila	-8.481388889	30.46138889
IWE8	F	Cunlon	Cunningtonia longiventralis	Ectodini	27.08.14	Ntingila	-8.481388889	30.46138889
IWE9	F	Cunlon	Cunningtonia longiventralis	Ectodini	27.08.14	Ntingila	-8.481388889	30.46138889
IWF1	NA	Lchaur	Limnochromis auritus	Limnochromini	27.08.14	Ntingila	-8.481388889	30.46138889
IWF2	NA	Lchaur	Limnochromis auritus	Limnochromini	27.08.14	Ntingila	-8.481388889	30.46138889
IWF3	NA	Lchaur	Limnochromis auritus	Limnochromini	28.08.14	Ndole Fishermen	-8.476694444	30.45566667
IWF4	M	Lamsig	Lamprologus signatus	Lamprologini	28.08.14	Chimba	-8.426111111	30.45666667
IWF5	M	Lamsig	Lamprologus signatus	Lamprologini	28.08.14	Chimba	-8.426111111	30.45666667
IWF6	M	Lamsig	Lamprologus signatus	Lamprologini	28.08.14	Chimba	-8.426111111	30.45666667
IWF7	M	Lamsig	Lamprologus signatus	Lamprologini	28.08.14	Chimba	-8.426111111	30.45666667
IWF8	M	Lamsig	Lamprologus signatus	Lamprologini	28.08.14	Chimba	-8.426111111	30.45666667
IWF9	M	Lamsig	Lamprologus signatus	Lamprologini	28.08.14	Chimba	-8.426111111	30.45666667
IWG2	F	Lamsig	Lamprologus signatus	Lamprologini	28.08.14	Chimba	-8.426111111	30.45666667
IWG3	F	Lamsig	Lamprologus signatus	Lamprologini	28.08.14	Chimba	-8.426111111	30.45666667
IWG6	NA	Gralem	Grammatotria lemairii	Ectodini	28.08.14	Ndole Fishermen	-8.476694444	30.45566667
IWG7	NA	Lepcun	Lepidiolamprologus cunningtoni	Lamprologini	28.08.14	Ndole Fishermen	-8.476694444	30.45566667
IWG8	NA	Gnapfe	Gnathochromis pfefferi	Tropheini	28.08.14	Chimba village	-8.421388889	30.45722222
IWG9	NA	Gnapfe	Gnathochromis pfefferi	Tropheini	28.08.14	Chimba village	-8.421388889	30.45722222
IWH1	NA	Gnapfe	Gnathochromis pfefferi	Tropheini	28.08.14	Chimba village	-8.421388889	30.45722222
IWH2	F	Psccur	Pseudosimochromis curvifrons	Tropheini	28.08.14	Chimba village	-8.421388889	30.45722222
IWH3	F	Psccur	Pseudosimochromis curvifrons	Tropheini	28.08.14	Chimba village	-8.421388889	30.45722222
IWH4	M	Pscple	Pseudosimochromis babaulti (South)	Tropheini	28.08.14	Chimba village	-8.421388889	30.45722222
IWH5	F	Pscple	Pseudosimochromis babaulti (South)	Tropheini	28.08.14	Chimba village	-8.421388889	30.45722222
IWH6	NA	Pettre	Petrochromis trewavasae	Tropheini	28.08.14	Chimba village	-8.421388889	30.45722222
IWH7	NA	Pettre	Petrochromis trewavasae	Tropheini	28.08.14	Chimba village	-8.421388889	30.45722222
IWH8	NA	Pettre	Petrochromis trewavasae	Tropheini	28.08.14	Chimba village	-8.421388889	30.45722222
IWH9	NA	Pettre	Petrochromis trewavasae	Tropheini	28.08.14	Chimba village	-8.421388889	30.45722222
IWI1	NA	Pettre	Petrochromis trewavasae	Tropheini	28.08.14	Chimba village	-8.421388889	30.45722222
IWI4	M	Lamsig	Lamprologus signatus	Lamprologini	29.08.14	Kabyolwe	-8.569166667	30.75055556
IWI5	F	Lamsig	Lamprologus signatus	Lamprologini	29.08.14	Kabyolwe	-8.569166667	30.75055556
IWI6	F	Petfas	Petrochromis fasciolatus	Tropheini	29.08.14	Kabyolwe	-8.569166667	30.75055556
IWI7	F	Trioto	Triglachromis otostigma	Limnochromini	29.08.14	Kabyolwe	-8.569166667	30.75055556
IWI8	M	Trioto	Triglachromis otostigma	Limnochromini	29.08.14	Kabyolwe	-8.569166667	30.75055556
IXA3	M	Treuni	Trematocara unimaculatum	Trematocarini	27.07.14	Chipwa Fishermen	-8.606166667	31.18611111
IXA4	M	Perecc	Perissodus eccentricus	Perissodini	27.07.14	Chipwa Fishermen	-8.606166667	31.18611111
IXA5	F	Batmin	Bathybates minor	Bathybatini	27.07.14	Chipwa Fishermen	-8.606166667	31.18611111
IXA6	F	Treuni	Trematocara unimaculatum	Trematocarini	27.07.14	Chipwa Fishermen	-8.606166667	31.18611111
IXB5	F	Gwcbel	Greenwoodochromis bellcrossi	Limnochromini	27.07.14	Chipwa Fishermen	-8.606166667	31.18611111
IXB6	M	Lchsta	Limnochromis staneri	Limnochromini	27.07.14	Chipwa Fishermen	-8.606166667	31.18611111
IXB8	M	Benmel	Benthochromis melanoides	Benthochromini	27.07.14	Chipwa Fishermen	-8.606166667	31.18611111
IXB9	M	Xencau	Xenotilapia caudafasciata	Ectodini	27.07.14	Chipwa Fishermen	-8.606166667	31.18611111
IXC1	F	Xencau	Xenotilapia caudafasciata	Ectodini	27.07.14	Chipwa Fishermen	-8.606166667	31.18611111
IXC2	M	Hemste	Hemibates stenosoma	Bathybatini	27.07.14	Chipwa Fishermen	-8.606166667	31.18611111
IXC3	F	Hemste	Hemibates stenosoma	Bathybatini	27.07.14	Chipwa Fishermen	-8.606166667	31.18611111
IXC5	M	Hemste	Hemibates stenosoma	Bathybatini	27.07.14	Chipwa Fishermen	-8.606166667	31.18611111
IXC6	M	Hemste	Hemibates stenosoma	Bathybatini	27.07.14	Chipwa Fishermen	-8.606166667	31.18611111
IXC7	M	Hemste	Hemibates stenosoma	Bathybatini	27.07.14	Chipwa Fishermen	-8.606166667	31.18611111
IXC8	M	Hemste	Hemibates stenosoma	Bathybatini	27.07.14	Chipwa Fishermen	-8.606166667	31.18611111
IXC9	M	HemstZ	Hemibates koningsi	Bathybatini	27.07.14	Chipwa Fishermen	-8.606166667	31.18611111
IXD5	NA	Gnaper	Gnathochromis permaxillaris	Limnochromini	27.07.14	Chipwa Fishermen	-8.606166667	31.18611111
IXD6	NA	Gnaper	Gnathochromis permaxillaris	Limnochromini	27.07.14	Chipwa Fishermen	-8.606166667	31.18611111
IXD7	NA	Gnaper	Gnathochromis permaxillaris	Limnochromini	27.07.14	Chipwa Fishermen	-8.606166667	31.18611111

IXD8	NA	Gnaper	Gnathochromis permaxillaris	Limnochromini	27.07.14	Chipwa Fishermen	-8.606166667	31.18611111
IXD9	NA	Gnaper	Gnathochromis permaxillaris	Limnochromini	27.07.14	Chipwa Fishermen	-8.606166667	31.18611111
IXE1	NA	Gnaper	Gnathochromis permaxillaris	Limnochromini	27.07.14	Chipwa Fishermen	-8.606166667	31.18611111
IXE2	NA	Gnaper	Gnathochromis permaxillaris	Limnochromini	27.07.14	Chipwa Fishermen	-8.606166667	31.18611111
IXE3	NA	Gnaper	Gnathochromis permaxillaris	Limnochromini	27.07.14	Chipwa Fishermen	-8.606166667	31.18611111
IXE4	NA	Gnaper	Gnathochromis permaxillaris	Limnochromini	27.07.14	Chipwa Fishermen	-8.606166667	31.18611111
IXE5	M	Tremac	Trematocara macrostoma	Trematocarini	27.07.14	Chipwa Fishermen	-8.606166667	31.18611111
IXE6	M	Tremac	Trematocara macrostoma	Trematocarini	27.07.14	Chipwa Fishermen	-8.606166667	31.18611111
IXE8	M	Tremac	Trematocara macrostoma	Trematocarini	27.07.14	Chipwa Fishermen	-8.606166667	31.18611111
IXE9	F	Treuni	Trematocara unimaculatum	Trematocarini	27.07.14	Chipwa Fishermen	-8.606166667	31.18611111
IXF1	NA	Treuni	Trematocara unimaculatum	Trematocarini	27.07.14	Chipwa Fishermen	-8.606166667	31.18611111
IXF2	M	Treuni	Trematocara unimaculatum	Trematocarini	27.07.14	Chipwa Fishermen	-8.606166667	31.18611111
IXF3	M	Treuni	Trematocara unimaculatum	Trematocarini	27.07.14	Chipwa Fishermen	-8.606166667	31.18611111
IXF4	F	XenniS	Xenotilapia nigrolabiata	Ectodini	27.07.14	Chipwa Fishermen	-8.606166667	31.18611111
IXF5	M	Treuni	Trematocara unimaculatum	Trematocarini	27.07.14	Chipwa Fishermen	-8.606166667	31.18611111
IXF6	F	Treuni	Trematocara unimaculatum	Trematocarini	27.07.14	Chipwa Fishermen	-8.606166667	31.18611111
IXF7	NA	Treuni	Trematocara unimaculatum	Trematocarini	27.07.14	Chipwa Fishermen	-8.606166667	31.18611111
IXF9	NA	Treuni	Trematocara unimaculatum	Trematocarini	27.07.14	Chipwa Fishermen	-8.606166667	31.18611111
IXG1	M	Treuni	Trematocara unimaculatum	Trematocarini	27.07.14	Chipwa Fishermen	-8.606166667	31.18611111
IXG2	NA	Batgra	Bathybates graueri	Bathybatini	27.07.14	Chipwa Fishermen	-8.606166667	31.18611111
IXG3	NA	Batgra	Bathybates graueri	Bathybatini	27.07.14	Chipwa Fishermen	-8.606166667	31.18611111
IXG4	NA	Xencau	Xenotilapia caudafasciata	Ectodini	27.07.14	Chipwa Fishermen	-8.606166667	31.18611111
IXG5	NA	Xencau	Xenotilapia caudafasciata	Ectodini	27.07.14	Chipwa Fishermen	-8.606166667	31.18611111
IXG6	NA	Benmel	Benthochromis melanoides	Benthochromini	27.07.14	Chipwa Fishermen	-8.606166667	31.18611111
IXG7	NA	Gwcchr	Greenwoodochromis christyi	Limnochromini	27.07.14	Chipwa Fishermen	-8.606166667	31.18611111
IXG8	NA	Lchsta	Limnochromis staneri	Limnochromini	27.07.14	Chipwa Fishermen	-8.606166667	31.18611111
IXG9	NA	Lchsta	Limnochromis staneri	Limnochromini	27.07.14	Chipwa Fishermen	-8.606166667	31.18611111
IXH1	NA	Lchsta	Limnochromis staneri	Limnochromini	27.07.14	Chipwa Fishermen	-8.606166667	31.18611111
IXH2	NA	Lchsta	Limnochromis staneri	Limnochromini	27.07.14	Chipwa Fishermen	-8.606166667	31.18611111
IXH3	NA	Lchsta	Limnochromis staneri	Limnochromini	27.07.14	Chipwa Fishermen	-8.606166667	31.18611111
IXH4	NA	Lchsta	Limnochromis staneri	Limnochromini	27.07.14	Chipwa Fishermen	-8.606166667	31.18611111
IXH5	NA	Gwcbel	Greenwoodochromis bellcrossi	Limnochromini	27.07.14	Chipwa Fishermen	-8.606166667	31.18611111
IXH6	NA	Gwcbel	Greenwoodochromis bellcrossi	Limnochromini	27.07.14	Chipwa Fishermen	-8.606166667	31.18611111
IXH7	NA	Gwcbel	Greenwoodochromis bellcrossi	Limnochromini	27.07.14	Chipwa Fishermen	-8.606166667	31.18611111
IXH8	NA	Gwcbel	Greenwoodochromis bellcrossi	Limnochromini	27.07.14	Chipwa Fishermen	-8.606166667	31.18611111
IXI1	M	Gwcbel	Greenwoodochromis bellcrossi	Limnochromini	28.07.14	Chipwa Fishermen	-8.606166667	31.18611111
IXI2	F	Gwcbel	Greenwoodochromis bellcrossi	Limnochromini	28.07.14	Chipwa Fishermen	-8.606166667	31.18611111
IXI3	NA	Benmel	Benthochromis melanoides	Benthochromini	28.07.14	Chipwa Fishermen	-8.606166667	31.18611111
IXI4	NA	Benmel	Benthochromis melanoides	Benthochromini	28.07.14	Chipwa Fishermen	-8.606166667	31.18611111
IXI5	NA	Benmel	Benthochromis melanoides	Benthochromini	28.07.14	Chipwa Fishermen	-8.606166667	31.18611111
IXI6	NA	Benmel	Benthochromis melanoides	Benthochromini	28.07.14	Chipwa Fishermen	-8.606166667	31.18611111
IXI7	NA	Benmel	Benthochromis melanoides	Benthochromini	28.07.14	Chipwa Fishermen	-8.606166667	31.18611111
IXI8	NA	Benmel	Benthochromis melanoides	Benthochromini	28.07.14	Chipwa Fishermen	-8.606166667	31.18611111
IYA4	F	Neosav	Neolamprologus savoryi	Lamprologini	29.07.14	Toby's Place	-8.623222222	31.20044444
IYA5	M	Peteph	Petrochromis ephippium	Tropheini	29.07.14	Toby's Place	-8.623222222	31.20044444
IYA6	F	Petfam	Petrochromis famula	Tropheini	29.07.14	Toby's Place	-8.623222222	31.20044444
IYA7	M	Petfam	Petrochromis famula	Tropheini	29.07.14	Toby's Place	-8.623222222	31.20044444
IYA8	F	Cteben	Ctenochromis benthicola	Cyphotilapiini	29.07.14	Chipwa Fishermen	-8.606166667	31.18611111
IYA9	NA	Neochr	Neolamprologus christyi	Lamprologini	29.07.14	Toby's Place	-8.623222222	31.20044444
IYB1	NA	Neochr	Neolamprologus christyi	Lamprologini	29.07.14	Toby's Place	-8.623222222	31.20044444
IYB2	NA	Neosav	Neolamprologus savoryi	Lamprologini	29.07.14	Toby's Place	-8.623222222	31.20044444
IYB3	M	Neosav	Neolamprologus savoryi	Lamprologini	29.07.14	Toby's Place	-8.623222222	31.20044444
IYB4	F	Regcal	Reganochromis calliurus	Limnochromini	29.07.14	Chipwa Fishermen	-8.606166667	31.18611111
IYB5	NA	Varmoo	Variabilichromis moorii	Lamprologini	29.07.14	Toby's Place	-8.623222222	31.20044444
IYB6	NA	Varmoo	Variabilichromis moorii	Lamprologini	29.07.14	Toby's Place	-8.623222222	31.20044444
IYB7	M	Neochr	Neolamprologus christyi	Lamprologini	29.07.14	Toby's Place	-8.623222222	31.20044444
IYB8	NA	Neochr	Neolamprologus christyi	Lamprologini	29.07.14	Toby's Place	-8.623222222	31.20044444
IYB9	NA	Loblab	Lobochilotes labiatus	Tropheini	29.07.14	Toby's Place	-8.623222222	31.20044444
IYC1	NA	Simdia	Simochromis diagramma	Tropheini	29.07.14	Toby's Place	-8.623222222	31.20044444
IYC2	NA	Varmoo	Variabilichromis moorii	Lamprologini	29.07.14	Toby's Place	-8.623222222	31.20044444
IYC3	NA	Varmoo	Variabilichromis moorii	Lamprologini	29.07.14	Toby's Place	-8.623222222	31.20044444
IYC4	NA	Varmoo	Variabilichromis moorii	Lamprologini	29.07.14	Toby's Place	-8.623222222	31.20044444
IYC5	NA	Chabri	Chalinochromis brichardi	Lamprologini	29.07.14	Toby's Place	-8.623222222	31.20044444
IYC6	NA	Chabri	Chalinochromis brichardi	Lamprologini	29.07.14	Toby's Place	-8.623222222	31.20044444
IYC7	NA	Varmoo	Variabilichromis moorii	Lamprologini	29.07.14	Toby's Place	-8.623222222	31.20044444
IYC8	NA	Varmoo	Variabilichromis moorii	Lamprologini	29.07.14	Toby's Place	-8.623222222	31.20044444
IYC9	NA	Altcom	Altolamprologus compressiceps	Lamprologini	29.07.14	Toby's Place	-8.623222222	31.20044444
IYD1	M	Petpol	Petrochromis polyodon	Tropheini	29.07.14	Toby's Place	-8.623222222	31.20044444
IYD2	F	Petpol	Petrochromis polyodon	Tropheini	29.07.14	Toby's Place	-8.623222222	31.20044444
IYD3	F	Cyafur	Cyathopharynx furcifer	Ectodini	29.07.14	Toby's Place	-8.623222222	31.20044444
IYD4	M	Petpol	Petrochromis polyodon	Tropheini	29.07.14	Toby's Place	-8.623222222	31.20044444
IYD5	F	Petpol	Petrochromis polyodon	Tropheini	29.07.14	Toby's Place	-8.623222222	31.20044444
IYD7	NA	Chabri	Chalinochromis brichardi	Lamprologini	29.07.14	Toby's Place	-8.623222222	31.20044444
IYD8	NA	Altcom	Altolamprologus compressiceps	Lamprologini	29.07.14	Toby's Place	-8.623222222	31.20044444
IYE2	NA	Loblab	Lobochilotes labiatus	Tropheini	29.07.14	Toby's Place	-8.623222222	31.20044444
IYE3	M	Psccur	Pseudosimochromis curvifrons	Tropheini	29.07.14	Toby's Place	-8.623222222	31.20044444
IYE5	NA	Intloo	Interochromis loocki	Tropheini	29.07.14	Toby's Place	-8.623222222	31.20044444
IYE7	NA	Altcom	Altolamprologus compressiceps	Lamprologini	29.07.14	Toby's Place	-8.623222222	31.20044444
IYE8	NA	Altcom	Altolamprologus compressiceps	Lamprologini	29.07.14	Toby's Place	-8.623222222	31.20044444
IYE9	NA	Petpol	Petrochromis polyodon	Tropheini	29.07.14	Toby's Place	-8.623222222	31.20044444
IYF1	M	Neochr	Neolamprologus christyi	Lamprologini	29.07.14	Toby's Place	-8.623222222	31.20044444
IYF2	M	Neosav	Neolamprologus savoryi	Lamprologini	29.07.14	Toby's Place	-8.623222222	31.20044444
IYF4	NA	Petfam	Petrochromis famula	Tropheini	29.07.14	Toby's Place	-8.623222222	31.20044444
IYF5	NA	Neosav	Neolamprologus savoryi	Lamprologini	29.07.14	Toby's Place	-8.623222222	31.20044444
IYF6	NA	Neochr	Neolamprologus christyi	Lamprologini	29.07.14	Toby's Place	-8.623222222	31.20044444
IYF7	NA	Intloo	Interochromis loocki	Tropheini	29.07.14	Toby's Place	-8.623222222	31.20044444
IYF8	NA	Intloo	Interochromis loocki	Tropheini	29.07.14	Toby's Place	-8.623222222	31.20044444
IYF9	M	Loblab	Lobochilotes labiatus	Tropheini	29.07.14	Toby's Place	-8.623222222	31.20044444
IYG1	NA	Simdia	Simochromis diagramma	Tropheini	29.07.14	Toby's Place	-8.623222222	31.20044444
IYG2	F	Loblab	Lobochilotes labiatus	Tropheini	29.07.14	Toby's Place	-8.623222222	31.20044444
IYG3	F	Loblab	Lobochilotes labiatus	Tropheini	29.07.14	Toby's Place	-8.623222222	31.20044444
IYG4	M	Psccur	Pseudosimochromis curvifrons	Tropheini	29.07.14	Toby's Place	-8.623222222	31.20044444
IYG5	F	Petpol	Petrochromis polyodon	Tropheini	29.07.14	Toby's Place	-8.623222222	31.20044444
IYG6	M	Petfam	Petrochromis famula	Tropheini	29.07.14	Toby's Place	-8.623222222	31.20044444
IYG7	NA	Neofas	Neolamprologus fasciatus	Lamprologini	29.07.14	Toby's Place	-8.623222222	31.20044444
IYG8	NA	Intloo	Interochromis loocki	Tropheini	29.07.14	Toby's Place	-8.623222222	31.20044444
IYG9	NA	Intloo	Interochromis loocki	Tropheini	29.07.14	Toby's Place	-8.623222222	31.20044444
IYH5	NA	Auldew	Aulonocranus dewindti	Ectodini	29.07.14	Toby's Place	-8.623222222	31.20044444
IYH6	NA	TelteS	Telmatochromis temporalis	Lamprologini	29.07.14	Toby's Place	-8.623222222	31.20044444
IYH7	NA	Neochr	Neolamprologus christyi	Lamprologini	29.07.14	Toby's Place	-8.623222222	31.20044444
IYH8	NA	Varmoo	Variabilichromis moorii	Lamprologini	29.07.14	Toby's Place	-8.623222222	31.20044444
IYH9	NA	Neosav	Neolamprologus savoryi	Lamprologini	29.07.14	Toby's Place	-8.623222222	31.20044444
IYI1	NA	Auldew	Aulonocranus dewindti	Ectodini	29.07.14	Toby's Place	-8.623222222	31.20044444
IYI2	NA	Auldew	Aulonocranus dewindti	Ectodini	29.07.14	Toby's Place	-8.623222222	31.20044444
IYI3	NA	Xenspi	Xenotilapia spilopterus	Ectodini	29.07.14	Toby's Place	-8.623222222	31.20044444
IYI4	NA	Xenspi	Xenotilapia spilopterus	Ectodini	29.07.14	Toby's Place	-8.623222222	31.20044444
IYI5	NA	Xenspi	Xenotilapia spilopterus	Ectodini	29.07.14	Toby's Place	-8.623222222	31.20044444
IYI6	NA	Auldew	Aulonocranus dewindti	Ectodini	29.07.14	Toby's Place	-8.623222222	31.20044444
IYI7	NA	Xenspi	Xenotilapia spilopterus	Ectodini	29.07.14	Toby's Place	-8.623222222	31.20044444
IYI8	NA	Neochr	Neolamprologus christyi	Lamprologini	29.07.14	Toby's Place	-8.623222222	31.20044444
IZA1	M	Astbur	Astatotilapia burtoni	Haplochromini	28.07.14	Kalambo Lake / Chipwa	-8.601741667	31.18701111
IZA2	F	Benmel	Benthochromis melanoides	Benthochromini	28.07.14	Chipwa Fishermen	-8.606166667	31.18611111
IZA4	F	Benmel	Benthochromis melanoides	Benthochromini	28.07.14	Chipwa Fishermen	-8.606166667	31.18611111
IZA5	NA	HemstZ	Hemibates koningsi	Bathybatini	28.07.14	Chipwa Fishermen	-8.606166667	31.18611111
IZA6	F	Lchaur	Limnochromis auritus	Limnochromini	28.07.14	Chipwa Fishermen	-8.606166667	31.18611111
IZA8	F	Plemul	Plecodus multidentatus	Perissodini	28.07.14	Chipwa Fishermen	-8.606166667	31.18611111
IZA9	M	Plemul	Plecodus multidentatus	Perissodini	28.07.14	Chipwa Fishermen	-8.606166667	31.18611111
IZB2	M	Perecc	Perissodus eccentricus	Perissodini	28.07.14	Chipwa Fishermen	-8.606166667	31.18611111
IZB4	NA	Perecc	Perissodus eccentricus	Perissodini	28.07.14	Chipwa Fishermen	-8.606166667	31.18611111
IZB5	NA	Regcal	Reganochromis calliurus	Limnochromini	28.07.14	Chipwa Fishermen	-8.606166667	31.18611111
IZB6	NA	Boumic	Boulengerochromis microlepis	Boulengerochromini	28.07.14	Chipwa Fishermen	-8.606166667	31.18611111
IZB8	M	Xchhec	Xenochromis hecqui	Perissodini	28.07.14	Chipwa Fishermen	-8.606166667	31.18611111
IZB9	M	Xchhec	Xenochromis hecqui	Perissodini	28.07.14	Chipwa Fishermen	-8.606166667	31.18611111
IZC1	M	Xchhec	Xenochromis hecqui	Perissodini	28.07.14	Chipwa Fishermen	-8.606166667	31.18611111

IZC2	M	Xchhec	Xenochromis hecqui	Perissodini	28.07.14	Chipwa Fishermen	-8.606166667	31.18611111
IZC3	NA	Xencau	Xenotilapia caudafasciata	Ectodini	28.07.14	Chipwa Fishermen	-8.606166667	31.18611111
IZC5	F	Astbur	Astatotilapia burtoni	Haplochromini	28.07.14	Kalambo Lake / Chipwa	-8.601741667	31.18701111
IZC7	M	XenniS	Xenotilapia nigrolabiata	Ectodini	28.07.14	Chipwa Fishermen	-8.606166667	31.18611111
IZC9	NA	Gwcbel	Greenwoodochromis bellcrossi	Limnochromini	28.07.14	Chipwa Fishermen	-8.606166667	31.18611111
IZD1	NA	Gwcbel	Greenwoodochromis bellcrossi	Limnochromini	28.07.14	Chipwa Fishermen	-8.606166667	31.18611111
IZD2	NA	Gwcbel	Greenwoodochromis bellcrossi	Limnochromini	28.07.14	Chipwa Fishermen	-8.606166667	31.18611111
IZD3	NA	Gwcbel	Greenwoodochromis bellcrossi	Limnochromini	28.07.14	Chipwa Fishermen	-8.606166667	31.18611111
IZD4	M	Batfas	Bathybates fasciatus	Bathybatini	28.07.14	Chipwa Fishermen	-8.606166667	31.18611111
IZE1	M	Tresti	Trematocara stigmaticum	Trematocarini	28.07.14	Chipwa Fishermen	-8.606166667	31.18611111
IZE4	M	Gwcchr	Greenwoodochromis christyi	Limnochromini	28.07.14	Chipwa Fishermen	-8.606166667	31.18611111
IZF1	F	Gwcchr	Greenwoodochromis christyi	Limnochromini	28.07.14	Chipwa Fishermen	-8.606166667	31.18611111
IZF2	NA	Gwcchr	Greenwoodochromis christyi	Limnochromini	28.07.14	Chipwa Fishermen	-8.606166667	31.18611111
IZF3	NA	Gwcchr	Greenwoodochromis christyi	Limnochromini	28.07.14	Chipwa Fishermen	-8.606166667	31.18611111
IZF4	NA	Gwcchr	Greenwoodochromis christyi	Limnochromini	28.07.14	Chipwa Fishermen	-8.606166667	31.18611111
IZF9	M	Tresti	Trematocara stigmaticum	Trematocarini	28.07.14	Chipwa Fishermen	-8.606166667	31.18611111
IZG1	M	Tresti	Trematocara stigmaticum	Trematocarini	28.07.14	Chipwa Fishermen	-8.606166667	31.18611111
IZG2	M	Tresti	Trematocara stigmaticum	Trematocarini	28.07.14	Chipwa Fishermen	-8.606166667	31.18611111
IZG3	M	Tresti	Trematocara stigmaticum	Trematocarini	28.07.14	Chipwa Fishermen	-8.606166667	31.18611111
IZG4	M	Tresti	Trematocara stigmaticum	Trematocarini	28.07.14	Chipwa Fishermen	-8.606166667	31.18611111
IZG5	M	Tresti	Trematocara stigmaticum	Trematocarini	28.07.14	Chipwa Fishermen	-8.606166667	31.18611111
IZG6	NA	TeldhS	Telmatochromis dhonti	Lamprologini	28.07.14	Kalambo Lake / Chipwa	-8.601741667	31.18701111
IZG7	NA	TeldhS	Telmatochromis dhonti	Lamprologini	28.07.14	Kalambo Lake / Chipwa	-8.601741667	31.18701111
IZG8	NA	TeldhS	Telmatochromis dhonti	Lamprologini	28.07.14	Kalambo Lake / Chipwa	-8.601741667	31.18701111
IZG9	NA	TeldhS	Telmatochromis dhonti	Lamprologini	28.07.14	Kalambo Lake / Chipwa	-8.601741667	31.18701111
IZH1	NA	TeldhS	Telmatochromis dhonti	Lamprologini	28.07.14	Kalambo Lake / Chipwa	-8.601741667	31.18701111
IZH2	NA	TeldhS	Telmatochromis dhonti	Lamprologini	28.07.14	Kalambo Lake / Chipwa	-8.601741667	31.18701111
IZH3	NA	TeldhS	Telmatochromis dhonti	Lamprologini	28.07.14	Chipwa Fishermen	-8.606166667	31.18611111
IZH4	NA	TeldhS	Telmatochromis dhonti	Lamprologini	28.07.14	Chipwa Fishermen	-8.606166667	31.18611111
IZH5	NA	TeldhS	Telmatochromis dhonti	Lamprologini	28.07.14	Kalambo Lake / Chipwa	-8.601741667	31.18701111
IZH6	NA	TeldhS	Telmatochromis dhonti	Lamprologini	28.07.14	Kalambo Lake / Chipwa	-8.601741667	31.18701111
IZH7	M	Erecya	Eretmodus cyanostictus	Eretmodini	29.07.14	Toby's Place	-8.623222222	31.20044444
IZI3	F	Erecya	Eretmodus cyanostictus	Eretmodini	29.07.14	Toby's Place	-8.623222222	31.20044444
IZI7	M	Lamlem	Lamprologus lemairii	Lamprologini	29.07.14	Toby's Place	-8.623222222	31.20044444
IZI8	M	Neochr	Neolamprologus christyi	Lamprologini	29.07.14	Toby's Place	-8.623222222	31.20044444
JAA1	F	Xencau	Xenotilapia caudafasciata	Ectodini	29.07.14	Chipwa Fishermen	-8.606166667	31.18611111
JAA2	NA	Xencau	Xenotilapia caudafasciata	Ectodini	29.07.14	Chipwa Fishermen	-8.606166667	31.18611111
JAA3	NA	Xencau	Xenotilapia caudafasciata	Ectodini	29.07.14	Chipwa Fishermen	-8.606166667	31.18611111
JAA4	NA	Xencau	Xenotilapia caudafasciata	Ectodini	29.07.14	Chipwa Fishermen	-8.606166667	31.18611111
JAB1	F	Lamcal	Lamprologus callipterus	Lamprologini	30.07.14	Toby's Place	-8.623222222	31.20044444
JAB6	M	Oretan	Oreochromis tanganicae	Oreochromini	30.07.14	Chipwa Fishermen	-8.606166667	31.18611111
JAB7	M	Baicen	Baileychromis centropomoides	Limnochromini	30.07.14	Chipwa Fishermen	-8.606166667	31.18611111
JAB8	F	Baicen	Baileychromis centropomoides	Limnochromini	30.07.14	Chipwa Fishermen	-8.606166667	31.18611111
JAB9	M	Lamcal	Lamprologus callipterus	Lamprologini	30.07.14	Toby's Place	-8.623222222	31.20044444
JAC2	M	Tremac	Trematocara macrostoma	Trematocarini	30.07.14	Chipwa Fishermen	-8.606166667	31.18611111
JAC4	NA	Plemul	Plecodus multidentatus	Perissodini	30.07.14	Chipwa Fishermen	-8.606166667	31.18611111
JAC5	NA	Gnaper	Gnathochromis permaxillaris	Limnochromini	30.07.14	Chipwa Fishermen	-8.606166667	31.18611111
JAC7	F	Oretan	Oreochromis tanganicae	Oreochromini	30.07.14	Chipwa Fishermen	-8.606166667	31.18611111
JAC8	NA	Xchhec	Xenochromis hecqui	Perissodini	30.07.14	Chipwa Fishermen	-8.606166667	31.18611111
JAC9	NA	Hapmic	Haplotaxodon microlepis	Perissodini	30.07.14	Toby's Place	-8.623222222	31.20044444
JAD1	NA	Xencau	Xenotilapia caudafasciata	Ectodini	30.07.14	Toby's Place	-8.623222222	31.20044444
JAD2	NA	Lchaur	Limnochromis auritus	Limnochromini	30.07.14	Chipwa Fishermen	-8.606166667	31.18611111
JAD3	NA	Lchabe	Limnochromis abeelei	Limnochromini	30.07.14	Chipwa Fishermen	-8.606166667	31.18611111
JAD4	F	Simdia	Simochromis diagramma	Tropheini	30.07.14	Toby's Place	-8.623222222	31.20044444
JAD5	NA	TelteS	Telmatochromis temporalis	Lamprologini	30.07.14	Toby's Place	-8.623222222	31.20044444
JAD6	NA	Xenspi	Xenotilapia spilopterus	Ectodini	30.07.14	Toby's Place	-8.623222222	31.20044444
JAD7	F	Permic	Perissodus microlepis	Perissodini	30.07.14	Toby's Place	-8.623222222	31.20044444
JAD8	NA	Permic	Perissodus microlepis	Perissodini	30.07.14	Toby's Place	-8.623222222	31.20044444
JAD9	M	Ctehor	Ctenochromis horei	Tropheini	30.07.14	Toby's Place	-8.623222222	31.20044444
JAE1	F	Petfas	Petrochromis fasciolatus	Tropheini	30.07.14	Toby's Place	-8.623222222	31.20044444
JAE2	F	Simdia	Simochromis diagramma	Tropheini	30.07.14	Toby's Place	-8.623222222	31.20044444
JAE3	NA	Neofas	Neolamprologus fasciatus	Lamprologini	30.07.14	Toby's Place	-8.623222222	31.20044444
JAE7	F	Boumic	Boulengerochromis microlepis	Boulengerochromini	31.07.14	Chipwa Fishermen	-8.606166667	31.18611111
JAE9	F	Baicen	Baileychromis centropomoides	Limnochromini	31.07.14	Chipwa Fishermen	-8.606166667	31.18611111
JAF5	M	Lchaur	Limnochromis auritus	Limnochromini	31.07.14	Chipwa Fishermen	-8.606166667	31.18611111
JAF7	M	Xenfla	Xenotilapia flavipinnis	Ectodini	31.07.14	Toby's Place	-8.623222222	31.20044444
JAF9	F	Xenfla	Xenotilapia flavipinnis	Ectodini	31.07.14	Toby's Place	-8.623222222	31.20044444
JAG2	M	Tylpol	Tylochromis polylepis	Tylochromini	31.07.14	Chipwa Fishermen	-8.606166667	31.18611111
JAG3	M	Baicen	Baileychromis centropomoides	Limnochromini	31.07.14	Chipwa Fishermen	-8.606166667	31.18611111
JAG4	M	Regcal	Reganochromis calliurus	Limnochromini	31.07.14	Chipwa Fishermen	-8.606166667	31.18611111
JAG6	M	Xenbou	Xenotilapia boulengeri	Ectodini	31.07.14	Toby's Place	-8.623222222	31.20044444
JAG7	M	Xenbou	Xenotilapia boulengeri	Ectodini	31.07.14	Toby's Place	-8.623222222	31.20044444
JAG8	F	Xenbou	Xenotilapia boulengeri	Ectodini	31.07.14	Toby's Place	-8.623222222	31.20044444
JAG9	M	Xenbou	Xenotilapia boulengeri	Ectodini	31.07.14	Toby's Place	-8.623222222	31.20044444
JAH2	F	Xenbou	Xenotilapia boulengeri	Ectodini	31.07.14	Toby's Place	-8.623222222	31.20044444
JAH3	F	Xenbou	Xenotilapia boulengeri	Ectodini	31.07.14	Toby's Place	-8.623222222	31.20044444
JAH5	F	Tylpol	Tylochromis polylepis	Tylochromini	31.07.14	Chipwa Fishermen	-8.606166667	31.18611111
JAH6	M	Regcal	Reganochromis calliurus	Limnochromini	31.07.14	Chipwa Fishermen	-8.606166667	31.18611111
JAH7	F	Xchhec	Xenochromis hecqui	Perissodini	31.07.14	Chipwa Fishermen	-8.606166667	31.18611111
JAH9	NA	Neopul	Neolamprologus pulcher	Lamprologini	31.07.14	Toby's Place	-8.623222222	31.20044444
JAI1	NA	Neopul	Neolamprologus pulcher	Lamprologini	31.07.14	Toby's Place	-8.623222222	31.20044444
JAI2	NA	Neopul	Neolamprologus pulcher	Lamprologini	31.07.14	Toby's Place	-8.623222222	31.20044444
JAI3	NA	Neopul	Neolamprologus pulcher	Lamprologini	31.07.14	Toby's Place	-8.623222222	31.20044444
JAI5	M	Lchabe	Limnochromis abeelei	Limnochromini	31.07.14	Chipwa Fishermen	-8.606166667	31.18611111
JAI6	M	Lchabe	Limnochromis abeelei	Limnochromini	31.07.14	Chipwa Fishermen	-8.606166667	31.18611111
JAI7	F	Lchabe	Limnochromis abeelei	Limnochromini	31.07.14	Chipwa Fishermen	-8.606166667	31.18611111
JAI8	F	Batvit	Bathybates vittatus	Bathybatini	31.07.14	Chipwa Fishermen	-8.606166667	31.18611111
JAI9	F	Lamlem	Lamprologus lemairii	Lamprologini	31.07.14	Toby's Place	-8.623222222	31.20044444
JBA1	M	Neobif	Neolamprologus bifasciatus	Lamprologini	30.08.14	Cape Chaitika Fishermen	-8.568888889	30.79705556
JBA2	M	Cphgib	Cyphotilapia gibberosa	Cyphotilapiini	30.08.14	Cape Chaitika Fishermen	-8.568888889	30.79705556
JBA3	M	Cphgib	Cyphotilapia gibberosa	Cyphotilapiini	30.08.14	Cape Chaitika Fishermen	-8.568888889	30.79705556
JBA4	F	Cphgib	Cyphotilapia gibberosa	Cyphotilapiini	30.08.14	Cape Chaitika Fishermen	-8.568888889	30.79705556
JBA5	NA	Cphgib	Cyphotilapia gibberosa	Cyphotilapiini	30.08.14	Cape Chaitika Fishermen	-8.568888889	30.79705556
JBA7	M	Telbra	Telmatochromis brachygnathus	Lamprologini	30.08.14	Kabyolwe	-8.569166667	30.75055556
JBA8	M	Telbra	Telmatochromis brachygnathus	Lamprologini	30.08.14	Kabyolwe	-8.569166667	30.75055556
JBA9	M	Plestr	Plecodus straeleni	Perissodini	30.08.14	Kabyolwe	-8.569166667	30.75055556
JBB1	F	Trioto	Triglachromis otostigma	Limnochromini	30.08.14	Kabyolwe	-8.569166667	30.75055556
JBB2	M	Trioto	Triglachromis otostigma	Limnochromini	30.08.14	Kabyolwe	-8.569166667	30.75055556
JBB3	M	Trioto	Triglachromis otostigma	Limnochromini	30.08.14	Kabyolwe	-8.569166667	30.75055556
JBB6	M	Lepken	Lepidiolamprologus kendalli	Lamprologini	30.08.14	Misepa	-8.588888889	30.80305556
JBB7	M	Lepken	Lepidiolamprologus kendalli	Lamprologini	30.08.14	Misepa	-8.588888889	30.80305556
JBB8	F	Lepken	Lepidiolamprologus kendalli	Lamprologini	30.08.14	Misepa	-8.588888889	30.80305556
JBB9	NA	Petfas	Petrochromis fasciolatus	Tropheini	30.08.14	Misepa	-8.588888889	30.80305556
JBC1	F	Psccur	Pseudosimochromis curvifrons	Tropheini	30.08.14	Misepa	-8.588888889	30.80305556
JBC2	M	Psccur	Pseudosimochromis curvifrons	Tropheini	30.08.14	Misepa	-8.588888889	30.80305556
JBC3	F	Psccur	Pseudosimochromis curvifrons	Tropheini	30.08.14	Misepa	-8.588888889	30.80305556
JBC4	F	Gralem	Grammatotria lemairii	Ectodini	31.08.14	Chitweshiba	-8.595833333	30.8075
JBC5	M	Gralem	Grammatotria lemairii	Ectodini	31.08.14	Chitweshiba	-8.595833333	30.8075
JBC6	M	Gralem	Grammatotria lemairii	Ectodini	31.08.14	Chitweshiba	-8.595833333	30.8075
JBC7	M	Telbra	Telmatochromis brachygnathus	Lamprologini	31.08.14	Chitweshiba	-8.595833333	30.8075
JBC8	M	Telbra	Telmatochromis brachygnathus	Lamprologini	31.08.14	Chitweshiba	-8.595833333	30.8075
JBC9	M	Telbra	Telmatochromis brachygnathus	Lamprologini	31.08.14	Chitweshiba	-8.595833333	30.8075
JBD2	NA	Pscple	Pseudosimochromis babaulti (South)	Tropheini	31.08.14	Chitweshiba	-8.595833333	30.8075
JBD3	NA	Pscple	Pseudosimochromis babaulti (South)	Tropheini	31.08.14	Chitweshiba	-8.595833333	30.8075
JBD4	M	Petfas	Petrochromis fasciolatus	Tropheini	31.08.14	Chitweshiba	-8.595833333	30.8075
JBD5	M	Telvit	Telmatochromis vittatus	Lamprologini	31.08.14	Chitweshiba	-8.595833333	30.8075
JBD6	F	Telvit	Telmatochromis vittatus	Lamprologini	31.08.14	Chitweshiba	-8.595833333	30.8075
JBD7	NA	Telvit	Telmatochromis vittatus	Lamprologini	31.08.14	Chitweshiba	-8.595833333	30.8075
JBD8	NA	Telvit	Telmatochromis vittatus	Lamprologini	31.08.14	Chitweshiba	-8.595833333	30.8075
JBD9	NA	Telvit	Telmatochromis vittatus	Lamprologini	31.08.14	Chitweshiba	-8.595833333	30.8075
JBE1	NA	Telvit	Telmatochromis vittatus	Lamprologini	31.08.14	Chitweshiba	-8.595833333	30.8075
JBE2	NA	Telvit	Telmatochromis vittatus	Lamprologini	31.08.14	Chitweshiba	-8.595833333	30.8075
JBE3	NA	Telvit	Telmatochromis vittatus	Lamprologini	31.08.14	Chitweshiba	-8.595833333	30.8075
JBE5	M	Leppro	Lepidiolamprologus profundicola	Lamprologini	31.08.14	Chitweshiba	-8.595833333	30.8075

JBE6	M	Mdcrot	Microdontochromis rotundiventralis	Ectodini	31.08.14	Nakaku	-8.643444444	30.87280556
JBE7	F	Mdcrot	Microdontochromis rotundiventralis	Ectodini	31.08.14	Nakaku	-8.643444444	30.87280556
JBE8	M	Telbra	Telmatochromis brachygnathus	Lamprologini	31.08.14	Nakaku	-8.643444444	30.87280556
JBE9	F	Telbra	Telmatochromis brachygnathus	Lamprologini	31.08.14	Nakaku	-8.643444444	30.87280556
JBF2	NA	Mdcrot	Microdontochromis rotundiventralis	Ectodini	31.08.14	Nakaku	-8.643444444	30.87280556
JBF3	NA	Mdcrot	Microdontochromis rotundiventralis	Ectodini	31.08.14	Nakaku	-8.643444444	30.87280556
JBF4	NA	Mdcrot	Microdontochromis rotundiventralis	Ectodini	31.08.14	Nakaku	-8.643444444	30.87280556
JBF5	NA	Mdcrot	Microdontochromis rotundiventralis	Ectodini	31.08.14	Nakaku	-8.643444444	30.87280556
JBF6	NA	Limdar	Limnotilapia dardennii	Tropheini	31.08.14	Nakaku	-8.643444444	30.87280556
JBF8	F	Pethor	Petrochromis horii	Tropheini	01.09.14	Kanfonki	-8.702777778	30.9225
JBF9	F	Pethor	Petrochromis horii	Tropheini	01.09.14	Kanfonki	-8.702777778	30.9225
JBG1	NA	Cphgib	Cyphotilapia gibberosa	Cyphotilapiini	01.09.14	Kanfonki	-8.702777778	30.9225
JBG3	M	Batmin	Bathybates minor	Bathybatini	01.09.14	Chezi Fishermen	-8.778888889	31.00694444
JBG4	M	Lchabe	Limnochromis abeelei	Limnochromini	01.09.14	Chezi Fishermen	-8.778888889	31.00694444
JBG5	M	Lchabe	Limnochromis abeelei	Limnochromini	01.09.14	Chezi Fishermen	-8.778888889	31.00694444
JBG6	M	Lamlap	Lamprologus laparogramma	Lamprologini	01.09.14	Kombe	-8.793888889	31.01583333
JBG7	M	Lamlap	Lamprologus laparogramma	Lamprologini	01.09.14	Kombe	-8.793888889	31.01583333
JBG8	M	Lamlap	Lamprologus laparogramma	Lamprologini	01.09.14	Kombe	-8.793888889	31.01583333
JBH1	M	Lamlap	Lamprologus laparogramma	Lamprologini	01.09.14	Kombe	-8.793888889	31.01583333
JBH2	M	Lamlap	Lamprologus laparogramma	Lamprologini	01.09.14	Kombe	-8.793888889	31.01583333
JBH3	F	Lamlap	Lamprologus laparogramma	Lamprologini	01.09.14	Kombe	-8.793888889	31.01583333
JBH4	M	Tromoo	Tropheus moorii	Tropheini	02.09.14	Mbita Island W	-8.753333333	31.08630556
JBH5	F	Tromoo	Tropheus moorii	Tropheini	02.09.14	Mbita Island W	-8.753333333	31.08630556
JBH6	M	Tromoo	Tropheus moorii	Tropheini	02.09.14	Mbita Island W	-8.753333333	31.08630556
JBH7	M	Tromoo	Tropheus moorii	Tropheini	02.09.14	Mbita Island W	-8.753333333	31.08630556
JBH9	NA	Tromoo	Tropheus moorii	Tropheini	02.09.14	Mbita Island W	-8.753333333	31.08630556
JBI1	NA	Tromoo	Tropheus moorii	Tropheini	02.09.14	Mbita Island W	-8.753333333	31.08630556
JBI2	NA	Julorn	Julidochromis ornatus	Lamprologini	02.09.14	Mbita Island W	-8.753333333	31.08630556
JBI3	NA	Julorn	Julidochromis ornatus	Lamprologini	02.09.14	Mbita Island W	-8.753333333	31.08630556
JBI4	NA	Julorn	Julidochromis ornatus	Lamprologini	02.09.14	Mbita Island W	-8.753333333	31.08630556
JBI5	NA	Julorn	Julidochromis ornatus	Lamprologini	02.09.14	Mbita Island W	-8.753333333	31.08630556
JBI6	NA	Julorn	Julidochromis ornatus	Lamprologini	02.09.14	Mbita Island W	-8.753333333	31.08630556
JBI7	NA	Boumic	Boulengerochromis microlepis	Boulengerochromini	02.09.14	Mbita Island W	-8.753333333	31.08630556
JBI8	NA	Boumic	Boulengerochromis microlepis	Boulengerochromini	02.09.14	Mbita Island W	-8.753333333	31.08630556
JCA1	NA	Lchaur	Limnochromis auritus	Limnochromini	31.07.14	Chipwa Fishermen	-8.606166667	31.18611111
JCA2	M	Psccur	Pseudosimochromis curvifrons	Tropheini	31.07.14	Toby's Place	-8.623222222	31.20044444
JCA5	NA	Xenfla	Xenotilapia flavipinnis	Ectodini	31.07.14	Toby's Place	-8.623222222	31.20044444
JCA6	NA	Xenfla	Xenotilapia flavipinnis	Ectodini	31.07.14	Toby's Place	-8.623222222	31.20044444
JCA7	NA	Xenfla	Xenotilapia flavipinnis	Ectodini	31.07.14	Toby's Place	-8.623222222	31.20044444
JCA8	NA	Xenfla	Xenotilapia flavipinnis	Ectodini	31.07.14	Toby's Place	-8.623222222	31.20044444
JCA9	NA	Xenfla	Xenotilapia flavipinnis	Ectodini	31.07.14	Toby's Place	-8.623222222	31.20044444
JCB1	NA	Xenfla	Xenotilapia flavipinnis	Ectodini	31.07.14	Toby's Place	-8.623222222	31.20044444
JCB2	NA	Xenfla	Xenotilapia flavipinnis	Ectodini	31.07.14	Toby's Place	-8.623222222	31.20044444
JCB3	NA	Xenfla	Xenotilapia flavipinnis	Ectodini	31.07.14	Toby's Place	-8.623222222	31.20044444
JCB5	F	Batvit	Bathybates vittatus	Bathybatini	31.07.14	Chipwa Fishermen	-8.606166667	31.18611111
JCB6	NA	Gwcchr	Greenwoodochromis christyi	Limnochromini	31.07.14	Chipwa Fishermen	-8.606166667	31.18611111
JCB7	NA	Lamlem	Lamprologus lemairii	Lamprologini	31.07.14	Toby's Place	-8.623222222	31.20044444
JCB8	M	Enamel	Enantiopus melanogenys	Ectodini	31.07.14	Toby's Place	-8.623222222	31.20044444
JCB9	M	Enamel	Enantiopus melanogenys	Ectodini	31.07.14	Toby's Place	-8.623222222	31.20044444
JCC1	M	Enamel	Enantiopus melanogenys	Ectodini	31.07.14	Toby's Place	-8.623222222	31.20044444
JCC2	M	Enamel	Enantiopus melanogenys	Ectodini	31.07.14	Toby's Place	-8.623222222	31.20044444
JCC3	M	Enamel	Enantiopus melanogenys	Ectodini	31.07.14	Toby's Place	-8.623222222	31.20044444
JCC6	M	Baicen	Baileychromis centropomoides	Limnochromini	31.07.14	Chipwa Fishermen	-8.606166667	31.18611111
JCC7	M	Baicen	Baileychromis centropomoides	Limnochromini	31.07.14	Chipwa Fishermen	-8.606166667	31.18611111
JCC8	M	Baicen	Baileychromis centropomoides	Limnochromini	31.07.14	Chipwa Fishermen	-8.606166667	31.18611111
JCC9	F	Baicen	Baileychromis centropomoides	Limnochromini	31.07.14	Chipwa Fishermen	-8.606166667	31.18611111
JCD1	NA	Baicen	Baileychromis centropomoides	Limnochromini	31.07.14	Chipwa Fishermen	-8.606166667	31.18611111
JCD3	M?	Regcal	Reganochromis calliurus	Limnochromini	31.07.14	Chipwa Fishermen	-8.606166667	31.18611111
JCD4	M	Regcal	Reganochromis calliurus	Limnochromini	31.07.14	Chipwa Fishermen	-8.606166667	31.18611111
JCD5	M	Regcal	Reganochromis calliurus	Limnochromini	31.07.14	Chipwa Fishermen	-8.606166667	31.18611111
JCD6	M	Benmel	Benthochromis melanoides	Benthochromini	31.07.14	Chipwa Fishermen	-8.606166667	31.18611111
JCD7	M	Benmel	Benthochromis melanoides	Benthochromini	31.07.14	Chipwa Fishermen	-8.606166667	31.18611111
JCD8	NA	Lchabe	Limnochromis abeelei	Limnochromini	31.07.14	Chipwa Fishermen	-8.606166667	31.18611111
JCD9	NA	Lchaur	Limnochromis auritus	Limnochromini	31.07.14	Chipwa Fishermen	-8.606166667	31.18611111
JCE1	NA	Lchaur	Limnochromis auritus	Limnochromini	31.07.14	Chipwa Fishermen	-8.606166667	31.18611111
JCE2	NA	Xencau	Xenotilapia caudafasciata	Ectodini	31.07.14	Chipwa Fishermen	-8.606166667	31.18611111
JCE3	NA	Xencau	Xenotilapia caudafasciata	Ectodini	31.07.14	Chipwa Fishermen	-8.606166667	31.18611111
JCE4	NA	Gwcchr	Greenwoodochromis christyi	Limnochromini	31.07.14	Chipwa Fishermen	-8.606166667	31.18611111
JCE6	NA	Gwcchr	Greenwoodochromis christyi	Limnochromini	31.07.14	Chipwa Fishermen	-8.606166667	31.18611111
JCE7	NA	Gwcchr	Greenwoodochromis christyi	Limnochromini	31.07.14	Chipwa Fishermen	-8.606166667	31.18611111
JCE8	NA	Gwcchr	Greenwoodochromis christyi	Limnochromini	31.07.14	Chipwa Fishermen	-8.606166667	31.18611111
JCE9	M	Tylpol	Tylochromis polylepis	Tylochromini	31.07.14	Chipwa Fishermen	-8.606166667	31.18611111
JCF1	M	Oretan	Oreochromis tanganicae	Oreochromini	31.07.14	Chipwa Fishermen	-8.606166667	31.18611111
JCF2	M	Boumic	Boulengerochromis microlepis	Boulengerochromini	01.08.14	Chipwa Fishermen	-8.606166667	31.18611111
JCF4	NA	Oretan	Oreochromis tanganicae	Oreochromini	01.08.14	Chipwa Fishermen	-8.606166667	31.18611111
JCF5	NA	Oretan	Oreochromis tanganicae	Oreochromini	01.08.14	Chipwa Fishermen	-8.606166667	31.18611111
JCF6	NA	Calmac	Callochromis macrops	Ectodini	01.08.14	Toby's Place	-8.623222222	31.20044444
JCF7	NA	Calmac	Callochromis macrops	Ectodini	01.08.14	Toby's Place	-8.623222222	31.20044444
JCF8	M	Calmac	Callochromis macrops	Ectodini	01.08.14	Toby's Place	-8.623222222	31.20044444
JCF9	NA	Julorn	Julidochromis ornatus	Lamprologini	01.08.14	Toby's Place	-8.623222222	31.20044444
JCG1	NA	Julorn	Julidochromis ornatus	Lamprologini	01.08.14	Toby's Place	-8.623222222	31.20044444
JCG2	NA	Peteph	Petrochromis ephippium	Tropheini	01.08.14	Toby's Place	-8.623222222	31.20044444
JCG3	NA	Peteph	Petrochromis ephippium	Tropheini	01.08.14	Toby's Place	-8.623222222	31.20044444
JCG4	NA	Peteph	Petrochromis ephippium	Tropheini	01.08.14	Toby's Place	-8.623222222	31.20044444
JCG5	NA	Peteph	Petrochromis ephippium	Tropheini	01.08.14	Toby's Place	-8.623222222	31.20044444
JCG6	NA	Peteph	Petrochromis ephippium	Tropheini	01.08.14	Toby's Place	-8.623222222	31.20044444
JCG7	NA	Peteph	Petrochromis ephippium	Tropheini	01.08.14	Toby's Place	-8.623222222	31.20044444
JCG8	NA	Peteph	Petrochromis ephippium	Tropheini	01.08.14	Toby's Place	-8.623222222	31.20044444
JCG9	NA	Petfam	Petrochromis famula	Tropheini	01.08.14	Toby's Place	-8.623222222	31.20044444
JCH1	NA	Petfam	Petrochromis famula	Tropheini	01.08.14	Toby's Place	-8.623222222	31.20044444
JCH2	NA	Petfam	Petrochromis famula	Tropheini	01.08.14	Toby's Place	-8.623222222	31.20044444
JCH4	NA	Petfam	Petrochromis famula	Tropheini	01.08.14	Toby's Place	-8.623222222	31.20044444
JCH5	M	Calmac	Callochromis macrops	Ectodini	01.08.14	Toby's Place	-8.623222222	31.20044444
JCH6	NA	Simdia	Simochromis diagramma	Tropheini	01.08.14	Toby's Place	-8.623222222	31.20044444
JCH7	NA	Peteph	Petrochromis ephippium	Tropheini	01.08.14	Toby's Place	-8.623222222	31.20044444
JCH8	M	Calmac	Callochromis macrops	Ectodini	01.08.14	Toby's Place	-8.623222222	31.20044444
JCH9	M	Calmac	Callochromis macrops	Ectodini	01.08.14	Toby's Place	-8.623222222	31.20044444
JCI1	F	Calmac	Callochromis macrops	Ectodini	01.08.14	Toby's Place	-8.623222222	31.20044444
JCI2	NA	Julorn	Julidochromis ornatus	Lamprologini	01.08.14	Toby's Place	-8.623222222	31.20044444
JCI3	NA	Julorn	Julidochromis ornatus	Lamprologini	01.08.14	Toby's Place	-8.623222222	31.20044444
JCI4	NA	Calmac	Callochromis macrops	Ectodini	01.08.14	Toby's Place	-8.623222222	31.20044444
JCI5	M	Calmac	Callochromis macrops	Ectodini	01.08.14	Toby's Place	-8.623222222	31.20044444
JCI6	F	Calmac	Callochromis macrops	Ectodini	01.08.14	Toby's Place	-8.623222222	31.20044444
JCI7	NA	Peteph	Petrochromis ephippium	Tropheini	01.08.14	Toby's Place	-8.623222222	31.20044444
JCI8	NA	Petfam	Petrochromis famula	Tropheini	01.08.14	Toby's Place	-8.623222222	31.20044444
JDA1	F	Erecya	Eretmodus cyanostictus	Eretmodini	01.08.14	Toby's Place	-8.623222222	31.20044444
JDA2	F	Erecya	Eretmodus cyanostictus	Eretmodini	01.08.14	Toby's Place	-8.623222222	31.20044444
JDA3	F	Erecya	Eretmodus cyanostictus	Eretmodini	01.08.14	Toby's Place	-8.623222222	31.20044444
JDA4	M	Erecya	Eretmodus cyanostictus	Eretmodini	01.08.14	Toby's Place	-8.623222222	31.20044444
JDA5	F	Erecya	Eretmodus cyanostictus	Eretmodini	01.08.14	Toby's Place	-8.623222222	31.20044444
JDA6	M	Erecya	Eretmodus cyanostictus	Eretmodini	01.08.14	Toby's Place	-8.623222222	31.20044444
JDA7	M	Erecya	Eretmodus cyanostictus	Eretmodini	01.08.14	Toby's Place	-8.623222222	31.20044444
JDA8	M	Erecya	Eretmodus cyanostictus	Eretmodini	01.08.14	Toby's Place	-8.623222222	31.20044444
JDA9	F	Erecya	Eretmodus cyanostictus	Eretmodini	01.08.14	Toby's Place	-8.623222222	31.20044444
JDB1	F	Erecya	Eretmodus cyanostictus	Eretmodini	01.08.14	Toby's Place	-8.623222222	31.20044444
JDB2	M	Ctehor	Ctenochromis horei	Tropheini	01.08.14	Toby's Place	-8.623222222	31.20044444
JDB4	M	Oretan	Oreochromis tanganicae	Oreochromini	01.08.14	Toby's Place	-8.623222222	31.20044444
JDB5	M	Ctehor	Ctenochromis horei	Tropheini	01.08.14	Toby's Place	-8.623222222	31.20044444
JDB6	M	Ctehor	Ctenochromis horei	Tropheini	01.08.14	Toby's Place	-8.623222222	31.20044444
JDB7	M	Simdia	Simochromis diagramma	Tropheini	01.08.14	Toby's Place	-8.623222222	31.20044444
JDB8	F	Simdia	Simochromis diagramma	Tropheini	01.08.14	Toby's Place	-8.623222222	31.20044444
JDB9	F	Simdia	Simochromis diagramma	Tropheini	01.08.14	Toby's Place	-8.623222222	31.20044444
JDC1	NA	Simdia	Simochromis diagramma	Tropheini	01.08.14	Toby's Place	-8.623222222	31.20044444
JDC2	F	Simdia	Simochromis diagramma	Tropheini	01.08.14	Toby's Place	-8.623222222	31.20044444

JDC3	NA	Ctehor	Ctenochromis horei	Tropheini	01.08.14	Toby's Place	-8.623222222	31.20044444
JDC4	F	Neochr	Neolamprologus christyi	Lamprologini	01.08.14	Toby's Place	-8.623222222	31.20044444
JDC7	NA	Neomod	Neolamprologus modestus	Lamprologini	01.08.14	Toby's Place	-8.623222222	31.20044444
JDC8	NA	Ctehor	Ctenochromis horei	Tropheini	01.08.14	Toby's Place	-8.623222222	31.20044444
JDC9	NA	Asplep	Asprotilapia leptura	Ectodini	01.08.14	Toby's Place	-8.623222222	31.20044444
JDD2	NA	Psccur	Pseudosimochromis curvifrons	Tropheini	01.08.14	Toby's Place	-8.623222222	31.20044444
JDD6	NA	Julorn	Julidochromis ornatus	Lamprologini	01.08.14	Toby's Place	-8.623222222	31.20044444
JDD7	M	Gralem	Grammatotria lemairii	Ectodini	01.08.14	Toby's Place	-8.623222222	31.20044444
JDD8	F	Gralem	Grammatotria lemairii	Ectodini	01.08.14	Toby's Place	-8.623222222	31.20044444
JDD9	NA	Ctehor	Ctenochromis horei	Tropheini	01.08.14	Toby's Place	-8.623222222	31.20044444
JDE1	NA	Ctehor	Ctenochromis horei	Tropheini	01.08.14	Toby's Place	-8.623222222	31.20044444
JDE3	M	Bathor	Bathybates hornii	Bathybatini	02.08.14	Chipwa Fishermen	-8.606166667	31.18611111
JDE4	M?	Bathor	Bathybates hornii	Bathybatini	02.08.14	Chipwa Fishermen	-8.606166667	31.18611111
JDE6	M	Batvit	Bathybates vittatus	Bathybatini	14.08.14	Katoto	-8.806111111	31.02666667
JDE7	F	Batvit	Bathybates vittatus	Bathybatini	14.08.14	Katoto	-8.806111111	31.02666667
JDE8	NA	Lepatt	Lepidiolamprologus attenuatus	Lamprologini	14.08.14	Katoto	-8.806111111	31.02666667
JDE9	NA	Lepatt	Lepidiolamprologus attenuatus	Lamprologini	14.08.14	Katoto	-8.806111111	31.02666667
JDF1	NA	Lchabe	Limnochromis abeelei	Limnochromini	14.08.14	Katoto	-8.806111111	31.02666667
JDF2	NA	Boumic	Boulengerochromis microlepis	Boulengerochromini	14.08.14	Katoto	-8.806111111	31.02666667
JDF3	M	Neomee	Neolamprologus meeli	Lamprologini	14.08.14	Katoto	-8.806111111	31.02666667
JDF4	F	Neomee	Neolamprologus meeli	Lamprologini	14.08.14	Katoto	-8.806111111	31.02666667
JDF5	M	LamorS	Lamprologus sp. "ornatipinnis zambia"	Lamprologini	14.08.14	Katoto	-8.806111111	31.02666667
JDF7	F	Neomee	Neolamprologus meeli	Lamprologini	14.08.14	Katoto	-8.806111111	31.02666667
JDF8	NA	Neomee	Neolamprologus meeli	Lamprologini	14.08.14	Katoto	-8.806111111	31.02666667
JDF9	M	Neomee	Neolamprologus meeli	Lamprologini	14.08.14	Katoto	-8.806111111	31.02666667
JDG1	F	Neomee	Neolamprologus meeli	Lamprologini	14.08.14	Katoto	-8.806111111	31.02666667
JDG2	NA	Neomee	Neolamprologus meeli	Lamprologini	14.08.14	Katoto	-8.806111111	31.02666667
JDG4	F	LamorS	Lamprologus sp. "ornatipinnis zambia"	Lamprologini	14.08.14	Katoto	-8.806111111	31.02666667
JDG6	NA	Neomee	Neolamprologus meeli	Lamprologini	14.08.14	Katoto	-8.806111111	31.02666667
JDG7	NA	Neomee	Neolamprologus meeli	Lamprologini	14.08.14	Katoto	-8.806111111	31.02666667
JDG8	NA	Neomee	Neolamprologus meeli	Lamprologini	14.08.14	Katoto	-8.806111111	31.02666667
JDG9	NA	Neomee	Neolamprologus meeli	Lamprologini	14.08.14	Katoto	-8.806111111	31.02666667
JDH1	F	Neomee	Neolamprologus meeli	Lamprologini	14.08.14	Katoto	-8.806111111	31.02666667
JDH4	M	LamorS	Lamprologus sp. "ornatipinnis zambia"	Lamprologini	14.08.14	Katoto	-8.806111111	31.02666667
JDH5	F	LamorS	Lamprologus sp. "ornatipinnis zambia"	Lamprologini	14.08.14	Katoto	-8.806111111	31.02666667
JDH6	F	LamorS	Lamprologus sp. "ornatipinnis zambia"	Lamprologini	14.08.14	Katoto	-8.806111111	31.02666667
JDH7	F	Lamlap	Lamprologus laparogramma	Lamprologini	14.08.14	Katoto	-8.806111111	31.02666667
JDH8	F	Lamlap	Lamprologus laparogramma	Lamprologini	14.08.14	Katoto	-8.806111111	31.02666667
JDI1	F	Lamlap	Lamprologus laparogramma	Lamprologini	14.08.14	Katoto	-8.806111111	31.02666667
JDI2	M	Lamlap	Lamprologus laparogramma	Lamprologini	14.08.14	Katoto	-8.806111111	31.02666667
JDI4	M	Plepar	Plecodus paradoxus	Perissodini	15.08.14	Katoto	-8.806111111	31.02666667
JDI6	M	Lepatt	Lepidiolamprologus attenuatus	Lamprologini	15.08.14	Katoto	-8.806111111	31.02666667
JDI7	M	Lepatt	Lepidiolamprologus attenuatus	Lamprologini	15.08.14	Katoto	-8.806111111	31.02666667
JDI8	M	Lepatt	Lepidiolamprologus attenuatus	Lamprologini	15.08.14	Katoto	-8.806111111	31.02666667
JDI9	F	Lepatt	Lepidiolamprologus attenuatus	Lamprologini	15.08.14	Katoto	-8.806111111	31.02666667
JEA2	M	Hapmic	Haplotaxodon microlepis	Perissodini	20.08.14	Chitweshiba	-8.595833333	30.8075
JEA3	F	Hapmic	Haplotaxodon microlepis	Perissodini	20.08.14	Chitweshiba	-8.595833333	30.8075
JEA4	NA	Lamcal	Lamprologus callipterus	Lamprologini	20.08.14	Chitweshiba	-8.595833333	30.8075
JEA5	NA	Lamcal	Lamprologus callipterus	Lamprologini	20.08.14	Chitweshiba	-8.595833333	30.8075
JEA6	NA	Lamcal	Lamprologus callipterus	Lamprologini	20.08.14	Chitweshiba	-8.595833333	30.8075
JEA7	NA	Lamcal	Lamprologus callipterus	Lamprologini	20.08.14	Chitweshiba	-8.595833333	30.8075
JEA8	NA	Cphgib	Cyphotilapia gibberosa	Cyphotilapiini	20.08.14	Misepa	-8.588888889	30.80305556
JEA9	NA	Cphgib	Cyphotilapia gibberosa	Cyphotilapiini	20.08.14	Misepa	-8.588888889	30.80305556
JEB1	NA	Cphgib	Cyphotilapia gibberosa	Cyphotilapiini	20.08.14	Misepa	-8.588888889	30.80305556
JEB2	M	Cyppav	Cyprichromis pavo	Cyprichromini	20.08.14	Misepa	-8.588888889	30.80305556
JEB4	F	Cyppav	Cyprichromis pavo	Cyprichromini	20.08.14	Misepa	-8.588888889	30.80305556
JEB6	M	Cyppav	Cyprichromis pavo	Cyprichromini	20.08.14	Misepa	-8.588888889	30.80305556
JEB7	M	Cyppav	Cyprichromis pavo	Cyprichromini	20.08.14	Misepa	-8.588888889	30.80305556
JEB8	M	Cyppav	Cyprichromis pavo	Cyprichromini	20.08.14	Misepa	-8.588888889	30.80305556
JEB9	F	Cyppav	Cyprichromis pavo	Cyprichromini	20.08.14	Misepa	-8.588888889	30.80305556
JEC1	F	Cyppav	Cyprichromis pavo	Cyprichromini	20.08.14	Misepa	-8.588888889	30.80305556
JEC2	M	Cyppav	Cyprichromis pavo	Cyprichromini	20.08.14	Misepa	-8.588888889	30.80305556
JEC3	M	Cyppav	Cyprichromis pavo	Cyprichromini	20.08.14	Misepa	-8.588888889	30.80305556
JEC4	M	Cyppav	Cyprichromis pavo	Cyprichromini	20.08.14	Misepa	-8.588888889	30.80305556
JEC5	M	Cyppav	Cyprichromis pavo	Cyprichromini	20.08.14	Misepa	-8.588888889	30.80305556
JEC6	M	Cyppav	Cyprichromis pavo	Cyprichromini	20.08.14	Chitweshiba	-8.595833333	30.8075
JEC7	M	Cypcol	Cyprichromis coloratus	Cyprichromini	20.08.14	Chitweshiba	-8.595833333	30.8075
JEC8	M	Cypcol	Cyprichromis coloratus	Cyprichromini	20.08.14	Chitweshiba	-8.595833333	30.8075
JEC9	F	Cypcol	Cyprichromis coloratus	Cyprichromini	20.08.14	Chitweshiba	-8.595833333	30.8075
JED1	F	Cypcol	Cyprichromis coloratus	Cyprichromini	20.08.14	Chitweshiba	-8.595833333	30.8075
JED2	F	Cypcol	Cyprichromis coloratus	Cyprichromini	20.08.14	Chitweshiba	-8.595833333	30.8075
JED3	M	Leppro	Lepidiolamprologus profundicola	Lamprologini	20.08.14	Chitweshiba	-8.595833333	30.8075
JED4	M	NeoveS	Neolamprologus sp. "ventralis stripe"	Lamprologini	20.08.14	Chitweshiba	-8.595833333	30.8075
JED5	F	NeoveS	Neolamprologus sp. "ventralis stripe"	Lamprologini	20.08.14	Chitweshiba	-8.595833333	30.8075
JED6	M	Cphgib	Cyphotilapia gibberosa	Cyphotilapiini	21.08.14	Mibwebwe	-8.565	30.76111111
JED7	M	Hapmic	Haplotaxodon microlepis	Perissodini	21.08.14	Mibwebwe	-8.565	30.76111111
JED8	F	Hapmic	Haplotaxodon microlepis	Perissodini	21.08.14	Mibwebwe	-8.565	30.76111111
JED9	M	Hapmic	Haplotaxodon microlepis	Perissodini	21.08.14	Mibwebwe	-8.565	30.76111111
JEE1	M	Lepken	Lepidiolamprologus kendalli	Lamprologini	21.08.14	Mibwebwe	-8.565	30.76111111
JEE2	M	LamorS	Lamprologus sp. "ornatipinnis zambia"	Lamprologini	21.08.14	Kabyolwe	-8.569166667	30.75055556
JEE3	F	Lamcal	Lamprologus callipterus	Lamprologini	21.08.14	Mibwebwe	-8.565	30.76111111
JEE4	F	Lamcal	Lamprologus callipterus	Lamprologini	21.08.14	Mibwebwe	-8.565	30.76111111
JEE5	F	Lamcal	Lamprologus callipterus	Lamprologini	21.08.14	Mibwebwe	-8.565	30.76111111
JEE6	F	Lamcal	Lamprologus callipterus	Lamprologini	21.08.14	Mibwebwe	-8.565	30.76111111
JEF1	M	Pleela	Plecodus elaviae	Perissodini	21.08.14	Kabyolwe Fishermen	-8.567694444	30.75219444
JEF4	NA	Batmin	Bathybates minor	Bathybatini	22.08.14	Kasenga West Fishermen	-8.566694444	30.75644444
JEF5	NA	Batmin	Bathybates minor	Bathybatini	22.08.14	Kasenga West Fishermen	-8.566694444	30.75644444
JEF6	NA	Batmin	Bathybates minor	Bathybatini	22.08.14	Kasenga West Fishermen	-8.566694444	30.75644444
JEF7	NA	Batmin	Bathybates minor	Bathybatini	22.08.14	Kasenga West Fishermen	-8.566694444	30.75644444
JEF8	NA	Batmin	Bathybates minor	Bathybatini	22.08.14	Kasenga West Fishermen	-8.566694444	30.75644444
JEF9	NA	Batmin	Bathybates minor	Bathybatini	22.08.14	Kasenga West Fishermen	-8.566694444	30.75644444
JEG2	NA	Batmin	Bathybates minor	Bathybatini	22.08.14	Kasenga West Fishermen	-8.566694444	30.75644444
JEG4	NA	Batfas	Bathybates fasciatus	Bathybatini	22.08.14	Kasenga West Fishermen	-8.566694444	30.75644444
JEG5	F	Trioto	Triglachromis otostigma	Limnochromini	22.08.14	Kabyolwe	-8.569166667	30.75055556
JEG6	M	Trioto	Triglachromis otostigma	Limnochromini	22.08.14	Kabyolwe	-8.569166667	30.75055556
JEG7	F	Trioto	Triglachromis otostigma	Limnochromini	22.08.14	Kabyolwe	-8.569166667	30.75055556
JEH2	NA	Lchaur	Limnochromis auritus	Limnochromini	22.08.14	Kabyolwe	-8.569166667	30.75055556
JEH4	NA	Telbra	Telmatochromis brachygnathus	Lamprologini	22.08.14	Kabyolwe	-8.569166667	30.75055556
JEH5	NA	Telbra	Telmatochromis brachygnathus	Lamprologini	22.08.14	Kabyolwe	-8.569166667	30.75055556
JEH6	NA	LamorS	Lamprologus sp. "ornatipinnis zambia"	Lamprologini	22.08.14	Kabyolwe	-8.569166667	30.75055556
JEH7	NA	Lamoce	Lamprologus ocellatus	Lamprologini	22.08.14	Kabyolwe	-8.569166667	30.75055556
JEH8	M	Pscple	Pseudosimochromis babaulti (South)	Tropheini	22.08.14	Kabyolwe	-8.569166667	30.75055556
JEH9	NA	Loblab	Lobochilotes labiatus	Tropheini	22.08.14	Kabyolwe	-8.569166667	30.75055556
JEI1	NA	Neofas	Neolamprologus fasciatus	Lamprologini	22.08.14	Kabyolwe	-8.569166667	30.75055556
JEI2	M	Neofas	Neolamprologus fasciatus	Lamprologini	22.08.14	Kabyolwe	-8.569166667	30.75055556
JEI3	M	Neofas	Neolamprologus fasciatus	Lamprologini	22.08.14	Kabyolwe	-8.569166667	30.75055556
JEI4	M	Neobue	Neolamprologus buescheri	Lamprologini	23.08.14	Kachese	-8.490527778	30.4775
JEI5	F	Neobue	Neolamprologus buescheri	Lamprologini	23.08.14	Kachese	-8.490527778	30.4775
JEI6	M	Neofur	Neolamprologus furcifer	Lamprologini	23.08.14	Kachese	-8.490527778	30.4775
JEI8	F	Neofur	Neolamprologus furcifer	Lamprologini	23.08.14	Kachese	-8.490527778	30.4775
JEI9	F	Neofur	Neolamprologus furcifer	Lamprologini	23.08.14	Kachese	-8.490527778	30.4775
JUA1	M	Pscbab	Pseudosimochromis babaulti	Tropheini	05.01.15	Kitaza south	-3.625694444	29.34238889
JUA2	M	Pscbab	Pseudosimochromis babaulti	Tropheini	05.01.15	Kitaza south	-3.625694444	29.34238889
JUA3	M	Pscbab	Pseudosimochromis babaulti	Tropheini	05.01.15	Kitaza south	-3.625694444	29.34238889
JUA4	F	Pscbab	Pseudosimochromis babaulti	Tropheini	05.01.15	Kitaza south	-3.625694444	29.34238889
JUA5	M	Pscbab	Pseudosimochromis babaulti	Tropheini	05.01.15	Kitaza south	-3.625694444	29.34238889
JUA6	F	Pscbab	Pseudosimochromis babaulti	Tropheini	05.01.15	Kitaza south	-3.625694444	29.34238889
JUA9	M	Pscbab	Pseudosimochromis babaulti	Tropheini	05.01.15	Kitaza south	-3.625694444	29.34238889
JUB1	F	Pscbab	Pseudosimochromis babaulti	Tropheini	05.01.15	Kitaza south	-3.625694444	29.34238889
JUB2	F	Pscbab	Pseudosimochromis babaulti	Tropheini	05.01.15	Kitaza south	-3.625694444	29.34238889
JUB3	F	Pscbab	Pseudosimochromis babaulti	Tropheini	05.01.15	Kitaza south	-3.625694444	29.34238889
JUB4	F	Pscbab	Pseudosimochromis babaulti	Tropheini	05.01.15	Kitaza south	-3.625694444	29.34238889
JUB5	M	Pscbab	Pseudosimochromis babaulti	Tropheini	05.01.15	Kitaza south	-3.625694444	29.34238889
JUB6	M	Spaery	Spathodus erythrodon	Eretmodini	05.01.15	Kitaza south	-3.625694444	29.34238889

JUB7	F	Spaery	Spathodus erythrodon	Eretmodini	05.01.15	Kitaza south	-3.625694444	29.34238889
JUC1	M	Spaery	Spathodus erythrodon	Eretmodini	05.01.15	Kitaza south	-3.625694444	29.34238889
JUC2	F	Spaery	Spathodus erythrodon	Eretmodini	05.01.15	Kitaza south	-3.625694444	29.34238889
JUC3	M	Spaery	Spathodus erythrodon	Eretmodini	05.01.15	Kitaza south	-3.625694444	29.34238889
JUC4	M	Spaery	Spathodus erythrodon	Eretmodini	05.01.15	Kitaza south	-3.625694444	29.34238889
JUC5	M	Spaery	Spathodus erythrodon	Eretmodini	05.01.15	Kitaza south	-3.625694444	29.34238889
JUC6	F	Spaery	Spathodus erythrodon	Eretmodini	05.01.15	Kitaza south	-3.625694444	29.34238889
JUC7	M	Spaery	Spathodus erythrodon	Eretmodini	05.01.15	Kitaza south	-3.625694444	29.34238889
JUC8	M	Spaery	Spathodus erythrodon	Eretmodini	05.01.15	Kitaza south	-3.625694444	29.34238889
JUC9	F	Spaery	Spathodus erythrodon	Eretmodini	05.01.15	Kitaza south	-3.625694444	29.34238889
JUD1	F	Spaery	Spathodus erythrodon	Eretmodini	05.01.15	Kitaza south	-3.625694444	29.34238889
JUD4	M	TeldhN	Telmatochromis sp. "dhonti north"	Lamprologini	05.01.15	Kitaza south	-3.625694444	29.34238889
JUD5	F	TeldhN	Telmatochromis sp. "dhonti north"	Lamprologini	05.01.15	Kitaza south	-3.625694444	29.34238889
JUD7	NA	TeldhN	Telmatochromis sp. "dhonti north"	Lamprologini	05.01.15	Kitaza south	-3.625694444	29.34238889
JUD8	NA	TeldhN	Telmatochromis sp. "dhonti north"	Lamprologini	05.01.15	Kitaza south	-3.625694444	29.34238889
JUE5	NA	TeldhN	Telmatochromis sp. "dhonti north"	Lamprologini	05.01.15	Kitaza south	-3.625694444	29.34238889
JUE6	NA	TeldhN	Telmatochromis sp. "dhonti north"	Lamprologini	05.01.15	Kitaza south	-3.625694444	29.34238889
JUE7	NA	TeldhN	Telmatochromis sp. "dhonti north"	Lamprologini	05.01.15	Kitaza south	-3.625694444	29.34238889
JUF5	NA	TeldhN	Telmatochromis sp. "dhonti north"	Lamprologini	05.01.15	Kitaza south	-3.625694444	29.34238889
JUF6	NA	TeldhN	Telmatochromis sp. "dhonti north"	Lamprologini	05.01.15	Kitaza south	-3.625694444	29.34238889
JUF7	NA	TeldhN	Telmatochromis sp. "dhonti north"	Lamprologini	05.01.15	Kitaza south	-3.625694444	29.34238889
JUF8	NA	TeldhN	Telmatochromis sp. "dhonti north"	Lamprologini	05.01.15	Kitaza south	-3.625694444	29.34238889
JUH5	M	Neobri	Neolamprologus brichardi	Lamprologini	06.01.15	Nyaruhongoka	-3.691583333	29.32369444
JUH6	M	Neobri	Neolamprologus brichardi	Lamprologini	06.01.15	Nyaruhongoka	-3.691583333	29.32369444
JUH7	F	Neobri	Neolamprologus brichardi	Lamprologini	06.01.15	Nyaruhongoka	-3.691583333	29.32369444
JUH8	F	Neobri	Neolamprologus brichardi	Lamprologini	06.01.15	Nyaruhongoka	-3.691583333	29.32369444
JUH9	F	Neobri	Neolamprologus brichardi	Lamprologini	06.01.15	Nyaruhongoka	-3.691583333	29.32369444
JUI1	M	Neobri	Neolamprologus brichardi	Lamprologini	06.01.15	Nyaruhongoka	-3.691583333	29.32369444
JUI2	F	Neobri	Neolamprologus brichardi	Lamprologini	06.01.15	Nyaruhongoka	-3.691583333	29.32369444
JUI3	F	Neobri	Neolamprologus brichardi	Lamprologini	06.01.15	Nyaruhongoka	-3.691583333	29.32369444
JUI4	M	Neobri	Neolamprologus brichardi	Lamprologini	06.01.15	Nyaruhongoka	-3.691583333	29.32369444
JUI5	M	Neobri	Neolamprologus brichardi	Lamprologini	06.01.15	Nyaruhongoka	-3.691583333	29.32369444
JUI7	M	Neobri	Neolamprologus brichardi	Lamprologini	06.01.15	Nyaruhongoka	-3.691583333	29.32369444
JUI8	M	Neobri	Neolamprologus brichardi	Lamprologini	06.01.15	Nyaruhongoka	-3.691583333	29.32369444
JVA2	M	Neomon	Neolamprologus mondabu	Lamprologini	06.01.15	Nyaruhongoka	-3.691583333	29.32369444
JVA5	M	Neomon	Neolamprologus mondabu	Lamprologini	06.01.15	Nyaruhongoka	-3.691583333	29.32369444
JVA6	F	Neomon	Neolamprologus mondabu	Lamprologini	06.01.15	Nyaruhongoka	-3.691583333	29.32369444
JVA9	M	Neomon	Neolamprologus mondabu	Lamprologini	06.01.15	Nyaruhongoka	-3.691583333	29.32369444
JVB1	M	Neomon	Neolamprologus mondabu	Lamprologini	06.01.15	Nyaruhongoka	-3.691583333	29.32369444
JVB2	F	Neomon	Neolamprologus mondabu	Lamprologini	06.01.15	Nyaruhongoka	-3.691583333	29.32369444
JVB3	F	Neomon	Neolamprologus mondabu	Lamprologini	06.01.15	Nyaruhongoka	-3.691583333	29.32369444
JVB4	M	Neomon	Neolamprologus mondabu	Lamprologini	06.01.15	Nyaruhongoka	-3.691583333	29.32369444
JVB5	F	Neomon	Neolamprologus mondabu	Lamprologini	06.01.15	Nyaruhongoka	-3.691583333	29.32369444
JVB6	F	Neomon	Neolamprologus mondabu	Lamprologini	06.01.15	Nyaruhongoka	-3.691583333	29.32369444
JVB7	M	Neomon	Neolamprologus mondabu	Lamprologini	06.01.15	Nyaruhongoka	-3.691583333	29.32369444
JVB8	F	Neomon	Neolamprologus mondabu	Lamprologini	06.01.15	Nyaruhongoka	-3.691583333	29.32369444
JVC3	F	Tronig	Tropheus sp. "black"	Tropheini	06.01.15	Nyaruhongoka	-3.691583333	29.32369444
JVC4	NA	Tronig	Tropheus sp. "black"	Tropheini	06.01.15	Nyaruhongoka	-3.691583333	29.32369444
JVC5	F	Tronig	Tropheus sp. "black"	Tropheini	06.01.15	Nyaruhongoka	-3.691583333	29.32369444
JVC6	NA	Tronig	Tropheus sp. "black"	Tropheini	06.01.15	Nyaruhongoka	-3.691583333	29.32369444
JVC7	NA	Tronig	Tropheus sp. "black"	Tropheini	06.01.15	Nyaruhongoka	-3.691583333	29.32369444
JVC8	NA	Tronig	Tropheus sp. "black"	Tropheini	06.01.15	Nyaruhongoka	-3.691583333	29.32369444
JVC9	M	Tronig	Tropheus sp. "black"	Tropheini	06.01.15	Nyaruhongoka	-3.691583333	29.32369444
JVD1	NA	Tronig	Tropheus sp. "black"	Tropheini	06.01.15	Nyaruhongoka	-3.691583333	29.32369444
JVD2	NA	Tronig	Tropheus sp. "black"	Tropheini	06.01.15	Nyaruhongoka	-3.691583333	29.32369444
JVD3	NA	Tronig	Tropheus sp. "black"	Tropheini	06.01.15	Nyaruhongoka	-3.691583333	29.32369444
JVD5	NA	Tronig	Tropheus sp. "black"	Tropheini	06.01.15	Nyaruhongoka	-3.691583333	29.32369444
JVD6	NA	Tronig	Tropheus sp. "black"	Tropheini	06.01.15	Nyaruhongoka	-3.691583333	29.32369444
JVE1	M	Cypmic	Cyprichromis microlepidotus	Cyprichromini	07.01.15	Nyaruhongoka 2	-3.698611111	29.32008333
JVE2	M	Cypmic	Cyprichromis microlepidotus	Cyprichromini	07.01.15	Nyaruhongoka 2	-3.698611111	29.32008333
JVE4	M	Cypmic	Cyprichromis microlepidotus	Cyprichromini	07.01.15	Nyaruhongoka 2	-3.698611111	29.32008333
JVE6	M	Cypmic	Cyprichromis microlepidotus	Cyprichromini	07.01.15	Nyaruhongoka 2	-3.698611111	29.32008333
JVE7	M	Cypmic	Cyprichromis microlepidotus	Cyprichromini	07.01.15	Nyaruhongoka 2	-3.698611111	29.32008333
JVE9	M	Cypmic	Cyprichromis microlepidotus	Cyprichromini	07.01.15	Nyaruhongoka 2	-3.698611111	29.32008333
JVF1	M	Cypmic	Cyprichromis microlepidotus	Cyprichromini	07.01.15	Nyaruhongoka 2	-3.698611111	29.32008333
JVF2	F	Cypmic	Cyprichromis microlepidotus	Cyprichromini	07.01.15	Nyaruhongoka 2	-3.698611111	29.32008333
JVF3	M	Cypmic	Cyprichromis microlepidotus	Cyprichromini	07.01.15	Nyaruhongoka 2	-3.698611111	29.32008333
JVF5	M	Cypmic	Cyprichromis microlepidotus	Cyprichromini	07.01.15	Nyaruhongoka 2	-3.698611111	29.32008333
JVF6	M	Neofal	Neolamprologus falcicula	Lamprologini	07.01.15	Nyaruhongoka 2	-3.698611111	29.32008333
JVF7	F	Neofal	Neolamprologus falcicula	Lamprologini	07.01.15	Nyaruhongoka 2	-3.698611111	29.32008333
JVG1	NA	Lessta	Lestradea stappersii	Ectodini	07.01.15	Nyaruhongoka 2	-3.698611111	29.32008333
JVG2	NA	Lessta	Lestradea stappersii	Ectodini	07.01.15	Nyaruhongoka 2	-3.698611111	29.32008333
JVG3	NA	Lessta	Lestradea stappersii	Ectodini	07.01.15	Nyaruhongoka 2	-3.698611111	29.32008333
JVG4	NA	Lessta	Lestradea stappersii	Ectodini	07.01.15	Nyaruhongoka 2	-3.698611111	29.32008333
JVG5	NA	Lessta	Lestradea stappersii	Ectodini	07.01.15	Nyaruhongoka 2	-3.698611111	29.32008333
JVG6	NA	Lessta	Lestradea stappersii	Ectodini	07.01.15	Nyaruhongoka 2	-3.698611111	29.32008333
JVG7	NA	Lessta	Lestradea stappersii	Ectodini	07.01.15	Nyaruhongoka 2	-3.698611111	29.32008333
JVG8	NA	Lessta	Lestradea stappersii	Ectodini	07.01.15	Nyaruhongoka 2	-3.698611111	29.32008333
JVG9	NA	Lessta	Lestradea stappersii	Ectodini	07.01.15	Nyaruhongoka 2	-3.698611111	29.32008333
JVH1	NA	Lessta	Lestradea stappersii	Ectodini	07.01.15	Nyaruhongoka 2	-3.698611111	29.32008333
JVH2	F	Lessta	Lestradea stappersii	Ectodini	07.01.15	Nyaruhongoka 2	-3.698611111	29.32008333
JVH3	M	Lessta	Lestradea stappersii	Ectodini	07.01.15	Nyaruhongoka 2	-3.698611111	29.32008333
JVH4	M	Xenoch	Xenotilapia ochrogenys	Ectodini	07.01.15	Mireille fishermen	-3.403361111	29.35925
JVH5	M	Xenoch	Xenotilapia ochrogenys	Ectodini	07.01.15	Mireille fishermen	-3.403361111	29.35925
JVH6	M	Xenoch	Xenotilapia ochrogenys	Ectodini	07.01.15	Mireille fishermen	-3.403361111	29.35925
JVH7	M	Xenoch	Xenotilapia ochrogenys	Ectodini	07.01.15	Mireille fishermen	-3.403361111	29.35925
JVH9	M	Xenoch	Xenotilapia ochrogenys	Ectodini	07.01.15	Mireille fishermen	-3.403361111	29.35925
JVI1	M	Xenoch	Xenotilapia ochrogenys	Ectodini	07.01.15	Mireille fishermen	-3.403361111	29.35925
JVI3	M	Xenoch	Xenotilapia ochrogenys	Ectodini	07.01.15	Mireille fishermen	-3.403361111	29.35925
JVI4	F	Xenoch	Xenotilapia ochrogenys	Ectodini	07.01.15	Mireille fishermen	-3.403361111	29.35925
JVI5	F	Xenoch	Xenotilapia ochrogenys	Ectodini	07.01.15	Mireille fishermen	-3.403361111	29.35925
JVI6	F	Xenoch	Xenotilapia ochrogenys	Ectodini	07.01.15	Mireille fishermen	-3.403361111	29.35925
JVI7	F	Xenoch	Xenotilapia ochrogenys	Ectodini	07.01.15	Mireille fishermen	-3.403361111	29.35925
JVI8	F	Xenoch	Xenotilapia ochrogenys	Ectodini	07.01.15	Mireille fishermen	-3.403361111	29.35925
JVI9	M	Telbri	Telmatochromis brichardi	Lamprologini	07.01.15	Nyaruhongoka 2	-3.698611111	29.32008333
JWA1	M	Julunt	Julidochromis sp. "unterfels"	Lamprologini	NA	Kieso (Heinz)	NA	NA
JWA2	F	Julunt	Julidochromis sp. "unterfels"	Lamprologini	NA	Kieso (Heinz)	NA	NA
JWA3	M	LamorC	Lamprologus sp. "ornatipinnis congo"	Lamprologini	NA	Tembwe DRC	-7.239722	30.119444
JWA4	F	LamorC	Lamprologus sp. "ornatipinnis congo"	Lamprologini	NA	Tembwe DRC	-7.239722	30.119444
JWA5	M	Neovar	Neolamprologus variostigma	Lamprologini	NA	Tembwe DRC	-7.239722	30.119444
JWA6	F	Neovar	Neolamprologus variostigma	Lamprologini	NA	Tembwe DRC	-7.239722	30.119444
JWA7	M	Neopec	Neolamprologus pectoralis	Lamprologini	NA	Tembwe DRC	-7.239722	30.119444
JWA8	M	Lammel	Lamprologus meleagris	Lamprologini	NA	Kalubamba DRC	-7.379444444	30.18972222
JWA9	F	Lammel	Lamprologus meleagris	Lamprologini	NA	Kalubamba DRC	-7.379444444	30.18972222
JWC8	M	Tellon	Telmatochromis sp. "longola"	Lamprologini	NA	Longola	-7.481944444	30.21777778
JWC9	F	Tellon	Telmatochromis sp. "longola"	Lamprologini	NA	Longola	-7.481944444	30.21777778
JWD1	M	Pcytem	Paracyprichromis sp. "tembwe"	Cyprichromini	NA	Tembwe DRC	-7.239722	30.119444
JWD2	F	Pcytem	Paracyprichromis sp. "tembwe"	Cyprichromini	NA	Tembwe DRC	-7.239722	30.119444
JWD3	NA	Etingu	Etia nguti	Etini	NA	Cameroon: Mafue River / Nguti	5.337806	9.417389
JWD4	NA	Etrcan	Etroplus canarensis	Etroplini	NA	India	NA	NA
JWD5	M	Parpol	Paratilapia polleni "Andapa"	Paratilapini	NA	Madagaskar: Andapa	NA	NA
JWD7	NA	Andbis	Andinoacara biseriatus	Cichlasomini	NA	Peru	NA	NA
JWD8	M	Bujvit	Bujurquina vittata	Cichlasomini	NA	Paraguay	NA	NA
JWD9	M	Apidip	Apistogramma diplotaenia	Geophagini	NA	Venezuela	NA	NA
JWE1	M	Ampzal	Amphilophus zaliosus	Amphilophini	NA	Lake Apoyo	11.932861	-86.05425
JWE2	M	Aussci	Australoheros scitulus	Heroini	NA	Uruguay	NA	NA
JWE3	NA	Hetbut	Heterotilapia buettikoferi	Heterotilapini	NA	Liberia	NA	NA
JWE4	M	Bencon	Benitochromis conjunctus	Chromidotilapini	NA	Cameroon: Muyuka	4.278278	9.404083
JWE5	NA	Copbak	Coptodon bakossiorum	Coptodini	NA	Cameroon: Lake Bermin	5.156694	9.636361
JWE6	M	Copren	Coptodon rendalli	Coptodini	NA	Toby's Place	-8.623222222	31.20044444
JWE7	M	Gobeth	Gobiocichla ethelwynnae	Gobiocichlini	NA	Cameroon: Cross / Mamfe	5.765861	9.310667
JWE8	M	Steult	Steatocranus sp. "ultraslender"	Steatocranini	NA	Inga DRC	-5.513278	13.625139
JWE9	M	Hchelo	Hemichromis elongatus	Hemichromini	NA	Cameroon: Ayatto	4.149861	9.524222
JWF1	Juvenile	Htcmul	Heterochromis multidens	Heterochromini	NA	Cameroon: Boumba	3.220028	14.920167

JWF2	Juvenile	Pelmar	Pelmatolapia mariae	Pelmatolapini	NA	Cameroon: Cross / Mamfe	5.765861	9.310667
JWF3	M	Phaacu	Pharyngochromis acuticeps	Serranochromini	NA	Mambova / Zambezi	-17.743361	25.173778
JWF4	Juvenile	Sarcar	Sargochromis carlottae	Serranochromini	NA	Mambova / Zambezi	-17.743361	25.173778
JWF5	M	Sermac	Serranochromis macrocephalus	Serranochromini	NA	Mukambi / Kafue	-14.978444	25.993167
JWF6	F	Lamtig	Lamprologus tigripictilis	Lamprologini	NA	DRC: Congo river	NA	NA
JWF7	M	Tilspa	Tilapia sparmanii	Tilapiini	NA	Lake Chila Outflow	-8.835744	31.3804
JWF8	M	Thobra	Thoracochromis brauschi	Haplochromini	NA	Lac Fwa	-5.72875	23.350583
JWF9	F	Tilbre	Tilapia brevimanus	Gobiocichlini	NA	West-Africa	NA	NA
JWG1	M	Psephi	Pseudocrenilabrus philander	Haplochromini	NA	Mbulu	-8.85725	31.364667
JWG2	M	Ctepol	Ctenochromis polli	Haplochromini	NA	DRC	NA	NA
JWG3	M	Hplvan	Haplochromis vanheusdeni	Haplochromini	NA	Ruaha	-7.808222222	36.89655556
JWG4	M	Troann	Tropheus annectens	Tropheini	NA	Mukamba	-6.9475	29.711944
JWG5	F	Troann	Tropheus annectens	Tropheini	NA	Mukamba	-6.9475	29.711944
JWG8	F	Neohel	Neolamprologus helianthus	Lamprologini	12.10.15	Kamakonde DRC	-7.873611111	30.30388889
JWG9	M	Neohel	Neolamprologus helianthus	Lamprologini	12.10.15	Kamakonde DRC	-7.873611111	30.30388889
JWH1	F	Neogra	Neolamprologus gracilis	Lamprologini	12.10.15	Kalo DRC	-7.795278	30.266389
JWH2	M	Neogra	Neolamprologus gracilis	Lamprologini	12.10.15	Kalo DRC	-7.795278	30.266389
JWH3	M	Neomar	Neolamprologus marunguensis	Lamprologini	12.10.15	Kafitilila DRC	-7.715222	30.234139
JWH4	F	Neomar	Neolamprologus marunguensis	Lamprologini	12.10.15	Kafitilila DRC	-7.715222	30.234139
JWH5	F	Neooli	Neolamprologus olivaceous	Lamprologini	12.10.15	Kyeso DRC	-6.816666667	29.61472222
JWH6	M	Neooli	Neolamprologus olivaceous	Lamprologini	12.10.15	Kyeso DRC	-6.816666667	29.61472222
JWH9	NA	NeoleL	Neolamprologus leleupi	Lamprologini	12.10.15	Luhanga (Graz)	-3.499528	29.139917
JWI2	M	Neolon	Neolamprologus longicaudatus	Lamprologini	09.10.15	Kapamba (Mireille)	-7.630278	30.195556
JWI3	F	Neolon	Neolamprologus longicaudatus	Lamprologini	09.10.15	Kapamba (Mireille)	-7.630278	30.195556
JWI4	M	Peltae	Pelvicachromis taeniatus	Chromidotilapini	NA	Moliwe	NA	NA
JWI5	F	Peltae	Pelvicachromis taeniatus	Chromidotilapini	NA	Moliwe	NA	NA
JWI6	F	Neopec	Neolamprologus pectoralis	Lamprologini	NA	NA	NA	NA
JXA1	NA	Telbri	Telmatochromis brichardi	Lamprologini	07.01.15	Nyaruhongoka 2	-3.698611111	29.32008333
JXA2	NA	Telbri	Telmatochromis brichardi	Lamprologini	07.01.15	Nyaruhongoka 2	-3.698611111	29.32008333
JXA3	NA	Telbri	Telmatochromis brichardi	Lamprologini	07.01.15	Nyaruhongoka 2	-3.698611111	29.32008333
JXA4	F	Telbri	Telmatochromis brichardi	Lamprologini	07.01.15	Nyaruhongoka 2	-3.698611111	29.32008333
JXA5	M	Telbri	Telmatochromis brichardi	Lamprologini	07.01.15	Nyaruhongoka 2	-3.698611111	29.32008333
JXA6	M	Telbri	Telmatochromis brichardi	Lamprologini	07.01.15	Nyaruhongoka 2	-3.698611111	29.32008333
JXA8	M	Telbri	Telmatochromis brichardi	Lamprologini	07.01.15	Nyaruhongoka 2	-3.698611111	29.32008333
JXA9	M	Telbri	Telmatochromis brichardi	Lamprologini	07.01.15	Nyaruhongoka 2	-3.698611111	29.32008333
JXB2	M	Telbri	Telmatochromis brichardi	Lamprologini	07.01.15	Nyaruhongoka 2	-3.698611111	29.32008333
JXB3	M	Telbri	Telmatochromis brichardi	Lamprologini	07.01.15	Nyaruhongoka 2	-3.698611111	29.32008333
JXB4	M	Telbri	Telmatochromis brichardi	Lamprologini	07.01.15	Nyaruhongoka 2	-3.698611111	29.32008333
JXB5	M	JulmaN	Julidochromis marlieri	Lamprologini	07.01.15	Nyaruhongoka 2	-3.698611111	29.32008333
JXB6	NA	JulmaN	Julidochromis marlieri	Lamprologini	07.01.15	Nyaruhongoka 2	-3.698611111	29.32008333
JXB7	NA	JulmaN	Julidochromis marlieri	Lamprologini	07.01.15	Nyaruhongoka 2	-3.698611111	29.32008333
JXB8	NA	JulmaN	Julidochromis marlieri	Lamprologini	07.01.15	Nyaruhongoka 2	-3.698611111	29.32008333
JXB9	NA	JulmaN	Julidochromis marlieri	Lamprologini	07.01.15	Nyaruhongoka 2	-3.698611111	29.32008333
JXC1	F	JulmaN	Julidochromis marlieri	Lamprologini	07.01.15	Nyaruhongoka 2	-3.698611111	29.32008333
JXC2	NA	JulmaN	Julidochromis marlieri	Lamprologini	07.01.15	Nyaruhongoka 2	-3.698611111	29.32008333
JXC3	NA	JulmaN	Julidochromis marlieri	Lamprologini	07.01.15	Nyaruhongoka 2	-3.698611111	29.32008333
JXC4	NA	JulmaN	Julidochromis marlieri	Lamprologini	07.01.15	Nyaruhongoka 2	-3.698611111	29.32008333
JXC6	NA	JulmaN	Julidochromis marlieri	Lamprologini	07.01.15	Nyaruhongoka 2	-3.698611111	29.32008333
JXC7	NA	JulmaN	Julidochromis marlieri	Lamprologini	07.01.15	Nyaruhongoka 2	-3.698611111	29.32008333
JXC9	NA	JulmaN	Julidochromis marlieri	Lamprologini	07.01.15	Nyaruhongoka 2	-3.698611111	29.32008333
JXD2	F	Petpol	Petrochromis polyodon	Tropheini	07.01.15	Nyaruhongoka 2	-3.698611111	29.32008333
JXD4	M	Neofal	Neolamprologus falcicula	Lamprologini	08.01.15	Nyaruhongoka 2	-3.698611111	29.32008333
JXD5	NA	Neofal	Neolamprologus falcicula	Lamprologini	08.01.15	Nyaruhongoka 2	-3.698611111	29.32008333
JXD6	NA	Neofal	Neolamprologus falcicula	Lamprologini	08.01.15	Nyaruhongoka 2	-3.698611111	29.32008333
JXD7	F	Neofal	Neolamprologus falcicula	Lamprologini	08.01.15	Nyaruhongoka 2	-3.698611111	29.32008333
JXD8	NA	Neofal	Neolamprologus falcicula	Lamprologini	08.01.15	Nyaruhongoka 2	-3.698611111	29.32008333
JXD9	NA	Neofal	Neolamprologus falcicula	Lamprologini	08.01.15	Nyaruhongoka 2	-3.698611111	29.32008333
JXE1	NA	Neofal	Neolamprologus falcicula	Lamprologini	08.01.15	Nyaruhongoka 2	-3.698611111	29.32008333
JXE3	NA	Neofal	Neolamprologus falcicula	Lamprologini	08.01.15	Nyaruhongoka 2	-3.698611111	29.32008333
JXE4	NA	Neofal	Neolamprologus falcicula	Lamprologini	08.01.15	Nyaruhongoka 2	-3.698611111	29.32008333
JXE5	NA	Neofal	Neolamprologus falcicula	Lamprologini	08.01.15	Nyaruhongoka 2	-3.698611111	29.32008333
JXE7	NA	Neosav	Neolamprologus savoryi	Lamprologini	08.01.15	Nyaruhongoka 2	-3.698611111	29.32008333
JXE9	M	Eremar	Eretmodus marksmithi	Eretmodini	08.01.15	Nyaruhongoka 2	-3.698611111	29.32008333
JXF1	F	Eremar	Eretmodus marksmithi	Eretmodini	08.01.15	Nyaruhongoka 2	-3.698611111	29.32008333
JXF2	F	Eremar	Eretmodus marksmithi	Eretmodini	08.01.15	Nyaruhongoka 2	-3.698611111	29.32008333
JXF3	F	Eremar	Eretmodus marksmithi	Eretmodini	08.01.15	Nyaruhongoka 2	-3.698611111	29.32008333
JXF4	F	Eremar	Eretmodus marksmithi	Eretmodini	08.01.15	Nyaruhongoka 2	-3.698611111	29.32008333
JXF5	F	Eremar	Eretmodus marksmithi	Eretmodini	08.01.15	Nyaruhongoka 2	-3.698611111	29.32008333
JXF6	M	Eremar	Eretmodus marksmithi	Eretmodini	08.01.15	Nyaruhongoka 2	-3.698611111	29.32008333
JXF7	F	Eremar	Eretmodus marksmithi	Eretmodini	08.01.15	Nyaruhongoka 2	-3.698611111	29.32008333
JXF9	M	Eremar	Eretmodus marksmithi	Eretmodini	08.01.15	Nyaruhongoka 2	-3.698611111	29.32008333
JXG1	F	Eremar	Eretmodus marksmithi	Eretmodini	08.01.15	Nyaruhongoka 2	-3.698611111	29.32008333
JXG3	M	Eremar	Eretmodus marksmithi	Eretmodini	08.01.15	Nyaruhongoka 2	-3.698611111	29.32008333
JXG4	F	Eremar	Eretmodus marksmithi	Eretmodini	08.01.15	Nyaruhongoka 2	-3.698611111	29.32008333
JXG5	M	Lamkun	Lamprologus kungweensis	Lamprologini	08.01.15	Nyaruhongoka 2	-3.698611111	29.32008333
JXG6	M	Lamkun	Lamprologus kungweensis	Lamprologini	08.01.15	Nyaruhongoka 2	-3.698611111	29.32008333
JXG7	M	Lamkun	Lamprologus kungweensis	Lamprologini	08.01.15	Nyaruhongoka 2	-3.698611111	29.32008333
JXG8	M	Lamkun	Lamprologus kungweensis	Lamprologini	08.01.15	Nyaruhongoka 2	-3.698611111	29.32008333
JXG9	M	Lamkun	Lamprologus kungweensis	Lamprologini	08.01.15	Nyaruhongoka 2	-3.698611111	29.32008333
JXH1	F	Lamkun	Lamprologus kungweensis	Lamprologini	08.01.15	Nyaruhongoka 2	-3.698611111	29.32008333
JXH2	F	Lamkun	Lamprologus kungweensis	Lamprologini	08.01.15	Nyaruhongoka 2	-3.698611111	29.32008333
JXH3	F	Lamkun	Lamprologus kungweensis	Lamprologini	08.01.15	Nyaruhongoka 2	-3.698611111	29.32008333
JXH4	F	Petort	Petrochromis orthognathus	Tropheini	08.01.15	Nyaruhongoka 2	-3.698611111	29.32008333
JXH5	M	Petort	Petrochromis orthognathus	Tropheini	08.01.15	Nyaruhongoka 2	-3.698611111	29.32008333
JXH6	M	Petort	Petrochromis orthognathus	Tropheini	08.01.15	Nyaruhongoka 2	-3.698611111	29.32008333
JXH7	NA	Petort	Petrochromis orthognathus	Tropheini	08.01.15	Nyaruhongoka 2	-3.698611111	29.32008333
JXI1	NA	Petfam	Petrochromis famula	Tropheini	08.01.15	Nyaruhongoka 2	-3.698611111	29.32008333
JXI2	M	PcybrN	Paracyprichromis brieni	Cyprichromini	09.01.15	Nyaruhongoka 2	-3.698611111	29.32008333
JXI4	F	PcybrN	Paracyprichromis brieni	Cyprichromini	09.01.15	Nyaruhongoka 2	-3.698611111	29.32008333
JXI7	M	PcybrN	Paracyprichromis brieni	Cyprichromini	09.01.15	Nyaruhongoka 2	-3.698611111	29.32008333
JXI8	M	PcybrN	Paracyprichromis brieni	Cyprichromini	09.01.15	Nyaruhongoka 2	-3.698611111	29.32008333
JXI9	M	PcybrN	Paracyprichromis brieni	Cyprichromini	09.01.15	Nyaruhongoka 2	-3.698611111	29.32008333
JYA1	M	PcybrN	Paracyprichromis brieni	Cyprichromini	09.01.15	Nyaruhongoka 2	-3.698611111	29.32008333
JYA2	M	PcybrN	Paracyprichromis brieni	Cyprichromini	09.01.15	Nyaruhongoka 2	-3.698611111	29.32008333
JYA3	F	PcybrN	Paracyprichromis brieni	Cyprichromini	09.01.15	Nyaruhongoka 2	-3.698611111	29.32008333
JYA4	F	PcybrN	Paracyprichromis brieni	Cyprichromini	09.01.15	Nyaruhongoka 2	-3.698611111	29.32008333
JYA5	F	PcybrN	Paracyprichromis brieni	Cyprichromini	09.01.15	Nyaruhongoka 2	-3.698611111	29.32008333
JYA6	F	PcybrN	Paracyprichromis brieni	Cyprichromini	09.01.15	Nyaruhongoka 2	-3.698611111	29.32008333
JYA7	F	PcybrN	Paracyprichromis brieni	Cyprichromini	09.01.15	Nyaruhongoka 2	-3.698611111	29.32008333
JYC1	M	Neofur	Neolamprologus furcifer	Lamprologini	09.01.15	Nyaruhongoka 2	-3.698611111	29.32008333
JYC2	F	Ophnas	Ophthalmotilapia nasuta	Ectodini	09.01.15	Nyaruhongoka 2	-3.698611111	29.32008333
JYD1	NA	Altcom	Altolamprologus compressiceps	Lamprologini	09.01.15	Nyaruhongoka 2	-3.698611111	29.32008333
JYD2	NA	Altcom	Altolamprologus compressiceps	Lamprologini	07.01.15	Nyaruhongoka 2	-3.698611111	29.32008333
JYD3	M	Hplsta	Haplochromis stappersii	Haplochromini	10.01.15	Bujumbura Creek	-3.391916667	29.34941667
JYD5	F	Astbur	Astatotilapia burtoni	Haplochromini	10.01.15	Bujumbura Creek	-3.391916667	29.34941667
JYF4	NA	Cphfr5	Cyphotilapia sp. "5-bar frontosa"	Cyphotilapiini	10.01.15	Nyaruhongoka 2	-3.698611111	29.32008333
JYF5	F	Cphfr5	Cyphotilapia sp. "5-bar frontosa"	Cyphotilapiini	10.01.15	Nyaruhongoka 2	-3.698611111	29.32008333
JYF6	NA	Batfas	Bathybates fasciatus	Bathybatini	10.01.15	Nyaruhongoka 2	-3.698611111	29.32008333
JYF7	M	Ophpar	Ophthalmotilapia sp. "paranasuta"	Ectodini	11.01.15	Nyanza Lac	-4.240777778	29.55011111
JYF8	M	Ophpar	Ophthalmotilapia sp. "paranasuta"	Ectodini	11.01.15	Nyanza Lac	-4.240777778	29.55011111
JYF9	M	Ophpar	Ophthalmotilapia sp. "paranasuta"	Ectodini	11.01.15	Nyanza Lac	-4.240777778	29.55011111
JYG2	M	Ophpar	Ophthalmotilapia sp. "paranasuta"	Ectodini	11.01.15	Nyanza Lac	-4.240777778	29.55011111
JYG3	M	Ophpar	Ophthalmotilapia sp. "paranasuta"	Ectodini	11.01.15	Nyanza Lac	-4.240777778	29.55011111
JYG4	M	Ophpar	Ophthalmotilapia sp. "paranasuta"	Ectodini	11.01.15	Nyanza Lac	-4.240777778	29.55011111
JYG5	F	Ophpar	Ophthalmotilapia sp. "paranasuta"	Ectodini	11.01.15	Nyanza Lac	-4.240777778	29.55011111
JYG6	M	Ophpar	Ophthalmotilapia sp. "paranasuta"	Ectodini	11.01.15	Nyanza Lac	-4.240777778	29.55011111
JYG7	M	Ophpar	Ophthalmotilapia sp. "paranasuta"	Ectodini	11.01.15	Nyanza Lac	-4.240777778	29.55011111
JYG8	M	Ophpar	Ophthalmotilapia sp. "paranasuta"	Ectodini	11.01.15	Nyanza Lac	-4.240777778	29.55011111
JYG9	F	Ophpar	Ophthalmotilapia sp. "paranasuta"	Ectodini	11.01.15	Nyanza Lac	-4.240777778	29.55011111
JYH1	F	Ophpar	Ophthalmotilapia sp. "paranasuta"	Ectodini	11.01.15	Nyanza Lac	-4.240777778	29.55011111
JYH3	M	Tanirs	Tanganicodus irsacae	Eretmodini	11.01.15	Nyanza Lac	-4.240777778	29.55011111
JYH4	M	Tanirs	Tanganicodus irsacae	Eretmodini	11.01.15	Nyanza Lac	-4.240777778	29.55011111
JYH5	M	Tanirs	Tanganicodus irsacae	Eretmodini	11.01.15	Nyanza Lac	-4.240777778	29.55011111
JYH6	F	Tanirs	Tanganicodus irsacae	Eretmodini	11.01.15	Nyanza Lac	-4.240777778	29.55011111

JYH7	F	Tanirs	Tanganicodus irsacae	Eretmodini	11.01.15	Nyanza Lac	-4.240777778	29.55011111
JYH8	M	Tanirs	Tanganicodus irsacae	Eretmodini	11.01.15	Nyanza Lac	-4.240777778	29.55011111
JYH9	M	Tanirs	Tanganicodus irsacae	Eretmodini	11.01.15	Nyanza Lac	-4.240777778	29.55011111
JYI1	F	Tanirs	Tanganicodus irsacae	Eretmodini	11.01.15	Nyanza Lac	-4.240777778	29.55011111
JYI3	F	Tanirs	Tanganicodus irsacae	Eretmodini	11.01.15	Nyanza Lac	-4.240777778	29.55011111
JYI4	M	Tanirs	Tanganicodus irsacae	Eretmodini	11.01.15	Nyanza Lac	-4.240777778	29.55011111
JYI5	M	Tanirs	Tanganicodus irsacae	Eretmodini	11.01.15	Nyanza Lac	-4.240777778	29.55011111
JYI6	M	Tanirs	Tanganicodus irsacae	Eretmodini	11.01.15	Nyanza Lac	-4.240777778	29.55011111
JYI8	M	Trobri	Tropheus brichardi	Tropheini	11.01.15	Nyanza Lac	-4.240777778	29.55011111
JYI9	NA	Trobri	Tropheus brichardi	Tropheini	11.01.15	Nyanza Lac	-4.240777778	29.55011111
JZA1	NA	Trobri	Tropheus brichardi	Tropheini	11.01.15	Nyanza Lac	-4.240777778	29.55011111
JZA2	NA	Trobri	Tropheus brichardi	Tropheini	11.01.15	Nyanza Lac	-4.240777778	29.55011111
JZA3	F	Trobri	Tropheus brichardi	Tropheini	11.01.15	Nyanza Lac	-4.240777778	29.55011111
JZA4	NA	Trobri	Tropheus brichardi	Tropheini	11.01.15	Nyanza Lac	-4.240777778	29.55011111
JZA5	NA	Trobri	Tropheus brichardi	Tropheini	11.01.15	Nyanza Lac	-4.240777778	29.55011111
JZA6	NA	Trobri	Tropheus brichardi	Tropheini	11.01.15	Nyanza Lac	-4.240777778	29.55011111
JZA8	NA	Trobri	Tropheus brichardi	Tropheini	11.01.15	Nyanza Lac	-4.240777778	29.55011111
JZA9	NA	Trobri	Tropheus brichardi	Tropheini	11.01.15	Nyanza Lac	-4.240777778	29.55011111
JZB1	NA	Trobri	Tropheus brichardi	Tropheini	11.01.15	Nyanza Lac	-4.240777778	29.55011111
JZB2	NA	Trobri	Tropheus brichardi	Tropheini	11.01.15	Nyanza Lac	-4.240777778	29.55011111
JZB4	M	Spamar	Spathodus marlieri	Eretmodini	11.01.15	Nyanza Lac	-4.240777778	29.55011111
JZB5	M	Spamar	Spathodus marlieri	Eretmodini	11.01.15	Nyanza Lac	-4.240777778	29.55011111
JZB6	M	Spamar	Spathodus marlieri	Eretmodini	11.01.15	Nyanza Lac	-4.240777778	29.55011111
JZB7	M	Spamar	Spathodus marlieri	Eretmodini	11.01.15	Nyanza Lac	-4.240777778	29.55011111
JZB8	M	Spamar	Spathodus marlieri	Eretmodini	11.01.15	Nyanza Lac	-4.240777778	29.55011111
JZB9	F	Spamar	Spathodus marlieri	Eretmodini	11.01.15	Nyanza Lac	-4.240777778	29.55011111
JZC1	M	Spamar	Spathodus marlieri	Eretmodini	11.01.15	Nyanza Lac	-4.240777778	29.55011111
JZC2	F	Spamar	Spathodus marlieri	Eretmodini	11.01.15	Nyanza Lac	-4.240777778	29.55011111
JZC4	F	Spamar	Spathodus marlieri	Eretmodini	11.01.15	Nyanza Lac	-4.240777778	29.55011111
JZC5	F	Spamar	Spathodus marlieri	Eretmodini	11.01.15	Nyanza Lac	-4.240777778	29.55011111
JZC6	F	Spamar	Spathodus marlieri	Eretmodini	11.01.15	Nyanza Lac	-4.240777778	29.55011111
JZC8	NA	Petort	Petrochromis orthognathus	Tropheini	10.01.15	Nyaruhongoka 2	-3.698611111	29.32008333
JZC9	NA	Petort	Petrochromis orthognathus	Tropheini	10.01.15	Nyaruhongoka 2	-3.698611111	29.32008333
JZD1	NA	Petort	Petrochromis orthognathus	Tropheini	10.01.15	Nyaruhongoka 2	-3.698611111	29.32008333
JZD2	NA	Petort	Petrochromis orthognathus	Tropheini	10.01.15	Nyaruhongoka 2	-3.698611111	29.32008333
JZD3	F	Spamar	Spathodus marlieri	Eretmodini	11.01.15	Nyanza Lac	-4.240777778	29.55011111
JZD4	NA	Neotoa	Neolamprologus toae	Lamprologini	11.01.15	Nyanza Lac	-4.240777778	29.55011111
JZD5	M	Neotoa	Neolamprologus toae	Lamprologini	11.01.15	Nyanza Lac	-4.240777778	29.55011111
JZD6	F	Neotoa	Neolamprologus toae	Lamprologini	11.01.15	Nyanza Lac	-4.240777778	29.55011111
JZD7	M	Lamkun	Lamprologus kungweensis	Lamprologini	10.01.15	Nyaruhongoka 2	-3.698611111	29.32008333
JZD8	M	Lamkun	Lamprologus kungweensis	Lamprologini	10.01.15	Nyaruhongoka 2	-3.698611111	29.32008333
JZD9	M	Lamkun	Lamprologus kungweensis	Lamprologini	10.01.15	Nyaruhongoka 2	-3.698611111	29.32008333
JZE1	F	Lamkun	Lamprologus kungweensis	Lamprologini	10.01.15	Nyaruhongoka 2	-3.698611111	29.32008333
JZE2	M	Calple	Callochromis pleurospilus	Ectodini	12.01.15	Bujumbura fishmarket	-3.347833333	29.29777778
JZE4	F	Calple	Callochromis pleurospilus	Ectodini	12.01.15	Bujumbura fishmarket	-3.347833333	29.29777778
JZE6	M	Xenorn	Xenotilapia ornatipinnis	Ectodini	12.01.15	Bujumbura fishmarket	-3.347833333	29.29777778
JZE8	F	Xenorn	Xenotilapia ornatipinnis	Ectodini	12.01.15	Bujumbura fishmarket	-3.347833333	29.29777778
JZF1	M	Neople	Neolamprologus pleuromaculatus	Lamprologini	12.01.15	Bujumbura fishmarket	-3.347833333	29.29777778
JZF2	F	Neople	Neolamprologus pleuromaculatus	Lamprologini	12.01.15	Bujumbura fishmarket	-3.347833333	29.29777778
JZF3	M	Lamorn	Lamprologus ornatipinnis	Lamprologini	12.01.15	Bujumbura fishmarket	-3.347833333	29.29777778
JZF4	F	Lamorn	Lamprologus ornatipinnis	Lamprologini	12.01.15	Bujumbura fishmarket	-3.347833333	29.29777778
JZF5	M	Calple	Callochromis pleurospilus	Ectodini	12.01.15	Bujumbura fishmarket	-3.347833333	29.29777778
JZF6	M	Calple	Callochromis pleurospilus	Ectodini	12.01.15	Bujumbura fishmarket	-3.347833333	29.29777778
JZF7	M	Calple	Callochromis pleurospilus	Ectodini	12.01.15	Bujumbura fishmarket	-3.347833333	29.29777778
JZF8	M	Calple	Callochromis pleurospilus	Ectodini	12.01.15	Bujumbura fishmarket	-3.347833333	29.29777778
JZF9	M	Calple	Callochromis pleurospilus	Ectodini	12.01.15	Bujumbura fishmarket	-3.347833333	29.29777778
JZG1	M	Calple	Callochromis pleurospilus	Ectodini	12.01.15	Bujumbura fishmarket	-3.347833333	29.29777778
JZG2	F	Calple	Callochromis pleurospilus	Ectodini	12.01.15	Bujumbura fishmarket	-3.347833333	29.29777778
JZG3	F	Calple	Callochromis pleurospilus	Ectodini	12.01.15	Bujumbura fishmarket	-3.347833333	29.29777778
JZG4	F	Calple	Callochromis pleurospilus	Ectodini	12.01.15	Bujumbura fishmarket	-3.347833333	29.29777778
JZG5	F	Calple	Callochromis pleurospilus	Ectodini	12.01.15	Bujumbura fishmarket	-3.347833333	29.29777778
JZG6	M	Xenlon	Xenotilapia longispinis	Ectodini	12.01.15	Bujumbura fishmarket	-3.347833333	29.29777778
JZG7	F	Xenlon	Xenotilapia longispinis	Ectodini	12.01.15	Bujumbura fishmarket	-3.347833333	29.29777778
JZG8	NA	Neople	Neolamprologus pleuromaculatus	Lamprologini	12.01.15	Bujumbura fishmarket	-3.347833333	29.29777778
JZG9	NA	Neople	Neolamprologus pleuromaculatus	Lamprologini	12.01.15	Bujumbura fishmarket	-3.347833333	29.29777778
JZH1	NA	Neople	Neolamprologus pleuromaculatus	Lamprologini	12.01.15	Bujumbura fishmarket	-3.347833333	29.29777778
JZH2	M	Calmel	Callochromis melanostigma	Ectodini	12.01.15	Bujumbura fishmarket	-3.347833333	29.29777778
JZH3	F	Calmel	Callochromis melanostigma	Ectodini	12.01.15	Bujumbura fishmarket	-3.347833333	29.29777778
JZI1	M	Xenorn	Xenotilapia ornatipinnis	Ectodini	12.01.15	Bujumbura fishmarket	-3.347833333	29.29777778
JZI2	M	Xenorn	Xenotilapia ornatipinnis	Ectodini	12.01.15	Bujumbura fishmarket	-3.347833333	29.29777778
JZI3	M	Xenorn	Xenotilapia ornatipinnis	Ectodini	12.01.15	Bujumbura fishmarket	-3.347833333	29.29777778
JZI4	F	Xenorn	Xenotilapia ornatipinnis	Ectodini	12.01.15	Bujumbura fishmarket	-3.347833333	29.29777778
JZI5	F	Xenorn	Xenotilapia ornatipinnis	Ectodini	12.01.15	Bujumbura fishmarket	-3.347833333	29.29777778
JZI6	F	Xenorn	Xenotilapia ornatipinnis	Ectodini	12.01.15	Bujumbura fishmarket	-3.347833333	29.29777778
JZI7	F	Xenorn	Xenotilapia ornatipinnis	Ectodini	12.01.15	Bujumbura fishmarket	-3.347833333	29.29777778
JZI8	F	Xenorn	Xenotilapia ornatipinnis	Ectodini	12.01.15	Bujumbura fishmarket	-3.347833333	29.29777778
JZI9	F	Xenorn	Xenotilapia ornatipinnis	Ectodini	12.01.15	Bujumbura fishmarket	-3.347833333	29.29777778
KAA1	F	Xenorn	Xenotilapia ornatipinnis	Ectodini	12.01.15	Bujumbura fishmarket	-3.347833333	29.29777778
KAA2	NA	Lchaur	Limnochromis auritus	Limnochromini	12.01.15	Bujumbura fishmarket	-3.347833333	29.29777778
KAA5	NA	Lamorn	Lamprologus ornatipinnis	Lamprologini	12.01.15	Bujumbura fishmarket	-3.347833333	29.29777778
KAA6	NA	Lamorn	Lamprologus ornatipinnis	Lamprologini	12.01.15	Bujumbura fishmarket	-3.347833333	29.29777778
KAA7	NA	Lamorn	Lamprologus ornatipinnis	Lamprologini	12.01.15	Bujumbura fishmarket	-3.347833333	29.29777778
KAA8	NA	Lamorn	Lamprologus ornatipinnis	Lamprologini	12.01.15	Bujumbura fishmarket	-3.347833333	29.29777778
KAA9	NA	Lamorn	Lamprologus ornatipinnis	Lamprologini	12.01.15	Bujumbura fishmarket	-3.347833333	29.29777778
KAC4	F	Cphfr5	Cyphotilapia sp. "5-bar frontosa"	Cyphotilapiini	12.01.15	Nyaruhongoka 2	-3.698611111	29.32008333
KAC5	F	Cphfr5	Cyphotilapia sp. "5-bar frontosa"	Cyphotilapiini	12.01.15	Nyaruhongoka 2	-3.698611111	29.32008333
KAC6	NA	Neotoa	Neolamprologus toae	Lamprologini	11.01.15	Nyanza Lac	-4.240777778	29.55011111
KAC7	NA	Neotoa	Neolamprologus toae	Lamprologini	11.01.15	Nyanza Lac	-4.240777778	29.55011111
KAC8	NA	Neotoa	Neolamprologus toae	Lamprologini	11.01.15	Nyanza Lac	-4.240777778	29.55011111
KAC9	NA	Neotoa	Neolamprologus toae	Lamprologini	11.01.15	Nyanza Lac	-4.240777778	29.55011111
KAD1	NA	Neofur	Neolamprologus furcifer	Lamprologini	12.01.15	Nyaruhongoka 2	-3.698611111	29.32008333
KAD2	M	Leppro	Lepidiolamprologus profundicola	Lamprologini	12.01.15	Nyaruhongoka 2	-3.698611111	29.32008333
KAD3	F	Cphfr5	Cyphotilapia sp. "5-bar frontosa"	Cyphotilapiini	12.01.15	Nyaruhongoka 2	-3.698611111	29.32008333
KAD4	F	NeoveB	Neolamprologus ventralis (Burundi)	Lamprologini	14.01.15	Nyaruhongoka 2	-3.698611111	29.32008333
KAD5	F	NeoveB	Neolamprologus ventralis (Burundi)	Lamprologini	14.01.15	Nyaruhongoka 2	-3.698611111	29.32008333
KAD6	M	Batmin	Bathybates minor	Bathybatini	14.01.15	Bujumbura fishmarket	-3.347833333	29.29777778
KAD8	M	Cphfr5	Cyphotilapia sp. "5-bar frontosa"	Cyphotilapiini	14.01.15	Nyaruhongoka 2	-3.698611111	29.32008333
KAD9	M	Cphfr5	Cyphotilapia sp. "5-bar frontosa"	Cyphotilapiini	14.01.15	Nyaruhongoka 2	-3.698611111	29.32008333
KAE1	F	Batleo	Bathybates leo	Bathybatini	14.01.15	Bujumbura fishmarket	-3.347833333	29.29777778
KAE3	M	Trespn	Trematocara sp. "new species"	Trematocarini	14.01.15	Bujumbura fishmarket	-3.347833333	29.29777778
KAE4	M	Ctehor	Ctenochromis horei	Tropheini	14.01.15	Nyaruhongoka 2	-3.698611111	29.32008333
KAE5	NA	Lepelo	Lepidiolamprologus elongatus	Lamprologini	14.01.15	Nyaruhongoka 2	-3.698611111	29.32008333
KAE6	NA	Xenbou	Xenotilapia boulengeri	Ectodini	14.01.15	Nyaruhongoka 2	-3.698611111	29.32008333
KAE8	M	Arcstr	Astatoreochromis straeleni	Haplochromini	14.01.15	Rusizi 2 (Gatumba)	-3.337888889	29.27383333
KAF1	M	Carsch	Cardiopharynx schoutedeni	Ectodini	15.01.15	Bujumbura fishmarket	-3.347833333	29.29777778
KAF2	F	Carsch	Cardiopharynx schoutedeni	Ectodini	15.01.15	Bujumbura fishmarket	-3.347833333	29.29777778
KAF3	M	Calmel	Callochromis melanostigma	Ectodini	15.01.15	Bujumbura fishmarket	-3.347833333	29.29777778
KAF4	F	Calmel	Callochromis melanostigma	Ectodini	15.01.15	Bujumbura fishmarket	-3.347833333	29.29777778
KAF5	M	Xenlon	Xenotilapia longispinis	Ectodini	15.01.15	Bujumbura fishmarket	-3.347833333	29.29777778
KAF6	F	Xenlon	Xenotilapia longispinis	Ectodini	15.01.15	Bujumbura fishmarket	-3.347833333	29.29777778
KAG3	M	Cphfr5	Cyphotilapia sp. "5-bar frontosa"	Cyphotilapiini	15.01.15	Nyaruhongoka 2	-3.698611111	29.32008333
KAG4	M	Ophnas	Ophthalmotilapia nasuta	Ectodini	15.01.15	Nyaruhongoka 2	-3.698611111	29.32008333
KAG6	NA	Permic	Perissodus microlepis	Perissodini	15.01.15	Nyaruhongoka 2	-3.698611111	29.32008333
KAG7	M	NeoveB	Neolamprologus ventralis (Burundi)	Lamprologini	15.01.15	Nyaruhongoka 2	-3.698611111	29.32008333
KAG8	F	NeoveB	Neolamprologus ventralis (Burundi)	Lamprologini	15.01.15	Nyaruhongoka 2	-3.698611111	29.32008333
KAG9	F	NeoveB	Neolamprologus ventralis (Burundi)	Lamprologini	15.01.15	Nyaruhongoka 2	-3.698611111	29.32008333
KAH2	M	Xenlon	Xenotilapia longispinis	Ectodini	15.01.15	Bujumbura fishmarket	-3.347833333	29.29777778
KAH3	M	Xenlon	Xenotilapia longispinis	Ectodini	15.01.15	Bujumbura fishmarket	-3.347833333	29.29777778
KAH4	M	Xenlon	Xenotilapia longispinis	Ectodini	15.01.15	Bujumbura fishmarket	-3.347833333	29.29777778
KAH5	M	Xenlon	Xenotilapia longispinis	Ectodini	15.01.15	Bujumbura fishmarket	-3.347833333	29.29777778
KAH6	F	Xenlon	Xenotilapia longispinis	Ectodini	15.01.15	Bujumbura fishmarket	-3.347833333	29.29777778
KAH7	F	Xenlon	Xenotilapia longispinis	Ectodini	15.01.15	Bujumbura fishmarket	-3.347833333	29.29777778
KAH8	F	Xenlon	Xenotilapia longispinis	Ectodini	15.01.15	Bujumbura fishmarket	-3.347833333	29.29777778
KAH9	M	Xenlon	Xenotilapia longispinis	Ectodini	15.01.15	Bujumbura fishmarket	-3.347833333	29.29777778

KAI4	F	Calmel	Callochromis melanostigma	Ectodini	15.01.15	Bujumbura fishmarket	-3.347833333	29.29777778
KAI5	M	Calmel	Callochromis melanostigma	Ectodini	15.01.15	Bujumbura fishmarket	-3.347833333	29.29777778
KAI6	M	Calmel	Callochromis melanostigma	Ectodini	15.01.15	Bujumbura fishmarket	-3.347833333	29.29777778
KAI7	M	Calmel	Callochromis melanostigma	Ectodini	15.01.15	Bujumbura fishmarket	-3.347833333	29.29777778
KAI8	NA	Calmel	Callochromis melanostigma	Ectodini	15.01.15	Bujumbura fishmarket	-3.347833333	29.29777778
KAI9	NA	Trioto	Triglachromis otostigma	Limnochromini	15.01.15	Bujumbura fishmarket	-3.347833333	29.29777778
KCA1	NA	Trioto	Triglachromis otostigma	Limnochromini	15.01.15	Bujumbura fishmarket	-3.347833333	29.29777778
KCA2	NA	Tylpol	Tylochromis polylepis	Tylochromini	15.01.15	Bujumbura fishmarket	-3.347833333	29.29777778
KCA3	NA	Tylpol	Tylochromis polylepis	Tylochromini	15.01.15	Bujumbura fishmarket	-3.347833333	29.29777778
KCA4	M	Carsch	Cardiopharynx schoutedeni	Ectodini	15.01.15	Bujumbura fishmarket	-3.347833333	29.29777778
KCA5	M	Carsch	Cardiopharynx schoutedeni	Ectodini	15.01.15	Bujumbura fishmarket	-3.347833333	29.29777778
KCA6	F	Carsch	Cardiopharynx schoutedeni	Ectodini	15.01.15	Bujumbura fishmarket	-3.347833333	29.29777778
KCA7	F	Carsch	Cardiopharynx schoutedeni	Ectodini	15.01.15	Bujumbura fishmarket	-3.347833333	29.29777778
KCA8	F	Carsch	Cardiopharynx schoutedeni	Ectodini	15.01.15	Bujumbura fishmarket	-3.347833333	29.29777778
KCA9	F	Carsch	Cardiopharynx schoutedeni	Ectodini	15.01.15	Bujumbura fishmarket	-3.347833333	29.29777778
KCB1	F	Carsch	Cardiopharynx schoutedeni	Ectodini	15.01.15	Bujumbura fishmarket	-3.347833333	29.29777778
KCB2	F	Carsch	Cardiopharynx schoutedeni	Ectodini	15.01.15	Bujumbura fishmarket	-3.347833333	29.29777778
KCB3	F	Carsch	Cardiopharynx schoutedeni	Ectodini	15.01.15	Bujumbura fishmarket	-3.347833333	29.29777778
KCB4	F	Carsch	Cardiopharynx schoutedeni	Ectodini	15.01.15	Bujumbura fishmarket	-3.347833333	29.29777778
KCB8	NA	Batleo	Bathybates leo	Bathybatini	15.01.15	Bujumbura fishmarket	-3.347833333	29.29777778
KCB9	NA	Batleo	Bathybates leo	Bathybatini	15.01.15	Bujumbura fishmarket	-3.347833333	29.29777778
KCC1	NA	Batleo	Bathybates leo	Bathybatini	15.01.15	Bujumbura fishmarket	-3.347833333	29.29777778
KCC2	NA	Batleo	Bathybates leo	Bathybatini	15.01.15	Bujumbura fishmarket	-3.347833333	29.29777778
KCC5	NA	Batleo	Bathybates leo	Bathybatini	15.01.15	Bujumbura fishmarket	-3.347833333	29.29777778
KCC7	NA	Batleo	Bathybates leo	Bathybatini	15.01.15	Bujumbura fishmarket	-3.347833333	29.29777778
KCC9	NA	Neotoa	Neolamprologus toae	Lamprologini	16.01.15	Nyanza Lac	-4.240777778	29.55011111
KCD1	NA	Neotoa	Neolamprologus toae	Lamprologini	16.01.15	Nyanza Lac	-4.240777778	29.55011111
KCD2	NA	Neotoa	Neolamprologus toae	Lamprologini	16.01.15	Nyanza Lac	-4.240777778	29.55011111
KCD3	NA	Neotoa	Neolamprologus toae	Lamprologini	16.01.15	Nyanza Lac	-4.240777778	29.55011111
KCD4	NA	Lamorn	Lamprologus ornatipinnis	Lamprologini	16.01.15	Nyanza Lac	-4.240777778	29.55011111
KCD6	M	Neobou	Neolamprologus boulengeri	Lamprologini	16.01.15	Nyanza Lac	-4.240777778	29.55011111
KCD7	NA	Neobou	Neolamprologus boulengeri	Lamprologini	16.01.15	Nyanza Lac	-4.240777778	29.55011111
KCD8	NA	Neobou	Neolamprologus boulengeri	Lamprologini	16.01.15	Nyanza Lac	-4.240777778	29.55011111
KCE1	F	Neobou	Neolamprologus boulengeri	Lamprologini	16.01.15	Nyanza Lac	-4.240777778	29.55011111
KCE2	NA	Neotoa	Neolamprologus toae	Lamprologini	16.01.15	Nyanza Lac	-4.240777778	29.55011111
KCE3	NA	Calmel	Callochromis melanostigma	Ectodini	16.01.15	Nyanza Lac	-4.240777778	29.55011111
KCE4	NA	Calmel	Callochromis melanostigma	Ectodini	16.01.15	Nyanza Lac	-4.240777778	29.55011111
KCE5	F	Neobou	Neolamprologus boulengeri	Lamprologini	16.01.15	Nyanza Lac	-4.240777778	29.55011111
KCE7	M	Pscmar	Pseudosimochromis marginatus	Tropheini	16.01.15	Nyanza Lac	-4.240777778	29.55011111
KCE9	F	Pscmar	Pseudosimochromis marginatus	Tropheini	16.01.15	Nyanza Lac	-4.240777778	29.55011111
KCF1	NA	Pscmar	Pseudosimochromis marginatus	Tropheini	16.01.15	Nyanza Lac	-4.240777778	29.55011111
KCF2	NA	Pscmar	Pseudosimochromis marginatus	Tropheini	16.01.15	Nyanza Lac	-4.240777778	29.55011111
KCF3	F	Pscmar	Pseudosimochromis marginatus	Tropheini	16.01.15	Nyanza Lac	-4.240777778	29.55011111
KCF4	NA	Pscmar	Pseudosimochromis marginatus	Tropheini	16.01.15	Nyanza Lac	-4.240777778	29.55011111
KCF5	NA	Pscmar	Pseudosimochromis marginatus	Tropheini	16.01.15	Nyanza Lac	-4.240777778	29.55011111
KCF6	NA	Pscmar	Pseudosimochromis marginatus	Tropheini	16.01.15	Nyanza Lac	-4.240777778	29.55011111
KCF8	NA	Pscmar	Pseudosimochromis marginatus	Tropheini	16.01.15	Nyanza Lac	-4.240777778	29.55011111
KCF9	NA	Pscmar	Pseudosimochromis marginatus	Tropheini	16.01.15	Nyanza Lac	-4.240777778	29.55011111
KCG1	NA	Pscmar	Pseudosimochromis marginatus	Tropheini	16.01.15	Nyanza Lac	-4.240777778	29.55011111
KCG2	M	Lamspe	Lamprologus speciosus	Lamprologini	16.01.15	Nyanza Lac	-4.240777778	29.55011111
KCG3	F	Lamspe	Lamprologus speciosus	Lamprologini	16.01.15	Nyanza Lac	-4.240777778	29.55011111
KCG4	M	Lamspe	Lamprologus speciosus	Lamprologini	16.01.15	Nyanza Lac	-4.240777778	29.55011111
KCG5	NA	Lamspe	Lamprologus speciosus	Lamprologini	16.01.15	Nyanza Lac	-4.240777778	29.55011111
KCG6	NA	Lamspe	Lamprologus speciosus	Lamprologini	16.01.15	Nyanza Lac	-4.240777778	29.55011111
KCG7	NA	Lamspe	Lamprologus speciosus	Lamprologini	16.01.15	Nyanza Lac	-4.240777778	29.55011111
KCG8	NA	Lamspe	Lamprologus speciosus	Lamprologini	16.01.15	Nyanza Lac	-4.240777778	29.55011111
KCG9	NA	Lamspe	Lamprologus speciosus	Lamprologini	16.01.15	Nyanza Lac	-4.240777778	29.55011111
KCH1	NA	Lamspe	Lamprologus speciosus	Lamprologini	16.01.15	Nyanza Lac	-4.240777778	29.55011111
KCH2	NA	Lamspe	Lamprologus speciosus	Lamprologini	16.01.15	Nyanza Lac	-4.240777778	29.55011111
KCH5	NA	NeobrM	Neolamprologus sp. "brevis magara"	Lamprologini	16.01.15	Nyanza Lac	-4.240777778	29.55011111
KCH6	NA	NeobrM	Neolamprologus sp. "brevis magara"	Lamprologini	16.01.15	Nyanza Lac	-4.240777778	29.55011111
KCH7	NA	NeobrM	Neolamprologus sp. "brevis magara"	Lamprologini	16.01.15	Nyanza Lac	-4.240777778	29.55011111
KCH8	NA	NeobrM	Neolamprologus sp. "brevis magara"	Lamprologini	16.01.15	Nyanza Lac	-4.240777778	29.55011111
KCH9	NA	NeobrM	Neolamprologus sp. "brevis magara"	Lamprologini	16.01.15	Nyanza Lac	-4.240777778	29.55011111
KCI1	NA	NeobrM	Neolamprologus sp. "brevis magara"	Lamprologini	16.01.15	Nyanza Lac	-4.240777778	29.55011111
KCI2	NA	NeobrM	Neolamprologus sp. "brevis magara"	Lamprologini	16.01.15	Nyanza Lac	-4.240777778	29.55011111
KCI3	NA	NeobrM	Neolamprologus sp. "brevis magara"	Lamprologini	16.01.15	Nyanza Lac	-4.240777778	29.55011111
KCI4	NA	NeobrM	Neolamprologus sp. "brevis magara"	Lamprologini	16.01.15	Nyanza Lac	-4.240777778	29.55011111
KCI5	NA	NeobrM	Neolamprologus sp. "brevis magara"	Lamprologini	16.01.15	Nyanza Lac	-4.240777778	29.55011111
KCI6	M	NeobrM	Neolamprologus sp. "brevis magara"	Lamprologini	16.01.15	Nyanza Lac	-4.240777778	29.55011111
KCI7	F	NeobrM	Neolamprologus sp. "brevis magara"	Lamprologini	16.01.15	Nyanza Lac	-4.240777778	29.55011111
KDC6	M	Ortmaz	Orthochromis mazimeroensis	Haplochromini	18.01.15	Mazimoero	-3.884722	30.19775
KDF2	F	Cphfr5	Cyphotilapia sp. "5-bar frontosa"	Cyphotilapiini	22.01.15	Nyaruhongoka 2	-3.698611111	29.32008333
KDF3	M	NeoveB	Neolamprologus ventralis (Burundi)	Lamprologini	22.01.15	Nyaruhongoka 2	-3.698611111	29.32008333
KDF4	F	NeoveB	Neolamprologus ventralis (Burundi)	Lamprologini	22.01.15	Nyaruhongoka 2	-3.698611111	29.32008333
KDF5	F	NeoveB	Neolamprologus ventralis (Burundi)	Lamprologini	22.01.15	Nyaruhongoka 2	-3.698611111	29.32008333
KDF6	M	Petort	Petrochromis orthognathus	Tropheini	22.01.15	Nyaruhongoka 2	-3.698611111	29.32008333
KDF7	NA	Neople	Neolamprologus pleuromaculatus	Lamprologini	22.01.15	Bujumbura fishmarket	-3.347833333	29.29777778
KDF8	NA	Petort	Petrochromis orthognathus	Tropheini	22.01.15	Nyanza Lac	-4.240777778	29.55011111
KDF9	M	Cphfr5	Cyphotilapia sp. "5-bar frontosa"	Cyphotilapiini	24.01.15	Nyaruhongoka 2	-3.698611111	29.32008333
KDG1	M	Cphfr5	Cyphotilapia sp. "5-bar frontosa"	Cyphotilapiini	24.01.15	Nyaruhongoka 2	-3.698611111	29.32008333
KDG2	F	Cphfr5	Cyphotilapia sp. "5-bar frontosa"	Cyphotilapiini	24.01.15	Nyaruhongoka 2	-3.698611111	29.32008333
KDG3	F	Cyprmic	Cyprichromis microlepidotus	Cyprichromini	24.01.15	Nyaruhongoka 2	-3.698611111	29.32008333
KDG4	NA	Cyprmic	Cyprichromis microlepidotus	Cyprichromini	24.01.15	Nyaruhongoka 2	-3.698611111	29.32008333
KEA1	F	Petkas	Petrochromis sp. "kazumbae"	Tropheini	24.06.15	Kaku	-4.896388889	29.61166667
KEA2	F	Petkas	Petrochromis sp. "kazumbae"	Tropheini	24.06.15	Kaku	-4.896388889	29.61166667
KEA3	M	Petkas	Petrochromis sp. "kazumbae"	Tropheini	24.06.15	Kaku	-4.896388889	29.61166667
KEA4	F	Petkas	Petrochromis sp. "kazumbae"	Tropheini	24.06.15	Kaku	-4.896388889	29.61166667
KEA5	M	Petkas	Petrochromis sp. "kazumbae"	Tropheini	24.06.15	Kaku	-4.896388889	29.61166667
KEA6	M	Petkas	Petrochromis sp. "kazumbae"	Tropheini	24.06.15	Kaku	-4.896388889	29.61166667
KEA7	M	Petkas	Petrochromis sp. "kazumbae"	Tropheini	24.06.15	Kaku	-4.896388889	29.61166667
KEA9	M	Petkas	Petrochromis sp. "kazumbae"	Tropheini	24.06.15	Kaku	-4.896388889	29.61166667
KEB1	M	Petkas	Petrochromis sp. "kazumbae"	Tropheini	24.06.15	Kaku	-4.896388889	29.61166667
KEB2	M	Petkas	Petrochromis sp. "kazumbae"	Tropheini	24.06.15	Kaku	-4.896388889	29.61166667
KEB3	M	Petkas	Petrochromis sp. "kazumbae"	Tropheini	24.06.15	Kaku	-4.896388889	29.61166667
KEB4	M	Petkas	Petrochromis sp. "kazumbae"	Tropheini	24.06.15	Kaku	-4.896388889	29.61166667
KEB7	M	Neoleu	Neolamprologus longior	Lamprologini	25.06.15	Cape Kabogo	-5.460833333	29.7475
KEB8	F	Leppro	Lepidiolamprologus profundicola	Lamprologini	25.06.15	Cape Kabogo	-5.460833333	29.7475
KEB9	F	Leppro	Lepidiolamprologus profundicola	Lamprologini	25.06.15	Cape Kabogo	-5.460833333	29.7475
KEC1	M	Neosim	Neolamprologus similis	Lamprologini	25.06.15	Cape Kabogo	-5.460833333	29.7475
KEC2	F	Neosim	Neolamprologus similis	Lamprologini	25.06.15	Cape Kabogo	-5.460833333	29.7475
KEC3	NA	Neosim	Neolamprologus similis	Lamprologini	25.06.15	Cape Kabogo	-5.460833333	29.7475
KEC4	NA	Neosim	Neolamprologus similis	Lamprologini	25.06.15	Cape Kabogo	-5.460833333	29.7475
KEC5	NA	Neosim	Neolamprologus similis	Lamprologini	25.06.15	Cape Kabogo	-5.460833333	29.7475
KEC8	NA	Neosim	Neolamprologus similis	Lamprologini	25.06.15	Cape Kabogo	-5.460833333	29.7475
KEC9	NA	Neosim	Neolamprologus similis	Lamprologini	25.06.15	Cape Kabogo	-5.460833333	29.7475
KED1	NA	Neosim	Neolamprologus similis	Lamprologini	25.06.15	Cape Kabogo	-5.460833333	29.7475
KED2	NA	Neosim	Neolamprologus similis	Lamprologini	25.06.15	Cape Kabogo	-5.460833333	29.7475
KED3	NA	Neosim	Neolamprologus similis	Lamprologini	25.06.15	Cape Kabogo	-5.460833333	29.7475
KED4	NA	Neosim	Neolamprologus similis	Lamprologini	25.06.15	Cape Kabogo	-5.460833333	29.7475
KED5	NA	Neosim	Neolamprologus similis	Lamprologini	25.06.15	Cape Kabogo	-5.460833333	29.7475
KED6	M	Trolun	Tropheus sp. "lunatus"	Tropheini	25.06.15	Cape Kabogo	-5.460833333	29.7475
KED7	F	Trolun	Tropheus sp. "lunatus"	Tropheini	25.06.15	Cape Kabogo	-5.460833333	29.7475
KED8	M	Trolun	Tropheus sp. "lunatus"	Tropheini	25.06.15	Cape Kabogo	-5.460833333	29.7475
KED9	F	Trolun	Tropheus sp. "lunatus"	Tropheini	25.06.15	Cape Kabogo	-5.460833333	29.7475
KEE1	F	Trolun	Tropheus sp. "lunatus"	Tropheini	25.06.15	Cape Kabogo	-5.460833333	29.7475
KEE2	F	Trolun	Tropheus sp. "lunatus"	Tropheini	25.06.15	Cape Kabogo	-5.460833333	29.7475
KEE3	M	Trolun	Tropheus sp. "lunatus"	Tropheini	25.06.15	Cape Kabogo	-5.460833333	29.7475
KEE4	F	Trolun	Tropheus sp. "lunatus"	Tropheini	25.06.15	Cape Kabogo	-5.460833333	29.7475
KEE5	M	Trolun	Tropheus sp. "lunatus"	Tropheini	25.06.15	Cape Kabogo	-5.460833333	29.7475
KEE6	M	Trolun	Tropheus sp. "lunatus"	Tropheini	25.06.15	Cape Kabogo	-5.460833333	29.7475
KEE7	M	Trolun	Tropheus sp. "lunatus"	Tropheini	25.06.15	Cape Kabogo	-5.460833333	29.7475
KEE8	NA	Batvit	Bathybates vittatus	Bathybatini	26.06.15	Kabogo fishermen	-5.683055556	29.76991667
KEE9	M	Chando	Chalinochromis sp. "ndobhoi"	Lamprologini	26.06.15	Katumbi	-6.008611111	29.76083333

KEF1	F	Chando	Chalinochromis sp. "ndobhoi"	Lamprologini	26.06.15	Katumbi	-6.008611111	29.76083333
KEF2	M	Troluk	Tropheus sp. "lukuga"	Tropheini	26.06.15	Katumbi	-6.008611111	29.76083333
KEF3	F	Troluk	Tropheus sp. "lukuga"	Tropheini	26.06.15	Katumbi	-6.008611111	29.76083333
KEF4	F	Chando	Chalinochromis sp. "ndobhoi"	Lamprologini	26.06.15	Katumbi	-6.008611111	29.76083333
KEF5	M	Chando	Chalinochromis sp. "ndobhoi"	Lamprologini	26.06.15	Katumbi	-6.008611111	29.76083333
KEF6	M	Chando	Chalinochromis sp. "ndobhoi"	Lamprologini	26.06.15	Katumbi	-6.008611111	29.76083333
KEF7	F	Chando	Chalinochromis sp. "ndobhoi"	Lamprologini	26.06.15	Katumbi	-6.008611111	29.76083333
KEF8	F	Chando	Chalinochromis sp. "ndobhoi"	Lamprologini	26.06.15	Katumbi	-6.008611111	29.76083333
KEF9	M	Chando	Chalinochromis sp. "ndobhoi"	Lamprologini	26.06.15	Katumbi	-6.008611111	29.76083333
KEG1	F	Chando	Chalinochromis sp. "ndobhoi"	Lamprologini	26.06.15	Katumbi	-6.008611111	29.76083333
KEG2	F	Chando	Chalinochromis sp. "ndobhoi"	Lamprologini	26.06.15	Katumbi	-6.008611111	29.76083333
KEG3	F	Chando	Chalinochromis sp. "ndobhoi"	Lamprologini	26.06.15	Katumbi	-6.008611111	29.76083333
KEG4	F	Chando	Chalinochromis sp. "ndobhoi"	Lamprologini	26.06.15	Katumbi	-6.008611111	29.76083333
KEG5	F	Troluk	Tropheus sp. "lukuga"	Tropheini	26.06.15	Katumbi	-6.008611111	29.76083333
KEG6	M	Troluk	Tropheus sp. "lukuga"	Tropheini	26.06.15	Katumbi	-6.008611111	29.76083333
KEG7	M	Troluk	Tropheus sp. "lukuga"	Tropheini	26.06.15	Katumbi	-6.008611111	29.76083333
KEG8	F	Troluk	Tropheus sp. "lukuga"	Tropheini	26.06.15	Katumbi	-6.008611111	29.76083333
KEG9	F	Troluk	Tropheus sp. "lukuga"	Tropheini	26.06.15	Katumbi	-6.008611111	29.76083333
KEH1	M?	XenspN	Xenotilapia sp. "spilopterus north"	Ectodini	26.06.15	Katumbi	-6.008611111	29.76083333
KEH2	M?	XenspN	Xenotilapia sp. "spilopterus north"	Ectodini	26.06.15	Katumbi	-6.008611111	29.76083333
KEH3	M	Neoleu	Neolamprologus longior	Lamprologini	27.06.15	Bulu Point	-6.016111111	29.74638889
KEH4	M	Neoleu	Neolamprologus longior	Lamprologini	27.06.15	Bulu Point	-6.016111111	29.74638889
KEH5	M	Neoleu	Neolamprologus longior	Lamprologini	27.06.15	Bulu Point	-6.016111111	29.74638889
KEH8	NA	Neoleu	Neolamprologus longior	Lamprologini	27.06.15	Bulu Point	-6.016111111	29.74638889
KEH9	M	Plepar	Plecodus paradoxus	Perissodini	27.06.15	Bulu Point	-6.016111111	29.74638889
KEI1	M	Plepar	Plecodus paradoxus	Perissodini	27.06.15	Bulu Point	-6.016111111	29.74638889
KEI2	F	Troluk	Tropheus sp. "lukuga"	Tropheini	27.06.15	Bulu Point	-6.016111111	29.74638889
KEI5	M	Troluk	Tropheus sp. "lukuga"	Tropheini	27.06.15	Karilani Island	-6.020555556	29.7425
KEI6	F	Troluk	Tropheus sp. "lukuga"	Tropheini	27.06.15	Karilani Island	-6.020555556	29.7425
KEI7	F	Troluk	Tropheus sp. "lukuga"	Tropheini	27.06.15	Karilani Island	-6.020555556	29.7425
KEI8	F	Troluk	Tropheus sp. "lukuga"	Tropheini	27.06.15	Karilani Island	-6.020555556	29.7425
KEI9	M	Plepar	Plecodus paradoxus	Perissodini	27.06.15	Karilani Island	-6.020555556	29.7425
KFA1	M	Cypdwj	Cyprichromis sp. "dwarf jumbo"	Cyprichromini	20.06.15	Cave Kigoma	-4.886944444	29.61583333
KFA2	M	Cypdwj	Cyprichromis sp. "dwarf jumbo"	Cyprichromini	20.06.15	Cave Kigoma	-4.886944444	29.61583333
KFA3	M	Cypdwj	Cyprichromis sp. "dwarf jumbo"	Cyprichromini	20.06.15	Cave Kigoma	-4.886944444	29.61583333
KFA4	M	Cypdwj	Cyprichromis sp. "dwarf jumbo"	Cyprichromini	20.06.15	Cave Kigoma	-4.886944444	29.61583333
KFA5	M	Cypdwj	Cyprichromis sp. "dwarf jumbo"	Cyprichromini	20.06.15	Cave Kigoma	-4.886944444	29.61583333
KFA6	F	Cypdwj	Cyprichromis sp. "dwarf jumbo"	Cyprichromini	20.06.15	Cave Kigoma	-4.886944444	29.61583333
KFA7	M	Cypdwj	Cyprichromis sp. "dwarf jumbo"	Cyprichromini	20.06.15	Cave Kigoma	-4.886944444	29.61583333
KFA9	F	Cypdwj	Cyprichromis sp. "dwarf jumbo"	Cyprichromini	20.06.15	Cave Kigoma	-4.886944444	29.61583333
KFB2	F	Cypdwj	Cyprichromis sp. "dwarf jumbo"	Cyprichromini	20.06.15	Cave Kigoma	-4.886944444	29.61583333
KFB3	F	Cypdwj	Cyprichromis sp. "dwarf jumbo"	Cyprichromini	20.06.15	Cave Kigoma	-4.886944444	29.61583333
KFB4	F	Cypdwj	Cyprichromis sp. "dwarf jumbo"	Cyprichromini	20.06.15	Cave Kigoma	-4.886944444	29.61583333
KFB5	F	Cypdwj	Cyprichromis sp. "dwarf jumbo"	Cyprichromini	20.06.15	Cave Kigoma	-4.886944444	29.61583333
KFD2	F	Neowal	Neolamprologus walteri	Lamprologini	20.06.15	Tembo Rock	-4.886944444	29.6125
KFD4	M	Neowal	Neolamprologus walteri	Lamprologini	20.06.15	Tembo Rock	-4.886944444	29.6125
KFD6	M	Neowal	Neolamprologus walteri	Lamprologini	20.06.15	Tembo Rock	-4.886944444	29.6125
KFD7	M	Neowal	Neolamprologus walteri	Lamprologini	20.06.15	Tembo Rock	-4.886944444	29.6125
KFD8	M	Neowal	Neolamprologus walteri	Lamprologini	20.06.15	Tembo Rock	-4.886944444	29.6125
KFD9	M	Neowal	Neolamprologus walteri	Lamprologini	20.06.15	Tembo Rock	-4.886944444	29.6125
KFE1	M	Neowal	Neolamprologus walteri	Lamprologini	20.06.15	Tembo Rock	-4.886944444	29.6125
KFE2	M	Neowal	Neolamprologus walteri	Lamprologini	20.06.15	Tembo Rock	-4.886944444	29.6125
KFE3	F	Neowal	Neolamprologus walteri	Lamprologini	20.06.15	Tembo Rock	-4.886944444	29.6125
KFE4	F	Neowal	Neolamprologus walteri	Lamprologini	20.06.15	Tembo Rock	-4.886944444	29.6125
KFE5	F	Neowal	Neolamprologus walteri	Lamprologini	20.06.15	Tembo Rock	-4.886944444	29.6125
KFE6	F	Neowal	Neolamprologus walteri	Lamprologini	20.06.15	Tembo Rock	-4.886944444	29.6125
KFE8	M	Pscmrg	Pseudosimochromis marginatus (North)	Tropheini	20.06.15	Tembo Rock	-4.886944444	29.6125
KFF1	F	Pscmrg	Pseudosimochromis marginatus (North)	Tropheini	20.06.15	Tembo Rock	-4.886944444	29.6125
KFF2	M	Pscmrg	Pseudosimochromis marginatus (North)	Tropheini	20.06.15	Tembo Rock	-4.886944444	29.6125
KFF3	M	Pscmrg	Pseudosimochromis marginatus (North)	Tropheini	20.06.15	Tembo Rock	-4.886944444	29.6125
KFF4	F	JulreK	Julidochromis regani	Lamprologini	21.06.15	Kaku	-4.896388889	29.61166667
KFH4	M	Neotre	Neolamprologus tretocephalus	Lamprologini	21.06.15	Kaku	-4.896388889	29.61166667
KFH5	F	Neotre	Neolamprologus tretocephalus	Lamprologini	21.06.15	Kaku	-4.896388889	29.61166667
KFH7	F	Neotre	Neolamprologus tretocephalus	Lamprologini	21.06.15	Kaku	-4.896388889	29.61166667
KFH8	F	Neotre	Neolamprologus tretocephalus	Lamprologini	21.06.15	Kaku	-4.896388889	29.61166667
KFH9	F	Neotre	Neolamprologus tretocephalus	Lamprologini	21.06.15	Kaku	-4.896388889	29.61166667
KFI2	F	Neotre	Neolamprologus tretocephalus	Lamprologini	21.06.15	Kaku	-4.896388889	29.61166667
KFI3	F	Neotre	Neolamprologus tretocephalus	Lamprologini	21.06.15	Kaku	-4.896388889	29.61166667
KFI4	M	Neotre	Neolamprologus tretocephalus	Lamprologini	21.06.15	Kaku	-4.896388889	29.61166667
KFI5	M	Neotre	Neolamprologus tretocephalus	Lamprologini	21.06.15	Kaku	-4.896388889	29.61166667
KFI6	M	Neotre	Neolamprologus tretocephalus	Lamprologini	21.06.15	Kaku	-4.896388889	29.61166667
KFI7	F	Neotre	Neolamprologus tretocephalus	Lamprologini	21.06.15	Kaku	-4.896388889	29.61166667
KFI8	M	Neotre	Neolamprologus tretocephalus	Lamprologini	21.06.15	Kaku	-4.896388889	29.61166667
KFI9	F	JulreK	Julidochromis regani	Lamprologini	21.06.15	Kaku	-4.896388889	29.61166667
KHA4	M	Trodub	Tropheus duboisi	Tropheini	21.06.15	Kaku	-4.896388889	29.61166667
KHA5	F	Trodub	Tropheus duboisi	Tropheini	21.06.15	Kaku	-4.896388889	29.61166667
KHA6	F	Trodub	Tropheus duboisi	Tropheini	21.06.15	Kaku	-4.896388889	29.61166667
KHA7	M	Neochi	Neolamprologus chitamwebwai	Lamprologini	22.06.15	Mwamahunga	-4.911944444	29.59833333
KHA9	F	Neochi	Neolamprologus chitamwebwai	Lamprologini	22.06.15	Mwamahunga	-4.911944444	29.59833333
KHB2	F	Neochi	Neolamprologus chitamwebwai	Lamprologini	22.06.15	Mwamahunga	-4.911944444	29.59833333
KHB3	F	Neochi	Neolamprologus chitamwebwai	Lamprologini	22.06.15	Mwamahunga	-4.911944444	29.59833333
KHB4	M	Neochi	Neolamprologus chitamwebwai	Lamprologini	22.06.15	Mwamahunga	-4.911944444	29.59833333
KHB5	F	Neochi	Neolamprologus chitamwebwai	Lamprologini	22.06.15	Mwamahunga	-4.911944444	29.59833333
KHB6	F	Neochi	Neolamprologus chitamwebwai	Lamprologini	22.06.15	Mwamahunga	-4.911944444	29.59833333
KHB7	M	Neochi	Neolamprologus chitamwebwai	Lamprologini	22.06.15	Mwamahunga	-4.911944444	29.59833333
KHB8	M	Neochi	Neolamprologus chitamwebwai	Lamprologini	22.06.15	Mwamahunga	-4.911944444	29.59833333
KHB9	M	Neochi	Neolamprologus chitamwebwai	Lamprologini	22.06.15	Mwamahunga	-4.911944444	29.59833333
KHC1	F	Neochi	Neolamprologus chitamwebwai	Lamprologini	22.06.15	Mwamahunga	-4.911944444	29.59833333
KHC2	F	Neochi	Neolamprologus chitamwebwai	Lamprologini	22.06.15	Mwamahunga	-4.911944444	29.59833333
KHC3	F	JulreK	Julidochromis regani	Lamprologini	22.06.15	Mwamahunga	-4.911944444	29.59833333
KHC4	M	EctspN	Ectodus sp. "north"	Ectodini	22.06.15	Mwamahunga	-4.911944444	29.59833333
KHC5	F	EctspN	Ectodus sp. "north"	Ectodini	22.06.15	Mwamahunga	-4.911944444	29.59833333
KHC8	M	EctspN	Ectodus sp. "north"	Ectodini	22.06.15	Mwamahunga	-4.911944444	29.59833333
KHC9	M	EctspN	Ectodus sp. "north"	Ectodini	22.06.15	Mwamahunga	-4.911944444	29.59833333
KHD1	F	EctspN	Ectodus sp. "north"	Ectodini	22.06.15	Mwamahunga	-4.911944444	29.59833333
KHD2	F	EctspN	Ectodus sp. "north"	Ectodini	22.06.15	Mwamahunga	-4.911944444	29.59833333
KHD3	F	EctspN	Ectodus sp. "north"	Ectodini	22.06.15	Mwamahunga	-4.911944444	29.59833333
KHD4	F	EctspN	Ectodus sp. "north"	Ectodini	22.06.15	Mwamahunga	-4.911944444	29.59833333
KHD5	M	EctspN	Ectodus sp. "north"	Ectodini	22.06.15	Mwamahunga	-4.911944444	29.59833333
KHD6	F	EctspN	Ectodus sp. "north"	Ectodini	22.06.15	Mwamahunga	-4.911944444	29.59833333
KHD7	F	EctspN	Ectodus sp. "north"	Ectodini	22.06.15	Mwamahunga	-4.911944444	29.59833333
KHD8	F	EctspN	Ectodus sp. "north"	Ectodini	22.06.15	Mwamahunga	-4.911944444	29.59833333
KHD9	F	Trodub	Tropheus duboisi	Tropheini	22.06.15	Mwamahunga	-4.911944444	29.59833333
KHE1	M	Trodub	Tropheus duboisi	Tropheini	22.06.15	Mwamahunga	-4.911944444	29.59833333
KHE2	F	Trodub	Tropheus duboisi	Tropheini	22.06.15	Mwamahunga	-4.911944444	29.59833333
KHE3	F	Pscmrg	Pseudosimochromis marginatus (North)	Tropheini	22.06.15	Mwamahunga	-4.911944444	29.59833333
KHE4	M	Pscmrg	Pseudosimochromis marginatus (North)	Tropheini	22.06.15	Mwamahunga	-4.911944444	29.59833333
KHE5	M	Pscmrg	Pseudosimochromis marginatus (North)	Tropheini	22.06.15	Mwamahunga	-4.911944444	29.59833333
KHE6	M	JulreK	Julidochromis regani	Lamprologini	23.06.15	Nondwa Point	-4.864166667	29.60722222
KHE7	F	JulreK	Julidochromis regani	Lamprologini	23.06.15	Nondwa Point	-4.864166667	29.60722222
KHE8	F	JulreK	Julidochromis regani	Lamprologini	23.06.15	Nondwa Point	-4.864166667	29.60722222
KHE9	F	JulreK	Julidochromis regani	Lamprologini	23.06.15	Nondwa Point	-4.864166667	29.60722222
KHF1	F	JulreK	Julidochromis regani	Lamprologini	23.06.15	Nondwa Point	-4.864166667	29.60722222
KHF2	F	JulreK	Julidochromis regani	Lamprologini	23.06.15	Nondwa Point	-4.864166667	29.60722222
KHF3	F	JulreK	Julidochromis regani	Lamprologini	23.06.15	Nondwa Point	-4.864166667	29.60722222
KHF6	F	Trodub	Tropheus duboisi	Tropheini	23.06.15	Nondwa Point	-4.864166667	29.60722222
KHF7	F	Trodub	Tropheus duboisi	Tropheini	23.06.15	Nondwa Point	-4.864166667	29.60722222
KHF8	F	Trodub	Tropheus duboisi	Tropheini	23.06.15	Nondwa Point	-4.864166667	29.60722222
KHF9	M	Trodub	Tropheus duboisi	Tropheini	23.06.15	Nondwa Point	-4.864166667	29.60722222
KHG1	M	Trodub	Tropheus duboisi	Tropheini	23.06.15	Nondwa Point	-4.864166667	29.60722222
KHG2	M	Calmel	Callochromis melanostigma	Ectodini	23.06.15	George's Place	-4.885	29.62083333
KHG3	NA	Pscmrg	Pseudosimochromis marginatus (North)	Tropheini	23.06.15	George's Place	-4.885	29.62083333
KHG4	NA	Pscmrg	Pseudosimochromis marginatus (North)	Tropheini	23.06.15	George's Place	-4.885	29.62083333
KHI1	M	Cphfro	Cyphotilapia frontosa	Cyphotilapiini	23.06.15	Nondwa Point	-4.864166667	29.60722222

KHI2	M	Cphfro	Cyphotilapia frontosa	Cyphotilapiini	23.06.15	Nondwa Point	-4.864166667	29.60722222
KHI3	F	JulreK	Julidochromis regani	Lamprologini	24.06.15	Kaku	-4.896388889	29.61166667
KHI4	M	JulreK	Julidochromis regani	Lamprologini	24.06.15	Kaku	-4.896388889	29.61166667
KHI5	M	Lamspe	Lamprologus speciosus	Lamprologini	24.06.15	Kaku	-4.896388889	29.61166667
KHI6	M	Lamspe	Lamprologus speciosus	Lamprologini	24.06.15	Kaku	-4.896388889	29.61166667
KHI7	F	Trodub	Tropheus duboisi	Tropheini	24.06.15	Kaku	-4.896388889	29.61166667
KYA1	M	Neonig	Neolamprologus niger	Lamprologini	10.07.15	Nondwa Point	-4.864166667	29.60722222
KYA2	M	Neonig	Neolamprologus niger	Lamprologini	10.07.15	Nondwa Point	-4.864166667	29.60722222
KYA3	M	Neonig	Neolamprologus niger	Lamprologini	11.07.15	Kananiye	-4.794166667	29.59444444
KYA4	M	Neonig	Neolamprologus niger	Lamprologini	11.07.15	Kananiye	-4.794166667	29.59444444
KYA5	F	Neonig	Neolamprologus niger	Lamprologini	11.07.15	Kananiye	-4.794166667	29.59444444
KYA6	F	Neonig	Neolamprologus niger	Lamprologini	11.07.15	Kananiye	-4.794166667	29.59444444
KYA7	F	Neonig	Neolamprologus niger	Lamprologini	11.07.15	Kananiye	-4.794166667	29.59444444
KYA8	M	Neonig	Neolamprologus niger	Lamprologini	11.07.15	Kananiye	-4.794166667	29.59444444
KYA9	M	Neonig	Neolamprologus niger	Lamprologini	11.07.15	Kananiye	-4.794166667	29.59444444
KYB1	F	Neonig	Neolamprologus niger	Lamprologini	11.07.15	Kananiye	-4.794166667	29.59444444
KYB2	M	Telbif	Telmatochromis bifrenatus	Lamprologini	12.07.15	Nondwa Point	-4.864166667	29.60722222
KYB3	M	Telbif	Telmatochromis bifrenatus	Lamprologini	12.07.15	Nondwa Point	-4.864166667	29.60722222
KYB4	F	Cphfro	Cyphotilapia frontosa	Cyphotilapiini	12.07.15	Nondwa Point	-4.864166667	29.60722222
KYB5	F	Cphfro	Cyphotilapia frontosa	Cyphotilapiini	12.07.15	Nondwa Point	-4.864166667	29.60722222
KYB6	F	Cphfro	Cyphotilapia frontosa	Cyphotilapiini	12.07.15	Nondwa Point	-4.864166667	29.60722222
KYB7	M	Telbif	Telmatochromis bifrenatus	Lamprologini	12.07.15	Nondwa Point	-4.864166667	29.60722222
KYB8	F	Telbif	Telmatochromis bifrenatus	Lamprologini	12.07.15	Nondwa Point	-4.864166667	29.60722222
KYB9	M	Neobou	Neolamprologus boulengeri	Lamprologini	13.07.15	Ujiji Fishmarket	-4.904416667	29.66911111
KYC2	M	Neobou	Neolamprologus boulengeri	Lamprologini	13.07.15	Ujiji Fishmarket	-4.904416667	29.66911111
KYC3	M	Neobou	Neolamprologus boulengeri	Lamprologini	13.07.15	Ujiji Fishmarket	-4.904416667	29.66911111
KYC4	M	Neobou	Neolamprologus boulengeri	Lamprologini	13.07.15	Ujiji Fishmarket	-4.904416667	29.66911111
KYC5	M	Neobou	Neolamprologus boulengeri	Lamprologini	13.07.15	Ujiji Fishmarket	-4.904416667	29.66911111
KYC6	M	Neobou	Neolamprologus boulengeri	Lamprologini	13.07.15	Ujiji Fishmarket	-4.904416667	29.66911111
KYC7	M	Neobou	Neolamprologus boulengeri	Lamprologini	13.07.15	Ujiji Fishmarket	-4.904416667	29.66911111
KYC8	F	Batfas	Bathybates fasciatus	Bathybatini	13.07.15	Ujiji Fishmarket	-4.904416667	29.66911111
KYC9	F	Batfas	Bathybates fasciatus	Bathybatini	13.07.15	Ujiji Fishmarket	-4.904416667	29.66911111
KYD1	M	Batfas	Bathybates fasciatus	Bathybatini	13.07.15	Ujiji Fishmarket	-4.904416667	29.66911111
KYE2	M	Ortred	Orthochromis malagaraziensis	Haplochromini	16.07.15	Malagarasi 2 (Uvinza)	-5.109444	30.393611
KYE7	M	Ortuvi	Orthochromis uvinzae	Haplochromini	16.07.15	Malagarasi 2 (Uvinza)	-5.109444	30.393611
KYG1	M	Astpal	Astatotilapia paludinosa	Haplochromini	16.07.15	Malagarasi 2 (Uvinza)	-5.109444	30.393611
KYH4	F	Oremal	Oreochromis malagarasi	Oreochromini	17.07.15	Malagarasi 2 (Uvinza)	-5.109444	30.393611
LBA1	F	JulmaS	Julidochromis sp. "marlieri south"	Lamprologini	31.07.15	Toby's Place	-8.623222222	31.20044444
LBA2	F	JulmaS	Julidochromis sp. "marlieri south"	Lamprologini	31.07.15	Toby's Place	-8.623222222	31.20044444
LBA3	F	JulmaS	Julidochromis sp. "marlieri south"	Lamprologini	31.07.15	Toby's Place	-8.623222222	31.20044444
LBA4	F	JulmaS	Julidochromis sp. "marlieri south"	Lamprologini	31.07.15	Toby's Place	-8.623222222	31.20044444
LBA5	M	JulmaS	Julidochromis sp. "marlieri south"	Lamprologini	31.07.15	Toby's Place	-8.623222222	31.20044444
LBA6	F	Neocyl	Neolamprologus cylindricus	Lamprologini	01.08.15	Toby's Place	-8.623222222	31.20044444
LBA7	M	JulmaS	Julidochromis sp. "marlieri south"	Lamprologini	01.08.15	Toby's Place	-8.623222222	31.20044444
LBA8	F	JulmaS	Julidochromis sp. "marlieri south"	Lamprologini	01.08.15	Toby's Place	-8.623222222	31.20044444
LBA9	F	Pleela	Plecodus elaviae	Perissodini	01.08.15	Chipwa Fishermen	-8.606166667	31.18611111
LBB2	F	Batleo	Bathybates leo	Bathybatini	01.08.15	Chipwa Fishermen	-8.606166667	31.18611111
LBB3	M	Batvit	Bathybates vittatus	Bathybatini	01.08.15	Chipwa Fishermen	-8.606166667	31.18611111
LBB4	F	Batvit	Bathybates vittatus	Bathybatini	01.08.15	Chipwa Fishermen	-8.606166667	31.18611111
LBB5	M	Hemste	Hemibates stenosoma	Bathybatini	01.08.15	Chipwa Fishermen	-8.606166667	31.18611111
LBB6	F	Hemste	Hemibates stenosoma	Bathybatini	01.08.15	Chipwa Fishermen	-8.606166667	31.18611111
LBB7	F	Hemste	Hemibates stenosoma	Bathybatini	01.08.15	Chipwa Fishermen	-8.606166667	31.18611111
LBC1	F	Tremac	Trematocara macrostoma	Trematocarini	01.08.15	Chipwa Fishermen	-8.606166667	31.18611111
LBC2	F	Xensim	Xenotilapia sima	Ectodini	01.08.15	Chipwa Fishermen	-8.606166667	31.18611111
LBC3	NA	Xchhec	Xenochromis hecqui	Perissodini	01.08.15	Chipwa Fishermen	-8.606166667	31.18611111
LBC4	NA	Perecc	Perissodus eccentricus	Perissodini	01.08.15	Chipwa Fishermen	-8.606166667	31.18611111
LBC5	M	Neocyl	Neolamprologus cylindricus	Lamprologini	02.08.15	Toby's Place	-8.623222222	31.20044444
LBC6	M	Neocyl	Neolamprologus cylindricus	Lamprologini	02.08.15	Toby's Place	-8.623222222	31.20044444
LBC7	F	Neocyl	Neolamprologus cylindricus	Lamprologini	02.08.15	Toby's Place	-8.623222222	31.20044444
LBC8	M	Neocyl	Neolamprologus cylindricus	Lamprologini	02.08.15	Toby's Place	-8.623222222	31.20044444
LBC9	M	Neocyl	Neolamprologus cylindricus	Lamprologini	02.08.15	Toby's Place	-8.623222222	31.20044444
LBD1	F	JulmaS	Julidochromis sp. "marlieri south"	Lamprologini	02.08.15	Toby's Place	-8.623222222	31.20044444
LBD2	F	Neocyl	Neolamprologus cylindricus	Lamprologini	02.08.15	Toby's Place	-8.623222222	31.20044444
LBD3	M	Batvit	Bathybates vittatus	Bathybatini	02.08.15	Chipwa Fishermen	-8.606166667	31.18611111
LBD4	M	Xchhec	Xenochromis hecqui	Perissodini	02.08.15	Chipwa Fishermen	-8.606166667	31.18611111
LBD5	F	Hemste	Hemibates stenosoma	Bathybatini	02.08.15	Chipwa Fishermen	-8.606166667	31.18611111
LBD6	F	Hemste	Hemibates stenosoma	Bathybatini	02.08.15	Chipwa Fishermen	-8.606166667	31.18611111
LBD8	M	Tremar	Trematocara marginatum	Trematocarini	02.08.15	Chipwa Fishermen	-8.606166667	31.18611111
LBD9	M	Trenig	Trematocara nigrifrons	Trematocarini	02.08.15	Chipwa Fishermen	-8.606166667	31.18611111
LBE1	F	Trenig	Trematocara nigrifrons	Trematocarini	02.08.15	Chipwa Fishermen	-8.606166667	31.18611111
LBE2	M	Xensim	Xenotilapia sima	Ectodini	02.08.15	Chipwa Fishermen	-8.606166667	31.18611111
LBE3	M	Xensim	Xenotilapia sima	Ectodini	02.08.15	Chipwa Fishermen	-8.606166667	31.18611111
LBE4	M	Xensim	Xenotilapia sima	Ectodini	02.08.15	Chipwa Fishermen	-8.606166667	31.18611111
LBE5	M	Xensim	Xenotilapia sima	Ectodini	02.08.15	Chipwa Fishermen	-8.606166667	31.18611111
LBE6	M	Xensim	Xenotilapia sima	Ectodini	02.08.15	Chipwa Fishermen	-8.606166667	31.18611111
LBE9	F	Xensim	Xenotilapia sima	Ectodini	02.08.15	Chipwa Fishermen	-8.606166667	31.18611111
LBF1	F	Xensim	Xenotilapia sima	Ectodini	02.08.15	Chipwa Fishermen	-8.606166667	31.18611111
LBF2	F	Xensim	Xenotilapia sima	Ectodini	02.08.15	Chipwa Fishermen	-8.606166667	31.18611111
LBF3	M	JulmaS	Julidochromis sp. "marlieri south"	Lamprologini	03.08.15	Toby's Place	-8.623222222	31.20044444
LBF4	F	Baicen	Baileychromis centropomoides	Limnochromini	04.08.15	Chipwa Fishermen	-8.606166667	31.18611111
LBF5	M	Baicen	Baileychromis centropomoides	Limnochromini	04.08.15	Chipwa Fishermen	-8.606166667	31.18611111
LBF6	F	Plemul	Plecodus multidentatus	Perissodini	04.08.15	Chipwa Fishermen	-8.606166667	31.18611111
LBF7	F	TeldhS	Telmatochromis dhonti	Lamprologini	04.08.15	Lunzua Lake / Kapata	-8.749202778	31.17273889
LBF8	M	TeldhS	Telmatochromis dhonti	Lamprologini	04.08.15	Lunzua Lake / Kapata	-8.749202778	31.17273889
LBF9	M	Neopro	Neolamprologus prochilus	Lamprologini	29.07.15	Mpulungu Fishmarket	-8.760472222	31.11219444
LBG1	F	Neopro	Neolamprologus prochilus	Lamprologini	29.07.15	Mpulungu Fishmarket	-8.760472222	31.11219444
LBG2	M	Perecc	Perissodus eccentricus	Perissodini	04.08.15	Chipwa Fishermen	-8.606166667	31.18611111
LBG3	M	XenniS	Xenotilapia nigrolabiata	Ectodini	06.08.15	Chituta	-8.723611111	31.15
LBG4	M	XenniS	Xenotilapia nigrolabiata	Ectodini	06.08.15	Chituta	-8.723611111	31.15
LBG5	M	XenniS	Xenotilapia nigrolabiata	Ectodini	06.08.15	Chituta	-8.723611111	31.15
LBG6	F	XenniS	Xenotilapia nigrolabiata	Ectodini	06.08.15	Chituta	-8.723611111	31.15
LBG7	F	XenniS	Xenotilapia nigrolabiata	Ectodini	06.08.15	Chituta	-8.723611111	31.15
LBG8	M	XenniS	Xenotilapia nigrolabiata	Ectodini	06.08.15	Chituta	-8.723611111	31.15
LBH1	M	XenniS	Xenotilapia nigrolabiata	Ectodini	06.08.15	Chituta	-8.723611111	31.15
LBH2	F	XenniS	Xenotilapia nigrolabiata	Ectodini	06.08.15	Chituta	-8.723611111	31.15
LBH3	M	XenniS	Xenotilapia nigrolabiata	Ectodini	06.08.15	Chituta	-8.723611111	31.15
LBI5	M	Cypzon	Cyprichromis zonatus	Cyprichromini	06.08.15	Chituta	-8.723611111	31.15
LBI6	F	Cypzon	Cyprichromis zonatus	Cyprichromini	06.08.15	Chituta	-8.723611111	31.15
LBI7	M	Cypzon	Cyprichromis zonatus	Cyprichromini	06.08.15	Chituta	-8.723611111	31.15
LBI8	M	Cypzon	Cyprichromis zonatus	Cyprichromini	06.08.15	Chituta	-8.723611111	31.15
LBI9	M	Cypzon	Cyprichromis zonatus	Cyprichromini	06.08.15	Chituta	-8.723611111	31.15
LCA1	M	Neolou	Neolamprologus leloupi	Lamprologini	01.07.15	Kalila Nkwasi	-6.260555556	29.73666667
LCA2	F	Neolou	Neolamprologus leloupi	Lamprologini	01.07.15	Kalila Nkwasi	-6.260555556	29.73666667
LCA3	M	Neolou	Neolamprologus leloupi	Lamprologini	01.07.15	Kalila Nkwasi	-6.260555556	29.73666667
LCA4	M	Neolou	Neolamprologus leloupi	Lamprologini	01.07.15	Kalila Nkwasi	-6.260555556	29.73666667
LCA5	M	Neolou	Neolamprologus leloupi	Lamprologini	01.07.15	Kalila Nkwasi	-6.260555556	29.73666667
LCA6	M	Neolou	Neolamprologus leloupi	Lamprologini	01.07.15	Kalila Nkwasi	-6.260555556	29.73666667
LCA7	M	Neolou	Neolamprologus leloupi	Lamprologini	01.07.15	Kalila Nkwasi	-6.260555556	29.73666667
LCA8	M	Neolou	Neolamprologus leloupi	Lamprologini	01.07.15	Kalila Nkwasi	-6.260555556	29.73666667
LCA9	M	Neolou	Neolamprologus leloupi	Lamprologini	01.07.15	Kalila Nkwasi	-6.260555556	29.73666667
LCB1	F	Neolou	Neolamprologus leloupi	Lamprologini	01.07.15	Kalila Nkwasi	-6.260555556	29.73666667
LCB2	M	Neolou	Neolamprologus leloupi	Lamprologini	01.07.15	Kalila Nkwasi	-6.260555556	29.73666667
LCB3	NA	Neolou	Neolamprologus leloupi	Lamprologini	01.07.15	Kalila Nkwasi	-6.260555556	29.73666667
LCB4	M	NeogrM	Neolamprologus sp. "gracilis tanzania"	Lamprologini	01.07.15	Kalila Nkwasi	-6.260555556	29.73666667
LCB5	F	NeofaM	Neolamprologus sp. "falcicula mahale"	Lamprologini	01.07.15	Kalila Nkwasi	-6.260555556	29.73666667
LCB6	M	NeofaM	Neolamprologus sp. "falcicula mahale"	Lamprologini	01.07.15	Kalila Nkwasi	-6.260555556	29.73666667
LCB7	M	NeofaM	Neolamprologus sp. "falcicula mahale"	Lamprologini	01.07.15	Kalila Nkwasi	-6.260555556	29.73666667
LCB8	M	NeofaM	Neolamprologus sp. "falcicula mahale"	Lamprologini	01.07.15	Kalila Nkwasi	-6.260555556	29.73666667
LCB9	M	NeogrM	Neolamprologus sp. "gracilis tanzania"	Lamprologini	01.07.15	Kalila Nkwasi	-6.260555556	29.73666667
LCC1	M	NeofaM	Neolamprologus sp. "falcicula mahale"	Lamprologini	01.07.15	Kalila Nkwasi	-6.260555556	29.73666667
LCC2	M	NeofaM	Neolamprologus sp. "falcicula mahale"	Lamprologini	01.07.15	Kalila Nkwasi	-6.260555556	29.73666667
LCC3	F	NeogrM	Neolamprologus sp. "gracilis tanzania"	Lamprologini	01.07.15	Kalila Nkwasi	-6.260555556	29.73666667
LCC4	M	NeofaM	Neolamprologus sp. "falcicula mahale"	Lamprologini	01.07.15	Kalila Nkwasi	-6.260555556	29.73666667
LCC5	F	NeofaM	Neolamprologus sp. "falcicula mahale"	Lamprologini	01.07.15	Kalila Nkwasi	-6.260555556	29.73666667

LCC6	F	NeogrM	Neolamprologus sp. "gracilis tanzania"	Lamprologini	01.07.15	Kalila Nkwasi	-6.260555556	29.73666667
LCC7	M	NeogrM	Neolamprologus sp. "gracilis tanzania"	Lamprologini	01.07.15	Kalila Nkwasi	-6.260555556	29.73666667
LCC8	F	NeogrM	Neolamprologus sp. "gracilis tanzania"	Lamprologini	01.07.15	Kalila Nkwasi	-6.260555556	29.73666667
LCC9	F	NeogrM	Neolamprologus sp. "gracilis tanzania"	Lamprologini	01.07.15	Kalila Nkwasi	-6.260555556	29.73666667
LCD1	M	Petred	Petrochromis sp. "red"	Tropheini	01.07.15	Kalila Nkwasi	-6.260555556	29.73666667
LCD2	M	Petred	Petrochromis sp. "red"	Tropheini	01.07.15	Kalila Nkwasi	-6.260555556	29.73666667
LCD3	M	Petred	Petrochromis sp. "red"	Tropheini	01.07.15	Kalila Nkwasi	-6.260555556	29.73666667
LCD4	M	Petred	Petrochromis sp. "red"	Tropheini	01.07.15	Kalila Nkwasi	-6.260555556	29.73666667
LCD5	F	Petred	Petrochromis sp. "red"	Tropheini	01.07.15	Kalila Nkwasi	-6.260555556	29.73666667
LCD6	M	Batfer	Bathybates ferox	Bathybatini	02.07.15	Nganja	-6.173333333	29.74027778
LCD7	F	Batfer	Bathybates ferox	Bathybatini	02.07.15	Nganja	-6.173333333	29.74027778
LCD8	M	Batfer	Bathybates ferox	Bathybatini	02.07.15	Nganja	-6.173333333	29.74027778
LCD9	F	Batfer	Bathybates ferox	Bathybatini	02.07.15	Nganja	-6.173333333	29.74027778
LCE1	M	Batfer	Bathybates ferox	Bathybatini	02.07.15	Nganja	-6.173333333	29.74027778
LCE2	F	Batfer	Bathybates ferox	Bathybatini	02.07.15	Nganja	-6.173333333	29.74027778
LCE3	F	Batfer	Bathybates ferox	Bathybatini	02.07.15	Nganja	-6.173333333	29.74027778
LCE4	F	Batfer	Bathybates ferox	Bathybatini	02.07.15	Nganja	-6.173333333	29.74027778
LCE5	M	Batfer	Bathybates ferox	Bathybatini	02.07.15	Nganja	-6.173333333	29.74027778
LCE6	NA	Batfer	Bathybates ferox	Bathybatini	02.07.15	Nganja	-6.173333333	29.74027778
LCE7	F	Petred	Petrochromis sp. "red"	Tropheini	02.07.15	Nganja	-6.173333333	29.74027778
LCE8	F	Petred	Petrochromis sp. "red"	Tropheini	02.07.15	Nganja	-6.173333333	29.74027778
LCE9	M	Petred	Petrochromis sp. "red"	Tropheini	02.07.15	Nganja	-6.173333333	29.74027778
LCF1	M	Trokir	Tropheus sp. "kirschfleck"	Tropheini	02.07.15	Nganja	-6.173333333	29.74027778
LCF2	M	Trokir	Tropheus sp. "kirschfleck"	Tropheini	02.07.15	Nganja	-6.173333333	29.74027778
LCF3	F	Trokir	Tropheus sp. "kirschfleck"	Tropheini	02.07.15	Nganja	-6.173333333	29.74027778
LCF4	F	Trokir	Tropheus sp. "kirschfleck"	Tropheini	02.07.15	Nganja	-6.173333333	29.74027778
LCF5	M	Trokir	Tropheus sp. "kirschfleck"	Tropheini	02.07.15	Nganja	-6.173333333	29.74027778
LCF6	M	Petmos	Petrochromis sp. "moshi yellow"	Tropheini	02.07.15	Nganja	-6.173333333	29.74027778
LCF7	M	Petmos	Petrochromis sp. "moshi yellow"	Tropheini	02.07.15	Nganja	-6.173333333	29.74027778
LCF8	F	Petmos	Petrochromis sp. "moshi yellow"	Tropheini	02.07.15	Nganja	-6.173333333	29.74027778
LCF9	F	Petmos	Petrochromis sp. "moshi yellow"	Tropheini	02.07.15	Nganja	-6.173333333	29.74027778
LCG1	M	Petmos	Petrochromis sp. "moshi yellow"	Tropheini	02.07.15	Nganja	-6.173333333	29.74027778
LCG2	F	Petmos	Petrochromis sp. "moshi yellow"	Tropheini	02.07.15	Nganja	-6.173333333	29.74027778
LCG3	F	Petmos	Petrochromis sp. "moshi yellow"	Tropheini	02.07.15	Nganja	-6.173333333	29.74027778
LCG4	F	Petmos	Petrochromis sp. "moshi yellow"	Tropheini	02.07.15	Nganja	-6.173333333	29.74027778
LCG5	F	Petmos	Petrochromis sp. "moshi yellow"	Tropheini	02.07.15	Nganja	-6.173333333	29.74027778
LCG6	F	Petmos	Petrochromis sp. "moshi yellow"	Tropheini	02.07.15	Nganja	-6.173333333	29.74027778
LCG7	F	Leppro	Lepidiolamprologus profundicola	Lamprologini	04.07.15	Storo 1	-6.01	29.75861111
LCH5	M	Plemul	Plecodus multidentatus	Perissodini	05.07.15	Mugambo Fishermen	-5.976083333	29.83944444
LCH6	M	Plemul	Plecodus multidentatus	Perissodini	05.07.15	Mugambo Fishermen	-5.976083333	29.83944444
LCH7	M	Plemul	Plecodus multidentatus	Perissodini	05.07.15	Mugambo Fishermen	-5.976083333	29.83944444
LCH8	M	Trolun	Tropheus sp. "lunatus"	Tropheini	07.07.15	Kabogo 2	-5.476944444	29.76
LCI9	F	Leppro	Lepidiolamprologus profundicola	Lamprologini	07.07.15	Cape Kabogo	-5.460833333	29.7475
LDA1	M	Cypzon	Cyprichromis zonatus	Cyprichromini	06.08.15	Chituta	-8.723611111	31.15
LDA2	F	Cypzon	Cyprichromis zonatus	Cyprichromini	06.08.15	Chituta	-8.723611111	31.15
LDA3	F	Cypzon	Cyprichromis zonatus	Cyprichromini	06.08.15	Chituta	-8.723611111	31.15
LDA4	M	Petmac	Petrochromis macrognathus	Tropheini	06.08.15	Chituta	-8.723611111	31.15
LDA5	M	Petmac	Petrochromis macrognathus	Tropheini	06.08.15	Chituta	-8.723611111	31.15
LDA6	M	Petmac	Petrochromis macrognathus	Tropheini	06.08.15	Chituta	-8.723611111	31.15
LDA7	M	Bentri	Benthochromis tricoti	Benthochromini	07.08.15	Chipwa Fishermen	-8.606166667	31.18611111
LDA8	M	Bentri	Benthochromis tricoti	Benthochromini	07.08.15	Chipwa Fishermen	-8.606166667	31.18611111
LDA9	F	Bentri	Benthochromis tricoti	Benthochromini	07.08.15	Chipwa Fishermen	-8.606166667	31.18611111
LDB2	M	Bentri	Benthochromis tricoti	Benthochromini	07.08.15	Chipwa Fishermen	-8.606166667	31.18611111
LDB3	M	Bentri	Benthochromis tricoti	Benthochromini	07.08.15	Chipwa Fishermen	-8.606166667	31.18611111
LDB4	M	Bentri	Benthochromis tricoti	Benthochromini	07.08.15	Chipwa Fishermen	-8.606166667	31.18611111
LDB5	M	Bentri	Benthochromis tricoti	Benthochromini	07.08.15	Chipwa Fishermen	-8.606166667	31.18611111
LDB6	M	Bentri	Benthochromis tricoti	Benthochromini	07.08.15	Chipwa Fishermen	-8.606166667	31.18611111
LDB7	M	Bentri	Benthochromis tricoti	Benthochromini	07.08.15	Chipwa Fishermen	-8.606166667	31.18611111
LDB8	F	Bentri	Benthochromis tricoti	Benthochromini	07.08.15	Chipwa Fishermen	-8.606166667	31.18611111
LDB9	F	Neopro	Neolamprologus prochilus	Lamprologini	07.08.15	Toby's Place	-8.623222222	31.20044444
LDC1	F	Neopro	Neolamprologus prochilus	Lamprologini	07.08.15	Toby's Place	-8.623222222	31.20044444
LDC2	M	Neopro	Neolamprologus prochilus	Lamprologini	07.08.15	Toby's Place	-8.623222222	31.20044444
LDC3	M	Petmac	Petrochromis macrognathus	Tropheini	08.08.15	Isanga	-8.654555556	31.19183333
LDC4	M	Petmac	Petrochromis macrognathus	Tropheini	08.08.15	Isanga	-8.654555556	31.19183333
LDC5	M	Petmac	Petrochromis macrognathus	Tropheini	08.08.15	Isanga	-8.654555556	31.19183333
LDC6	M	Petgia	Petrochromis sp. "giant"	Tropheini	12.08.15	Fulwe	-7.955	30.8225
LDC7	M	Petgia	Petrochromis sp. "giant"	Tropheini	12.08.15	Fulwe	-7.955	30.8225
LDC8	M	Petgia	Petrochromis sp. "giant"	Tropheini	12.08.15	Fulwe	-7.955	30.8225
LDC9	M	Petgia	Petrochromis sp. "giant"	Tropheini	12.08.15	Fulwe	-7.955	30.8225
LDD1	M	Lepmim	Lepidiolamprologus mimicus	Lamprologini	12.08.15	Fulwe	-7.955	30.8225
LDD2	M	Lepmim	Lepidiolamprologus mimicus	Lamprologini	12.08.15	Fulwe	-7.955	30.8225
LDD3	M	Lepmim	Lepidiolamprologus mimicus	Lamprologini	12.08.15	Fulwe	-7.955	30.8225
LDD4	M	Lepmim	Lepidiolamprologus mimicus	Lamprologini	12.08.15	Fulwe	-7.955	30.8225
LDD5	M	Lepmim	Lepidiolamprologus mimicus	Lamprologini	12.08.15	Fulwe	-7.955	30.8225
LDD6	F	Lepmim	Lepidiolamprologus mimicus	Lamprologini	12.08.15	Fulwe	-7.955	30.8225
LDD7	M	Chacya	Chalinochromis cyanophleps	Lamprologini	12.08.15	Fulwe	-7.955	30.8225
LDD8	M	Chacya	Chalinochromis cyanophleps	Lamprologini	12.08.15	Fulwe	-7.955	30.8225
LDD9	F	Chabif	Chalinochromis sp. "bifrenatus"	Lamprologini	12.08.15	Fulwe	-7.955	30.8225
LDE1	M	Chabif	Chalinochromis sp. "bifrenatus"	Lamprologini	12.08.15	Fulwe	-7.955	30.8225
LDE2	F	Chabif	Chalinochromis sp. "bifrenatus"	Lamprologini	12.08.15	Fulwe	-7.955	30.8225
LDE3	M	Petkip	Petrochromis sp. "kipili brown"	Tropheini	12.08.15	Fulwe	-7.955	30.8225
LDE4	F	Petkip	Petrochromis sp. "kipili brown"	Tropheini	12.08.15	Fulwe	-7.955	30.8225
LDE5	F	Petkip	Petrochromis sp. "kipili brown"	Tropheini	12.08.15	Fulwe	-7.955	30.8225
LDE6	F	Petkip	Petrochromis sp. "kipili brown"	Tropheini	12.08.15	Fulwe	-7.955	30.8225
LDE7	M	Petkip	Petrochromis sp. "kipili brown"	Tropheini	12.08.15	Fulwe	-7.955	30.8225
LDE8	F	Chacya	Chalinochromis cyanophleps	Lamprologini	13.08.15	Twiyu	-7.581944444	30.62833333
LDE9	M	Neocyg	Neolamprologus sp. "cygnus"	Lamprologini	13.08.15	Twiyu	-7.581944444	30.62833333
LDF1	F	Neotim	Neolamprologus timidus	Lamprologini	13.08.15	Twiyu	-7.581944444	30.62833333
LDF2	F	Neotim	Neolamprologus timidus	Lamprologini	13.08.15	Twiyu	-7.581944444	30.62833333
LDF3	M	Neotim	Neolamprologus timidus	Lamprologini	13.08.15	Twiyu	-7.581944444	30.62833333
LDF4	F	NeofuU	Neolamprologus sp. "furcifer ulwile"	Lamprologini	13.08.15	Twiyu	-7.581944444	30.62833333
LDF5	M	NeofuU	Neolamprologus sp. "furcifer ulwile"	Lamprologini	13.08.15	Twiyu	-7.581944444	30.62833333
LDF6	F	NeofuU	Neolamprologus sp. "furcifer ulwile"	Lamprologini	13.08.15	Twiyu	-7.581944444	30.62833333
LDF7	M	NeofuU	Neolamprologus sp. "furcifer ulwile"	Lamprologini	13.08.15	Twiyu	-7.581944444	30.62833333
LDF8	F	NeofuU	Neolamprologus sp. "furcifer ulwile"	Lamprologini	13.08.15	Twiyu	-7.581944444	30.62833333
LDF9	F	NeofuU	Neolamprologus sp. "furcifer ulwile"	Lamprologini	13.08.15	Twiyu	-7.581944444	30.62833333
LDG1	F	NeofuU	Neolamprologus sp. "furcifer ulwile"	Lamprologini	13.08.15	Twiyu	-7.581944444	30.62833333
LDG2	M	NeocaK	Neolamprologus sp. "caudopunctatus kipili"	Lamprologini	13.08.15	Twiyu	-7.581944444	30.62833333
LDG3	F	NeocaK	Neolamprologus sp. "caudopunctatus kipili"	Lamprologini	13.08.15	Twiyu	-7.581944444	30.62833333
LDG4	F	NeocaK	Neolamprologus sp. "caudopunctatus kipili"	Lamprologini	13.08.15	Twiyu	-7.581944444	30.62833333
LDG5	F	NeocaK	Neolamprologus sp. "caudopunctatus kipili"	Lamprologini	13.08.15	Twiyu	-7.581944444	30.62833333
LDG6	M	NeocaK	Neolamprologus sp. "caudopunctatus kipili"	Lamprologini	13.08.15	Twiyu	-7.581944444	30.62833333
LDG7	F	NeocaK	Neolamprologus sp. "caudopunctatus kipili"	Lamprologini	13.08.15	Twiyu	-7.581944444	30.62833333
LDG8	F	NeocaK	Neolamprologus sp. "caudopunctatus kipili"	Lamprologini	13.08.15	Twiyu	-7.581944444	30.62833333
LDG9	M	NeocaK	Neolamprologus sp. "caudopunctatus kipili"	Lamprologini	13.08.15	Twiyu	-7.581944444	30.62833333
LDH1	F	NeocaK	Neolamprologus sp. "caudopunctatus kipili"	Lamprologini	13.08.15	Twiyu	-7.581944444	30.62833333
LDH2	M	NeocaK	Neolamprologus sp. "caudopunctatus kipili"	Lamprologini	13.08.15	Twiyu	-7.581944444	30.62833333
LDH3	M	Lepmim	Lepidiolamprologus mimicus	Lamprologini	13.08.15	Twiyu	-7.581944444	30.62833333
LDH4	F	Chabif	Chalinochromis sp. "bifrenatus"	Lamprologini	13.08.15	Twiyu	-7.581944444	30.62833333
LDH5	M	Chabif	Chalinochromis sp. "bifrenatus"	Lamprologini	13.08.15	Twiyu	-7.581944444	30.62833333
LDH6	M	Chabif	Chalinochromis sp. "bifrenatus"	Lamprologini	13.08.15	Twiyu	-7.581944444	30.62833333
LDH7	M	Chabif	Chalinochromis sp. "bifrenatus"	Lamprologini	13.08.15	Twiyu	-7.581944444	30.62833333
LDH8	F	Petkip	Petrochromis sp. "kipili brown"	Tropheini	13.08.15	Twiyu	-7.581944444	30.62833333
LDH9	F	Chabif	Chalinochromis sp. "bifrenatus"	Lamprologini	14.08.15	Korongwe	-7.136944444	30.50777778
LDI1	F	Chabif	Chalinochromis sp. "bifrenatus"	Lamprologini	14.08.15	Korongwe	-7.136944444	30.50777778
LDI2	M	Chabif	Chalinochromis sp. "bifrenatus"	Lamprologini	14.08.15	Korongwe	-7.136944444	30.50777778
LDI3	F	Neocyg	Neolamprologus sp. "cygnus"	Lamprologini	14.08.15	Korongwe	-7.136944444	30.50777778
LDI4	M	Julmrk	Julidochromis marksmithi	Lamprologini	14.08.15	Korongwe	-7.136944444	30.50777778
LDI5	M	Trompi	Tropheus sp. "mpimbwe"	Tropheini	14.08.15	Korongwe	-7.136944444	30.50777778
LDI6	M	Trompi	Tropheus sp. "mpimbwe"	Tropheini	14.08.15	Korongwe	-7.136944444	30.50777778
LDI7	F	Trompi	Tropheus sp. "mpimbwe"	Tropheini	14.08.15	Korongwe	-7.136944444	30.50777778
LDI8	F	Trompi	Tropheus sp. "mpimbwe"	Tropheini	14.08.15	Korongwe	-7.136944444	30.50777778
LDI9	F	Trompi	Tropheus sp. "mpimbwe"	Tropheini	14.08.15	Korongwe	-7.136944444	30.50777778
LEA1	M	Plepar	Plecodus paradoxus	Perissodini	27.06.15	Karilani Island	-6.020555556	29.7425

LEA2	M	Plepar	Plecodus paradoxus	Perissodini	27.06.15	Karilani Island	-6.020555556	29.7425
LEA3	M	XenspN	Xenotilapia sp. "spilopterus north"	Ectodini	27.06.15	Karilani Island	-6.020555556	29.7425
LEA4	F	XenspN	Xenotilapia sp. "spilopterus north"	Ectodini	27.06.15	Karilani Island	-6.020555556	29.7425
LEA5	M?	XenspN	Xenotilapia sp. "spilopterus north"	Ectodini	27.06.15	Karilani Island	-6.020555556	29.7425
LEA6	F?	XenspN	Xenotilapia sp. "spilopterus north"	Ectodini	27.06.15	Karilani Island	-6.020555556	29.7425
LEA7	F?	XenspN	Xenotilapia sp. "spilopterus north"	Ectodini	27.06.15	Karilani Island	-6.020555556	29.7425
LEA8	M?	XenspN	Xenotilapia sp. "spilopterus north"	Ectodini	27.06.15	Karilani Island	-6.020555556	29.7425
LEA9	M?	XenspN	Xenotilapia sp. "spilopterus north"	Ectodini	27.06.15	Karilani Island	-6.020555556	29.7425
LEB1	F?	XenspN	Xenotilapia sp. "spilopterus north"	Ectodini	27.06.15	Karilani Island	-6.020555556	29.7425
LEB2	F?	XenspN	Xenotilapia sp. "spilopterus north"	Ectodini	27.06.15	Karilani Island	-6.020555556	29.7425
LEB3	M?	XenspN	Xenotilapia sp. "spilopterus north"	Ectodini	27.06.15	Karilani Island	-6.020555556	29.7425
LEC6	NA	Plepar	Plecodus paradoxus	Perissodini	27.06.15	Karilani Island	-6.020555556	29.7425
LEC7	F	Plepar	Plecodus paradoxus	Perissodini	28.06.15	Bulu Fishermen	-6.017972222	29.73880556
LEC8	F	Plepar	Plecodus paradoxus	Perissodini	28.06.15	Bulu Fishermen	-6.017972222	29.73880556
LEC9	M	Neoleu	Neolamprologus longior	Lamprologini	28.06.15	Bulu Point	-6.016111111	29.74638889
LED1	M	Neoleu	Neolamprologus longior	Lamprologini	28.06.15	Bulu Point	-6.016111111	29.74638889
LED3	M	Neoleu	Neolamprologus longior	Lamprologini	28.06.15	Bulu Point	-6.016111111	29.74638889
LED4	M	Telbif	Telmatochromis bifrenatus	Lamprologini	29.06.15	Storo bay	-6.016944444	29.74944444
LED5	M	Telbif	Telmatochromis bifrenatus	Lamprologini	29.06.15	Storo bay	-6.016944444	29.74944444
LED6	M	Telbif	Telmatochromis bifrenatus	Lamprologini	29.06.15	Storo bay	-6.016944444	29.74944444
LED7	M	Telbif	Telmatochromis bifrenatus	Lamprologini	29.06.15	Storo bay	-6.016944444	29.74944444
LED8	M	Telbif	Telmatochromis bifrenatus	Lamprologini	29.06.15	Storo bay	-6.016944444	29.74944444
LEE1	F	Neoleu	Neolamprologus longior	Lamprologini	29.06.15	Bulu Point	-6.016111111	29.74638889
LEE4	NA	Telbif	Telmatochromis bifrenatus	Lamprologini	30.06.15	Storo bay	-6.016944444	29.74944444
LEE5	NA	Telbif	Telmatochromis bifrenatus	Lamprologini	30.06.15	Storo bay	-6.016944444	29.74944444
LEE6	NA	Telbif	Telmatochromis bifrenatus	Lamprologini	30.06.15	Storo bay	-6.016944444	29.74944444
LEE7	NA	Leppro	Lepidiolamprologus profundicola	Lamprologini	30.06.15	Storo bay	-6.016944444	29.74944444
LEE8	M	Neoleu	Neolamprologus longior	Lamprologini	01.07.15	Kalila Nkwasi	-6.260555556	29.73666667
LEE9	F	Neoleu	Neolamprologus longior	Lamprologini	01.07.15	Kalila Nkwasi	-6.260555556	29.73666667
LEF1	F	Neoleu	Neolamprologus longior	Lamprologini	01.07.15	Kalila Nkwasi	-6.260555556	29.73666667
LEF2	M	BenhoM	Benthochromis sp. "horii mahale"	Benthochromini	02.07.15	Nganja	-6.173333333	29.74027778
LEF3	M	Trokir	Tropheus sp. "kirschfleck"	Tropheini	02.07.15	Nganja	-6.173333333	29.74027778
LEF4	M	Trokir	Tropheus sp. "kirschfleck"	Tropheini	02.07.15	Nganja	-6.173333333	29.74027778
LEF5	F	Trokir	Tropheus sp. "kirschfleck"	Tropheini	02.07.15	Nganja	-6.173333333	29.74027778
LEF6	M	Trokir	Tropheus sp. "kirschfleck"	Tropheini	02.07.15	Nganja	-6.173333333	29.74027778
LEF7	F	Trokir	Tropheus sp. "kirschfleck"	Tropheini	02.07.15	Nganja	-6.173333333	29.74027778
LEF8	M	Tropol	Tropheus polli	Tropheini	05.07.15	Storo 1	-6.01	29.75861111
LEF9	F	Tropol	Tropheus polli	Tropheini	05.07.15	Storo 1	-6.01	29.75861111
LEG1	M	Tropol	Tropheus polli	Tropheini	05.07.15	Storo 1	-6.01	29.75861111
LEG2	F	Tropol	Tropheus polli	Tropheini	05.07.15	Storo 1	-6.01	29.75861111
LEG3	F	Tropol	Tropheus polli	Tropheini	05.07.15	Storo 1	-6.01	29.75861111
LEG4	F	Tropol	Tropheus polli	Tropheini	05.07.15	Storo 1	-6.01	29.75861111
LEG5	F	Tropol	Tropheus polli	Tropheini	05.07.15	Storo 1	-6.01	29.75861111
LEG6	F	Tropol	Tropheus polli	Tropheini	05.07.15	Storo 1	-6.01	29.75861111
LEG7	F	Tropol	Tropheus polli	Tropheini	05.07.15	Storo 1	-6.01	29.75861111
LEG8	F	Tropol	Tropheus polli	Tropheini	05.07.15	Storo 1	-6.01	29.75861111
LEG9	M	Tropol	Tropheus polli	Tropheini	05.07.15	Storo 1	-6.01	29.75861111
LEH1	F	Tropol	Tropheus polli	Tropheini	05.07.15	Storo 1	-6.01	29.75861111
LEH2	M	Neodev	Neolamprologus devosi	Lamprologini	08.07.15	Malagarasi 1 (Kigoma)	-5.211944	29.842222
LEI1	F	Pscmrg	Pseudosimochromis marginatus (North)	Tropheini	10.07.15	Kalalangabo	-4.843611111	29.60944444
LEI2	F	Pscmrg	Pseudosimochromis marginatus (North)	Tropheini	10.07.15	Kalalangabo	-4.843611111	29.60944444
LEI3	F	Pscmrg	Pseudosimochromis marginatus (North)	Tropheini	10.07.15	Kalalangabo	-4.843611111	29.60944444
LEI5	M	Cphfro	Cyphotilapia frontosa	Cyphotilapiini	10.07.15	Kalalangabo	-4.843611111	29.60944444
LEI6	F	Cphfro	Cyphotilapia frontosa	Cyphotilapiini	10.07.15	Nondwa Point	-4.864166667	29.60722222
LEI7	F	Cphfro	Cyphotilapia frontosa	Cyphotilapiini	10.07.15	Nondwa Point	-4.864166667	29.60722222
LEI8	F	Cphfro	Cyphotilapia frontosa	Cyphotilapiini	10.07.15	Nondwa Point	-4.864166667	29.60722222
LEI9	M	Cphfro	Cyphotilapia frontosa	Cyphotilapiini	10.07.15	Nondwa Point	-4.864166667	29.60722222
LFA1	M	Trompi	Tropheus sp. "mpimbwe"	Tropheini	14.08.15	Korongwe	-7.136944444	30.50777778
LFA2	F	Trompi	Tropheus sp. "mpimbwe"	Tropheini	14.08.15	Korongwe	-7.136944444	30.50777778
LFA3	F	Trompi	Tropheus sp. "mpimbwe"	Tropheini	14.08.15	Korongwe	-7.136944444	30.50777778
LFA4	M	Trompi	Tropheus sp. "mpimbwe"	Tropheini	14.08.15	Korongwe	-7.136944444	30.50777778
LFA5	M	Trompi	Tropheus sp. "mpimbwe"	Tropheini	14.08.15	Korongwe	-7.136944444	30.50777778
LFA6	M	Petiko	Petrochromis sp. "orthognathus ikola"	Tropheini	14.08.15	Korongwe	-7.136944444	30.50777778
LFA7	M	Petiko	Petrochromis sp. "orthognathus ikola"	Tropheini	14.08.15	Korongwe	-7.136944444	30.50777778
LFA8	F	Petiko	Petrochromis sp. "orthognathus ikola"	Tropheini	14.08.15	Korongwe	-7.136944444	30.50777778
LFA9	F	Petiko	Petrochromis sp. "orthognathus ikola"	Tropheini	14.08.15	Korongwe	-7.136944444	30.50777778
LFB1	F	Petiko	Petrochromis sp. "orthognathus ikola"	Tropheini	14.08.15	Msalaba	-7.116666667	30.49777778
LFB2	M	Petiko	Petrochromis sp. "orthognathus ikola"	Tropheini	14.08.15	Msalaba	-7.116666667	30.49777778
LFB3	F	Petiko	Petrochromis sp. "orthognathus ikola"	Tropheini	14.08.15	Msalaba	-7.116666667	30.49777778
LFB4	F	Petiko	Petrochromis sp. "orthognathus ikola"	Tropheini	14.08.15	Msalaba	-7.116666667	30.49777778
LFB5	M	Petiko	Petrochromis sp. "orthognathus ikola"	Tropheini	14.08.15	Msalaba	-7.116666667	30.49777778
LFB6	M	Petiko	Petrochromis sp. "orthognathus ikola"	Tropheini	14.08.15	Msalaba	-7.116666667	30.49777778
LFB7	M	Neoese	Neolamprologus sp. "eseki"	Lamprologini	14.08.15	Msalaba	-7.116666667	30.49777778
LFB8	M	Neoese	Neolamprologus sp. "eseki"	Lamprologini	14.08.15	Msalaba	-7.116666667	30.49777778
LFB9	F	Neoese	Neolamprologus sp. "eseki"	Lamprologini	14.08.15	Msalaba	-7.116666667	30.49777778
LFC1	F	Neoese	Neolamprologus sp. "eseki"	Lamprologini	14.08.15	Msalaba	-7.116666667	30.49777778
LFC2	F	Neoese	Neolamprologus sp. "eseki"	Lamprologini	14.08.15	Msalaba	-7.116666667	30.49777778
LFC3	F	Neoese	Neolamprologus sp. "eseki"	Lamprologini	14.08.15	Msalaba	-7.116666667	30.49777778
LFC4	M	Neoese	Neolamprologus sp. "eseki"	Lamprologini	14.08.15	Msalaba	-7.116666667	30.49777778
LFC5	M	Neoese	Neolamprologus sp. "eseki"	Lamprologini	14.08.15	Msalaba	-7.116666667	30.49777778
LFC6	M	Neoese	Neolamprologus sp. "eseki"	Lamprologini	14.08.15	Msalaba	-7.116666667	30.49777778
LFC7	M	Neoese	Neolamprologus sp. "eseki"	Lamprologini	14.08.15	Msalaba	-7.116666667	30.49777778
LFC8	M	Neocyg	Neolamprologus sp. "cygnus"	Lamprologini	14.08.15	Msalaba	-7.116666667	30.49777778
LFC9	M	Trezeb	Trematocara zebra	Trematocarini	15.08.15	Korongwe	-7.136944444	30.50777778
LFD2	M	Neocyg	Neolamprologus sp. "cygnus"	Lamprologini	15.08.15	Korongwe	-7.136944444	30.50777778
LFD3	M	Neocyg	Neolamprologus sp. "cygnus"	Lamprologini	15.08.15	Korongwe	-7.136944444	30.50777778
LFD4	F	Neocyg	Neolamprologus sp. "cygnus"	Lamprologini	15.08.15	Korongwe	-7.136944444	30.50777778
LFD5	M	Neocyg	Neolamprologus sp. "cygnus"	Lamprologini	15.08.15	Korongwe	-7.136944444	30.50777778
LFD6	F	Neocyg	Neolamprologus sp. "cygnus"	Lamprologini	15.08.15	Korongwe	-7.136944444	30.50777778
LFD7	M	Neocyg	Neolamprologus sp. "cygnus"	Lamprologini	15.08.15	Korongwe	-7.136944444	30.50777778
LFD8	F	Neocyg	Neolamprologus sp. "cygnus"	Lamprologini	15.08.15	Korongwe	-7.136944444	30.50777778
LFE4	F	Trezeb	Trematocara zebra	Trematocarini	15.08.15	Korongwe	-7.136944444	30.50777778
LFE5	F	Trezeb	Trematocara zebra	Trematocarini	15.08.15	Korongwe	-7.136944444	30.50777778
LFE6	F	Trezeb	Trematocara zebra	Trematocarini	15.08.15	Korongwe	-7.136944444	30.50777778
LFE7	F	Trezeb	Trematocara zebra	Trematocarini	15.08.15	Korongwe	-7.136944444	30.50777778
LFE8	F	Trezeb	Trematocara zebra	Trematocarini	15.08.15	Korongwe	-7.136944444	30.50777778
LFE9	F	Trezeb	Trematocara zebra	Trematocarini	15.08.15	Korongwe	-7.136944444	30.50777778
LFF2	F	Trezeb	Trematocara zebra	Trematocarini	15.08.15	Korongwe	-7.136944444	30.50777778
LFF3	F	Trezeb	Trematocara zebra	Trematocarini	15.08.15	Korongwe	-7.136944444	30.50777778
LFF5	M	Trezeb	Trematocara zebra	Trematocarini	15.08.15	Korongwe	-7.136944444	30.50777778
LFF6	F	Julmrk	Julidochromis marksmithi	Lamprologini	15.08.15	Korongwe	-7.136944444	30.50777778
LFF7	M	Lepkam	Lepidiolamprologus kamambae	Lamprologini	16.08.15	Kamamba Island	-7.3975	30.55416667
LFF8	F	Lepkam	Lepidiolamprologus kamambae	Lamprologini	16.08.15	Kamamba Island	-7.3975	30.55416667
LFF9	M	Lepkam	Lepidiolamprologus kamambae	Lamprologini	16.08.15	Kamamba Island	-7.3975	30.55416667
LFG1	F	Lepkam	Lepidiolamprologus kamambae	Lamprologini	16.08.15	Kamamba Island	-7.3975	30.55416667
LFG2	F	Lepkam	Lepidiolamprologus kamambae	Lamprologini	16.08.15	Kamamba Island	-7.3975	30.55416667
LFG3	F	Lepkam	Lepidiolamprologus kamambae	Lamprologini	16.08.15	Kamamba Island	-7.3975	30.55416667
LFG4	M	Lepkam	Lepidiolamprologus kamambae	Lamprologini	16.08.15	Kamamba Island	-7.3975	30.55416667
LFG5	M	Lepkam	Lepidiolamprologus kamambae	Lamprologini	16.08.15	Kamamba Island	-7.3975	30.55416667
LFG6	F	Lepkam	Lepidiolamprologus kamambae	Lamprologini	16.08.15	Kamamba Island	-7.3975	30.55416667
LFG7	M	Lepkam	Lepidiolamprologus kamambae	Lamprologini	16.08.15	Kamamba Island	-7.3975	30.55416667
LFG8	M	Julmrk	Julidochromis marksmithi	Lamprologini	16.08.15	Kamamba Island	-7.3975	30.55416667
LFG9	M	Julmrk	Julidochromis marksmithi	Lamprologini	16.08.15	Kamamba Island	-7.3975	30.55416667
LFH1	F	Julmrk	Julidochromis marksmithi	Lamprologini	16.08.15	Kamamba Island	-7.3975	30.55416667
LFH2	F	Julmrk	Julidochromis marksmithi	Lamprologini	16.08.15	Kamamba Island	-7.3975	30.55416667
LFH3	M	Julmrk	Julidochromis marksmithi	Lamprologini	16.08.15	Kamamba Island	-7.3975	30.55416667
LFH4	M	Julmrk	Julidochromis marksmithi	Lamprologini	16.08.15	Kamamba Island	-7.3975	30.55416667
LFH5	M	Julmrk	Julidochromis marksmithi	Lamprologini	16.08.15	Kamamba Island	-7.3975	30.55416667
LFH6	M	Pettex	Petrochromis sp. "polyodon texas"	Tropheini	17.08.15	Nkondwe	-7.378888889	30.54611111
LFH7	M	Pettex	Petrochromis sp. "polyodon texas"	Tropheini	17.08.15	Nkondwe	-7.378888889	30.54611111
LFH8	F	Julmrk	Julidochromis marksmithi	Lamprologini	17.08.15	Nkondwe	-7.378888889	30.54611111
LFH9	F	TrobrK	Tropheus sp. "brichardi kipili"	Tropheini	17.08.15	Nkondwe	-7.378888889	30.54611111
LFI1	M	TrobrK	Tropheus sp. "brichardi kipili"	Tropheini	17.08.15	Nkondwe	-7.378888889	30.54611111
LFI2	M	Pettex	Petrochromis sp. "polyodon texas"	Tropheini	17.08.15	Nkondwe	-7.378888889	30.54611111

LFI3	M	Pettex	Petrochromis sp. "polyodon texas"	Tropheini	17.08.15	Nkondwe	-7.378888889	30.54611111
LFI4	M	Ophboo	Ophthalmotilapia boops	Ectodini	17.08.15	Nkondwe	-7.378888889	30.54611111
LFI5	M	Ophboo	Ophthalmotilapia boops	Ectodini	17.08.15	Nkondwe	-7.378888889	30.54611111
LFI6	F	Ophboo	Ophthalmotilapia boops	Ectodini	17.08.15	Nkondwe	-7.378888889	30.54611111
LFI7	F	Ophboo	Ophthalmotilapia boops	Ectodini	17.08.15	Nkondwe	-7.378888889	30.54611111
LFI8	M	Ophboo	Ophthalmotilapia boops	Ectodini	17.08.15	Nkondwe	-7.378888889	30.54611111
LFI9	M	Ophboo	Ophthalmotilapia boops	Ectodini	17.08.15	Nkondwe	-7.378888889	30.54611111
LGA1	M	Ophboo	Ophthalmotilapia boops	Ectodini	17.08.15	Nkondwe	-7.378888889	30.54611111
LGA2	M	Ophboo	Ophthalmotilapia boops	Ectodini	17.08.15	Nkondwe	-7.378888889	30.54611111
LGA3	F	Ophboo	Ophthalmotilapia boops	Ectodini	17.08.15	Nkondwe	-7.378888889	30.54611111
LGA4	F	Ophboo	Ophthalmotilapia boops	Ectodini	17.08.15	Nkondwe	-7.378888889	30.54611111
LGA5	M	TrobrK	Tropheus sp. "brichardi kipili"	Tropheini	17.08.15	Nkondwe	-7.378888889	30.54611111
LGA6	F	TrobrK	Tropheus sp. "brichardi kipili"	Tropheini	17.08.15	Nkondwe	-7.378888889	30.54611111
LGA7	F	TrobrK	Tropheus sp. "brichardi kipili"	Tropheini	17.08.15	Nkondwe	-7.378888889	30.54611111
LGA8	F	TrobrK	Tropheus sp. "brichardi kipili"	Tropheini	17.08.15	Nkondwe	-7.378888889	30.54611111
LGA9	F	TrobrK	Tropheus sp. "brichardi kipili"	Tropheini	17.08.15	Nkondwe	-7.378888889	30.54611111
LGB1	M	TrobrK	Tropheus sp. "brichardi kipili"	Tropheini	17.08.15	Nkondwe	-7.378888889	30.54611111
LGB2	M	TrobrK	Tropheus sp. "brichardi kipili"	Tropheini	17.08.15	Nkondwe	-7.378888889	30.54611111
LGB3	F	TrobrK	Tropheus sp. "brichardi kipili"	Tropheini	17.08.15	Nkondwe	-7.378888889	30.54611111
LGB4	F	Petkip	Petrochromis sp. "kipili brown"	Tropheini	17.08.15	Nkondwe	-7.378888889	30.54611111
LGB5	M	Petrai	Petrochromis sp. "macrognathus rainbow"	Tropheini	17.08.15	Nkondwe	-7.378888889	30.54611111
LGB6	M	Petrai	Petrochromis sp. "macrognathus rainbow"	Tropheini	17.08.15	Nkondwe	-7.378888889	30.54611111
LGB7	M	Petrai	Petrochromis sp. "macrognathus rainbow"	Tropheini	17.08.15	Nkondwe	-7.378888889	30.54611111
LGB8	F	Petrai	Petrochromis sp. "macrognathus rainbow"	Tropheini	17.08.15	Nkondwe	-7.378888889	30.54611111
LGB9	M	Petrai	Petrochromis sp. "macrognathus rainbow"	Tropheini	17.08.15	Nkondwe	-7.378888889	30.54611111
LGC1	M	Petrai	Petrochromis sp. "macrognathus rainbow"	Tropheini	17.08.15	Nkondwe	-7.378888889	30.54611111
LGC2	F	Petrai	Petrochromis sp. "macrognathus rainbow"	Tropheini	17.08.15	Nkondwe	-7.378888889	30.54611111
LGC3	M	Petrai	Petrochromis sp. "macrognathus rainbow"	Tropheini	17.08.15	Nkondwe	-7.378888889	30.54611111
LGC4	M	Petrai	Petrochromis sp. "macrognathus rainbow"	Tropheini	17.08.15	Nkondwe	-7.378888889	30.54611111
LGC5	F	Petrai	Petrochromis sp. "macrognathus rainbow"	Tropheini	17.08.15	Nkondwe	-7.378888889	30.54611111
LGC7	M	Chacya	Chalinochromis cyanophleps	Lamprologini	18.08.15	Mvuna Island	-7.444166667	30.54388889
LGC8	M	Chacya	Chalinochromis cyanophleps	Lamprologini	18.08.15	Mvuna Island	-7.444166667	30.54388889
LGC9	F	Leppro	Lepidiolamprologus profundicola	Lamprologini	18.08.15	Mvuna Island	-7.444166667	30.54388889
LGD1	F	Leppro	Lepidiolamprologus profundicola	Lamprologini	18.08.15	Mvuna Island	-7.444166667	30.54388889
LGD2	M	Petkip	Petrochromis sp. "kipili brown"	Tropheini	18.08.15	Mvuna Island	-7.444166667	30.54388889
LGD3	F	Petkip	Petrochromis sp. "kipili brown"	Tropheini	18.08.15	Mvuna Island	-7.444166667	30.54388889
LGD4	M	Petkip	Petrochromis sp. "kipili brown"	Tropheini	18.08.15	Mvuna Island	-7.444166667	30.54388889
LGD5	M	Lepmim	Lepidiolamprologus mimicus	Lamprologini	18.08.15	Mvuna Island	-7.444166667	30.54388889
LGD7	F	Oretan	Oreochromis tanganicae	Oreochromini	18.08.15	Mvuna Island	-7.444166667	30.54388889
LGD8	F	Oretan	Oreochromis tanganicae	Oreochromini	18.08.15	Mvuna Island	-7.444166667	30.54388889
LGD9	F	Oretan	Oreochromis tanganicae	Oreochromini	18.08.15	Mvuna Island	-7.444166667	30.54388889
LGE2	M	Neotim	Neolamprologus timidus	Lamprologini	19.08.15	Ulwile Musi Point	-7.478888889	30.57638889
LGE3	F	Neotim	Neolamprologus timidus	Lamprologini	19.08.15	Ulwile Musi Point	-7.478888889	30.57638889
LGE4	F	Neotim	Neolamprologus timidus	Lamprologini	19.08.15	Ulwile Musi Point	-7.478888889	30.57638889
LGE5	F	Neotim	Neolamprologus timidus	Lamprologini	19.08.15	Ulwile Musi Point	-7.478888889	30.57638889
LGE6	F	Neotim	Neolamprologus timidus	Lamprologini	19.08.15	Ulwile Musi Point	-7.478888889	30.57638889
LGE7	F	Neotim	Neolamprologus timidus	Lamprologini	19.08.15	Ulwile Musi Point	-7.478888889	30.57638889
LGE8	F	Neotim	Neolamprologus timidus	Lamprologini	19.08.15	Ulwile Musi Point	-7.478888889	30.57638889
LGE9	NA	NeofuU	Neolamprologus sp. "furcifer ulwile"	Lamprologini	19.08.15	Ulwile Musi Point	-7.478888889	30.57638889
LGF1	M	NeofuU	Neolamprologus sp. "furcifer ulwile"	Lamprologini	19.08.15	Ulwile Musi Point	-7.478888889	30.57638889
LGF2	F	NeofuU	Neolamprologus sp. "furcifer ulwile"	Lamprologini	19.08.15	Ulwile Musi Point	-7.478888889	30.57638889
LGG4	M	Lepmim	Lepidiolamprologus mimicus	Lamprologini	19.08.15	Twiyu	-7.581944444	30.62833333
LGG5	M	Chacya	Chalinochromis cyanophleps	Lamprologini	19.08.15	Twiyu	-7.581944444	30.62833333
LGG6	M	Chacya	Chalinochromis cyanophleps	Lamprologini	19.08.15	Twiyu	-7.581944444	30.62833333
LGG7	F	Chacya	Chalinochromis cyanophleps	Lamprologini	19.08.15	Twiyu	-7.581944444	30.62833333
LGG8	F	Chacya	Chalinochromis cyanophleps	Lamprologini	19.08.15	Twiyu	-7.581944444	30.62833333
LGG9	F	Chacya	Chalinochromis cyanophleps	Lamprologini	19.08.15	Twiyu	-7.581944444	30.62833333
LGH1	M	Ophwhi	Ophthalmotilapia sp. "white cap"	Ectodini	19.08.15	Twiyu	-7.581944444	30.62833333
LGH2	M	Ophwhi	Ophthalmotilapia sp. "white cap"	Ectodini	19.08.15	Twiyu	-7.581944444	30.62833333
LGH3	F	Ophwhi	Ophthalmotilapia sp. "white cap"	Ectodini	19.08.15	Twiyu	-7.581944444	30.62833333
LGH4	M	Ophwhi	Ophthalmotilapia sp. "white cap"	Ectodini	19.08.15	Twiyu	-7.581944444	30.62833333
LGH5	M	Ophwhi	Ophthalmotilapia sp. "white cap"	Ectodini	19.08.15	Twiyu	-7.581944444	30.62833333
LGH6	M	Ophwhi	Ophthalmotilapia sp. "white cap"	Ectodini	19.08.15	Twiyu	-7.581944444	30.62833333
LGH7	M	Ophwhi	Ophthalmotilapia sp. "white cap"	Ectodini	19.08.15	Twiyu	-7.581944444	30.62833333
LGH8	M	Neopet	Neolamprologus petricola	Lamprologini	19.08.15	Twiyu	-7.581944444	30.62833333
LGH9	M	Neopet	Neolamprologus petricola	Lamprologini	19.08.15	Twiyu	-7.581944444	30.62833333
LGI1	F	Neopet	Neolamprologus petricola	Lamprologini	19.08.15	Twiyu	-7.581944444	30.62833333
LGI2	F	Neopet	Neolamprologus petricola	Lamprologini	19.08.15	Twiyu	-7.581944444	30.62833333
LGI3	M	Neopet	Neolamprologus petricola	Lamprologini	19.08.15	Twiyu	-7.581944444	30.62833333
LGI4	F	Neopet	Neolamprologus petricola	Lamprologini	19.08.15	Twiyu	-7.581944444	30.62833333
LGI5	M	Neopet	Neolamprologus petricola	Lamprologini	19.08.15	Twiyu	-7.581944444	30.62833333
LGI6	F	Neopet	Neolamprologus petricola	Lamprologini	19.08.15	Twiyu	-7.581944444	30.62833333
LGI7	F	Neopet	Neolamprologus petricola	Lamprologini	19.08.15	Twiyu	-7.581944444	30.62833333
LGI8	M	Neopet	Neolamprologus petricola	Lamprologini	19.08.15	Twiyu	-7.581944444	30.62833333
LGI9	M	LepmeK	Lepidiolamprologus sp. "meeli kipili"	Lamprologini	19.08.15	Twiyu	-7.581944444	30.62833333
LHA1	M	LepmeK	Lepidiolamprologus sp. "meeli kipili"	Lamprologini	19.08.15	Twiyu	-7.581944444	30.62833333
LHA2	F	LepmeK	Lepidiolamprologus sp. "meeli kipili"	Lamprologini	19.08.15	Twiyu	-7.581944444	30.62833333
LHA3	M	LepmeK	Lepidiolamprologus sp. "meeli kipili"	Lamprologini	19.08.15	Twiyu	-7.581944444	30.62833333
LHA4	M	LepmeK	Lepidiolamprologus sp. "meeli kipili"	Lamprologini	19.08.15	Twiyu	-7.581944444	30.62833333
LHA5	M	LepmeK	Lepidiolamprologus sp. "meeli kipili"	Lamprologini	19.08.15	Twiyu	-7.581944444	30.62833333
LHA6	M	LepmeK	Lepidiolamprologus sp. "meeli kipili"	Lamprologini	19.08.15	Twiyu	-7.581944444	30.62833333
LHA7	M	LepmeK	Lepidiolamprologus sp. "meeli kipili"	Lamprologini	19.08.15	Twiyu	-7.581944444	30.62833333
LHA8	M	LepmeK	Lepidiolamprologus sp. "meeli kipili"	Lamprologini	19.08.15	Twiyu	-7.581944444	30.62833333
LHA9	M	LepmeK	Lepidiolamprologus sp. "meeli kipili"	Lamprologini	19.08.15	Twiyu	-7.581944444	30.62833333
LHB1	M	Pettex	Petrochromis sp. "polyodon texas"	Tropheini	20.08.15	Twiyu	-7.581944444	30.62833333
LHB2	M	Pettex	Petrochromis sp. "polyodon texas"	Tropheini	20.08.15	Twiyu	-7.581944444	30.62833333
LHB3	F	Pettex	Petrochromis sp. "polyodon texas"	Tropheini	20.08.15	Twiyu	-7.581944444	30.62833333
LHB4	M	Pettex	Petrochromis sp. "polyodon texas"	Tropheini	20.08.15	Twiyu	-7.581944444	30.62833333
LHB5	F	Pettex	Petrochromis sp. "polyodon texas"	Tropheini	20.08.15	Twiyu	-7.581944444	30.62833333
LHB6	M	Pettex	Petrochromis sp. "polyodon texas"	Tropheini	20.08.15	Twiyu	-7.581944444	30.62833333
LHB7	F	Ophwhi	Ophthalmotilapia sp. "white cap"	Ectodini	20.08.15	Twiyu	-7.581944444	30.62833333
LHB8	M	Ophwhi	Ophthalmotilapia sp. "white cap"	Ectodini	20.08.15	Twiyu	-7.581944444	30.62833333
LHB9	M	Ophwhi	Ophthalmotilapia sp. "white cap"	Ectodini	20.08.15	Twiyu	-7.581944444	30.62833333
LHC1	M	TeldhT	Telmatochromis sp. "dhonti twiyu"	Lamprologini	20.08.15	Twiyu	-7.581944444	30.62833333
LHC2	M	TeldhT	Telmatochromis sp. "dhonti twiyu"	Lamprologini	20.08.15	Twiyu	-7.581944444	30.62833333
LHC3	M	TeldhT	Telmatochromis sp. "dhonti twiyu"	Lamprologini	20.08.15	Twiyu	-7.581944444	30.62833333
LHC4	M	TeldhT	Telmatochromis sp. "dhonti twiyu"	Lamprologini	20.08.15	Twiyu	-7.581944444	30.62833333
LHC5	M	TeldhT	Telmatochromis sp. "dhonti twiyu"	Lamprologini	20.08.15	Twiyu	-7.581944444	30.62833333
LHC6	M	TeldhT	Telmatochromis sp. "dhonti twiyu"	Lamprologini	20.08.15	Twiyu	-7.581944444	30.62833333
LHC7	M	TeldhT	Telmatochromis sp. "dhonti twiyu"	Lamprologini	20.08.15	Twiyu	-7.581944444	30.62833333
LHC8	M	TeldhT	Telmatochromis sp. "dhonti twiyu"	Lamprologini	20.08.15	Twiyu	-7.581944444	30.62833333
LHC9	M	TeldhT	Telmatochromis sp. "dhonti twiyu"	Lamprologini	20.08.15	Twiyu	-7.581944444	30.62833333
LHD1	M	TeldhT	Telmatochromis sp. "dhonti twiyu"	Lamprologini	20.08.15	Twiyu	-7.581944444	30.62833333
LHD2	F	Petgia	Petrochromis sp. "giant"	Tropheini	21.08.15	Fulwe	-7.955	30.8225
LHD3	M	Petgia	Petrochromis sp. "giant"	Tropheini	21.08.15	Fulwe	-7.955	30.8225
LHD4	F	Petgia	Petrochromis sp. "giant"	Tropheini	21.08.15	Fulwe	-7.955	30.8225
LHD5	F	Petgia	Petrochromis sp. "giant"	Tropheini	21.08.15	Fulwe	-7.955	30.8225
LHD6	F	Petgia	Petrochromis sp. "giant"	Tropheini	21.08.15	Fulwe	-7.955	30.8225
LHD7	F	Petgia	Petrochromis sp. "giant"	Tropheini	21.08.15	Fulwe	-7.955	30.8225
LHD8	M	Oretan	Oreochromis tanganicae	Oreochromini	21.08.15	Fulwe	-7.955	30.8225
LHD9	M	Tromor	Tropheus sp. "murago"	Tropheini	21.08.15	Wapembwe	-7.946666667	30.83761111
LHE1	M	Tromor	Tropheus sp. "murago"	Tropheini	21.08.15	Wapembwe	-7.946666667	30.83761111
LHE2	M	Tromor	Tropheus sp. "murago"	Tropheini	21.08.15	Wapembwe	-7.946666667	30.83761111
LHE3	F	Tromor	Tropheus sp. "murago"	Tropheini	21.08.15	Wapembwe	-7.946666667	30.83761111
LHE4	F	Tromor	Tropheus sp. "murago"	Tropheini	21.08.15	Wapembwe	-7.946666667	30.83761111
LHE5	M	Tromor	Tropheus sp. "murago"	Tropheini	21.08.15	Wapembwe	-7.946666667	30.83761111
LHE6	F	Tromor	Tropheus sp. "murago"	Tropheini	21.08.15	Wapembwe	-7.946666667	30.83761111
LHE7	M	Tromor	Tropheus sp. "murago"	Tropheini	21.08.15	Wapembwe	-7.946666667	30.83761111
LHE8	M	Tromor	Tropheus sp. "murago"	Tropheini	21.08.15	Wapembwe	-7.946666667	30.83761111
LHE9	F	Tromor	Tropheus sp. "murago"	Tropheini	21.08.15	Wapembwe	-7.946666667	30.83761111
LHF2	F	TeldhT	Telmatochromis sp. "dhonti twiyu"	Lamprologini	20.08.15	Twiyu	-7.581944444	30.62833333
LHF3	M	Tylpol	Tylochromis polylepis	Tylochromini	22.08.15	Malasa Island	-8.211944444	30.94638889
LHF4	F	Neobif	Neolamprologus bifasciatus	Lamprologini	22.08.15	Malasa Island	-8.211944444	30.94638889
LHF5	M	Neobif	Neolamprologus bifasciatus	Lamprologini	22.08.15	Malasa Island	-8.211944444	30.94638889

LHF6	M	Neobif	Neolamprologus bifasciatus	Lamprologini	22.08.15	Malasa Island	-8.211944444	30.94638889
LHF7	F	Neobif	Neolamprologus bifasciatus	Lamprologini	22.08.15	Malasa Island	-8.211944444	30.94638889
LHF8	M	Neobif	Neolamprologus bifasciatus	Lamprologini	22.08.15	Malasa Island	-8.211944444	30.94638889
LHF9	M	Neobif	Neolamprologus bifasciatus	Lamprologini	22.08.15	Malasa Island	-8.211944444	30.94638889
LHG1	M	Neobif	Neolamprologus bifasciatus	Lamprologini	22.08.15	Malasa Island	-8.211944444	30.94638889
LHG2	F	Neobif	Neolamprologus bifasciatus	Lamprologini	22.08.15	Malasa Island	-8.211944444	30.94638889
LHG3	M	Neobif	Neolamprologus bifasciatus	Lamprologini	22.08.15	Malasa Island	-8.211944444	30.94638889
LHG4	M	Mdcten	Microdontochromis tenuidentata	Ectodini	23.08.15	Malasa Bay	-8.209444444	30.96277778
LHG6	F	Mdcten	Microdontochromis tenuidentata	Ectodini	23.08.15	Malasa Bay	-8.209444444	30.96277778
LHG8	M	Mdcten	Microdontochromis tenuidentata	Ectodini	23.08.15	Malasa Bay	-8.209444444	30.96277778
LHG9	M	Mdcten	Microdontochromis tenuidentata	Ectodini	23.08.15	Malasa Bay	-8.209444444	30.96277778
LHH1	F	Mdcten	Microdontochromis tenuidentata	Ectodini	23.08.15	Malasa Bay	-8.209444444	30.96277778
LHH2	M	Mdcten	Microdontochromis tenuidentata	Ectodini	23.08.15	Malasa Bay	-8.209444444	30.96277778
LHH3	F	Mdcten	Microdontochromis tenuidentata	Ectodini	23.08.15	Malasa Bay	-8.209444444	30.96277778
LHH4	M	Mdcten	Microdontochromis tenuidentata	Ectodini	23.08.15	Malasa Bay	-8.209444444	30.96277778
LHH5	F	Mdcten	Microdontochromis tenuidentata	Ectodini	23.08.15	Malasa Bay	-8.209444444	30.96277778
LHH6	M	Mdcten	Microdontochromis tenuidentata	Ectodini	23.08.15	Malasa Bay	-8.209444444	30.96277778
LHH7	M	Mdcten	Microdontochromis tenuidentata	Ectodini	23.08.15	Malasa Bay	-8.209444444	30.96277778
LHH8	F	Mdcten	Microdontochromis tenuidentata	Ectodini	23.08.15	Malasa Bay	-8.209444444	30.96277778
LHH9	M	Neopro	Neolamprologus prochilus	Lamprologini	25.08.15	Toby's Place	-8.623222222	31.20044444
LHI1	M	Neopro	Neolamprologus prochilus	Lamprologini	25.08.15	Toby's Place	-8.623222222	31.20044444
LHI2	F	Neopro	Neolamprologus prochilus	Lamprologini	25.08.15	Toby's Place	-8.623222222	31.20044444
LHI3	M	Perecc	Perissodus eccentricus	Perissodini	25.08.15	Chipwa Fishermen	-8.606166667	31.18611111
LHI4	M	Pleela	Plecodus elaviae	Perissodini	25.08.15	Chipwa Fishermen	-8.606166667	31.18611111
LHI5	M	Pleela	Plecodus elaviae	Perissodini	25.08.15	Chipwa Fishermen	-8.606166667	31.18611111
LHI6	F	Pleela	Plecodus elaviae	Perissodini	25.08.15	Chipwa Fishermen	-8.606166667	31.18611111
LHI7	F	Pleela	Plecodus elaviae	Perissodini	25.08.15	Chipwa Fishermen	-8.606166667	31.18611111
LIA1	F	Pleela	Plecodus elaviae	Perissodini	25.08.15	Chipwa Fishermen	-8.606166667	31.18611111
LIA2	F	Pleela	Plecodus elaviae	Perissodini	25.08.15	Chipwa Fishermen	-8.606166667	31.18611111
LIA3	M	Pleela	Plecodus elaviae	Perissodini	25.08.15	Chipwa Fishermen	-8.606166667	31.18611111
LIA4	M	Pleela	Plecodus elaviae	Perissodini	25.08.15	Chipwa Fishermen	-8.606166667	31.18611111
LIA5	M	Batmin	Bathybates minor	Bathybatini	25.08.15	Chipwa Fishermen	-8.606166667	31.18611111
LIA6	F	Plemul	Plecodus multidentatus	Perissodini	26.08.15	Mpulungu Fishmarket	-8.760472222	31.11219444
LIA7	F?	Perecc	Perissodus eccentricus	Perissodini	26.08.15	Mpulungu Fishmarket	-8.760472222	31.11219444
LIA8	M	Perecc	Perissodus eccentricus	Perissodini	26.08.15	Mpulungu Fishmarket	-8.760472222	31.11219444
LIA9	M	Perecc	Perissodus eccentricus	Perissodini	26.08.15	Mpulungu Fishmarket	-8.760472222	31.11219444
LIB1	M	Perecc	Perissodus eccentricus	Perissodini	26.08.15	Mpulungu Fishmarket	-8.760472222	31.11219444
LIB2	M	Perecc	Perissodus eccentricus	Perissodini	26.08.15	Mpulungu Fishmarket	-8.760472222	31.11219444
LIB3	M	Oretan	Oreochromis tanganicae	Oreochromini	26.08.15	Mpulungu Fishmarket	-8.760472222	31.11219444
LIB4	F	Oretan	Oreochromis tanganicae	Oreochromini	26.08.15	Mpulungu Fishmarket	-8.760472222	31.11219444
LIB5	NA	Oretan	Oreochromis tanganicae	Oreochromini	26.08.15	Mpulungu Fishmarket	-8.760472222	31.11219444
LIC8	M	Tylpol	Tylochromis polylepis	Tylochromini	02.09.15	Mpulungu Fishmarket	-8.760472222	31.11219444
LIC9	M	Tylpol	Tylochromis polylepis	Tylochromini	02.09.15	Mpulungu Fishmarket	-8.760472222	31.11219444
LID1	M	Tylpol	Tylochromis polylepis	Tylochromini	02.09.15	Mpulungu Fishmarket	-8.760472222	31.11219444
LJA1	F	Tylpol	Tylochromis polylepis	Tylochromini	04.11.15	Mpulungu Fishmarket	-8.760472222	31.11219444
LJA7	M	Tchdha	Tangachromis dhanisi	Limnochromini	06.11.15	Chituta	-8.723611111	31.15
LJA8	F	Tchdha	Tangachromis dhanisi	Limnochromini	06.11.15	Chituta	-8.723611111	31.15
LJA9	M	Tchdha	Tangachromis dhanisi	Limnochromini	06.11.15	Chituta	-8.723611111	31.15
LJB1	F	Petmac	Petrochromis macrognathus	Tropheini	06.11.15	Chituta	-8.723611111	31.15
LJB2	F	Petmac	Petrochromis macrognathus	Tropheini	06.11.15	Chituta	-8.723611111	31.15
LJB3	F	Petmac	Petrochromis macrognathus	Tropheini	06.11.15	Chituta	-8.723611111	31.15
LJB4	M	Xensin	Xenotilapia singularis	Ectodini	12.11.15	Ndole bay harbor	-8.476138889	30.44933333
LJB5	M	Xensin	Xenotilapia singularis	Ectodini	12.11.15	Ndole bay harbor	-8.476138889	30.44933333
LJB6	M	Xensin	Xenotilapia singularis	Ectodini	12.11.15	Ndole bay harbor	-8.476138889	30.44933333
LJB7	M	Xensin	Xenotilapia singularis	Ectodini	12.11.15	Ndole bay harbor	-8.476138889	30.44933333
LJB8	F	Xensin	Xenotilapia singularis	Ectodini	12.11.15	Ndole bay harbor	-8.476138889	30.44933333
LJB9	F	Xensin	Xenotilapia singularis	Ectodini	12.11.15	Ndole bay harbor	-8.476138889	30.44933333
LJC1	F	Plemul	Plecodus multidentatus	Perissodini	14.11.15	Chipwa Fishermen	-8.606166667	31.18611111
LJC2	F	Jultra	Julidochromis transcriptus	Lamprologini	23.11.15	Pemba DRC	-3.610861	29.150694
LJC3	M	Neonve	Neolamprologus nigriventris	Lamprologini	NA	NA	NA	NA
LJC5	F	HemstZ	Hemibates koningsi	Bathybatini	NA	Mpulungu Fishmarket	-8.760472222	31.11219444
LJC6	NA	Trecap	Trematocara caparti	Trematocarini	NA	NA	NA	NA
LJC7	NA	Trecap	Trematocara caparti	Trematocarini	NA	NA	NA	NA
LJC8	NA	Trecap	Trematocara caparti	Trematocarini	NA	NA	NA	NA
LJC9	NA	Neocan	Neolamprologus cancellatus	Lamprologini	NA	Wonzye Point	-8.724722222	31.13305556
LJD1	NA	Neocan	Neolamprologus cancellatus	Lamprologini	NA	Wonzye Point	-8.724722222	31.13305556
LJD2	M	Astfla	Astatotilapia flaviijosephi	Haplochromini	NA	NA	NA	NA
LJD3	M	Neospl	Neolamprologus splendens	Lamprologini	NA	Kasu	-7.316667	30.15
LJE8	M	Hplkil	Haplochromis sp. "kilossana"	Haplochromini	NA	Wami river	NA	NA
LNE7	NA	Perecc	Perissodus eccentricus	Perissodini	22.08.16	Toby's Place	-8.623222222	31.20044444
LNF5	NA	Varmoo	Variabilichromis moorii	Lamprologini	22.08.16	Toby's Place	-8.623222222	31.20044444
LNF6	NA	Peteph	Petrochromis ephippium	Tropheini	22.08.16	Toby's Place	-8.623222222	31.20044444
LNH3	F	Xchhec	Xenochromis hecqui	Perissodini	23.08.16	Chipwa Fishermen	-8.606166667	31.18611111
LNH7	NA	Batvit	Bathybates vittatus	Bathybatini	23.08.16	Chipwa Fishermen	-8.606166667	31.18611111
LNH9	M	Batvit	Bathybates vittatus	Bathybatini	23.08.16	Chipwa Fishermen	-8.606166667	31.18611111
LOE1	M	XenorS	Xenotilapia ornatipinnis (South)	Ectodini	26.08.16	Chipwa Fishermen	-8.606166667	31.18611111
LPA4	M	Telvit	Telmatochromis vittatus	Lamprologini	23.08.16	Toby's Place	-8.623222222	31.20044444
MOB4	F	Xennas	Xenotilapia nasus	Ectodini	30.08.16	Chituta	-8.723611111	31.15
MOD4	NA	Bathor	Bathybates hornii	Bathybatini	01.09.16	Mpulungu Fishmarket	-8.760472222	31.11219444
MOD7	F	Cypkan	Cyprichromis sp. "jumbo"	Cyprichromini	02.09.16	Kanfonki	-8.702777778	30.9225
MOD8	F	Cypkan	Cyprichromis sp. "jumbo"	Cyprichromini	02.09.16	Kanfonki	-8.702777778	30.9225
MOD9	M	Cypkan	Cyprichromis sp. "jumbo"	Cyprichromini	02.09.16	Kanfonki	-8.702777778	30.9225
MOE1	M	Cypkan	Cyprichromis sp. "jumbo"	Cyprichromini	02.09.16	Kanfonki	-8.702777778	30.9225
MOE2	NA	NeoveS	Neolamprologus sp. "ventralis stripe"	Lamprologini	03.09.16	Kabwensolo	-8.609722222	30.82916667
MOE5	M	NeoveS	Neolamprologus sp. "ventralis stripe"	Lamprologini	04.09.16	Misepa	-8.588888889	30.80305556
MOE6	M	NeoveS	Neolamprologus sp. "ventralis stripe"	Lamprologini	04.09.16	Misepa	-8.588888889	30.80305556
MOE7	M	NeoveS	Neolamprologus sp. "ventralis stripe"	Lamprologini	04.09.16	Misepa	-8.588888889	30.80305556
MOE8	F	NeoveS	Neolamprologus sp. "ventralis stripe"	Lamprologini	04.09.16	Misepa	-8.588888889	30.80305556
MOH3	F	Trored	Tropheus sp. "red"	Tropheini	06.09.16	Chimba	-8.426111111	30.45666667
MPB2	M	Telshe	Telmatochromis sp. "shell"	Lamprologini	07.09.16	Chibwensolo	-8.442777778	30.45472222
MPD8	F	Lepnka	Lepidiolamprologus nkambae	Lamprologini	09.09.16	Kachese	-8.490527778	30.4775
MUA4	M	Ophhet	Ophthalmotilapia heterodonta	Ectodini	08.08.16	Pemba DRC	-3.610861	29.150694
OME9	NA	Petred	Petrochromis sp. "red"	Tropheini	02.02.17	Nganja	-6.173333333	29.74027778
OMF6	M	BenhoM	Benthochromis sp. "horii mahale"	Benthochromini	04.02.17	Kalila Nkwasi	-6.260555556	29.73666667
OMF7	M	BenhoM	Benthochromis sp. "horii mahale"	Benthochromini	04.02.17	Kalila Nkwasi	-6.260555556	29.73666667
OMF8	M	BenhoM	Benthochromis sp. "horii mahale"	Benthochromini	04.02.17	Kalila Nkwasi	-6.260555556	29.73666667
OMF9	M	BenhoM	Benthochromis sp. "horii mahale"	Benthochromini	04.02.17	Kalila Nkwasi	-6.260555556	29.73666667
OMG1	F	BenhoM	Benthochromis sp. "horii mahale"	Benthochromini	04.02.17	Kalila Nkwasi	-6.260555556	29.73666667
OMG2	F	BenhoM	Benthochromis sp. "horii mahale"	Benthochromini	04.02.17	Kalila Nkwasi	-6.260555556	29.73666667
OMG3	F	BenhoM	Benthochromis sp. "horii mahale"	Benthochromini	04.02.17	Kalila Nkwasi	-6.260555556	29.73666667
OMG4	F	BenhoM	Benthochromis sp. "horii mahale"	Benthochromini	04.02.17	Kalila Nkwasi	-6.260555556	29.73666667
OMG5	M	BenhoM	Benthochromis sp. "horii mahale"	Benthochromini	04.02.17	Kalila Nkwasi	-6.260555556	29.73666667
OMG6	F	Petred	Petrochromis sp. "red"	Tropheini	04.02.17	Kalila Nkwasi	-6.260555556	29.73666667
OMH3	M	NeogrM	Neolamprologus sp. "gracilis tanzania"	Lamprologini	04.02.17	Kalila Nkwasi	-6.260555556	29.73666667
OMH4	M	NeogrM	Neolamprologus sp. "gracilis tanzania"	Lamprologini	04.02.17	Kalila Nkwasi	-6.260555556	29.73666667
OMH5	M	NeogrM	Neolamprologus sp. "gracilis tanzania"	Lamprologini	04.02.17	Kalila Nkwasi	-6.260555556	29.73666667
OMH6	F	NeogrM	Neolamprologus sp. "gracilis tanzania"	Lamprologini	04.02.17	Kalila Nkwasi	-6.260555556	29.73666667
OMH7	M	NeofaM	Neolamprologus sp. "falcicula mahale"	Lamprologini	04.02.17	Kalila Nkwasi	-6.260555556	29.73666667
OMH8	F	NeofaM	Neolamprologus sp. "falcicula mahale"	Lamprologini	04.02.17	Kalila Nkwasi	-6.260555556	29.73666667
OMH9	F	NeofaM	Neolamprologus sp. "falcicula mahale"	Lamprologini	04.02.17	Kalila Nkwasi	-6.260555556	29.73666667
OMI1	M	NeofaM	Neolamprologus sp. "falcicula mahale"	Lamprologini	04.02.17	Kalila Nkwasi	-6.260555556	29.73666667
ONE7	M	Lamorn	Lamprologus ornatipinnis	Lamprologini	21.01.17	Kalalangabo	-4.843611111	29.60944444
ONE8	M	Lamorn	Lamprologus ornatipinnis	Lamprologini	21.01.17	Kalalangabo	-4.843611111	29.60944444
ONE9	M	Lamorn	Lamprologus ornatipinnis	Lamprologini	21.01.17	Kalalangabo	-4.843611111	29.60944444
ONF1	M	Lamorn	Lamprologus ornatipinnis	Lamprologini	21.01.17	Kalalangabo	-4.843611111	29.60944444
Z03	M	Punmac	Pungu maclareni	Oreochromini	NA	NA	NA	NA
Z05	M	Sthloh	Sarotherodon lohbergeri	Oreochromini	NA	NA	NA	NA
Z06	F	Sthloh	Sarotherodon lohbergeri	Oreochromini	NA	NA	NA	NA
Z07	M	Sthste	Sarotherodon steinbachi	Oreochromini	NA	NA	NA	NA
Z09	M	Stopin	Stomatepia pindu	Oreochromini	NA	NA	NA	NA
Z17	M	Sthcar	Sarotherodon caroli	Oreochromini	NA	NA	NA	NA

CHAPTER 3

Supplementary information on the characterisation of the genomic repeat content of Lake Tanganyika cichlids

The genomic repeat content of Lake Tanganyika cichlids

Virginie Ricci

Introduction

Transposable Elements (TEs) are features of the repeat content that can make up to 50% of eukaryotic genomes (Sotero-Caio, Platt, Suh, & Ray, 2017). They are selfish DNA elements able to move and spread within the host genome and hence considered to be drivers of the host genome evolution (see reviews Bourque, 2009; Bourque et al., 2018; Levin & Moran, 2011; Sotero-Caio et al., 2017). TEs can be autonomous or non-autonomous mobile elements and are usually classified in two classes depending on whether the intermediate is RNA or DNA molecule. Class I comprises retrotransposons spreading via a "copy-and-paste" mechanism with 5 orders currently characterized: LTR, DIRS, PLE, LINE and SINE elements. On the other hand, class II includes (DNA) transposons moving via a "cut-and-paste" mechanism. The spread of TEs depends on whether the host uses repressive mechanisms (e.g., methylation of TE promoter) and on the ability of TEs to transpose between non-homologous and homologous genomic sites. The probability that homologous recombinations occur can increase with the copy number of a given TE. Yet, overtime, each copy can acquire mutations resulting in polymorphic TEs (fragmented, divergent and mosaic TE copies) or non-mobile TE fossils. Overall, TEs can affect the sequence, the size, and the structure of the host genome. More specifically, transposable element activity induces structural genomic variations including deletions, duplications, inversions and translocations. Such genomic alterations can modify the regulation, function and coding ability of an existing gene, as well as create new RNA and protein-coding features potentially leading to new phenotypes. Due to the implication of TEs in the host genome evolution, it has been hypothesised that TEs might be involved in evolutionary processes such as adaptation, diversification and speciation (D. C. Ferreira, Porto-Foresti, Oliveira, & Foresti, 2011; Serrato-Capuchina & Matute, 2018; Sotero-Caio et al., 2017). Notably, it has been suggested that the radiating African cichlid lineages are characterised by an increase of TE content (Brawand et al., 2014). In Ronco et al. (2021) (Ronco et al., 2021), we characterised the repeat content in the massive adaptive radiation of Lake Tanganyika cichlid fishes and tested for an association between TE content and per-tribe species richness. Here, I provided further details on the TE content and families identified.

Method

The method is available in the Supplementary Methods section of Ronco et al. (2021) (Ronco et al., 2021). The code used to characterise the repeat content are available on GitHub (https://github.com/cichlidx/ronco_et_al/tree/master/transposable_elements).

Results and discussion

Making use of available genome assemblies, we characterised the TE content in 245 cichlid species occurring in Lake Tanganyika. Overall, we found that approximately 14% of the cichlid host genome are TEs (**Table 1**) (**Figure 4a** of Ronco et al., 2021). DNA transposons constituted the largest part of TEs (>63%), followed by the retrotransposons LINEs, LTR elements, and SINEs (**Table 2**) (**Extended Data Figure 9a** of Ronco et al., 2021). These results were congruent with a previous study on five East African cichlid reference genomes (Brawand et al., 2014).

Furthermore, we found that the TE content of Lake Tanganyika cichlids included families belonging to both Class I and II (**Table 3**). More specifically, 32 DNA transposons elements and 32 retrotransposons were identified. Overall, the three most abundant TE families were two DNA transposons (TcMar.Tc1 [Tc1-Mariner] and hAT.Ac [hAT]) and one retrotransposon (L2 [LINE-2]) (**Figure 2**). A previous study on the TE content of six African cichlid species (Carleton et al., 2020) also found that Tc1-Mariner and hAT were among the top three TE families (with Rex1/Babar LINE retrotransposons).

In addition to an increase of TEs in the radiating African cichlid lineages, it has been suggested that TEs are implicated with the evolution and emergence of sex chromosomes in fish (Böhne et al., 2019; Chalopin, Volff, Galiana, Anderson, & Schartl, 2015; I. A. Ferreira & Martins, 2008; Harvey et al., 2003) and with cichlid visual diversity (TEs found in the promotor region of visual opsins underlying changes in expression) (Carleton et al., 2020). Hence, future projects should examine the distribution of TEs in the cichlids' genome and the genomic alterations caused by TEs.

References

Böhne, A., Weber, A. A. T., Rajkov, J., Rechsteiner, M., Riss, A., Egger, B., & Salzburger, W. (2019). Repeated evolution versus common ancestry: Sex chromosome evolution in the haplochromine CICHLIDX Pseudocrenilabrus philander. *Genome Biology and Evolution*, *11*(2), 439–458. doi: 10.1093/gbe/evz003

Bourque, G. (2009). Transposable elements in gene regulation and in the evolution of vertebrate genomes. *Current Opinion in Genetics and Development*, *19*(6), 607–612. doi: 10.1016/j.gde.2009.10.013

Bourque, G., Burns, K. H., Gehring, M., Gorbunova, V., Seluanov, A., Hammell, M., … Feschotte, C. (2018). Ten things you should know about transposable elements. *Genome Biology*, *19*(1), 1–12. doi: 10.1186/s13059-018-1577-z

Brawand, D., Wagner, C. E., Li, Y. I., Malinsky, M., Keller, I., Fan, S., … Di Palma, F. (2014). The genomic substrate for adaptive radiation in African cichlid fish. *Nature*, *513*(7518), 375–381. doi: 10.1038/nature13726

Carleton, K. L., Conte, M. A., Malinsky, M., Nandamuri, S. P., Sandkam, B. A., Meier, J. I., … Kocher, T. D. (2020). Movement of transposable elements contributes to cichlid diversity. *Molecular Ecology*, *29*(24), 4956–4969. doi: 10.1111/mec.15685

Chalopin, D., Volff, J. N., Galiana, D., Anderson, J. L., & Schartl, M. (2015). Transposable elements and early evolution of sex chromosomes in fish. *Chromosome Research*, *23*(3), 545–560. doi: 10.1007/s10577-015-9490-8

Ferreira, D. C., Porto-Foresti, F., Oliveira, C., & Foresti, F. (2011). Transposable elements as a potential source for understanding the fish genome. *Mobile Genetic Elements*, *1*(2), 112–117. doi: 10.4161/mge.1.2.16731

Ferreira, I. A., & Martins, C. (2008). Physical chromosome mapping of repetitive DNA sequences in Nile tilapia Oreochromis niloticus: Evidences for a differential distribution of repetitive elements in the sex chromosomes. *Micron*, *39*(4), 411–418. doi: 10.1016/j.micron.2007.02.010

Harvey, S. C., Boonphakdee, C., Campos-Ramos, R., Ezaz, M. T., Griffin, D. K., Bromage, N. R., & Penman, D. J. (2003). Analysis of repetitive DNA sequences in the sex chromosomes of Oreochromis niloticus. *Cytogenetic and Genome Research*, *101*(3–4), 314–319. doi: 10.1159/000074355

Levin, H. L., & Moran, J. V. (2011). Dynamic interactions between transposable elements and their hosts. *Nature Reviews Genetics*, *12*(9), 615–627. doi: 10.1038/nrg3030

Ronco, F., Matschiner, M., Böhne, A., Boila, A., Büscher, H. H., El Taher, A., … Salzburger, W. (2021). Drivers and dynamics of a massive adaptive radiation in cichlid fishes. *Nature*, *589*, 76–81. doi: 10.1038/s41586-020-2930-4

Serrato-Capuchina, A., & Matute, D. R. (2018). The role of transposable elements in speciation. *Genes*, *9*(5). doi: 10.3390/genes9050254

Sotero-Caio, C. G., Platt, R. N., Suh, A., & Ray, D. A. (2017). Evolution and diversity

of transposable elements in vertebrate genomes. *Genome Biology and Evolution*, *9*(1), 161–177. doi: 10.1093/gbe/evw264

Table 1 **Proportion [%] of TEs in the host genome.**

	Minimum	1st quartile	Median	Mean	3rd quartile	Max
TEs	12.030	13.650	14.010	13.975	14.330	15.200

Table 2 **Proportion [%] of TE classes (with respect to all TEs).**

		Minimum	1st quartile	Median	Mean	3rd quartile	Max
Retrotransposons	**LINEs**	26.118	28.582	29.462	29.308	30.065	32.431
	SINEs	0.493	0.964	1.226	1.240	1.503	2.411
	LTR elements	1.932	2.273	2.407	2.428	2.557	3.194
DNA transposons		63.750	66.186	66.953	67.023	67.929	70.228

Table 3 **TE families identified in the cichlid species of Lake Tanganyika.** Retrotransposons include SINEs, LINEs, and LTR elements.

DNA transposons
Academ.1
CMC.Chapaev
CMC.Chapaev.3
CMC.EnSpm
Dada
DNA
hAT
hAT.Ac
hAT.Blackjack
hAT.Charlie
hAT.hAT5
hAT.hATx
hAT.Tag1
hAT.Tip100
hAT.Tol2
Helitron
Kolobok
Kolobok.T2
MuLE.MuDR
P
PIF.Harbinger
PIF.ISL2EU
PiggyBac
Sola
TcMar.Fot1
TcMar.ISRm11
TcMar.Mariner
TcMar.Tc1
TcMar.Tc2
TcMar.Tigger
Zisupton
Zisupton.hAT.hybrid

Retrotransposons		
LINEs	**SINEs**	**LTR elements**
CR1	SINE	Copia
CR1.Zenon	tRNA.Core	DIRS
Dong.R4	tRNA.Core.L2	ERV1
I	tRNA.Mermaid	ERV4
I.Nimb	tRNA.V	Gypsy
Jockey		Gypsy.Cigr
L1		LTR
L1.Tx1		Ngaro
L2		Pao
LINE		
Penelope		
Proto2		
R1		
R2		
R2.Hero		
Rex.Babar		
RTE.BovB		
RTE.X		

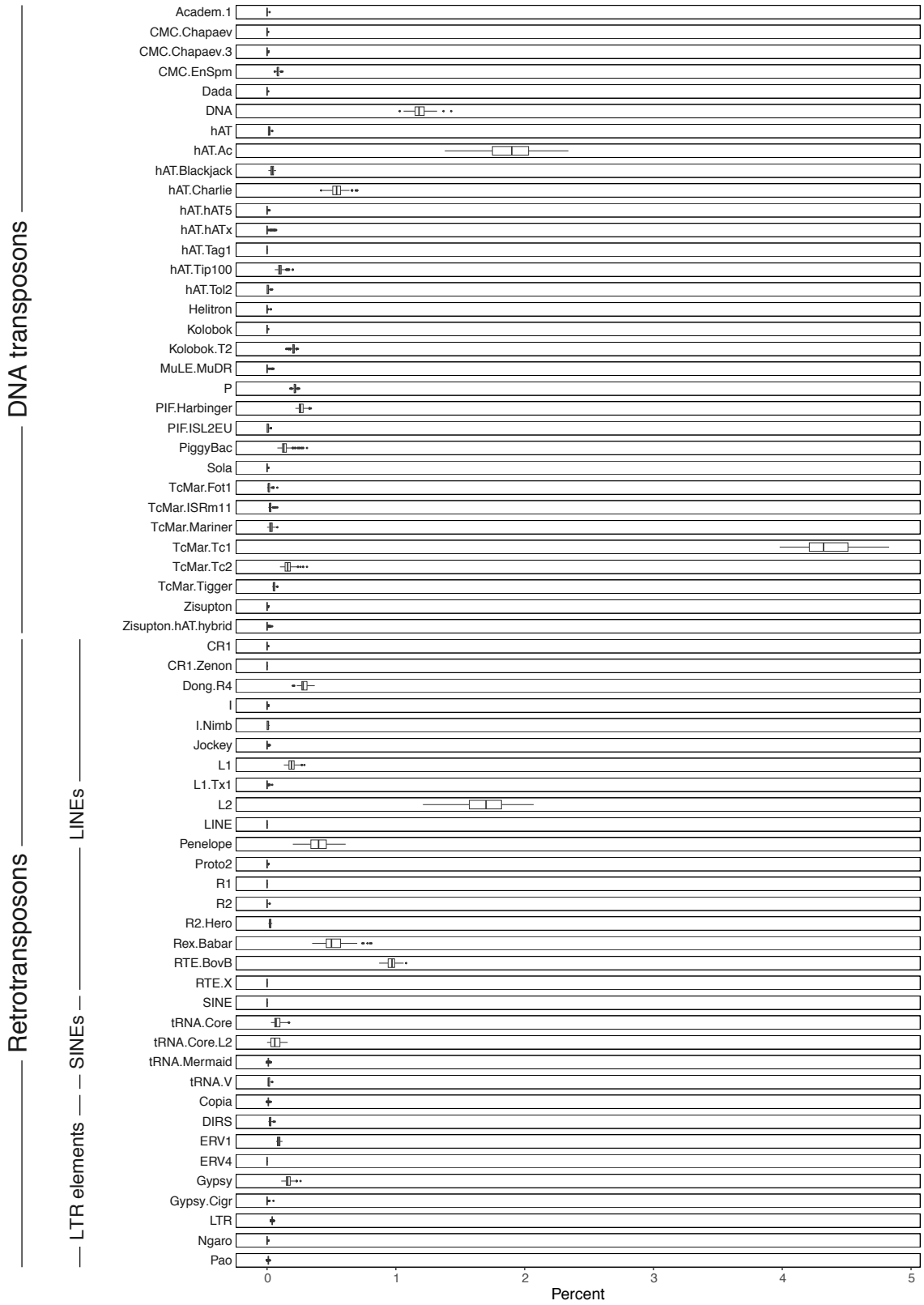

Figure 1 **Proportion of TE families within the genome of 245 cichlid species of Lake Tanganyika.**

Extended Figures

The extended figures represent the TE content per genome assembly using RepeatMasker and RepeatMasker combined with RepeatModeler. For each tribe and species, the stacked barplots show (1) the total length of TEs (in bp), (2) the TE proportion (in %) in relation to the genome size, (3) the proportion (in %) of each TE category in relation to the total TE content, and (4) the proportion (in %) of each TE feature in relation to the genome size. The barplots are colour-coded according to the main TE categories (retrotransposons: SINEs, LINEs, and LTR elements; and DNA transposons).

1

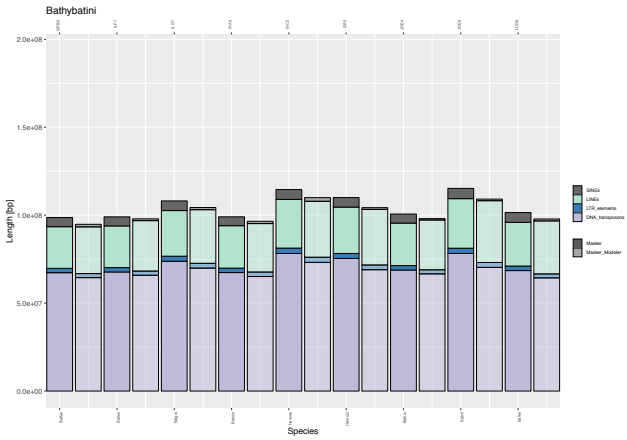
Bathybatini
Length [bp]
Species
SINEs
LINEs
LTR_elements
DNA_transposons
Masker
Masker_Modeler

3

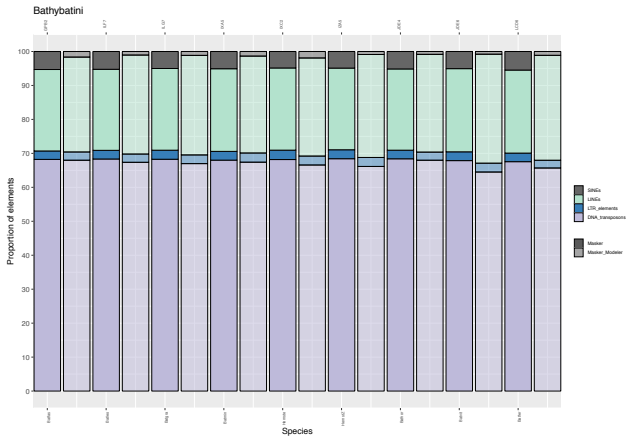
Bathybatini
Proportion of elements
Species
SINEs
LINEs
LTR_elements
DNA_transposons
Masker
Masker_Modeler

2

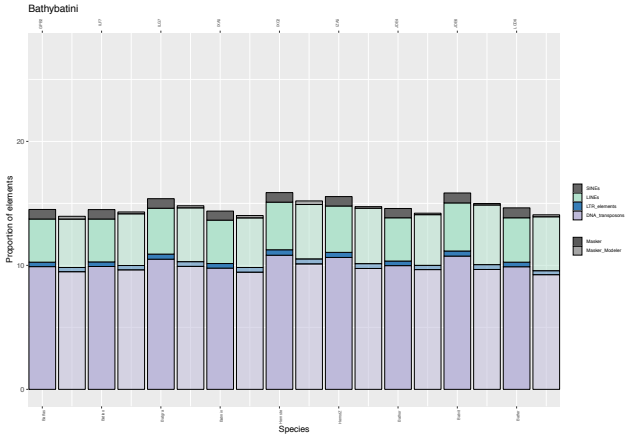
Bathybatini
Proportion of elements
Species
SINEs
LINEs
LTR_elements
DNA_transposons
Masker
Masker_Modeler

4

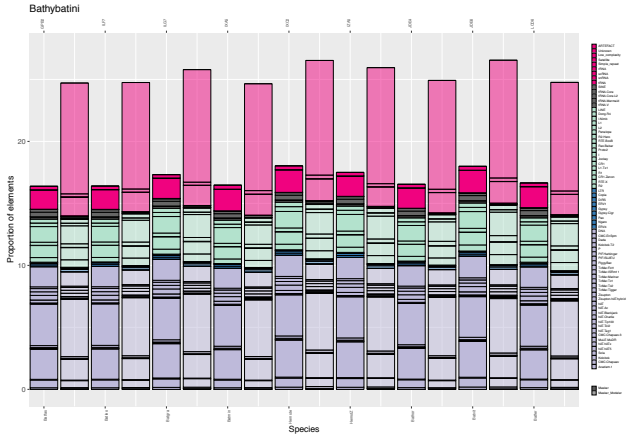
Bathybatini
Proportion of elements
Species

1

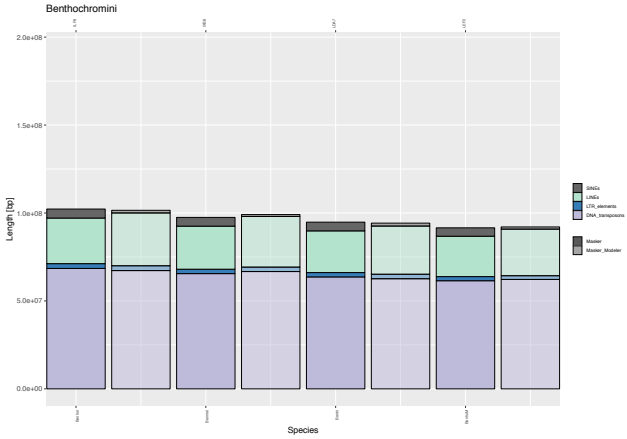
Benthochromini
Length [bp]
Species
SINEs
LINEs
LTR_elements
DNA_transposons
Masker
Masker_Modeler

3

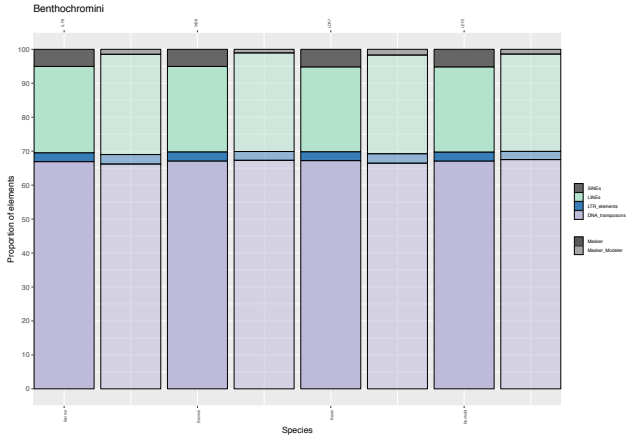
Benthochromini
Proportion of elements
Species
SINEs
LINEs
LTR_elements
DNA_transposons
Masker
Masker_Modeler

2

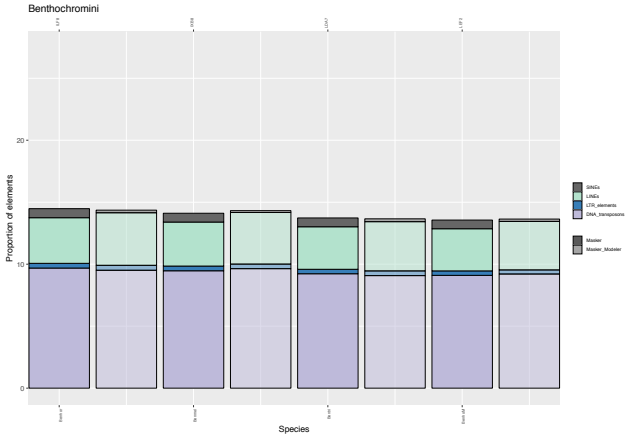
Benthochromini
Proportion of elements
Species
SINEs
LINEs
LTR_elements
DNA_transposons
Masker
Masker_Modeler

4

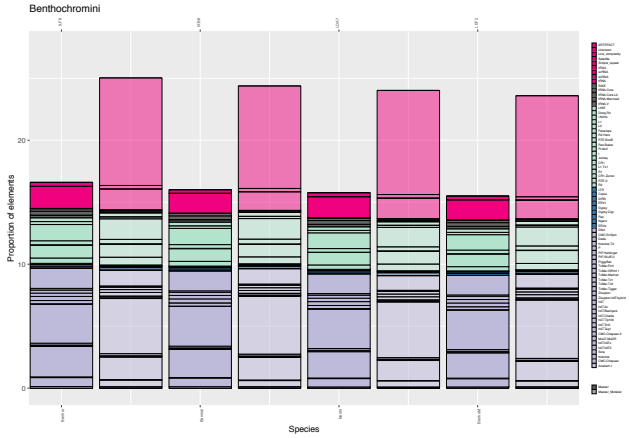
Benthochromini
Proportion of elements
Species

1

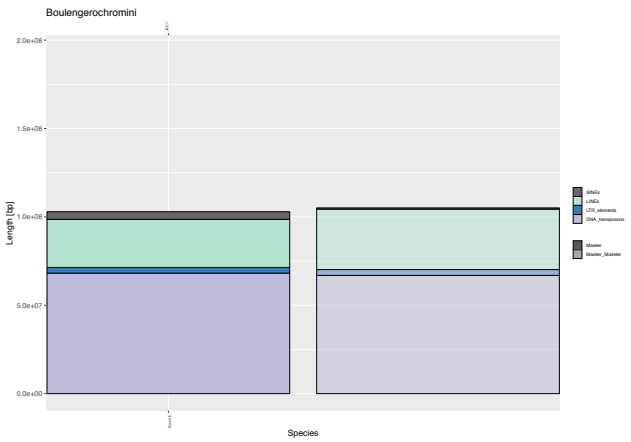
Boulengerochromini
Length [bp]
2.0e+08
1.5e+08
1.0e+08
5.0e+07
0.0e+00
Species
SINEs
LINEs
LTR_elements
DNA_transposons
Masker
Masker_Modeler

3

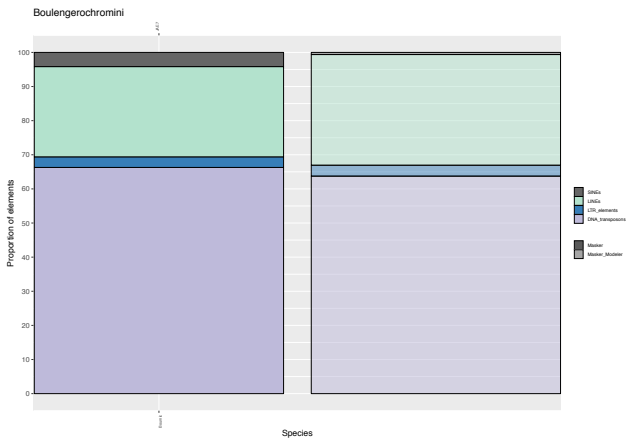
Boulengerochromini
Proportion of elements
100
90
80
70
60
50
40
30
20
10
0
Species
SINEs
LINEs
LTR_elements
DNA_transposons
Masker
Masker_Modeler

2

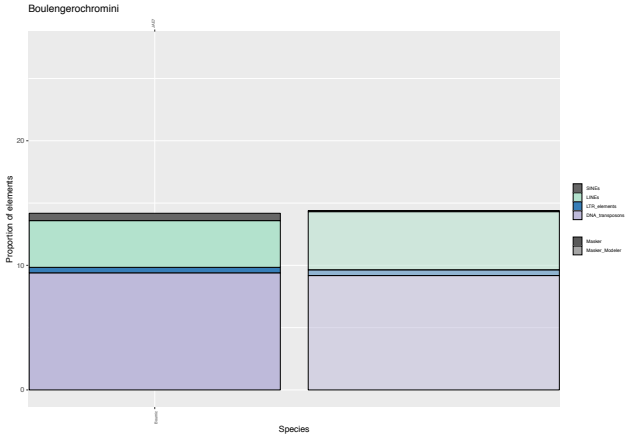
Boulengerochromini
Proportion of elements
20
10
0
Species
SINEs
LINEs
LTR_elements
DNA_transposons
Masker
Masker_Modeler

4

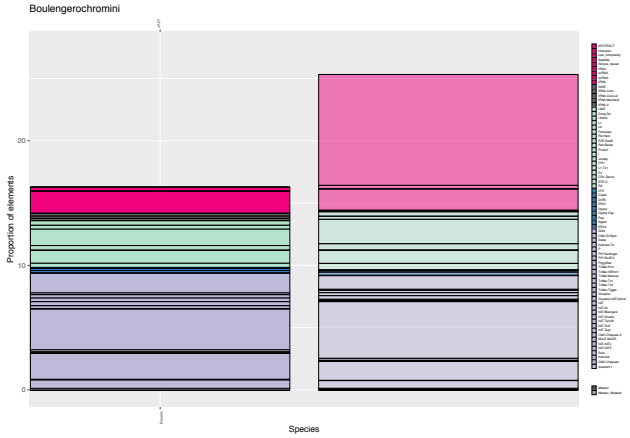
Boulengerochromini
Proportion of elements
20
10
0
Species

1

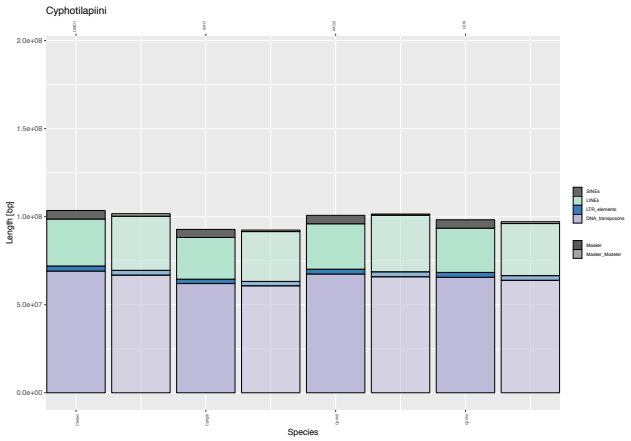
Cyphotilapiini
Length [bp]
2.0e+08
1.5e+08
1.0e+08
5.0e+07
0.0e+00
Species
SINEs
LINEs
LTR_elements
DNA_transposons
Masker
Masker_Modeler

3

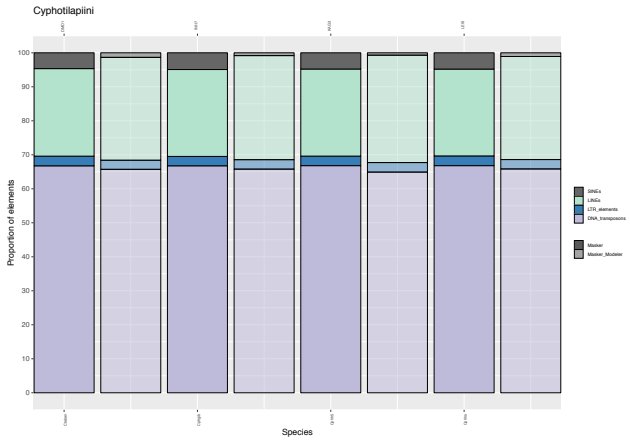
Cyphotilapiini
Proportion of elements
100
90
80
70
60
50
40
30
20
10
0
Species
SINEs
LINEs
LTR_elements
DNA_transposons
Masker
Masker_Modeler

2

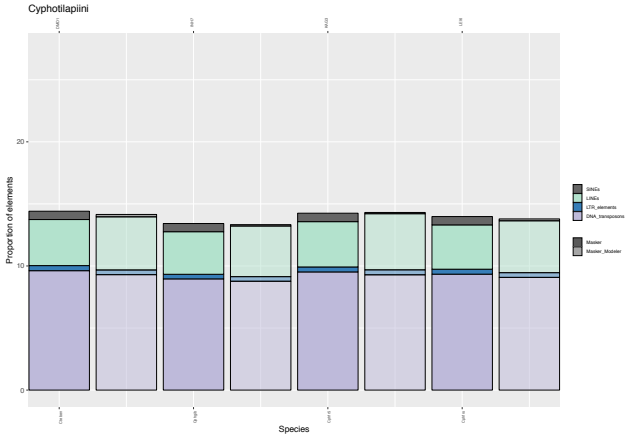
Cyphotilapiini
Proportion of elements
20
10
0
Species
SINEs
LINEs
LTR_elements
DNA_transposons
Masker
Masker_Modeler

4

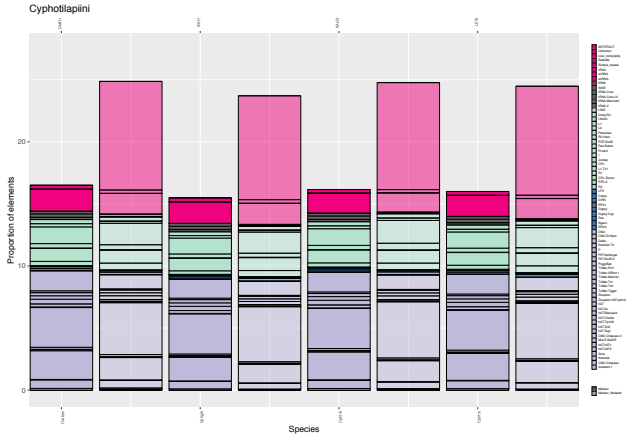
Cyphotilapiini
Proportion of elements
20
10
0
Species

1

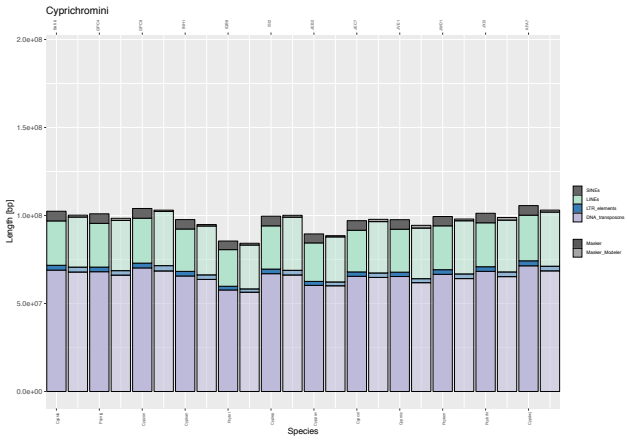
Cyprichromini
Length (bp)
Species
SINEs
LINEs
LTR_elements
DNA_transposons
Maskier
Maskier_Modeler

3

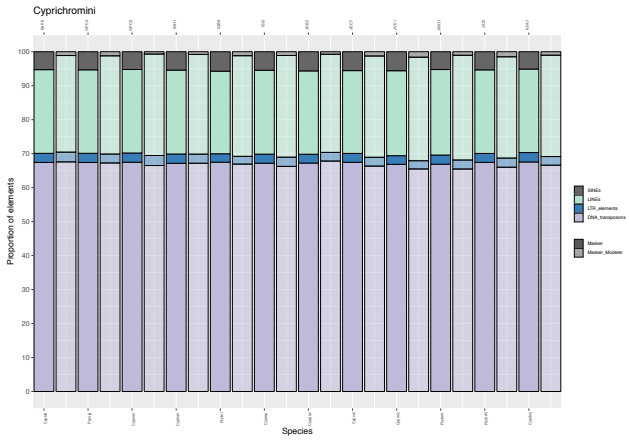
Cyprichromini
Proportion of elements
Species
SINEs
LINEs
LTR_elements
DNA_transposons
Maskier
Maskier_Modeler

2

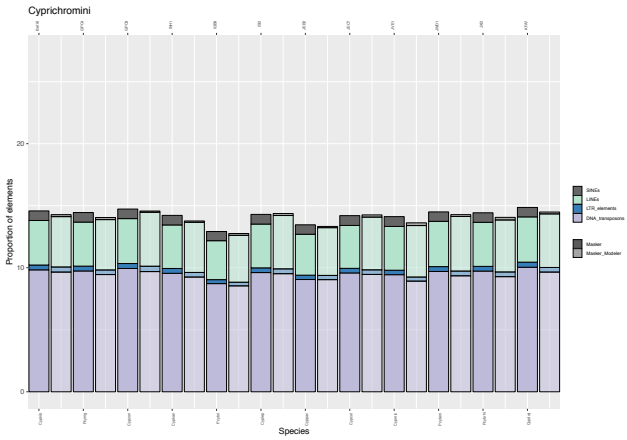
Cyprichromini
Proportion of elements
Species
SINEs
LINEs
LTR_elements
DNA_transposons
Maskier
Maskier_Modeler

4

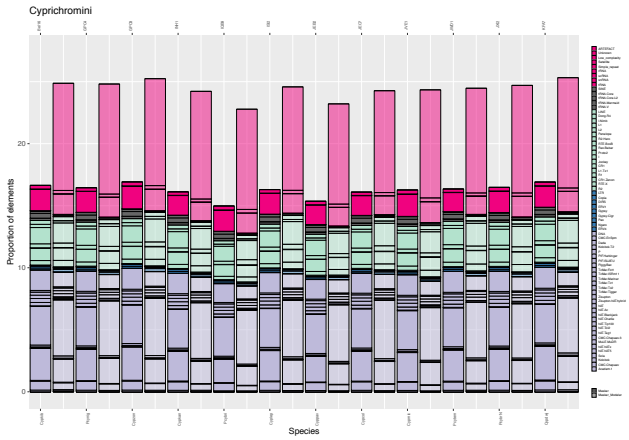
Cyprichromini
Proportion of elements
Species

1

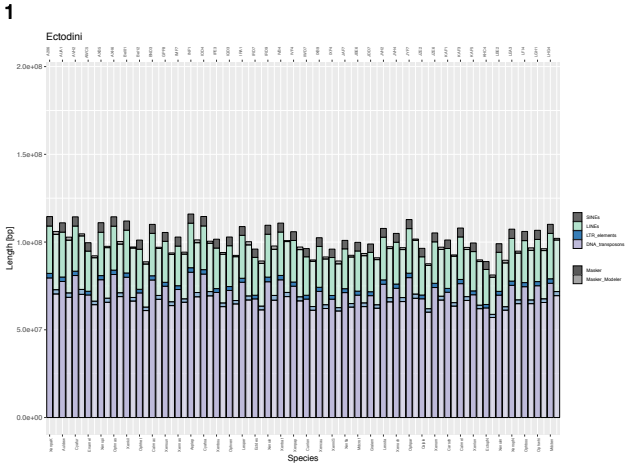
Ectodini
Length (bp)
Species
SINEs
LINEs
LTR_elements
DNA_transposons
Maskier
Maskier_Modeler

3

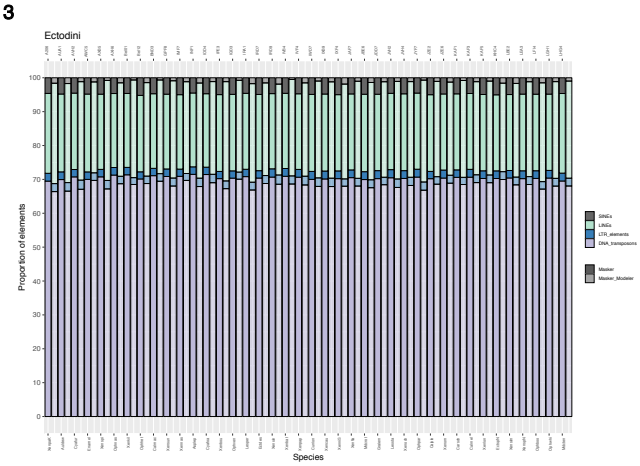
Ectodini
Proportion of elements
Species
SINEs
LINEs
LTR_elements
DNA_transposons
Maskier
Maskier_Modeler

2

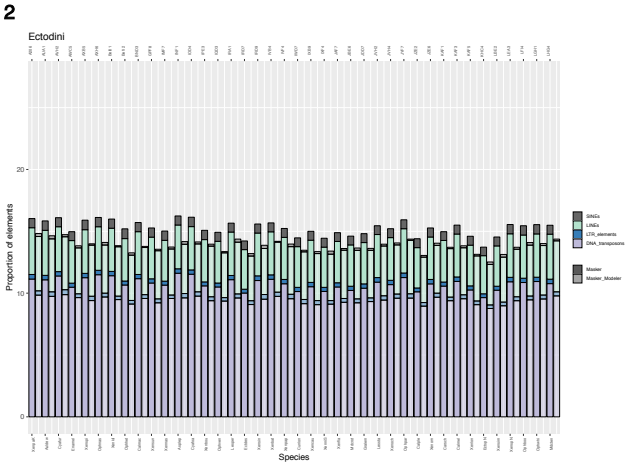
Ectodini
Proportion of elements
Species
SINEs
LINEs
LTR_elements
DNA_transposons
Maskier
Maskier_Modeler

4

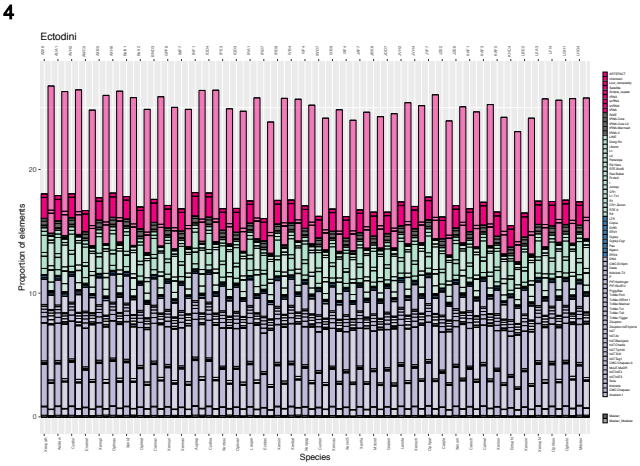
Ectodini
Proportion of elements
Species

1

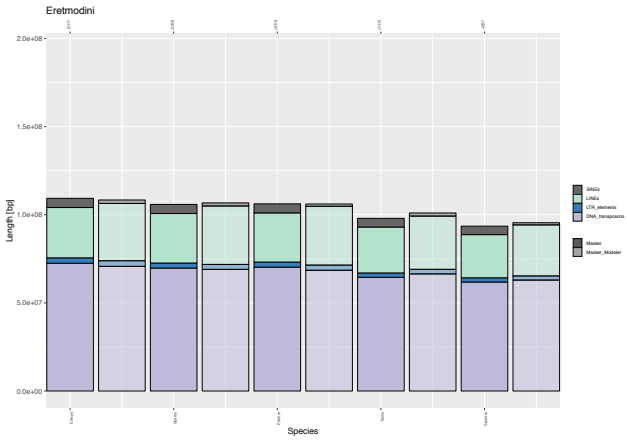
Eretmodini
Length [bp]
Species
SINEs
LINEs
LTR_elements
DNA_transposons
Maskier
Maskier_Modeler

3

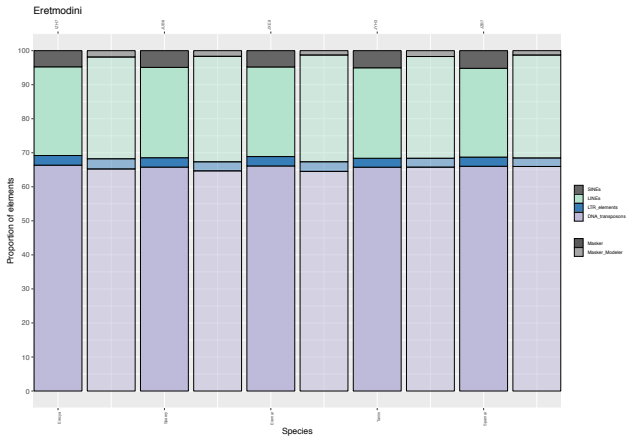
Eretmodini
Proportion of elements
Species
SINEs
LINEs
LTR_elements
DNA_transposons
Maskier
Maskier_Modeler

2

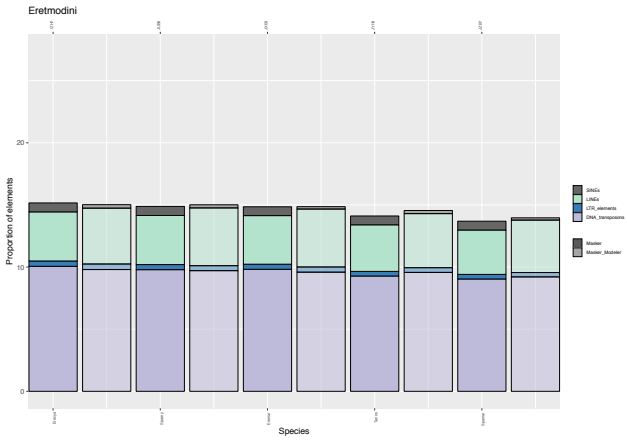
Eretmodini
Proportion of elements
Species
SINEs
LINEs
LTR_elements
DNA_transposons
Maskier
Maskier_Modeler

4

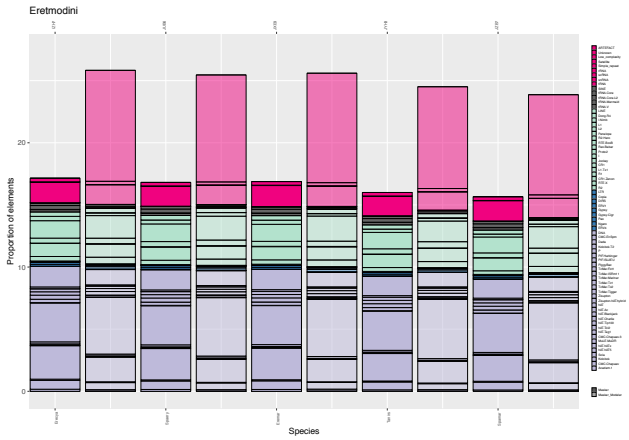
Eretmodini
Proportion of elements
Species

1

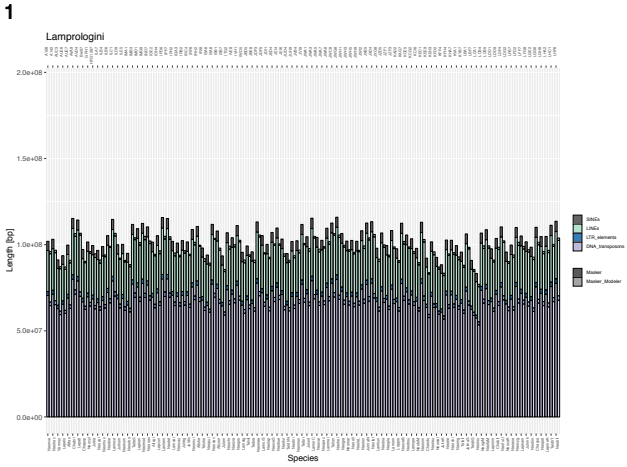
Lamprologini
Length [bp]
Species
SINEs
LINEs
LTR_elements
DNA_transposons
Maskier
Maskier_Modeler

3

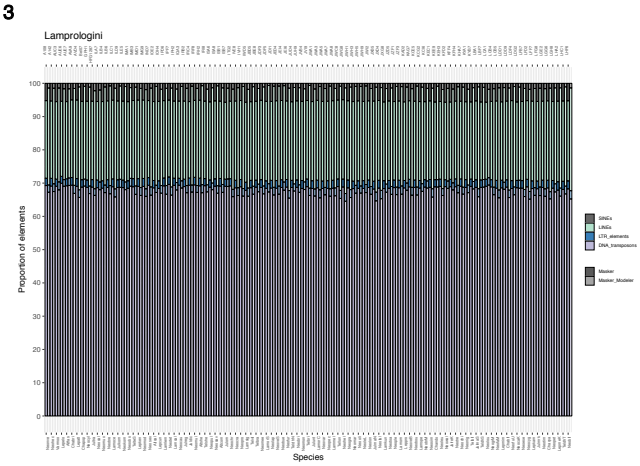
Lamprologini
Proportion of elements
Species
SINEs
LINEs
LTR_elements
DNA_transposons
Maskier
Maskier_Modeler

2

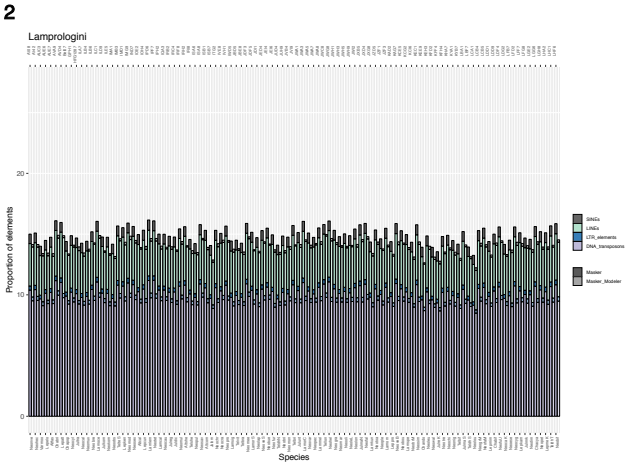
Lamprologini
Proportion of elements
Species
SINEs
LINEs
LTR_elements
DNA_transposons
Maskier
Maskier_Modeler

4

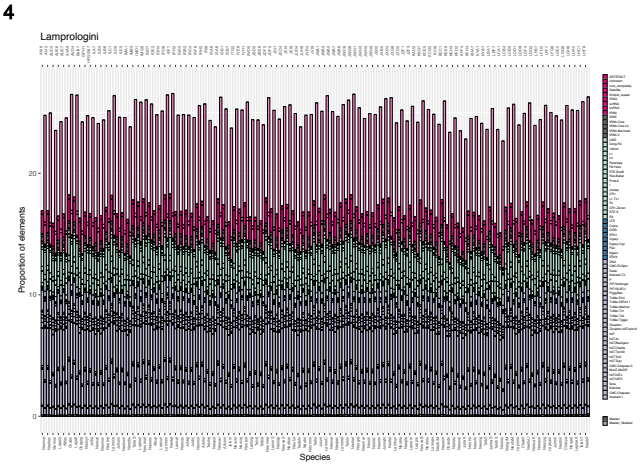
Lamprologini
Proportion of elements
Species

1

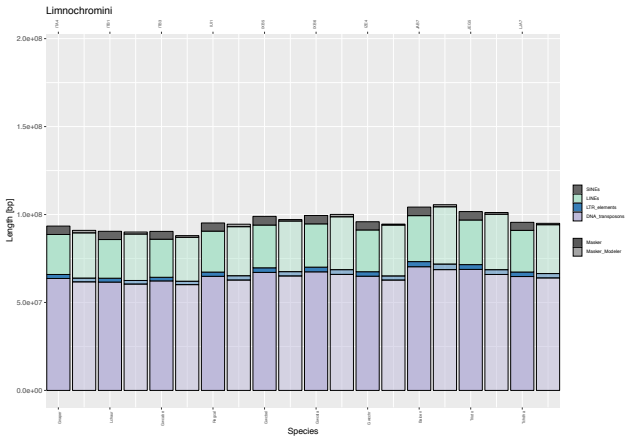
Limnochromini
Length [bp]
Species
SINEs
LINEs
LTR_elements
DNA_transposons
Maskier
Maskier_Modeler

3

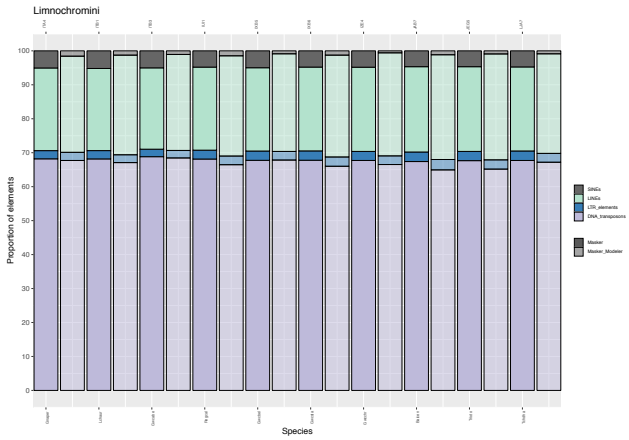
Limnochromini
Proportion of elements
Species
SINEs
LINEs
LTR_elements
DNA_transposons
Maskier
Maskier_Modeler

2

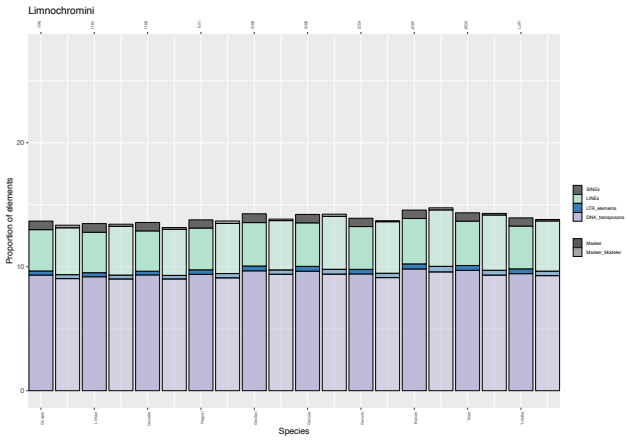
Limnochromini
Proportion of elements
Species
SINEs
LINEs
LTR_elements
DNA_transposons
Maskier
Maskier_Modeler

4

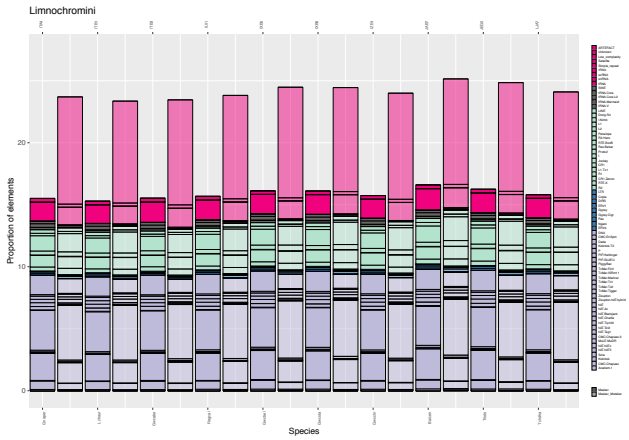
Limnochromini
Proportion of elements
Species

1

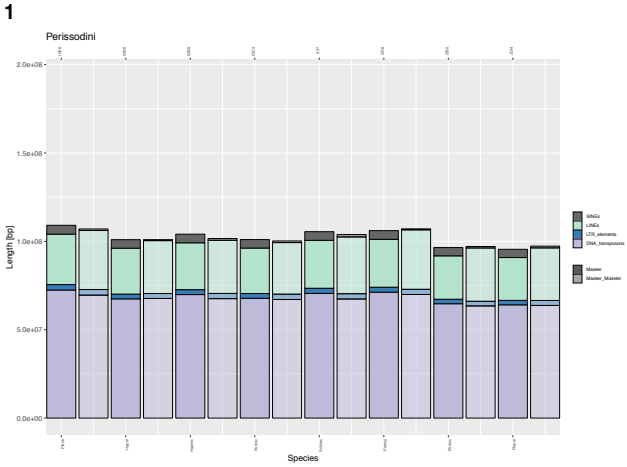
Perissodini
Length [bp]
Species
SINEs
LINEs
LTR_elements
DNA_transposons
Maskier
Maskier_Modeler

3

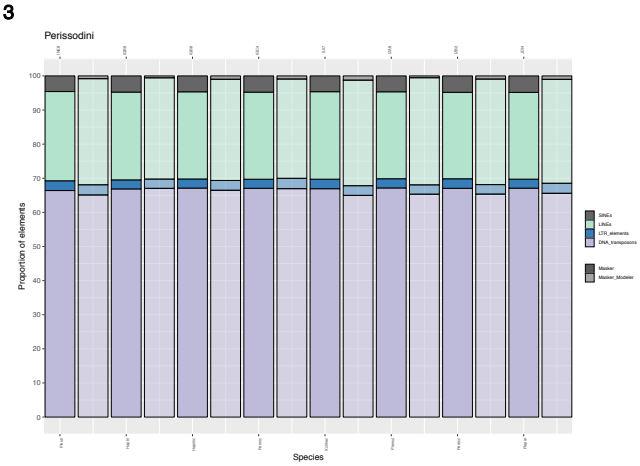
Perissodini
Proportion of elements
Species
SINEs
LINEs
LTR_elements
DNA_transposons
Maskier
Maskier_Modeler

2

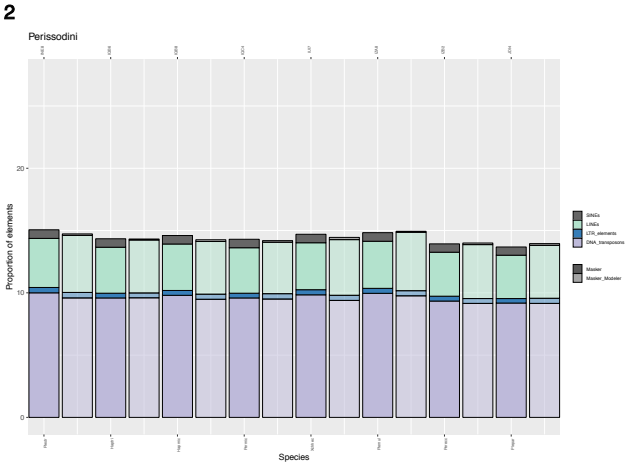
Perissodini
Proportion of elements
Species
SINEs
LINEs
LTR_elements
DNA_transposons
Maskier
Maskier_Modeler

4

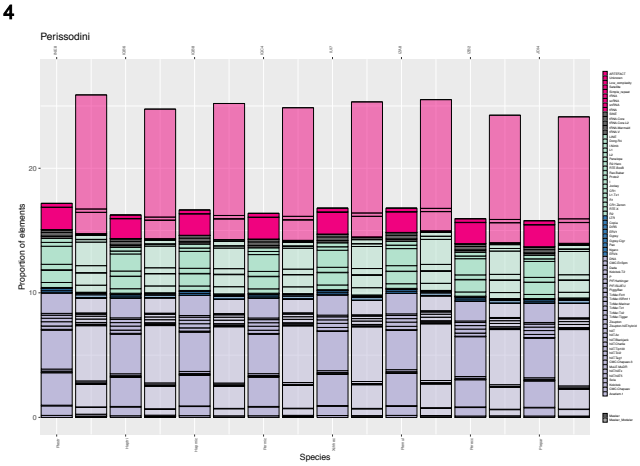
Perissodini
Proportion of elements
Species

1

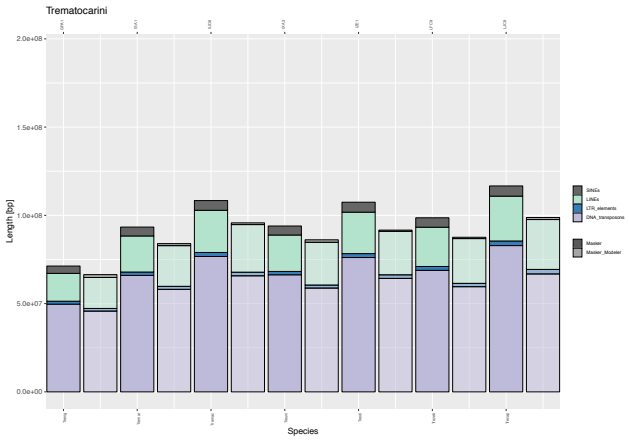
Trematocarini
Length [bp]
Species
SINEs
LINEs
LTR_elements
DNA_transposons
Masker
Masker_Modeler

3

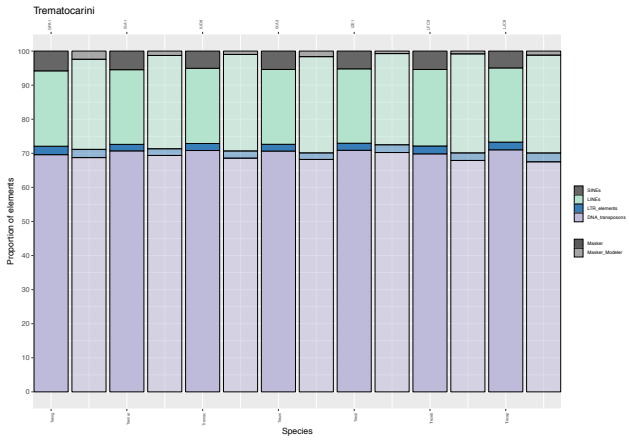
Trematocarini
Proportion of elements
Species
SINEs
LINEs
LTR_elements
DNA_transposons
Masker
Masker_Modeler

2

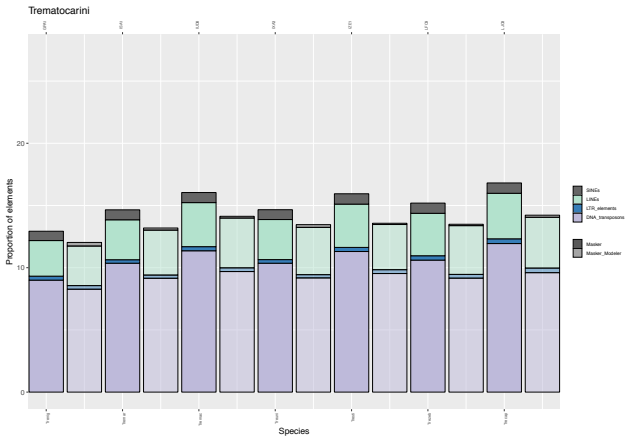
Trematocarini
Proportion of elements
Species
SINEs
LINEs
LTR_elements
DNA_transposons
Masker
Masker_Modeler

4

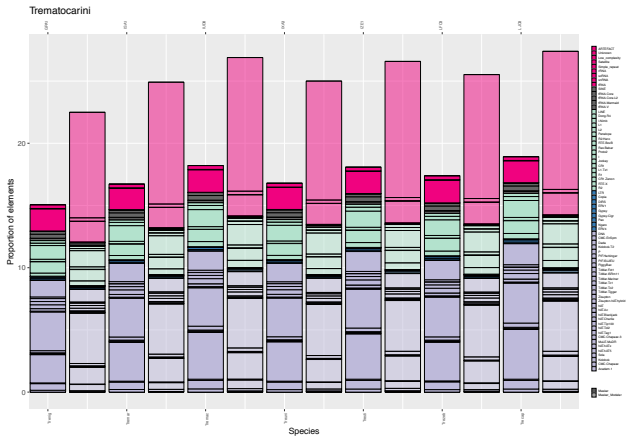
Trematocarini
Proportion of elements
Species

1

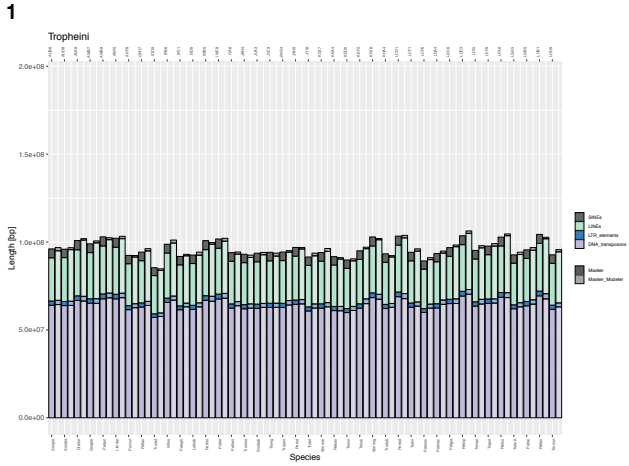
Tropheini
Length [bp]
Species
SINEs
LINEs
LTR_elements
DNA_transposons
Masker
Masker_Modeler

3

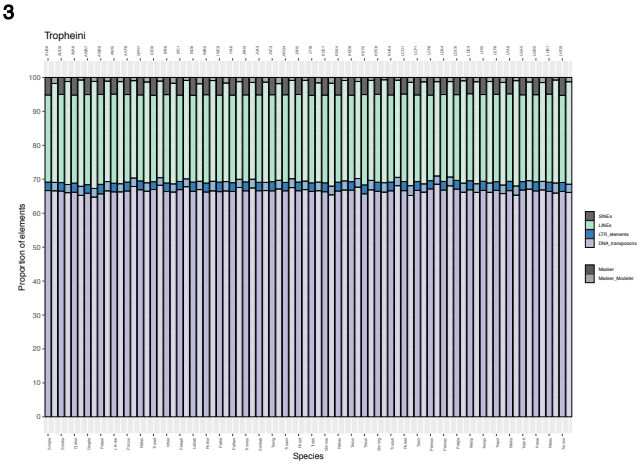
Tropheini
Proportion of elements
Species
SINEs
LINEs
LTR_elements
DNA_transposons
Masker
Masker_Modeler

2

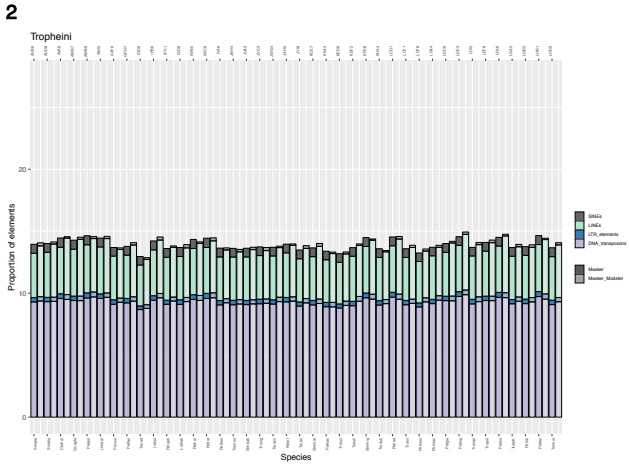
Tropheini
Proportion of elements
Species
SINEs
LINEs
LTR_elements
DNA_transposons
Masker
Masker_Modeler

4

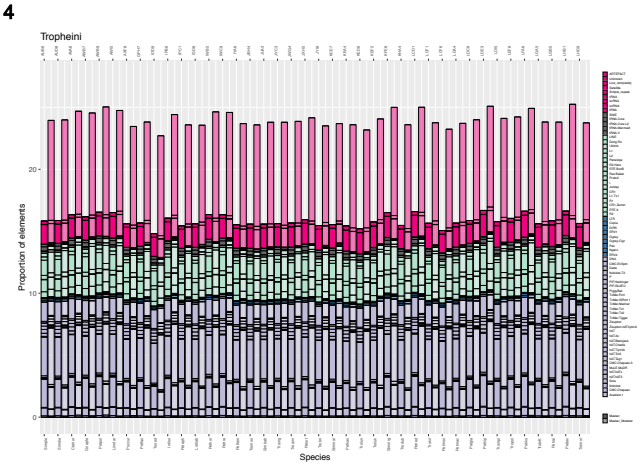
Tropheini
Proportion of elements
Species

CHAPTER 4

QTL study reveals candidate genes underlying host resistance in a Red Queen model system

Maridel Fredericksen, Peter D. Fields, Louis Du Pasquier, **Virginie Ricci** & Dieter Ebert

PLOS Genetics (2023)

PLOS GENETICS

RESEARCH ARTICLE

QTL study reveals candidate genes underlying host resistance in a Red Queen model system

Maridel Fredericksen*, Peter D. Fields, Louis Du Pasquier, Virginie Ricci, Dieter Ebert

University of Basel, Department of Environmental Sciences, Zoology, Basel, Switzerland

* maridel.fredericksen@unibas.ch

OPEN ACCESS

Citation: Fredericksen M, Fields PD, Du Pasquier L, Ricci V, Ebert D (2023) QTL study reveals candidate genes underlying host resistance in a Red Queen model system. PLoS Genet 19(2): e1010570. https://doi.org/10.1371/journal.pgen.1010570

Editor: Harmit S. Malik, Fred Hutchinson Cancer Research Center, UNITED STATES

Received: July 11, 2022

Accepted: December 14, 2022

Published: February 2, 2023

Peer Review History: PLOS recognizes the benefits of transparency in the peer review process; therefore, we enable the publication of all of the content of peer review and author responses alongside final, published articles. The editorial history of this article is available here: https://doi.org/10.1371/journal.pgen.1010570

Data Availability Statement: Scripts for the QTL analysis, RepeatModeler analysis, codon-based sequence alignment, differential expression analysis, and transcript mapping as well as

Abstract

Specific interactions of host and parasite genotypes can lead to balancing selection, maintaining genetic diversity within populations. In order to understand the drivers of such specific coevolution, it is necessary to identify the molecular underpinnings of these genotypic interactions. Here, we investigate the genetic basis of resistance in the crustacean host, *Daphnia magna*, to attachment and subsequent infection by the bacterial parasite, *Pasteuria ramosa*. We discover a single locus with Mendelian segregation (3:1 ratio) with resistance being dominant, which we call the F locus. We use QTL analysis and fine mapping to localize the F locus to a 28.8-kb region in the host genome, adjacent to a known resistance supergene. We compare the 28.8-kb region in the two QTL parents to identify differences between host genotypes that are resistant versus susceptible to attachment and infection by the parasite. We identify 13 genes in the region, from which we highlight eight biological candidates for the F locus, based on presence/absence polymorphisms and differential gene expression. The top candidates include a fucosyltransferase gene that is only present in one of the two QTL parents, as well as several Cladoceran-specific genes belonging to a large family that is represented in multiple locations of the host genome. Fucosyltransferases have been linked to resistance in previous studies of *Daphnia–Pasteuria* and other host–parasite systems, suggesting that *P. ramosa* spore attachment could be mediated by changes in glycan structures on *D. magna* cuticle proteins. The Cladoceran-specific candidate genes suggest a resistance strategy that relies on gene duplication. Our results add a new locus to a growing genetic model of resistance in the *D. magna–P. ramosa* system. The identified candidate genes will be used in future functional genetic studies, with the ultimate aim to test for cycles of allele frequencies in natural populations.

Author summary

Identifying the genes under selection is often a necessary step toward understanding the processes that drive evolution. In the case of coevolving hosts and parasites, the host genes under selection are those that confer resistance to the parasite. Here, we aim to identify genes conferring resistance in a coevolving host–parasite system. We map a newly discovered resistance locus to a region adjacent to a previously described resistance supergene, and we validate the locus with additional genetic crosses. By comparing the genes present

associated data files are available on GitHub (https://github.com/maf8a/Flocus_QTL) and archived through Zenodo (doi: 10.5281/zenodo.7437819). Assembled and annotated haplotypes of the F-locus region, as well as additional Sanger sequencing data from iF, are available on GenBank (xF accession number: OP831933; iF accession number: OP831934; Sanger accession numbers: OP795832, OP795833, OP795834).

Funding: This work was funded by the Swiss National Science Foundation (https://www.snf.ch), grants 310030B_166677 and 310030_188887 to DE. The funders had no role in study design, data collection and analysis, decision to publish, or preparation of the manuscript.

Competing interests: The authors have declared that no competing interests exist.

in resistant versus susceptible hosts and by analyzing gene expression data, we identify eight biological candidates. One of the top candidates represents a newly identified gene family that is only found in closely related species and is duplicated in several areas in the genome, and another top candidate strengthens a working hypothesis that resistance might depend on sugar molecules. This work broadens our perspective on the complexity and diversity of resistance loci in this host–parasite system, and it pinpoints intriguing candidates that will be tested in future gene knock-out experiments. Follow-up population genetic studies will help us better understand how parasites coevolve with their hosts in natural populations.

Introduction

Understanding how diversity is maintained in natural populations is a major goal of evolutionary biology. One way that diversity may be maintained is through coevolution with parasites. For example, the Red Queen hypothesis predicts host and parasite allele frequencies cycle under negative frequency-dependent selection (NFDS), meaning that common genotypes are selected against. A key prerequisite to testing various models of coevolution, including the Red Queen hypothesis, is to identify the loci determining host resistance and parasite infectivity, because these are the loci under selection during coevolution [1]. Despite their importance for understanding coevolution, genetic variants responsible for resistance/susceptibility polymorphisms have only been identified in a few systems, such as R genes in plants [2–4], MHC genes mediating HIV progression in humans [5,6], and viral resistance genes in *Drosophila* [7,8].

The cyclically parthenogenetic freshwater crustacean, *Daphnia magna*, and its bacterial parasite, *Pasteuria ramosa*, have been studied extensively as a natural host–parasite system likely coevolving under NFDS [9–11]. Early studies suggested resistance in this system may have a relatively simple genetic basis. Variation in host resistance depends largely on a single step in the infection process, in which parasite spores attach to a susceptible host's cuticle [12]. This spore attachment is determined by the combination of host and parasite genotypes, with negligible environmental effects [13–15]. Furthermore, genetic crosses demonstrated that host resistance to two *P. ramosa* genotypes shows Mendelian segregation [11]. The combination of Mendelian segregation and little to no effects of the environment suggested that resistance may be controlled by few loci with strong effect.

However, subsequent studies with additional *P. ramosa* genotypes have begun to reveal an increasingly complex genetic architecture of host resistance. The current model includes five resistance loci (A, B, C, D, and E), located on three separate chromosomes and explaining resistance to four *P. ramosa* genotypes (C1, C19, P15, and P20). Moreover, resistance to each genotype is explained by at least two of the loci, which interact through dominance and epistasis [16–18]. An additional layer of complexity is the attachment sites: it was first thought that *P. ramosa* attaches exclusively to the foregut of its host (this is the case for genotypes C1, C19, and P20), but genotype P15 was found to attach to the host's hindgut [18]. A recent study found that *P. ramosa* can infect its host through at least three additional attachment sites [19], suggesting that studies so far have only scratched the surface of the diversity of host–parasite interactions in this system. Despite the insights into the genetic architecture of resistance, mapping efforts have not yet identified the gene(s) responsible for host resistance, in part because the regions containing the loci are structurally complex [16,17].

For this study, we investigate *D. magna* resistance to a fifth *P. ramosa* genotype, P21, which shows a distinct pattern of attachment specificity compared to the four genotypes studied

previously. Genotype P21 offers a new opportunity to map the genetic basis of resistance, and we aim to identify candidate genes that can be tested in functional studies. Initial QTL analyses revealed a single, strong peak on a 2.3-Mb scaffold. Subsequent fine mapping narrowed the QTL to a 28.8-kb region, which we call the F-locus region. The F-locus region contains 13 putative genes (positional candidates) and is adjacent to, but distinguished from, a 50-kb *Pasteuria*-resistance region that was previously described as a supergene (due to apparent lack of recombination), and which contains the A, B, and C loci [16]. By analyzing structural differences between the F-locus haplotypes from the QTL parents, and by comparing gene expression data, we highlight eight of the 13 genes as biological candidates. Our findings reveal candidate genes that can be tested in functional studies, and they also add another locus to our current genetic model, thus bringing us a step closer to understanding the genetic basis of host resistance in this system.

Results

Resistance polymorphism maps to a 28.8-kb region downstream of the ABC supergene

The F2 panel of *D. magna* clones had been previously created by crossing clone Xinb3 (reference genotype), susceptible to *P. ramosa* genotype P21, with clone Iinb1, resistant to P21 [20]. In preparation for QTL mapping, we scored the clones in this F2 panel for their hindgut attachment phenotype (attachment positive = susceptible, attachment negative = resistant) to *P. ramosa* genotype P21. The F2 panel consists of a "core panel", comprising a random set of F2 clones created from a genetic cross, and an "extended panel", comprising a specific subset of F2 clones, chosen in a previous study, that are susceptible to *P. ramosa* genotype C19 [16,18]. In total, 178 of 340 (52%) F2 clones were scored as susceptible to P21, including 41 of 191 (21%) in the core panel and 137 of 149 (92%) in the extended panel (S1 File). The 150:41 ratio (79%:21%) of resistant to susceptible clones in the core panel is not significantly different from the 3:1 ratio expected under a classic genetic cross with Mendelian segregation (χ^2 = 1.27, p = 0.26). These results suggest resistance to P21 is dominant, as is also the case for resistance to C19 [21], and resistance to P21 is possibly influenced by only one major-effect locus. Moreover, the very high percentage of susceptible clones in the extended panel suggests that the resistances to *P. ramosa* genotypes C19 and P21 are linked in some form.

Initial interval mapping with a single-locus model revealed a major QTL (Fig 1A) with a peak LOD score of 63.5 (p-value between 0.0 and 0.004 (permutation test), 5% LOD threshold = 3.74) at position 157 centiMorgans (cM) on linkage group 3 in the genetic map (S1 File) created from *D. magna* draft genome version 2.4 (from QTL parent clone Xinb3, GenBank accession: GCA_001632505.1). Setting the major QTL as a covariate suggested the presence of an interacting locus on linkage group 4, but multiple-QTL mapping revealed that the single-QTL model consistently yielded the maximum penalized LOD score (full QTL analysis procedure available on GitHub). This single peak spanned 426 kb between the flanking markers scaffold00288_965 and scaffold01464_354 at positions 154 cM and 161 cM, respectively, and this major QTL explained 57% of the variance in the attachment phenotype (Fig 1A, S1 File). An effect plot revealed that heterozygotes were largely resistant (Fig 1A, inset), reinforcing our suggestion that resistance to P21 is dominant.

We next performed fine mapping by recombination breakpoint analysis, in which we scored additional markers within the QTL region and checked for a perfect association between genotype and phenotype. This approach allowed us to narrow our region of interest from the 426-kb QTL peak to a 28.8-kb region (Fig 1B, S1 and S2 Files). Fine-mapping markers U0_55 and D16 (S1 File) define the closest recombination breakpoints at positions

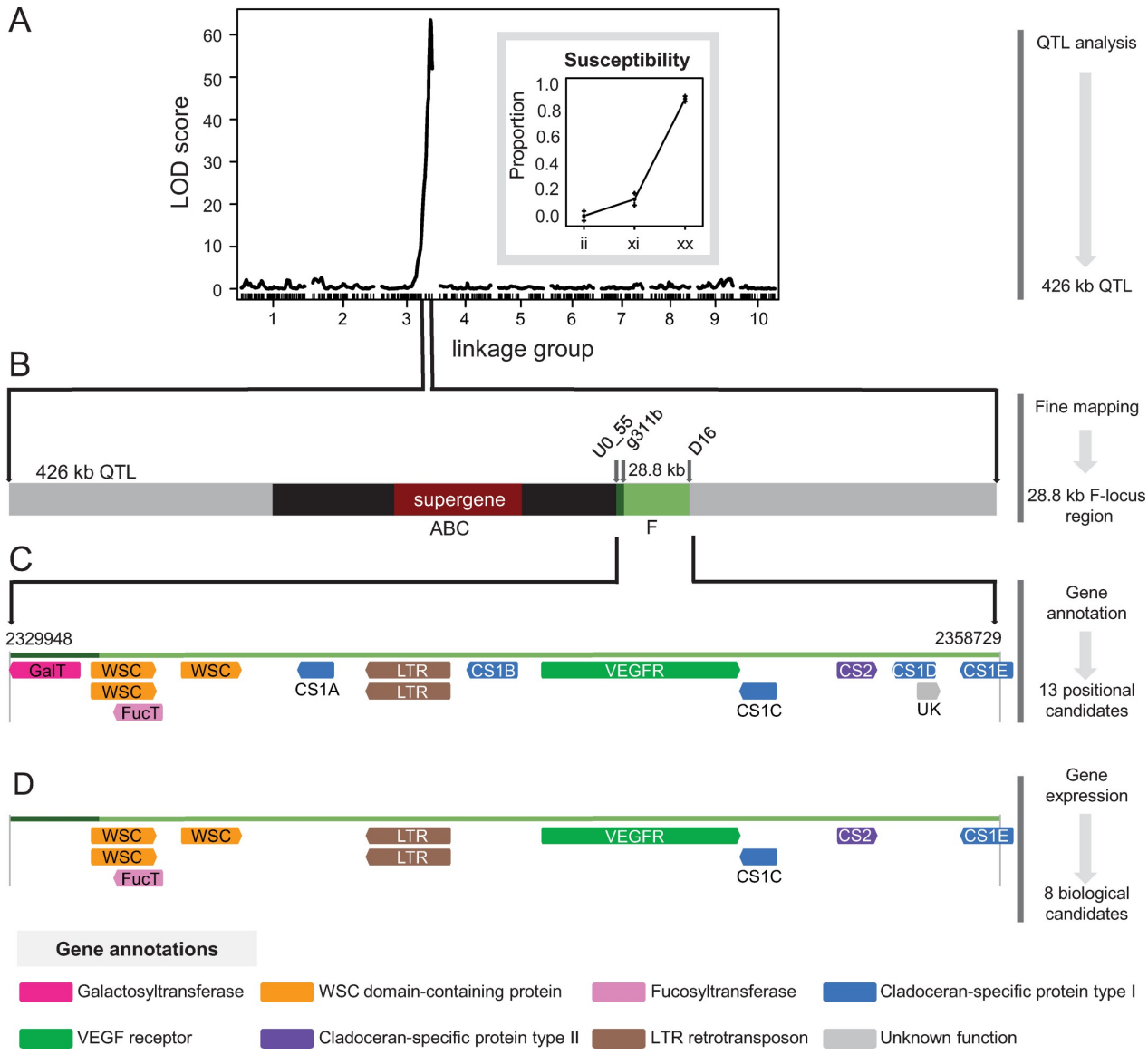

Fig 1. QTL mapping of the polymorphism in *Daphnia magna* resistance to *Pasteuria ramosa* genotype P21. Overview of the workflow used in this study to narrow in on candidate genes underlying a resistance polymorphism. Using QTL mapping and recombination breakpoint mapping with additional markers, we associated the polymorphism in resistance phenotype (attachment of *Pasteuria ramosa* genotype P21 to the hindgut of *Daphnia magna* hosts) to a 28.8-kb region at the end of linkage group 3 (*Daphnia magna* genome version 2.4) which we call the F-locus region. **A)** Results of the single-QTL genome scan (i.e., interval mapping), showing LOD score (log_{10} likelihood ratio) plotted at each SNP marker position in the *D. magna* genetic map. A strong peak with LOD score 63 explains 57% of the phenotypic variance in resistance to P21. The horizontal dashed line indicates the calculated threshold (LOD = 3.74) used to identify significant ($\alpha = 0.05$) QTL. Effect plot (inset) of the SNP marker with the highest LOD score, showing proportion of F2 clones in each genotype group (ii = homozygous for Iinb1 parent clone; xi = heterozygous; xx = homozygous for Xinb3 parent clone) that are susceptible to hindgut attachment by P21. Error bars indicate ± 1 standard error. **B)** Enlarged schematic view of the 426-kb QTL containing the resistance locus (*D. magna* genome version 3.0). The fine-mapped location of the F locus, delimited by SNP markers U0_55 and D16, is shown in green. This F-locus region slightly overlaps with the previously described ABC region (black), which is delimited by SNP marker g311b. The ABC region includes the 50-kb ABC supergene (red), which contains the A, B, and C loci. **C)** Enlarged schematic of the F-locus region, which lies between positions 2,329,948 and 2,358,729 on contig 000011F and contains 13 putative genes (colored by functional annotation), plus two splice variants, in the reference genome (version 3.0) of clone Xinb3. The region colored in dark green indicates the overlap with the ABC region. **D)** Sequence comparisons and differential gene expression analysis between the two QTL parent clones identified eight biological candidate genes in the F-locus region.

https://doi.org/10.1371/journal.pgen.1010570.g001

2,329,948 and 2,358,729 of contig 000011F in the *D. magna* draft genome version 3.0 (from QTL parent clone Xinb3; BioProject ID: PRJNA624896; Fields et al., in prep.). We call this newly discovered interval the "F-locus region" (i.e., the region containing the F locus), following from the previously described loci A, B, C, D, and E [16–18]. The F-locus region contains 13 annotated protein-coding genes (in Xinb3 genome version 3.0), including those that encode putative glycosyltransferases, cell wall integrity and stress response component (WSC) domain-containing proteins (predicted to bind to sugar molecules [22]), a long terminal repeat (LTR) retrotransposon, a vascular endothelial growth factor (VEGF) receptor, and several uncharacterized genes (Fig 1C). Six of the uncharacterized genes (colored in blue and purple in Fig 1C) were found to be part of a large family that occurs in multiple locations of the *D. magna* genome (S1 Fig and S1 Methods) and seems specific to Cladocera [23], the order comprising waterfleas [24]. The F-locus region is located at the end of its linkage group, directly downstream of (and overlapping by 2,541 bp) the 130-kb ABC region (previously called PR-locus), which contains the 50-kb ABC supergene that underlies resistance to *P. ramosa* genotype C19 [19]. One gene in the F-locus region (a putative galactosyltransferase (GalT); colored in magenta in Fig 1C) occurs in the 2.5-kb region overlapping the ABC region. The ABC supergene is, however, about 17 kb distant from the F-locus region (Fig 2).

There is a small chance that apparent differences in resistance to C19 and P21 occurred because of phenotyping errors, which can never be fully excluded. To validate our fine-mapping data and thus confirm that the F locus is indeed independent of the closely located A, B, and C loci (S1 Methods), we selfed selected F2 clones to produce F3 offspring. We selected two QTL F2 panel clones that were expected to have experienced a recombination event between the ABC supergene and the F locus, resulting in one locus being homozygous and the other heterozygous. We selfed the two selected F2 clones and phenotyped the cloned F3 offspring. If recombination had occurred between the loci, the heterozygous loci should segregate in Mendelian proportions. All offspring of one F2 clone (nr. 693) tested as susceptible to C19, but showed Mendelian segregation of resistance to P21, with 8 susceptible (= 28%) and 21 resistant F3 offspring genotypes (S2 File). These results confirm that the resistance phenotypes to *P. ramosa* genotypes C19 and P21 are coded by two separate loci, located close to each other.

We also noted a slight distortion of segregation for resistance to *P. ramosa* genotype P15 hindgut attachment, which is coded by the D locus; two of the tested F3 offspring of F2 clone 693 were susceptible, even though the F2 parent was homozygous recessive (genotype dd; note that resistance to P15 is recessive), which predicts zero susceptible offspring (see S2 File). Previous work suggested that P15 resistance is mainly affected by the D locus, but partly affected by the dominant allele at the C locus of the ABC supergene [18]. However, in our experiments, the parent clone was homozygous recessive at the C locus (genotype cc), suggesting that the distortion in P15 resistance could instead be caused by the nearby F locus. We could not test this possibility with our current dataset, but we were able to test the opposite interaction: whether a host's genotype at the D locus affects P21 resistance. We therefore tested the QTL panel for evidence of epistasis between the loci coding for resistance to P15 and P21. Results suggest a weak epistatic interaction (LOD = 2.48) in which clones that are homozygous recessive at both D and F loci (genotype ddff) are slightly more likely to be resistant to P21 attachment than clones with a dominant allele at the D locus (genotype D_ff, see S2 Fig).

The F-locus region shows structural variation between QTL parent clones

Indel polymorphisms and structural rearrangements have resulted in areas of non-homology throughout the F-locus region, including several private genes (unique to either the xF or iF haplotype; see Table 1). Such structural differences represent conspicuous starting points for

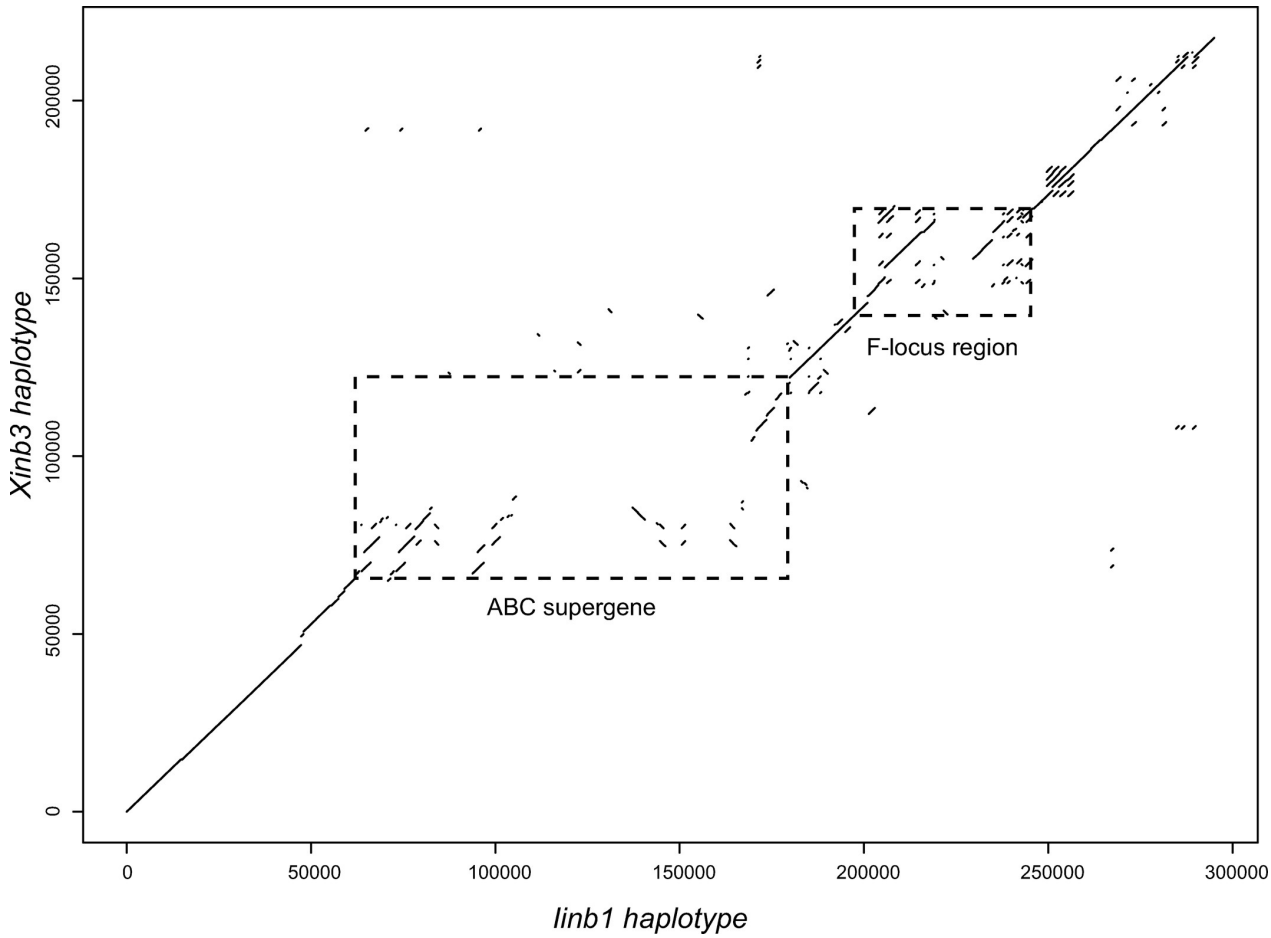

Fig 2. Compared alignments at ABC supergene and F-locus region. Dot plots of aligned DNA sequences show regions of homology between QTL parent clones Xinb3 and Iinb1. The depicted alignment includes the ABC region (which contains the ABC supergene) and the neighboring F-locus region, plus 50 kb beyond the F-locus region to aid visual comparison. Axes indicate base-pair position along each respective haplotype. Dashed boxes denote the ABC supergene and F-locus region. This figure has been modified from a previously published figure (Fig 3 in [16]) to specifically compare the location and alignment structure of the ABC supergene and F-locus region.

https://doi.org/10.1371/journal.pgen.1010570.g002

evaluating potential candidates explaining the resistance phenotype, though it is important to point out that even small genetic differences could be functionally relevant. The most obvious structural difference between iF and xF is that iF is 60% larger (Fig 3). This size difference is due to a combination of duplications and insertions. Both xF and iF have intra-locus duplications (i.e., the sequence in question is duplicated within the F-locus region), but these duplications are more abundant in iF compared to xF (Fig 3B and 3C). A 10.5-kb region in xF maps at two positions (10,057–21,095 and 31,603–39,899) in iF (yellow highlight in Fig 3A and 3C). This duplicated region includes homologs to three xF genes (23.9, 23.23, and 23.10). Despite this large duplication, each of the three genes appears to only be expressed once in iF, with the second copy being lost or pseudogenized through gaining or losing stop codons (Fig 3A). Pseudogenization is common following gene duplication, since functional redundancy relaxes selection against deleterious mutations [25–27].

Indeed, all iF private genes appear to be pseudogenes (Table 1), since they were found to be fragments of larger genes located elsewhere in the genome. Some of these fragments (iF 2589,

Table 1. Private genes within the F-locus region of the QTL parent clones.

Gene (xF)	Gene (iF)	Gene annotation	Complete gene?	Expression (counts)	Protein length	N glycosylation	O glycosylation
23.84–1		WSC domain-containing protein 1	complete	164.1	167	0	1
23.20		Alpha(1,3) fucosyltransferase C-like	complete	99.6	390	6	0
23.94–1		LTR retrotransposon	complete	1.6	542	5	37
23.113		Protein of unknown function	uncertain	—	67	0	1
	2596	Protein of unknown function	fragment				
	2597	Protein of unknown function	fragment				
	2598	Lactosylceramide 4-alpha-galactosyltransferase-like	fragment				
	2599	VEGF receptor 3	fragment				
	2600	VEGF receptor 3	fragment				
	2601	VEGF receptor 3	fragment				

Summarized characteristics of genes found in either the xF or iF haplotypes of the F-locus region. For genes with splice variants (23.84 and 23.94), we represent the transcript with the longer coding sequence. Several of the annotated genes seem to be incomplete (pseudogenes), because they were found to be fragments of larger genes elsewhere in the genome. Gene expression is presented as mean of normalized counts across all treatments. These values are based on Xinb3 RNA-seq reads mapped to the Xinb3 genome-based transcriptome. Dash indicates that no RNA-seq reads mapped to this gene (xF 23.113).

https://doi.org/10.1371/journal.pgen.1010570.t001

2599, 2600, and 2601) mapped to genes within the F-locus region. Other fragments (iF 2596 and 2597) mapped to genes outside the F-locus region (i.e., extra-locus duplications, indicated with black and grey bars in Fig 3; see also S3 Fig and S3 File).

In addition to annotated genes, we looked for annotated repeat elements in the F-locus region of both the Xinb3 and Iinb1 genomes. Results indicate that xF and iF each contain a private LTR retrotransposon (S4 File and S3 Fig and S3 File). The retrotransposon private to iF is located in a 7.2-kb insertion (position 24,375–31,602 within iF) that did not contain any gene annotations (Fig 3A). The retrotransposon private to xF was annotated as gene 23.94. These retrotransposons contain the most extra-locus duplications in the F-locus region (S3 Fig and S3 File).

Besides the retrotransposon 23.94, xF contains three additional private genes (Table 1). Genes 23.84 and 23.20 are overlapping genes on opposite strands, and they are predicted to encode a WSC-domain-containing protein and a fucosyltransferase, respectively. Overlapping genes share at least one nucleotide in their primary transcripts, and they are widespread in prokaryotic, eukaryotic, and viral genomes [28]. Genes 23.84 and 23.20 were likely lost from iF, as suggested by a segment in iF that maps to the 5' untranslated region of gene 23.84 in xF (orange highlight in Fig 3A). Additionally, gene xF 23.113, which overlaps with gene xF 23.53, is also absent from the annotation of iF (Fig 3A). However, this gene does not show evidence of expression (Table 1), and the predicted protein is quite small (67 aa), thus it may be a pseudogenized gene fragment.

Overall, by comparing the annotated genetic sequences of the QTL parent haplotypes, we identified many structural polymorphisms, including three expressed private genes (xF 23.84, 23.20, and 23.94). These genes may encode functionally relevant differences between the QTL parents, and thus they represent our first three biological candidates.

Gene sequence and expression comparisons identify additional biological candidates

In order to investigate functional differences between shared genes in xF and iF, we characterized differences in mRNA and protein sequences by calculating similarity measures such as

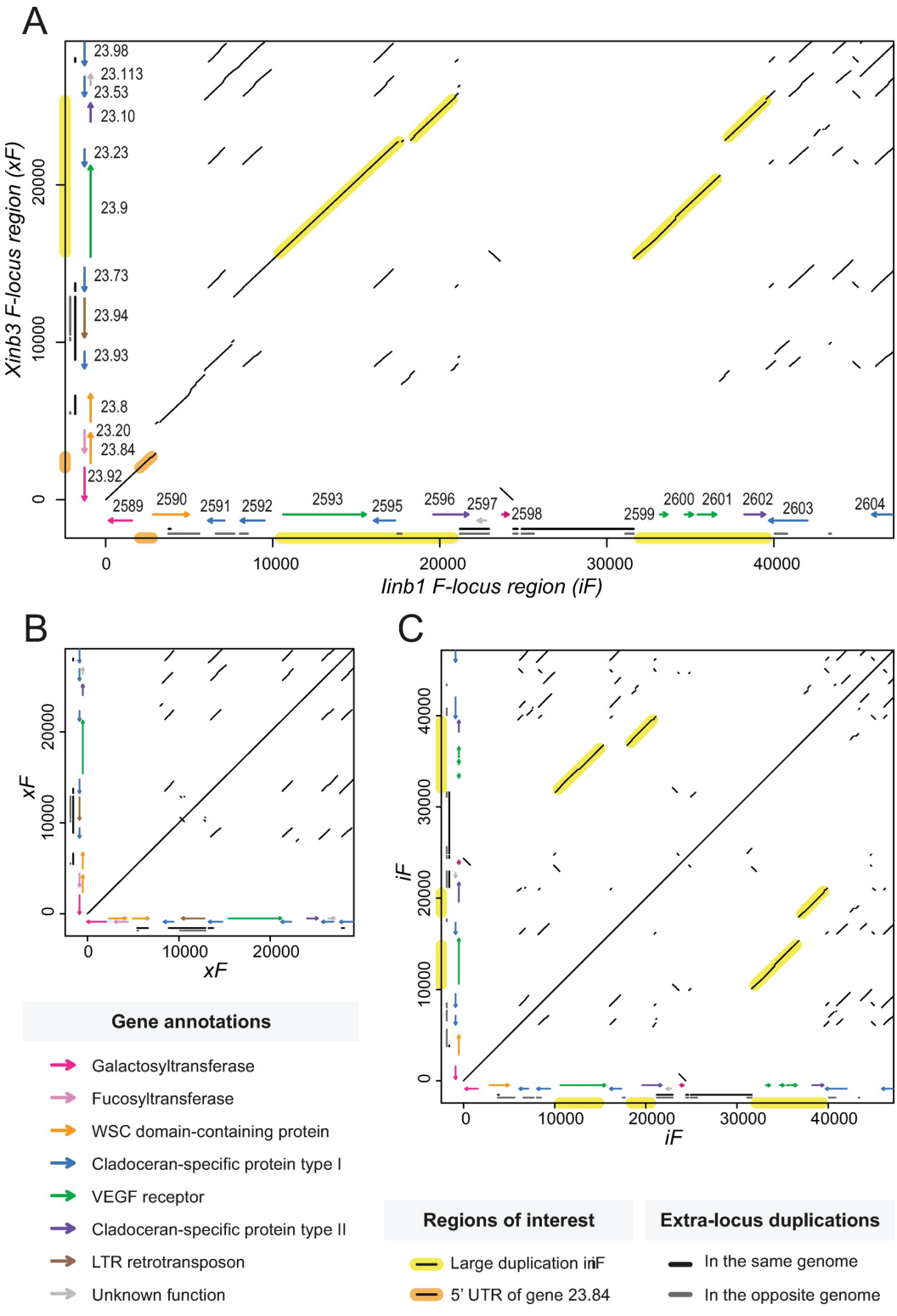
A
Xinb3 F-locus region (xF)
23.98
23.113
23.53
23.10
23.23
23.9
23.73
23.94
23.93
23.8
23.20
23.84
23.92
2589
2590
2591
2592
2593
2595
2596
2597
2598
2599
2600
2601
2602
2603
2604
0
10000
20000
30000
40000
Iinb1 F-locus region (iF)
B
xF
C
iF
Gene annotations
Galactosyltransferase
Fucosyltransferase
WSC domain-containing protein
Cladoceran-specific protein type I
VEGF receptor
Cladoceran-specific protein type II
LTR retrotransposon
Unknown function
Regions of interest
Large duplication in iF
5' UTR of gene 23.84
Extra-locus duplications
In the same genome
In the opposite genome

Fig 3. Dot plots of the F-locus region reveal genetic structure in QTL parent clones. Dot plots of aligned DNA sequences show regions of homology in the F-locus region from QTL parent clones Xinb3 (xF haplotype, containing susceptible allele) and Iinb1 (iF haplotype, containing resistant allele). Axes indicate base-pair position along each respective haplotype. Homologous regions with a negative slope correspond to inversions. Arrows represent putative genes, colored by functional annotation. Gray and black bars represent regions that are duplicated outside the F-locus region in the same genome and the opposite genome (genome of the other parent clone), respectively. **A)** Alignment of xF and iF. The difference in length of 18.2 kb between xF and iF can be largely attributed to an ~8 kb region of non-homology in iF (~24000–32000) and a large intra-locus duplication in iF (yellow highlight). Part of the 5' untranslated region of gene 23.84 is present in iF (orange highlight), suggesting that this xF private gene was likely lost in iF. **B)** Alignment of xF to itself. Central diagonal line indicates 1:1 homology. Elements outside the central diagonal line indicate intralocus duplications, the largest of which reveal a family of five uncharacterized genes specific to Cladocerans (blue arrows). **C)** Alignment of iF to itself. The abundance of elements compared to panel B indicates that intralocus duplications are more prevalent in iF compared to xF.

https://doi.org/10.1371/journal.pgen.1010570.g003

percent identity and piN/piS (nucleotide site diversity within species), and we compared predicted protein structural traits such as number of glycosylation sites (Table 2, S4 and S5 Figs). Most shared genes had very similar sequences, with percent identity above 90% for mRNA and protein (Table 2). Gene xF 23.53 (iF 2603) is an exception, but this gene is not expressed in either parent and we do not consider it further. Nearly all genes had piN/piS values below 1, the one exception being gene xF 23.10 (iF 2602).

The F-locus region contains six Cladoceran-specific uncharacterized genes (xF 23.93, 23.73, 23.23, 23.53, 23.98, and 23.10, and their iF positional homologs; colored in blue and purple in Fig 3A and Table 2) that can be divided into two types belonging to the same large gene family. Protein products from the first five of these genes (CS1) share high sequence similarity (> 40% similarity to at least one other member of this group and > 35% similarity to all members) and likely arose from recent duplication events (S4 and S5 Figs). Topological similarities between these five paralogs include a predicted transmembrane domain near the C-terminal end as well as a shared intracellular amino acid motif YXXC (YXVC and FXVC in our dataset, see

Table 2. Shared genes within the F-locus region of the QTL parent clones.

Gene (xF)	Gene (iF)	Gene annotation	Expression (counts)		% ID mRNA	% ID protein	Protein length		piN/piS	N glycosylation		O glycosylation	
			xF	iF	xF vs iF	xF vs iF	xF	iF	xF vs iF	xF	iF	xF	iF
23.92	2589	Lactosylceramide 4-alpha-galactosyltransferase-like	62.0	67.2	95.18	98.90	365	365	0.55	4	4	**3**	**2**
23.8	2590	WSC domain-containing protein 1	**224.9**	**175.0**	93.02	94.32	357	352	0.37	3	3	4	4
23.93	2591*	Cladoceran-specific protein type 1 (CS1A)	1.5	1.4	97.40	94.12	272	272	0.83	1	1	**9**	**2**
23.73	2592*	Cladoceran-specific protein type 1 (CS1B)	14.8	13.1	95.14	96.85	316	316	0.29	**1**	**0**	**11**	**10**
23.9	2593*	VEGF receptor 3	**144.8**	**163.2**	83.21	96.41	946	925	0.21	**9**	**12**	**13**	**11**
23.23	2595	Cladoceran-specific protein type 1 (CS1C)	**6.4**	**0.2**	86.30	93.72	239	252	0.44	1	1	**0**	**9**
23.10	2602	Cladoceran-specific protein type 2 (CS2)	**51.0**	**110.7**	96.67	92.33	287	287	**1.73**	0	0	**0**	**5**
23.53	2603	Cladoceran-specific protein type 1 (CS1D)	—	—	**54.06**	**45.16**	**298**	**365**	0.75	1	1	**6**	**11**
23.98	2604	Cladoceran-specific protein type 1 (CS1E)	**12.7**	**5.2**	97.27	96.18	314	312	0.32	1	1	**9**	**4**

Summarized characteristics of genes found in both the xF and iF haplotypes of the F-locus region. Bold type and gray shadings indicate notable differences between xF and iF, with light gray indicating a relatively low value and dark gray indicating a relatively high value. Expression is presented as mean of normalized counts across all treatments. These values are based on Xinb3 and Iinb1 RNA-seq reads mapped to the Xinb3 genome-based transcriptome. Dashes indicate that no RNA-seq reads mapped to this gene. Differential expression is based on Benjamini-Hochberg-adjusted p-value < 0.05 between xF and iF homologs across all treatment groups (see main text and Fig 3 for further information). Percent identities were calculated in relation to length of the aligned region (including gaps). piN/piS values represent nucleotide site diversity within species.

* Genes whose mRNA and protein sequences have been corrected, based on Sanger sequencing data (See S9 Fig).

https://doi.org/10.1371/journal.pgen.1010570.t002

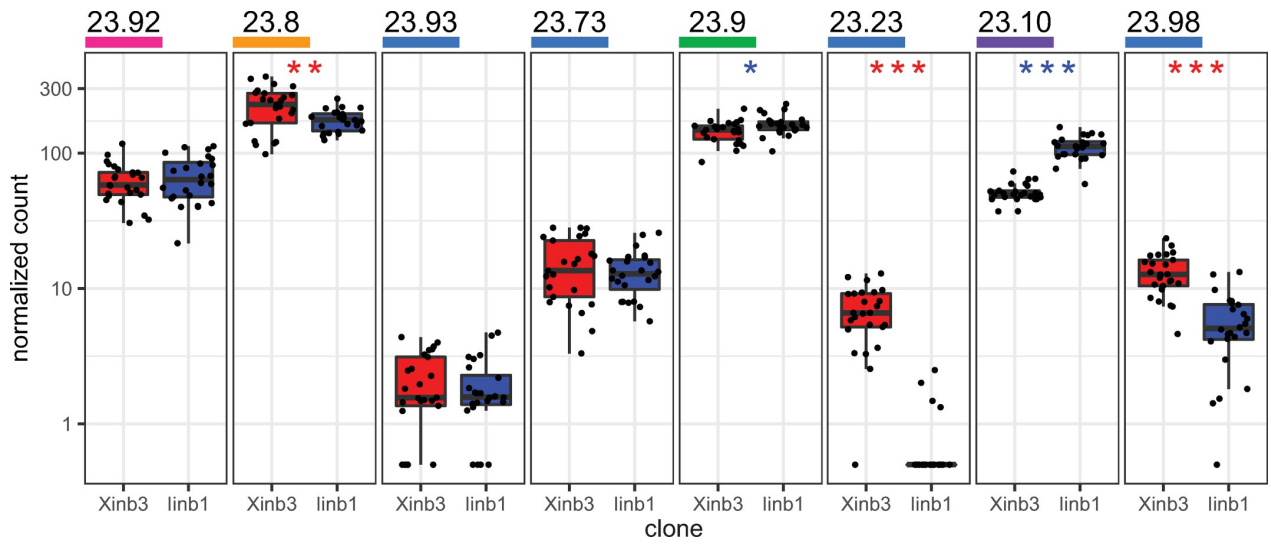

Fig 4. Differential gene expression of shared genes between QTL parent clones. Boxplots showing gene expression data collected for a previous study [30], with raw RNA-seq reads from QTL parent clones Xinb3 and Iinb1 mapped to the genome-based transcriptome from clone Xinb3. Gene names are underlined with colors corresponding to functional annotation (see Fig 1). Y-axes from each plot show normalized read counts with a pseudocount of 0.5 added to allow for log-scale plotting. Each plotted point represents a *Daphnia magna* individual from the respective clone. Box edges indicate first and third quartiles, central line indicates median, and whiskers extend to 1.5 x interquartile range. Asterisks indicate genes that show significant differential expression (non-zero logarithmic fold change in mean expression across all treatments combined) between QTL parent clones Xinb3 (n = 25) and Iinb1(n = 24), with clone Xinb3 as reference after correcting for multiple tests: Benjamini-Hochberg-adjusted p-value < 0.05 (*), < 0.01 (**), < 0.001 (***). Asterisks are colored according to the parent clone which shows higher expression (red = susceptible parent Xinb3; blue = resistant parent Iinb1). Wald test statistics and Benjamini-Hochberg-adjusted p-values are as follows: **23.92:** z = 0.425, p = 0.498; **23.8:** z = -2.78, p = 9.96E-03; **23.93:** z = -0.488, p = 0.690; **23.73:** z = -0.898, p = 0.442; **23.9** z = 2.59, p = 0.0167; **23.23** z = -8.89, p = 4.00E-18; **23.10** z = 13.23, p = 8.51e-39; **23.98** z = -6.23, p = 1.80E-09. For the same expression data presented separately for each treatment condition, see S6 Fig.

https://doi.org/10.1371/journal.pgen.1010570.g004

S4 Fig), which is thought to be involved in the JAK/STAT signaling pathway [29]. Predicted protein products from genes xF 23.10 and iF homolog, 2602, do not have this STAT motif and have lower sequence similarity to the CS1 paralogs (< 30% similarity to all CS1 proteins; S5 Fig), thus we categorize these as type II Cladoceran-specific proteins (CS2). Despite the similarities in sequence and overall topology between the CS1 paralogs (within each genome), pairs of xF and iF homologs (between genomes) from all six Cladoceran-specific proteins differ in their predicted number of O-glycosylation sites (Table 2), and any of these differences could be functionally relevant for the resistance polymorphism.

In addition to the gene sequence comparisons, we performed a differential gene expression analysis to investigate functional differences between homologs in xF and iF. We used RNA-seq data that had been previously collected from Xinb3 and Iinb1 individuals that were exposed to a variety of stressful conditions [30]. We mapped the raw RNA-seq reads to the genome-based transcriptomes from both clones. We present here the results from the analysis in which all reads were mapped to the Xinb3 transcriptome (Figs 4 and S6, and S5 File). Mapping the reads to the Iinb1 transcriptome produced qualitatively similar results (S7 Fig and S5 File). Because the attachment phenotype depends on the host genotype, rather than on environmental factors [14], we included all treatments in our differential expression analysis so that we could analyze constitutive expression differences (independent of environmental treatment) between resistant and susceptible clones. Such constitutive expression differences were previously shown for genes in the ABC region [16].

Five genes in the F-locus region showed significant differential expression between the QTL parent clones (p-value < 0.05, Fig 4, Table 2 and S5 File). The VEGF receptor gene (xF

23.9; Fig 4E) and the CS2 gene (xF 23.10; Fig 4G) showed higher expression in the resistant parent (Iinb1). Two CS1 genes, CS1C (xF 23.23; Fig 4F) and CS1E (xF 23.98; Fig 4H) showed higher expression in the susceptible parent (Xinb3), as did gene xF 23.8 (Fig 4B), which encodes a putative WSC domain-containing protein. The two genes showing the strongest upregulation in each respective parent clone were the CS2 gene (xF 23.10; Fig 4G) in the resistant parent, and gene CS1C (xF 23.23; Fig 4F) in the susceptible parent.

In summary, from the 13 positional candidate genes in the F-locus region, we identified eight biological candidates that appear to harbor functional differences and thus may underlie the resistance polymorphism studied here. These eight candidates include three private genes (xF genes 23.84, 23.20, and 23.94) that are present and expressed in only one QTL parent (Table 1). The other five candidates (xF genes 23.8, 23.9, 23.23, 23.10, and 23.98) are shared between both QTL parents (Table 2) but show difference in gene expression (Fig 4).

Discussion

In this study, we identified and described a single genetic locus, which underlies *Daphnia magna* resistance to *Pasteuria ramosa* genotype P21. The "F locus" shows Mendelian segregation and maps to a 28.8-kb region containing 13 genes. Detailed comparison of gene annotations and expression data from QTL parent clones elevated eight of these positional candidates to biological candidate genes. Putative protein products of these biological candidates include a fucosyltransferase, two WSC-domain-containing proteins, an LTR retrotransposon, a VEGF receptor, and several uncharacterized but related proteins that are unique to the waterflea clade, Cladocera.

A dominant resistance locus with Mendelian segregation

Our discovery of the F locus adds to the genetic model of *D. magna* resistance to *P. ramosa*. With the newly added F locus, the model now describes the dominance patterns and epistatic interactions of six loci in *D. magna* that explain resistance to five genotypes of *P. ramosa*. Each locus added to this model creates a more complete picture of the genetic variation in *D. magna* resistance. The F locus in particular revealed that hindgut attachment is mediated by different host loci (D or F) depending on the parasite genotype (P15 or P21, respectively). All other known resistance loci mediate attachment to the host's foregut. Additionally, the proximity between the F locus and ABC supergene demonstrated that resistance loci may be located physically close to each other even if they mediate resistance to different attachment sites. Clustering of immune-related genes has been reported for other systems as well, e.g., the MHC genes in vertebrates [31,32] and R genes in plants [33,34], and such clustering may be adaptive, as recombination rates are strongly reduced.

Characterizing the diversity of loci that underlie resistance in this system will help us better understand how these resistance loci arise and are maintained within populations during coevolution. For example, selection on the ABC supergene may influence the F locus and vice-versa because they are physically linked in the genome. Indeed, the flanking sequences of the ABC region (including the F-locus region) were previously shown to have elevated genetic diversity and signals of balancing selection compared to other genomic regions [35]. Future studies may test to what extent the F locus itself contributes to this elevated genetic diversity and signals of balancing selection and to what extent it is influenced by the nearby supergene.

Our analysis showed that resistance at the F locus is dominant when tested against *Pasteuria ramosa* genotype P21. Dominant resistance was also shown for loci B and C against *P. ramosa* genotypes C19 and C1, respectively [16]. In contrast, resistance is recessive for loci D and E against genotypes P15 and P20 [17,18]. For the A locus, on the other hand, dominance

depends on the parasite genotype [11]). Although this context-dependent dominance makes the A locus unique regarding resistance to the five parasite genotypes described so far, such a genetic architecture may also be the case for the other resistance loci. Once a greater diversity of *P. ramosa* genotypes [19,36] is incorporated into studies of host resistance, we may find that dominance at other resistance loci also changes with the parasite genotype tested.

The described resistance loci A–E interact with each other epistatically, and the F locus also shows evidence of such interactions. Previous work demonstrated epistasis between loci A, B, C, and E, all of which determine parasite attachment to the host's foregut. The D and F loci, on the other hand, determine attachment to the host's hindgut, and here we found evidence suggesting the F-locus genotype may interact with the D locus (S2 Fig and S2 File). A previous study suggested that the C locus, or another tightly linked locus, may interact with the D locus [18]. Instead, here we suggest this effect may have been caused by the F locus, which is strongly physically linked to the C locus.

Our finding that resistance at the F locus shows Mendelian segregation suggests that the polymorphism has a simple genetic basis. Indeed, each attachment phenotype studied so far is a binary trait mediated by few loci, with negligible environmental effects [16–18]. Thus, if one considers resistance to each parasite genotype as a separate trait, then the underlying genetics may be straightforward. Such an approach may be necessary for uncovering the genetic mechanisms underlying resistance. However, to understand coevolution between *D. magna* and *P. ramosa* in natural populations, the relevant trait to consider is overall resistance, since this is the trait under selection. Resistance to each *P. ramosa* genotype studied so far is coded by different loci, with epistatic interactions between loci. So far, the more we investigate overall resistance to *P. ramosa*, the more complex this trait becomes. While it is not yet clear what this increasing complexity implies for coevolution, it is clear that to understand *Daphnia–Pasteuria* coevolution, we must continue to characterize the diversity of resistance phenotypes.

Candidate genes to be tested in functional studies

The complexity of *D. magna* resistance to *P. ramosa* does not end with the genetic model of overall resistance; rather, the individual genetic regions containing the resistance loci are also highly complex [16,17], a trend which has hindered efforts to identify candidate genes underlying resistance. In the current study, we were fortunate to find that the F-locus region is largely homologous, which allowed us to compare gene content and gene expression between the QTL parent clones to ultimately identify eight biological candidate genes that may be tested in forthcoming functional studies. These candidates include three private genes of the Xinb3 parent (Table 1) and five differentially expressed shared genes (Table 2).

Given that resistance to P21 hindgut attachment is dominant, can we speculate which of our biological candidate genes is more likely to contain the F locus? Most genes are expected to show higher expression in individuals with the dominant phenotype [37]. These genes are haplosufficient, i.e., one working copy is sufficient for gene function. Genes 23.9 and 23.10 would thus be good candidates to confer resistance, because they show higher expression in the resistant parent, Iinb1, than in the susceptible parent, Xinb3 (Table 2, Fig 2). Alternatively, the gene responsible for the resistance polymorphism could be haploinsufficient. In this case, two copies of the gene would confer susceptibility, and we would expect higher expression in the susceptible parent. Several of our biological candidates would fit these criteria: the three genes private to the Xinb3 (genes 23.84, 23.20, and 23.94), and the three genes that showed higher expression in Xinb3 than in Iinb1 (genes 23.8, 23.23, and 23.10). In contrast to haplosufficiency, haploinsufficiency is relatively rare in nature, with only a few hundred such genes described in humans [38] and a mere 3% of the genes in yeast [39]. Even so, prominent

examples of haploinsufficient genes exist in several disease systems. Such examples include the HIV-1 coreceptor CCR5 in humans [40], as well as the A1S subunit of a voltage-gated calcium channel in mice, which affects arenavirus entry and infection [41]. In the following, we use haplosufficiency as one criterion to roughly rank the eight biological candidates. Other criteria include differences in gene expression or protein structure, as well as whether similar genes were previously identified in other *Pasteuria* resistance loci.

Among the eight biological candidates, the gene encoding a type II Cladoceran-specific protein (CS2: gene xF 23.10/iF 2602) stands out for several reasons. First, it was one of only two candidates (the other being the VEGF receptor xF 23.9/ iF 2593) that showed higher expression in the resistant parent (Fig 4), which is the expected differential expression pattern for haplosufficient genes given that resistance is dominant at the F locus. Compared to the VEGF receptor gene (xF 23.9/ iF 2593), the CS2 gene (xF 23.10/ iF 2602) showed larger expression differences between the two QTL parents (Fig 4E and 4G). Second, this gene is unique among the candidates shared between xF and iF in that it has a strongly elevated piN/piS of 1.79, the only gene in the F-locus region exceeding 1 for this metric (Table 2). Such a high piN/piS value indicates that the xF and iF versions of this gene are remarkably diverged at nonsynonymous sites and suggests that selection might be driving the divergence between these two alleles. Third, the protein sequences differ in their predicted O-glycosylation sites (Table 2). Differential glycosylation has been associated with resistance polymorphisms in other systems reviewed in [42]. Moreover, differential glycosylation has been linked to the attachment specificity of *P. ramosa*: a predicted N-glycosylation site in the *P. ramosa* gene PCL7 showed perfect association with the parasite's ability to attach to its host [36]. Finally, the CS2 gene belongs to an uncharacterized Cladoceran-specific gene family that has been found in several other locations in the *D. magna* genome, including within the ABC region and the D-locus region [18]. The presence of the Cladoceran-specific gene family in the vicinity of multiple known *Pasteuria*-resistance regions suggests that the evolution of *P. ramosa* resistance in this system may be influenced by gene duplication.

Another strong candidate is the alpha(1,3)fucosyltransferase, coded by xF private gene 23.20. This candidate is of particular interest, because it supports previous findings from the ABC region, in which several putative fucosyltransferase genes were present only in the susceptible QTL parent haplotype [16]. This previous finding led to a working hypothesis that fucosyltransferase genes are among the top candidates for explaining the resistance polymorphism, and our current findings are consistent with this hypothesis. Fucosyltransferases are a family of glycosyltransferases, which are enzymes that assemble glycan chains (polysaccharides) by transferring sugars to another sugar, a protein, or a lipid [43]. Alpha(1,3)fucosyltransferases (including the xF private gene 23.20), in particular, transfer a fucose sugar as the final step in building glycan chains [44–46]. Fucosyltransferases often play a critical role in resistance polymorphisms since they attach sugars mostly at peripheral positions in glycan sequences such that these sugars may interact directly with pathogens attaching to them [47,48]. This is the case in the bacterial pathogen *Helicobacter pylori*, which infects mammalian epithelial cells by attaching to glycans on ABO blood group antigens [49–51].

Thus, one plausible mechanism underlying attachment in the *D. magna*–*P. ramosa* system is that parasite spores may attach to glycosylated proteins on the host cuticle, and variations in glycosylation may confer the variations in attachment phenotype we observe among different host genotypes. Specifically, in the case of attachment by *P. ramosa* genotype P21 to the host's hindgut, we can speculate that the parasite spores may only attach to glycans that contain a fucose transferred by the fucosyltransferase encoded by gene xF 23.20. The presence of fucosyltransferase genes in multiple resistance loci and the plausible molecular mechanism of attachment make gene 23.20 a strong biological candidate. However, note that since the gene is only

found in the susceptible parent haplotype xF (and sequence evidence indicates it was likely lost in iF rather than gained in xF), it would need to be haploinsufficient to confer dominant resistance.

Two other candidates (CS1C (xF 23.23/iF 2595) and CS1E (xF 23.98/ iF 2604)) show strong differential gene expression and predicted O-linked glycosylation (Table 2, Fig 4F and 4H), though both genes are more highly expressed in the susceptible parent, meaning that, like the fucosyltransferase candidate, these genes would need to be haploinsufficient (or experienced gain-of-function mutations [52]). Like gene CS2 (xF 23.10/ iF 2602), these candidates also encode Cladoceran-specific proteins. Specifically, they belong to the group of five genes that were identified as paralogs of each other, due, in part, to a conserved transmembrane domain followed by a STAT motif (S4 Fig). The STAT motif is implicated in the recruitment and activation of the transcription regulator STAT3 [29], which is part of the JAK/STAT signaling pathway that acts in embryonic development but also in arthropod innate immunity [53,54]. The presence of this STAT motif suggests that the five paralogs in the F-locus region could be part of a signaling pathway; these proteins might communicate between the outside and inside of the cell. It seems unlikely that membrane proteins such as these would interact directly with attachment of *P. ramosa* spores, because the attachment occurs at the surface of the host cuticle, which is non-cellular. However, these proteins could still play a role in modulating host resistance, for example by affecting cuticle organization [55].

The gene candidate encoding a putative vascular endothelial growth factor (VEGF) receptor (xF 23.9/iF 2593) shows the expected pattern of higher gene expression in the resistant parent (happlosufficient), but the expression difference is not very strong. Like the Cladoceran-specific proteins described above, VEGF receptors have a transmembrane domain, giving them access to both the interior and exterior of the cell [56]. VEGF receptors in *Drosophila* play a role in forming the epithelium [57], suggesting that these receptors could also affect development of the cuticle, which is secreted by epithelial cells. Perhaps also in *D. magna*, VEGF receptors like gene 23.9 affect how this host's cuticle develops and thus affect the ability of *P. ramosa* spores to attach to the cuticle. The final three candidate genes (xF 23.94, 23.84, and 23.8) would be haploinsufficient, and they do not stand out among the biological candidates in terms of predicted protein structure or function.

While the above considerations help use rank the eight candidate genes to some degree, none of the given arguments is waterproof. Thus, the next step requires experimental manipulation using genetic tools to knock out the candidate genes and assess the effect on the attachment phenotype [58,59]. Knockout strategies would have to differ depending on the predicted haplosufficiency of the candidate gene: for a haplosufficient candidate like gene CS2 (xF 23.10/ iF 2602), one could select a (resistant) heterozygote and knock out the gene to test whether susceptibility is induced. For a haploinsufficient candidate like the fucosyltransferase gene 23.20, one would choose a (susceptible) homozygote and knock out one copy to test whether resistance is induced. In addition, lectin staining along with glycoproteomics could determine which glycans may be involved in attachment.

Conclusion

Here we describe the sixth polymorphic resistance locus of *D. magna* against the virulent and wide-spread bacterial parasite *Pasteuria ramosa*. The high resolution of sequence polymorphism we reached for the F locus is new for this system and adds nicely to what we know about the system as a whole. The six loci are believed to be under selection during host–parasite coevolution, and their identification can therefore aid us to shed light on the coevolutionary process. With more of these loci being described, we see more patterns, which may allow

us to formulate testable hypotheses. All of the resistance loci show Mendelian segregation when their effects are isolated from other loci, but segregation patterns of all loci can be strongly distorted by epistatic interactions with other loci. Resistance can be dominant or recessive and, in all cases, seems to be unaffected by environmental variation. However, so far, GWAS and QTL approaches where in no case able to pinpoint the actual genetic polymorphism. This is, in part, because the resistance regions are highly diverse, including structural polymorphisms. Furthermore, resistance loci seem to be placed in regions of low genetic recombination: four of the six loci (A, B, C, and F) cluster tightly together, and the ABC and the E loci seem to be located in supergenes. This reduced recombination hinders our attempts to fine map the location of these resistance loci. High genetic diversity, perfect dominance and epistasis, strong phenotypic effects without environmental effects, and reduced recombination rates have all been suggested to promote Red Queen dynamics, strengthening the suggestion that these loci evolve under negative frequency-dependent coevolution.

Besides the population genetic aspects, with more loci being identified, we can also speculate about the molecular mechanisms at work. Two of the six resistance loci mediate attachment to the hindgut; the other four mediate attachment to the foregut. Both these sections of the gut are of ectodermal origin, meaning they are part of the molted cuticle. Therefore, candidate genes may code either for proteins expressed on the surface of the cuticle or for enzymes that modify these proteins, e.g. by glycosylation. Across the genomic regions containing the six described *D. magna* resistance loci, both these types of proteins are represented, including the fucosyltransferase candidates described here for the F locus. If resistance involves polymorphisms in proteins of both types (presence/ absence of cuticle proteins with or without modification), these protein interactions may give rise to the changing patterns of dominance and epistasis that we observe among the resistance loci. The right combination may determine if the parasite can attach or not.

Methods

QTL and fine mapping

Quantitative Trait Locus (QTL) mapping was performed using a standing *Daphnia magna* QTL panel [20]. This panel was created by crossing a Finnish mother clone (FI-Xinb3 (here called Xinb3), susceptible to *Pasteuria ramosa* genotype P21) with a German father clone (DE-Iinb1 (here called Iinb1), resistant to *P. ramosa* genotype P21), and all offspring were genotyped at 1,324 SNP markers (S1 File) based on the *D. magna* draft genome version 2.4 (GenBank accession: GCA_001632505.1). Note that genome version 2.4 was used for QTL mapping only; all fine mapping and subsequent analyses were performed using the more recent version, 3.0 (both genome versions are from clone Xinb3). For the QTL analysis, we tested the hindgut attachment phenotype by spores from *P. ramosa* genotype P21 for a total of 340 clones from the F2 "core" panel (randomly selected F2 lines) and the "extended" panel (F2 clones susceptible to *P. ramosa* genotype C19) [13] using the *Pasteuria* attachment test [14]. An infection experiment confirmed that attachment by P21 spores to the host's hindgut is highly correlated with infection outcome (S1 Fig and S1 File and S1 Methods). The spores from *P. ramosa* genotype P21 were obtained from a *D. magna* population in the Aegelsee, Switzerland [17]. We performed the QTL analysis, which tests the association of the phenotype data to each marker in the genetic map, using the R Statistical Software (version 3.4.3) [60] package qtl (version 1.42–8) [61], with a binary phenotype model and Haley-Knott regression [62] as described previously [21]. As part of the R/qtl analysis, a genome-wide significant ($\alpha = 0.05$) LOD score was calculated at 3.74 using 1,000 permutation tests. We performed the QTL mapping using both a single-locus model (function scanone) and two-locus model (function scantwo), and the

results from these analyses informed our final multiple-QTL mapping (function stepwiseqtl), which employs a penalized LOD score approach for model selection.

In order to fine map the resulting major QTL, we designed additional genetic markers (S1 File) using the Xinb3 reference genome (version 3.0) and the Iinb1 draft genome, and we placed these new markers between the QTL-flanking markers. We then genotyped the F2 clones that had a recombination event within this region (i.e., F2 clones whose genotype differs between the two markers flanking the major QTL). We analyzed size-polymorphic markers and SNP markers using PCR followed by capillary electrophoresis (Applied Biosystems 3130xl Genetic Analyzer) and Sanger sequencing (Microsynth; Basel, Switzerland), respectively. We then used these genotype data to locate the recombination breakpoints in each of the selected F2 clones, assuming a perfect association between genotype and phenotype.

In order to validate that resistance to *P. ramosa* genotype P21 is conferred by a locus that is separate from the previously characterized ABC supergene [16], we produced F3 offspring (S1 Methods) by selfing several F2 clones that had a recombination event between the C locus (underlying resistance to foregut attachment by *P. ramosa* genotype C19) and the putative F locus (underlying resistance to hindgut attachment by *P. ramosa* genotype P21). We then phenotyped the F3 offspring for resistance to C19 foregut attachment and P21 hindgut attachment to infer the parent clone's genotype according to the segregation pattern of the offspring. Offspring which segregated for P21 resistance but not for C19 resistance were inferred to come from a parent clone that is heterozygous at the F locus and homozygous at the C locus, indicating that the F locus and C locus are indeed distinct. We also tested the F3 offspring for resistance to P15 hindgut attachment in order to check for possible epistasis between the F and D loci. Previous work suggested that loci C and D may interact such that P15 hindgut resistance (mainly coded by the D locus) may be partially explained by the dominant allele at the C locus [18]. In the current experiment, both of the tested F2 clones were homozygous at the C and D loci but potentially heterozygous at the putative F locus. Thus, if the F3 offspring segregate in their resistance to P15, this could due to an effect from the F locus, rather than from the nearby C locus.

Characterizing the F locus

We characterized differences in the F-locus region between the Xinb3 and Iinb1 haplotypes, here called "xF" and "iF", respectively. We extracted the xF and iF haplotype sequences from the respective genomes, and we aligned these nucleotide sequences to themselves and to each other using LASTZ (version 1.04.03) [63] under default settings. Because much of the nearby ABC supergene consists of duplications [16], we also checked the F-locus haplotypes for intra-locus and extra-locus duplications in both genomes. We define an intra-locus duplication as a sequence that is fully contained in the F-locus region in at least two locations. An extra-locus duplication occurs outside the F-locus region. Specifically, we used BLASTN (version 2.7.1+, blast.ncbi.nlm.nih.gov) to query each F-locus haplotype (xF and iF) against each entire genome. Hits with an e-value of less than 10^{-20} were considered homologous [64] and thus classified as a duplication. Besides the BLAST approach, we also used the program RepeatModeler2 (version 2.0.1) [65] with RepeatMasker (version 4.1.0) [66] to identify repeat elements such as transposable elements in both xF and iF haplotypes.

Finally, we annotated the genes in the F-locus region of both xF and iF to help identify biological candidates underlying the resistance polymorphism. Annotations of the QTL parent genomes Xinb3 (version 3.0) and Iinb1 were performed using the MAKER2 pipeline (version 2.31.10) [67], including ab-initio gene predictors by AUGUSTUS (version 3.3.3) [68], SNAP (version 2006-07-28) [69], and GeneMark (version 4.28) [70]. Upon visual inspection of these

gene annotations, we determined that several annotated genes were actually fragments of complete genes that occurred elsewhere in the genome, and other annotations were incomplete (e.g., missing UTRs). We manually curated the incomplete annotations using a combination of transcriptomic data, protein structure predictions, and alignment to homologous genes (see S1 Methods and S6 File). Additionally, we corrected the coding sequences of three genes (2591, 2592, and 2593) from clone Iinb1 based on Sanger sequencing data (S9 Fig). All downstream analyses were based on the curated gene annotations.

Gene and protein sequence comparisons

We compared curated gene and protein sequences between xF and iF haplotypes. We aligned mRNA and protein sequences of positional homologs (determined by relative position in the respective haplotypes) using MAFFT (version 7.450) [71] under the following settings in Geneious (version 2022.1.1) (algorithm: FFT-NS-1, scoring matrix: 200PAM/k = 2 (for mRNA; for proteins, scoring matrix = BLOSUM62), gap open penalty: 1.53, offset value: 0.123) and then calculated percent identity in relation to the length of the aligned region (including gaps) for each gene pair.

Alignments of orthologous coding sequences between xF and iF were made using a custom R script which initially utilized the R (version 4.0.3) package seqinr (version 3.6–1) [72] to import individual coding sequences for each respective genotype, followed by identification of the correct reading frame, and finally, a codon-based alignment using R package prank (version 170427) [73,74]. We calculated piN/piS in DnaSP (version 6.12.03) [75] on each alignment. We also characterized protein topology by predicting presence and location of transmembrane domains using CCTOP (version s.1.00) [76], and by locating putative N- and O-linked glycosylation sites with NetNGlyc1.0 [77] and NetOGlyc4.0 [78], respectively.

Gene expression analysis

We quantified gene expression for complete genes in the F-locus region from each parent clone using raw RNA-seq reads collected previously for *D. magna* individuals from parent clones Xinb3 (n = 25 individuals) and Iinb1 (n = 24 individuals) [30]. These RNA-seq reads were mapped separately to the Xinb3 and Iinb1 *in-silico* derived transcriptome, i.e., transcript sequences were generated using the aforementioned annotation by using the program gffread (version 0.11.4) [79] to extract transcript sequences from the gff file. Transcripts were mapped and quantified using the program kallisto (version 0.46.1) [80], and counts were analyzed for differential gene expression between clones Xinb3 and Iinb1 using the R/Bioconductor package DESeq2 (version 1.28.1) [81]. P-values were adjusted for multiple testing using the Benjamini-Hochberg method [82].

Scripts for the QTL analysis, RepeatModeler analysis, codon-based sequence alignment, differential expression analysis, and transcript mapping as well as associated data files are available on GitHub (https://github.com/maf8a/Flocus_QTL) and archived through Zenodo (doi: 10.5281/zenodo.7437819). Assembled and annotated haplotypes of the F-locus region, as well as additional Sanger sequencing data from iF, are available on GenBank (xF accession number: OP831933; iF accession number: OP831934; Sanger accession numbers: OP795832, OP795833, OP795834).

Supporting information

S1 Methods. Supplementary materials and methods with supporting literature.
(DOCX)

S1 Fig. Alignment of Cladoceran-specific protein sequences. Clustal Omega alignment of amino acid sequences from 53 Cladoceran-specific genes located on contigs 000011F (containing the ABC supergene and the F locus) and 000018F (containing the D locus). cov: coverage; pid: percent identity. Residues of note: cysteine: yellow; charged amino acids: red; serine and threonine: light blue. Consensus sequence is indicated below the alignment and is particularly notable between positions 400 and 720.
(HTML)

S2 Fig. Effect plot and epistasis test between P15 and P21 resistance. Effect plot showing mean susceptibility (± 1 *SE*) as a function of genotype at two putative QTL explaining host variation in hindgut attachment of *Pasteuria ramosa* genotype P21. The x axis shows variation at on the QTL detected on linkage group 3 (lg3) at position 157.0 (near F locus), and different colors represent the genotypes at the QTL on lg9 at position 105.3 (near D locus). The Xinb3 QTL parent is known to be susceptible to both parasite genotypes, with genotype ff at lg3 and DD at lg9. The Iinb1 QTL parent is known to be resistant to both parasite genotypes, with genotype FF at lg3 and dd at lg9. Table shows estimated support of each QTL after dropping one term at a time from a binary multiple-QTL model with both QTL (lg3 @ 157.0 and lg9 @ 105.3) and an interaction term (lg3 x lg9) between them. For each model term, we give the degrees of freedom (df), the $\log_{10}$ likelihood ratio (LOD) comparing the full model to reduced models, the estimated percent of phenotypic variance explained by the term, and a p-value that is based on the LOD score and assumes a χ^2 distribution of LOD x (2ln10). Note that p-values are pointwise, meaning they do not account for the search over the whole genome. We therefore consider them with caution.
(PDF)

S3 Fig. Extra-locus duplication mappings. Extra-locus duplications from the F-locus region and their mapping locations in the respective QTL parent genome (for full BLAST results see S2 File). Duplicated segments (black) are separated and labeled according to the contig to which they map (leading zeroes in contig names are omitted). Colored arrows indicate annotated genes in the F-locus region (see Fig 1 for color code). A) Extra-locus duplications from xF and their mapping locations in the Xinb3 (susceptible QTL parent) genome. B) Extra-locus duplications from iF and their mapping locations in the Iinb1 (resistant QTL parent) genome.
(PDF)

S4 Fig. Alignment of five Cladoceran-specific paralogs. Predicted sequences of five Cladoceran-specific (type I) paralogs from each of xF and iF were aligned using MAFFT in Geneious. The predicted transmembrane domain and STAT motif are indicated (pink and green, respectively).
(PDF)

S5 Fig. Heatmaps of percent identity for six Cladoceran-specific genes. Heatmaps comparing percent identities of six Cladoceran-specific genes, including five type I (blue) and one type II (purple) from each of xF and iF. Percent identities were calculated from pairwise alignments of full mRNA sequences (A) and predicted protein sequences (B). Bold black outline indicates positional homologs (compared in Table 2).
(PDF)

S6 Fig. Differential gene expression of shared genes between QTL parent clones across treatment conditions (mapped to Xinb3). Boxplots showing gene expression data collected across multiple stressful conditions for a previous study [30], with raw RNA-seq reads from QTL parent clones Xinb3 and Iinb1 mapped to the genome-based transcriptome from clone

Xinb3. Gene names are underlined with colors corresponding to functional annotation (see Fig 1). Y-axes from each plot show normalized read counts with a pseudocount of 0.5 added to allow for log-scale plotting. Each plotted point represents a *Daphnia magna* individual from the respective clone. Box edges indicate first and third quartiles, central line indicates median, and whiskers extend to 1.5 x interquartile range. Asterisks indicate genes that show significant differential expression (non-zero logarithmic fold change in mean expression across all treatments combined) between QTL parent clones Xinb3 (n = 25) and Iinb1(n = 24), with clone Xinb3 as reference after correcting for multiple tests: Benjamini-Hochberg-adjusted p-value < 0.05 (*), < 0.01 (**), < 0.001 (***). Asterisks are colored according to the parent clone which shows higher expression (red = susceptible parent Xinb3; blue = resistant parent Iinb1). Wald test statistics and Benjamini-Hochberg-adjusted p-values are as follows: **A)** z = 0.425, p = 0.498; **B)** z = -2.78, p = 9.96E-03; **C)** z = -0.488, p = 0.690; **D)** z = -0.898, p = 0.442; **E)** z = 2.59, p = 0.0167; **F)** z = -8.89, p = 4.00E-18; **G)** z = 13.23, p = 8.51e-39; **H)** z = -6.23, p = 1.80E-09.
(PDF)

S7 Fig. Differential gene expression of shared genes between QTL parent clones across treatment conditions (mapped to Iinb1). Boxplots showing gene expression data collected across multiple stressful conditions for a previous study [30], with raw RNA-seq reads from QTL parent clones Xinb3 and Iinb1 mapped to the genome-based transcriptome from clone Iinb1. Gene names are underlined with colors corresponding to functional annotation (see Fig 1). Y-axes from each plot show normalized read counts with a pseudocount of 0.5 added to allow for log-scale plotting. Each plotted point represents a *Daphnia magna* individual from the respective clone. Box edges indicate first and third quartiles, central line indicates median, and whiskers extend to 1.5 x interquartile range. Asterisks indicate genes that show significant differential expression (non-zero logarithmic fold change in mean expression across all treatments combined) between QTL parent clones Xinb3 (n = 25) and Iinb1(n = 24), with clone Iinb1 as reference after correcting for multiple tests: Benjamini-Hochberg-adjusted p-value < 0.05 (*), < 0.01 (**), < 0.001 (***). Asterisks are colored according to the parent clone which shows higher expression (red = susceptible parent Xinb3; blue = resistant parent Iinb1). Wald test statistics and Benjamini-Hochberg-adjusted p-values are as follows: **A)** z = -1.44, p = 0.204; **B)** z = 2.36, p = 0.0312; **C)** z = -1.11, p = 0.339; **D)** z = 1.24, p = 0.279; **E)** z = -4.61, p = 1.19E-05; **F)** z = 8.51, p = 1.26E-16; **G)** z = -18.82, p = 2.29e-77; **H)** z = 4.80, p = 5.01E-06.
(PDF)

S8 Fig. Correlation between attachment phenotype and infection outcome. Scatterplot showing percent of individuals with positive attachment to the hindgut and percent of exposed individuals showing disease symptoms five weeks after infection. Each point represents one of 40 *Daphnia magna* clones from the QTL F2 panel, tested against spores from the *Pasteuria ramosa* genotype P21. The linear regression line is shown in black, with gray shading indicating the 95% confidence interval. Positive attachment was strongly correlated with subsequent infection (Spearman's rho = 0.76, $P < 0.001$, $n = 40$).
(PDF)

S9 Fig. Corrections of three Iinb1 gene sequences based on Sanger sequencing data. Nucleotide sequence alignments showing the iF haplotype extracted from the Iinb1 reference genome (upper sequence in each panel) aligned to Sanger-sequencing data (lower sequence in each panel), which were used to correct the sequences of iF genes 2591 (A), 2592 (B), and 2593 (C) for comparison with xF homologs (summarized in Table 2). Sanger sequencing results include associated chromatograms, colored by the nucleotide base called at the given peak.

Annotations above the aligned sequences indicate the consensus sequence (colored by base identity and numbered according to the position in the iF haplotype) and the identity score of the alignments (green indicates 100% identity and gaps indicate polymorphisms). Raw sequencing data can be accessed at the GenBank link provided at the end of the manuscript. Figure was created using Geneious Prime software.
(PDF)

S1 File. QTL and Fine-mapping data README) Column descriptions for following tables QTL phenotypes). Attachment test results (*Pasteuria ramosa* P21 hindgut attachment) for all *Daphnia magna* clones from the QTL panel. Red and blue shading correspond to susceptible (attachment positive) and resistant (attachment negative) phenotypes, respectively. QTL SNP map) QTL mapping data containing clone names, attachment phenotype, (1 = susceptible, 0 = resistant), and genetic markers with corresponding genotypes (AA = matching resistant parent, BB = matching susceptible parent, AB = heterozygous). Infection experiment) Attachment and infection results for 40 *Daphnia magna* clones from the QTL panel. Thirty individuals from each clone were exposed to spores from *Pasteuria ramosa* genotype P21 and assessed for disease symptoms after five weeks. Marker primers) Primer information for all size-polymorphic (microsatellite) and SNP markers used for fine mapping. Finemap microsat) Fine-mapping results from size-polymorphic (microsatellite) markers. A subset of clones from the QTL panel was selected for genotyping at eight markers within the QTL region (See S1 Methods for additional description of fine-mapping procedures). Red cells (B) indicate a haplotype matching the susceptible parent Xinb3, dark blue cells (A) indicate a match to the resistant parent (Iinb1), and light blue cells (H) indicate heterozygotes. Clones 177 and 693 (delimited) identify the limits of this fine-mapping effort at markers D42 and U1, respectively. Finemap Sanger) Fine-mapping results from SNP markers. Clones 177 and 693 were selected for further fine mapping at 13 additional markers. Recombination breakpoints were localized within markers U0_55 and D16_9.
(XLSX)

S2 File. Selfing. We selfed two F2 panel clones (94 and 693) with a recombination event in the F-locus region to test the independence of the ABC supergene and the F locus, and to attempt additional fine mapping. **README)** Column descriptions for following tables. **Collection)** Selfing is performed by collecting ephippia (sexually produced resting eggs) and hatching them after a period of dormancy. Ephippia were collected across four dates in 2019 and 2020. **Attachment tests)** Selfed offspring were tested for resistance to attachment by *Pasteuria ramosa* genotypes C19, P15, and P21. Resistance to these genotypes is known to segregate in the QTL panel. Red and blue shading correspond to susceptible (attachment positive) and resistant (attachment negative) phenotypes, respectively. **Summary)** Summary table of resistance to each of the three *P. ramosa* genotypes. We inferred the genotype of each locus predicted to confer resistance to the parasite genotypes, according to the genetic model of resistance and assuming Mendelian segregation.
(XLSX)

S3 File. Duplications. BLASTn output of F-locus haplotypes against the whole genome from each QTL parent. Tables include both intra-locus and extra-locus duplications, and output is sorted by query start position. **README)** Column descriptions for following tables. **xFvsXinb3)** BLASTn output for Xinb3 F-locus region against whole Xinb3 genome (version 3.0). **iFvsIinb1)** BLASTn output for Iinb1 F-locus region against whole Iinb1 genome. **xFvsIinb1)** BLASTn output for Xinb3 F-locus region against whole Iinb1 genome. **iFvsXinb3)**

BLASTn output for Iinb1 F-locus region against whole Xinb3 genome (version 3.0).
(XLSX)

S4 File. RepeatMasker output. README) Column descriptions for following tables. Xinb3) RepeatMasker output for Xinb3 F-locus region. **Iinb1)** RepeatMasker output for Iinb1 F-locus region
(XLSX)

S5 File. DESeq2 output (differential gene expression). README) Column descriptions for following tables. **Mapped to Xinb3)** Output from differential gene expression analysis in which all RNA-seq reads were mapped to the Xinb3 genome (version 3.0). Full results have been filtered to only include the genes in the F-locus region. **Mapped to Iinb1)** Output from differential gene expression analysis in which all RNA-seq reads were mapped to the Iinb1 genome. Full results have been filtered to only include the genes in the F-locus region.
(XLSX)

S6 File. Hand-curation of gene annotations from F-locus region. README) Column descriptions for following tables. Xinb3) Hand-curation for Xinb3 F-locus region. Iinb1) Hand-curation for Iinb1 F-locus region
(XLSX)

Acknowledgments

The authors would like to thank Jürgen Hottinger, Michelle Krebs, Urs Stiefel, and Kristina Müller for assistance in the laboratory, as well as Meret Halter, Pascal Angst, Joana Santos, and Jeremias Brand for assistance with coding. We also thank members of the Ebert group for helpful feedback on the manuscript.

Author Contributions

Conceptualization: Maridel Fredericksen, Dieter Ebert.

Data curation: Peter D. Fields, Louis Du Pasquier.

Formal analysis: Maridel Fredericksen, Peter D. Fields, Louis Du Pasquier, Virginie Ricci.

Funding acquisition: Dieter Ebert.

Investigation: Maridel Fredericksen.

Software: Peter D. Fields, Virginie Ricci.

Supervision: Dieter Ebert.

Visualization: Maridel Fredericksen, Virginie Ricci.

Writing – original draft: Maridel Fredericksen, Dieter Ebert.

Writing – review & editing: Maridel Fredericksen, Peter D. Fields, Louis Du Pasquier, Virginie Ricci, Dieter Ebert.

References

1. Lythgoe KA, Read AF. Catching the Red Queen? The advice of the Rose. Trends in Ecology & Evolution. 1998; 13:473–4. https://doi.org/10.1016/s0169-5347(98)01486-4 PMID: 21238400
2. Jones JDG, Dangl JL. The plant immune system. Nature. 2006; 444:323–9. https://doi.org/10.1038/nature05286 PMID: 17108957

3. Hammond-Kosack KE, Jones JD. Resistance gene-dependent plant defense responses. The Plant Cell. 1996; 8:1773–91. https://doi.org/10.1105/tpc.8.10.1773 PMID: 8914325
4. Dodds PN, Lawrence GJ, Catanzariti AM, Teh T, Wang CIA, Ayliffe MA, et al. Direct protein interaction underlies gene-for-gene specificity and coevolution of the flax resistance genes and flax rust avirulence genes. Proceedings of the National Academy of Sciences. 2006; 103:8888–93. https://doi.org/10.1073/pnas.0602577103 PMID: 16731621
5. McLaren PJ, Fellay J. HIV-1 and human genetic variation. Nature Reviews Genetics. 2021; 22:645–57. https://doi.org/10.1038/s41576-021-00378-0 PMID: 34168330
6. McLaren PJ, Coulonges C, Bartha I, Lenz TL, Deutsch AJ, Bashirova A, et al. Polymorphisms of large effect explain the majority of the host genetic contribution to variation of HIV-1 virus load. Proceedings of the National Academy of Sciences. 2015; 112:14658–63. https://doi.org/10.1073/pnas.1514867112 PMID: 26553974
7. Martins NE, Faria VG, Nolte V, Schlötterer C, Teixeira L, Sucena É, et al. Host adaptation to viruses relies on few genes with different cross-resistance properties. Proceedings of the National Academy of Sciences. 2014; 111:5938–43. https://doi.org/10.1073/pnas.1400378111 PMID: 24711428
8. Brosh O, Fabian DK, Cogni R, Tolosana I, Day JP, Olivieri F, et al. A novel transposable element-mediated mechanism causes antiviral resistance in *Drosophila* through truncating the Veneno protein. Proceedings of the National Academy of Sciences. 2022; 119:e2122026119.
9. Carius HJ, Little TJ, Ebert D. Genetic variation in a host-parasite association: potential for coevolution and frequency-dependent selection. Evolution. 2001; 55:1136–45. https://doi.org/10.1111/j.0014-3820.2001.tb00633.x PMID: 11475049
10. Decaestecker E, Gaba S, Raeymaekers JAM, Stoks R, Van Kerckhoven L, Ebert D, et al. Host–parasite 'Red Queen' dynamics archived in pond sediment. Nature. 2007; 450:870–3. https://doi.org/10.1038/nature06291 PMID: 18004303
11. Luijckx P, Fienberg H, Duneau D, Ebert D. A matching-allele model explains host resistance to parasites. Current Biology. 2013; 23:1085–8. https://doi.org/10.1016/j.cub.2013.04.064 PMID: 23707426
12. Ebert D, Duneau D, Hall MD, Luijckx P, Andras JP, Du Pasquier L, et al. A population biology perspective on the stepwise infection process of the bacterial pathogen *Pasteuria ramosa* in *Daphnia*. Advances in parasitology. 2016; 91:265–310.
13. Hall MD, Routtu J, Ebert D. Dissecting the genetic architecture of a stepwise infection process. Molecular Ecology. 2019; 28:3942–57. https://doi.org/10.1111/mec.15166 PMID: 31283079
14. Duneau D, Luijckx P, Ben-Ami F, Laforsch C, Ebert D. Resolving the infection process reveals striking differences in the contribution of environment, genetics and phylogeny to host-parasite interactions. BMC biology. 2011; 9:11. https://doi.org/10.1186/1741-7007-9-11 PMID: 21342515
15. Luijckx P, Fienberg H, Duneau D, Ebert D. Resistance to a bacterial parasite in the crustacean *Daphnia magna* shows Mendelian segregation with dominance. Heredity. 2012; 108:547–51.
16. Bento G, Routtu J, Fields P, Bourgeois Y, Du Pasquier L, Ebert D. The genetic basis of resistance and matching-allele interactions of a host-parasite system: The *Daphnia magna*-Pasteuria ramosa model. PLOS Genetics 2017;13.
17. Ameline C, Bourgeois Y, Vögtli F, Savola E, Andras J, Engelstädter J, et al. A two-locus system with strong epistasis underlies rapid parasite-mediated evolution of host resistance. Molecular Biology and Evolution. 2021; 38:1512–28. https://doi.org/10.1093/molbev/msaa311 PMID: 33258959
18. Bento G, Fields PD, Duneau D, Ebert D. An alternative route of bacterial infection associated with a novel resistance locus in the *Daphnia–Pasteuria* host–parasite system. Heredity. 2020;1–11.
19. Fredericksen M, Ameline C, Krebs M, Hüssy B, Fields PD, Andras JP, et al. Infection phenotypes of a coevolving parasite are highly diverse, structured, and specific. Evolution. 2021; 75:2540–54. https://doi.org/10.1111/evo.14323 PMID: 34431523
20. Routtu J, Hall MD, Albere B, Beisel C, Bergeron RD, Chaturvedi A, et al. An SNP-based second-generation genetic map of Daphnia magna and its application to QTL analysis of phenotypic traits. BMC Genomics. 2014; 15:1033. https://doi.org/10.1186/1471-2164-15-1033 PMID: 25431334
21. Routtu J, Ebert D. Genetic architecture of resistance in *Daphnia* hosts against two species of host-specific parasites. Heredity. 2015; 114:241–8.
22. Ponting CP, Hofmann K, Bork P. A latrophilin/CL-1-like GPS domain in polycystin-1. Current Biology. 1999; 9:R585–8. https://doi.org/10.1016/s0960-9822(99)80379-0 PMID: 10469603
23. Colbourne JK, Pfrender ME, Gilbert D, Thomas WK, Tucker A, Oakley TH, et al. The ecoresponsive genome of *Daphnia pulex*. Science. 2011; 331:555–61.
24. Van Damme K, Cornetti L, Fields PD, Ebert D. Whole-genome phylogenetic reconstruction as a powerful tool to reveal homoplasy and ancient rapid radiation in waterflea evolution. Systematic Biology. 2021;syab094.

25. Ohno S. Evolution by gene duplication. Heidelberg, Germany: Springer-Verlag; 1970.
26. Lynch M, Conery JS. The evolutionary fate and consequences of duplicate genes. Science. 2000; 290:1151–5. https://doi.org/10.1126/science.290.5494.1151 PMID: 11073452
27. Zhang J. Evolution by gene duplication: an update. Trends in Ecology & Evolution. 2003; 18:292–8.
28. Wright BW, Molloy MP, Jaschke PR. Overlapping genes in natural and engineered genomes. Nature Reviews Genetics 2021;1–15.
29. Chakraborty A, Dyer KF, Cascio M, Mietzner TA, Tweardy DJ. Identification of a novel Stat3 recruitment and activation motif within the granulocyte colony-stimulating factor receptor. Blood. 1999; 93:15–24. PMID: 9864141
30. Orsini L, Gilbert D, Podicheti R, Jansen M, Brown JB, Solari OS, et al. *Daphnia magna* transcriptome by RNA-Seq across 12 environmental stressors. Scientific Data. 2016; 3:160030.
31. Kelley J, Trowsdale J. Features of MHC and NK gene clusters. Transplant Immunology. 2005; 14:129–34. https://doi.org/10.1016/j.trim.2005.03.001 PMID: 15982554
32. Kumánovics A, Takada T, Lindahl KF. Genomic organization of the mammalian MHC. Annual Review of Immunology. 2003; 21:629–57. https://doi.org/10.1146/annurev.immunol.21.090501.080116 PMID: 12500978
33. Michelmore RW, Meyers BC. Clusters of resistance genes in plants evolve by divergent selection and a birth-and-death process. Genome Research. 1998; 8:1113–30. https://doi.org/10.1101/gr.8.11.1113 PMID: 9847076
34. van Wersch S, Li X. Stronger when together: clustering of plant NLR disease resistance genes. Trends in Plant Science. 2019; 24:688–99. https://doi.org/10.1016/j.tplants.2019.05.005 PMID: 31266697
35. Bourgeois Y, Fields PD, Bento G, Ebert D. Balancing selection for pathogen resistance reveals an intercontinental signature of Red Queen coevolution. Molecular Biology and Evolution. 2021; 38:4918–33. https://doi.org/10.1093/molbev/msab217 PMID: 34289047
36. Andras JP, Fields PD, Du Pasquier L, Fredericksen M, Ebert D. Genome-wide association analysis identifies a genetic basis of infectivity in a model bacterial pathogen. Molecular Biology and Evolution. 2020; 37:3439–52. https://doi.org/10.1093/molbev/msaa173 PMID: 32658956
37. Morrill SA, Amon A. Why haploinsufficiency persists. Proceedings of the National Academy of Sciences. 2019; 116:11866–71. https://doi.org/10.1073/pnas.1900437116 PMID: 31142641
38. Dang VT, Kassahn KS, Marcos AE, Ragan MA. Identification of human haploinsufficient genes and their genomic proximity to segmental duplications. European Journal of Human Genetics. 2008; 16:1350–7. https://doi.org/10.1038/ejhg.2008.111 PMID: 18523451
39. Deutschbauer AM, Jaramillo DF, Proctor M, Kumm J, Hillenmeyer ME, Davis RW, et al. Mechanisms of haploinsufficiency revealed by genome-wide profiling in yeast. Genetics. 2005; 169:1915–25. https://doi.org/10.1534/genetics.104.036871 PMID: 15716499
40. Samson M, Libert F, Doranz BJ, Rucker J, Liesnard C, Farber CM, et al. Resistance to HIV-1 infection in Caucasian individuals bearing mutant alleles of the CCR-5 chemokine receptor gene. Nature. 1996; 382:722–5. https://doi.org/10.1038/382722a0 PMID: 8751444
41. Sarute N, Ross SR. CACNA1S haploinsufficiency confers resistance to New World arenavirus infection. Proceedings of the National Academy of Sciences. 2020; 117:19497–506. https://doi.org/10.1073/pnas.1920551117 PMID: 32719120
42. Taylor SL, McGuckin MA, Wesselingh S, Rogers GB. Infection's sweet tooth: how glycans mediate infection and disease susceptibility. Trends in Microbiology. 2018; 26:92–101. https://doi.org/10.1016/j.tim.2017.09.011 PMID: 29079498
43. Rini JM, Esko JD. Glycosyltransferases and glycan-processing enzymes. In: Varki A, Cummings RD, Esko JD, Stanley P, Hart GW, Aebi M, et al., editors. Essentials of Glycobiology. Cold Spring Harbor (NY): Cold Spring Harbor Laboratory Press; 2015.
44. de Vries T, Knegtel RMA, Holmes EH, Macher BA. Fucosyltransferases: structure/function studies. Glycobiology. 2001; 11:119R–128R. https://doi.org/10.1093/glycob/11.10.119r PMID: 11588153
45. Ma B, Simala-Grant JL, Taylor DE. Fucosylation in prokaryotes and eukaryotes. Glycobiology. 2006; 16:158R–184R. https://doi.org/10.1093/glycob/cwl040 PMID: 16973733
46. Li J, Hsu HC, Mountz JD, Allen JG. Unmasking fucosylation: from cell adhesion to immune system regulation and diseases. Cell Chemical Biology. 2018; 25:499–512. https://doi.org/10.1016/j.chembiol.2018.02.005 PMID: 29526711
47. Brockhausen I, Stanley P. O-GalNAc glycans. In: Varki A, Cummings RD, Esko JD, Stanley P, Hart GW, Aebi M, et al., editors. Essentials of Glycobiology. Cold Spring Harbor (NY): Cold Spring Harbor Laboratory Press; 2015.

48. Audfray A, Varrot A, Imberty A. Bacteria love our sugars: Interaction between soluble lectins and human fucosylated glycans, structures, thermodynamics and design of competing glycocompounds. Comptes Rendus Chimie. 2013; 16:482–90.

49. Matos R, Amorim I, Magalhães A, Haesebrouck F, Gärtner F, Reis CA. Adhesion of Helicobacter species to the human gastric mucosa: a deep look into glycans role. Frontiers in molecular biosciences. 2021; 8:386.

50. Magalhães A, Rossez Y, Robbe-Masselot C, Maes E, Gomes J, Shevtsova A, et al. Muc5ac gastric mucin glycosylation is shaped by FUT2 activity and functionally impacts *Helicobacter pylori* binding. Scientific Reports. 2016; 6:25575.

51. Magalhães A, Gomes J, Ismail MN, Haslam SM, Mendes N, Osório H, et al. Fut2-null mice display an altered glycosylation profile and impaired BabA-mediated *Helicobacter pylori* adhesion to gastric mucosa. Glycobiology. 2009; 19:1525–36.

52. Read AP. Haploinsufficiency. In: eLS. John Wiley & Sons, Ltd; 2017. page 1–5.

53. Hillmer EJ, Zhang H, Li HS, Watowich SS. STAT3 signaling in immunity. Cytokine & growth factor reviews. 2016; 31:1–15. https://doi.org/10.1016/j.cytogfr.2016.05.001 PMID: 27185365

54. Kingsolver MB, Hardy RW. Making connections in insect innate immunity. Proceedings of the National Academy of Sciences. 2012; 109:18639–40. https://doi.org/10.1073/pnas.1216736109 PMID: 23100537

55. Noh MY, Muthukrishnan S, Kramer KJ, Arakane Y. A chitinase with two catalytic domains is required for organization of the cuticular extracellular matrix of a beetle. PLOS Genetics. 2018; 14:e1007307. https://doi.org/10.1371/journal.pgen.1007307 PMID: 29590098

56. Mustonen T, Alitalo K. Endothelial receptor tyrosine kinases involved in angiogenesis. Journal of Cell Biology. 1995; 129:895–8. https://doi.org/10.1083/jcb.129.4.895 PMID: 7538139

57. Rosin D, Schejter E, Volk T, Shilo BZ. Apical accumulation of the *Drosophila* PDGF/VEGF receptor ligands provides a mechanism for triggering localized actin polymerization. Development. 2004; 131:1939–48.

58. Naitou A, Kato Y, Nakanishi T, Matsuura T, Watanabe H. Heterodimeric TALENs induce targeted heritable mutations in the crustacean *Daphnia magna*. Biology Open. 2015; 4:364–9.

59. Kumagai H, Nakanishi T, Matsuura T, Kato Y, Watanabe H. CRISPR/Cas-mediated knock-in via non-homologous end-joining in the crustacean *Daphnia magna*. PLOS ONE. 2017; 12:e0186112.

60. R Core Team. R: a language and environment for statatistical computing. Vienna, Austria: R Foundation for Statistical Computing; 2020.

61. Broman KW, Wu H, Sen S, Churchill GA. R/qtl: QTL mapping in experimental crosses. Bioinformatics. 2003; 19:889–90. https://doi.org/10.1093/bioinformatics/btg112 PMID: 12724300

62. Haley CS, Knott SA. A simple regression method for mapping quantitative trait loci in line crosses using flanking markers. Heredity. 1992; 69:315–24. https://doi.org/10.1038/hdy.1992.131 PMID: 16718932

63. Harris RS. Improved pairwise alignment of genomic DNA. The Pennsylvania State University; 2007.

64. Pearson WR. An introduction to sequence similarity ("homology") searching. Current protocols in bioinformatics. 2013;0 3. https://doi.org/10.1002/0471250953.bi0301s42 PMID: 23749753

65. Flynn JM, Hubley R, Goubert C, Rosen J, Clark AG, Feschotte C, et al. RepeatModeler2 for automated genomic discovery of transposable element families. Proceedings of the National Academy of Sciences. 2020; 117:9451–7. https://doi.org/10.1073/pnas.1921046117 PMID: 32300014

66. Smith A, Hubley R, Green P. RepeatMasker Open-4.0. RepeatMasker Open-4.0. 2013;

67. Holt C, Yandell M. MAKER2: an annotation pipeline and genome-database management tool for second-generation genome projects. BMC Bioinformatics. 2011; 12:491. https://doi.org/10.1186/1471-2105-12-491 PMID: 22192575

68. Keller O, Kollmar M, Stanke M, Waack S. A novel hybrid gene prediction method employing protein multiple sequence alignments. Bioinformatics. 2011; 27:757–63. https://doi.org/10.1093/bioinformatics/btr010 PMID: 21216780

69. Li S, Ma L, Li H, Vang S, Hu Y, Bolund L, et al. Snap: an integrated SNP annotation platform. Nucleic Acids Research. 2007; 35:D707–10. https://doi.org/10.1093/nar/gkl969 PMID: 17135198

70. Borodovsky M, McIninch J. GENMARK: Parallel gene recognition for both DNA strands. Computers & Chemistry. 1993; 17:123–33.

71. Katoh K, Standley DM. MAFFT multiple sequence alignment software version 7: improvements in performance and usability. Molecular Biology and Evolution. 2013; 30:772–80. https://doi.org/10.1093/molbev/mst010 PMID: 23329690

72. Charif D, Lobry JR. SeqinR 1.0–2: a contributed package to the R project for statistical computing devoted to biological sequences retrieval and analysis. In: Structural approaches to sequence evolution. Springer; 2007. page 207–32.

73. Löytynoja A, Goldman N. An algorithm for progressive multiple alignment of sequences with insertions. Proceedings of the National Academy of Sciences. 2005; 102:10557–62. https://doi.org/10.1073/pnas.0409137102 PMID: 16000407

74. Löytynoja A, Goldman N. Phylogeny-aware gap placement prevents errors in sequence alignment and evolutionary analysis. Science. 2008; 320:1632–5. https://doi.org/10.1126/science.1158395 PMID: 18566285

75. Rozas J, Ferrer-Mata A, Sánchez-DelBarrio JC, Guirao-Rico S, Librado P, Ramos-Onsins SE, et al. DnaSP 6: DNA sequence polymorphism analysis of large data sets. Molecular Biology and Evolution. 2017; 34:3299–302. https://doi.org/10.1093/molbev/msx248 PMID: 29029172

76. Dobson L, Reményi I, Tusnády GE. CCTOP: a consensus constrained TOPology prediction web server. Nucleic Acids Research. 2015; 43:W408–12. https://doi.org/10.1093/nar/gkv451 PMID: 25943549

77. Gupta R, Brunak S. Prediction of glycosylation across the human proteome and the correlation to protein function. In: Pacific Symposium on Biocomputing. 2001. page 310–22.

78. Steentoft C, Vakhrushev SY, Joshi HJ, Kong Y, Vester-Christensen MB, Schjoldager KTBG, et al. Precision mapping of the human O-GalNAc glycoproteome through SimpleCell technology. The EMBO Journal. 2013; 32:1478. https://doi.org/10.1038/emboj.2013.79 PMID: 23584533

79. Pertea G, Pertea M. GFF utilities: GffRead and GffCompare. F1000Research. 2020; 9:304. https://doi.org/10.12688/f1000research.23297.2 PMID: 32489650

80. Bray NL, Pimentel H, Melsted P, Pachter L. Near-optimal probabilistic RNA-seq quantification. Nature Biotechnology. 2016; 34:525–7. https://doi.org/10.1038/nbt.3519 PMID: 27043002

81. Love MI, Huber W, Anders S. Moderated estimation of fold change and dispersion for RNA-seq data with DESeq2. Genome Biology. 2014; 15:550. https://doi.org/10.1186/s13059-014-0550-8 PMID: 25516281

82. Benjamini Y, Hochberg Y. Controlling the false discovery rate: a practical and powerful approach to multiple testing. Journal of the Royal Statistical Society. Series B (Methodological). 1995; 57:289–300.

S1 Methods: Supplementary materials and methods

Infection experiment

We used an arbitrary subset of 40 F2 clones (20 attachment positive, and 20 attachment negative) from the QTL panel to test whether P21 hindgut attachment predicts infection outcome (S1_File). Thirty *Daphnia magna* individuals from each clone were housed in three separate 100-mL jars (ten individuals per jar) and exposed to 5,000 spores of the *Pasteuria ramosa* genotype P21 per day for three days (total 15,000 spores per individual). Animals were fed daily with 2 million cells of algae (*Tetradesmus obliquus*) until 10 days post infection, after which they were fed 10 million cells per day until the end of the experiment. Five weeks after infection, we scored all individuals for presence of diseases symptoms (empty brood pouch, red coloration), and a sample of individuals were also crushed and examined under a binocular microscope to confirm the presence of *P. ramosa* spores.

QTL mapping

Phenotyping panel

We phenotyped all clones in the F2 panel using the attachment test [1]. Isolate P21 attaches to the hindgut of its host, so clones were considered susceptible if fluorescent spores were visible in the hindgut, and otherwise they were considered resistant. At least four individuals were scored for each clone. For clones with ambiguous results, additional individuals were scored.

Mapping with R/qtl

Phenotype data were combined with the genetic map data and analyzed using the R package qtl (version 1.42-8) [2]. Single QTL interval mapping was performed with a binary model. LOD significance thresholds were determined using permutation tests (1,000 permutations), and upper confidence limits on true p-values were determined using a binomial test. The QTL location (in cM) was estimated using a LOD support interval of 1.8, which is recommended for QTL panels created from an intercross.

A further genome scan using the QTL marker as an interactive covariate identified an additional QTL on linkage group 4 (position 20.4 cM; LOD 4.68; p-value 0.033) that may interact with the main effect QTL on linkage group 3. However, a 2-dimensional scan using a 2-QTL model failed to identify any linked loci or loci with marginal effects, and both manual and automated model search methods confirmed that the model with the single QTL at linkage group 3 had the maximum penalized LOD score.

Fine mapping

Concept

Fine mapping is simply QTL mapping on a finer scale, and thus both methods rely on the same logic. QTL mapping works by crossing the parents (which differ in a phenotype of interest) and then selfing the resulting F1 generation to produce an F2 generation with random recombination events between the parental genotypes throughout the genome. By genotyping the F2 panel at genetic markers throughout the genome, the phenotype of interest can be associated with a genotype at a certain locus (under the assumption that F2 clones with the phenotype of interest have the same genotype as the parent clone with that phenotype). The goal of fine mapping, then, is to increase the resolution of the genetic map in the specific region that encompasses the QTL. This is accomplished by adding genetic markers within the QTL region and genotyping these markers in the informative clones from the QTL (F2) panel. The informative clones are those which show a phenotype-altering recombination event within the QTL region (i.e., in this study, such informative clones are expected to be susceptible to P21 attachment if the F locus is on one side of the recombination breakpoint, and resistant if the F locus is on the other side of the breakpoint). Using these informative clones, the QTL region can then be narrowed down by associating the phenotype to the matching genotype (based on the genotype/phenotype combination of the parent clones). The fine mapping has reached its limit when there are no more recombination events between the two markers, as these recombination "breakpoints" delimit the boundaries of the locus (for the particular collection of F2 clones). The ideal scenario is that the recombination events happen to be spaced such that the QTL can be fine mapped to the level of the gene which underlies the phenotype of interest. In this case, some clones must have a recombination event just upstream of the gene, and others must have a recombination event just downstream of the gene.

Experimental design

From the QTL analysis results, we narrowed down the region of interest to approximately 426 kb (Fig 1A), between the SNP markers scaffold00288_965 and scaffold01464_326 of the QTL map (S1_File, sheet "QTL SNP map"). Additional genotype data from a previous fine mapping effort [3] allowed us to reduce the region further to 350 kb (using the downstream flanking marker P24). We then began fine mapping using microsatellite analysis. We started by re-sequencing all the informative F2 clones (those which had previously shown a phenotype-altering recombination event in the region of interest [4]) at flanking markers P24 and 965D1 (just 165 bp downstream of previously used marker scaffold00288_965) in order to check the recorded genotypes of these clones (S1_File, sheet "Marker primers"). According to our results, only 18 of the 28 informative clones showed recombination events in the 350 kb region (S1_File, sheet "Finemap microsat"). We repeated the PCRs and sequencing analysis a second time and got the same results for all clones. We also sequenced the 28 F2 clones at markers from both ends of the ABC region (markers P34new

and U1 (5.3 kb upstream of the forward primer from marker g311b that was previously used to delimit the ABC region [3])), to determine whether our locus of interest is upstream or downstream of this region. Lastly, we placed two additional markers on each side of the ABC region (markers 44154 and 90815 upstream and markers D16 and D42 downstream) to narrow the region down even further.

This first round of microsatellite sequencing (S1_File, sheet "Finemap microsat") narrowed down the locus to a 58-kb region just downstream of (and overlapping the last 5.3 kb of) the ABC region (between markers U1 and D42), with just two informative clones remaining (clones 177 and 693). Clone 693 provides information on the upstream boundary of the locus, with a recombination breakpoint in the 5.3 kb between markers U1 and g311b (S1_File, sheet "Marker primers"). Clone 177 provides information on the downstream boundary, with a recombination breakpoint in the 25.7 kb between markers D16 and D42.

We next used Sanger sequencing for further fine mapping (S1_File, sheet "Finemap Sanger"). We re-sequenced clone 693 at marker g311b to confirm the location of the upstream boundary, and we sequenced clone 177 at two additional markers (D22 and D32) between D16 and D42 to narrow in on the downstream boundary. This reduced the locus to 40.4 kb, with the downstream boundary in the 8 kb between markers D16 and D22. In the second round of Sanger sequencing, we placed two additional markers (D16_5 and D19) between markers D16 and D22, which reduced the window of the downstream boundary from 8 kb to 6 kb. We also placed three additional markers (U0_5, U0_6, and U0_7) between markers U1 and g311b, which reduced the window of the upstream boundary from 5.3 kb to 2.5 kb. In the third and final round of Sanger sequencing, we placed 3 additional markers (D16_9, D17_1, D18) between markers D16_5 and D19, and we placed 2 additional markers (U0_55 and U0_54) between markers U0_5 and U0_6. The upstream recombination breakpoint was mapped to within 116 bp downstream of the SNP at position 2,329,948 (contig 000011F) in marker U0_55, and the downstream breakpoint was mapped to within 70 upstream of the SNP at position 2,361,178 (also contig 000011F) in marker D16_9.

Later evidence from F3 clones (see "Producing Selfed Offspring" below) allowed us to determine that the F locus is upstream of marker D16 (at position 2,358,729), thus narrowing the region by another 2.4 kb.

Marker creation

Microsatellite markers

Size-polymorphic markers were created for analysis with capillary electrophoresis (S1_File, sheet "Marker primers"). These markers are similar to microsatellites in that they are size polymorphic between the two parent clones, and the target region is smaller than that for SNP markers, which are sequenced with Sanger sequencing. We aligned the F-locus region (between markers scaffold00288_965 and P24) of the parent clones Xinb3 and Iinb1 in MEGA (version X) [5] using ClustalW alignment [6]. We then manually searched for size polymorphisms (gaps in alignment) between the two clones in the genomic areas where we wanted

to place our markers. Only gaps larger than 3 bp were considered in order to minimize the risk of including spurious gaps that were the result of assembly errors (both genomes were sequenced using PacBio technology, which is susceptible to such errors). A 400-bp region surrounding each gap was searched for primers using Primer3Web (version 4.1.0) [7,8], and we checked that the primer pairs were identical between the parent clones. Target sizes varied from 142 bp to 339 bp. Primer pairs were also checked for mis-priming using BLASTN (version 2.7.1+, blast.ncbi.nlm.nih.gov) against the Xinb3 reference genome version 3.0. We used the program Multiple Primer Analyzer (ThermoFisher) to check for possible cross-primer dimers in order to optimize the primer pair combinations in each of two multiplex runs. Unlabeled primers were used to optimize PCR conditions, and 5' fluorescently-labeled forward primers were used for capillary electrophoresis.

SNP markers for Sanger Sequencing

Sanger sequencing-appropriate primers were created to amplify regions containing at least one SNP between the QTL parent clones (S1_File, sheet "Marker primers"). We searched a region of approximately 1 kb for primers with product sizes between 150 and 700 bp. Chosen product sizes ranged from 128 bp to 557 bp. QTL F2 panel clones 693 or 177 were sequenced at each of the created markers, and sequences were compared to those of the QTL parent clones (Xinb3 and Iinb1) to determine the genotype at each marker position.

Marker sequencing

DNA was extracted from whole *Daphnia magna* using Chelex beads (Bio-Rad), as adapted from Walsh et al. [9]. Individual *D. magna* were placed in 96-well plates with a drop of water and crushed using plastic pestles. To each well was added 150 µL of 5-10 % (w/v) Chelex beads and 10 µL of 20 % (w/v) proteinase K, and samples were incubated for 2 hours at 55 °C followed by 10 minutes at 99 °C. Sample plates were centrifuged for 5 minutes at 7,000 rpm to separate DNA from the Chelex beads, and 75-100 µL of the supernatant was removed for PCR amplification.

For the first round of fine mapping, we used a microsatellite sequencing protocol as described in Andras and Ebert [10] to amplify markers that were size polymorphic between the QTL parents Xinb3 and Iinb1. Forward primers from eight primer pairs were uniquely labeled with fluorescent dyes and combined in multiplex PCR reactions (two runs of four primers). Primers, DNA, and master mix (2x Qiagen Multiplex PCR Master Mix) were combined and heated to 95°C for 15 minutes to activate the Taq polymerase. This initial heating was followed by 30 PCR cycles as follows: 30 seconds at 94°C (denature), 90 seconds at 60°C (anneal), 90 seconds at 72°C (extend). Optimal annealing temperature had been determined previously using a gradient PCR for all primer pairs. After all PCR cycles were complete, samples were incubated for 10 minutes at 72°C for the final extension. PCR products were added to a microsatellite master mix (containing Applied Biosystems Hi-Di formamide and GeneScan500LIZ dye size standard) and

incubated for 4 min at 94°C and then snap cooled on ice for 4 minutes. The PCR product was then analyzed with capillary electrophoresis (Applied Biosystems 3130xl Genetic Analyzer), and the resulting electropherogram peaks were interpreted using GeneMapper Software (version 4.1, Applied Biosystems) to distinguish the homozygotes and the heterozygotes.

For the second and third rounds of fine mapping, PCRs were performed as previously described, but with a separate reaction for each primer pair, and with an annealing temperature of 58°C (again determined with gradient PCR for this new set of primers). PCR products were run on an agarose gel to confirm the presence of sufficient DNA for sequencing. PCR products were then sent for Sanger Sequencing (Microsynth; Basel, Switzerland). Chromatogram results were examined visually for sequencing accuracy and to check for overlapping peaks in the case of potential heterozygotes.

Producing selfed offspring

We produced F3 offspring from clones 693 and 94 of the QTL F2 panel, primarily to validate that the F locus and ABC supergene are separate loci, and secondarily to further refine the interval of the F-locus region and to check for possible epistasis between the D and F loci (S2_File). We chose F2 clones 693 and 94 because they were predicted to have experienced recombination between the F locus and the ABC supergene (recombination is necessary to demonstrate that the two loci are different) and they were also potentially heterozygous at the F locus (heterozygosity is necessary to produce segregating offspring that can be used for further fine mapping). Selfed offspring were produced by collecting and hatching the sexually-produced ephippia (resting eggs) from single-clone jars of these F2 clones (S2_File, sheet "Collection"). To stimulate ephippia production, we placed the animals in modified laboratory conditions, with a lower temperature (18 °C instead of 20 °C) and shorter day (8:16 hour light/dark instead of 18:6 hour light/dark). Ephippia were collected four times at approximately two-week intervals. Collected ephippia were placed in 1.5 mL plastic tubes and stored in the dark at 4 °C for at least six weeks to simulate winter. After this dormancy period, ephippia were dried by placing them on suspended coffee filters in a well-aerated room for 4 – 5 days. Then ephippia were stimulated to hatch by first placing them in a 50 % bleach solution (in deionized water) for four minutes, then rinsing thoroughly in deionized water for one minute and placing them in artificial Daphnia medium (ADaM) [11,12] until hatching (after approximately 5 – 10 days). Newly hatched offspring were transferred individually to new 100 mL jars and cared for under standard laboratory conditions [12].

All 74 F3 offspring of F2 clone 94 were resistant to P21 attachment, strongly suggesting that clone 94 is homozygous dominant (genotype FF) and indicating that the F locus is upstream of marker D16 (because clone 94 is heterozygous at this marker). In contrast, the F3 offspring of F2 clone 693 segregated for P21 resistance: 8 out of 29 (28%) offspring tested were susceptible to P21 attachment. This strongly suggests

that clone 693 is heterozygous at the F locus and confirms that the F and C loci are separate, because clone 693 is homozygous recessive at the C locus, which was inferred previously [3] and was supported by our result showing that 22 out of 22 (100%) of F3 offspring from clone 693 were susceptible to C19 attachment. Two out of 22 (8 %) of the F3 offspring from F2 clone 693 were susceptible to P15 hindgut attachment, although the D-locus genotype (dd) of clone 693 predicted zero susceptible offspring. This slight distortion of segregation suggests that the F locus could have an effect on P15 attachment.

Cladoceran-specific protein family

The Cladoceran-specific (CS) proteins described here form a large family of molecules (over 100 members detected so far), the genes of which are distributed in multiple locations of the *D. magna* genome. These include gene islets linked to *Pasteuria ramosa* resistance loci ABC and F (located on contig 000011F (2991638 bp) in the Xinb3 reference genome version 3.0) as well as to the D locus (located on contig 000018F (2589983 bp) in the Xinb3 reference genome version 3.0), which we aligned using Clustal Omega [13] (S1_Figure). Some of the CS proteins are membrane bound, thanks to a hydrophobic segment. Many others are susceptible to be secreted. As their name suggests, homologs of these genes have so far been found only in Cladocerans.

The sequence of a CS (one example below) shows some highly conserved features:

- An average predicted sequence length of about 190 – 300 amino acids (with a few exceptions reaching up to 1148 aa)
- A high percentage of amino acid identities (from 35 – 70 %)
- A richness in T and S residues, suggesting a high level of glycosylation
- Some (4) highly conserved cysteine residues at positions 442 – 472 and 708 – 718 (see sequence below and S1_Figure)
- Some highly conserved charged residues (K and R) at positions 473 – 483 (S1_Figure)

>11F23.93 CS
MEFTFILLSALVAVSQQQFRRHPSEGMFWLASYYSPPSATINPYLTSNYNNDELVVMPFFRQLPRDDPDVEEIFGGTQLR
NKEMNRYQPFRQDKARLVVNFSSRSYLLNKVKTISFTITSSVTLTKVESCIPSHQFSASFASVTCRRKRGGIAELPVTNW
KDIQLATKPTNVQPVEPTIVSALNSPTGSAELPQISSSKDEDLLNEKQSSQVIPPSQQARMKRLLFHFVATTTVVSYTFFSA
TSTKTVSLLSVADQGPGFLICRPEGYSVCS

Gene annotation

Software-generated annotations were manually curated using a combination of transcriptomic data, protein structure predictions, and alignment to homologous genes (S6_File). Briefly, RNAseq reads sequenced previously [14] were assembled *de novo* to their respective genomes using TRINITY (version 2.11.0) [15]

and rnaSPADES (version 3.14.1) [16]. Each sample was assembled as an independent transcriptome, and then all these transcriptomes were combined and de-duplicated to produce a consensus transcriptome for each QTL parent clone (Xinb3 and Iinb1). We then mapped the resulting transcripts back to their respective genome using minimap2 (version 2.17-r941) [17] with the splice:hq option (long-read splice alignment for PacBio CCS reads), filtering out transcripts with bit flag 0x100 (secondary alignments) and mapQ score below 60 to retain only uniquely mapped transcripts. We then used the mapped transcripts to curate the structural gene annotations. For example, sometimes two neighboring genes were found to have transcripts spanning both sequences, suggesting that they should be instead annotated as a single gene. Also, many genes did not have their flanking untranslated regions (UTRs) annotated, so in some cases we could use the transcripts to add these UTR annotations. This hand curation was also important for making accurate comparisons between homologous genes in xF and iF (e.g., for percent identity and piN/piS calculations). A summary of the manual curations for each QTL parent genome is listed below (see S6_File for additional details):

Xinb3 genes (all on contig 000011F)

23.92: extended 3' UTR by 183 bp to match transcript contig71687.1

23.84: extended 5' UTR by 24 bp to match transcript contig153863.1. I did this for both mRNA-1 and mRNA-2 because the transcript evidence does not favor one over the other.

23.20: annotated 5' UTR based on transcript contig173441.1 and annotated 3' UTR based on transcript contig140187.1

23.8: extended 5' UTR by 7 bp to match transcript contig149714.1

23.93: annotated 3' UTR based on transcript contig188817.1

23.73: made 5' end of gene match the annotation for Iinb1 homolog 2592. This involved joining the two 5' exons and making them 5' UTR rather than CDS. Evidence for changes comes from alignment with Iinb1 homolog and other paralogs in F locus: protein alignment shows unusually long leader and unusually short first CDS.

23.23: annotated 5' UTR based on transcript contig110083.1

23.10: annotated 5' UTR based on transcript contig115927.1

Iinb1 genes (all on contig 129)

2589: Annotated both UTRs based on transcript contig16355.1

2590: Annotated 3' UTR based on transcript contig14710.1

2591: Extended second CDS by 8 bp based on transcript contig36462.1 and alignment with Xinb3 homolog 23.93. This caused premature stop codon in protein sequence, so next CDS shortened and 3' UTR lengthened accordingly.

2593: Combined genes 2593 and 2594 into one single gene based on transcript evidence, alignment to Xinb3 homolog 23.9, and predicted functional annotation as VEGF receptor. Shifted some exons and added one exon based on transcript contig5457.1. Shifted 5' CDS and added 5' UTR based on transcripts contig5353.1 and contig49933.1. Changed last seven exons into 3' UTR based on a 1-bp deletion (relative to transcripts and Xinb3 reference) between

positions 728968 and 728969 in the Iinb1 reference sequence that caused a frame shift and premature stop codon in the reference haplotype.

2603: Removed two 5' CDS regions based on protein structure prediction (leader is unusually long) as well as alignment to Xinb3 homolog 23.53 and to the other Cladoceran-specific paralogs (see S4_Figure).

Besides using the transcript evidence to curate the structural annotations, we also refined the functional annotations by examining the translated protein structures using a combination of programs including INTERPROSCAN (version 5.39-77.0) [18], PROSITE (version 2019_11) [19], SWISS-MODEL (version 2021-12-17) [20,21], and SMART (version 8.0) [22]. These methods revealed that gene 23.92 is similar to a lactosylceramide 4-alpha-galactosyltransferase (previously annotated as an alpha(1,3)fucosyltransferase) and that gene 23.9 is likely a VEGF receptor (previously annotated as brain chitinase and chia).

References

1. Duneau D, Luijckx P, Ben-Ami F, Laforsch C, Ebert D. Resolving the infection process reveals striking differences in the contribution of environment, genetics and phylogeny to host-parasite interactions. BMC biology. 2011;9:11.
2. Broman KW, Wu H, Sen S, Churchill GA. R/qtl: QTL mapping in experimental crosses. Bioinformatics. 2003;19:889–90.
3. Bento G, Routtu J, Fields P, Bourgeois Y, Du Pasquier L, Ebert D. The genetic basis of resistance and matching-allele interactions of a host-parasite system: The *Daphnia magna*-*Pasteuria ramosa* model. PLOS Genetics. 2017;13.
4. Routtu J, Hall MD, Albere B, Beisel C, Bergeron RD, Chaturvedi A, et al. An SNP-based second-generation genetic map of *Daphnia magna* and its application to QTL analysis of phenotypic traits. BMC Genomics. 2014;15:1033.
5. Kumar S, Stecher G, Li M, Knyaz C, Tamura K. MEGA X: Molecular Evolutionary Genetics Analysis across computing platforms. Molecular Biology and Evolution. 2018;35:1547–9.
6. Thompson JD, Gibson TJ, Higgins DG. Multiple sequence alignment using ClustalW and ClustalX. Current protocols in bioinformatics. 2003;2–3.
7. Untergasser A, Cutcutache I, Koressaar T, Ye J, Faircloth BC, Remm M, et al. Primer3—new capabilities and interfaces. Nucleic Acids Research. 2012;40:e115.
8. Koressaar T, Remm M. Enhancements and modifications of primer design program Primer3. Bioinformatics. 2007;23:1289–91.

9. Walsh PS, Metzger DA, Higuchi R. Chelex 100 as a medium for simple extraction of DNA for PCR-based typing from forensic material. BioTechniques. 1991;10:506–13.
10. Andras JP, Ebert D. A novel approach to parasite population genetics: Experimental infection reveals geographic differentiation, recombination and host-mediated population structure in *Pasteuria ramosa*, a bacterial parasite of *Daphnia*. Molecular Ecology. 2013;22:972–86.
11. Klüttgen B, Dülmer U, Engels M, Ratte HT. ADaM, an artificial freshwater for the culture of zooplankton. Water Research. 1994;28:743–6.
12. Ebert D, Zschokke-Rohringer CD, Carius HJ. Within- and between-population variation for resistance of *Daphnia magna* to the bacterial endoparasite *Pasteuria ramosa*. Proceedings of the Royal Society B: Biological Sciences. 1998;265:2127–34.
13. Madeira F, Pearce M, Tivey ARN, Basutkar P, Lee J, Edbali O, et al. Search and sequence analysis tools services from EMBL-EBI in 2022. Nucleic acids research. 2022;gkac240.
14. Orsini L, Gilbert D, Podicheti R, Jansen M, Brown JB, Solari OS, et al. *Daphnia magna* transcriptome by RNA-Seq across 12 environmental stressors. Scientific Data. 2016;3:160030.
15. Grabherr MG, Haas BJ, Yassour M, Levin JZ, Thompson DA, Amit I, et al. Full-length transcriptome assembly from RNA-Seq data without a reference genome. Nature biotechnology. 2011;29:644–52.
16. Bushmanova E, Antipov D, Lapidus A, Prjibelski AD. rnaSPAdes: a de novo transcriptome assembler and its application to RNA-Seq data. GigaScience. 2019;8:giz100.
17. Li H. Minimap2: pairwise alignment for nucleotide sequences. Bioinformatics. 2018;34:3094–100.
18. Apweiler R, Attwood TK, Bairoch A, Bateman A, Birney E, Biswas M, et al. The InterPro database, an integrated documentation resource for protein families, domains and functional sites. Nucleic Acids Research. 2001;29:37–40.
19. Sigrist CJ, Cerutti L, Hulo N, Gattiker A, Falquet L, Pagni M, et al. PROSITE: a documented database using patterns and profiles as motif descriptors. Briefings in bioinformatics. 2002;3:265–74.
20. Waterhouse A, Bertoni M, Bienert S, Studer G, Tauriello G, Gumienny R, et al. SWISS-MODEL: homology modelling of protein structures and complexes. Nucleic Acids Research. 2018;46:W296–303.

21. Guex N, Peitsch MC, Schwede T. Automated comparative protein structure modeling with SWISS-MODEL and Swiss-PdbViewer: a historical perspective. Electrophoresis. 2009;30 Suppl 1:S162-173.
22. Letunic I, Bork P. 20 years of the SMART protein domain annotation resource. Nucleic Acids Research. 2018;46:D493–6.

Figures S1-S9

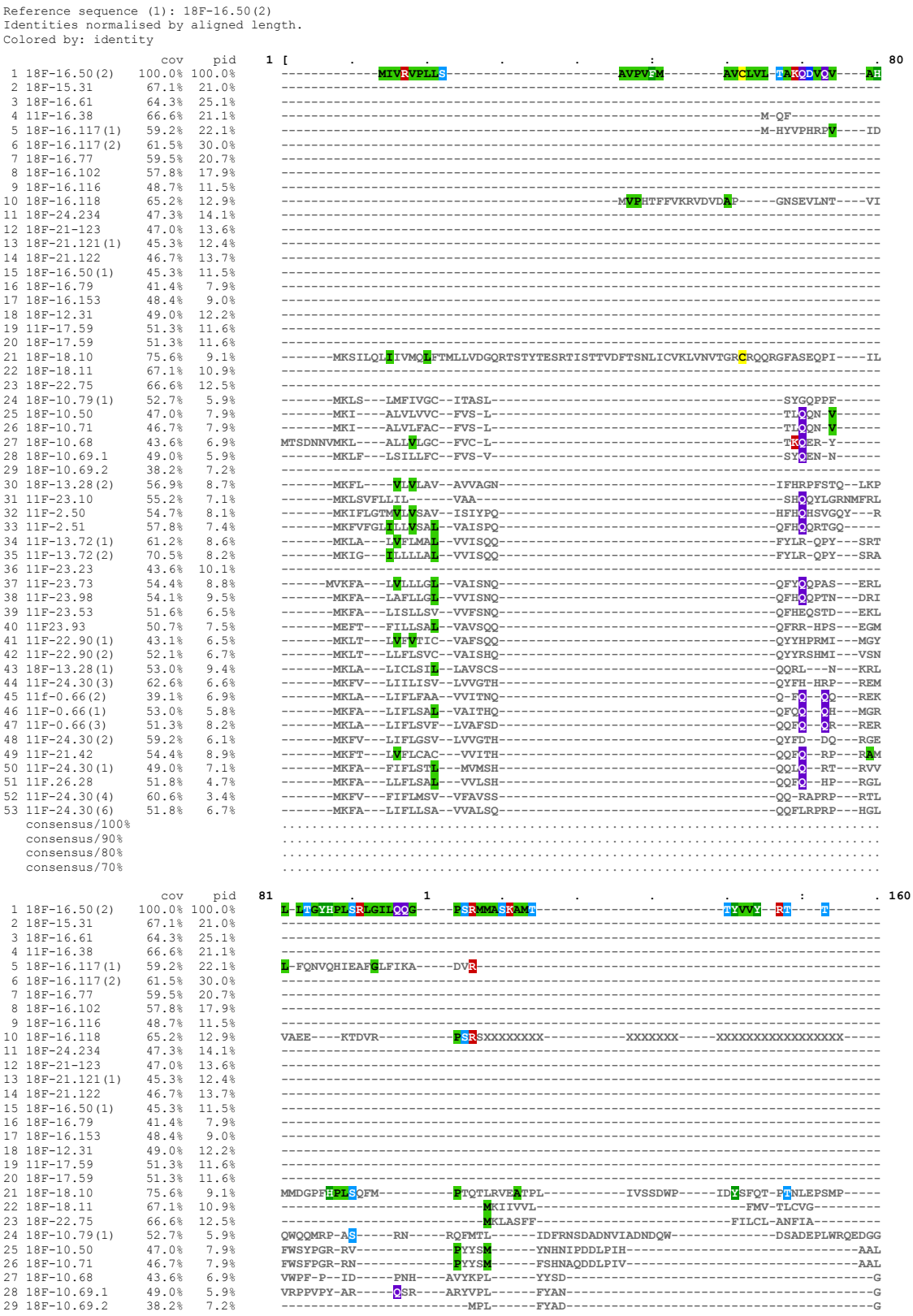

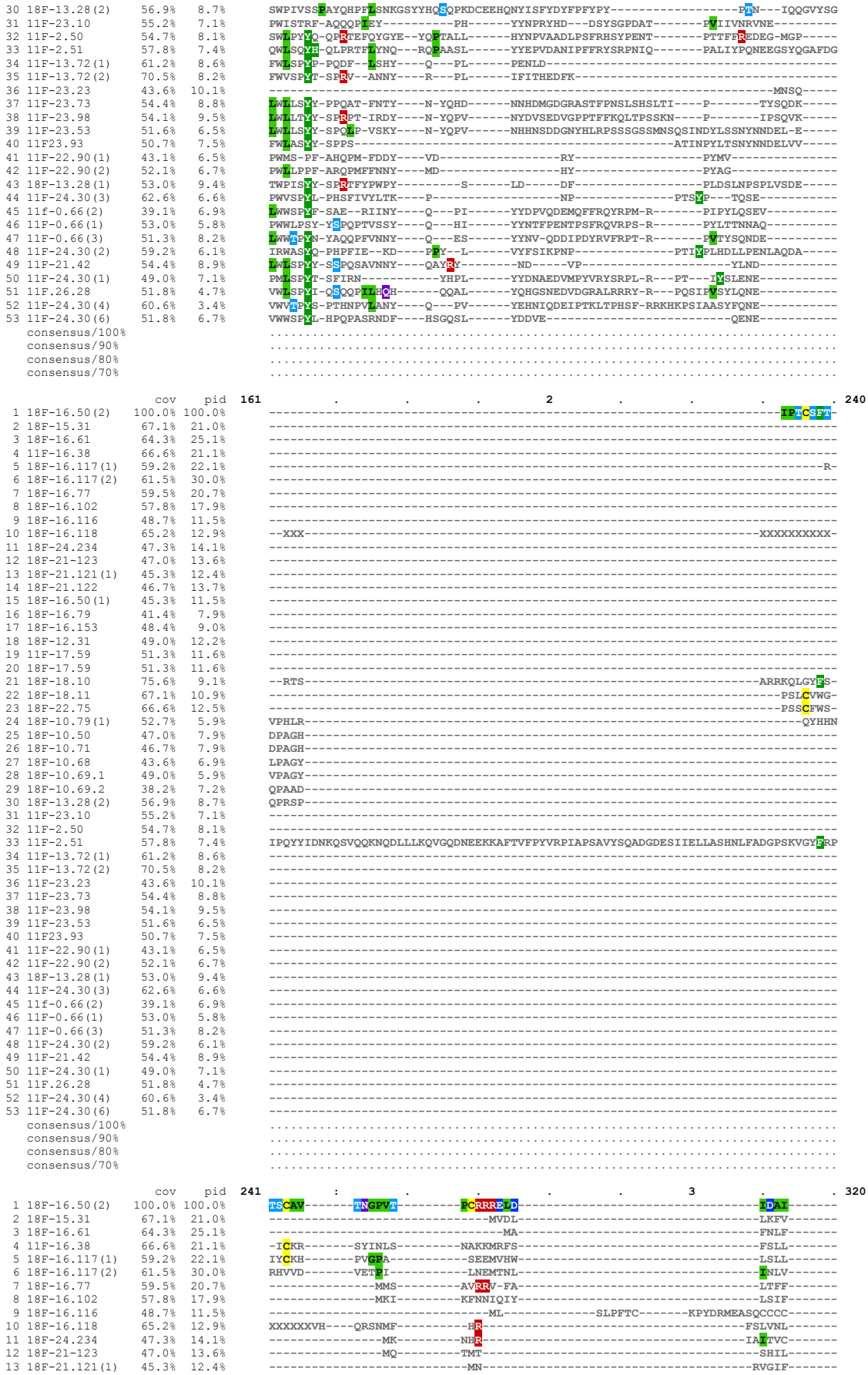

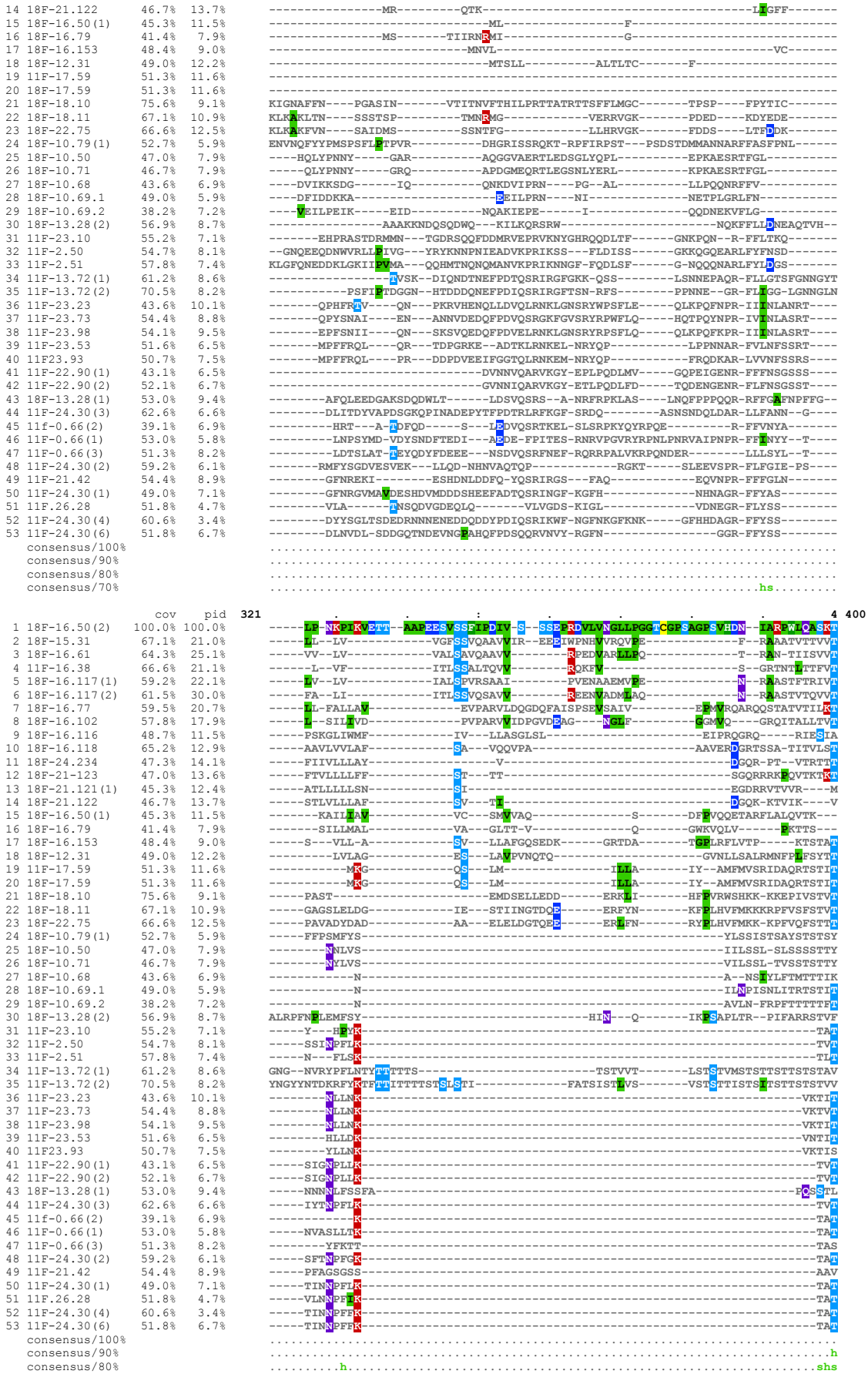

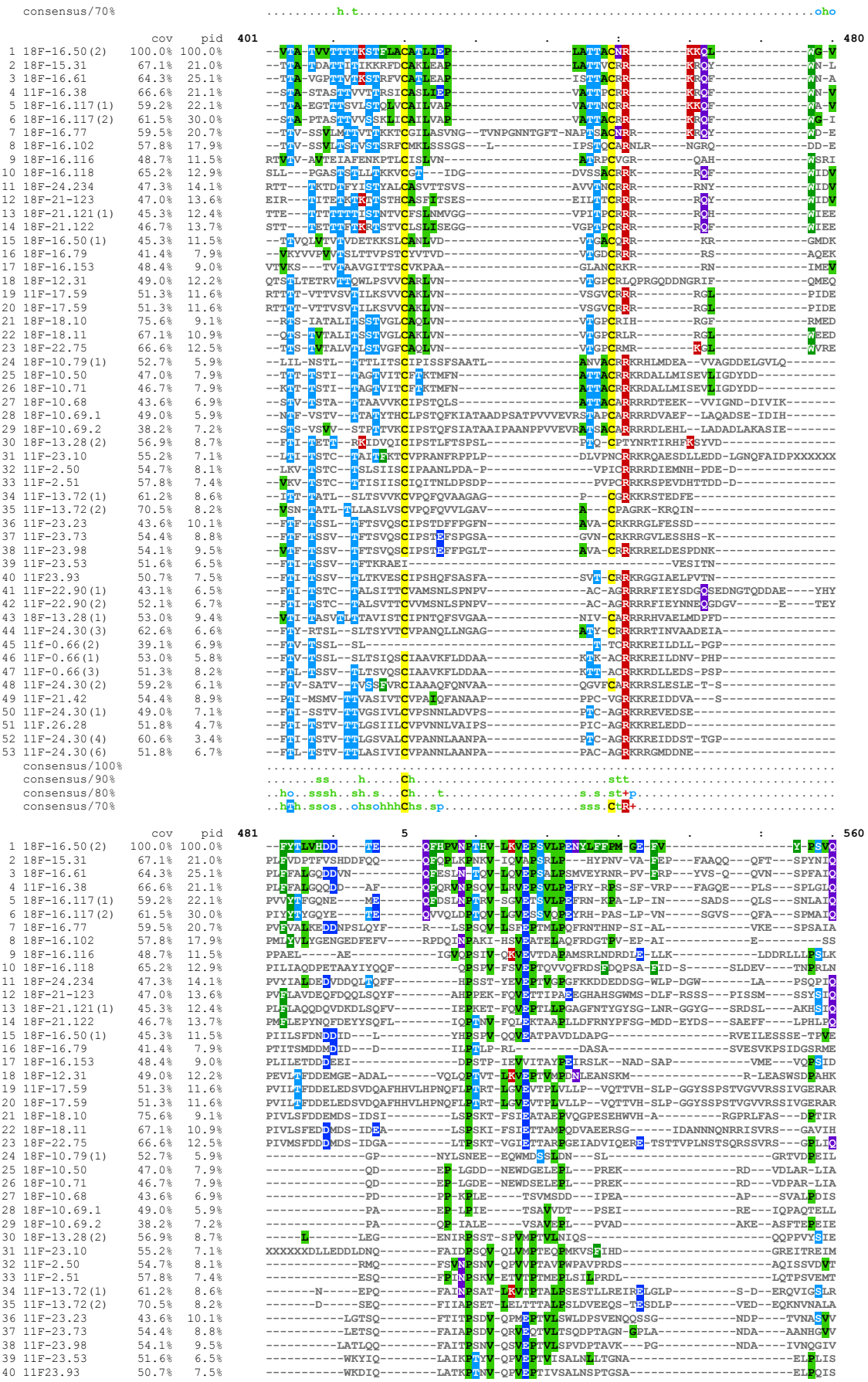

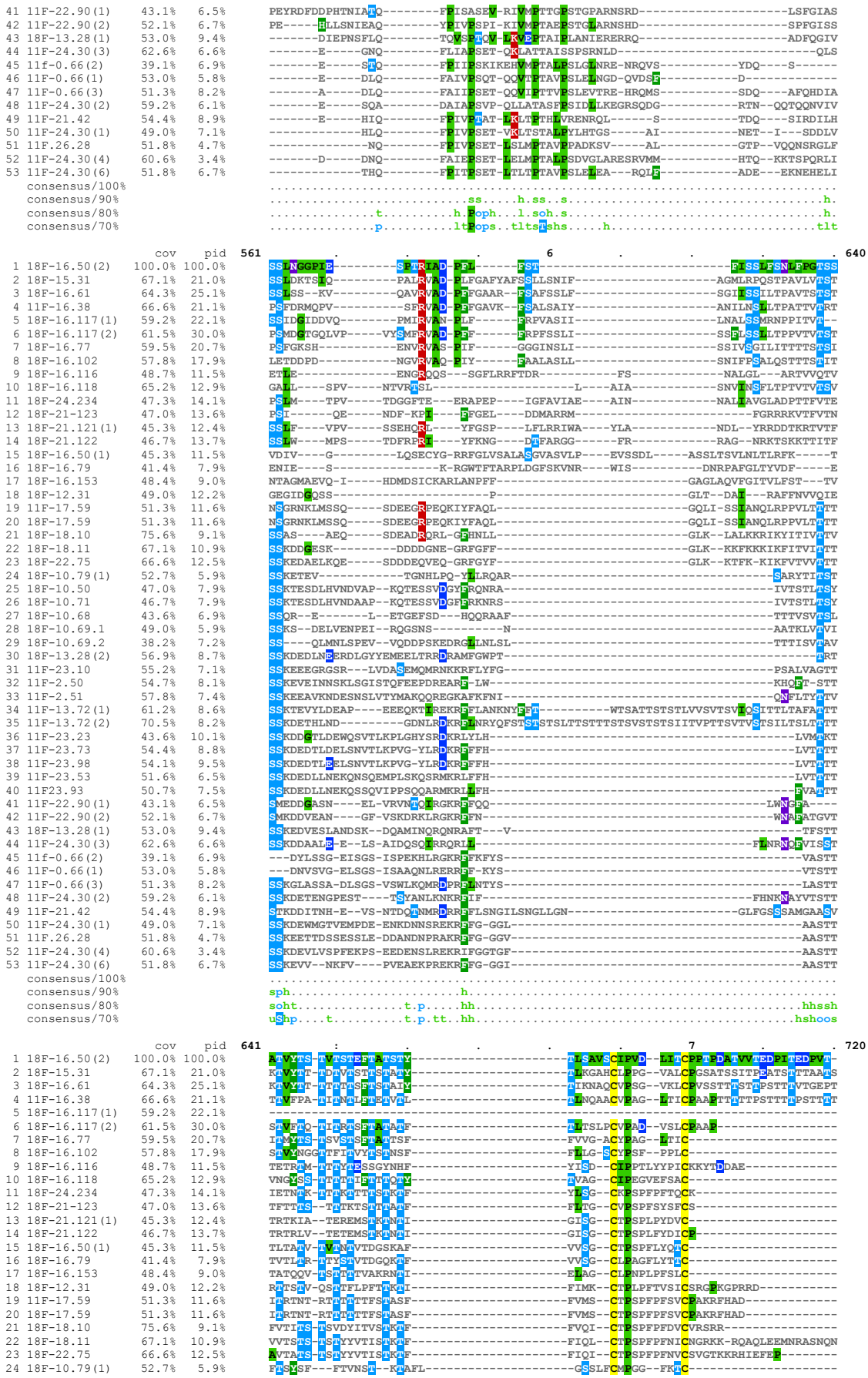

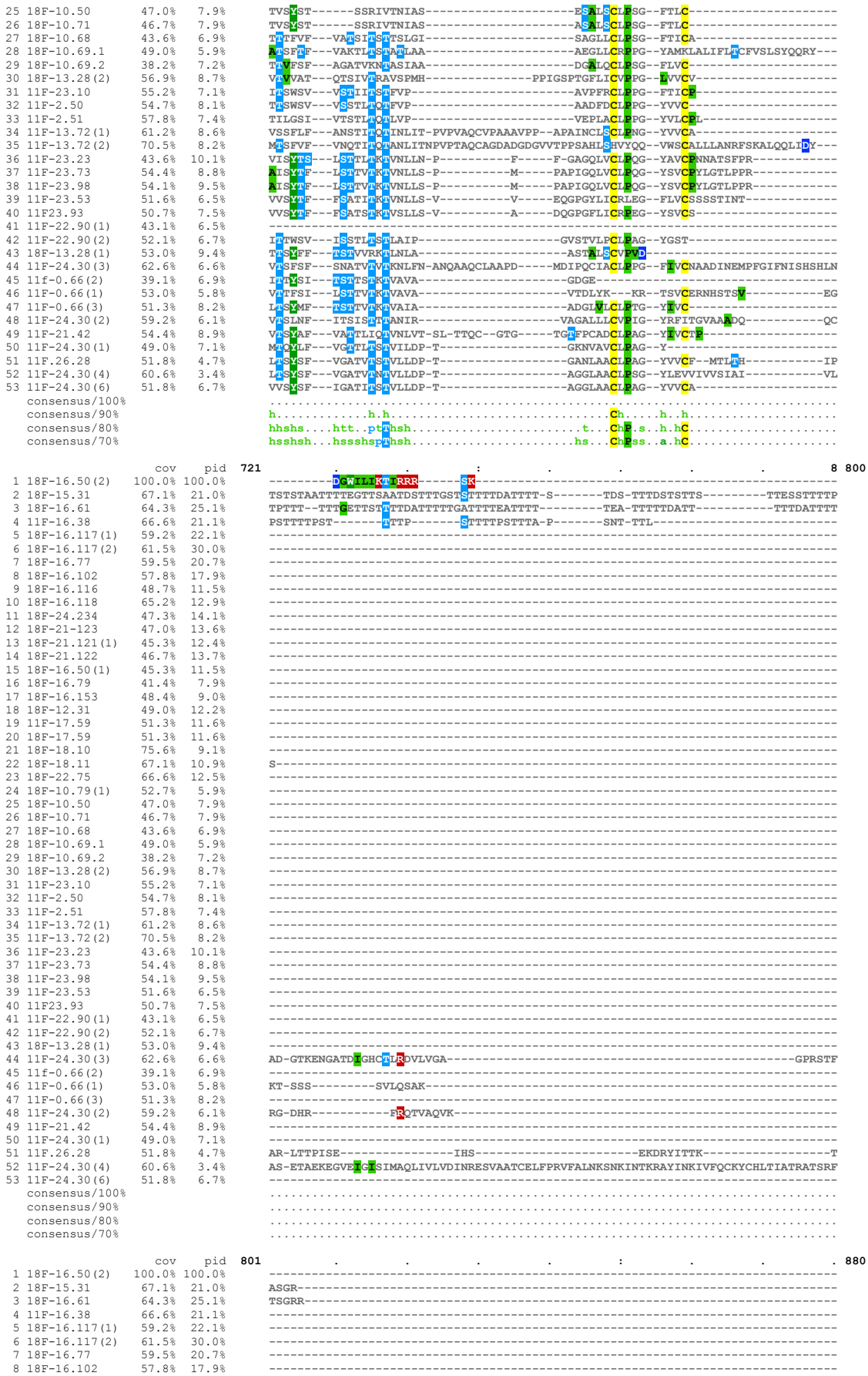

```
 9 18F-16.116      48.7%  11.5%      ----------------------------------------------------------------------------------------
10 18F-16.118      65.2%  12.9%      ----------------------------------------------------------------------------------------
11 18F-24.234      47.3%  14.1%      ----------------------------------------------------------------------------------------
12 18F-21-123      47.0%  13.6%      ----------------------------------------------------------------------------------------
13 18F-21.121(1)   45.3%  12.4%      ----------------------------------------------------------------------------------------
14 18F-21.122      46.7%  13.7%      ----------------------------------------------------------------------------------------
15 18F-16.50(1)    45.3%  11.5%      ----------------------------------------------------------------------------------------
16 18F-16.79       41.4%   7.9%      ----------------------------------------------------------------------------------------
17 18F-16.153      48.4%   9.0%      ----------------------------------------------------------------------------------------
18 18F-12.31       49.0%  12.2%      ----------------------------------------------------------------------------------------
19 11F-17.59       51.3%  11.6%      ----------------------------------------------------------------------------------------
20 18F-17.59       51.3%  11.6%      ----------------------------------------------------------------------------------------
21 18F-18.10       75.6%   9.1%      ----------------------------------------------------------------------------------------
22 18F-18.11       67.1%  10.9%      ----------------------------------------------------------------------------------------
23 18F-22.75       66.6%  12.5%      ----------------------------------------------------------------------------------------
24 18F-10.79(1)    52.7%   5.9%      ----------------------------------------------------------------------------------------
25 18F-10.50       47.0%   7.9%      ----------------------------------------------------------------------------------------
26 18F-10.71       46.7%   7.9%      ----------------------------------------------------------------------------------------
27 18F-10.68       43.6%   6.9%      ----------------------------------------------------------------------------------------
28 18F-10.69.1     49.0%   5.9%      ------------------------------------VWPMPYAPRAHL----------------------------------------
29 18F-10.69.2     38.2%   7.2%      ----------------------------------------------------------------------------------------
30 18F-13.28(2)    56.9%   8.7%      ----------------------------------------------------------------------------------------
31 11F-23.10       55.2%   7.1%      ----------------------------------------------------------------------------------------
32 11F-2.50        54.7%   8.1%      ----------------------------------------------------------------------------------------
33 11F-2.51        57.8%   7.4%      ----------------------------------------------------------------------------------------
34 11F-13.72(1)    61.2%   8.6%      ----------------------------------------------------------------------------------------
35 11F-13.72(2)    70.5%   8.2%      ----------------------------------------------------------------------------------------
36 11F-23.23       43.6%  10.1%      ----------------------------------------------------------------------------------------
37 11F-23.73       54.4%   8.8%      ----------------------------------------------------------------------------------------
38 11F-23.98       54.1%   9.5%      ----------------------------------------------------------------------------------------
39 11F-23.53       51.6%   6.5%      ----------------------------------------------------------------------------------------
40 11F23.93        50.7%   7.5%      ----------------------------------------------------------------------------------------
41 11F-22.90(1)    43.1%   6.5%      ----------------------------------------------------------------------------------------
42 11F-22.90(2)    52.1%   6.7%      ----------------------------------------------------------------------------------------
43 18F-13.28(1)    53.0%   9.4%      ----------------------------------------------------------------------------------------
44 11F-24.30(3)    62.6%   6.6%      STVEQIEYT-QKFHLLLK----------------------------------------------------------------------
45 11f-0.66(2)     39.1%   6.9%      ----------------------------------------------------------------------------------------
46 11F-0.66(1)     53.0%   5.8%      ----------------------------------------------------------------------------------------
47 11F-0.66(3)     51.3%   8.2%      ----------------------------------------------------------------------------------------
48 11F-24.30(2)    59.2%   6.1%      ----------------------------------------------------------------------------------------
49 11F-21.42       54.4%   8.9%      ----------------------------------------------------------------------------------------
50 11F-24.30(1)    49.0%   7.1%      ----------------------------------------------------------------------------------------
51 11F.26.28       51.8%   4.7%      PLWRLSKYNAMKLTLILLVCFVGVTY------QQGYAWSP-FHRH-SPR--LYLSNNYHENDRQLP--------AKSA
52 11F-24.30(4)    60.6%   3.4%      SSHSCLKF--MKFVLLFVTSVLSVSTHQYLHKTPAGLVWLSPYMSKQKPVLHKYQQVLYEPVDPDMPYFRYSKPLHPAVT
53 11F-24.30(6)    51.8%   6.7%      ----------------------------------------------------------------------------------------
   consensus/100%                    ........................................................................................
   consensus/90%                     ........................................................................................
   consensus/80%                     ........................................................................................
   consensus/70%                     ........................................................................................

                     cov    pid  881         .        9        .        .        .        .        :        . 960
 1 18F-16.50(2)   100.0% 100.0%      ----------------------------------------------------------------------------------------
 2 18F-15.31       67.1%  21.0%      ----------------------------------------------------------------------------------------
 3 18F-16.61       64.3%  25.1%      ----------------------------------------------------------------------------------------
 4 11F-16.38       66.6%  21.1%      ----------------------------------------------------------------------------------------
 5 18F-16.117(1)   59.2%  22.1%      ----------------------------------------------------------------------------------------
 6 18F-16.117(2)   61.5%  30.0%      ----------------------------------------------------------------------------------------
 7 18F-16.77       59.5%  20.7%      ----------------------------------------------------------------------------------------
 8 18F-16.102      57.8%  17.9%      ----------------------------------------------------------------------------------------
 9 18F-16.116      48.7%  11.5%      ----------------------------------------------------------------------------------------
10 18F-16.118      65.2%  12.9%      ----------------------------------------------------------------------------------------
11 18F-24.234      47.3%  14.1%      ----------------------------------------------------------------------------------------
12 18F-21-123      47.0%  13.6%      ----------------------------------------------------------------------------------------
13 18F-21.121(1)   45.3%  12.4%      ----------------------------------------------------------------------------------------
14 18F-21.122      46.7%  13.7%      ----------------------------------------------------------------------------------------
15 18F-16.50(1)    45.3%  11.5%      ----------------------------------------------------------------------------------------
16 18F-16.79       41.4%   7.9%      ----------------------------------------------------------------------------------------
17 18F-16.153      48.4%   9.0%      ----------------------------------------------------------------------------------------
18 18F-12.31       49.0%  12.2%      ----------------------------------------------------------------------------------------
19 11F-17.59       51.3%  11.6%      ----------------------------------------------------------------------------------------
20 18F-17.59       51.3%  11.6%      ----------------------------------------------------------------------------------------
21 18F-18.10       75.6%   9.1%      ----------------------------------------------------------------------------------------
22 18F-18.11       67.1%  10.9%      ----------------------------------------------------------------------------------------
23 18F-22.75       66.6%  12.5%      ----------------------------------------------------------------------------------------
24 18F-10.79(1)    52.7%   5.9%      ----------------------------------------------------------------------------------------
25 18F-10.50       47.0%   7.9%      ----------------------------------------------------------------------------------------
26 18F-10.71       46.7%   7.9%      ----------------------------------------------------------------------------------------
27 18F-10.68       43.6%   6.9%      ----------------------------------------------------------------------------------------
28 18F-10.69.1     49.0%   5.9%      ----------------------------------------------------------------------------------------
29 18F-10.69.2     38.2%   7.2%      ----------------------------------------------------------------------------------------
30 18F-13.28(2)    56.9%   8.7%      ----------------------------------------------------------------------------------------
31 11F-23.10       55.2%   7.1%      ----------------------------------------------------------------------------------------
32 11F-2.50        54.7%   8.1%      ----------------------------------------------------------------------------------------
33 11F-2.51        57.8%   7.4%      ----------------------------------------------------------------------------------------
34 11F-13.72(1)    61.2%   8.6%      ----------------------------------------------------------------------------------------
35 11F-13.72(2)    70.5%   8.2%      ----------------------------------------------------------------------------------------
36 11F-23.23       43.6%  10.1%      ----------------------------------------------------------------------------------------
37 11F-23.73       54.4%   8.8%      ----------------------------------------------------------------------------------------
38 11F-23.98       54.1%   9.5%      ----------------------------------------------------------------------------------------
39 11F-23.53       51.6%   6.5%      ----------------------------------------------------------------------------------------
40 11F23.93        50.7%   7.5%      ----------------------------------------------------------------------------------------
41 11F-22.90(1)    43.1%   6.5%      ----------------------------------------------------------------------------------------
42 11F-22.90(2)    52.1%   6.7%      ----------------------------------------------------------------------------------------
43 18F-13.28(1)    53.0%   9.4%      ----------------------------------------------------------------------------------------
44 11F-24.30(3)    62.6%   6.6%      ----------------------------------------------------------------------------------------
45 11f-0.66(2)     39.1%   6.9%      ----------------------------------------------------------------------------------------
46 11F-0.66(1)     53.0%   5.8%      ----------------------------------------------------------------------------------------
47 11F-0.66(3)     51.3%   8.2%      ----------------------------------------------------------------------------------------
48 11F-24.30(2)    59.2%   6.1%      ----------------------------------------------------------------------------------------
49 11F-21.42       54.4%   8.9%      ----------------------------------------------------------------------------------------
50 11F-24.30(1)    49.0%   7.1%      ----------------------------------------------------------------------------------------
51 11F.26.28       51.8%   4.7%      YDFELADSLATYDD---DEIASSLSDVQARIPFGS-ARKAQKKFFVTSVFPNSLFPFNFRPVTVTTLTTTALSVITSTAV
```

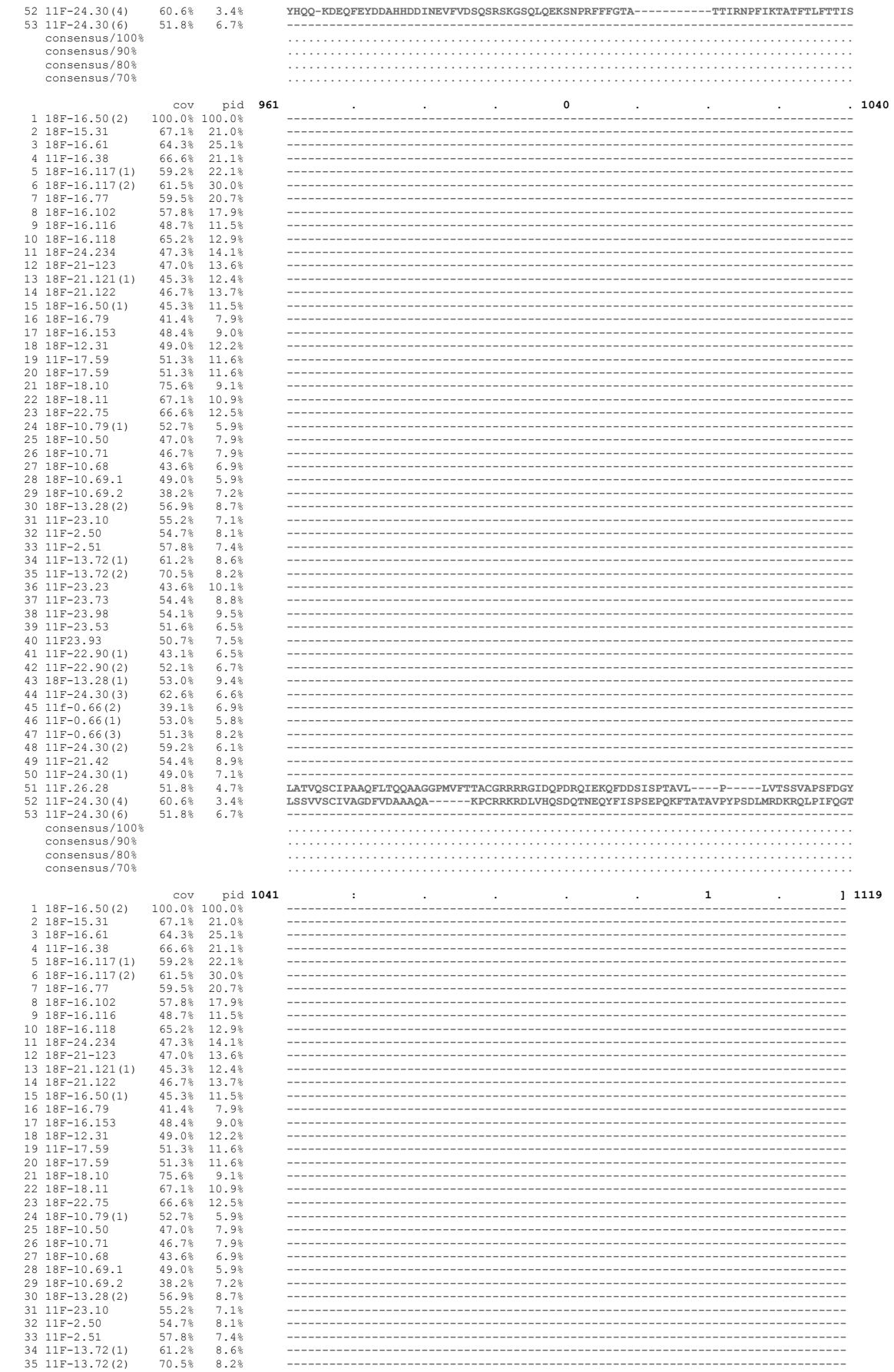
52 11F-24.30(4) 60.6% 3.4% YHQQ-KDEQFEYDDAHHDDINEVFVDSQSRSKGSQLQEKSNPRFFFGTA----------TTIRNPFIKTATFTLFTTIS
53 11F-24.30(6) 51.8% 6.7%
consensus/100%
consensus/90%
consensus/80%
consensus/70%
cov pid 961 . . . 0 1040
1 18F-16.50(2) 100.0% 100.0%
2 18F-15.31 67.1% 21.0%
3 18F-16.61 64.3% 25.1%
4 11F-16.38 66.6% 21.1%
5 18F-16.117(1) 59.2% 22.1%
6 18F-16.117(2) 61.5% 30.0%
7 18F-16.77 59.5% 20.7%
8 18F-16.102 57.8% 17.9%
9 18F-16.116 48.7% 11.5%
10 18F-16.118 65.2% 12.9%
11 18F-24.234 47.3% 14.1%
12 18F-21-123 47.0% 13.6%
13 18F-21.121(1) 45.3% 12.4%
14 18F-21.122 46.7% 13.7%
15 18F-16.50(1) 45.3% 11.5%
16 18F-16.79 41.4% 7.9%
17 18F-16.153 48.4% 9.0%
18 18F-12.31 49.0% 12.2%
19 11F-17.59 51.3% 11.6%
20 18F-17.59 51.3% 11.6%
21 18F-18.10 75.6% 9.1%
22 18F-18.11 67.1% 10.9%
23 18F-22.75 66.6% 12.5%
24 18F-10.79(1) 52.7% 5.9%
25 18F-10.50 47.0% 7.9%
26 18F-10.71 46.7% 7.9%
27 18F-10.68 43.6% 6.9%
28 18F-10.69.1 49.0% 5.9%
29 18F-10.69.2 38.2% 7.2%
30 18F-13.28(2) 56.9% 8.7%
31 11F-23.10 55.2% 7.1%
32 11F-2.50 54.7% 8.1%
33 11F-2.51 57.8% 7.4%
34 11F-13.72(1) 61.2% 8.6%
35 11F-13.72(2) 70.5% 8.2%
36 11F-23.23 43.6% 10.1%
37 11F-23.73 54.4% 8.8%
38 11F-23.98 54.1% 9.5%
39 11F-23.53 51.6% 6.5%
40 11F23.93 50.7% 7.5%
41 11F-22.90(1) 43.1% 6.5%
42 11F-22.90(2) 52.1% 6.7%
43 18F-13.28(1) 53.0% 9.4%
44 11F-24.30(3) 62.6% 6.6%
45 11f-0.66(2) 39.1% 6.9%
46 11F-0.66(1) 53.0% 5.8%
47 11F-0.66(3) 51.3% 8.2%
48 11F-24.30(2) 59.2% 6.1%
49 11F-21.42 54.4% 8.9%
50 11F-24.30(1) 49.0% 7.1%
51 11F.26.28 51.8% 4.7% LATVQSCIPAAQFLTQQAAGGPMVFTTACGRRRRGIDQPDRQIEKQFDDSISPTAVL----P-----LVTSSVAPSFDGY
52 11F-24.30(4) 60.6% 3.4% LSSVVSCIVAGDFVDAAAQA------KPCRRKRDLVHQSDQTNEQYFISPSEPQKFTATAVPYPSDLMRDKRQLPIFQGT
53 11F-24.30(6) 51.8% 6.7%
consensus/100%
consensus/90%
consensus/80%
consensus/70%
cov pid 1041 : . . . . 1 .] 1119
1 18F-16.50(2) 100.0% 100.0%
2 18F-15.31 67.1% 21.0%
3 18F-16.61 64.3% 25.1%
4 11F-16.38 66.6% 21.1%
5 18F-16.117(1) 59.2% 22.1%
6 18F-16.117(2) 61.5% 30.0%
7 18F-16.77 59.5% 20.7%
8 18F-16.102 57.8% 17.9%
9 18F-16.116 48.7% 11.5%
10 18F-16.118 65.2% 12.9%
11 18F-24.234 47.3% 14.1%
12 18F-21-123 47.0% 13.6%
13 18F-21.121(1) 45.3% 12.4%
14 18F-21.122 46.7% 13.7%
15 18F-16.50(1) 45.3% 11.5%
16 18F-16.79 41.4% 7.9%
17 18F-16.153 48.4% 9.0%
18 18F-12.31 49.0% 12.2%
19 11F-17.59 51.3% 11.6%
20 18F-17.59 51.3% 11.6%
21 18F-18.10 75.6% 9.1%
22 18F-18.11 67.1% 10.9%
23 18F-22.75 66.6% 12.5%
24 18F-10.79(1) 52.7% 5.9%
25 18F-10.50 47.0% 7.9%
26 18F-10.71 46.7% 7.9%
27 18F-10.68 43.6% 6.9%
28 18F-10.69.1 49.0% 5.9%
29 18F-10.69.2 38.2% 7.2%
30 18F-13.28(2) 56.9% 8.7%
31 11F-23.10 55.2% 7.1%
32 11F-2.50 54.7% 8.1%
33 11F-2.51 57.8% 7.4%
34 11F-13.72(1) 61.2% 8.6%
35 11F-13.72(2) 70.5% 8.2%

```
36 11F-23.23        43.6%  10.1%      ------------------------------------------------------------------------------
37 11F-23.73        54.4%   8.8%      ------------------------------------------------------------------------------
38 11F-23.98        54.1%   9.5%      ------------------------------------------------------------------------------
39 11F-23.53        51.6%   6.5%      ------------------------------------------------------------------------------
40 11F23.93         50.7%   7.5%      ------------------------------------------------------------------------------
41 11F-22.90(1)     43.1%   6.5%      ------------------------------------------------------------------------------
42 11F-22.90(2)     52.1%   6.7%      ------------------------------------------------------------------------------
43 18F-13.28(1)     53.0%   9.4%      ------------------------------------------------------------------------------
44 11F-24.30(3)     62.6%   6.6%      ------------------------------------------------------------------------------
45 11f-0.66(2)      39.1%   6.9%      ------------------------------------------------------------------------------
46 11F-0.66(1)      53.0%   5.8%      ------------------------------------------------------------------------------
47 11F-0.66(3)      51.3%   8.2%      ------------------------------------------------------------------------------
48 11F-24.30(2)     59.2%   6.1%      ------------------------------------------------------------------------------
49 11F-21.42        54.4%   8.9%      ------------------------------------------------------------------------------
50 11F-24.30(1)     49.0%   7.1%      ------------------------------------------------------------------------------
51 11F.26.28        51.8%   4.7%      DDVQPELRSSQTNLEEDQRQIFRVDAGNARQRRGL--SLVLTVTLTSTSYSFSTTTLKKTVNLSGTGQLSCLPAGFAVC
52 11F-24.30(4)     60.6%   3.4%      SLWNKDIIES--TKEENDVSYFWP-AKNRKEQRFLFENSHYVASTTVTSYNFVSTTVTKTVDVAIDVGLNCVPTGYV--
53 11F-24.30(6)     51.8%   6.7%      ------------------------------------------------------------------------------
   consensus/100%                     ..............................................................................
   consensus/90%                      ..............................................................................
   consensus/80%                      ..............................................................................
   consensus/70%                      ..............................................................................
```

MView 1.63, Copyright © 1997-2018 Nigel P. Brown

S1 Figure

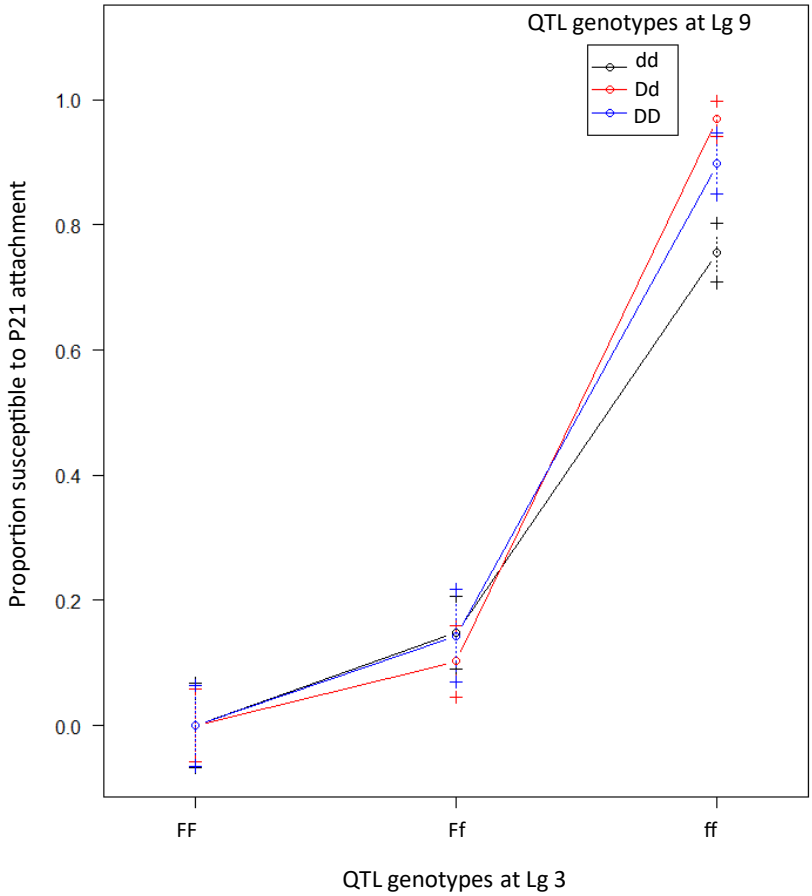

	df	LOD	% variance	P-value (Chi²)
Lg 3 @ 157.0 (F locus QTL)	6	65.115	56.844	< 2e-16
Lg 9 @ 105.3 (D locus QTL)	6	4.481	2.513	0.00213
Lg 3 x Lg 9	4	2.478	1.371	0.02231

S2 Figure

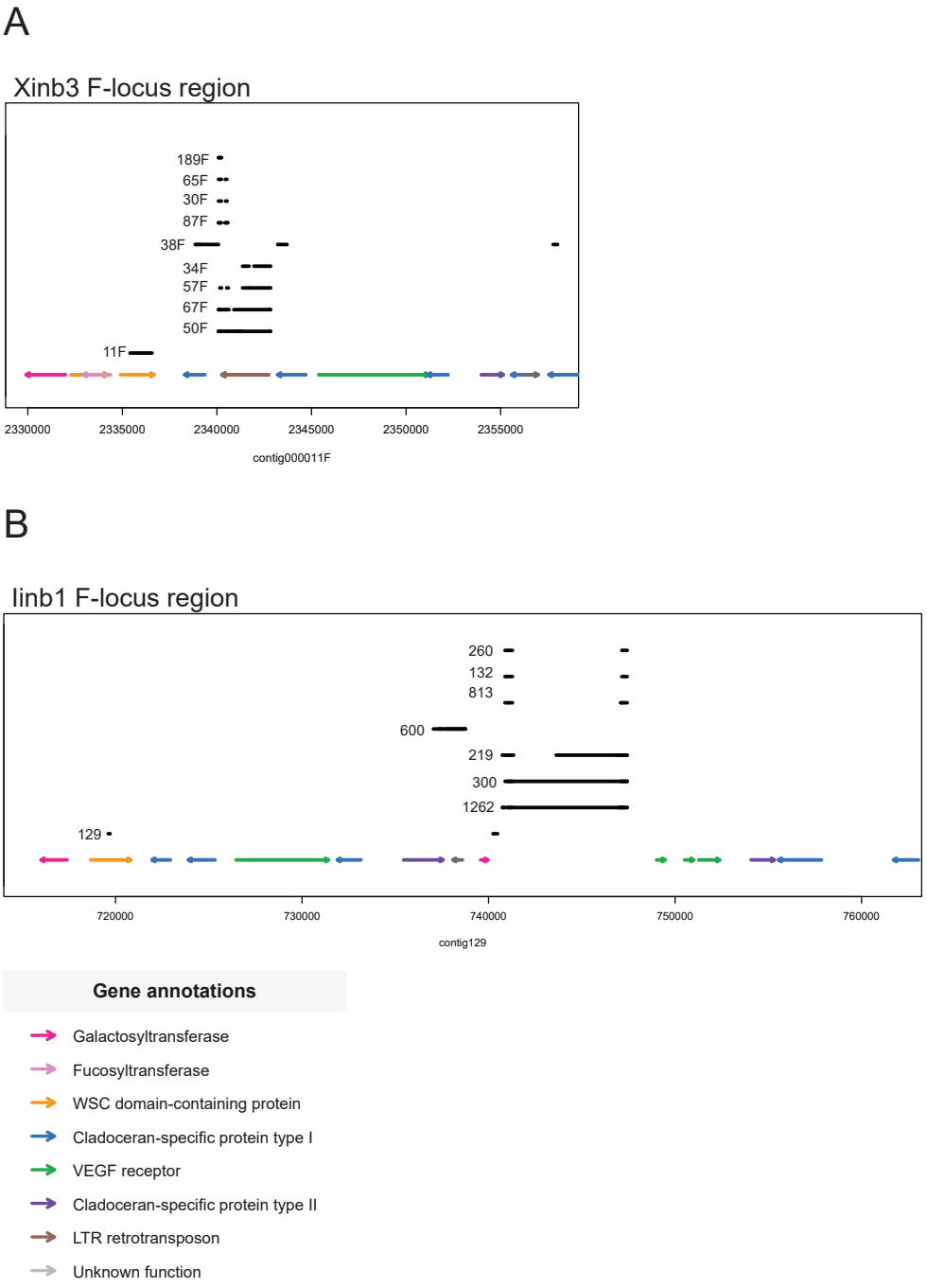
A
Xinb3 F-locus region
189F
65F
30F
87F
38F
34F
57F
67F
50F
11F
2330000
2335000
2340000
2345000
2350000
2355000
contig000011F
B
linb1 F-locus region
260
132
813
600
219
300
1262
129
720000
730000
740000
750000
760000
contig129
Gene annotations
Galactosyltransferase
Fucosyltransferase
WSC domain-containing protein
Cladoceran-specific protein type I
VEGF receptor
Cladoceran-specific protein type II
LTR retrotransposon
Unknown function

S3 Figure

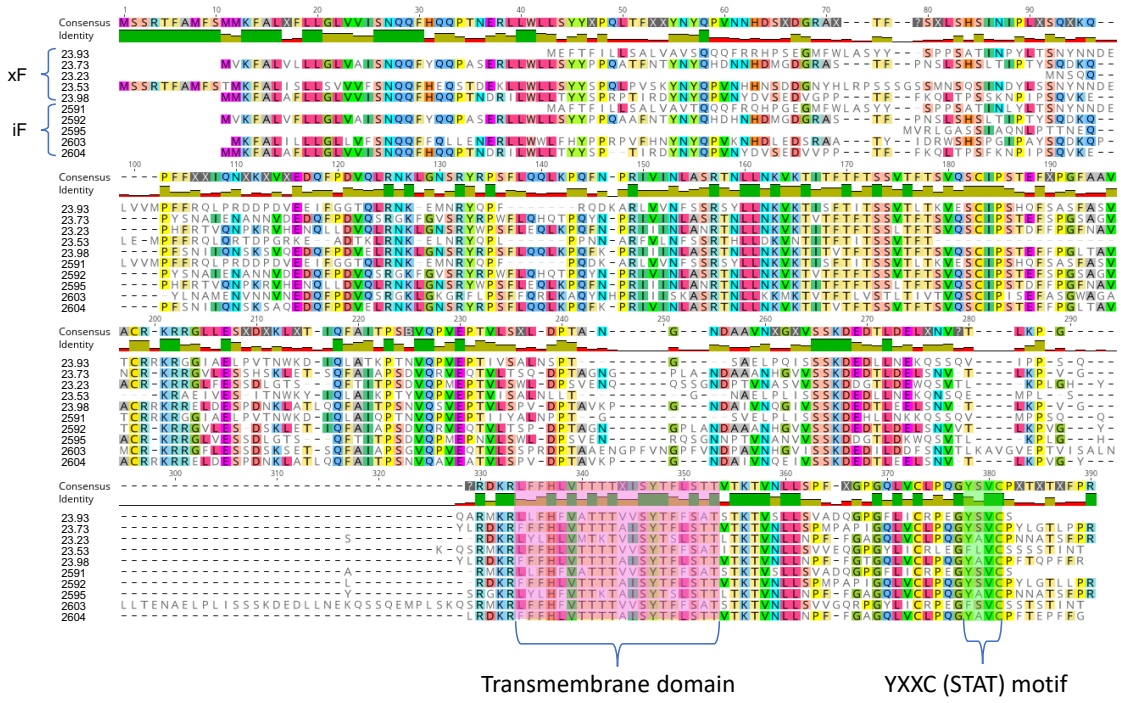
xF
iF
Consensus
Identity
Transmembrane domain
YXXC (STAT) motif

S4 Figure

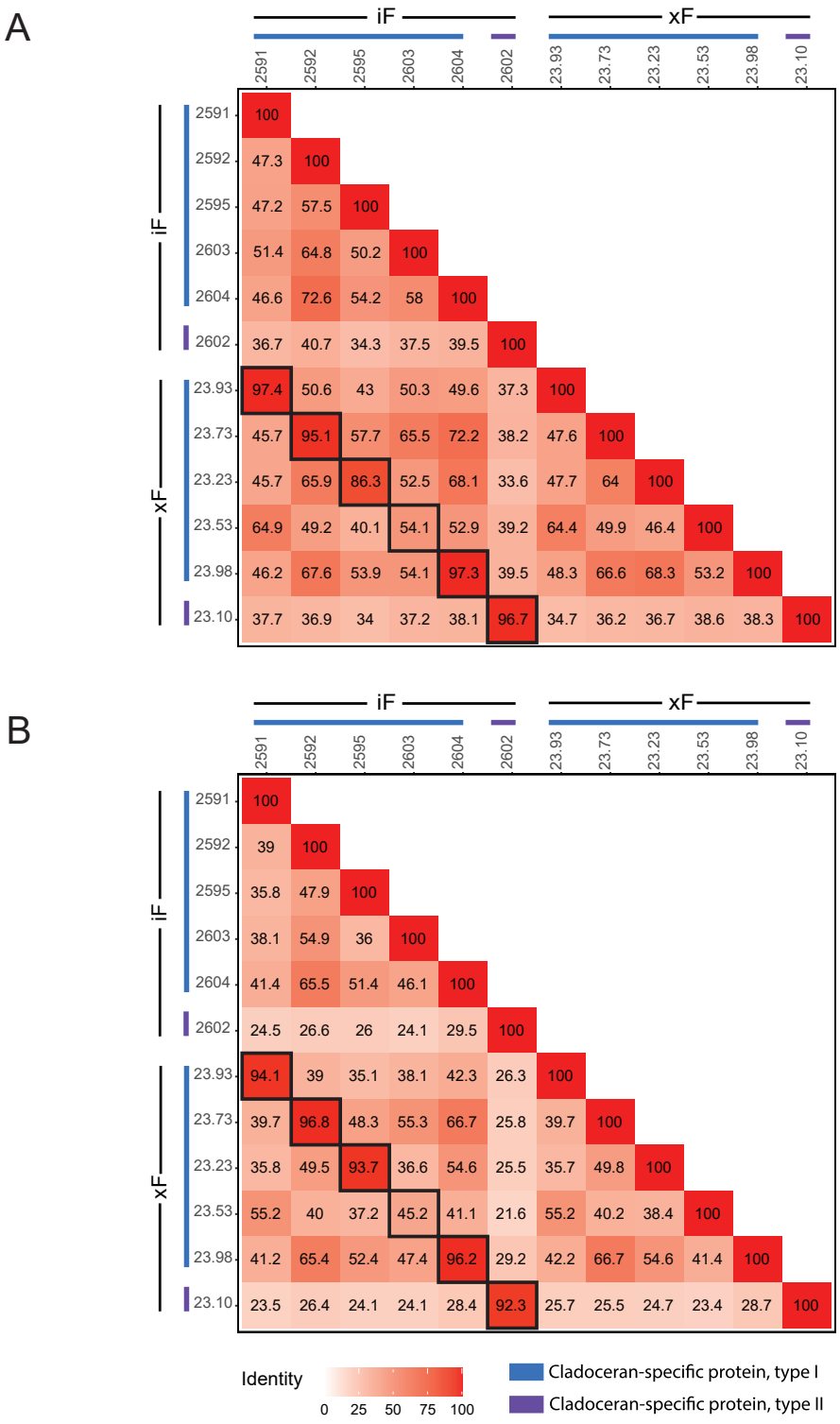
A
iF
xF
2591 2592 2595 2603 2604 2602 23.93 23.73 23.23 23.53 23.98 23.10
2591 100
2592 47.3 100
2595 47.2 57.5 100
2603 51.4 64.8 50.2 100
2604 46.6 72.6 54.2 58 100
2602 36.7 40.7 34.3 37.5 39.5 100
23.93 97.4 50.6 43 50.3 49.6 37.3 100
23.73 45.7 95.1 57.7 65.5 72.2 38.2 47.6 100
23.23 45.7 65.9 86.3 52.5 68.1 33.6 47.7 64 100
23.53 64.9 49.2 40.1 54.1 52.9 39.2 64.4 49.9 46.4 100
23.98 46.2 67.6 53.9 54.1 97.3 39.5 48.3 66.6 68.3 53.2 100
23.10 37.7 36.9 34 37.2 38.1 96.7 34.7 36.2 36.7 38.6 38.3 100
B
iF
xF
2591 2592 2595 2603 2604 2602 23.93 23.73 23.23 23.53 23.98 23.10
2591 100
2592 39 100
2595 35.8 47.9 100
2603 38.1 54.9 36 100
2604 41.4 65.5 51.4 46.1 100
2602 24.5 26.6 26 24.1 29.5 100
23.93 94.1 39 35.1 38.1 42.3 26.3 100
23.73 39.7 96.8 48.3 55.3 66.7 25.8 39.7 100
23.23 35.8 49.5 93.7 36.6 54.6 25.5 35.7 49.8 100
23.53 55.2 40 37.2 45.2 41.1 21.6 55.2 40.2 38.4 100
23.98 41.2 65.4 52.4 47.4 96.2 29.2 42.2 66.7 54.6 41.4 100
23.10 23.5 26.4 24.1 24.1 28.4 92.3 25.7 25.5 24.7 23.4 28.7 100
Identity
0 25 50 75 100
Cladoceran-specific protein, type I
Cladoceran-specific protein, type II

S5 Figure

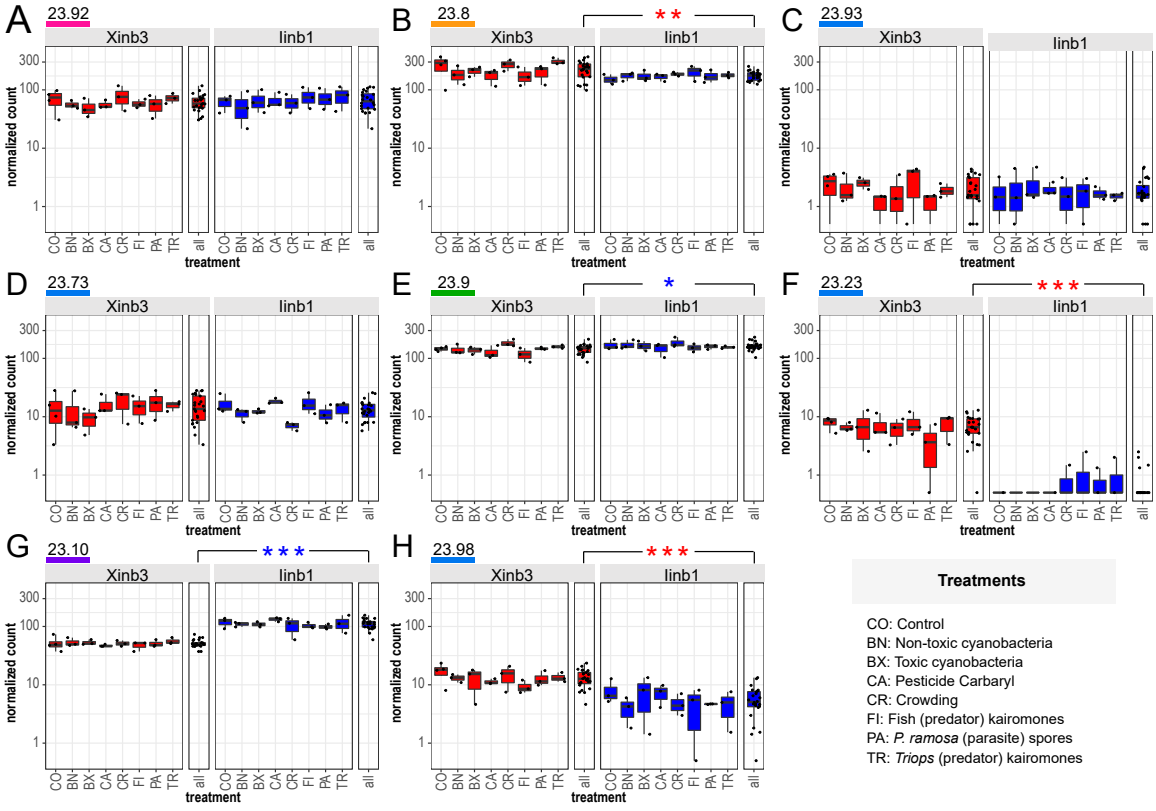
A
23.92
Xinb3
linb1
B
23.8
**
C
23.93
D
23.73
E
23.9
*
F
23.23
***
G
23.10
***
H
23.98
***
normalized count
300
100
10
1
CO
BN
BX
CA
CR
FI
PA
TR
all
treatment
Treatments
CO: Control
BN: Non-toxic cyanobacteria
BX: Toxic cyanobacteria
CA: Pesticide Carbaryl
CR: Crowding
FI: Fish (predator) kairomones
PA: P. ramosa (parasite) spores
TR: Triops (predator) kairomones

S6 Figure

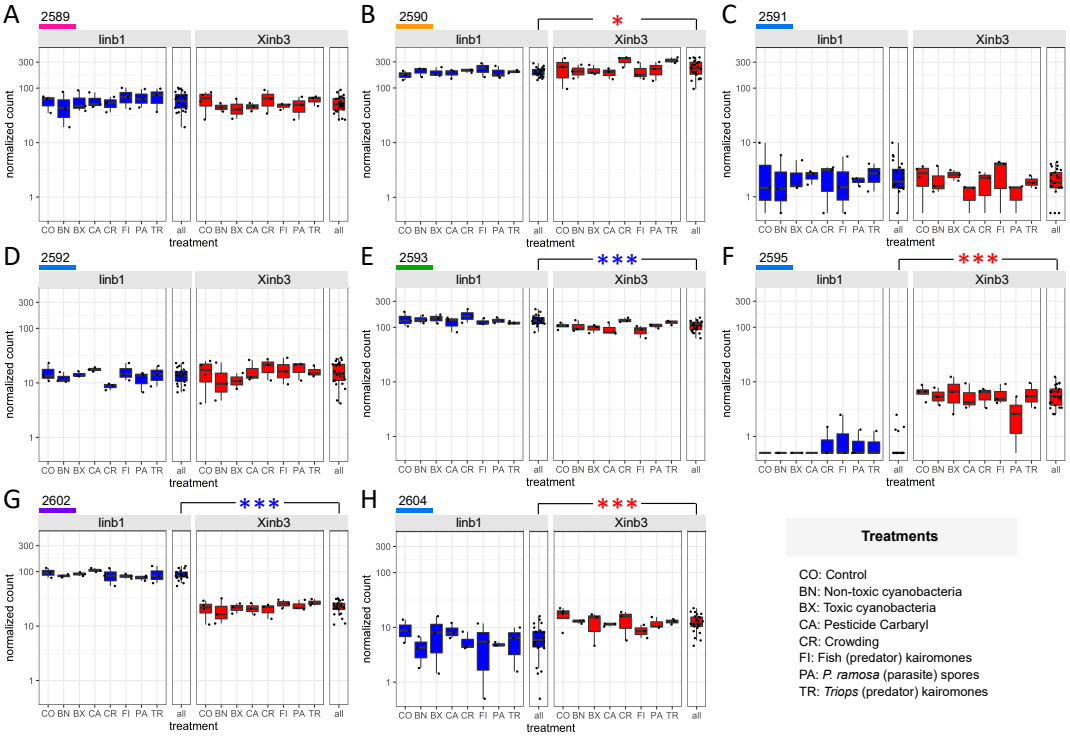
A
2589
linb1
Xinb3
B
2590
*
C
2591
D
2592
E
2593
***
F
2595
***
G
2602
***
H
2604
***
normalized count
300
100
10
1
CO BN BX CA CR FI PA TR all
treatment
Treatments
CO: Control
BN: Non-toxic cyanobacteria
BX: Toxic cyanobacteria
CA: Pesticide Carbaryl
CR: Crowding
FI: Fish (predator) kairomones
PA: P. ramosa (parasite) spores
TR: Triops (predator) kairomones

S7 Figure

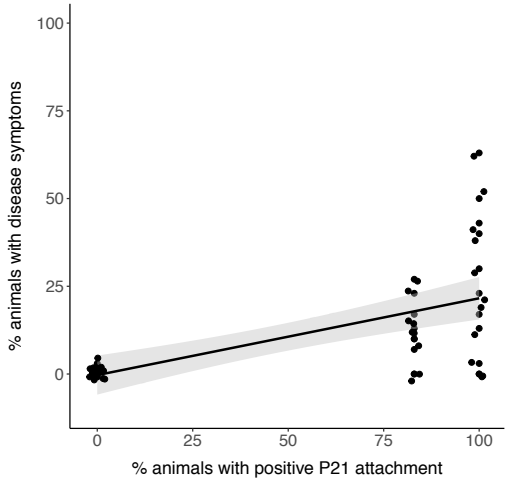
100
75
50
25
0
% animals with disease symptoms
0
25
50
75
100
% animals with positive P21 attachment

S8 Figure

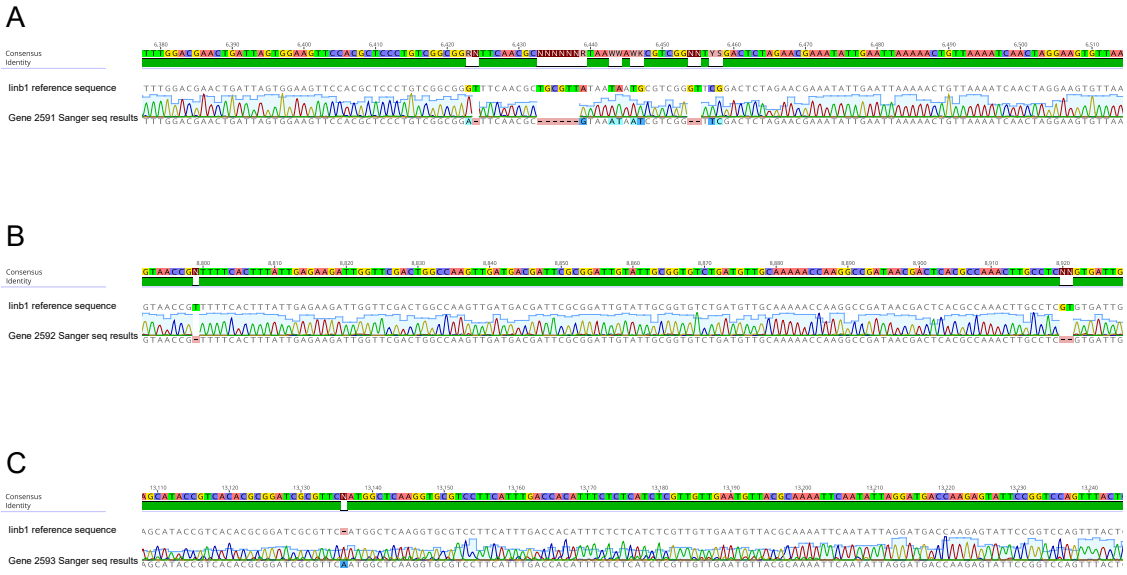

S9 Figure

Files S1-S6 will be publicly available upon publication.

DISCUSSION

My doctoral thesis comprises the first comprehensive analyses of the molecular adaptations of the visual system in the massive adaptive radiation of Lake Tanganyika cichlid fishes (**Chapter 1**: "Molecular evolution and depth-related adaptations of rhodopsin in the adaptive radiation of cichlid fishes in Lake Tanganyika" and **Chapter 2**: "Visual opsin gene expression evolution in the adaptive radiation of cichlid fishes of Lake Tanganyika"). With colleagues and collaborators, I examined visual opsin molecular changes reflecting advantageous phenotypic and ecological adaptations. **Chapter 1** shed light on the diversity and the deep-water adaptations of the rhodopsin and **Chapter 2** uncovered the transcriptomic dynamics and eco-morphological adaptations of rod and cone opsins. Here, I review the main results and conclusions of **Chapter 1** and **Chapter 2**, and I discuss the implications of the overall findings and address the future perspectives.

In **Chapter 1**, we examined the intron-less RH1 in 517 specimens representing 271 cichlid species of Lake Tanganyika. A single RH1 copy per species was retrieved with a great degree of amino acid sequence identity among all pairs of individuals. Among the variable sites that showed signals of positive selection, we found amino acid variants in dependence on the water depth at three key tuning sites, one site implicated in the protein stability, as well as 11 novel candidate sites.

In **Chapter 2**, we examined the retinal transcriptomic profiles of 753 specimens representing 112 cichlid species of Lake Tanganyika. We found that cone opsins, but not the rhodopsin, contribute to most of the variance in gene expression. We retrieved the three visual palettes previously identified in cichlids, in addition to two novel visual palettes exclusive to shallow- and deep-water living species. Furthermore, we detected a correlation between expression levels of particular opsins and eco-morphological traits.

In **Chapter 1** and **Chapter 2**, we primarily used the depth habitat and the stable carbon isotope composition per species to assess the habitat light conditions in the relatively clear waters of Lake Tanganyika. Yet, the ecological variables are not directly comparable but give similar overviews on the environmental light content. The presence of light in the range of UV to red is confined in the shallow water, as well as in the littoral zone of the lake. In contrast, blue and blue-green light prevails in deep waters and in the open-water benthic zone of the lake. The stable nitrogen isotope composition also informed us on the environmental light content. Indeed, species feeding on algae, plants and phytoplankton mostly occur in the shallow water where photosynthesis can happen. The eye size did not inform us on the light conditions, but rather suggests that species primarily living in dim-light environments might have bigger eyes in order to increase the catch of photons (see Musilova,

Cortesi, et al., 2019; Musilova, Salzburger, & Cortesi, 2021). Yet, no correlation between habitat and eye size was detected.

Taken together, the findings of **Chapter 1** and **Chapter 2** emphasised different strategies to improve the visual performance of Lake Tanganyika cichlids both in dim- and bright-light conditions.

The visual performance of the scotopic vision in Lake Tanganyika cichlids was examined at the level of RH1 protein sequences (**Chapter 1**) and gene expression levels (**Chapter 2**). We retrieved amino acid variants at sites very likely involved in deep-water adaptations, notably at key-tuning sites 292 and 299. Yet, no correlation between gene expression level and ecological traits has been detected. These results suggest that species living in bright- and dim-light habitats likely express differently tuned RH1s at relatively similar levels. Deep-water living species most probably express a blue-shifted RH1 (spectral shift due to the amino acid substitutions A292S and/or S299A) (Sugawara et al., 2005). The exact maximal spectral sensitivity should be estimated in the future with spectroscopy to confirm the effect of both the adaptive amino acid substitutions at key tuning sites (Yokoyama, 2008).

The adaptation and optimisation of the photopic vision in Lake Tanganyika cichlids was solely examined at the transcriptomic level (**Chapter 2**). In addition to the short-, medium-, and long-wavelength visual palettes, we newly identified a visual palette (SWS1+RH2B+LWS) – sensitive to both ends of the UV and visible light spectrum – exclusively expressed in five shallow-water living species (one Lamprologini and four Eretmodini species), and a visual palette (SWS2A+RH2B+RH2As) – sensitive to the central waveband of the spectrum – exclusively expressed in eight deep-water living species of the tribes Bathybatini, Limnochromini, and Trematocarini. Furthermore, we observed that species living in benthic/littoral (shallow) areas of the lake expressed less green-sensitive RH2As (opposite result in species living in the pelagic zone and/or in the depth of the lake). We also found that species feeding on plants and algae and thereby rather living in shallow waters expressed more of the UV-sensitive SWS1 and less of the blue-sensitive SWS2A (opposite result in more predatorial species). Overall, these results show that the environmental light conditions are implicated with changes in expression level of cone opsins sensitive to all types of wavelength. Future research should investigate the cone opsin amino acid variants at (key tuning) sites putatively in dependence on the water depth. So far, we only know that Lake Tanganyika cichlids harbour a single copy of each cone opsin, either complete or pseudogenized (see **Chapter 2**). Future studies should primarily focus on the sequence diversity of the UV-sensitive SWS1 and the red-sensitive LWS. Indeed, previous studies showed that the protein-coding sequences of cone opsins sensitive to the edge of the light spectrum are particularly variable (K. L. Carleton, Escobar-Camacho, Stieb, Cortesi, & Marshall, 2020; Hofmann et al.,

2009), reflecting shift in the maximal spectral sensitivity. This is very likely due to the relatively rapid absorption and scattering of UV and red light with water depth.

Regarding the eye size, we found that Lake Tanganyika cichlid species with bigger eyes expressed more RH1. These results suggest either an increase of RH1 expression per rods or a higher number of rods with a relatively steady RH1 expression level. A previous study on cardinal fish observed that bigger eyes haver larger retinas containing a higher density of photoreceptor cells (Fishelson, Ayalon, Zverdling, & Holzman, 2004). This scenario was as well suggested in coral reef fishes (Myrberg & Fuiman, 2002). The respective density of cones and rods in the retina as well as the expression of opsin genes per photoreceptor cells should be addressed with images of the retinal mosaic and single-cell sequencing.

In addition to opsin genes, whole retina RNA-sequencing enabled us to investigate the expression of important water depth-related genes. We found that in addition to cone opsins, several vision-, oxygen-, and circadian-related genes are differentially expressed in shallow- and deep-water living species. These results highlight the optimisation of the overall retinal transcriptome of Lake Tanganyika cichlids in relation to the different water properties found along the depth, especially the light and dissolved oxygen content. We also investigated the expression level of the enzyme responsible for the conversion of vitamin A1- and A2-derived chromophores [CYP27C1]. The change of chromophore from A1 to A2 shifts the maximal spectral sensitivity of all visual pigments towards longer wavelengths. Previous studies found that the CYP27C1 expression level correlates with the level of vitamin A2 and is higher in cichlid species living in turbid (red-shifted) water than in clear water (K. L. Carleton & Yourick, 2020; Härer, Meyer, & Torres-Dowdall, 2018; Torres-Dowdall et al., 2017). Our results revealed no significant association between the expression level of CYP27C1 and each of the ecological and morphological proxies (**Figure 2**).

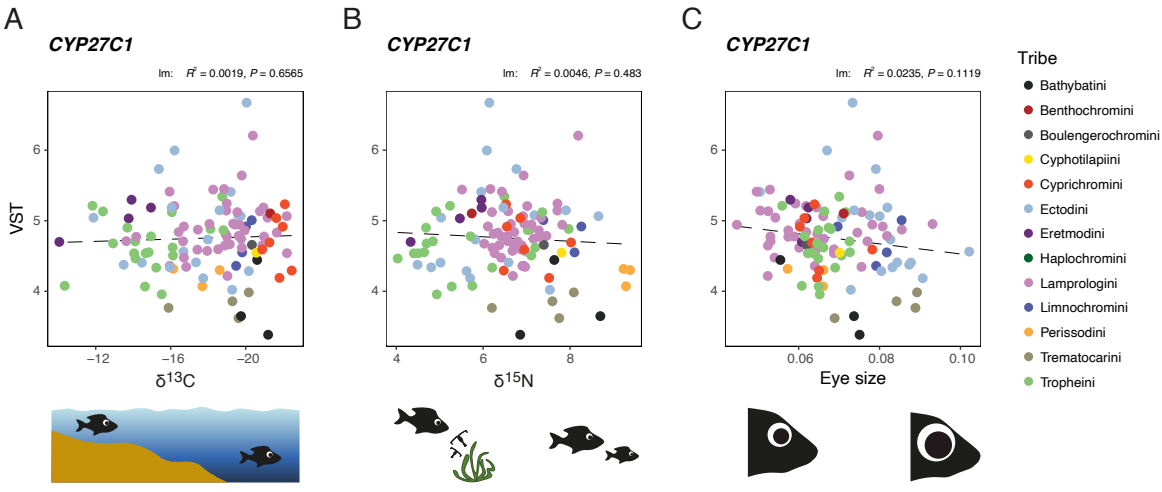

Figure 1 CYP27C1 gene expression and its correlation with ecology and eye size. Linear regression (lm) analyses showing the associations between CYP27C1 gene expression (VST-normalized count) and (**A**) **δ**^{13}C-

values as habitat proxy for a species' position along the benthic-pelagic axis, (**B**) δ^{15}N-values as proxy for the relative trophic level of a species, and (**C**) eye size. We considered significant results if $P < 0.05$ (linear regression depicted as a continuous black line); each dot represents a species and is colour-coded according to tribes. In the bottom panel, a schematic summary that illustrates the macrohabitat (**A**), trophic level (**B**) and eye size (**C**). The primarily riverine haplochromine *A. burtoni* as well as the more distantly related species *O. tanganicae* and *T. polylepis* were excluded from this analysis. For each correlation test, the R-squared (R^2) and the p-value (*P*) are indicated.

In addition to the eco-morphological traits used in our analyses, other environmental factors and species life-history traits are undoubtedly implicated in the adaptive evolution of the visual system and need attention in future projects. The key drivers of environmental light variation are spatial and temporal. Along the day, the light spectrum and intensity vary more in shallow and clear waters than in deep and turbid waters (Abate & Noakes, 2021; Musilova et al., 2021). In the temperate zone, the length of the day is shorter (and thus the light duration) and the water is clearer (free of algae and phytoplankton) in winter compared to summer. Furthermore, the lunar cycle, the weather, and the type of habitat (rocky, sandy, or the presence of vegetation) have also an effect on the local light conditions. Relative to phenotypic traits, the circadian rhythm is highly dependent on light environmental cues and has been detected in the retina of fish (e.g., diurnal rhythm of opsin expression) (Frøland Steindal & Whitmore, 2019; Halstenberg et al., 2005; Yourick et al., 2019). Lastly, body coloration (colour sexual dimorphism with typically brightly coloured males in cichlids) has been suggested to drive the evolution of the visual system through sexual selection, as mate choice would drive the evolution of the visual sensitivity, which in turn drives the evolution of the mate preference and so forth. In this respect, the sensory drive hypothesis explains how the visual system adapts to the local light environment and possibly leads to species divergence (e.g., colour polymorphism) and supposedly results in speciation (Boughman, 2002; Maan, Hofker, Van Alphen, & Seehausen, 2006; Schneider, Rometsch, Torres-Dowdall, & Meyer, 2020; Seehausen et al., 2008; Wright et al., 2020).

In addition to natural and/or sexual selection, the adaptation of the visual sensory system can be based on plasticity. Phenotypic plasticity can promote an individual phenotypic response to changing environments (e.g., variation in habitat light conditions) without a change in the individual genotype (Grenier, Barre, & Litrico, 1991; Perry, Schield, & Castoe, 2018). Phenotypic plasticity was not the focus of the present thesis and we would not be able to speculate on the contribution of plasticity to our findings. Yet, plasticity is suggested to facilitate adaptive evolution and therefore should be investigated in the adaptive evolution of cichlid fish to the different ecological niches in Lake Tanganyika (previous studies on plasticity in cichlids: Hofmann, O'Quin, Smith, & Carleton, 2010; Nandamuri, Yourick, & Carleton, 2017).

Overall, my doctoral thesis further contributed to the understanding of the genetic basis underlying the diversification of cichlids in Lake Tanganyika. My findings provided additional evidence that ecological speciation is implicated in the adaptive radiation of the African Great Lakes cichlids.

Making use of the established dataset of this thesis, future projects might be considered, such as:

- The validation of RH1 amino acid substitutions putatively shifting the maximal spectral sensitivity with the use of spectrometry (Musilova, Cortesi, et al., 2019)
- The examination of the cone opsin coding-protein sequences, the possible pseudogenes (Karen L. Carleton et al., 2008; Spady et al., 2005) and the deep-water adaptations in terms of amino acid variants (Cortesi et al., 2015; Fabrin, Gasques, Prioli, & Prioli, 2016; Spady et al., 2005), plus the validation of potential shifts in the maximal spectral sensitivity
- The incorporation of additional ecological and morphological/physiological traits potentially adaptive in the visual system. Notably, comparing the expression level of visual opsins with the circadian rhythm currently examined in Basel would be a great start.
- The examination of the spatial retinal distribution of photoreceptor cells and especially the retinal mosaic to investigate the putative loss of mosaic in deep-water living species (Musilova, Indermaur, et al., 2019; Musilova et al., 2021)
- The exploration of phenotypic plasticity of the visual system (Grenier et al., 1991; Nandamuri et al., 2017; Perry et al., 2018)
- The investigation of visual opsins in cichlids occurring in other rivers and lakes to investigate convergent evolution and the putative constraints of the visual system (O'Quin, Hofmann, Hofmann, & Carleton, 2010)
- The incorporation of additional transcriptomic analyses with larval and juvenile specimens to investigate differential gene expression throughout the different life stages (wild or lab raised individuals) (Lupše et al., 2021)
- The examination of opsin regulatory elements (Hofmann et al., 2009; O'Quin et al., 2012), including TE activity (Karen L. Carleton et al., 2020)
- The investigation of the expression of non-visual opsins (Feuda, Menon, & Göpfert, 2022)

Lastly, I generated various scripts to analyse both genomic and transcriptomic data. Most codes included custom-made functions in combination with existing software and modules. They were developed to be applied on hundreds of files and can be of great help in future studies. Generic version of the main scripts used in the different projects are available on GitHub (https://github.com/cichlidx/ronco_et_al, https://github.com/Ninet93/RH1_Ricci_et_al, https://github.com/Ninet93/RNASeq_Ricci_et_al).

References

Abate, M. E., & Noakes, D. L. G. (2021). *The Behavior , Ecology and Evolution of Cichlid Fishes*. Springer.

Boughman, J. W. (2002). How sensory drive can promote speciation. *Trends in Ecology and Evolution*, *17*(12), 571–577. doi: 10.1016/S0169-5347(02)02595-8

Carleton, K. L., Escobar-Camacho, D., Stieb, S. M., Cortesi, F., & Marshall, N. J. (2020). Seeing the rainbow: mechanisms underlying spectral sensitivity in teleost fishes. *Journal of Experimental Biology*, *223*. doi: 10.1242/jeb.193334

Carleton, K. L., & Yourick, M. R. (2020). Axes of visual adaptation in the ecologically diverse family Cichlidae. *Seminars in Cell and Developmental Biology*, *106*, 43–52. doi: 10.1016/j.semcdb.2020.04.015

Carleton, Karen L., Conte, M. A., Malinsky, M., Nandamuri, S. P., Sandkam, B. A., Meier, J. I., … Kocher, T. D. (2020). Movement of transposable elements contributes to cichlid diversity. *Molecular Ecology*, *29*(24), 4956–4969. doi: 10.1111/mec.15685

Carleton, Karen L., Spady, T. C., Streelman, J. T., Kidd, M. R., McFarland, W. N., & Loew, E. R. (2008). Visual sensitivities tuned by heterochronic shifts in opsin gene expression. *BMC Biology*, *6*, 1–14. doi: 10.1186/1741-7007-6-22

Cortesi, F., Musilová, Z., Stieb, S. M., Hart, N. S., Siebeck, U. E., Malmstrøm, M., … Salzburger, W. (2015). Ancestral duplications and highly dynamic opsin gene evolution in percomorph fishes. *Proceedings of the National Academy of Sciences of the United States of America*, *112*(5), 1493–1498. doi: 10.1073/pnas.1417803112

Fabrin, T. M. C., Gasques, L. S., Prioli, S. M. A. P., & Prioli, A. J. (2016). Opsin genes: Research perspectives with neotropical cichlids (perciformes: Cichlidae) and their relevance in floodplain studies. *Acta Scientiarum - Biological Sciences*, *38*(2), 241–246. doi: 10.4025/actascibiolsci.v38i2.28295

Feuda, R., Menon, A. K., & Göpfert, M. C. (2022). Rethinking Opsins. *Molecular Biology and Evolution*, *39*(3), 1–10. doi: 10.1093/molbev/msac033

Fishelson, L., Ayalon, G., Zverdling, A., & Holzman, R. (2004). Comparative Morphology of the Eye (with Particular Attention to the Retina) in Various Species of Cardinal Fish (Apogonidae, Teleostei). *Anatomical Record - Part A Discoveries in Molecular, Cellular, and Evolutionary Biology*, *277*(2), 249–261. doi: 10.1002/ar.a.20005

Frøland Steindal, I. A., & Whitmore, D. (2019). Circadian clocks in fish-what have we learned so far? *Biology*, *8*(1). doi: 10.3390/biology8010017

Grenier, S., Barre, P., & Litrico, I. (1991). Phenotypic Plasticity and Selection: Nonexclusive Mechanisms of Adaptation. *Scientifica*, *2016*.

Halstenberg, S., Lindgren, K. M., Samagh, S. P. S., Nadal-Vicens, M., Balt, S., & Fernald, R. D. (2005). Diurnal rhythm of cone opsin expression in the teleost fish Haplochromis burtoni. *Visual Neuroscience*, *22*(2), 135–141. doi:

10.1017/S0952523805222022

Härer, A., Meyer, A., & Torres-Dowdall, J. (2018). Convergent phenotypic evolution of the visual system via different molecular routes: How Neotropical cichlid fishes adapt to novel light environments. *Evolution Letters*, *2*(4), 341–354. doi: 10.1002/evl3.71

Hofmann, C. M., O'Quin, K. E., Justin Marshall, N., Cronin, T. W., Seehausen, O., & Carleton, K. L. (2009). The eyes have it: Regulatory and structural changes both underlie cichlid visual pigment diversity. *PLoS Biology*, *7*(12). doi: 10.1371/journal.pbio.1000266

Hofmann, C. M., O'Quin, K. E., Smith, A. R., & Carleton, K. L. (2010). Plasticity of opsin gene expression in cichlids from Lake Malawi. *Molecular Ecology*, *19*(10), 2064–2074. doi: 10.1111/j.1365-294X.2010.04621.x

Lupše, N., Cortesi, F., Freese, M., Marohn, L., Pohlmann, J. D., Wysujack, K., … Musilova, Z. (2021). Visual Gene Expression Reveals a cone-to-rod Developmental Progression in Deep-Sea Fishes. *Molecular Biology and Evolution*, *38*(12), 5664–5677. doi: 10.1093/molbev/msab281

Maan, M. E., Hofker, K. D., Van Alphen, J. J. M., & Seehausen, O. (2006). Sensory Drive in Cichlid Speciation. *The American Naturalist*, *167*(6), 947–954. doi: https://doi.org/10.1086/503532

Musilova, Z., Cortesi, F., Matschiner, M., Davies, W. I. L., Patel, J. S., Stieb, S. M., … Salzburger, W. (2019). Vision using multiple distinct rod opsins in deep-sea fishes. *Science*, *364*(6440), 588–592. doi: 10.1126/science.aav4632

Musilova, Z., Indermaur, A., Bitja-Nyom, A. R., Omelchenko, D., Kłodawska, M., Albergati, L., … Salzburger, W. (2019). Evolution of the visual sensory system in cichlid fishes from crater lake Barombi Mbo in Cameroon. *Molecular Ecology*, *28*, 5010–5031. doi: 10.1111/mec.15217

Musilova, Z., Salzburger, W., & Cortesi, F. (2021). The Visual Opsin Gene Repertoires of Teleost Fishes: Evolution, Ecology, and Function. *Annual Review of Cell and Developmental Biology*, *37*(1), 441–468. doi: 10.1146/annurev-cellbio-120219-024915

Myrberg, A. A., & Fuiman, L. A. (2002). The Sensory World of Coral Reef Fishes. *Coral Reef Fishes*, 123–148. doi: 10.1016/b978-012615185-5/50009-8

Nandamuri, S. P., Yourick, M. R., & Carleton, K. L. (2017). Adult plasticity in African cichlids: Rapid changes in opsin expression in response to environmental light differences. *Molecular Ecology*, *26*(21), 6036–6052. doi: 10.1111/mec.14357

O'Quin, K. E., Hofmann, C. M., Hofmann, H. A., & Carleton, K. L. (2010). Parallel Evolution of opsin gene expression in African cichlid fishes. *Molecular Biology and Evolution*, *27*(12). doi: 10.1093/molbev/msq171

O'Quin, K. E., Schulte, J. E., Patel, Z., Kahn, N., Naseer, Z., Wang, H., … Carleton, K. L. (2012). Evolution of cichlid vision via trans-regulatory divergence. *BMC Evolutionary Biology*, *12*(1). doi: 10.1186/1471-2148-12-251

Perry, B. W., Schield, D. R., & Castoe, T. A. (2018). Evolution: Plasticity versus

Selection, or Plasticity and Selection? *Current Biology*, *28*(18), R1104–R1106. doi: 10.1016/j.cub.2018.07.050

Schneider, R. F., Rometsch, S. J., Torres-Dowdall, J., & Meyer, A. (2020). Habitat light sets the boundaries for the rapid evolution of cichlid fish vision, while sexual selection can tune it within those limits. *Molecular Ecology*, *29*(8), 1476–1493. doi: 10.1111/mec.15416

Seehausen, O., Terai, Y., Magalhaes, I. S., Carleton, K. L., Mrosso, H. D. J., Miyagi, R., … Okada, N. (2008). Speciation through sensory drive in cichlid fish. *Nature*, *455*(7213), 620–626. doi: 10.1038/nature07285

Spady, T. C., Seehausen, O., Loew, E. R., Jordan, R. C., Kocher, T. D., & Carleton, K. L. (2005). Adaptive molecular evolution in the opsin genes of rapidly speciating cichlid species. *Molecular Biology and Evolution*, *22*(6), 1412–1422. doi: 10.1093/molbev/msi137

Sugawara, T., Terai, Y., Imai, H., Turner, G. F., Koblmüller, S., Sturmbauer, C., … Okada, N. (2005). Parallelism of amino acid changes at the RH1 affecting spectral sensitivity among deep-water cichlids from Lakes Tanganyika and Malawi. *Proceedings of the National Academy of Sciences of the United States of America*, *102*(15), 5448–5453. doi: 10.1073/pnas.0405302102

Torres-Dowdall, J., Pierotti, M. E. R., Härer, A., Karagic, N., Woltering, J. M., Henning, F., … Meyer, A. (2017). Rapid and Parallel Adaptive Evolution of the Visual System of Neotropical Midas Cichlid Fishes. *Molecular Biology and Evolution*, *34*(10), 2469–2485. doi: 10.1093/molbev/msx143

Wright, D. S., van Eijk, R., Schuart, L., Seehausen, O., Groothuis, T. G. G., & Maan, M. E. (2020). Testing sensory drive speciation in cichlid fish: Linking light conditions to opsin expression, opsin genotype and female mate preference. In *Journal of Evolutionary Biology* (Vol. 33). doi: 10.1111/jeb.13577

Yokoyama, S. (2008). Evolution of dim-light and color vision pigments. *Annual Review of Genomics and Human Genetics*, *9*, 259–282. doi: 10.1146/annurev.genom.9.081307.164228

Yourick, M. R., Sandkam, B. A., Gammerdinger, W. J., Escobar-Camacho, D., Nandamuri, S. P., Clark, F. E., … Carleton, K. L. (2019). Diurnal variation in opsin expression and common housekeeping genes necessitates comprehensive normalization methods for quantitative real-time PCR analyses. *Molecular Ecology Resources*, *19*(6), 1447–1460. doi: 10.1111/1755-0998.13062

ACKNOWLEDGEMENTS

The PhD brought me intellectual and emotional challenges, but everything is possible with an expanding group of supporting, loving and lovable people.

First of all, I would like to thank my supervisor, **Walter Salzburger**, who gave me a golden opportunity to do my PhD thesis in his group. *I am genuinely grateful for your guidance (underwater in Lake Tanganyika as well) and help throughout the past four-five years. Merci infiniment.*

I would like to thank from the bottom of my heart "my sister from another egg", **Fabrizia Ronco**. *You have been the most exceptional co-supervisor, but also the most encouraging and motivating sister. I am thankful for everything you showed me, taught me and helped me with. Merci du fond du coeur.*

Since good things come in threes. I would like to sincerely thank my co-supervisor, **Patrick Tschopp**, for his valuable help and feedback as a co-supervisor. *Merci beaucoup.*

I would like to thank **Nicolas Boileau** for being "all-in-one". *You have been an amazing office buddy, lab buddy, co-author, and friend. Merci mille fois.*

I would like to truly thank my co-author **Zuzana Musilova**, as well as **Fabio Cortesi**, for completing the "Team Cichlid Vision". *Merci pour tout.*

I would like to thank very much my co-author **Maridel Fredericksen** for her precious support and presence. *Grand merci.*

I would like to thank my office buddies, **Telma Laurentino** and **Grégoire Vernaz**, for entertaining and softening my PhD life on a daily basis. *Obrigada, merci.*

I would like to thank Mama **Joana Santos** for her precious love and support. *Muito obrigada.*

I would like to thank all former and present members of the Salzburger Lab and the Zoological Institute, and notably **Attila Rüegg**, **Athimed El Taher**, **Marcos da Silva**, **Adrian Indermaur**, **Charlotte Huyghe**, **Antoine Fages**, **Frédéric Schedel**, **Tomasz Mamos**, **Daniela Souza**, **Lily Fogg**, **Anja Häfeli**, **James Lusana**, **Maëva Luxey**, and **Dieter Ebert**, for the constant support. *Vielen Dank.*

I would like to thank the **sciCORE team** for their help and advice, as well as **Christian Beisel** and **Elodie Burcklen,** and the **D-BSSE team** for the retina RNA-sequencing. *Merci*.

I would like to thank my **Räppli Huus family**, including **Christian Feregrino** and **Bianka Berki**, for their support and the happiness and joy you all brought in my life. *Merci pour tout*.

I would like to thank everyone at **UNIL** who has believed in me as a scientist, especially **Nicolas Salamin**, **Anna Marcionetti**, **Anthony Sonrel**, and **Cyril Matthey-Doret**. *Merci à tous*.

I would like to thank **my friends** and **my EA family** for the valuable support. Notably, I would like to thank my lovely friend, **Vivi L.**, for her loving support. *Merci beaucoup.*

I would like to thank my long-lasting friends, **Marie D.**, **Laurence S.** and **Daniel B.**, for your endless love and support. *Merci merci merci*.

I would like to thank the incredible **Thibault T.** for actually proving that vision is overrated. *Merci cousin*.

Finally, I would like to thank **my family** for their presence, advice, encouragement, and love. In French : *Merci à ma famille pour votre présence, vos conseils, vos encouragements, et votre amour. Merci maman.*

Visual system adaptations in the cichlid fish fauna of Lake Tanganyika

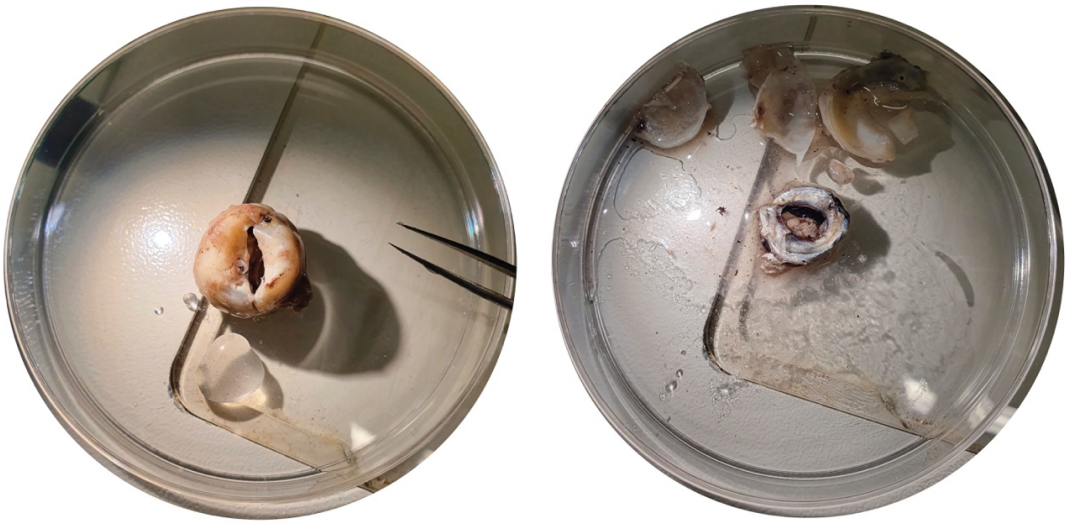

Eye dissection (*Oreochromis tanganicae*)

Inauguraldissertation zur
Erlangung der Würde eines Doktors der Philosophie
vorgelegt der Philosophisch-Naturwissenschaftlichen Fakultät
der Universität Basel von

Virginie Micheline Irène **Ricci**

betreut von
Prof. Dr. Walter Salzburger

evaluiert von
Prof. Dr. Walter Salzburger, Prof. Dr. Patrick Tschopp,
Dr. Maude Baldwin & Dr. Fabrizia Ronco

Basel, 2023